New and unusual co-ordination of main group elements

Helen Goodwin

How to cite:

Goodwin, Helen (1990) New and unusual co-ordination of main group elements. Doctoral thesis, Durham University.

NEW AND UNUSUAL CO-ORDINATION OF MAIN GROUP ELEMENTS

by

Helen Goodwin, B.Sc.(Dunelm)

University of Durham

A Thesis submitted in part fulfillment of the requirements for the degree of Doctor of Philosophy at the University of Durham.

February 1990

STATEMENT OF COPYRIGHT.

DECLARATION

The work described in this thesis was carried out in the Department of Chemistry at the University of Durham between October 1986 and October 1989. All the work is my own, unless stated to the contrary, and it has not been submitted previously for a degree at this or any other University.

(The part of the work carried out in Toulouse was with official permission).

To Mum and Dad.

ACKNOWLEDGEMENTS

I would like to thank Dr. K.B. Dillon, for his continual help and encouragement, and Professor R.D. Chambers for his ideas and interest in this work. I would also like to express my thanks to Dr. R. Matthews and J. Banks for NMR data and allowing my access to the NMR facilities. Thankyou to Dr. M. Jones and V. McNeilly for mass spectra, and B. Coult and M. Cox for elemental analyses.

My special thanks for technical assistance by D. Hunter, J. Lincoln and R. Plumb, glass blowing by R. Hart and G. Haswell and Professor W.S. Sheldrick for crystal structure data.

Many thanks are due to all my colleagues. I would especially like to thank Mr. Paul Wight for his help with the MNDO calculations.

I am very grateful to Nigel Smith and my sister Angela for all their work in typing, to my Dad for his helpful discussions, and to my Mum and Dad for their endless help and support.

J'aimerais remercier le groupe de M. Guy Bertrand pour m'avoir donné la chance, de traveiller dans le laboratoire de chemie de coordination du C.N.R.S. à Toulouse. Je tiens particulièrement à remercier Guy Bertrand et Antoine Baceiredo pour leur aide précieuse, ainsi que pour leur grande disponibilité, ce que m'a ainsi permis de mener à bien mon travail.

ABSTRACT

NEW AND UNUSUAL CO-ORDINATION OF MAIN GROUP ELEMENTS.

There is considerable current interest in the chemistry of low coordinate main group elements, the extensive development of which was highlighted at last year's Euchem Conference Psiblocs in Paris-Palaiseau (August 1988).

This area has been stimulated by the isolation of low coordination compounds stabilised by the use of bulky groups, for example, Supermes, mes (see Chapters 3 and 4).

Following the synthesis of 1,3,5 tris-trifluoromethyl benzene (ArH) by R.D. Chambers *et al.* (Chapter 1), and the facilities available to synthesise this material it seemed very worthwhile to study the influence of this substituent on low coordinate main group species.

As a result, this group has been incorporated into phosphines, diphosphenes, phosphaalkenes, antimony and boron derivatives. Its involvement in other systems, for example borinium and phosphoranide species, and its incorporation into the cation associated with halo and pseudohalo borate anions, have also been examined. In particular, the low coordination chemistry of phosphorus has involved the synthesis, isolation and full characterisation of the new diphosphene (19) [prepared independently by Edelmann *et al.*]† and the unsymmetrical diphosphene (20) (Figure C1). The 2,6-bis(trifluoromethylphenyl) substituent has been employed by Escudié *et al.*‡

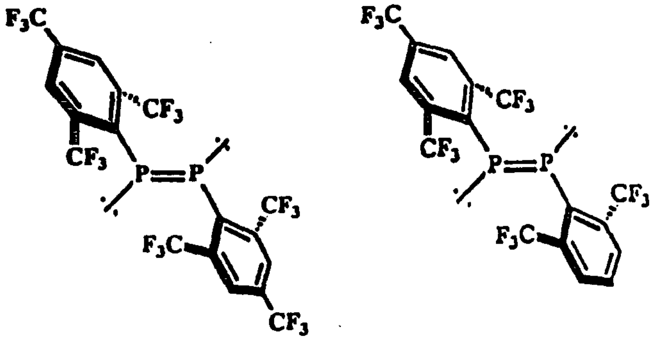

Figure C1: *The Ar-substituted symmetrical and unsymmetrical diphosphenes.*

---

†M. Scholz, H.W. Roesky, D. Stalke, K. Keller and F.T. Edelmann, *J.Organometallic Chem.*, 366, 73-85 (1989).

‡J. Escudié, C. Couret, H. Ranaivonjatovo, M. Lazraq and J. Satgé, *Phosphorus and Sulfur*, 31, 27-31 (1987).

The formation of the species ArP=PMes (21) and $ArP=PNiPr_2$ (22) [where Ar ≡ $(CF_3)_3C_6H_2$], in solution has been demonstrated by NMR.

The first phosphaalkene containing the Aryl group on phosphorus stable to vacuum distillation has been prepared *ie.* $ArP=C(Cl)_2$ (31) and a synthetic route to other phosphaalkenes containing the Ar group has been elucidated (Chapter 4). Where appropriate, the structure, characteristics of stabilisation, spectroscopic parameters and transition-metal coordination have been critically examined.

The first nitrileimines containing boron with phosphorus and silicon respectively were synthesised (Chapter 11). Their reactivity was studied, including their use as synthons for heterocycles, and their rearrangement by photolysis to new carbodiimides.

In view of the wide range of studies included it was decided to present the various aspects as separate chapters. The references are given at the end of each chapter. Experimental details and suggestions for further work are also provided within the appropriate chapters.

Helen Goodwin (February 1990)

ABBREVIATIONS

Ar	2,4,6-Tris(trifluoromethyl)phenyl
Ar'	2,6-Bis(trifluoromethyl)phenyl
Ar"	2-Trifluoromethylphenyl
Mes	2,4,6-Tri - (methyl)phenyl
Supermes	2,4,6-Tri-(t-butyl)phenyl
tmp	Tetramethylpiperidine
THF	Tetrahydrofuran
TCOQ	Tetrachloroorthoquinone
DBU	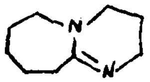
DABCO	
HOMO	Highest Occupied Molecular Orbital
LUMO	Lowest Occupied Molecular Orbital
MNDO	Modified Neglect of Diatomic Overlap
AM1	Austin Model 1
LDA	Lithium diisopropylamide
UHF	Unrestricted Hartree-Fock
RHF	Restricted Hartree-Fock
NI	Nitrileimine
CD	Carbodiimide
CA	Cycloadduct
DCD	Dewar-Chatt-Duncanson

CONTENTS PAGE

CHAPTER THREE - DIPHOSPHENES 32

CHAPTER ONE

ORGANOLITHIUM STARTING MATERIALS

1.1 THE 2,4,6-TRIS(TRIFLUOROMETHYL)PHENYL SUBSTITUENT

1,3,5-Tris(trifluoromethyl)benzene (ArH) (1) was prepared using high pressure techniques by R.D. Chambers *et al.*[1] (Figure 1.1). Some aspects of the chemistry of this species have been investigated [1]. It was shown to lithiate directly when treated with butyl or methyl lithium forming 2,4,6-tris(trifluoromethyl)phenyllithium (ArLi) (2) [1]. The lithium compound could then be used to prepare organometallic derivatives for example with Sn(IV) and Cu(I).

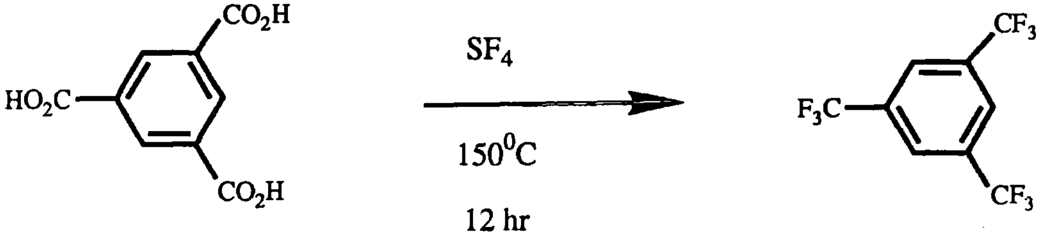

(1)

Figure 1.1: *The synthesis of ArH (1).*

For the first time it was hoped to study the influence of this substituent on the possible stabilisation of low coordinate complexes, and its introduction into phosphorus, antimony and boron compounds. Some of the work on phosphorus was independently carried out by Edelmann *et al.* [2]. Some of the selective reactions carried out in this work illustrate the behaviour of Ar as an electron withdrawing group (A), and its behaviour as a sterically hindering moiety (B).

(A) No normal oxidative fluorination of chlorophosphines occurs with strongly electronegative groups attached to phosphorus. [3]. $ArPF_2$ (3) was prepared as shown (Figure 1.2) and details are given in Section 2.3.1.

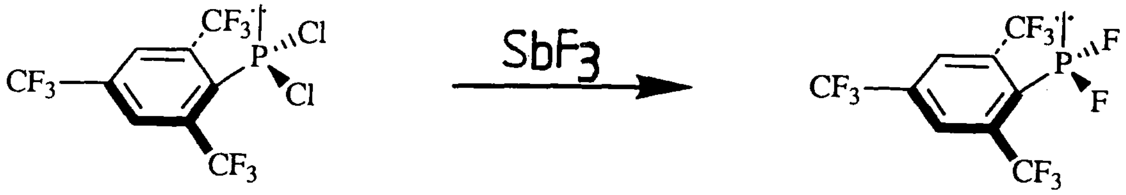

(12) (3)

Figure 1.2: *The synthetic route to $ArPF_2$.*

(B) No formation of Ar_3P was observed (Equation 1.1), attributed to steric crowding around the phosphorus atom. The ^{19}F NMR data for Ar_2BCl (4) (Equation 1.2) shows an inequivalence of the ortho-trifluoromethyl groups, similarly ascribed to steric crowding around the trigonal boron, also observed in the MNDO calculation (Section 8.7).

$$3\ \mathrm{ArLi}\ (2) + \mathrm{PCl_3} \xrightarrow{\ X\ } \mathrm{Ar_3P} \qquad (1.1)$$

$$2\ \mathrm{ArLi}\ (2) + \mathrm{BCl_3} \longrightarrow \mathrm{Ar_2BCl}\ (4) \qquad (1.2)$$

1.2 INTRODUCTION TO ORGANOLITHIUM COMPOUNDS

An excellent up-to-date review on the preparation of organolithium species is available [4]. The methods may be summarised as follows:

1) (a) Preparation from organo halides (Equation 1.3);

(b) Metal/halogen exchange (Equation 1.4). Early work has been comprehensively reviewed in this area by G. Köbrich [5].

$$\mathrm{RX} + 2\mathrm{Li} \longrightarrow \mathrm{RLi} + \mathrm{LiX} \qquad (1.3)$$

$$\mathrm{RLi} + \mathrm{R'X} \rightleftharpoons \mathrm{R'Li} + \mathrm{RX} \qquad (1.4)$$

$$\mathrm{RLi} + \mathrm{R'H} \longrightarrow \mathrm{RH} + \mathrm{R'Li} \qquad (1.5)$$

2) Preparation by metallation (Equation 1.5) [6]. A reaction occurs with a relatively strongly acidic hydrocarbon and when a proton is activated by an α- or β-heteroatom, thus increasing the kinetic or

thermodynamic acidity of a particular hydrogen atom [4]. Lithiation takes place with alkyl-lithium, *eg*. BuLi. However, when nucleophilic character is incompatible, for example in the presence of a carbonyl functionality, reagents with high basicity but relatively low nucleophilicity are employed, for example lithium diisopropyl amide (LDA).

3) Three less widely used methods are:
   (a) Preparation from other organometallic compounds [6] (Equation 1.6).
   (b) From ethers and thioethers (Equation 1.7) and
   (c) From sulphonylhydrazone (Equation 1.8)[4]

$$(CH_2{=}CH)_4Sn + 4\ BuLi \longrightarrow 4CH_2{=}CHLi + Bu_4Sn \qquad (1.6)$$

$$CH_2CHCH_2OPh + 2Li \longrightarrow CH_2{=}CHCH_2Li + LiOPh \qquad (1.7)$$

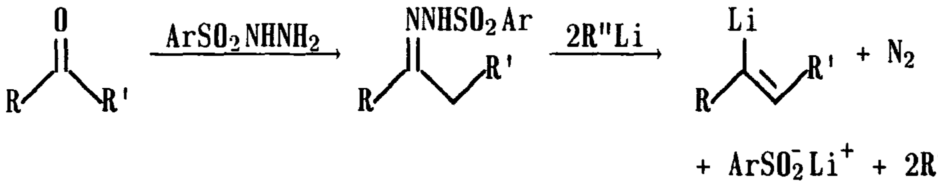

(1.8)

1.3 ArLi SYNTHESIS AND STRUCTURE

ArLi (2) was generated *via* route 2 (Equation 1.5) [1]. The species is ideally set up for this reaction because of the ortho-trifluoromethyl groups which significantly increase the acidity of the proton. In THF, ArH would not lithiate on the addition of BuLi. It is unclear why this should be so. In order to attempt isolation of ArLi in a crystalline form, TMEDA was added to the ArLi solution in ether. No crystals were formed even on cooling. In comparison, 2,4,6-tri(t-butyl)phenyllithium·TMEDA, is soluble in ether down to -100 °C [7]. Lower temperatures may allow isolation of the ArLi·TMEDA complex and hence its structural elucidation.

To compare the ArLi (2) with other lithium compounds: 2,4,6-tri-(t-butyl)phenyllithium (5) is monomeric in THF, and 2,4,6-(trimethyl) phenyl lithium (6), due to its solubility problems, could only be recorded by NMR in the presence of TMEDA, so it was not surprising that a monomeric structure was found [7] (Figure 1.3).

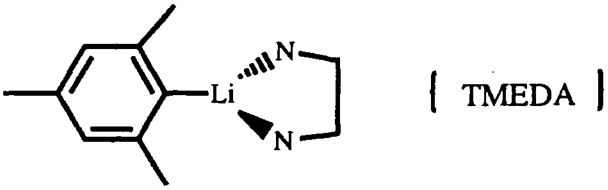

Figure 1.3: *MesLi Compound (6).*

For ArLi (2), because of the electron density which must exist around the ortho-trifluoromethyl groups, a monomeric structure is postulated with the association of ether.

Attempts to remove the bulk diethylether at 40 °C from ArLi (2) *in vacuo* led to an explosion, attributed to the removal of the stabilising coordinated ether molecules. However, the prevalence of ether explosions due to peroxides may provide an alternative explanation. Isolation of a crystalline solid from ether failed due to its long term decomposition over 2 months in this solvent system, even with cooling (see Section 1.8.5). Numerous attempts have been made to identify the products of decomposition, primarily by NMR analysis. Unfortunately this gave no information on the mechanism of decomposition, or indeed on the species formed. A mixture of products was evident, interestingly in the "fluoride" region of the ^{19}F NMR spectrum (Figure 1.13).

After a prolonged time in solution attack of 2,4,6-tris(trifluoromethyl)phenyllithium (2) on a second molecule [or indeed on the small amount of 1,3,5-tris(trifluoromethyl)benzene (1) present] may be postulated [Figure 1.4(a)] or a possible intramolecular decomposition *via* LiF elimination [Figure 1.4(b)].

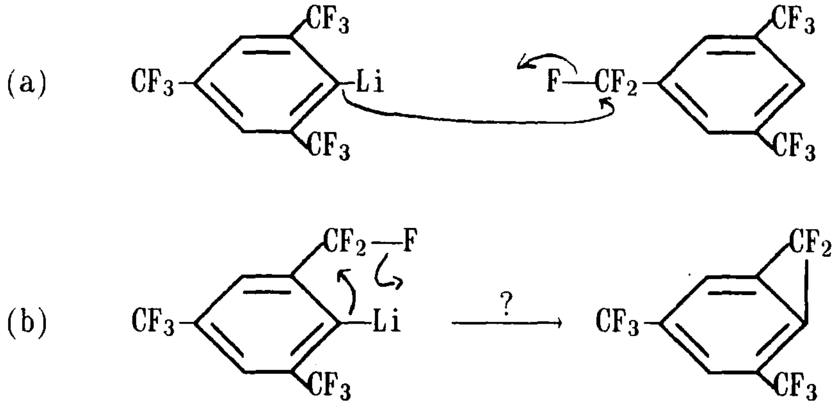

Figure 1.4: *"Decomposition" of ArLi.*

The stability of ArLi (2), however, is in marked contrast to pentafluorophenyllithium which readily loses lithium fluoride, a decomposition mode which is common in compounds containing lithium and fluorine in a vicinal position. Pentafluorophenyllithium is usually prepared at -78 °C, since even at -10 °C 25% decomposition occurs within forty minutes [8].

1.4 NMR STUDIES

1.4.1 ^{7}Li NMR

The ^{7}Li NMR of ArLi showed a single peak indicative of a symmetrical aggregate environment of the lithium, or a monomeric structure. Considerable broadening attributed to interactions with the fluorine was observed.

1.4.2 ^{19}F NMR

The ^{19}F NMR gave two signals in a 2:1 intensity ratio, characteristic of equivalent ortho trifluoromethyls (integral 2) and a non equivalent para-trifluoromethyl (integral 1) (see Section 1.8.2). The spectrum (Figure 1.5) illustrates a conversion of *ca.* 50%. In general the percentage conversion to ArLi was calculated from the ^{19}F integration. Average values of ~85% conversion were achieved. It is interesting to compare these data with those for the 2,4,6-tri(t-butyl)phenyl lithio derivative. The ortho-protons in this case resonate down field, postulated as being a result of their close proximity to the more positively charged lithium (Li^{+}) [7]. An exactly similar downfield shift of the ortho fluorines is observed in ArLi (2) which may be ascribed in a similar way to reduced π-electron density and increased σ-electron density at the metallated carbon. The π-electron density is polarised away from the ipso-carbon - illustrated in the MNDO calculation (Section 1.7).

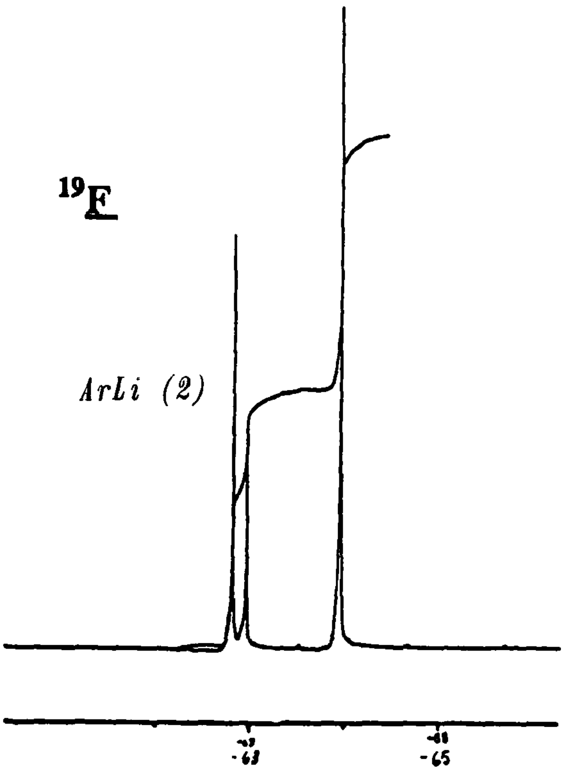

Figure 1.5: *^{19}F NMR spectrum of ArLi (2) in diethylether.*

1.4.3 A Predicted 2D-NMR Spectrum

By using two-dimensional Heteronuclear Overhauser Spectroscopy the interaction between lithium and fluorine may be determined, *ie.* ^{6}Li *via* ^{19}F. A two channel NMR would be required for this which was not available in Durham. The predicted features of the 2D-NMR are presented in Figure 1.6, reflecting the close contact between the two groups [9],[7]

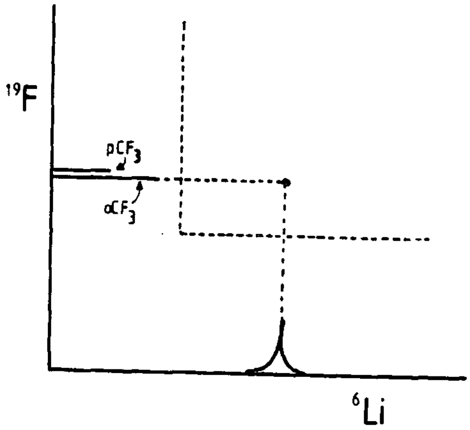

Figure 1.6: *Predicted 2D Heteronuclear Overhauser Spectrum of ArLi (2), ^{6}Li versus ^{19}F.*

The structure and possible aggregation of the ArLi species is of particular interest. Ideally the isolation of a crystalline solid was sought. This failed and hence other methods were tried.

1.4.4 ^{13}C NMR

Using ^{13}C NMR it should be possible by looking directly at the coupling of the quaternary carbon with lithium to determine the number of lithiums to which it is coupled, and hence the number of molecules in the aggregate. Work on the more reactive organolithium species (*eg.* R = Bu) has to be carried out at very low temperatures. In this case in diethylether, the quaternary carbon is split into seven lines as a

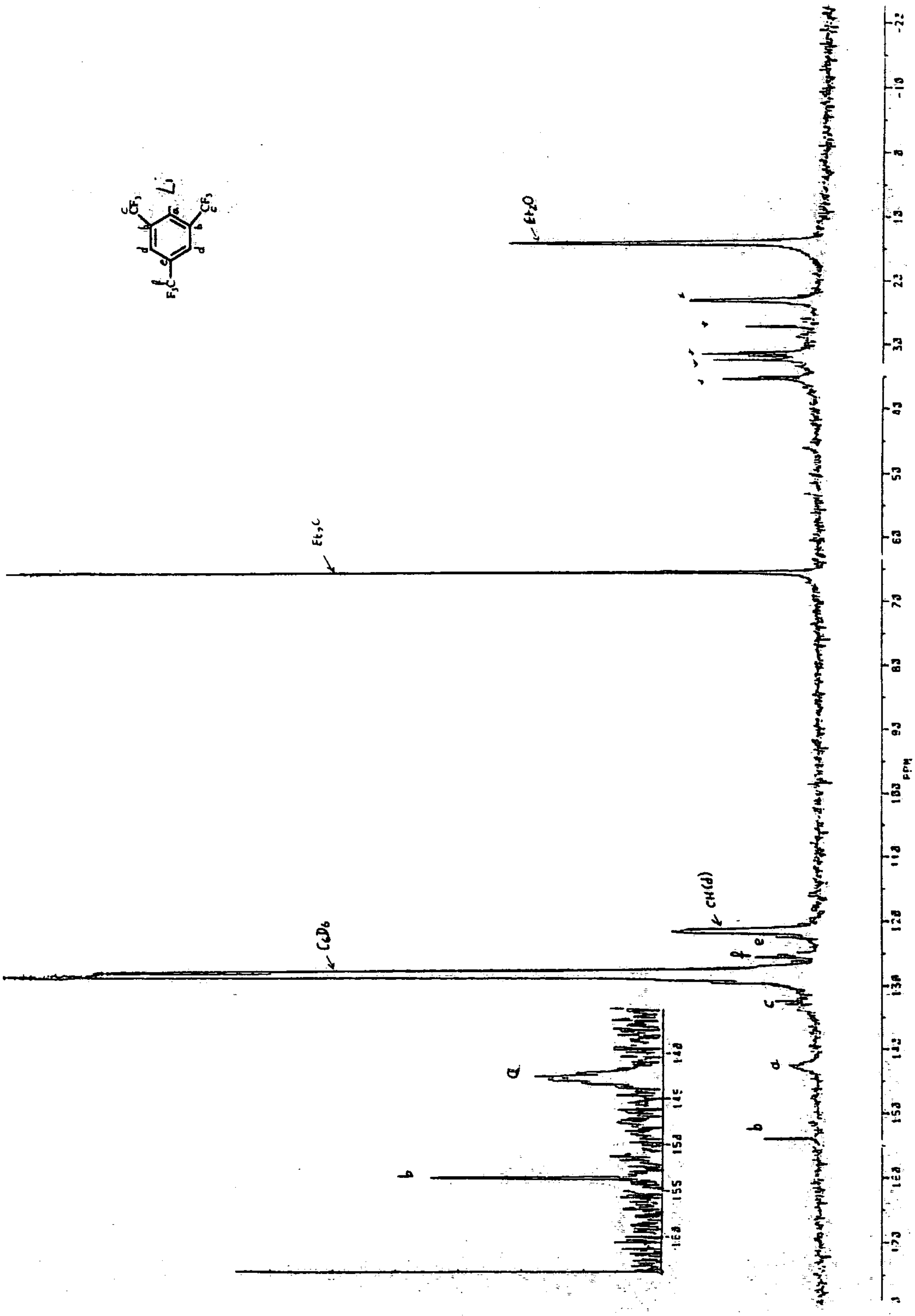

Figure 1.7: ^{13}C *NMR spectrum of ArLi (2) in deuterobenzene.*

result of its coupling to two ^{7}Li isotopes. Hence a dimeric structure can be assigned[7].

As discussed earlier, attempts to isolate 2,4,6-tris(trifluoromethyl)phenyllithium (2) by removal of Et_2O resulted in an explosion. However, with a small quantity of material (20 mmol) and by exercising great caution it was maintained *in vacuo* for 12 hours without incident. The ^{13}C NMR of the resulting pale brown powdery solid is presented in Figure 1.7. It is evident that Et_2O remains coordinated. No ^{13}C-^{7}Li or ^{13}C-^{6}Li coupling is clearly resolved.

1.5 OTHER TRIFLUOROMETHYL SUBSTITUTED BENZENES

It is interesting to compare the electronic properties of the compounds (7), (1) and (8) (Table 1.1).

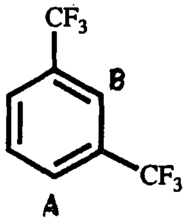 (7)‡	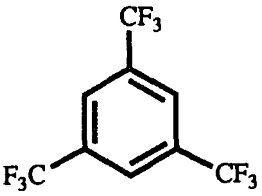 (1)*	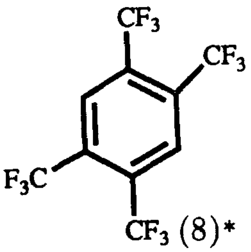 (8)*
Liquid Bpt 116 °C	Liquid Bpt 119 °C (ref.1).	White solid Mpt: 92-94°C.
Proton A: most kinetically favourable proton, least hindered most accessible.	All 3 positions equally activated for lithiation.	Both positions equally favoured and disfavoured for lithiation.
TMEDA promotes the removal of the most thermodynamically favourable proton B.		(Even by increasing the base strength it is <u>not</u> possible to see any lithiation). This solid was difficult to purify.

Table 1.1: *Electronic properties of compounds (1), (7) and (8); ‡Commercially available from Aldrich; *Synthesised via high pressure techniques (ref.10).*

1.6 PREPARATION OF FURTHER ORGANOLITHIUM DERIVATIVES

A great deal of work was directed toward the preparation of organolithium species in view of the synthesis of many secondary phosphines, as precursors to phosphaalkenes (Chapter 4). Some of the species prepared and the general routes by which they were synthesised are given in Table 1.2. For experimental details see Section 4.12.1 and 4.12.2.

SPECIES		PREPARATIVE ROUTE
$LiCHCl_2$	(9)	1 (Section 4.12.2)
$PhCH_2Li \cdot TMEDA$	(10)	2 (Section 4.12.1)
$Ph_2CHLi \cdot TMEDA$	(11)	3 (Section 4.12.1)

Table 1.2

The importance of controlling temperature, concentration and solvent to reduce unwanted side reactions and increase yields was realised [11-13]. For example, there is the possibility of THF cleavage with prolonged reaction of organolithium species at 65 °C [13]. Concentrations exceeding 0.3 M may cause loss of yield due to the Wurtz reaction, and result in the formation of a gelatinous precipitate [11,12].

1.7 MNDO CALCULATIONS ON ArLi

MNDO studies on the ArLi (2) species are presented below. AM1 calculations on ArLi (2) did not give a great deal of information. In this calculation type, the Li^+ is treated as a point charge so that any lithium-fluorine interaction is entirely electrostatic. In MNDO, however, the lithium is assigned with 2s and 2p orbitals and therefore it has orbital coefficient values. The molecular geometry is shown in

Figure 1.8.

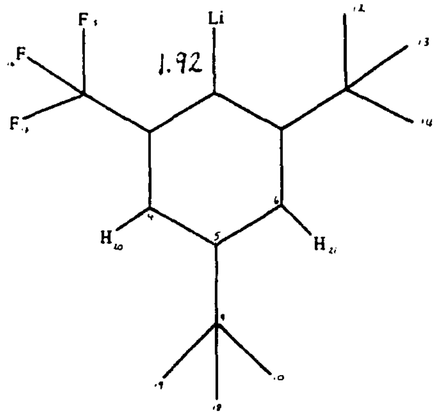

Figure 1.8: *ArLi (2) geometry from MNDO calculations.*

The HOMO and HOMO-1 are shown in Figure 1.9. The HOMO is π-bonding around the ring system with a small amount of p_z lithium coefficient. There is more lithium involvement in the HOMO-1 and it is possible to see direct lithium-fluorine bond interaction and a lithium-carbon bond.

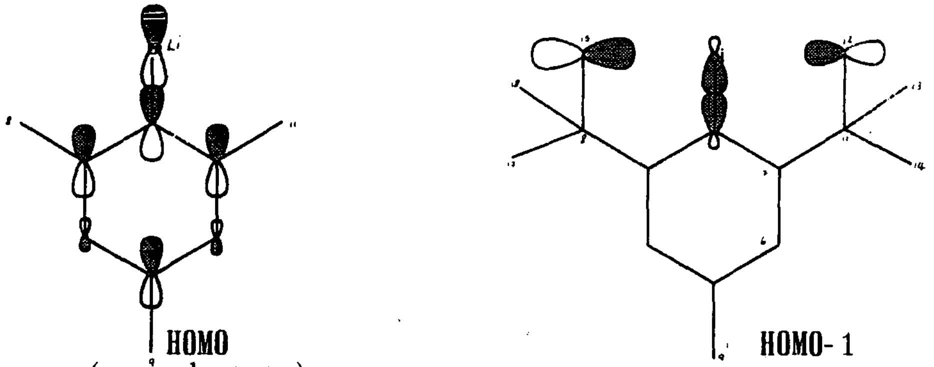

HOMO
(ground state)

HOMO-1

Figure 1.9: *Predicted HOMO's for ArLi (2).*

Charges and Bond Order are shown in Figure 1.10. Note the alternating charges around the ring (*cf.* benzene). The calculation assigns negative charge α to a -CF_3 group. The para fluorines all have a charge of -0.23 [F(18), F(19) and F(10)]. This is the same for the ortho CF_3 groups [F(16), F(17), F(13), F(14)]. F(15) and F(12) donate negative charge toward the lithium and hence have a reduced value of -0.16, this correlates well with the ^{19}F NMR data (Figure 1.5).

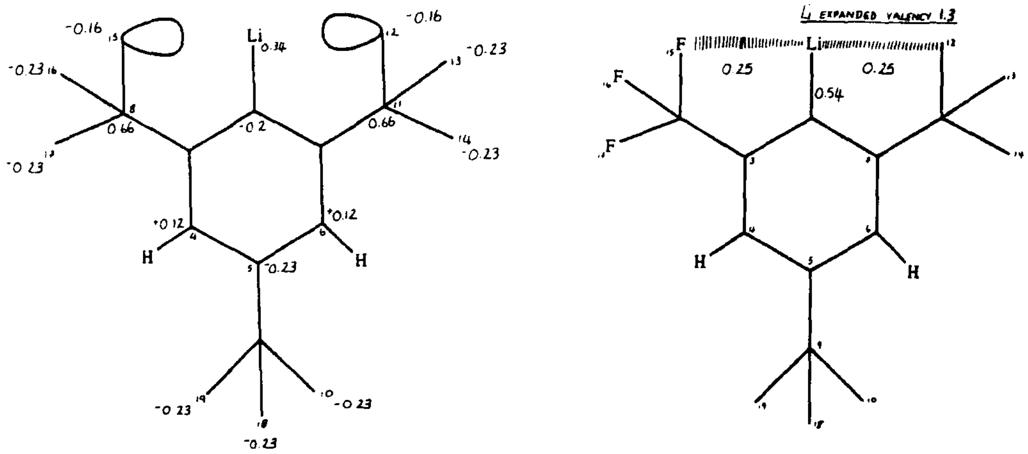

Charges

Bond Order

Figure 1.10: *Predicted charge separation and bond orders for ArLi (2).*

1.8 EXPERIMENTAL

1.8.1 Preparation of 1,3,5-Tris(trifluoromethyl)benzene (ArH) (High Pressure Technique)

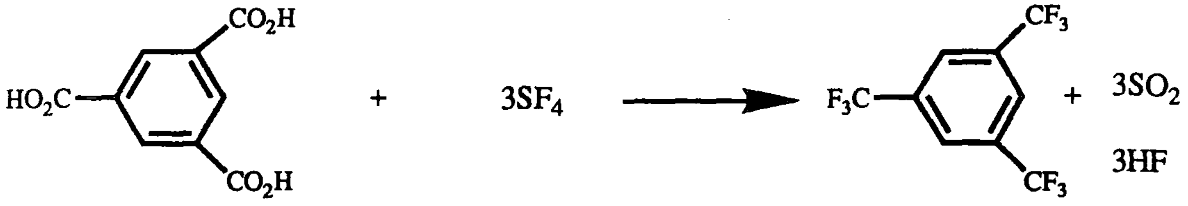

A steel vacuum line was designed specifically for work involving sulphur tetrafluoride. Its constitution is outlined below (Figure 1.11). The upper reservoir has a known capacity (425 cm^3) and holds *ca.* 150 g of SF_4. After evacuation this cylinder was allowed to fill completely with SF_4 over a period of 30 minutes. Subsequently its contents were condensed into a small sample bottle. From its tare the accurate weight of SF_4 collected could be determined. This process was repeated until the required quantity of SF_4 [550g (3.9 mole) - 3 sample bottles] had been obtained.

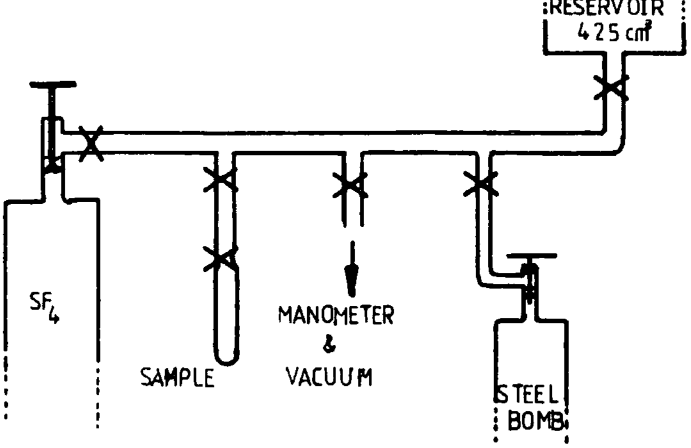

Figure 1.11: *The apparatus used for the manipulation of SF_4.*

A 1 litre steel bomb was charged with 150 g (0.71 mole) trimesic acid (benzene-1,3,5-tricarboxylic acid). This vessel was evacuated and cooled to -190 ^{0}C by liquid air. The bomb design used is shown in Figure 1.12.

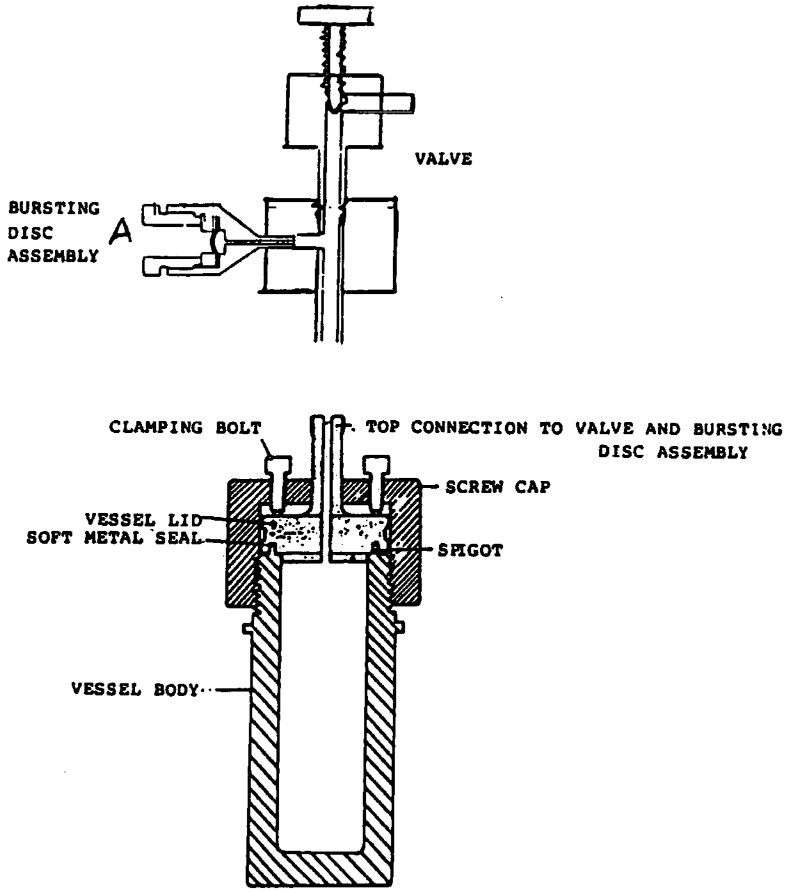

Figure 1.12: *The 1-litre steel bomb.*

An aspect of particular interest is the recent safety introduction of the bursting valve (A).

The contents of the four weighed small cylinders were condensed into the bomb. After completion the bomb was transferred at -190 °C in a large Dewar of liquid air to the high pressure reaction chamber. Within the high pressure cell the bomb was allowed to equilibrate to ambient temperature, before thermocouples enabled a temperature of 150 °C to be maintained for a maximum period of 12 hours. The bomb was vented in an efficient hood to release any unreacted sulphur tetrafluoride, sulphur dioxide and hydrogen fluoride, before the liquid contents of the bomb were poured onto crushed ice (to remove any unreacted trimesic acid and HF). This mixture was filtered to discard any solid impurities. The filtrate was treated with 4 aliquots of 150 ml NaOH (2M) and washed well with water. The oily product was subsequently dried with anhydrous magnesium sulphate. Distillation yielded pure product (1) 159.5g (80%); Bpt 119 °C (760 mm Hg); ^{19}F ($CDCl_3$) δ: -65.3 ppm (s, CF_3); ^{1}H ($CDCl_3$) δ: +8.1 ppm (s,CH ring) [1].

This technique was modified to maximise the yields obtained. This is of particular significance (as in all preparative chemistry) because of the high cost of these materials. A few selective reactions illustrating the effect of variation in reaction conditions are presented in Table 1.3. Reaction yields were maximised (increasing the viability of this technique) with prolonged reaction times, and slightly larger quantities of SF_4 relative to the trimesic acid starting material. The effect of increase in reaction time with yield was also recognised by Edelmann *et al.* [2] (reaction time 24 hours). In our hands it was found that no significant increase in yield was achieved by extending the reaction period beyond 12 hours.

REACTION NUMBER	TEMP	MASS OF SF_4 /g	REACTION TIME	YIELD ‡
1	150	480	6 hours	55%
2	150	500	6 hours	65%
3	150	550	6 hours	67%
4	150	550	6 hours	70%
5	150	450	10 hours	72%
6	150	550	12 hours	80%
7	150	550	18 hours	80%

Table 1.3: *Conditions used for the preparation of ArH (1);*
‡These may be compared to yields of 33% (ref.1).

1.8.2 Preparation of 2,4,6-Tris(trifluoromethyl)phenyllithium (2)

$$\underset{(1)}{\mathrm{ArH}} + \mathrm{BuLi} \xrightarrow{\mathrm{Et_2O}} \underset{(2)}{\mathrm{ArLi}} + \mathrm{BuH}$$

BuLi (2.5M in hexane, 31.2 ml, 78.0 mmol) was added dropwise over 5 minutes to a stirred solution of ArH (20.0g, 71.0 mmol) in Et_2O (100 ml) at -10 ^{o}C. The solution was allowed to reach room temperature and stirred for 5 hours, yielding a deep brown gelatinous solution (with a larger volume of ether it remains free-flowing). The percentage conversion was determined by ^{19}F NMR. The ArLi (2) was not isolated, but used from this stage *in situ* (0.54 M). Consistent yields of the order 85%-90% were achieved, calculated from the distinctive ^{19}F NMR. ^{19}F NMR (Et_2O) δ: -62.6 (s,6F,o-CF_3), -62.8 (s,3F,p-CF_3) ppm; ^{7}Li NMR (Et_2O) δ: +0.2 ppm.

1.8.3 Attempted Reaction of ArH with BuLi in THF

BuLi (2.5M in hexane, 15.6 ml, 39.0 mmol) was added dropwise over 5 minutes to a stirred solution of ArH (10.0g, 35.5 mmol) in THF (100 ml) at -10 ^{o}C. This reaction mixture was stirred at room temperature for 5 hours. The solution became deep brown, but no reaction of ArH had occurred. ^{19}F NMR (THF) δ: -65.0 (s) ppm. This mixture was brought to reflux for 2 hours and no change in the ^{19}F NMR was observed.

1.8.4 Addition of TMEDA to ArLi/Et$_2$O (2) Solution

TMEDA (6.9 ml, 45.7 mmol) in Et$_2$O (25 ml) was added dropwise over 5 minutes to a stirred solution of ArLi/Et$_2$O (0.45 M, 102.0 ml, 45.9 mmol) at -10 ^{o}C. Copious amounts of solid appeared to form. This mixture was cooled to -50 ^{o}C and filtered. The separation process was not successful, and only a brown oil collected on the frit, which appeared to contain ArLi. It was not proven whether TMEDA was coordinated. Attempts to recrystallise the oil from Et$_2$O (*ca.* 10 ml) at -40 ^{o}C failed.

1.8.5 Attempted Isolation of ArLi (2)

ArLi was prepared as described in Section 1.8.2. Attempts to concentrate this solution [initially 20 ml (0.54 M) which was reduced to half-volume by the removal of ether *in vacuo*] and cooling gave no precipitate (a viscous brown oil was produced). ^{19}F (Et$_2$O) δ: -62.6 (s,6F,o-CF$_3$), -62.8 (s,3F,p-CF$_3$) ppm.

An ArLi sample (approximately 1 M) was allowed to stand at room temperature (inert atmosphere) for 8 weeks. Clear transparent crystals (*ca.* 50 mg) were isolated from below a supernatant liquid. Mpt. 110-111 ^{o}C; Analysis found: C, 15.60; H, 3.74; (No lithium detected); Required for $C_9H_2F_9Li$: C, 37.53; H, 0.70%. The ^{19}F spectrum of the supernatant liquid is shown in Figure 1.13. It is clear that many products are present. The large crystals were cut and mounted for X-ray analysis. (The crystals showed a unit cell smaller than that expected

Figure 1.13: *Illustrating the* ^{19}F *NMR spectrum of the supernatant liquid obtained from the decomposition mixture.*

for ArLi, but larger than for LiOH and Li_2O). The crystal structure remained incomplete. It was assumed to be a decomposition product and was not further investigated by crystallography. (The peak at -111 ppm (^{19}F) may represent a fluoride ion).

Refluxing the ArLi (2) (0.7 M, 25 ml, 17.5 mmol) over a period of 2 days gave no evidence of LiF elimination. The ArLi (2) remained intact apart from a small amount of hydrolysis (approximately 7%) to ArH (1). This was observed by ^{19}F NMR. ^{19}F (Et_2O) ArLi δ: -62.6 (s,6F,o-CF_3), -62.8 (s,3F,p-CF_3) ppm; ArH δ: -65.3 (s,CF_3) ppm.

1.8.6 ArLi/Et_2O Standing at Room Temperature

A solution of ArLi in Et_2O (0.7 M, 50 ml, 35 mmol) remained standing in a glove box for a period of two months. Its ^{19}F NMR was recorded every few days. The solution darkened on standing and a sticky black solid precipitated which was redissolved in Et_2O for analysis by NMR. The decomposition process postulated (Section 1.3) was not repeated. Gradual hydrolysis of ArLi to ArH (a single peak in the ^{19}F NMR) was observed. ^{19}F NMR (Et_2O) δ: -65.3 (s,CF_3) ppm. ArH (1).

1.8.7 ^{13}C Studies on ArLi (2)

An ArLi/ArH Et_2O solution (0.7 M, 100 ml, 70 mmol) was placed *in vacuo* in order to remove the diethyl ether. The resultant oily residue was warmed gradually to 40 ^{o}C with an oil bath to remove any remaining solvent and inherent ArH. This resulted in an explosion. With a small quantity of the lithium species (2) (1 M) in diethylether (20 ml, 20 mmol) and executing great caution the mixture was allowed to pump *in vacuo* for a period of 12 hours at room temperature to yield a powdery pale brown solid. 25 mg of this material was redissolved in deuterobenzene, C_6D_6 (2 ml) and its ^{13}C NMR was recorded (Figure 1.7).

1.9 REFERENCES

1. G.E. Carr, R.D. Chambers, T.F. Holmes and D.G. Parker, *J. Organometallic Chem.*, 325, 13 (1987).
2. M. Scholz, H.W. Roesky, D. Stalke, K. Keller and F.T. Edelmann, *J.Organometallic Chem.*, 366, 73 (1989).
3. a) R. Schmutzler, *Chem. and Industry*, 1868 (1962).

   b) L. Heuer and R. Schmutzler, *J. of Fluorine Chemistry*, 39, 197 (1988).

   c) L. Heuer, M. Sell, R. Schmutzler and D. Schomburg, *Polyhedron*, 6(6), 1295-1307 (1987).
4. B.J. Wakefield, *Best Synthetic Methods: Organolithium Methods*, Academic Press, Chapter 3, p.21 (1988).
5. G. Köbrich, *Angew.Chem. Int.Ed.Engl.*, 11(6), 473 (1972).
6. J.M. Mallan and R.L. Bebb, *Chemical Reviews*, 69, 693 (1969).
7. W. Bauer, W.R. Winchester and P. von Ragué Schleyer, *Organometallics*, 6, 2371 (1987).
8. M. Hudlicky, "*Chemistry of Organic Fluorine Compounds*", Ellis Horwood, New York, 2nd Edition.
9. H. Günther, D. Moskau, P. Bast and D. Schmalz, *Angew.Chem. Int.Ed. Engl.*, 26, 1212 (1987).
10. R.D. Chambers, T.F. Holmes and T. Straw, unpublished work, University of Durham, South Road, Chemistry Department (1988).
11. H. Gilman and G.L. Schwebke, *J.Chem.Soc.*, 27, 4259 (1962).
12. H. Gilman and H.A. McNinch, *J.Chem.Soc.*, 26, 3723 (1961).
13. J.J. Eisch, *J.Org.Chem.*, 28, 707-710 (1963).

CHAPTER TWO

ORGANOHALOPHOSPHINES

2.1 INTRODUCTION

There are many preparative routes available for organohalophosphorus compounds [1] and many species are known [2]. This work has concentrated on their synthesis using:

(A) The action of organocadmium or organozinc reagents on PCl_3 (Equation 2.1) [3,4].

(B) Cleavage of phosphinous/phosphonous amides with anhydrous HX and an inert solvent (Equation 2.2) [5].

(C) Exchange methods (Equation 2.3).

$$R_2Cd + 2PCl_3 \longrightarrow 2RPCl_2 + CdCl_2 \qquad (2.1)$$

$$R_2PNR_2 + 2HCl \longrightarrow R_2PCl + R_2NH.HCl \qquad (2.2)$$

$$RPCl_2 + 2AgCN \longrightarrow RP(CN)_2 + 2AgCl \qquad (2.3)$$

Many phosphines have been prepared throughout this work as:

(1) Synthons to observe their acceptor properties (Chapter 6), *eg.* $ArPCl_2$ (12), CF_3PCl_2 (13), $i\text{-}Pr_2NPCl_2$, $(i\text{-}Pr_2N)_2PCl$, $(Et_2N)PCl_2$, $(Et_2N)_2PCl$ and their respective cyano derivatives.

(2) Synthons for attempts at unsymmetrical diphosphene preparation (Chapter 3), *eg.* $t\text{-}BuPCl_2$, $C_6F_5PCl_2$, $MesPCl_2$, $t\text{-}BuPH_2$, $Ar'PCl_2$, $Ar'PH_2$ [where Ar' = 2,6-bis(trifluoromethyl)phenyl].

(3) Synthons for phosphaalkene preparation, *eg.* $Me_3SiCH_2PCl_2$, $PhCH_2PCl_2$, CH_3PCl_2 and many secondary phosphines were prepared from these starting materials (Chapter 4).

Other phosphines were precursors for the synthesis of the P(V) derivatives as counterions in halo and pseudohalo borate chemistry (Chapter 10). Of particular interest are the new phosphines containing the aryl group, 2,4,6-tris(trifluoromethyl)phenyl: *ie.* $ArPCl_2$ (12), Ar_2PCl (14), $ArPF_2$ (3), $ArPH_2$ (15) and $ArP(CN)_2$ (16). These are discussed in more detail in the next section.

2.2 Ar SUBSTITUTED PHOSPHINES

2.2.1 $ArPF_2$ (3)

$ArPF_2$ (3) was prepared by the action of SbF_3 on $ArPCl_2$ (12). No oxidative fluorination to yield the fluorophosphorane, $ArPF_4$ was observed (see Section 2.3.1).

This represents an example of a stable fluorophosphine attributed to the increase in Lewis acidity of the P(III) compound bearing an electron-withdrawing substituent, Ar [6,7]. An alternative synthetic route could be *via* the organo lithium reagent with $ClPF_2$ [6].

This is a particularly interesting compound since difluorophosphines have become known only relatively recently, due not so much to the synthetic problems but to their inherent instability, as indicated by a recent scheme by R. Schmutzler [6]. Such difficulties were not experienced here and $ArPF_2$ (3) was comparatively stable.

2.2.2 $ArPH_2$ (15)

This was prepared in high yield *via* one of two routes from $ArPCl_2$ (12) (Equations 2.4 and 2.5) [8,9] (Section 2.3.2). The structure of $ArPH_2$ and its ^{31}P NMR parameters are shown in Figure 2.1.

$$ArPCl_2 + 2Bu_3SnH \longrightarrow ArPH_2\ (15) + 2Bu_3SnCl \qquad (2.4)$$

$$ArPCl_2 + 1/2LiAlH_4 \longrightarrow ArPH_2\ (15) + 1/2LiAlCl_4 \qquad (2.5)$$

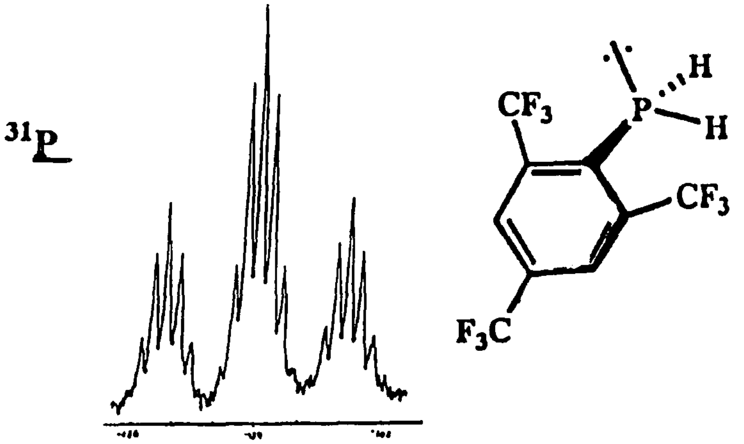

Figure 2.1: *The structure and ^{31}P NMR spectrum of ArPH$_2$ (15); ^{31}P δ: -139.8 ppm (triplet of septets), $^4J(PF)$ 28.9 Hz, $^1J(PH)$ 217.9 Hz.*

The second route (Equation 2.5) was employed with anticipation of CF_3 cleavage, since it was reported [8] that in the 2,6-bis(trifluoromethyl)Ph derivative there was attack at the CF_3 group. This was not observed here. A clear liquid with a very pungent smell was obtained. Compare this with 2,4,6-tri(^{t}butyl)phenylphosphine (17) which is an odourless white solid (Mpt. 150-152 °C) [10].

2.2.3 ArPCl$_2$ (12)

Representatives of this class of dichlorophosphines (Equation 2.6) have been in the literature since the 19th Century [11]. This new dichlorophosphine was obtained as a clear oil (Figure 2.2) (Section 2.3.3).

$$\text{ArLi (2)} + \text{PCl}_3 \longrightarrow \text{ArPCl}_2 \text{ (12)} \qquad (2.6)$$

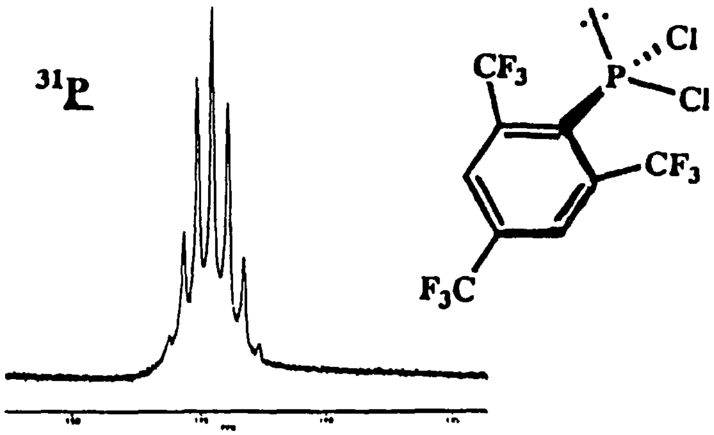

Figure 2.2: *^{31}P NMR spectrum of $ArPCl_2$ (12); ^{31}P δ: +144.4 ppm (septet), $^{4}J(PF)$ 61.4 Hz.*

A variable temperature NMR experiment to low temperature (-60 °C) was carried out. The aim of this experiment was to attempt to "freeze" ring rotation to cause inequivalence in the ortho-CF_3 groups. The ^{31}P NMR was observed (Table 2.1). No change was detected - inequivalence of the CF_3 groups would have been expected to increase the complexity of this spectrum.

TEMPERATURE	^{31}P /ppm	$^{4}J(PF)$ /Hz
294	144.4 (septet)	61.4
273	144.4 (septet)	61.4
253	144.4 (septet)	61.4
233	144.4 (septet)	61.4
213	144.4 (septet)	61.4

Table 2.1 *A variable temperature NMR study on $ArPCl_2$*

The results indicate either continuation of ring rotation, or the "freezing" of the ring with a symmetrical geometry. It would be interesting to carry out this experiment on Ar_2PCl (14) (Section 2.2.4) where the greater steric limitations may cause ring "freezing" at a higher temperature.

2.2.4 Ar_2PCl (14)

The use of ArLi in slight excess of two-fold stoichiometry gave high yields of Ar_2PCl as a pure white crystalline solid (Equation 2.7). ^{31}P NMR spectral data is presented in Figure 2.3.

$$2ArLi\ (2) + PCl_3 \longrightarrow Ar_2PCl\ (14) \qquad (2.7)$$

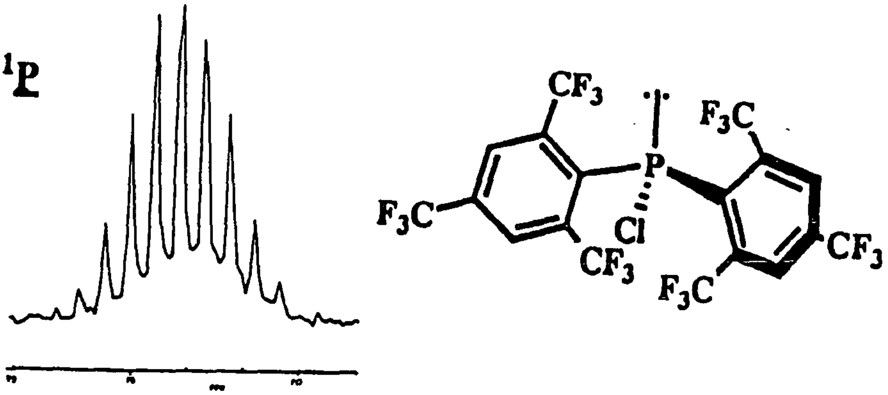

Figure 2.3: *^{31}P NMR spectrum of Ar_2PCl (14); ^{31}P δ: -74.2 ppm (13 line multiplet), $^4J(PF)$ 42.0 Hz.*

The attachment of two such bulky groups geminal on one phosphorus is unusual [12-14]. The first successful preparation of a compound carrying two very bulky geminal 2,4,6-tri-^{t}butylphenyl groups on one element was achieved for the synthesis of bis(2,4,6-tri-^{t}butylphenyl)phosphinic chloride [12]. Ar_3P does not appear to form even by the use of a large excess of ArLi and refluxing the reaction mixture in ether. This may be attributed to the steric requirement of the aryl group in the tetrahedral environment. Trimesitylphosphine is the largest tertiary phosphine known and was synthesised as early as 1901 [13].

2.2.5 $ArP(CN)_2$ (16)

This was prepared via chlorine substitution in $ArPCl_2$ by cyanide (Equation 2.8).

$$\underset{(12)}{ArPCl_2} \xrightarrow{2AgCN} \underset{(16)}{ArP(CN)_2} + 2AgCl \qquad (2.8)$$

The ^{31}P shift of -87 ppm is indicative of the higher degree of shielding in the cyanide species. However, the increase in electrophilicity of the phosphorus and apparent increase in its susceptibility to hydrolysis can be attributed to the electronegativity of cyanide.

2.2.6 'ArP(H)Cl'

To complete this series of phosphines it would be interesting to consider the chemistry of ArP(H)Cl. In general RP(H)A, where R is a hydrocarbon group and A an electronegative group, are normally unstable as they tend to lose AH to give the corresponding cyclopolyphosphine $(RP)_n$ [15]. Significant exceptions exist with R as a highly electronegative group, *eg*. R = CF_3; A = Cl, Br [16], or when RP(H)Hal is co-ordinated to a transition metal [15]. A third consideration is the stability of SupermesP(H)Cl [15b] which may be explained in terms of a possible bimolecular decomposition process with HCl elimination to form cyclopolyphosphines, and therefore with very bulky R groups formation of the transition state is precluded. The steric and electron-withdrawing nature of Ar = 1,3,5-tris(trifluoromethyl)benzene should allow its isolation and indeed a facile route to its preparation has been suggested [17], involving the refluxing of $ArPH_2$ in the presence of an excess of CCl_4 and a catalytic quantity of the radical initiator AIBN possibly by the route shown in Figure 2.4. This, however, was not successful, and irradiation with gamma rays gave very low yields (Section 7.3).

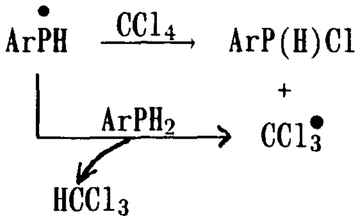

Figure 2.4: *Proposed synthetic route to ArPH(Cl).*

2.3 EXPERIMENTAL PROCEDURES

2.3.1 Preparation of $ArPF_2$ (3)

$$\underset{(12)}{ArPCl_2} \xrightarrow{SbF_3} \underset{(3)}{ArPF_2}$$

SbF_3 (2.3g, 13.0 mmol) was added to a stirred solution of $ArPCl_2$ (3.8g, 10.0 mmol) in CH_2Cl_2 (50 ml) at room temperature. The SbF_3 was only sparingly soluble in CH_2Cl_2. The mixture was refluxed overnight for a period of 12 hours to ensure complete conversion to $ArPF_2$. The solution was filtered to remove the excess SbF_3, and the CH_2Cl_2 removed by distillation at atmospheric pressure. The product was obtained by distillation at reduced pressure and collected as a clear pure oil at 54 ^{o}C (8 mm Hg). Yield was 2.2g (63%). Analysis found: C, 30.97; H, 0.37; Required for $C_9H_2F_9PF_2$: C, 30.88; H, 0.58%; IR (Film) ν_{max}: 1400-1150 (s,CF_3), 900 (s,P-F) cm^{-1}; UV-Vis (CCl_4) λ_{max} (ϵ): 262 (39877) nm; MS (Intensity%) EI: 331 (100,$ArPF^+$), 262 (40,$Ar\text{-}F^+$); ^{31}P ($CDCl_3$) δ: +184.6 ppm (doublet of septets), $^1J_{PF}$ 1179.6 , $^4J_{PF}$ 50.6 Hz; ^{19}F δ: -55.5 ppm (6F, doublet of triplets), $^4J_{PF}$ 50.6, $^5J_{FF}$ 18.6 Hz, -64.5 ppm (s,3F), -90.9 (2F, doublet of septets), $^1J_{PF}$ 1179.6, $^5J_{FF}$ 18.6 Hz; ^1H ($CDCl_3$) δ: 8.13 (s) ppm.

The preparation was also attempted by the reaction of $ArPCl_2$ with LiF:

$$ArPCl_2 + 4LiF \xrightarrow{\times} ArPF_2$$

Lithium fluoride (0.55g, 21.2 mmol) was added to a stirred solution of $ArPCl_2$ (1.8g, 4.7 mmol) in CH_2Cl_2 (50 ml). This mixture was refluxed overnight. There was no evidence of fluorination and unchanged $ArPCl_2$ was recovered.

2.3.2 Preparations of $ArPH_2$ (15)

2.3.2.1 $$\underset{(12)}{ArPCl_2} + 1/2LiAlH_4 \longrightarrow \underset{(15)}{ArPH_2} + 1/2LiAlCl_4$$

$LiAlH_4$ (2.6 ml, 1M solution in Et_2O, 2.6 mmol) was added dropwise over 5 minutes, to a stirred solution of $ArPCl_2$ (2.0g, 5.2 mmol) in Et_2O (50 ml) at 0 °C. A white precipitate ($LiAlCl_4$) was seen to form almost instantaneously. This was filtered with a fine sinter yielding a yellowish filtrate, which gave a signal in the $^{31}P\{^1H\}$ NMR at -139.8 ppm (septet). The Et_2O was removed by distillation at atmospheric pressure and $ArPH_2$ was distilled, as a clear oil, at 56 °C (12 mm Hg). Yield was *ca.* 1.0g (61%). (As is clear from these results, and the ^{19}F NMR of the filtrate there was no inherent attack at CF_3 by $LiAlH_4$) [9].

2.3.2.2 $$\underset{(12)}{ArPCl_2} + 2Bu_3SnH \longrightarrow \underset{(15)}{ArPH_2} + 2Bu_3SnCl$$

Bu_3SnH (1.62 ml, 6.0 mmol) in Et_2O (10 ml) was added dropwise over 5 minutes to a stirred solution of $ArPCl_2$ (1.15g, 3.0 mmol) in Et_2O (15 ml) at 0 °C. The mixture was stirred at 0 °C for 30 minutes and then allowed to reach room temperature. The solution turned from colourless to yellow. The clear solution was attributed to the solubility of Bu_3SnCl in Et_2O. The ether was removed by distillation at atmospheric pressure. $ArPH_2$ was distilled directly from the crude $ArPH_2/Bu_3SnCl$ residue. Yield of clear oil was 0.61g (65%). Bpt. 48 ^oC (5 mm Hg); Analysis found: C, 34.48; H, 1.00; Required for $C_9H_2F_9PH_2$: C, 34.42; H, 1.28%; IR (Film) ν_{max}: 3100 (w,ArCH), 2360 (s,P-H), 1630 and 1570 (m,ArC=C), 1400-1000 (m,C-F), *ca.* 900 (m,ArCH) cm^{-1}; UV-Vis (CCl_4) λ_{max} (ϵ): 340 (13688), 262 (54753) nm; MS (Intensity%) EI: 314 (90,$ArPH_2^+$), 295 (26.9,$ArPH_2$-F^+), 263 (98.0,Ar-F^+); CI^+: 314 (100,$ArPH_2^+$), 371 (20.0), 357 (47.0); ^{31}P ($CDCl_3$) δ: -139.8 (triplet of septets), $^4J_{PF}$ 28.9 Hz, $^1J_{PH}$ 217.9 Hz; ^{19}F δ: -61.4 ppm (6F,doublet of triplets), -63.8 ppm (s,3F), $^4J_{PF}$ 28.9 Hz, $^5J_{FH}$ 5.5 Hz; ^1H ($CDCl_3$) δ: 7.95 (s) ppm.

2.3.3 Preparation of $ArPCl_2$ (12)

2.3.3.1

$$\underset{(2)}{ArLi} + PCl_3 \xrightarrow{-LiCl} \underset{(12)}{ArPCl_2}$$

ArLi (0.72 M, 100 ml, 72.0 mmol) solution in Et_2O was added dropwise over 10 minutes to a stirred solution of PCl_3 (12.6 ml, 19.8g, 0.14 mole) in Et_2O (150 ml) at -78 ^oC. On allowing the reaction mixture to warm gradually to room temperature a precipitate was formed. The reaction mixture was stirred for 2 hours, filtered through a fine sinter to remove LiCl, and the volatile material, Et_2O excess PCl_3 and the small amount of residual ArH were removed from the filtrate *in vacuo*. A yellowish oil: crude $ArPCl_2$ remained. This was purified by vacuum distillation. Yield was 19.8g (72%); Bpt 62 ^oC (0.5 mm Hg); IR (Film) : ν_{max}: 3100 (w,ArCH), 1630 and 1570 (m,ArC=C), 580 and 440 (m,P-Cl) cm^{-1}; UV-Vis (CCl_4) λ_{max} (ϵ): 295 (10802), 280 (13904), 273

(13262) nm; MS (Intensity%) EI: 382 (13.5,$ArPCl_2^+$), 262 (100,$Ar-F^+$); ^{31}P ($CDCl_3$) δ: +144.4 ppm (septet), $^4J_{PF}$ 61.4 Hz; ^{19}F δ: -53.3 ppm (6F,doublet,o-CF_3), $^4J_{PF}$ 61.4, -64.5 ppm (s,3F,p-CF_3); ^1H ($CDCl_3$) δ: 8.25 (s) ppm.

2.3.3.2 Variable Temperature studies on $ArPCl_2$ (12)

$CDCl_3$ (1 ml) was added to a small volume of $ArPCl_2$ (0.5g, 1.3 mmol), making it possible to lock on in the NMR and cool to a lower temperature without freezing. Results are described in Section 2.2.3.

2.3.4 Preparation of Ar_2PCl (14)

$$\underset{(2)}{2ArLi} + PCl_3 \longrightarrow \underset{(14)}{Ar_2PCl}$$

ArLi (0.52 M, 150 ml, 78 mmol) as a solution in Et_2O was added dropwise over 10 minutes to a stirred solution of PCl_3 (5.3g, 38.5 mmol) at 0 °C. A visible precipitate of LiCl was observed. The mixture was stirred at room temperature for a period of six hours. The insoluble LiCl was removed by filtration through a fine sinter, and the resulting yellowish filtrate concentrated by the removal of Et_2O *in vacuo*, yielding a yellowish sticky solid of crude Ar_2PCl. This was most effectively purified by distillation (as often an inherent small amount of $ArPCl_2$ remained which complicated sublimation attempts). By the use of an air condenser in the standard distillation apparatus Ar_2PCl was obtained as a pure colourless oil with a boiling point of 110-112 °C (0.1 mm Hg) which solidified in the receiver flask as a white crystalline solid. Yield was 17.2g (71%). Crystallisation of this product at low temperature (-40 °C) from a small volume of CH_2Cl_2 (10 ml) yielded crystals suitable for X-ray analysis. These were subsequently mounted in 0.3 μm Lindemann capillaries and submitted for crystallographic analysis. BPt. 110-112 °C (0.1 mm Hg); MPt. 91-92 °C; Analysis found: C, 34.87; H, 0.67; Cl, 5.23; Required for $C_{18}H_4F_{18}PCl$: C, 34.39; H, 0.64; Cl, 5.63%; IR (Nujol) ν_{max}: 3100 (w,ArCH), 1630 and 1580 (s,ArC=C), 1400-1000 (s,C-F), 540 (m,PCl) cm^{-1}; UV-Vis (CCl_4) λ_{max} (ϵ): 282 (34685) nm; MS (Intensity%) EI: 628 (32.7,Ar_2PCl^+), 593 (12.3,Ar_2P^+), 347 (12,$ArPCl^+$); CI^+: 628 (10.7, Ar_2PCl^+), 377 (100); ^{31}P ($CDCl_3$) δ: +73.3 (13 line multiplet), $^4J_{PF}$ 42.0 Hz; ^{19}F δ: -54.9 ppm (d,12F), $^4J_{PF}$ 42.0 Hz, -64.8 (s,6F) ppm; Solid state ^{31}P NMR δ: +73.2 (13 line multiplet), $^4J_{PF}$ 42.0 Hz.

See Chapter 6 for the preparation of $ArP(CN)_2$ (16).

2.4 REFERENCES

1. M. Fild and R. Schmutzler, "*Halo and Pseudohalophosphines*", in "*Organic Phosphorus Compounds*", G.M. Kosolapoff and L. Maier (Eds.), Wiley-Interscience (1972), Chapter 8, pp.75-153.

2. M.M. Crutchfield, C.H. Dungan, J.H. Letcher, V. Mark and J.R. Van Wazer, "^{31}*P Nuclear Magnetic Resonance*", John Wiley and Sons (1967).

3. a) J. Carson, *J.Amer.Chem.Soc.*, 68, 2078 (1946).

   b) R.B. Fox, *J.Amer.Chem.Soc.*, 72, 4147 (1950).

4. Th. Weil, B. Prijis and H. Erlenmeyer, *Helv.Chim.Acta.*, 175, 1412 (1952).

5. a) E.M. Evleth, Jr., L.D. Freeman and R.I. Wagner, *J.Org.Chem.*, 27, 2192 (1962).

   b) Th. A. van der Knapp, Th. C. Klebach, F. Visser, F. Bickelhaupt, P. Ros, E.J. Baerends, C.H. Stam and M. Konijn, *Tetrahedron*, 40(4), 765-776 (1984).

6. a) L. Heuer and R. Schmutzler, *J.Fluorine Chem.*, 39, 197 (1988).

b) L. Heuer, M. Sell, R. Schmutzler and D. Schomberg, *Polyhedron*, 6(6), 1295-1307 (1987).

7. L. Heuer and R. Schmutzler, *Euchem Conference*, *PSIBLOCS*, *Paris-Palaiseau*, 22nd August 1988.

8. J. Escudié, C. Couret, H. Ranaivonjato, M. Lazraq and J. Satgé, *Phosphorus and Sulphur*, 31, 27 (1987).

9. M. Scholtz, H.W. Roesky, D. Stalke, K. Keller and F.T. Edelmann, *J.Organometallic Chem.*, 366, 73 (1989).

10. M. Yoshifuji, K. Shibayama and N. Inamoto, *J.Amer.Chem.Soc.*, 105, 2495-2497 (1983).

11. G.M. Kosolapoff and L. Maier, "*Organic Phosphorus Compounds*", Wiley-Interscience, 4, 75 (1972).

12. M. Yoshifuji, I. Shimai and N. Inamoto, *Tetrahedron Lett.*, 41, 3963 (1979).

13. E.C. Alyea and J. Malito, "*International Conference on Phosphorus Chemistry*", Bonn, Federal Republic of Germany, August 31st - September 6th (1986), R. Appel (General Chairman), Abstracts of posters; Poster A59.

14. A.H. Cowley and R.A. Kemp, *Inorg.Chem.*, 22, 547 (1983).

15. a) A. Marinetti and F. Mathey, *Organometallics*, 1, 1488 (1982); and references therein.

b) A.H. Cowley, J.E. Kilduff, N.C. Norman and M. Pakulski, *J.Chem. Soc.Dalton Trans.*, 1801-1808 (1986).

16. R.C. Dobbie, P.D. Gosling and B.P. Straughan, *J.Chem.Soc.Dalton Trans.*, 2368 (1975).

17. J. Escudié, personal communication to K.B. Dillon, September 1989.

CHAPTER THREE

DIPHOSPHENES

3.1 INTRODUCTION

A brief historical perspective of diphosphene identification is first presented:

1877	$C_6H_5PH_2$ and $C_6H_5PCl_2$ were coupled to form a "phosphabenzene" formulated as $C_6H_5P{=}PC_6H_5$ [1].
1957	The oligomeric structure of phosphabenzene was elucidated $(C_6H_5P)_4$, $(C_6H_5P)_5$ [2].
1964	X-ray studies showed that "phosphabenzene" had pentameric or hexameric structure [3].
1966-67	Compounds of composition P_2H_2 were detected in mass spectrometry from the thermolysis of P_2H_4 [4,5].
1968	P_2H_4 gave P_2H_2 by photolysis at room temperature [6].
1981	The first stable diphosphene was prepared (Supermes P)$_2$ [7].
1983	The first heteroatom substituted diphosphene was prepared $(R_1R_2NP)_2$ where $R_1{=}R_2$ = $SiMe_3$ [8].

3.2 DIPHOSPHENE SYNTHESIS

There are many synthetic routes to diphosphenes. These are considered here in three major parts (Table 3.1):

1) The formation of symmetrical diphosphenes.
2) The formation of unsymmetrical diphosphenes.
3) The use of a diphosphene as the preparative starting material for further derivatives.

A considerable overlap exists between these classifications, for example (2a) allows the selective synthesis of both symmetrical and unsymmetrical diphosphenes [9,20], (see Sections 3.10.2.2, 3.10.5.1/2). Side reactions have been indicated where they are known to occur.

$$RPCl_2 \xrightarrow{Mg} RP{=}PR \quad [R \equiv \text{Supermes}, (Me_3Si)_3C, Ar'] \quad [7] \qquad \textbf{(1a)}$$

$$tmpPCl_2 + Hg(SiMe_3)_2 \xrightarrow{-Hg,\,-2Me_3SiCl} (tmp)_2P_2 \quad [12] \qquad \textbf{(1b)}$$

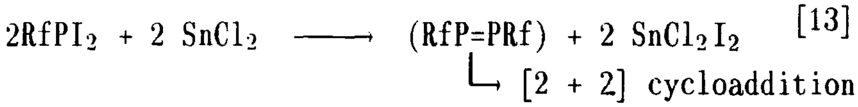

$$2RfPI_2 + 2\,SnCl_2 \longrightarrow (RfP{=}PRf) + 2\,SnCl_2I_2 \quad [13]$$
$$\hookrightarrow [2+2]\ \text{cycloaddition}$$

(1c)

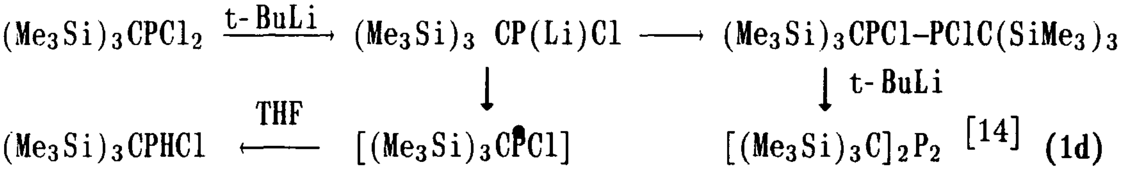

$$\begin{tikzcd}
(Me_3Si)_3CPCl_2 \arrow[r, "t\text{-}BuLi"] & (Me_3Si)_3\,CP(Li)Cl \arrow[r] \arrow[d] & (Me_3Si)_3CPCl\text{-}PClC(SiMe_3)_3 \arrow[d, "t\text{-}BuLi"] \\
(Me_3Si)_3CPHCl & {[(Me_3Si)_3C\dot{P}Cl]} \arrow[l, "THF"'] & {[(Me_3Si)_3C]_2P_2}
\end{tikzcd}$$

[14] **(1d)**

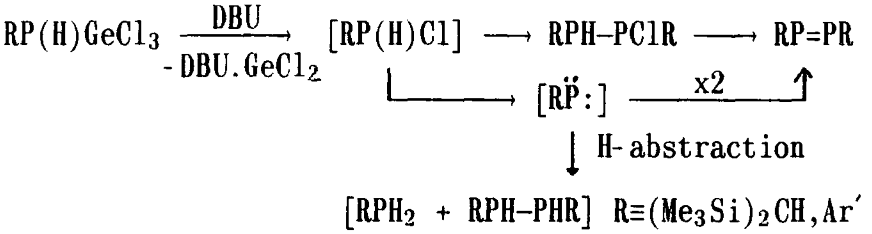

$$\begin{tikzcd}
RP(H)GeCl_3 \arrow[r, "DBU", "-DBU.GeCl_2"'] & {[RP(H)Cl]} \arrow[r] \arrow[dr] & RPH\text{-}PClR \arrow[r] & RP{=}PR \\
& & {[R\ddot{P}:]} \arrow[ur, "x2"] \arrow[d, "H\text{-abstraction}"] & \\
& & {[RPH_2 + RPH\text{-}PHR]\ R{\equiv}(Me_3Si)_2CH,Ar'} &
\end{tikzcd}$$

(1e)

(1e) avoids isolating the possibly unstable intermediate [RPHCl] [10,15]

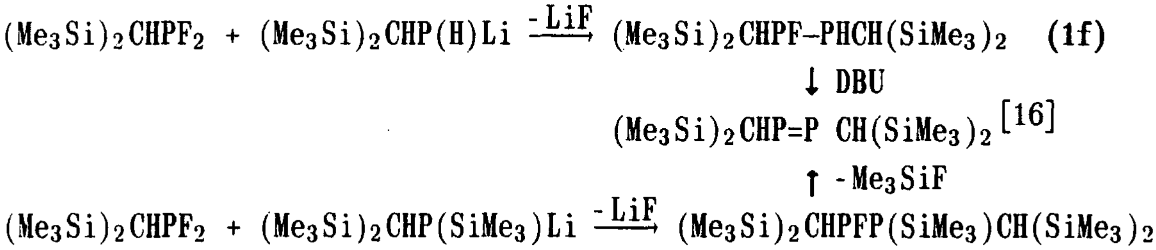

$$\begin{tikzcd}
(Me_3Si)_2CHPF_2 + (Me_3Si)_2CHP(H)Li \arrow[r, "-LiF"] & (Me_3Si)_2CHPF\text{-}PHCH(SiMe_3)_2 \arrow[d, "DBU"] \\
& (Me_3Si)_2CHP{=}P\ CH(SiMe_3)_2 \\
(Me_3Si)_2CHPF_2 + (Me_3Si)_2CHP(SiMe_3)Li \arrow[r, "-LiF"] & (Me_3Si)_2CHPFP(SiMe_3)CH(SiMe_3)_2 \arrow[u, "-Me_3SiF"']
\end{tikzcd}$$

(1f) [16]

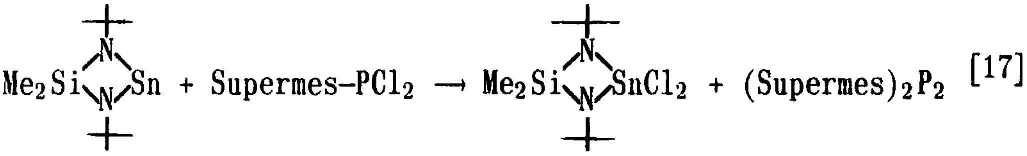

Me₂Si(N^tBu)₂Sn + Supermes–PCl₂ → Me₂Si(N^tBu)₂SnCl₂ + (Supermes)₂P₂ [17] **(1g)**

Table 3.1: *Synthetic routes to diphosphenes; in Table 3.1, Ar',Ar" refer to aryl species generally.*

$$\text{SupermesPCl}_2 + \text{GeI}_2 \rightarrow (\text{Supermes})_2\text{P}_2 + \text{SupermesPH}_2 + \text{GeI}_2\text{Cl}_2$$ [17] **(1h)**

$$(\text{SiMe}_3)_2\text{NPH–PClN}(\text{SiMe}_3)_2 \xrightarrow{\text{LiN(SiMe}_3)^t\text{Bu}} [(\text{Me}_3\text{Si})_2\text{NP}]_2 \xrightarrow{\text{x2}} \text{Dimer}$$ [12] **(1i)**

$$\text{PCl}_3 + 2\text{Li(Supermes)} \xrightarrow{\Delta} [\text{Supermes}\ddot{\text{P}}:] \xrightarrow{\text{x2}} \text{Supermes}_2\text{P}_2$$ [18a] **(1j)**

$$2\text{PArCl}_2 \xrightarrow[-\text{Q}]{\frac{1}{2}\text{P}} 2\text{ArPClPClAr} \xrightarrow{\frac{1}{2}\text{P}} \text{ArP=PAr}$$ [19] **(1k)**

where:

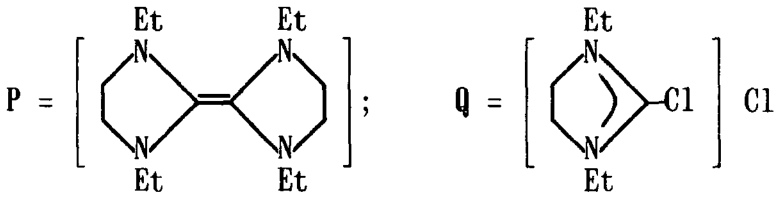

$$\text{ArPH}_2 + \text{Ar'PCl}_2 \xrightarrow[-\text{DBU.HCl}]{\text{DBU}} \text{ArP=PAr'} \quad \begin{bmatrix}\text{Ar} \equiv \text{Supermes}\\ \text{Ar'} \equiv \text{Mes}\end{bmatrix}$$ [20] **(2a)**

$$\underset{(\text{A})}{\text{SupermesP(H)GeCl}_3} + \underset{(\text{B})}{\text{Ar'P(H)GeCl}_3} \longrightarrow \text{AA, BB, AB}$$ [10] **(2b)**

(2b) is unselective, generating both symmetrical and unsymmetrical species.

$$\text{SupermesPCl}_2 + (\text{Me}_3\text{Si})_2\text{PMes} \xrightarrow{-2\text{Me}_3\text{SiCl}} \text{SupermesP=PMes}$$ [11] **(2c)**

$$\llcorner\!\longrightarrow \text{Supermes–P(Cl)SiMe}_3 \xrightarrow{\text{x2}} (\text{Supermes})_2\text{P}_2$$

$$\underset{(\text{A})}{(\text{Me}_3\text{Si})_3\text{CPCl}_2} + \underset{(\text{B})}{\text{SupermesPCl}_2} \xrightarrow[\text{naphthalenide}]{\text{sodium}} \text{AA, BB, AB}$$ [21] **(2d)**

(2d) A phosphaalkene formed using the lithium reagent $(\text{Me}_3\text{Si})_3\text{CLi}$

Table 3.1: *Synthetic routes to diphosphenes (cont'd).*

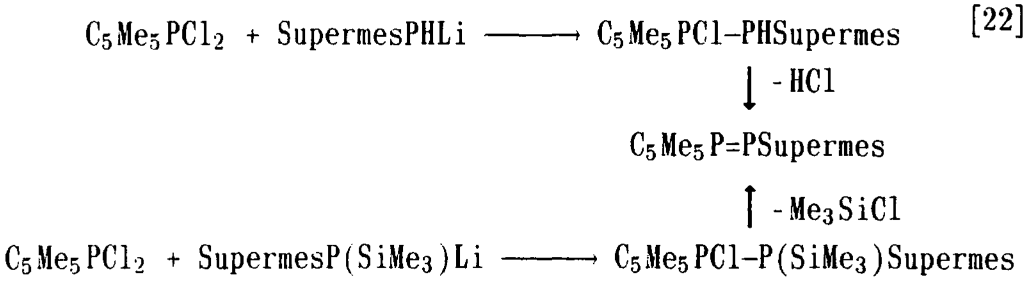

(2e)

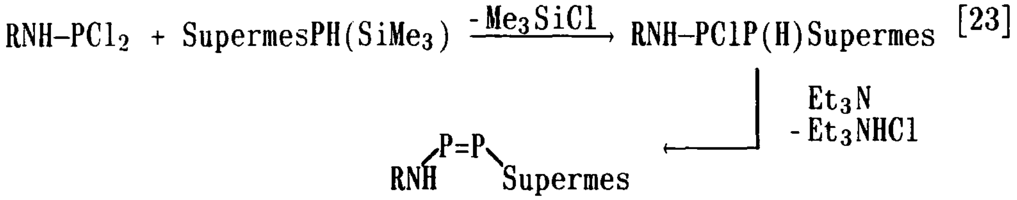

(2f)

(2f) The first synthetic route to a diphosphene with a cis conformation. The conformation is substituent dependent.

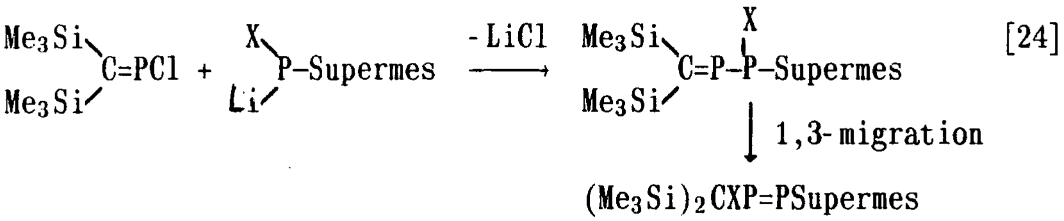

(2g)

(2g) An interesting isomerisation to a diphosphene, based on 1,3 "X" migration, for example X ≡ SiMe3. If the group on phosphorus is small (*eg.* butyl), no migration occurs.

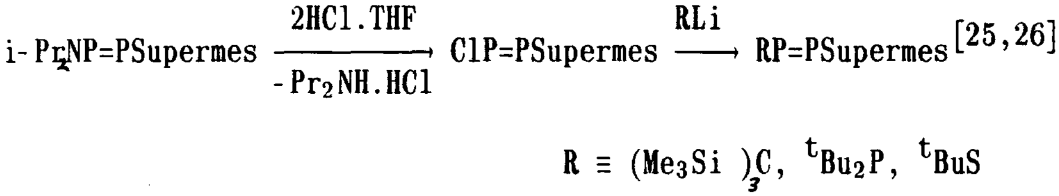

(3a)

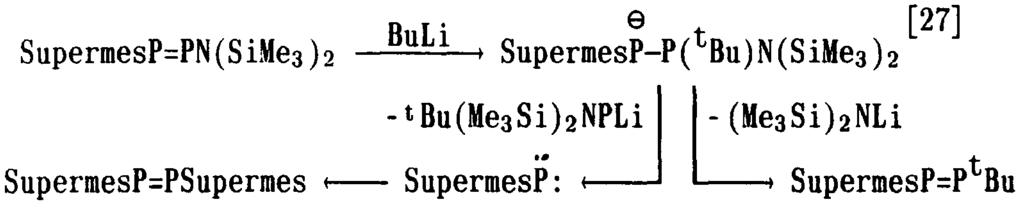

(3b)

Table 3.1: *Synthetic routes to diphosphenes (cont'd).*

3.3 DIPHOSPHENE STABILITY

The classical Double-bond rule states that "*elements having a principal quantum number greater than two should not be able to form a* $P\pi$-$P\pi$ *bond with themselves or other elements*" [28]. This is essentially correct for simple unprotected molecules, *eg*. HP=PH and HP=CH$_2$. However, the Pπ hybrid state can be stabilised by one (or a combination) of the following approaches:

1. Incorporation into a delocalised system
2. Incorporation into a charged system
3. Coordination to a metal centre
4. Steric protection by bulky groups.

Points 1-3 relate to stabilisation of a thermodynamic nature, and point 4 to kinetically derived stabilisation. For non-coordinated moieties points 1 and 4 are applicable.

The new diphosphenes synthesised in this work include ArP=PAr (19), ArP=PAr' (20), ArP=PMes (21) and ArP=PN^{i}Pr$_2$ (22). Their stabilisation is attributed to the large steric demand of the Ar substituent. In (20), (21) and (22) the large size of Ar', mesityl, and ^{i}Pr$_2$N respectively, may contribute to stabilise the system. The electron-withdrawing nature of the aryl ring may also offer a degree of electronic, (thermodynamic) stabilisation by decreasing the availability of the lone pairs, and hence their susceptibility to attack. In the diphosphene (22), stabilisation by delocalisation may be possible as a result of the nitrogen directly attached to phosphorus. Predominantly, stabilisation in systems (19-22) is kinetic, however another factor to be considered is that some thermodynamic stabilisation may originate from the lesser steric interaction in diphosphenes than in the cyclic species.

The chemistry of these diphosphenes has been developed and will be considered here in four major parts:

1. Synthetic routes (Section 3.4)
2. Characterisation and structure (MNDO) (Section 3.5/6)
3. Reactivity (Section 3.9)
4. Coordination chemistry with transition metal fragments (Chapter 5).

3.4 SYNTHETIC ROUTES TO NEW DIPHOSPHENES

The diphosphene (19) was synthesised by the three major routes outlined below:

(1) dechlorination with bisimidazolidine (an electron rich olefin) [Table 3.1, reaction (1k)] [19]. It was thought that the mechanism of this reaction was unlikely to proceed through a phosphinidene intermediate [19]. The proposed route is shown in Equation 3.1.

$$\begin{tikzcd} 2PArCl_2 \arrow[r] & 2ArP^{\bullet}Cl \arrow[r] \arrow[dr, "X"] & ArPCl\text{-}PClAr \arrow[r] & Ar_2P_2 \\ & & {[Ar\ddot{P}:]} \arrow[ur] & \end{tikzcd} \qquad (3.1)$$

(2) coupling of $ArPH_2$ and $ArPCl_2$ by dehydrochlorination with DBU (Equation 3.2) [Table 3.1, reaction (2a)] [9,20].

$$ArPCl_2 + ArPH_2 \xrightarrow{2DBU} ArP{=}PAr \qquad (3.2)$$

(3) dechlorination by magnesium (Equation 3.3) [Table 3.1, reaction (1a)] [7,11]

$$2ArPCl_2 \xrightarrow{Mg} ArP{=}PAr \qquad (3.3)$$

This reaction gave a brown inhomogeneous mixture showing predominantly the characteristic diphosphene signal in the ^{31}P NMR (+473 ppm), and a small peak at -139 ppm corresponding to the reduction product $ArPH_2$.

The highest yields were obtained from method (1) of the order of 72%. Method (2) is arguably the most convenient route to the diphosphene since the precursors have been synthesised (Section 2.3.2/3) and DBU is commercially available (yield 68-70%), whereas the bisimidazolidine is not.

The diphosphene (19) has also been synthesised and isolated *via* the following indirect routes:

(4) $$\underset{(15)}{ArPH_2} + \underset{(23)}{C_6Cl_5PCl_2} \xrightarrow{DBU} \underset{(19)}{ArP{=}PAr}$$ [conversion 38% wrt $ArPH_2$ (15)]

(5) $$\underset{(15)}{ArPH_2} + Ph_2CCl_2 \xrightarrow{DBU} \underset{(19)}{ArP{=}PAr}$$ (Section 4.3.4)

(6) Following the distillation of Ar_2PCl (14) the residual solid was analysed as Ar_2P_2 (19). This was attributed to a possible concentration effect, with the coupling to form the diphosphene preceded by phosphinidene formation [Table 3.1, reaction (1j)] [18] (for example, see Figure 3.1)

$$\begin{tikzcd}
{} & Ar_2PCl \arrow[r] & Ar_2P\bullet + Cl\bullet \arrow[d] & {} \\
ArCl & {} & Ar\bullet + Ar\ddot{P}: \arrow[ll, "(\bullet Cl\bullet)"'] \arrow[r] & ArP{=}PAr
\end{tikzcd}$$

Figure 3.1

No mechanistic studies were carried out on the formation of the diphosphene. However, on the basis of previous results an intramolecular dehydrochlorination or dechlorination [Figure 3.2(a)] (as suggested in Equation 3.1), or an intermolecular process *via* the phosphinidene intermediate [Figure 3.2(c)] may be postulated. A proposed rationalisation for the diphosphene formation in (4) and (5)

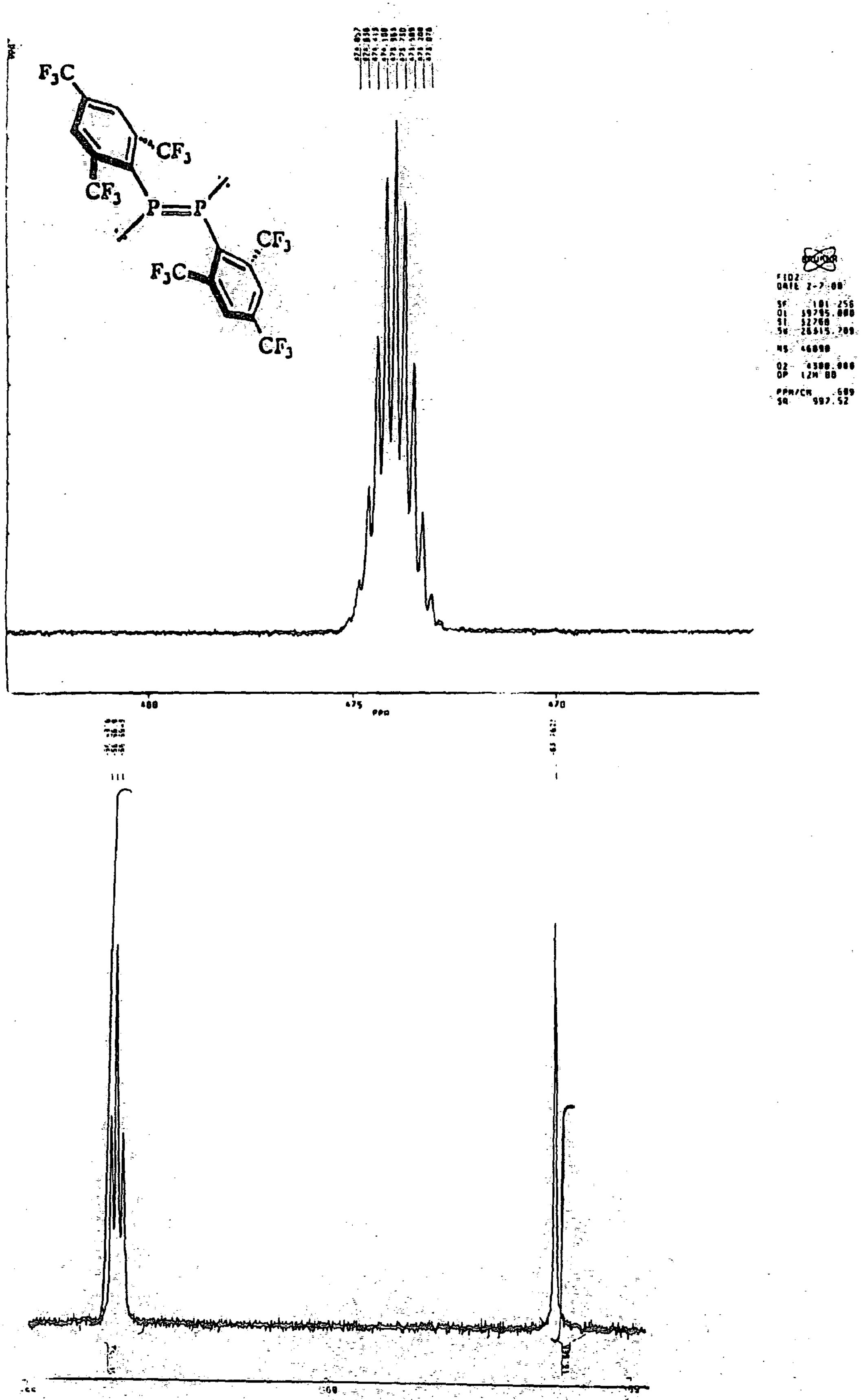

Figure 3.3: *(a)* ^{31}P *NMR and (b)* ^{19}F *NMR parameters of the diphosphene (19) in* $CDCl_3$.

(and further examples) has been given in Section 7.3

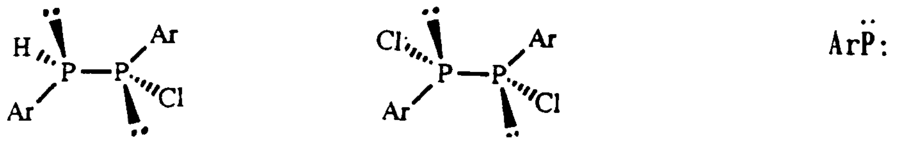
(a) (b) (c)

Figure 3.2: *Intramolecular dehydrochlorination (a) or dechlorination (b) and the phosphinidene intermediate (c); (refs.9,11,20).*

3.5 SPECTROSCOPIC DATA FOR THE SYMMETRICAL DIPHOSPHENE

3.5.1 ^{19}F and ^{31}P NMR

A significantly deshielded thirteen line multiplet was observed in the ^{31}P NMR at +473 ppm. This characteristic ^{31}P chemical shift is due to a significant increase in the paramagnetic shielding term caused by the existence of low-lying excited states. This is a dominant effect in multiply bonded compounds [29].

A pseudo-triplet was observed in the ^{19}F NMR with a through-space coupling from fluorine to phosphorus $^{4}J_{PF}$ + $^{5}J_{PF}$ = 45Hz. This phenomenon exists in many systems, for example, the Escudié diphosphene Ar'_2P_2 [10], $(CH_3)_2P$-$P(CH_3)_2$ [30a], and is observed in the $^{13}C\{1H\}$ NMR spectrum of (Supermes)$_2P_2$ [7]. The NMR parameters (^{31}P and ^{19}F) for the diphosphene (19) are shown in Figure 3.3(a) and 3.3(b) respectively.

3.5.2 Solid state ^{31}P NMR

The solid state NMR of the diphosphene (19) is presented in Figure 3.4. The static solid state NMR of this species would be extremely broad and of a characteristic shape. By the technique of magic angle spinning this is split into a set of lines consisting of a centre band

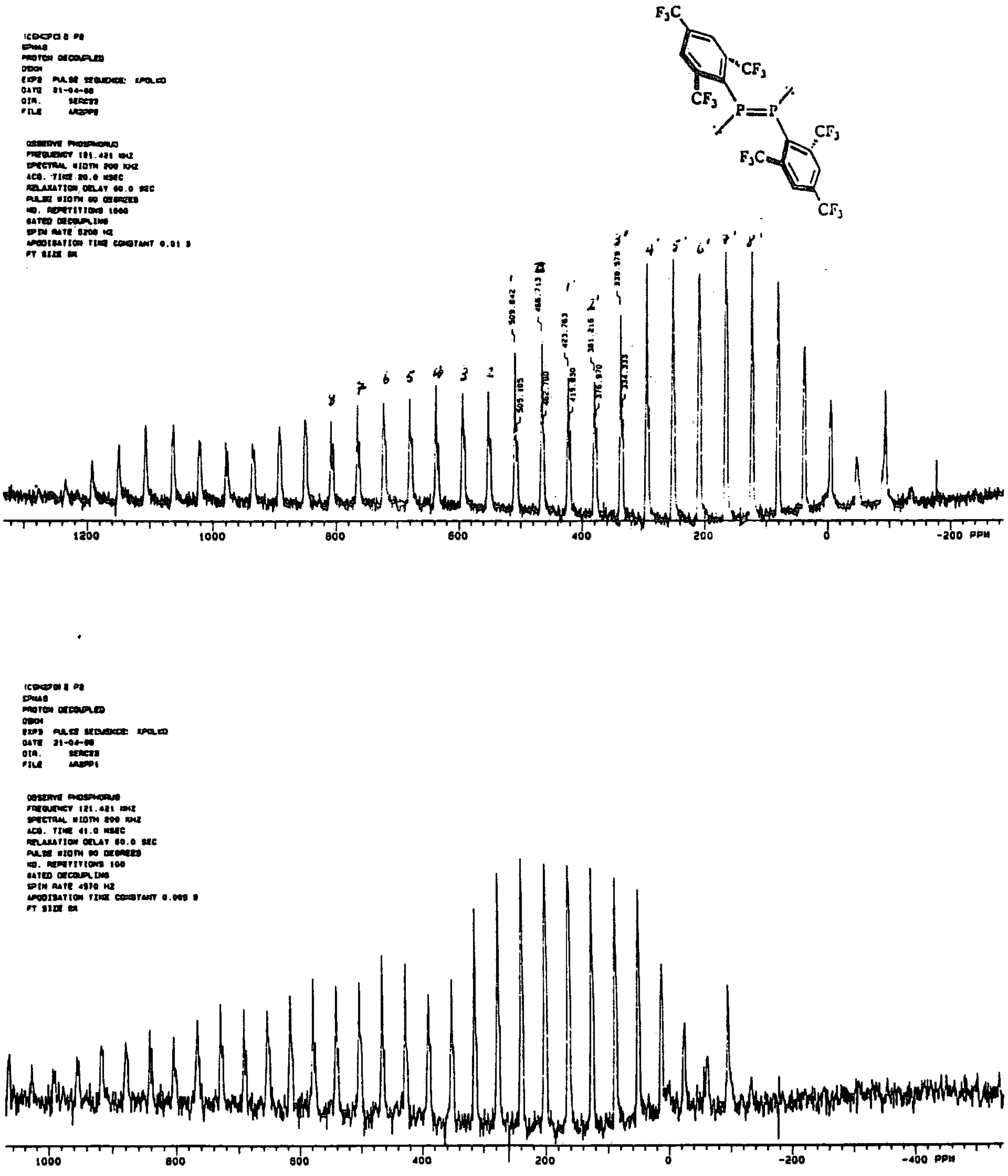

[illegible]
CPMAS
PROTON DECOUPLED
[illegible]
EXP2 PULSE SEQUENCE: [illegible]
DATE 21-04-88
DIR. [illegible]
FILE [illegible]

OBSERVE PHOSPHORUS
FREQUENCY 121.421 MHZ
SPECTRAL WIDTH 200 KHZ
ACQ. TIME 20.0 MSEC
RELAXATION DELAY 60.0 SEC
PULSE WIDTH 90 DEGREES
NO. REPETITIONS 1000
GATED DECOUPLING
SPIN RATE 5200 HZ
APODISATION TIME CONSTANT 0.01 S
FT SIZE 8K

[illegible]
CPMAS
PROTON DECOUPLED
[illegible]
EXP3 PULSE SEQUENCE: [illegible]
DATE 21-04-88
DIR. [illegible]
FILE [illegible]

OBSERVE PHOSPHORUS
FREQUENCY 121.421 MHZ
SPECTRAL WIDTH 200 KHZ
ACQ. TIME 41.0 MSEC
RELAXATION DELAY 60.0 SEC
PULSE WIDTH 90 DEGREES
NO. REPETITIONS 100
GATED DECOUPLING
SPIN RATE 4970 HZ
APODISATION TIME CONSTANT 0.005 S
FT SIZE 8K

Figure 3.4: *The ^{31}P solid state NMR spectrum of diphosphene (19).*

and spinning side bands [30b]. [The centre band has been denoted by o and the spinning side-bands at distances nf_R from the centre bands by n and n', f_R is the sample rotation frequency].

The isotopic shift has been obtained from a comparison of the spectra measured at slightly different sample rotation rates, and its value is +466.7 ppm. The total width of the spinning side-band pattern indicates that the chemical shift anisotropy is large spanning 1320 ppm (from -100 to +1220 ppm) [31]. (The smaller the anisotropy the smaller the number of side bands observed). It would be of interest to calculate the principal elements of the chemical shielding tensor for the diphosphene (19). Procedures exist to derive these elements from the intensities of the spinning side-bands [32a,b]. Problems, however, may be anticipated due to the simultaneous effect of dipolar coupling (P-P and P-F) and the chemical shift anisotropy. The simultaneous presence of the dipolar interaction and the anisotropic chemical shielding is known to considerably distort the NMR line shapes. This results in a poor agreement between theory and experiment: as the theoretical calculation considers only the chemical shift anisotropy [32].

3.5.3 Electronic Spectra and Molecular Orbitals of Diphosphenes

Ab initio calculations (MO) on the model diphosphene, *trans*-P_2H_2 [33-37], reveal the LUMO possesses appreciable *p*-*p*π* character[38].

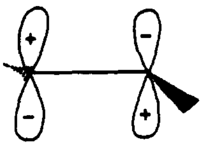

2b$_g$

The two HOMOs are closely spaced, with their order dependent on the calculation method.

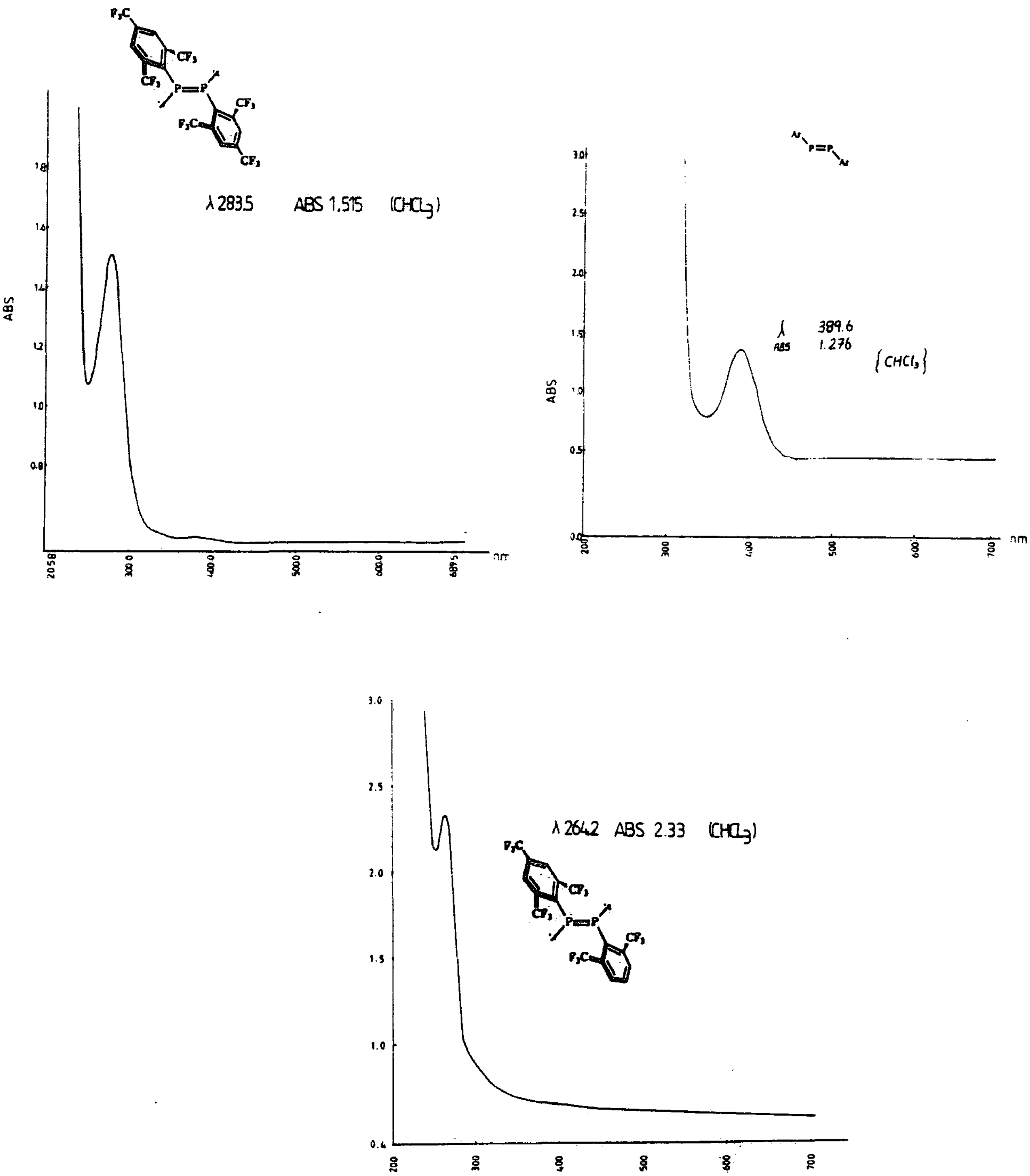

Figure 3.5: *Visible and ultraviolet absorption for the diphosphenes ArP=PAr (19) and ArP=PAr' (20).*

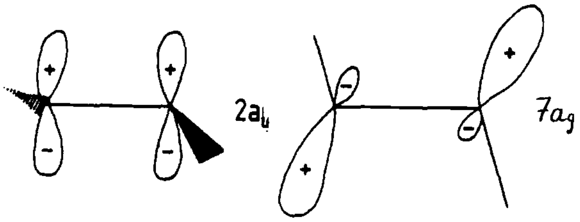

The electronic spectral data show that the longer wavelength is much less intense. (The lone pair combination as the HOMO can therefore be deduced, since the corresponding n-π^* transition is symmetry forbidden (g → g the Laporte selection rule) π-π^* is symmetry allowed and therefore of a greater intensity. The red, orange and yellow colours of the diphosphenes are therefore a direct result of these n-π^* and π-π^* "P=P" transitions, (as the wavelengths are greater than 300 nm they lie outside the π-π^* aromatic region). Some values of UV λ_{max} for known diphosphenes are given in Table 3.2.

COMPOUND	λ(max)/nm	ϵ	REF
Supermes–P=P–Supermes	460 340	1360 7690	[7,38]
$(Me_3Si)_3C$-P=P-$C(SiMe_3)_3$	484 353	63 9474	[38]
Supermes–P=P-C(H)$(SiMe_3)_2$	427 325	370 13000	[38]
Supermes–P=P–Mes	456 326	220 2500	[20]
$Me_5C_5P=PC_5Me_5$	407 275	1995 12589	[39]

Table 3.2: *UV λ(max) values for known diphosphenes.*

Data obtained from this study are shown in Table 3.3 and the UV/Visible spectra are presented in Figure 3.5.

The UV spectral absorption for n–π^* and π –π^* transitions is about 70 nm less than for most other diphosphenes. The shift observed is hypsochromic (to shorter wavelength).

COMPOUND	COLOUR	λ(max)	ε	REF
ArP=PAr (19)	pale yellow crystals	389.6 283.5	5694 6763	this work
ArP=PAr' (20)	white ‡ crystals	264.2	40451	this work
Ar'P=PAr' (24)	pale yellow	394 277	NM NM	[10]

Table 3.3: *UV data on diphosphenes (19),(20) and (24); ‡No $n-\pi^*$ transition was observed; NM=not measured.*

Another interesting feature of the UV-Visible data is that λ_{max} for arylated and alkylated diphosphenes (Tables 3.2 and 3.3) are similar. This suggests that there is little conjugation between aryl groups and the "P=P" double bond. This is further supported by MNDO studies on the species Ar_2P_2 (19), $ArAr'P_2$ (20) and Ar'_2P_2 (24) in this study (Section 3.6).

3.5.4 Vibrational Spectroscopy

A resonance Raman study of $(Supermes)_2P_2$ has attributed a 610 cm^{-1} band to the P=P stretch [40]. This vibration is symmetric with respect to the C-P=P-C linkage, consequently this band does not appear strongly in the infrared. This situation appears analogous for Ar_2P_2 and $ArAr'P_2$ (Experimental, Section 3.10). The nature of the P=P in $(Supermes)_2P_2$ has been studied using ESCA [41] (low 2p binding energy).

3.6 STRUCTURE

The structure of the three diphosphenes Ar_2P_2 (19), $ArAr'P_2$ (20) and Ar'_2P_2 (24) have been elucidated by MNDO calculations. The MNDO structure of the symmetrical diphosphene (19) and the unsymmetrical diphosphene ArAr'P_2 (20) [illustrated in Figure 3.6(a) and 3.6(b) respectively] shows, in each case, the two rings to be parallel and not conjugated with the double bond.

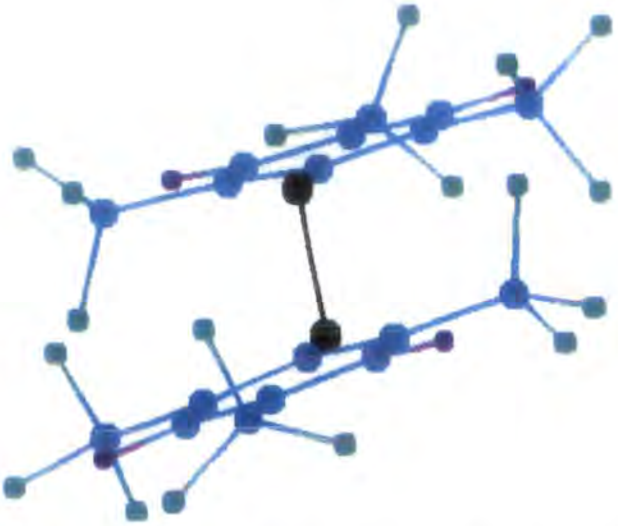

Figure 3.6(a): *The MNDO structure of diphosphene (19).*

3.6.1 Ar_2P_2 (19)

The geometry as calculated by **MNDO** is illustrated in Figure 3.6(a). The **HOMO** in this species appears to lie much lower in energy than for the diphosphene (24), hence the compound is more difficult to ionise.

<u>HOMO</u>: the phosphorus lone pair Energy -10.92 eV

<u>HOMO-1</u>: The π-system Energy -11.74 eV

CHEN-5 JULY 1986

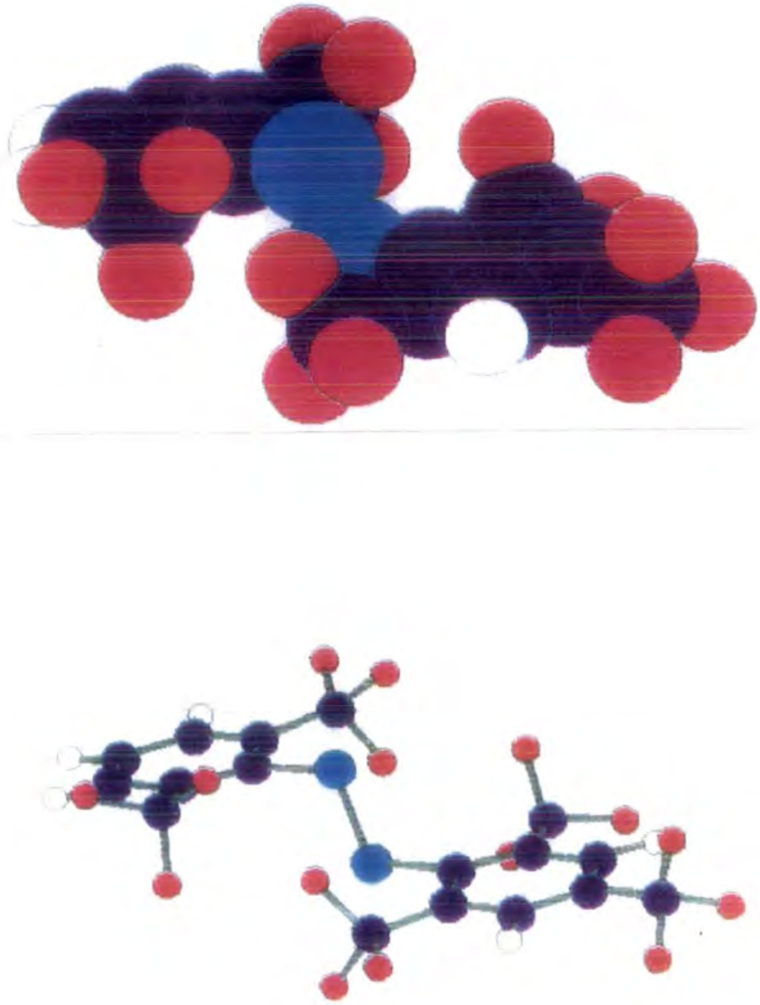

Figure 3.6(b): *The predicted geometry of the unsymmetrical diphosphene Ar'ArP$_2$ (20) by MNDO calculation.*

Charge: The phosphorus atoms are positively charged

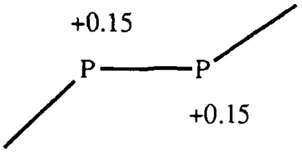

Geometry: The Ar groups are orthogonal to the plane of the P=P.

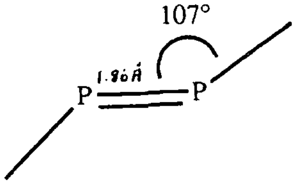

The potential surface at minimum energy (90^0) is relatively flat, suggesting that the rings can twist slightly from this conformation.

π-bond order

The total calculated π-electron density on P_1 is 1.09 of which 0.98 originates from P_2. There is therefore only a very small π-electron contribution from the ring.

The d-orbital on phosphorus is empty and available for electron donation from a metal (d-orbitals however are not considered in the MNDO calculation).

3.6.2 Ar'ArP$_2$ (20)

The geometry as calculated by MNDO is illustrated in Figure 3.6(b).

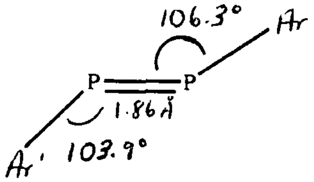

P=P bond length
calculated 1.8 Å

Delocalised HOMO: The phosphorus lone pair

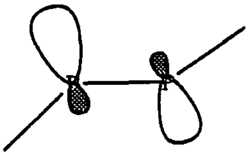

Energy -10.14 eV
(Ionisation potential)

HOMO-1: The π-orbital (pπ–pπ overlap)

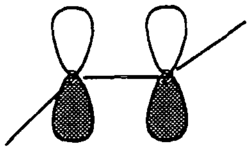

Energy -11.06 eV
(p-pσ -16.80 eV)

Charge

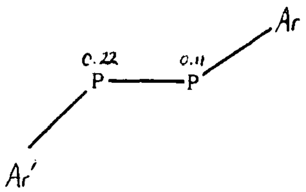

3.6.3 Ar'_2P_2 (24)

The two rings are orthogonal to the plane of the P=P bond (compare this with the X-ray structure) [42].

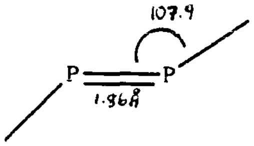

P=P bond length
calculated 1.86Å

Delocalised HOMO: The phosphorus lone pair

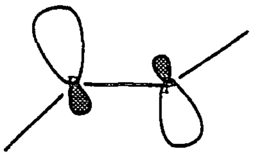

Energy -10.14 eV
(Ionisation potential)

HOMO-1: The π-orbital (pπ–pπ overlap)

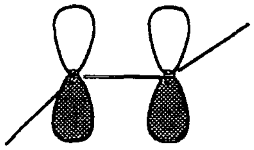

Energy -11.16 eV
(p-pσ -16.85 eV)

Charge

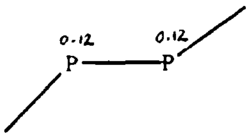

It has been suggested that due to the close proximity between the phosphorus and the fluorines, the Ar'_2P_2 (24) appears the most crowded of the known diphosphenes [42]. Nevertheless, the exceptional lack of reactivity (Section 3.9) observed for both (19) and (24) indicates that

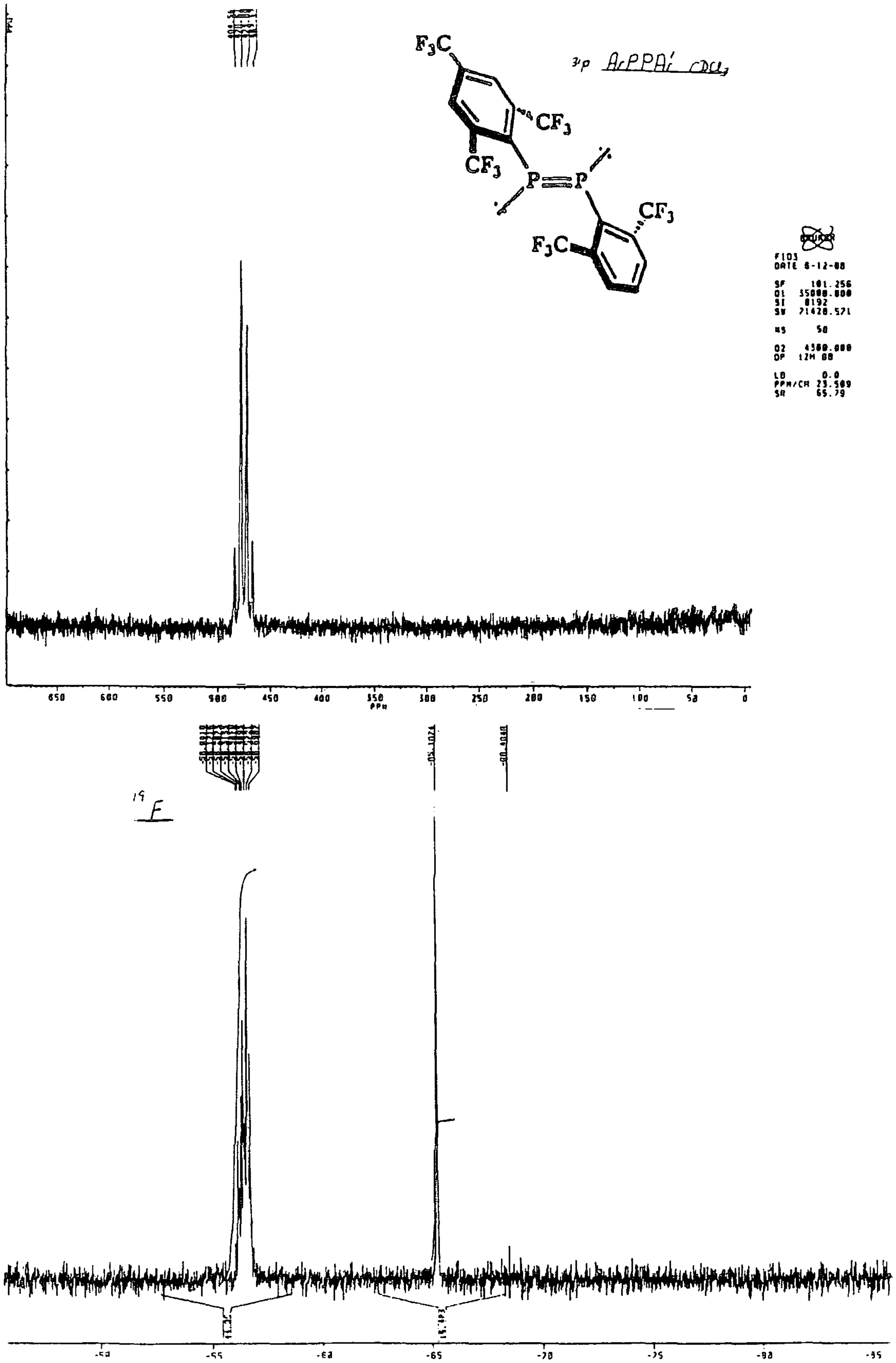

Figure 3.7(a): *(i) ^{31}P NMR and (ii) ^{19}F NMR spectra for the unsymmetrical diphosphene, ArAr'P_2 (20) in $CDCl_3$.*

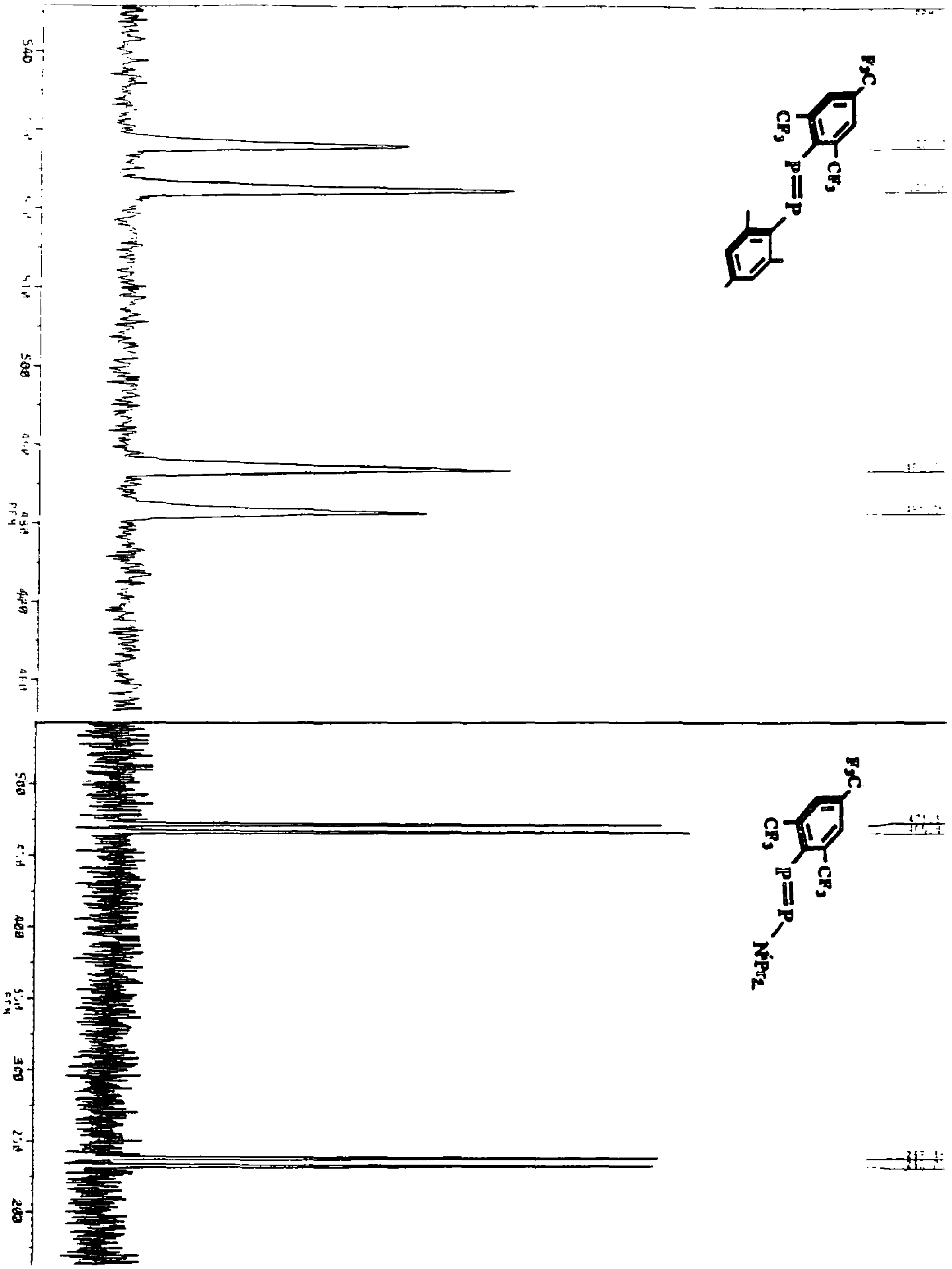

Figure 3.7(b): *The ^{31}P NMR data of (i) ArP=PMes (21) and (ii) i-Pr$_2$NP=PAr (22) in CDCl$_3$.*

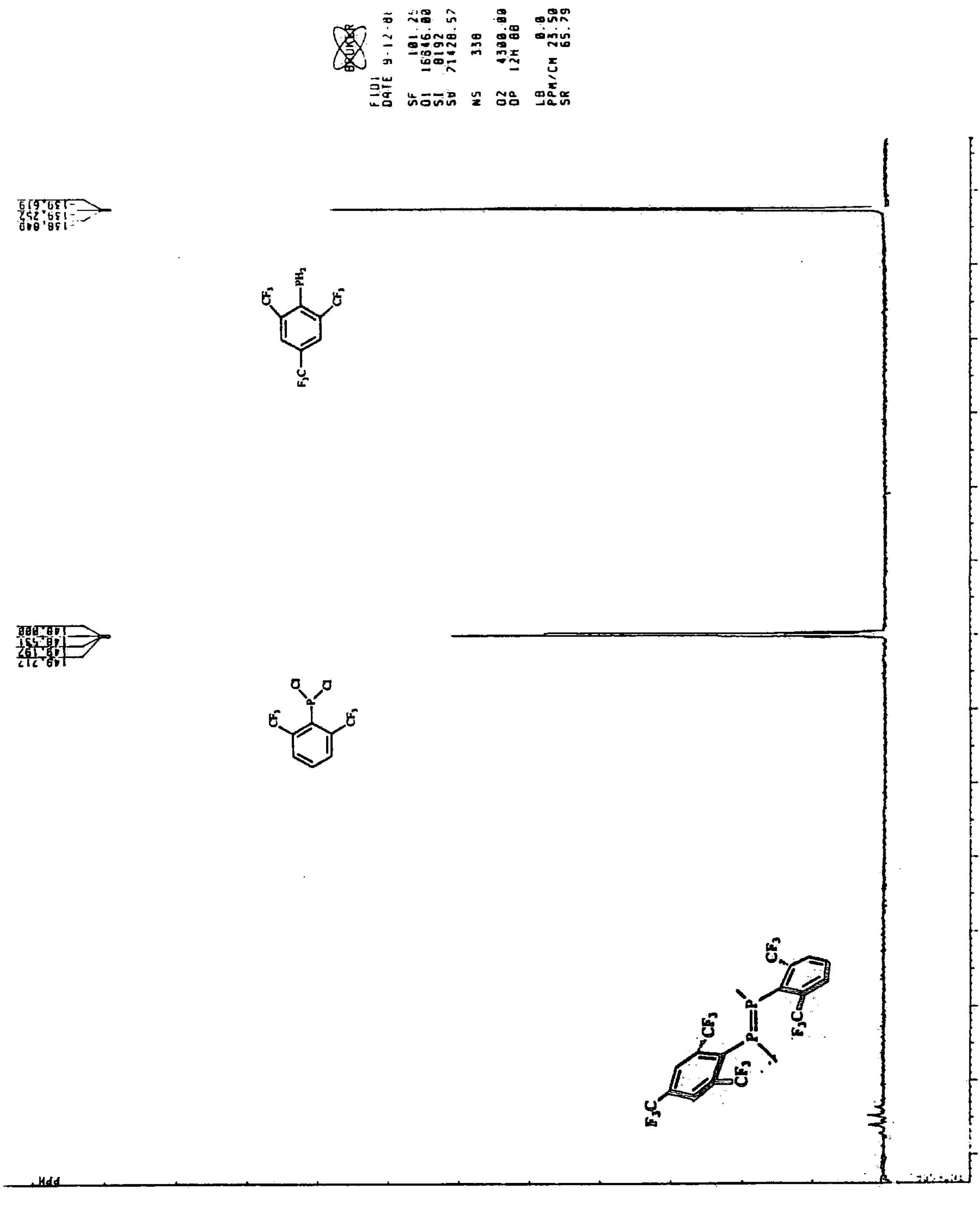

Figure 3.8: *Mixing $Ar'PCl_2$ and $ArPH_2$ in THF at ambient temperature. The ^{31}P NMR spectrum of the solution.*

the electronic effects give an important contribution to the stability.

The interactions of the fluorines in Ar_2P_2 (19) and Ar'_2P_2 (24) may be anticipated to cause a longer bond, however, Escudié *et al.*[42] suggested that the electronic effects could cause a shortening of the normal "P=P" length. This may be a result of reduced electron density around the phosphorus atom with electron-withdrawing substituents attached. The X-ray structure shows the "P=P" bond length to be 2.019 Å in Ar'_2P_2 (24) and within the normal range (see Table 3.4).

COMPOUND	P=P (Å)	$\text{P-}\hat{\text{P}}\text{-C}$ (^{o})	REF
$(Supermes)_2P_2$	2.034	102.8	[7]
$[(Me_3Si)_3C]_2P_2$	2.014 * 2.004	108.1 108.9	[38]
$Ar'Ar'P_2$	2.019	98.0	[42]

Table 3.4: *Bond lengths and angles of some selected diphosphenes; *two crystallographically independent molecules per unit cell.*

This is also clearly illustrated for $ArAr'P_2$ (20) and Ar_2P_2 (19). The normal bond length is a probable result of the two competing effects.

3.7 UNSYMMETRICAL DIPHOSPHENES

As mentioned in Section 3.3, three unsymmetrical diphosphenes were synthesised: ArP=PAr' (20), ArP=PMes (21) and $ArP{=}PN^iPr_2$ (22). The latter two species were characterised by spectroscopic data only (Figure 3.7, Table 3.5). The coupling reactions (Equations 3.4 and 3.5) allowed the successful isolation of the unsymmetrical diphosphene, ArP=PAr' (20). As illustrated in Figure 3.8, this was somewhat surprisingly observed by simply mixing the two phosphorus components. Similarly the derivative bearing the mesityl group (21) was prepared as shown in Equation 3.6 [Figure 3.7b(i)].

$$Ar'PH_2 + ArPCl_2 \xrightarrow{DBU} Ar'P{=}PAr\ (20) \qquad (3.4)$$

$$Ar'PCl_2 + ArPH_2 \xrightarrow{DBU} Ar'P{=}PAr\ (20) \qquad (3.5)$$

$$MesPCl_2 + ArPH_2 \xrightarrow{DBU} ArP{=}PMes\ (21) \qquad (3.6)$$

Diphosphene (21) appeared less stable than (19). Its life time in solution appeared to be only of the order of a few days. $Ar'ArP_2$ (20) appeared stable in air over a few days, and indefinitely when stored in an inert atmosphere at ambient temperature.

Diphosphene $^{i}Pr_2NP{=}PAr$ (22) was obtained by dehydrochlorination between $^{i}Pr_2NPCl_2$ and $ArPH_2$ (15). (22) is a particularly interesting species since it is stabilised both by delocalisation attributed to the attached nitrogen, giving interesting spectral parameters *ie.* one phosphorus is significantly more shielded [23] [see Figure 3.7b(ii)], and by the kinetic stabilisation of the large Ar group. The stability of this compound (22) appeared to be analogous to that of species (21). It would be interesting to vary the nature of R on the nitrogen, to study its effect on diphosphene conformation. This has been investigated in similar systems [43]. The large $^{1}J_{PP}$ coupling constant observed in the species (20), (21) and (22) is evidence for the special bonding situation *ie.* σ between the 2 sp^2 hybridised phosphorus atoms, the high s-character and rather short "P-P" bond length due to the additional π-bond. A similar correlation exists between s-character and $^{1}J_{CC}$ coupling constants [11]. The diphosphene NMR data has been presented in Table 3.5.

	R	R'	^{31}P	$^{1}J_{PP}$	REF
(19)	Ar	Ar	+473.9	---	This work
(20)	Ar	Ar'	+489.0 +478.2	552	This work
(21)	Ar	Mes	+524.7 +484.4	566.8	This work
(24)	Ar'	Ar'	+477.1	---	Escudié [10,42]
(22)	Ar	NR_2	+468.5 +234.7	542.1	This work

Table 3.5: *^{31}P NMR parameters of new diphosphenes (See Figure 3.7).*

3.8 OTHER DIPHOSPHENES

An attempt was made at the synthesis of unsymmetrical diphosphenes with smaller groups forming direct phosphorus-carbon bonds, in general *via* the coupling reaction $ArPH_2 + RPCl_2 \longrightarrow ArP{=}PR$ [where R ≡ ^{t}Bu (25), 2,$(CF_3)C_6H_4$(Ar") (26), C_6Cl_5 (27) and C_6F_5 (28)]. The requirement of two ortho substituents for diphosphene stabilisation with direct substitution by an aromatic species is well known [7,9-11]. It has been shown that two ortho ^{t}butyl groups plus two ortho methyl groups can stabilise the diaryldiphosphene, whereas two ortho ^{i}propyl groups at each aryl ring are insufficient [11]. It was of interest to study the possible stabilising effect by ortho chlorines (27) and ortho fluorines (28). Due to the stability of Ar'_2P_2 (24) and $Ar'ArP_2$ (20), the reaction of $Ar''PCl_2$ (26) with $ArPH_2$ (15) was also investigated.

In the ^{t}butyl case no diphosphene was isolated, only upfield shifts were observed. The ^{t}butyl group (25) was considered too small to offer a significant degree of stabilisation with its geometry offering very little shielding of the attached phosphorus (Figure 3.9) (compare with the substituents $C(SiMe_3)_3$ and Supermes, used in the formation of the very first unsymmetrical diphosphene) [21].

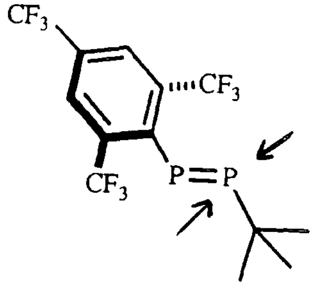

Figure 3.9: *Geometry of a proposed t-butyl substituted diphosphene.*

For the coupling $^tBuP^1Cl_2$ and ArP^2H_2, the mechanism would be expected to proceed *via* the initial attack of P^2 on P^1. The effectiveness of P^2 as a nucleophile is reduced by the presence of Ar (an electron-withdrawing substituent). Hence the coupling reaction $^tBuP^1H_2$ and ArP^2Cl_2 was attempted. Nucleophilic attack at P^2 is now favoured by the presence of three electron-withdrawing substituents. Even with the application of a stronger base, *eg*. DABCO, similar results were obtained. No unsymmetrical diphosphene was obtained by similar coupling reactions (Equations 3.7 and 3.8).

$$ArPH_2 \ (15) + C_6Cl_5PCl_2 \ (27) \xrightarrow{DBU} \tag{3.7}$$

$$ArPH_2 \ (15) + C_6F_5PCl_2 \ (28) \xrightarrow{DBU} \tag{3.8}$$

The reaction with $C_6Cl_5PCl_2$ (27) again gave no evidence of the unsymmetrical diphosphene even at low temperature (213 K). Only peaks at -84 and -89 ppm were observed. As this reaction mixture reached room temperature, the symmetrical diphosphene (19) was isolated. It appears that Ar" (a single ortho CF_3 substituent), and both chlorine and fluorine do not give the unsymmetrical diphosphene, instead other reactions intervene. The presence of the upfield peaks (-84, -89 ppm) observed here, has been seen in many other cases on reaction of a chlorine species with $ArPH_2$ and DBU. An attempted rationalisation of this is made in Section 7.3

3.9 DIPHOSPHENE REACTIVITY.

Despite the requisite steric hindrance, many diphosphenes exhibit a varied and interesting reaction chemistry [44]. The reactivity patterns can be divided into three main areas: electrophilic attack, *eg.* with sulphur [45], selenium [46] or $Au[PEt_3]^+$ (isolobal with H^+)[47], oxygen [48]; nucleophilic attack, *eg.* H^- [49], BuLi, MeLi [50]; and coordination chemistry (see Chapter 5). There is a vast amount of reactivity exhibited by the first kinetically stabilised diphosphene, $(Supermes)_2P_2$ [7,50] containing a localised P=P bond.

It was therefore somewhat surprising when the diphosphene Ar_2P_2 (19) was treated with either strong acids, for example CF_3COOH and $HBF_4 \cdot Et_2O$, or with S_8 under mild conditions, that no reaction occurred. This was further supported by Edelmann *et al.*[9] who similarly observed no protonation with $HBF_4 \cdot Et_2O$ and no reaction with Vanadocene. Further investigation into the reactivity of the diphosphene should involve the addition of methoxide ($MeO^- Na^+$), or methyllithium, *ie.* small nucleophiles which may be expected to react with Ar_2P_2 (19) (LOW-LYING LUMO). The reaction of the diphosphene (19) with a carbene in an attempt to generate a cyclic diphosphirane was carried out [51]. A general scheme is shown in Figure 3.10.

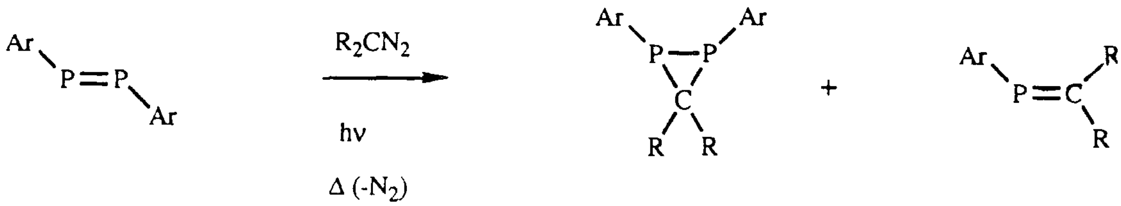

Figure 3.10: *General scheme for the formation of a diphosphirane by the reaction of a carbene with a diphosphene; R ≡ Cl, Br, Ph and Ar ≡ Supermes.*

The absence of [2+3] cycloadducts in this reaction, and the fact that cyclopropanation reactions only take place under conditions in which carbenes are formed, *eg.* Δ and $h\nu$ indicate a direct carbene attack at a P=P double bond. In this work $(^{i}Pr_2N)_2PC(N_2)SiMe_3$ was synthesised as the starting material (Section 11.4.2).

This was irradiated at 300 nm in pentane, in the presence of the diphosphene for 8 hours [*ie.* the nucleophilic $Me_3Si\text{-}C\text{:-}P(NR_2)_2$ carbene was generated *in situ*]. (Carbenes have a vacant orbital and lone pair of electrons and hence can be nucleophilic or electrophilic: Moss carbene scale). The resulting solution showed the characteristic signal due to the carbene at -42 ppm (^{31}P NMR) [52] and the presence of the unreacted diphosphene. The use of toluene to increase the solubility of the diphosphene showed a similar lack of reactivity. The specific diazo compound was used primarily because of its synthetic availability. It must not be overlooked that this lack of reactivity may be due to the nature of the carbene. It would be interesting to parallel the experiment, using the same diazo species as those in which the diphosphirane was observed [51] with the starting material, $(Supermes)_2P_2$.

3.10 EXPERIMENTAL

3.10.1 1,3,1',3'-Tetraethyl-2,2'-bis(imidazolidine) [19]

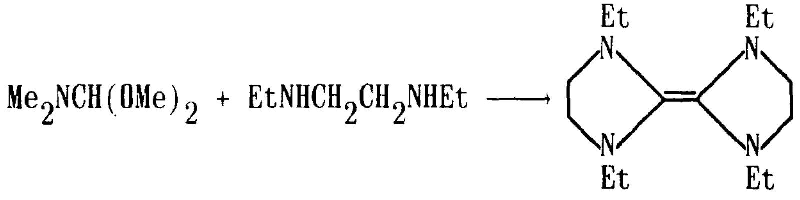

N,N-dimethylformamide dimethylacetal (17.9g, 20 cm^3, 151 mmol) was added in one portion to a stirred solution of N,N'-diethylethylene diamine (15.1g, 18.3 ml, 130 mmol) in dry benzene (35 ml). This reaction mixture was heated in a distillation vessel to 110 °C for three hours, and the methanol/benzene azeotrope that was produced was collected. The vessel was cooled and the remaining benzene was removed *in vacuo*. The residue was distilled under vacuum to give 1,3,1',3'-tetraethyl-2,2'-bis(imidazolidine). Yield was 11.7g (71%); Bpt. 87-88 °C (3 mm Hg). This was a low melting point, moisture and air sensitive solid, Mpt. 48 °C [19].

3.10.2 Preparation of Diphosphene, ArP=PAr (19)

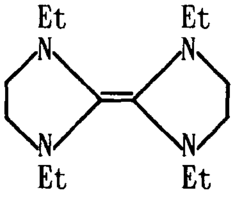

3.10.2.1 $2ArPCl_2$ (12) $\xrightarrow{\hspace{3cm}}$ ArP=PAr (19)

Bisimidazolidine (0.41g, 1.6 mmol) in toluene (10 ml) was added dropwise over 5 minutes to a stirred solution of $ArPCl_2$ (1.22g, 3.2 mmol) in toluene (20 ml) at ambient temperature. On addition of the base the solution turned yellow/orange immediately with a visible white precipitate. It was warmed to reflux by the use of an oil bath.

All the solid dissolved and the solution became a clear dark red. After refluxing for 1 hour[1] the stirred solution was allowed to cool to ambient temperature. Quantitative conversion was observed by ^{31}P NMR (+473.9 ppm). The solid was removed by filtration, and the toluene removed from the filtrate *in vacuo*. To the resulting yellowish/orange oil (crude yield 76%) a small volume of toluene (7 ml) was added. On cooling the solution to -40 ^{o}C crystals (pale yellow needles) of the diphosphene, ArP=PAr were obtained (0.65g, 65%). This yield could be increased by obtaining a second batch of crystals from the supernatant liquid. Total yield 72% (an additional 0.07g collected). It was very difficult to form crystals suitable for X-ray analysis. A solution of diphosphene (from several batches) (1.7g) in toluene (16 ml) was placed in a ripple tank oscillating between +10 and -20 ^{o}C. The crystals obtained were submitted for X-ray analysis. The diphosphene is a pale yellow needle-like crystalline solid, which is stable in air.

Ar_2P_2: Mpt. 185 ^{o}C; Analysis Found: C, 34.97; H, 0.87. Required for $C_{18}H_4F_{18}P_2$: C, 34.64; H, 0.65%; IR (KBr) ν_{max}: 3100 (w,ArCH), 1630 and 1570 (m,ArC=C), 1400-1000 (s,CF_3), 780 and 680 (w,"P=P") cm^{-1}; UV-Vis ($CHCl_3$) $\lambda_{max}(\epsilon)$: 283.5 (6763), 389.6 (5696) nm; MS EI (Intensity%): 343 (36,ArP_2^+); ^{31}P ($CDCl_3$) δ: +473.9 (13 line multiplet), $^{4}J_{PF}$ + $^{5}J_{PF}$ 45.0 Hz; ^{31}P (solid state) δ: +466.7 ppm, shielding anisotropy +1240 to -100 ppm; ^{19}F ($CDCl_3$) δ: -56.5 (triplet,12F), -63.8 (s,6F); ^{1}H ($CDCl_3$) δ: +8.3 (s).

---

[1] It was possible to obtain exactly similar yields without refluxing the solution. The reaction mixture was stirred at ambient temperature for 1.5 hours.

3.10.2.2 $\mathrm{ArPH_2} + \mathrm{ArPCl_2} \xrightarrow[\text{-2DBU.HCl}]{\text{2DBU}} \mathrm{ArP{=}PAr}$

DBU (1.44g, 1.41 ml, 9.46 mmol) in THF (50 ml) was added dropwise over 10 minutes to a stirred solution of $\mathrm{ArPH_2}$ (1.49g, 4.75 mmol) and $\mathrm{ArPCl_2}$ (1.82g, 4.75 mmol) in THF (50 ml) at 0 ^{0}C. The solution became yellow and a white precipitate was formed. The reaction mixture was stirred at room temperature for 1 hour. The precipitate was removed by filtration and the solvent removed *in vacuo* to give a yellow viscous oil which was redissolved in toluene (7 ml) and recrystallised at -40 ^{0}C to yield 2.01 g (68.0%). $\mathrm{Ar_2P_2}$ data as previously detailed.

3.10.2.3 $2\mathrm{ArPCl_2} \xrightarrow[\text{-2MgCl}_2]{\text{2Mg}} \mathrm{ArP{=}PAr}$ (19)

Magnesium (0.71g, 29.2 mmol) was added to a stirred solution of $\mathrm{ArPCl_2}$ (11.2g, 29.2 mmol) in THF (150 ml) at 0 ^{0}C and the mixture was allowed to warm to room temperature over 30 minutes. The mixture became dark brown and was stirred for a further 10 minutes. The solution was concentrated to half volume and the ^{31}P NMR recorded. This showed almost quantitative conversion to the diphosphene (δ = +473.8 ppm) with a very small peak at -138 ppm which may be attributed to $\mathrm{ArPH_2}$ (coupling with hydrogen yielded a triplet $^{1}J_{PH}$ 217.9 Hz). The product (19) was not isolated.

3.10.3 2,6-Bis(trifluoromethyl)phenyl dichlorophosphine, Ar'PCl$_2$

$$\mathrm{Ar'H + BuLi{\cdot}TMEDA \longrightarrow Ar'Li{\cdot}TMEDA \xrightarrow{PCl_3} Ar'PCl_2}$$

TMEDA (7.74 ml, 5.96g, 51.3 mmol) was added to a stirred solution of BuLi (1.6 M in hexane, 32.0 ml, 51.3 mmol) in diethylether (50 ml) to generate the BuLi·TMEDA complex. This solution was added dropwise over 10 minutes to a stirred solution of 1,5-bis(trifluoromethyl)benzene (Ar'H) (7.97 ml, 10.98g, 51.3 mmol) in diethylether (50 ml) at 0 ^{o}C. This mixture was stirred at room temperature for 8 hours (and became deep brown). It was then added dropwise over 10 minutes to a stirred solution of phosphorus trichloride (9.4 ml, 14.79g, 0.107 mole) in diethyl ether (50 ml) at -78 ^{o}C. The reaction mixture was allowed to warm to room temperature. All the volatiles were removed *in vacuo* and the product (a clear oil) was distilled from the brown oil/solid residue. Yield 5.2g (32%); Bpt 80 ^{o}C (10^{-1} mm Hg); ^{1}H NMR (CDCl$_3$) δ: 7.3-7.9 (m,aromatic H); ^{31}P {^{1}H} δ: 146.6 (sept), $^4J_{PF}$ 61.0 Hz; ^{19}F δ: -53.14 ppm (d,o-CF$_3$) $^4J_{PF}$ 61.0 Hz.

3.10.4 Preparation 2,6-Bis(trifluoromethyl)phenyl-phosphine, Ar'PH$_2$

$$\mathrm{Ar'PCl_2 \xrightarrow{2Bu_3SnH} Ar'PH_2}$$

Tributyltinhydride (5.11 ml, 5.53g, 19.0 mmol) was added dropwise over 5 minutes to a stirred solution of Ar'PCl$_2$ (3.0 g, 9.5 mmol) in diethylether (30 ml) at 0 ^{o}C. This reaction mixture was then stirred for 2 hours at room temperature and distilled to yield 1.9g Ar'PH$_2$ (81.3%). Bpt 70 ^{o}C (20 mm Hg); IR (Film) ν_{max}: 2370 (P-H) cm^{-1}; ^{1}H (CDCl$_3$) δ: 3.9 (sept d,PH) $^1J_{PH}$ 214.0 Hz $^5J_{PF}$ 5.1 Hz, 6.9-7.6 (m,arom

H); $^{31}P\ \{^{1}H\}$ δ: -142.7 ppm (sept) $^{4}J_{PF}$ 29.4 Hz; ^{19}F δ: -61.5 (doublet of triplets) $^{4}J_{PF}$ 29.4, $^{5}J_{PH}$ 5.0 Hz.

3.10.5 Preparation of Unsymmetrical Diphosphene, $Ar'ArP_2$ (20)

3.10.5.1 $$Ar'PH_2 + ArPCl_2 \xrightarrow[-2DBU.HCl]{2DBU} ArP{=}PAr'\ (20)$$

DBU (1.44 ml, 9.63 mmol) in THF (15 ml) was added dropwise over 5 minutes to a stirred solution of $Ar'PH_2$ (1.18g, 4.80 mmol) and $ArPCl_2$ (1.84g, 4.80 mmol) in THF (45 ml) at 0 °C. The solution turned a brown/yellow colour, with the formation of a precipitate. This mixture was stirred for 30 minutes at room temperature. The solid was removed by filtration and the filtrate concentrated to yield a pale yellow powder, (1.9g, 3.4 mmol) - crude yield of (20) was 70%. This solid was washed with several aliquots of diethylether (10 ml), (it had a very limited solubility in this solvent), to yield a pure white solid 1.2 g (44%). Recrystallisation of this powder from CH_2Cl_2 (10 ml) gave a crystalline material, but only very small crystals were obtained.

The reverse coupling, *ie.*

3.10.5.2 $$ArPH_2 + Ar'PCl_2 \xrightarrow[-2DBU.HCl]{2DBU} ArP{=}PAr'$$

gave identical results and a similar yield. Quantities used were: $Ar'PCl_2$ (1.98g, 6.3 mmol), $ArPH_2$ (1.97g, 6.3 mmol), DBU (1.90 ml, 12.7 mmol), THF (100 ml) and the yield was 1.64g (46%).

Employing the ripple tank oscillation technique between +10 and -30 °C for several days for the diphosphene (0.9g) in toluene (7 ml) again yielded only small crystals.

$ArAr'P_2$: Mpt. 131 °C; Analysis Found: C, 36.33; H, 0.60. Required for $C_{17}H_5F_{15}P_2$: C, 36.72; H, 0.91%; IR (Nujol) ν_{max}: 3100 (w,ArCH), 1400-1000 (s,CF_3), 915 (m,CH ring), 710 and 685 (w, C–F "P=P") cm^{-1}; UV-Vis ($CHCl_3$) $\lambda_{max}(\epsilon)$: 264.2 (40451) nm; MS EI (Intensity%): 343 (10.5,ArP_2^+), 324 (20,ArP_2^+-F), (Ar ring fragmentation); ^{31}P ($CDCl_3$) δ: +489.0 (P_1), 478.2 (P_2) ppm $^1J_{PP}$ 552 Hz; ^{19}F ($CDCl_3$) δ: *ca.* -53 (o-CF_3,12F)[2], -64.1 (p-CF_3,3F). No $^4J_{PF}$ coupling was resolved.

3.10.6 Preparation of Mesityl Dihalophosphine

$$3MesMgBr + 3PCl_3 \longrightarrow MesPBr_2 + MesPClBr + MesPCl_2$$

Mesityl magnesium bromide (45 ml, 45 mmol, 1 M solution in THF) was added dropwise over 5 minutes to a stirred solution of phosphorus trichloride (6.2g, 3.9 ml, 45 mmol) in diethylether (150 ml) at -78 °C. This mixture was stirred for one hour. It was allowed to reach room temperature. A yellow solution with a precipitate formed. The latter was removed by filtration, and the solvent removed from the resultant filtrate *in vacuo*, to yield a crude yellow oil. ^{31}P NMR indicated the presence of $MesPBr_2$ (168.4 ppm) MesPClBr (162.5 ppm) and $MesPCl_2$ (154.2 ppm) in the ratio 3:2:1 respectively. Yield *ca.* 8.8 g (70%).

The following stage of the reaction to form the unsymmetrical diphosphene MesP=PAr, involved dehydrohalogenation, and the ease of abstraction of HBr made it unnecessary to convert the $MesPBr_2$/MesPBrCl and $MesPCl_2$ mixture entirely to the dichloro-derivative.

---

[2] complex o-CF_3 region consisting of two superimposed doublet of doublets, see Figure 3.8(a).

3.10.7 Preparation of MesP=PAr (21)

$$\underset{(X=Br,Cl)}{MesPX_2} + ArPH_2 \xrightarrow[-2DBU.HCl]{2DBU} MesP{=}PAr\ (21)$$

DBU (0.96 ml, 0.98g, 6.4 mmol) in THF (20 ml) was added dropwise to a stirred solution of $MesPX_2$ ($X \equiv Br, Cl$) (*ca.* 0.9g, 3.2 mmol) and $ArPH_2$ (1.0g, 3.2 mmol) in THF (50 ml). A bright orange solution was formed with a white precipitate. The solid was removed by filtration. The solvent was removed from the resulting filtrate *in vacuo* to yield a yellowish oil. Yield of crude product *ca.* 0.62 g (42%); IR (Film) ν_{max}: 3100 (w,CH Ar ring), 2910 (m,CH alkyl,CH_3), 1600-1620 (m,C=C Ar), 1400-1000 (s,C–F), 700 (s,sharp), 680 (s,sharp), 550 (mbr,"P=P") cm^{-1}; UV-Vis (CCl_4) λ_{max}: 400, 260 nm; ^{31}P ($CDCl_3$) δ: +524.7 (P_1), 484.4 (P_2) ppm $^1J_{PP}$ 566.8 Hz; ^{19}F ($CDCl_3$) δ: -53.5 (d of d poorly resolved,6F, o-CF_3), -64.0 (s,3F,p-CF_3) ppm; ^1H ($CDCl_3$) δ: 8.9 (2H,CH Ar ring), 8.8 (2H,CH Mes ring), 2.8 (9H,CH_3-groups).

3.10.8 Preparation of Unsymmetrical Diphosphene, $^{i}Pr_2N$–P=P–Ar (22)

Diisopropyl dichlorophosphine, $^{i}Pr_2NPCl_2$, was prepared as described in Section 6.4.9. DBU (0.96 ml, 6.4 mmol) in THF (15 ml) was added dropwise over 5 minutes to a stirred solution of $^{i}Pr_2NPCl_2$ (0.64g, 3.2 mmol) and $ArPH_2$ (1.0g, 3.2 mmol) at room temperature. An orange solution with a white precipitate was formed. The solid was removed by filtration and the solvent removed in vacuo, to yield a yellowish oil. Yield of crude product was *ca.* 0.77 g (54%). IR (Film) ν_{max}: 3100 (vw,CH Ar), 2960 (m,CH alkyl), 1600 and 1620 (w,C=C Ar), 1260 (s), 1260-1000 (s,br,Ar–CF_3), 800 (s), 700 (w,"P=P") cm^{-1}; ^{31}P (THF) δ: +468.5

(P_1), 234.7 (P_2) ppm $^1J_{PP}$ 542.1; ^{19}F ($CDCl_3$) δ: -54.9 (not resolved, 6F,o-CF_3), -63.0 (s,3F,p-CF_3) ppm.

3.10.9 Preparation of $^tBuPH_2$

$$^tBuPCl_2 + 2Bu_3SnH \xrightarrow{THF} t\text{-}BuPH_2 + 2Bu_3SnCl$$

$^tBuPCl_2$ was prepared according to S.H. Metzger *et al.* [53] [Bpt. 145-150 ^oC (760 mm Hg), ^{31}P δ: +190.0 ppm]. Bu_3SnH (7.02 ml, 7.6g, 26.1 mmol) in THF (20 ml) was added dropwise over 5 minutes to a stirred solution of $^tBuPCl_2$ (2.1g, 13.2 mmol) in THF (50 ml) at -10 ^oC. The solution was allowed to reach room temperature and stirred for 1 hour. A THF solution of $^tBuPH_2$ was collected by vacuum transfer (*ca.* 1g) and used *in situ*. $^{31}P\{^1H\}$ δ: -90.23 ppm (s) $^1J_{PH}$ 195 Hz.

3.10.10 Attempted Preparations of Other Unsymmetrical Diphosphenes

3.10.10.1

$$^tBuPCl_2 + ArPH_2 \xrightarrow[0^oC]{2DBU}$$

DBU (1.47 ml, 9.83 mmol) in THF (10 ml) was added dropwise over 5 minutes, to a stirred solution of $ArPH_2$ (1.54g, 4.91 mmol) and $^tBuPCl_2$ (0.78g, 4.91 mmol) in THF (50 ml) at 0 ^oC. The solution became deep red with the formation of a precipitate. As the mixture warmed to room temperature, it became clear pale yellow and the solid redissolved. $^{31}P\{^1H\}$ δ: -74.9 (triplet) J 138.9 Hz, major signal +473.4 ppm [symmetrical diphosphene (19)]; ^{31}P δ: +190 ppm (unreacted $^tBuPCl_2$).

3.10.10.2 $^{t}BuPH_2 + ArPCl_2 \xrightarrow{2DBU}$

DBU (3.9 ml, 26.1 mmol) in THF (15 ml) was added dropwise over 5 minutes to a stirred solution of $^{t}BuPH_2$ (*ca.* 1 g, 12 mmol) in THF (70 ml) and $ArPCl_2$ (4.9g, 12.8 mmol) in THF (50 ml) at -10 ^{o}C. A precipitate formed, but on warming to room temperature it redissolved to yield a clear yellow liquid. $^{31}P\{^{1}H\}$ δ: +206.5 (s) -31(s), -89(s, unreacted $^{t}BuPH_2$) $^{1}J_{PH}$ 193.6 Hz. [Product(s) unassigned].

3.10.10.3 $ArPH_2 + Ar''PCl_2 \xrightarrow{2DBU}$

DBU (1.56 ml, 10.4 mmol) in THF (15 ml) was added dropwise over 5 minutes to a stirred solution of $ArPH_2$ (1.6g, 5.1 mmol) and $Ar''PCl_2$ (1.61g, 5.1 mmol) in THF (50 ml) at 0 ^{o}C. The solution became dark orange with a solid formed. The solution became yellow on warming to room temperature. The ^{31}P spectrum indicated the presence of the symmetrical diphosphene Ar_2P_2 (19). $^{31}P\{^{1}H\}$ δ: + 473.8 ppm $^{4}J_{PF}$ + $^{5}J_{PF}$ 45.0 Hz (major signal). Other minor species δ: +61.2, +30 (s), unassigned), +157.1 (q) $^{4}J_{PF}$ 86.6 Hz (unreacted $Ar''PCl_2$).

3.10.10.4 $C_6F_5PCl_2 + ArPH_2 \xrightarrow{2DBU}$

DBU (1.23 ml, 8.2 mmol) in THF (15 ml) was added dropwise over 5 minutes to a stirred solution of $ArPH_2$ (1.3g, 4.1 mmol) and $C_6F_5PCl_2$ (1.1g, 4.1 mmol) in THF (50 ml) at 0 ^{o}C. A solid was precipitated and the solution became orange. On allowing to warm to room temperature it became clear and yellow. ^{31}P δ: +473 (small signal), -83.8, -89.2 ppm (approximate intensity ratio 3:1) observed as singlets,no $^{4}J_{PF}$ resolved.

3.10.11 Variable Temperature Study of $C_6Cl_5PCl_2$ + $ArPH_2$ (DBU)

DBU (1.5 ml, 10.0 mmol) in THF (15 ml) was added dropwise over 5 minutes to a stirred solution of $C_6Cl_5PCl_2$ (1.76g, 5.0 mmol) and $ArPH_2$ (1.57g, 5.0 mmol) in THF (50 ml) cooled to -40 ^{o}C. A yellow solution was formed (it was difficult to assess whether the solid present was formed in the course of the reaction, or as a result of the insolubility of $C_6Cl_5PCl_2$ in THF). The ^{31}P NMR at -40 ^{o}C showed only *two*[3] signals at -83.8 (3P) and -89.2 (1P) ppm. The mixture was allowed to reach room temperature and the ^{31}P NMR was re-recorded: 473.8 ppm (major product); 2.3, 0.3, -12.3, -27.8, -83.8 ppm (smaller peaks). It was then filtered, and all the volatile material removed *in vacuo*. The symmetrical diphosphene was extracted into CH_2Cl_2 (10 ml) and isolated by crystallisation at -40 ^{o}C. Yield was 1.2g (38% based on $ArPH_2$). Characterisation data as detailed in Section 3.10.2.1.

3.10.12 Reactions of Diphosphene Ar_2P_2 (19)

3.10.12.1 $ArP{=}PAr + 1/8\ S_8 \longrightarrow$

A five-fold excess of elemental sulphur (0.16g, 5.0 mmol) was added to a stirred solution of ArP=PAr (19) (0.64g, 1.0 mmol). This was stirred at room temperature for 6 hours. The ^{31}P NMR showed no evidence of reaction (unreacted starting material, δ: +473.8 ppm).

---

[3] singlets are only possible for *symmetrical* cyclic polyphosphines. A peak at *ca.* -83 ppm would indicate a hydrogen atom still attached to phosphorus (see Section 7.4).

3.10.12.2 $ArP{=}PAr + CF_3COOH \longrightarrow$

A large excess of liquid trifluoro~~methyl~~acetic acid, CF_3COOH (2.2g, 1.5 ml, 19.3 mmol) was added, with stirring, to $ArP{=}PAr$ (19) (0.82g, 1.3 mmol) in THF (15 ml) at room temperature. No reaction was detected by ^{31}P NMR (unreacted starting material, δ: +473 ppm).

3.10.12.3 $ArP{=}PAr + HBF_4{\cdot}Et_2O \longrightarrow$

An approximate six-fold excess of tetrafluoroboric acid-diethyl ether complex, $HBF_4{\cdot}Et_2O$ (0.92g, 5.7 mmol) was added to a stirred solution of $ArP{=}PAr$ (0.62g, 1 mmol) in Et_2O (20 ml) at -10 ^oC. An orange solution was formed. The reaction mixture was allowed to reach room temperature and stirred for 4 hours. ^{31}P NMR showed uniquely unreacted diphosphene (δ: +473 ppm).

3.10.12.4

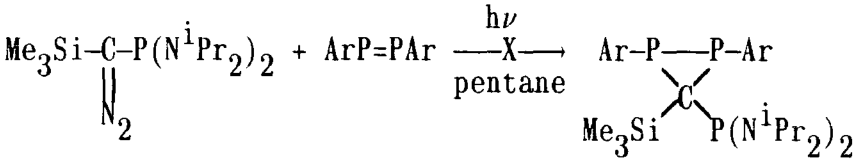

$Me_3SiC(N_2)P(N^iPr_2)_2$ (0.55g, 1.6 mmol) in pentane (7 ml) was added in one portion to a stirred solution of Ar_2P_2 (1.0g, 1.6 mmol) in pentane (50 ml). The mixture was irradiated at 300 nm for 6 hours. ^{31}P δ: -42 ppm $(Me_3Si)\underset{\cdot\cdot}{C}P(N^iPr_2)_2$ (carbene) [52], $ArP{=}PAr$ 473.8 ppm. These two species remained *in situ* without reaction. (The same procedure was repeated in toluene and analogous results were obtained).

3.11 REFERENCES

1. H. Köhler and A. Michaelis, *Ber.Dtsch.Chem.Ges.*, 10, 807 (1877).

2. W. Mahler and A.B. Burg, *J.Amer.Chem.Soc.*, 79, 251 (1957); 80, 6161 (1958).

3. J.J. Daly, *J.Chem.Soc.*, 6147 (1964).

4. T.P. Fehlner, *J.Amer.Chem.Soc.*, 88, 1819 (1966).

5. T.P. Fehlner, *J.Amer.Chem.Soc.*, 89, 6477 (1967).

6. T.P. Fehlner, *J.Amer.Chem.Soc.*, 90, 6062 (1968).

7. M. Yoshifuji, I. Shima and N. Inamoto, *J.Amer.Chem.Soc.*, 103, 4587 (1981).

8. E. Niecke and R. Rüger, *Angew.Chem. Int.Ed.Engl.*, 22, 155 (1983).

9. M. Scholz, H.W. Roesky, D. Stalke, K. Keller and F.T. Edelmann, *J.Organometallic Chem.*, 366, 73-85 (1989).

10. J. Escudié, C. Couret, H. Ranaivonjatovo, M. Lazraq and J. Satgé, *Phosphorus and Sulfur*, 31, 27-31 (1987).

11. a) C.N. Smit, Th. A. van der Knapp and F. Bickelhaupt, *Tetrahedron Lett.*, 24(19), 2031 (1983).

    b) M. Baudler, B. Carlsohn, W. Böhm and G. Reuschenbach, *Z.Naturforsch B*, 31, 558 (1976).

12. V.D. Romanenko, E.O. Klebanskii, V.F. Shul'gin and L.N. Markovskii, *Z.Obs.Khim.*, 54(2), 465 (1984).

13. J. Grobe, D. Le Van and J. Schulze, *Z.Naturforsch B*, 40(12), 1753-1755 (1985).

14. J. Jaud, C. Couret and J. Escudié, *J.Organometallic Chem.*, 249, C25-C27 (1983).

15. C. Couret, J Escudié, H. Ranaivonjatovo and J. Satgé, *Organometallics*, 5, 113-117 (1986).

16. H. Ranaivonjatovo, J. Escudié, C. Couret and J. Satgé, *Phosphorus and Sulfur*, 31, 81-87 (1987).

17. M. Veith, V. Huch, J.P. Majoral, G. Bertrand and G. Manuel, *Tetrahedron Lett.*, 24(39), 4219-22 (1983).

18. a) S. Cetinkaya, P.B. Hitchcock, M.F. Lappert, A.J. Thorne and H. Goldwhite, *J.Chem.Soc.Chem.Commun.*, 691-692 (1982).

    b) S. Cetinkaya, A. Hudson, M.F. Lappert and H. Goldwhite, *J.Chem.Soc.Chem.Commun.*, 609-610 (1982).

19. H. Goldwhite, J. Kaminski, G. Millhauser, J. Ortiz, M. Vargas, L. Vertal, M.F. Lappert and S.J. Smith, *J.Organometallic Chem.*, 310, 21-25 (1986).

20. M. Yoshifuji, K. Shibayama, N. Inamoto, T. Matsushita and K. Nishimoto, *J.Amer.Chem.Soc.*, 105, 2495-2497 (1983).

21. A.H. Cowley, J.E. Kilduff, M. Pakulski and C.A. Stewart, *J.Amer. Chem.Soc.*, 105, 1655-56 (1983).

22. P. Jutzi and U. Meyer, *J.Organometallic Chem.*, 326, C6-C8 (1987).

23. E. Niecke, B. Kramer and M. Nieger, *Angew.Chem. Int.Ed.Engl.*, 28(2), 215-217 (1989).

24. a) A.V. Ruban, L.K. Polyachenko, V.D. Romanenko and L.N. Markovskii, *Z.Obs.Khim.*, 55(5), 1190-1191 (1985).

b) V.D. Romanenko, A.V. Ruban, S.V. Iksanova, L.K. Polyachenko and L.N. Markovskii, ***Phosphorus and Sulphur***, 22, 365-368 (1985).

25. L.N. Markovskii, V.D. Romanenko and A.V. Ruban, ***Phosphorus and Sulfur***, 30, 447-50 (1987).

26. L.N. Markovskii, V.D. Romanenko, M.I. Povolotskii, A.V. Ruban and E.O. Kebanskii, *Z.Obs.Khim.*, 56(9), 2157-2158 (1986).

27. V.D. Romanenko, E.O. Klebanskii and L.N. Markovskii, *Z.Obs.Khim.*, 56(9), 2159-60 (1986).

28. a) K.S. Pitzer, *J.Amer.Chem.Soc.*, 70, 2140 (1948).

b) R.S. Mulliken, *J.Amer.Chem.Soc.*, 72, 4493 (1950).

29. A.H. Cowley, ***Polyhedron***, 3(4), 389-432 (1984), page 423..

30. a) R.K. Harris personnel communication - Durham University (September 1989).

b) R.K. Harris and B.E. Mann, "***NMR and the Periodic Table***", Academic Press (1978).

31. K.W. Zilm, G.G. Webb, A.H. Cowley, M. Pakulski and A. Orendt, *J.Amer.Chem.Soc.*, 110, 2032-38 (1988).

32. a) H.W. Kroto, S.I. Klein, M.F. Meidine, J.F. Nixon, R.K. Harris, K.J. Packer and P. Reams, *J.Organometallic Chem.*, 280, 281-287 (1985).

b) Th. A. van der Knapp, F. Bickelhaupt, J.G. Kraaykamp, G. von Kroten, J.P.C. Bernards, H.T. Edzes, W.S. Veeman, E. de Boer and E.J. Baerends, ***Organometallics***, 3, 1804-1811 (1984).

33. T.K. Ha, M.T. Nguyen and P. Ruelle, ***Chem.Phys.***, 87, 23-29 (1984).

34. V. Galasso, ***Chem.Phys.***, 83, 407-413 (1984).

35. D. Gonbeau and G. Pfister-Guillouzo, *J.Elect.Spect. and Related Phenomenon*, 33, 279-83 (1984).

36. M. Yoshifuji, N. Inamoto, K. Itq and S. Nagase, *Chem.Lett.*, 437-440 (1985).

37. T.L. Allen, A.C. Scheiner, Y. Yamaguchi and H.F. Schaefer III, *J.Amer. Chem.Soc.*, 108, 7579-7588 (1986).

38. A.H. Cowley, J.E. Kilduff, J.G. Lasch, S.K. Mehrotra, N.C. Norman, M. Pakulski, B.R. Whittlesey, J.L. Atwood and W.E. Hunter, *Inorg. Chem.*, 23, 2582 (1984).

39. P. Jutzi, U. Meyer, B. Krebs and M. Dartmann, *Angew.Chem. Int.Ed. Engl.*, 25, 919 (1986).

40. H. Hamaguchi, M. Tasumi, M. Yoshifuji and N. Inamoto, *J.Amer.Chem.Soc.*, 106, 508 (1984).

41. M. Yoshifuji, I. Shima, N. Inamoto, M. Yamada and H. Kuroda, *Phosphorus and Sulfur*, 16, 157-159 (1983).

42. A. Dubourg, J.P. Declercq, H. Ranaivonjatovo, J. Escudié, C. Couret and M. Lazraq, *Acta Cryst.*, C44, 2004 (1988).

43. E. Niecke, W. Kramer, M. Nieger, H. Westermann, W.W. Schoeller and J. Busch, *Euchem Conference*, *PSIBLOCS*, Paris-Palaiseau, August 22nd, 1988.

44. A.H. Cowley, J.E. Kilduff, N.C. Norman and M. Pakulski, *J.Chem. Soc.Dalton Trans.*, 1801-8 (1986).

45. a) M. Yoshifuji, K. Ando, K. Shibayama, N. Inamoto, K. Hirotsu and T. Higuchi, *Angew.Chem. Int.Ed.Engl.*, 22(5), 418-419 (1983).

    b) A.H. Cowley and M. Pakulski, *Tetrahedron Lett.*, 25(20), 2125-2126 (1984).

    c) M. Yoshifuji, K. Shibayama, N. Inamoto, K. Hirotsu and T. Higuchi, *J.Chem.Soc.Chem.Commun.*, 862-863 (1983).

46. M. Yoshifuji, K. Shibayama and N. Inamoto, *Chem.Lett.*, 603-606 (1984).

47. a) A.H. Cowley, N.C. Norman, M. Pakulski, *J.Chem.Soc.Chem. Commun.*, 1054-1055 (1984).

    b) A.H. Cowley, J.E. Kilduff, N.C. Norman and M. Pakulski, *J.Amer. Chem.Soc.*, 105, 4845-4846 (1983).

48. a) M. Koenig, G. Etemad-Moghadam, C. Tachon and J. Bellan, *Phosphorus and Sulfur*, 30, 425-428 (1987).

    b) M. Yoshifuji, K. Ando, K. Toyota, I. Shima and N. Inamoto, *J.Chem.Soc.Chem.Commun.*, 419-420 (1983).

49. M. Yoshifuji, K. Shibayama, N. Inamoto and T. Watanabe, *Chem. Lett.*, 585-588 (1983).

50. a) M. Yoshifuji, K. Shibayama and N. Inamoto, *Chem.Lett.*, 115-118 (1984).

b) A.H. Cowley and M.R. Pakulski, *J.Amer.Chem.Soc.*, 106, 1491-1492 (1984).

51. a) G. Etemad-Moghadam, J. Bellan, C. Tachon and M. Koenig, *Tetrahedron*, 43(8), 1793-97 (1987).

b) M. Gouygon, J. Bellan, J. Escudié, C. Couret, A. Dubourg, J.P. Declercq and M. Koenig, *J.Chem.Soc.Chem.Commun.*, 593-595 (1989).

52. A, Igau, H. Grutzmacher, A. Baceiredo and G. Bertrand, *J.Amer.Chem.Soc.*, 110, 6463-6466 (1988).

53. S.H. Metzger, O.H. Basedow and A.F. Isbell, *J.Org.Chem.*, 29, 627 (1964).

CHAPTER FOUR

PHOSPHAALKENES

4.1 INTRODUCTION

The most important highlights within the development of phosphaalkene chemistry [1] are now outlined.

1964	Delocalised C_{2p}- P_{3p} π-bond in phosphamethine cyanine cations. The first P=C containing compound stable at room temperature [Figure 4.1(a)] [2]. The structure was determined by X-ray analysis [3].
1966 and 1971	The synthesis of 2,4,6-trisubstituted phosphabenzene [Figure 4.1(b)]. The (p-p) π-bonds are stabilised by forming part of an aromatic ring [4,5].

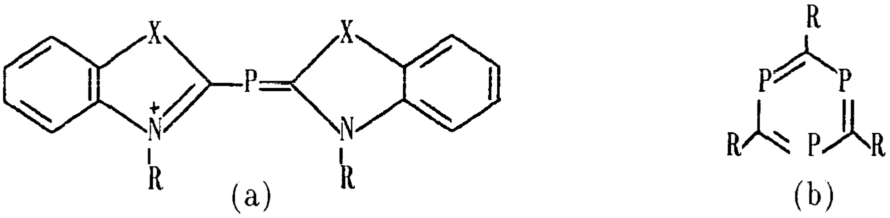

Figure 4.1: *Early phosphaalkenes; (a) X = S, NR , -CH=CH- and R = CH_3, C_2H_5; (b) R = Ar (ref.4), H (ref.5).*

1976	Becker initiated the breakthrough to isolable acyclic compounds with a localised P=C bond, by observation of the migration from phosphorus to oxygen in P-silylated acylphosphanes, and obtained the first example of the structural type: $PhP=C(OSiMe_3)^tBu$ [6].

A vast amount of work and development has taken place in this area by J.F. Nixon, F. Bickelhaupt, R. Appel, M. Yoshifuji and many others (see References, Section 4.13). This work concentrates on the synthesis of the first phosphaalkene compound containing the Ar group.

4.2 SYNTHESIS OF PHOSPHAALKENES: LITERATURE SURVEY

The aim of the detailed literature survey of the synthetic routes to phosphaalkenes is to illustrate the vast number of these compound types available. Tables 4.1-4.7 summarise the major developments in phosphaalkene synthesis and provide a fairly comprehensive list of the range of compounds previously described. Ar on phosphorus has been studied (Section 4.4). It would be interesting to study the effect on structure and reactivity of the trifluoromethyl aryl group on the carbon end of the molecule. Preliminary studies in this area have begun (Section 4.11).

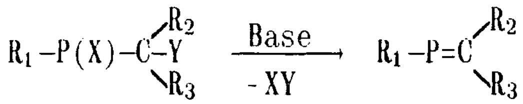

$$R_1{-}P(X){-}C(R_2)(R_3){-}Y \xrightarrow[-XY]{Base} R_1{-}P{=}C(R_2)(R_3)$$

R_1	R_2	R_3	Y	REF	BASE
Supermes	Ph	Ph	H	7,8	DBU
t-Bu	SAlkyl	SAlkyl	H	7	DBU
Cl	SAlkyl	SAlkyl	H	9	Et_3N
Mes	— fluorenyl —		H	10	DBU
Supermes	Cl	Cl	H	11	DBU
Cl	H	Cl	H	12	$2(Me_3Si)_2NNa$
Mes	Mes	Mes	H	13	[X] DBU no HCl elimination.
$(Me_3Si)_2N$	Cl	H	H	12	$(Me_3Si)_2NNa$ $-NaX, -(Me_3Si)_2NH$
Ph	$SiMe_3$	$SiMe_3$	Cl	7	Li (THF)
Cl	$SiMe_3$	$SiMe_3$	$SiMe_3$	14	T>100°C, $-Me_3SiCl$
Ar (Ar≡Ph,Mes)	R (H,CH_3)	NMe_2	OR	15,32	-ROH ‡

Table 4.1: *1,2-Elimination reactions (-HX); X = Cl [‡X = H]; Ar and Ar' refer to aryl species generally.*

$$CF_3PH_2 \xrightarrow{KOH/-HF} CF_2{=}PH \xrightarrow{KOH/-HF} FC{\equiv}P \quad (ref.16)$$

$$(CF_3)_2PH \xrightarrow{-HF} F_3CP{=}CF_2 \quad (refs.17,18)$$

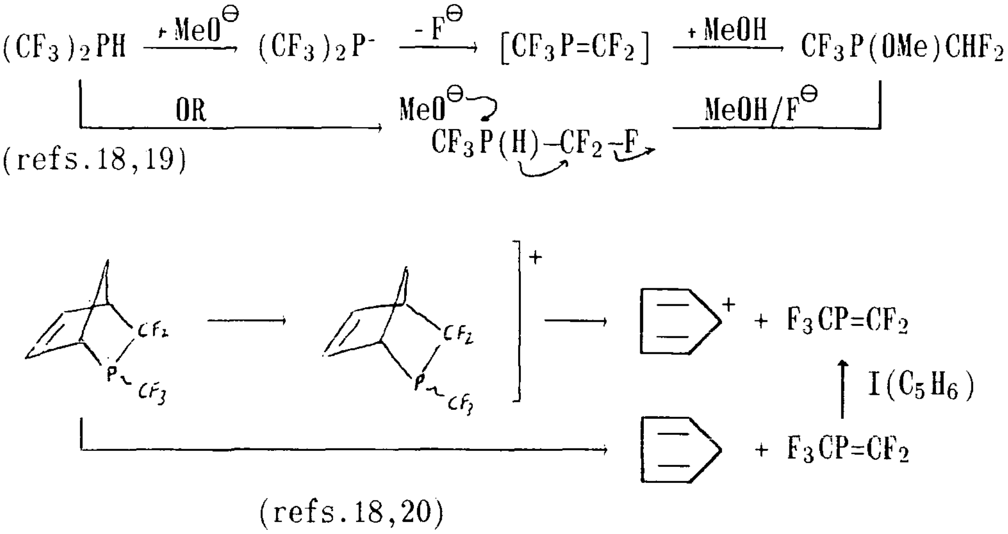

$$(CF_3)_2PH \xrightarrow{+MeO^{\ominus}} (CF_3)_2P^- \xrightarrow{-F^{\ominus}} [CF_3P{=}CF_2] \xrightarrow{+MeOH} CF_3P(OMe)CHF_2$$

$$Me_3SnP(CF_3)_2 \xrightarrow{320^{o}C/10^{-3}T} Me_3SnF + F_3CP{=}CF_2{}^{*}$$

(refs.18,21)

$$Me_3SnP(C_2F_5)_2 \xrightarrow{320^{o}C/10^{-3}T} Me_3SnF + F_5C_2P{=}C(F)CF_3 \quad ^{\ddagger}$$

(refs.18,22,23)

Table 4.2: *1,2-Elimination to reactive phosphaalkenes; ‡Careful observation of thermolysis of $Me_3SnP(CF_3)CF_2H$, $Me_3SnP(CF_3)C_2F_5$ and $Me_3SnP(CF_3)CF(CF_3)_2$ illustrates a preference for CF_3 preservation and attack of CF_2X or $CF(CF_3)_2$ (the perfluoro effect); *nucleophilic initiated H^- shift from phosphorus to an α-carbon atom.*

$$R_1-P\genfrac{}{}{0pt}{}{\nearrow R_2}{\searrow R_3} + O=C\genfrac{}{}{0pt}{}{\nearrow R_4}{\searrow R_5} \longrightarrow R_1-P=C\genfrac{}{}{0pt}{}{\nearrow R_4}{\searrow R_5} + R_2R_3O$$

R_1	R_2	R_3	R_4	R_5	REF
Ph,Mes	$SiMe_3$	$SiMe_3$	Ph,Mes Supermes	Ph,Mes Supermes	7,25 [a]
Ph	$SiMe_3$	$SiMe_3$	Me_2N	H	24 [a]
^tBu,Mes	$SiMe_3$	$SiMe_3$	Me_2N	H	24,25 [a]
$C_6H_4NH_2$	H	H	R [b]	Cl (-HCl)	15,32
Supermes	H	H	H	C_6H_4Y [c]	26
Supermes	H	H	H	Ar [f]	27
Supermes	H	H	—— fluorenyl ——		27
Mes	$SiMe_3$	Li	H	NMe_2	25
Supermes	$SiMe_2Bu^t$	Li	H	Ph	29
Supermes, Mes	$SiMe_3$	Li	C_6H_5Y	C_6H_5X	28

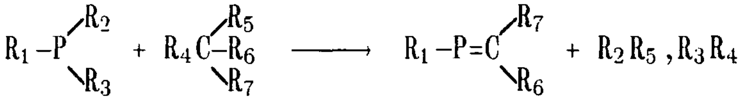

$$R_1-P\genfrac{}{}{0pt}{}{\nearrow R_2}{\searrow R_3} + R_4C\genfrac{}{}{0pt}{}{\nearrow R_5}{\searrow R_7}-R_6 \longrightarrow R_1-P=C\genfrac{}{}{0pt}{}{\nearrow R_7}{\searrow R_6} + R_2R_5, R_3R_4$$

R_1	R_2	R_3	R_4	R_5	R_6	R_7	REF
Supermes	H	H	Cl	Cl	Cl	H [d]	30,31
Supermes	H	H	Cl	Cl	H	H [d]	30,31
Ph	H	H	OMe	OMe	← 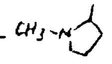 →		32
Ph,Mes	H	H	OMe	OMe	NMe_2	H	32
Ph,Mes	H	H	OMe	OMe	NMe_2	Me	15,32
R_1 [e]	$SiMe_3$	$SiMe_3$	F	F	NR_2	NR_2	7

Table 4.3: *Addition and Condensation; a) with the elimination of hexamethyldisiloxane; b) R=H,CH_3,Ph,Me_2N; c) Y=H,OCH_3,NMe_2; d) analogous to the isocyanate reaction; e) R_1=Me_3Si,^tBu,Ph; f) Ar≡2,4$(MeO)_2C_6H_3$.*

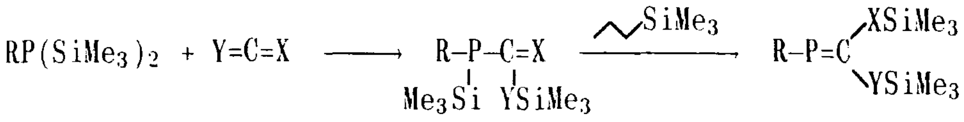

R	X	Y	REF
Ph	S	S	33
Ph,^{t}Bu	O	O	34
Me,^{t}Bu	NAlkyl	NAryl	7

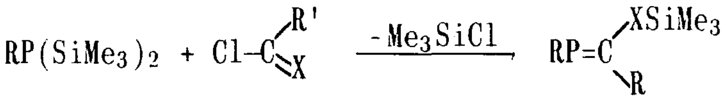

R	X	R'	REF
Ph	NC_6H_4Cl	Cl	7,35 *
Ph	NPh	Cl	7,35 *
^{t}Bu,Ph	O	^{t}Bu	36,37
Me_3Si	O	^{t}Bu	36,37

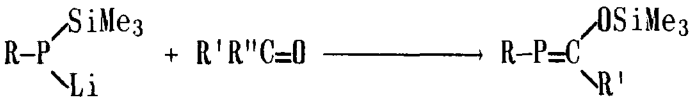

R	R'R"C=O	REF	
Me_3Si	^{t}Bu–CO(Cl)	38	(-LiCl)
Me_3Si	$Me_2C(COCl)_2$	39	(-LiCl)
^{t}Bu,Ph	$CpRe(CO)_2NO$	40	(-Li^+)
Me_3Si	$CpRe(CO)_2NO$	40	(-Li^+)
	Ph–C(=O)Cl	41	(-LiCl)
	Mes–C(=O)Cl	41	(-LiCl)
	CH_3–C(=O)Cl	41	(-LiCl)

Table 4.4: *Condensation and 1,3-migration of the Me_3Si group;*
**the second chlorine atom may be further substituted.*

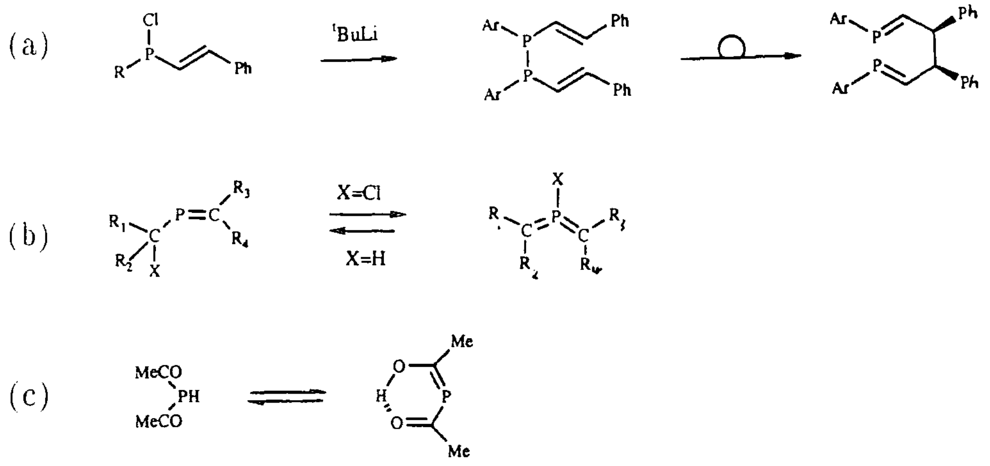

Table 4.5: *Rearrangement and isomerisation to yield phosphaalkenes; (a) via Cope rearrangment (ref.42); (b) Isomerisation R_1-R_4 = Me_3Si (refs.7,43); (c) Keto-Enol isomerisation (P=C stabilised by intramolecular H-bonding) (ref.7).*

$$R_1{-}P{=}C\begin{matrix}R_2\\ R_3\end{matrix} \longrightarrow R_1{-}P{=}C\begin{matrix}R_4\\ R_3\end{matrix}$$

R_1	R_2	R_3	R_4	CONDITIONS	REF
Supermes	$SiMe_3$	R ‡	H	KF (DMF,H_2O),-$\frac{1}{2}$$TMS_2O$	53
CF_3	F	F	NR_2	+$2R_2NH$,-R_2NH_2F	54
Supermes	Br/Cl	Br/Cl	$SiMe_3$	+BuLi,+TMSCl,-LiCl	11
Supermes	Br/Cl	Br/Cl	CH_3	+BuLi,+CH_3I,-LiCl	11

Table 4.6: *Altering group at carbon*; ‡*R* ≡ *Ph*, *$SiMe_3$*, *Br*; **R* ≡ *Et*, *^{i}Pr*.

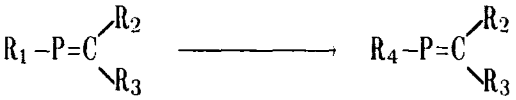

$$R_1{-}P{=}C\begin{smallmatrix}\diagup R_2\\ \diagdown R_3\end{smallmatrix} \longrightarrow R_4{-}P{=}C\begin{smallmatrix}\diagup R_2\\ \diagdown R_3\end{smallmatrix}$$

R_1	R_2	R_3	R_4	CONDITIONS	REF
$SiMe_3$	R_2N [R≡Et,Me]	R_2N	$P(^tBu)_2$	$+ClP(^tBu)_2$ $-Me_3SiCl$	46
$SiMe_3$	R_2N [R≡Me]	R_2N	H	triethanolsilanol $+Et_3SiOH$ $-Et_3SiOSiMe_3$	46
Cl	Ph	$SiMe_3$	$-C_6H_4{}^tBu$	-MgBrCl	45
Cl	Ph	$SiMe_3$	RR'N ‡	$RR'NH/Et_3N$	46-48
Cl	Ph	$SiMe_3$	OR	ROH/Et_3N	46,48
Cl	Ph	$SiMe_3$	$-N(R)-P{=}\underset{\underset{SiMe_3}{\vert}}{C}-Ph$	$\frac{1}{2}RNH_2/Et_3N$	48
Cl	Ph	$SiMe_3$	PR_2 or PRR'	HPR_2/Et_3N or $LiPR_2$(-LiCl) or $Me_3SiPR(R')$ $(-Me_3SiCl)$	48
Cl	Ph	$SiMe_3$	Supermes	-LiCl	48
Cl	Ph	$SiMe_3$	R *	(RMgBr)	48,49
Cl	$SiMe_3$	$SiMe_3$	$-C{\equiv}C{-}SiMe_3$	-LiCl	49
Cl	Ph	Me_3Si	$RN(H){-}N{\diagdown}{-}R$	NEt_3, $-NEt_3{\cdot}HCl$	50
Me_3Si	$OSiMe_3$	CMe_3	Cl	$+C_2Cl_6$,$-Me_3SiCl$ $-C_2Cl_4$	46
$(Me_3Si)_2N$	H	$SiMe_3$	Supermes	+ArLi $-(Me_3Si)_2NLi$	51
$(Me_3Si)_2N$	H	$SiMe_3$	$^iPr_2N$	$+^iPr_2NLi$ $-(Me_3Si)_2NLi$	51
Cl	SR	SR	$^tBu_2P$	$-^tBu_2PH$ (Et_3N),$-Et_3N{\cdot}HCl$	9 52a,b
Cl	SR	SR	$^tBu_2As$	$^tBu_2AsLi$	9,52b
Cl	SR	SR	$(Me_3Si)_2N$	$(Me_3Si)_2NLi$,-LiCl	52a

Table 4.7: *Altering group at phosphorus;‡R=R'=^{i}Pr or R≡H, R'≡^{t}Bu; *R≡Et,^{n}Bu,Ph.*

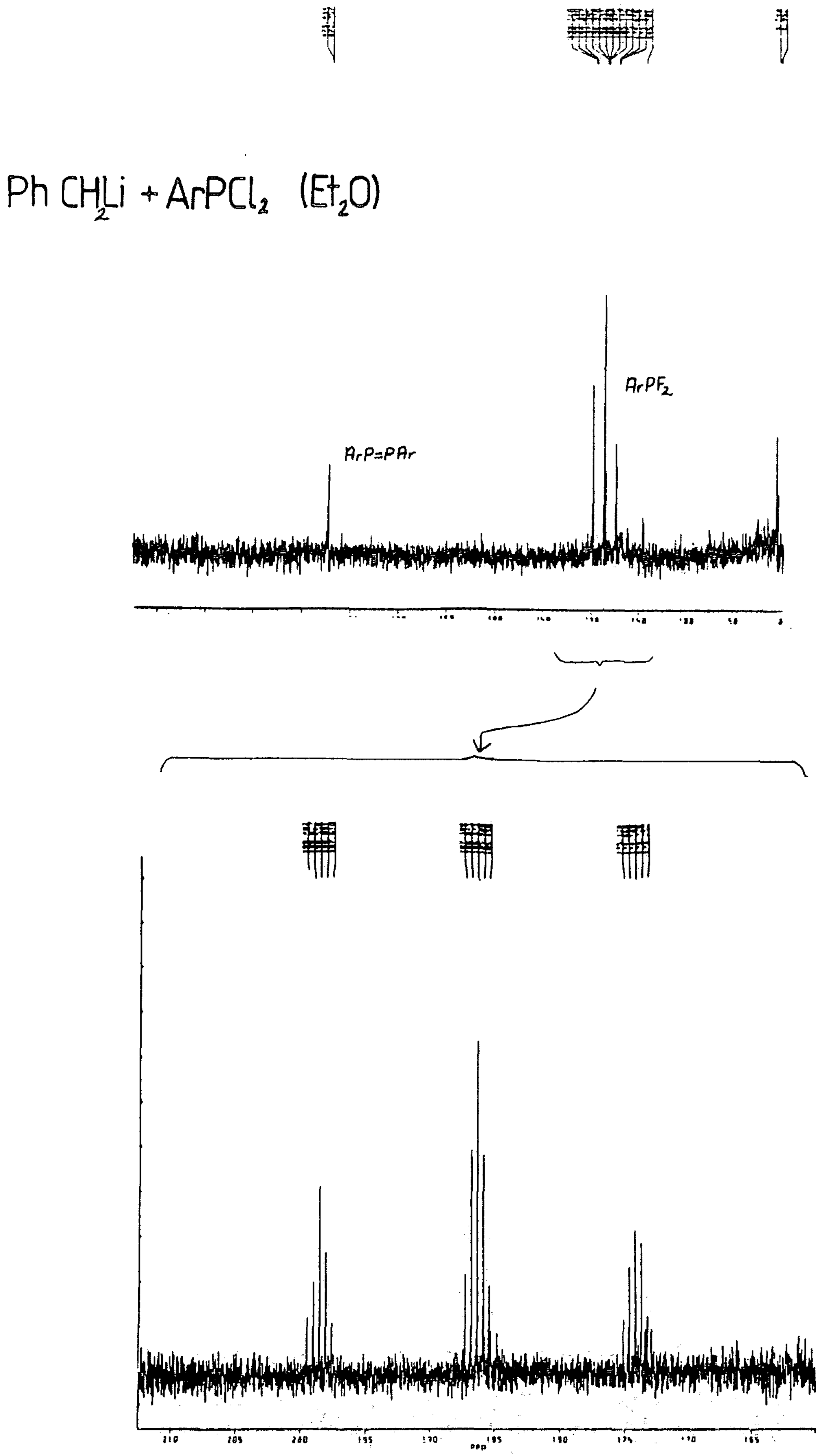

Figure 4.1: ^{31}P *NMR spectrum of* $ArPF_2$ *(3) generated by the addition of* $PhCH_2Li \cdot TMEDA$ *to* $ArPCl_2$ *(12) in* Et_2O.

4.3 SYNTHETIC PROCEDURES USED FOR PHOSPHAALKENES

The following methods (1-4) were used in the attempted synthesis of phosphaalkenes with Ar attached to phosphorus.

4.3.1 Method 1: Attempted Formation of a P-C Bond by Reaction of RLi with $ArPCl_2$

The first method employed for phosphaalkene synthesis is shown in Equation 4.1(a). Overall two major synthetic problems were encountered: (i) the inherent preference for tertiary phosphine formation [55] [Equation 4.1(b)] and (ii) attack at fluorine atoms on the ring system thought to be due to attack by the lithium species.

$$RR_1CHLi + ArPCl_2 \longrightarrow RR_1CH\text{-}PAr(Cl) \xrightarrow{DBU} R_1RC{=}PAr \qquad (4.1a)$$

$$(R{=}Ph,\ R_1{=}Ph,H).$$

$$2RR_1CHLi + ArPCl_2 \longrightarrow ArP(RR_1CH)_2 + 2LiCl \qquad (4.1b)$$

Ph_2CHLi (11) and $PhCH_2Li$ (10) were generated in the presence of TMEDA [56] and used *in situ* by dropwise addition to excess $ArPCl_2$ (12) dissolved in diethylether. $ArPF_2$ (3) was present in the ^{31}P and ^{19}F NMR spectra, and by concentrating the mixture it could be isolated, and its identify confirmed by measuring its boiling point and NMR parameters (Figure 4.1). On addition of $PhCH_2Li{\cdot}TMEDA$ (10) to $ArPCl_2$ some diphosphene (19) with its characteristic ^{31}P shift (473.8 ppm) was observed in the NMR (Figure 4.2).

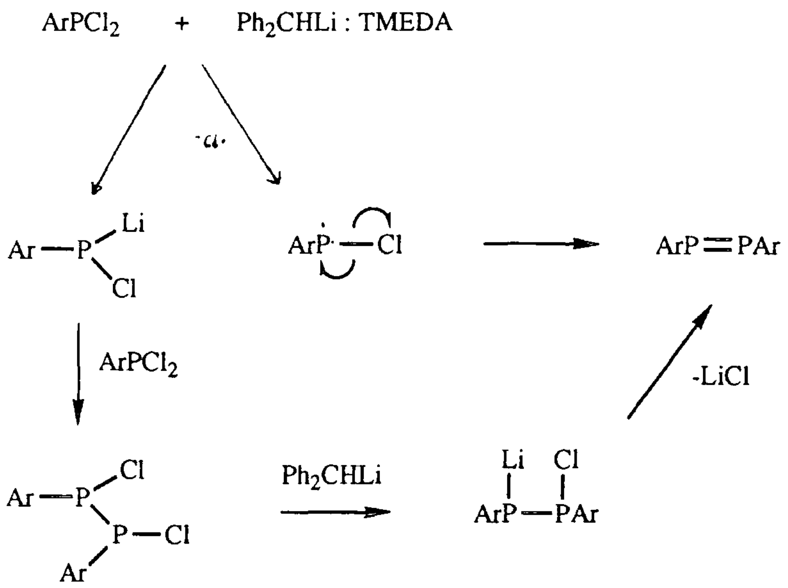

Figure 4.2: *Possible routes for $PhCH_2Li$ attack on $ArPCl_2$.*

With $Ph_2CHLi \cdot TMEDA$ (11) a similar reaction was apparent, with the ^{19}F NMR possessing a very complex "CF_3" region and a doublet of septets [δ:-90.9 ppm, $^1J_{PF}$ 1179.6, $^5J_{FF}$ 18.6 Hz, *cf.* $ArPF_2$ (3)] corresponding to a possible "P-F" species. This problem, (aside from loss of yield due to tertiary phosphine formation)[55] was not seen with Cl_2CHLi addition to $ArPCl_2$. It is also interesting to note that no attack at the ring fluorines occurs on addition of butyllithium and methyllithium.

Attack on the ring was seen with lithium species in the presence of TMEDA. In general organolithium compounds (4 orbitals, 2 electrons) form aggregates. TMEDA is a good electron source and partially due to its steric demands will cause Ph_2CHLi (11) and $PhCH_2Li$ (10) to be monomeric. (It must be noted that BuLi·TMEDA does not attack CF_3[57]). This may be attributed to an increase in the reactivity of the monomeric organolithium species. However, to develop this argument, information on the mechanism of attack for aggregates would be required. For example, do they break up before attacking as nucleophiles?

There are many other variables which may account for these results. The order of decreasing basicity in the lithio compounds used in this study is: Me > Bu > $CHCl_2$ > $PhCH_2$ > Ph_2CH. [$CHCl_2Li$ (9) is generated by BuLi reaction with CH_2Cl_2, and hence butyllithium is the more basic]. $ArPCl_2$ has two distinctive electrophilic sites for nucleophilic attack, *ie*. P-Cl and C-F (Figure 4.3)

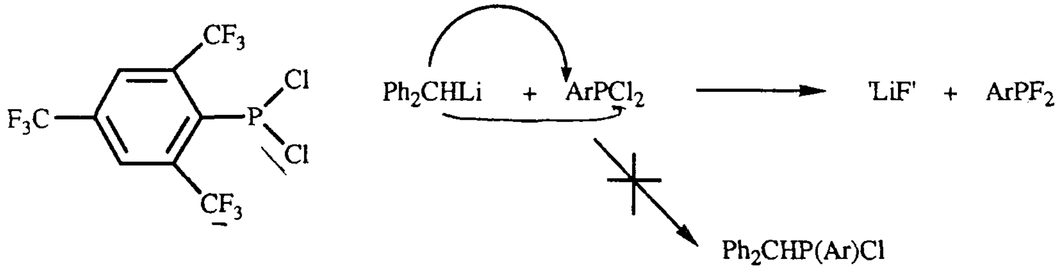

Figure 4.3: *Two possible sites for nucleophilic attack in* $ArPCl_2$.

It is not clear if steric effects do play a part, since Ph_2CHLi and $PhCH_2Li$ are certainly the larger of the lithio species used, especially with TMEDA coordinated. However, it is assumed that the attack takes place at the ortho-CF_3 groups since peaks in the ^{19}F NMR corresponding to the para-CF_3 groups appear to remain intact.

4.3.2 Method 2: Attempted Formation of a P-C Bond by the Reaction of a Geminal Dichlorocarbon Species with an Ar-Substituted Phosphide

One standard route to phosphaalkenes involves the action of the phosphide (29) on the geminal dichlorocarbon species (30). The process (Equation 4.2) is followed by treatment with base to eliminate HCl (Table 4.1) [7-15].

$$\underset{(29)}{ArP(H)Li} + \underset{(30)}{Cl_2CR_1R_2} \longrightarrow ArP(H)C(Cl)R_1R_2 \qquad (4.2)$$

Cooling $ArPH_2$ (15) to -78 °C in THF, and addition of 1 equivalent of butyllithium dropwise, resulted in an immediate black colouration. On addition of the carbon species (30) (R_1R_2 = Ph), and allowing it gradually to reach room temperature only a very broad signal indicative of decomposition was observed in the ^{19}F NMR. This was attributed to the attack of phosphide (29) on a second molecule at the CF_3. The inherent instability of the phosphide even at very low temperature was also apparent with 2,6-bis(trifluoromethylphenyl) as the substituent. This has since been verified by J Escudié [58].

4.3.3 Method 3: Reaction of $ArPCl_2$ with Dichlorocarbon Species

In view of the apparent attack by lithio species on the CF_3 groups, the following coupling reactions were attempted:

(1) $Ph_2CCl_2 + ArPCl_2 \xrightarrow{Mg}$ symmetrical diphosphene.

The copious amount of solid formed was attributed to possible Ph_2CCl_2 coupling with itself.

(2) $CCl_4 + ArPCl_2 \xrightarrow{Mg}$

Some diphosphene was formed and a signal was observed in the ^{31}P NMR possibly corresponding to $ArP{=}C(Cl)_2$ (conversion to the phosphaalkene was ~ 50% w.r.t ^{31}P NMR spectrum).

(3) $CH_2Cl_2 + ArPCl_2 \xrightarrow{Mg}$ symmetrical diphosphene + small peak possibly due to $Ar{-}P{=}C{-}(H)_2$

Attempts to isolate products from (2) and (3) were not successful. The inherent competing symmetrical diphosphene (19) reaction (Equation 3.3, Section 3.4) illustrates the unsuitability of this reaction for phosphaalkene synthesis. In all cases preference for the initial formation of a P-C bond would be anticipated (Table 4.1).

The route to the phosphaalkene where it appeared to have formed may proceed *via* an initial carbon or even a "phosphorus based" Grignard, or *via* carbene generation, for example the greater stability [59] of Ph_2C: over Cl_2C: in (1) may induce its more selective coupling to give $Ph_2C{=}CPh_2$ instead of forming a phosphaalkene.

4.3.4 Method 4 Reaction of ArPH$_2$ with Dichlorocarbon species

More selective coupling was attempted by intermolecular dehydrohalogenation, *ie.* by the following routes:

(1) $HCCl_3 + ArPH_2 \xrightarrow{DBU}$

Signals upfield *ca.* -84 and -89 ppm (intensity ratio 3:1) were obtained (see Section 7.3).

(2) $Ph_2CCl_2 + ArPH_2 \xrightarrow{DBU} ArP{=}P{-}Ar$ (19) symmetrical diphosphene.

The upfield signals in (1), and the symmetrical diphosphene (19) formation in (2) are interesting observations. $ArPH_2$ (15) in the presence of DBU gives only a signal in the ^{31}P NMR corresponding to unchanged $ArPH_2$, no diphosphene is formed. In (2), therefore, a chlorine exchange process may be postulated (see Section 7.3).

4.3.5 Method 5: Reaction of ArPH$_2$ with KOH and CHCl$_3$

The failure of the phosphaalkene synthetic route [30,31] (Equation 4.3) was attributed to the strong nucleophilic base character of KOH.

$$ArPH_2\ (15) + CHCl_3 \xrightarrow{KOH} X \rightarrow ArP{=}C(H)Cl \qquad (4.3)$$

The complex ^{19}F NMR is possibly indicative of OH^- attack at the fluorine site, causing decomposition (Figure 4.4).

Synthesis of Phospha-alkene

The dichloro-substituted phospha-alkene was synthesised by initial P-C bond formation followed by dehydrohalogenation.

a) $CH_2Cl_2 \xrightarrow{BuLi} LiCHCl_2$ (4.4)

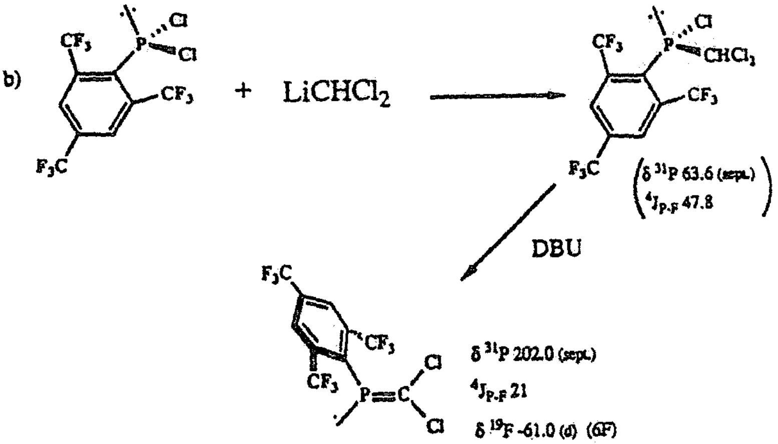

(31)

MNDO Structure [31]

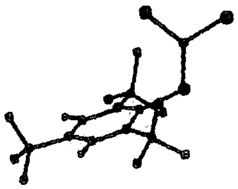

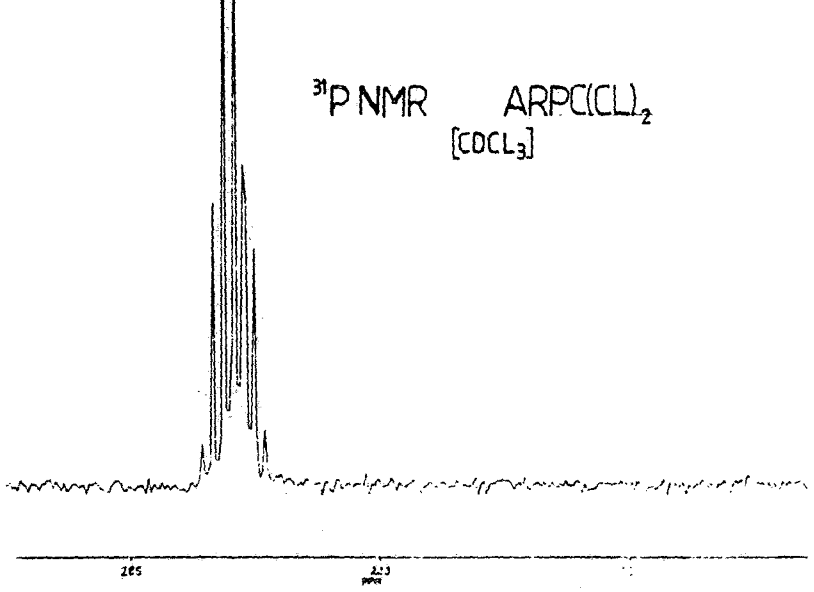

Figure 4.5: *The synthesis and ^{31}P NMR data of the new phospha-alkene, Ar–P=C(Cl)$_2$ (31).*

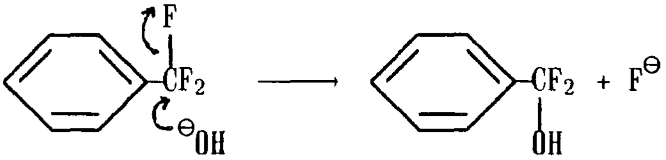

Figure 4.4: *Postulated nucleophilic attack at CF_3 by OH^-.*

4.3.6 Method 6: Acid Catalysed Reaction Between $ArPH_2$ and Carbonyls

A further route to phosphaalkenes is shown in Equation 4.4 (see also Table 4.3) [15,24-27].

$$Ph_2C{=}O + ArPH_2 \xrightarrow[\text{catalyst}]{H^{+}\ \times} \tag{4.4}$$

This reaction was not successful, even using benzaldehyde (greater δ^+ carbon and smaller steric demand). This may be attributed to the reduced nucleophilic character of the phosphorus bearing an electron withdrawing group (Ar).

4.4 SYNTHESIS OF THE PHOSPHAALKENE $ArP{=}C(Cl)_2$ (31)

4.4.1 Characterisation

The first phosphaalkene containing the Ar group was synthesised according to the scheme depicted in Figure 4.5 (see Table 4.1). Its ^{31}P NMR data and mass spectrum are illustrated in Figures 4.5 and 4.6 respectively. Phosphaalkene (31) was stable to vacuum distillation and fully characterised (see Section 4.12.3).

i

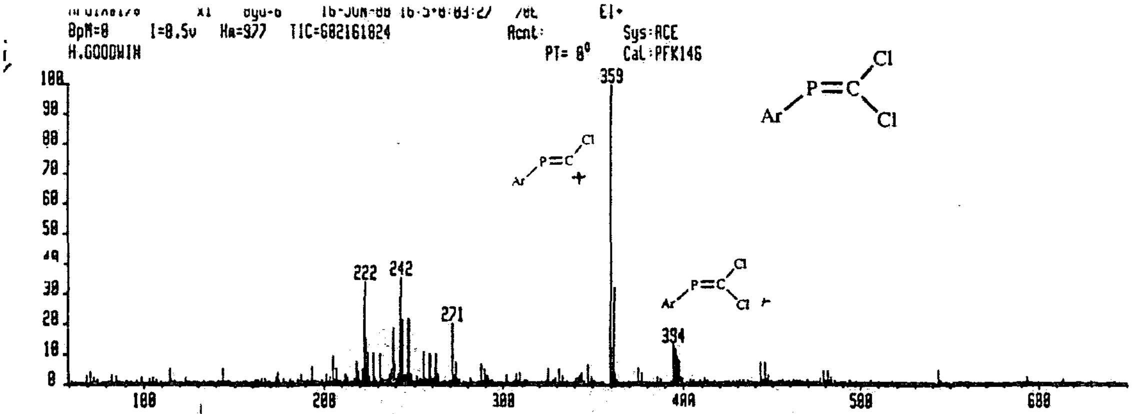

212.17	3.25	251.27	2.65	353.30	0.45	390.93	0.04	441.37	0.87	475.41	0.63
213.19	2.24	255.22	10.59	353.68	0.03	391.32	0.65	441.85	0.04	475.97	0.03
218.30	7.58	258.34	9.89	354.32	0.23	392.38	0.27	443.20	7.00	476.43	0.23
219.28	4.25	259.21	9.63	354.79	0.05	393.29	1.09	444.27	1.38	477.32	1.96
221.19	4.88	261.24	5.29	355.31	0.71	394.22	13.08	445.25	7.14	479.11	4.29
222.33	34.07	262.30	10.10	355.89	0.04	395.23	11.93	446.30	1.28	480.27	1.09
223.27	14.83	263.28	3.61	359.33	100.00	396.22	9.61	447.28	2.78	481.28	4.21
224.20	10.49	271.18	20.22	360.24	11.81	397.24	8.16	448.32	0.57	482.30	1.01
225.21	2.45	272.20	2.95	361.23	31.99	398.24	2.59	449.37	1.00	483.30	2.11
227.27	10.33	273.20	7.43	362.24	3.94	399.26	1.96	450.43	0.30	485.09	1.09
228.28	2.21			362.71	0.05	399.73	0.02	451.40	0.75	486.39	0.44
231.24	10.17			362.80	0.02	400.31	0.41			486.94	0.05
236.21	3.18			363.28	1.53	400.67	0.05			487.41	0.46
237.21	5.17			363.70	0.03	401.35	0.99			488.40	0.24
238.38	18.41			364.29	0.43						
239.31	6.37										
241.27	3.44										
242.35	35.21										
243.28	21.47										
244.29	2.94										
245.28	3.23										
246.35	21.89										
247.30	21.47										
248.30	3.28										

ii

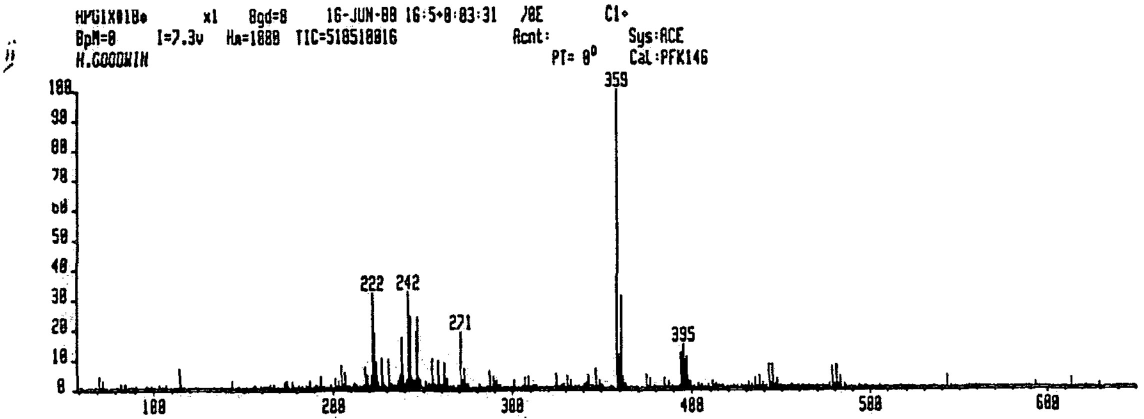

355.29	0.59	386.71	0.04	440.32	0.40	475.87	0.03
355.72	0.03	386.85	0.04	441.34	1.14	476.04	0.04
355.85	0.04	387.26	2.54	443.17	8.15	476.38	0.23
356.00	0.07	387.72	0.04	444.24	1.63	476.73	0.03
356.33	0.26	388.27	0.48	445.20	8.27	477.28	1.69
359.19	100.00	389.30	0.98	446.23	1.35	479.12	7.09
360.20	11.51	389.70	0.06	447.21	3.30	480.20	1.45
361.19	31.09	390.30	0.25	448.23	0.53	481.21	8.01
362.21	3.84	390.58	0.09	449.29	0.93	482.23	1.35
362.68	0.04	391.29	0.80	450.38	0.24	483.36	3.93
363.25	1.82	392.32	0.24	450.87	0.03	485.49	1.35
363.67	0.07	393.26	1.20	451.36	0.73	486.84	0.04
364.26	0.36	394.18	12.23	452.36	0.24	487.34	0.40
		395.19	14.84			488.03	0.05
		396.19	9.67			488.38	0.15
		397.21	10.58			488.76	0.03
		397.79	0.05			488.91	0.04
		398.21	2.64			489.41	0.77
		398.78	0.06			489.97	0.02
		399.23	2.42				
		399.72	0.04				
		400.27	0.44				

Figure 4.6: *Mass spectra of the new phosphaalkene, Ar–P=C(Cl)$_2$ (31); (i) electron impact (EI); (ii) positive ion chemical ionisation (CI$^+$).*

4.4.2 MNDO Calculation

The molecular geometry resulting from an MNDO calculation on this new compound is now presented [Figure 4.7(a)]. The stability of Ar-P=C(Cl)$_2$ [where Ar = 2,4,6-tris(trifluoromethyl)phenyl] may be attributed to the resonance form shown in Figure 4.7(b).

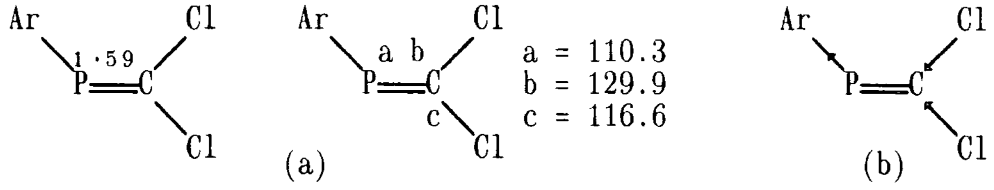

Figure 4.7: *MNDO calculations on ArP=C(Cl)$_2$ (31); (a) molecular geometry and (b) resonance stabilisation.*

High stability is associated with π-acceptance at phosphorus and π-donation at carbon, and *vice versa*.[60a,b] Characteristically carbon attached to another atom Y [Y(R)C=PAr, *eg*. Y = Cl, N, O] leads to an increase in shielding of the phosphorus nuclei attributed to conjugation of the atom Y with the π-bond. This is most pronounced when the substituent at phosphorus is electron-withdrawing, *eg*. Ar. [This effect is illustrated by the shift sequence obtained in this work, *ie*. ArP=CCl$_2$ (31) +202 ppm, ArP=C(Ph)H (32) +218 ppm, ArP=C(SiMe$_3$)H (33) +283 ppm].

4.5 ATTEMPTS TO SUBSTITUTE CHLORINE AT CARBON ON ArP=C(Cl)$_2$

In many similar systems of formula ArP=CCl$_2$, direct chlorine substitution for other organo groups, for example Me$_3$Si, Bu (see Table 4.5) provides a useful facile route to other phosphaalkene derivatives.

4.5.1 Substitution By Me_3Si

BuLi was added to the new species $ArP{=}C(Cl)_2$ [Ar = 2,4,6-tris-(trifluoromethyl)phenyl] at -78 ^{o}C. The solution blackened immediately even with maintenance of the low temperature. Dropwise addition of Me_3SiCl and allowing to warm to room temperature showed no reaction proceeding as shown (Equation 4.5).

$$\underset{(31)}{\text{Ar–P=C(Cl)}_2} \xrightarrow{\text{BuLi}} \underset{(34)}{\text{Ar–P=C(Cl)Li}} \overset{\text{Me}_3\text{SiCl}}{-\!\!-\!\!\text{X}\!\!-\!\!\!\longrightarrow} \underset{(35)}{\text{Ar–P=C(Cl)SiMe}_3} \qquad (4.5)$$

Decomposition was indicated by a broad absorption in the ^{19}F NMR, attributed to the inherent instability of the lithio derivative (34). This was possibly a result of LiCl elimination from (34) generating a reactive carbene, or an intermolecular reaction resulting in fluorine attack by the lithium species on a second molecule.

4.5.2 Substitution by Ar

The reaction $ArP{=}C(Cl)_2$ + ArLi did not generate the required product *ie*. Ar-P=C(Cl)Ar. This was as expected because of the low basicity of ArLi, illustrated by the reaction $ArLi + CCl_4 \longrightarrow ArCl$ and by the reaction of ArLi (2) with Cl_2 or C_2Cl_6 respectively [60c]. Indeed in this case $ArP{=}C(Cl)_2$ was the only phosphorus containing species observed in the ^{31}P NMR. The ^{19}F NMR also showed the presence of ArCl [61].

4.6 OVERCOMING THE SYNTHETIC PROBLEMS

To avoid the presence of lithium species *in situ* with the aryl group, or strong bases, or the requirement of a nucleophilic phosphorus, several possibilities were considered.

(1) The preparation of a secondary chlorophosphine with an R group bearing on α-H, and subsequent HCl elimination with DBU: (a) the R group could be introduced primarily onto PCl_3 followed by subsequent addition of ArLi (2) (ArLi is selective enough to allow mono substitution into a primary phosphine) or, (b) *via* a less reactive organometallic species, for example a Grignard, organocadmium or organozinc reagent substituting directly into $ArPCl_2$ (12).

(2) Preparation of the halomethylene-phosphine, Cl-P=C(R)R' with the aim to substitute chlorine for aryl in the final stage.

The first route (1) was chosen since it allowed purification of the secondary phosphine before phosphaalkene generation. The species formed in (2) may be unstable and therefore require the maintenance of low temperature, for example $Cl_2C=PCl$. (However, halomethylenephosphines with two Me_3Si groups or a Me_3Si and a Ph group on carbon, are thermally stable and can be vacuum distilled without decomposition) [7].

4.7 PHOSPHAALKENE PREPARATIONS FROM SECONDARY PHOSPHINES

4.7.1 Synthetic Routes

Preparations were attempted of RArPCl [R = Me_3SiCH_2 (36), $PhCH_2$ (37), vinyl (38) and $CHCl_2$ (39)]. The R group may be introduced *via* many routes (Chapter 2). The two employed in this case (Equations 4.6

and Equations 4.7) are now discussed. Slightly higher yields were obtained (from Equation 4.6) by the use of the lithio derivative.

$$(Et_2N)_2PCl \xrightarrow[RMgBr]{LiR\ or} (Et_2N)_2PR \xrightarrow[-2Et_2NH_2^+Cl^-]{4HCl}$$

$$RPCl_2 \xrightarrow[-LiCl]{ArLi} RP(Ar)Cl \qquad (4.6)$$

$$\begin{array}{ll} (a) & R_2Cd + 2PCl_3 \longrightarrow 2RPCl_2 \xrightarrow{ArLi} 2RP(Ar)Cl \\ (b) & R_2Cd + 2ArPCl_2 \longrightarrow 2ArP(R)Cl \end{array} \qquad (4.7)$$

4.7.2 Specific Synthetic Problems

A disadvantage of the first method was that removal of all the amine salt, *ie.* $Et_2NH_2^+Cl^-$ proved difficult, and subsequent reaction with ArLi resulted in a loss of yield (Experimental, Section 4.12.5.1). This was overcome by the use of ArLi in a slight excess. Specific examples in which a particular preparative route is not applicable include the following: Equation 4.6 should not be used for the trimethylsilylmethyl substituent (36) since reaction with hydrogen chloride to remove the amine groups may cleave the carbon silicon bond. Equations 4.6 and 4.7(a) could not be used in the presence of vinyl (38) since this group must be introduced last [Equation 4.7(b)], as ArLi (2) may add across the unsaturated "C=C" functionality. Equations 4.6 and 4.7(a) are also not suitable for the synthesis of $ArP(CHCl_2)Cl$ (39), since ArLi (2) reacts with $CHCl_2PCl_2$ causing ArCl formation, and [in Equation 4.6] would possibly induce rearrangement associated with a nucleophilic three-coordinated phosphorus atom, with an electrophilic atom in an α-position [12]. The possible rearrangement is illustrated in Figure 4.8 and is known for X = $SiMe_3$ [12], although it may not occur for X = Et.

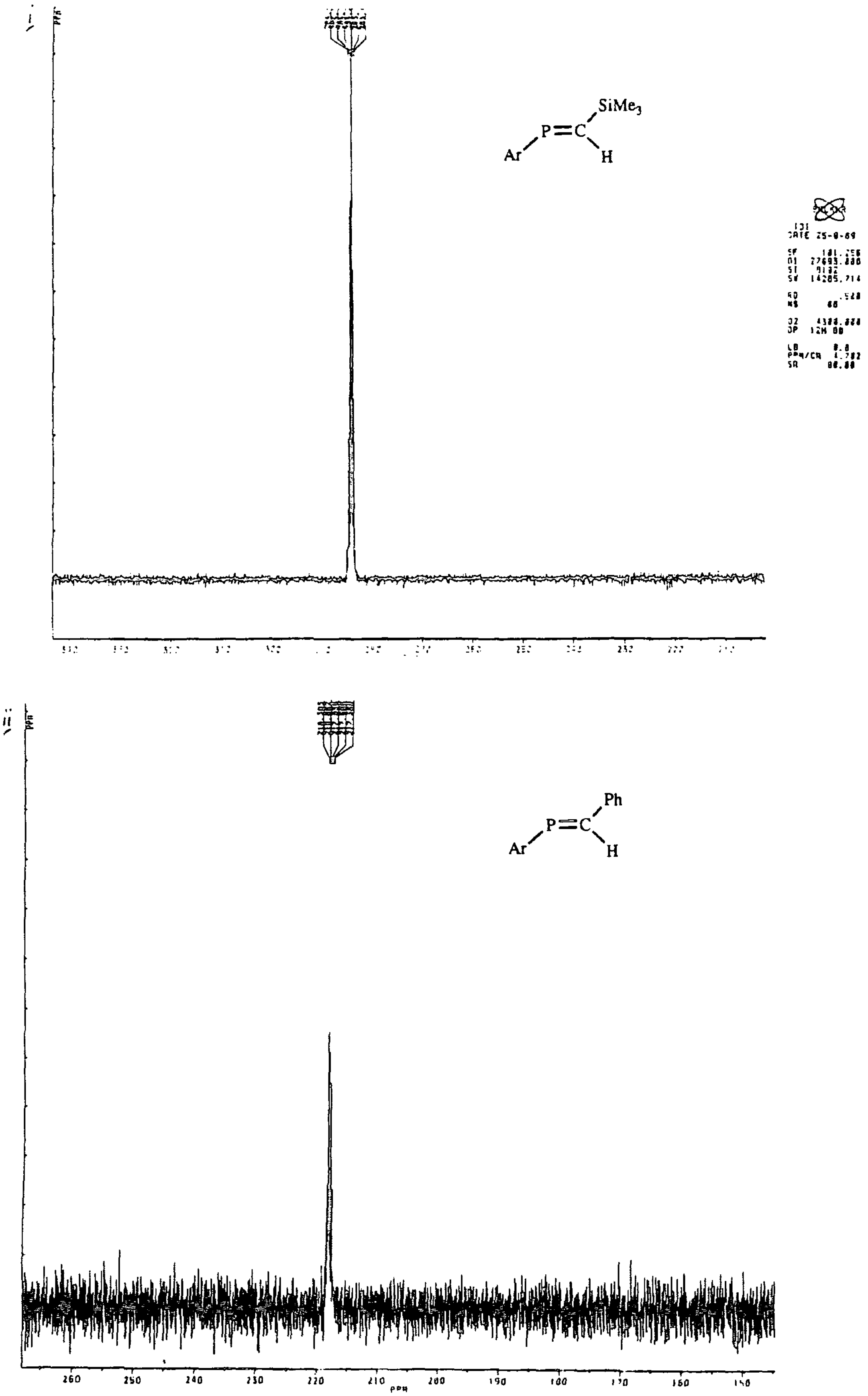

Figure 4.11: ^{31}P *NMR spectra of compounds shown in Table 4.8; (i) ArP=C(SiMe$_3$)(H) (33); (ii) ArP=C(Ph)(H) (32) recorded as solutions in THF.*

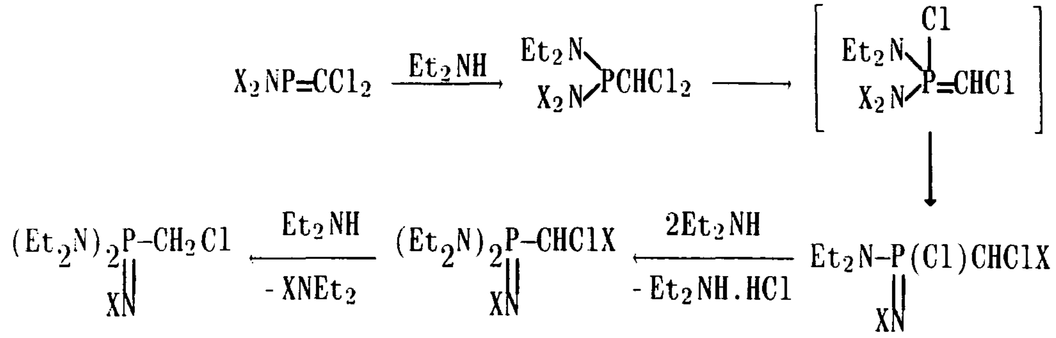

Figure 4.8: *Possible rearrangement for* $(Et_2N)_2P(CHCl_2)$.

4.7.3 Products Obtained

The secondary phosphines shown in Table 4.8 were isolated. Dehydrochlorination with DBU did not appear to be problematic. Preliminary studies and attempts at the isolation of these compounds have begun (Figure 4.11). Limited coordination data is available on species (32) and (33). The vinyl derivative is a special case and is discussed separately (Section 4.10). In each case only one isomeric form was observed with respect to the ^{31}P and ^{13}C NMR parameters. This was assigned to the E-conformation (minimising non-bonding repulsions).

Secondary phosphines		Phosphaalkenes
$PhCH_2P(Ar)Cl$ (37)	$\xrightarrow[-DBU.HCl]{DBU}$	$PhCH{=}PAr$ (32)
$Me_3SiCH_2P(Cl)Ar$ (36)	$\xrightarrow[-DBU.HCl]{DBU}$	$Me_3SiCH{=}PAr$ (33)
VinylP(Cl)Ar (38)	$\xrightarrow[-DBU.HCl]{DBU}$	(Section 4.10)

Table 4.8

Secondary phosphine (36) is a particularly interesting moiety, since there also exists the possibility of Me_3SiCl elimination [7-12] with the generation of the new phosphaalkene Ar-P=CH_2.

4.8 THE EFFECT OF THE Ar GROUP ON CARBON POLARITY

Within phosphaalkene synthetic chemistry, the requirement of at least one substituent other than H β-displaced to phosphorus to allow HCl elimination, is well-known [1,7].

In view of the electron-withdrawing nature of the Ar group, it was considered valuable to study its influence on the acidity of the hydrogen atom at the carbon, from an increase in the P-C bond polarity (Figure 4.9).

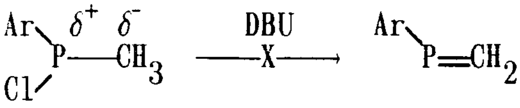

Figure 4.9
Ar group effect on P-C bond polarity.

The secondary phosphine MeP(Cl)Ar (40), was prepared by the addition of ArLi to $MePCl_2$. No apparent HCl abstraction was observed even by increasing the base strength *ie.* using DBU, DABCO and LDA. Signals in the upfield region of the ^{31}P NMR were observed. This may be attributed to the nucleophilic displacement of the chlorine on phosphorus, particularly in the case of LDA (Figure 4.10).

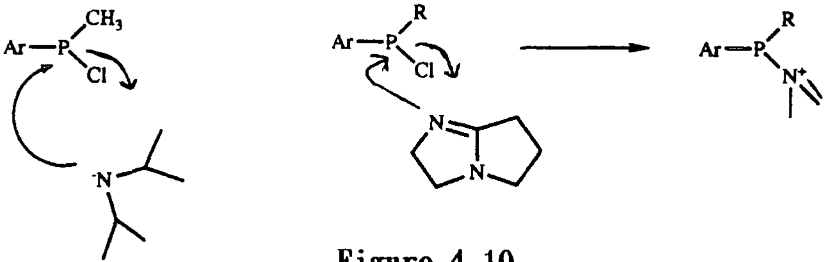

Figure 4.10
Nucleophilic displacement of Cl

The phosphaalkene ClP=CH_2 has been obtained from the starting material Cl_2PCH_3 by thermolysis [62]. This technique may have a possible application here.

4.9 PHOSPHAALKENE REACTIVITY

An interesting area to develop would involve a study of the reactivity of the phosphaalkene species. Many reactions of other phosphaalkenes are known. The presence of a weakly bonded π-system is responsible for their pronounced tendency to form new σ-bonds [46]. Figure 4.12 illustrates five types of reactions of phosphaalkenes distinguished here in terms of the change in the coordination number (σ) and valence (λ) of the phosphorus atom in the course of the chemical conversion. Each class of these reactions has been extensively reviewed.

(a) *1,2-Addition at the P=C bond:* $\sigma^2\lambda^3 \rightarrow \sigma^3\lambda^3$

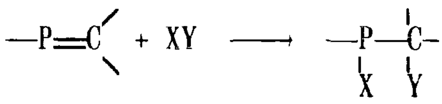

(b) *Formation of tri-coordinated pentavalent phosphorus:* $\sigma^2\lambda^3 \rightarrow \sigma^3\lambda^5$

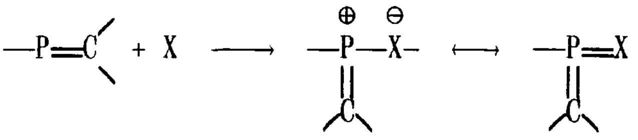

(c) *Formation of tetra-coordinated pentavalent phosphorus:* $\sigma^2\lambda^3 \rightarrow \sigma^4\lambda^5$

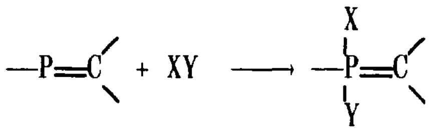

(d) *Functionalisation occurring without a change in valence or coordination of phosphorus:* $\sigma^2\lambda^3 \rightarrow \sigma^2\lambda^3$

(e) *1,2-Elimination leading to compounds of mono-coordinated phosphorus:* $\sigma^2\lambda^3 \rightarrow \sigma^1\lambda^3$

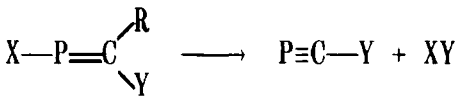

Figure 4.12

This work has involved a study of the coordination chemistry of $ArP=CCl_2$ (31), $ArP=CH(Ph)$ (32) and $ArP=CH(SiMe_3)$ (33) with the Pt(II) dimer, $(PEt_3)_2Pt_2Cl_4$ (Chapter 5).

It is obvious that more work is required to purify $ArP=CH(Ph)$ and $ArP=CH(SiMe_3)$ to enable their full characterisation. However, it was considered appropriate to present the data and properties of these materials obtained so far, for completeness of this section of work.

4.10 PHOSPHAALLENES

4.10.1 Introduction

Many stable 1-phosphaallenes are known [63-67] and synthetic routes to these species are shown in Equation 4.8 [63,64] and (*via* a phosphaketene) Equation 4.9 [64,65] and 4.10 [67].

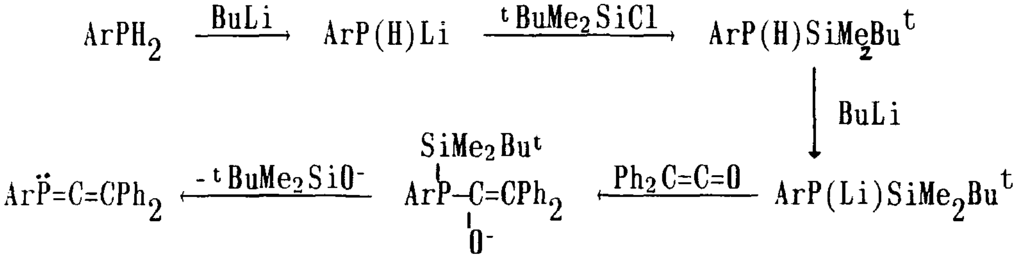

$$\begin{tikzcd} ArPH_2 \arrow[r, "BuLi"] & ArP(H)Li \arrow[r, "{}^tBuMe_2SiCl"] & ArP(H)SiMe_2Bu^t \arrow[d, "BuLi"] \\ Ar\ddot{P}=C=CPh_2 & Ar\overset{SiMe_2Bu^t}{P}-\underset{O^-}{C}=CPh_2 \arrow[l, "-{}^tBuMe_2SiO^-"'] & ArP(Li)SiMe_2Bu^t \arrow[l, "Ph_2C=C=O"'] \end{tikzcd}$$

(4.8)

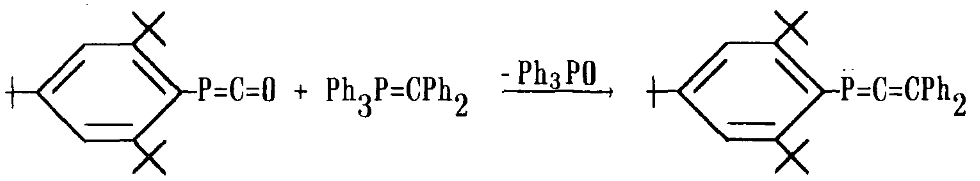

(4.9)

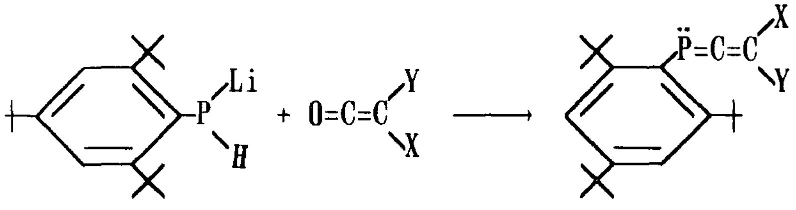

(4.10)

4.10.2 Attempted Preparation of 1-Phosphaallenes from a Secondary Vinyl Phosphine

The secondary chlorovinyl phosphine, $ArP(Cl)CH{=}CH_2$ (38) was isolated and fully characterised. This species was stable to vacuum distillation.

A possible route to the formation of a phosphaallene was postulated by the elimination of HCl from this molecule. This is a standard route used for the preparation of phosphaalkenes [7-15], from the phosphorus bearing an organo-group with an *α*-H (and a substituent other than H increasing its acidity), together with a bond directly to chlorine. A similar method was used in the synthesis of a 1-phosphadiene [68].

4.10.3 Results

Following the addition of DBU in THF at 0 °C to(38), no phosphaallene with a characteristic ^{31}P shift in the range ~75-80 ppm was observed [63-67]. Shielding with respect to the initial secondary phosphine would be expected, attributed to the resonance structure:

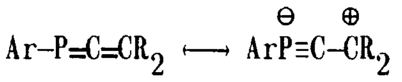

$$\mathrm{Ar{-}P{=}C{=}CR_2} \longleftrightarrow \mathrm{Ar\overset{\ominus}{P}{\equiv}C{-}\overset{\oplus}{C}R_2}$$

Instead, a clean reaction yielding a septet downfield at +221 ppm in the ^{31}P NMR was observed. Unfortunately time did not allow isolation of the compound, although it appeared stable in solution for a few days. It may be postulated that a phosphaalkene has been formed, possibly by the initial formation of the allene *via* HCl abstraction followed by either addition of further HCl, [Figure 4.13(a)] or by dimerisation [Figure 4.13(b)]. Other points of consideration include a possible Michael addition [Figure 4.13(c,d)].

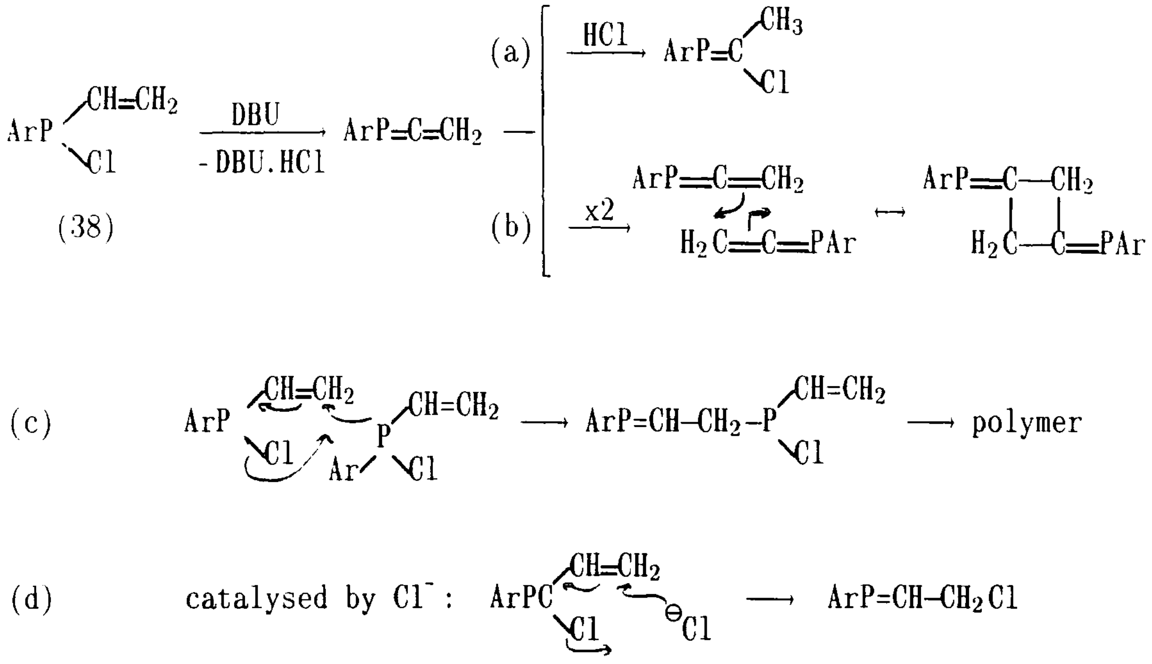

Figure 4.13

A very recent publication [69] reports the observation of an unprecedented thermal isomerisation of a secondary vinylphosphine into a phosphaalkene *via* a radical mechanism (Figure 4.14). It is obvious here that further work must be carried out to isolate the postulated 'phosphaalkene' species.

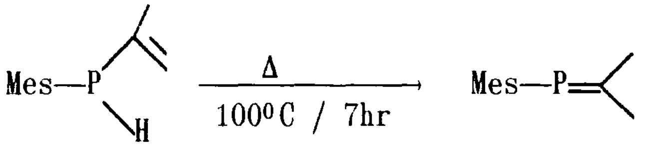

Figure 4.14: *Thermal isomerisation of a secondary vinylphosphine into a phosphaalkene;* ^{31}P *NMR* δ*: 210.5 ppm.*

4.11 THE Ar GROUP ON CARBON

4.11.1 Aryl Substituted Methyl Groups

In the hope of preparing phosphaalkenes with the carbon end bearing the new Ar substituent, the following substituted methyl derivatives were prepared: $ArCH_3$ (41), $ArCH_2OH$ (42), $ArCH(CH_3)OH$ (43), ArCHPhOH (44) and $ArCH_2Br$ (45).

Very recently the preparation of the phenol derivative (Equations 4.11 and 4.12) has been reported [70].

$$Me_3SiO{-}OSiMe_3 + C_6H_2(CF_3)_3Li \longrightarrow C_6H_2(CF_3)_3OSiMe_3 + Me_3SiOLi \tag{4.11}$$

$$C_6H_2(CF_3)_3OSiMe_3 \xrightarrow{HCl} C_6H_2(CF_3)_3OH \tag{4.12}$$

4.11.2 Potential Synthons for Phosphaalkenes

These should allow the formation of organometallic substituted methyl derivatives, and hence *via* secondary phosphines to phosphaalkenes, utilising the well-established phosphaalkene synthesis *via* HCl elimination (Figure 4.15).

$$\begin{tikzcd}
 & ArC(R)H(OH) \arrow[r] & ArC(R)H(Br) \arrow[r, "Mg"] & ArC(R)H(MgBr)^{\ddagger} \arrow[d, "PCl_3"] \\
 & ArCH_3 \arrow[r, "BuLi"] & ArCH_2Li \arrow[r, "PCl_3"] & ArC(R)H(PCl_2) \arrow[dl, "DBU", "-DBU\cdot HCl"'] \\
 & & Ar(R)C{=}P{-}Cl &
\end{tikzcd}$$

Figure 4.15: *Proposed route to phosphaalkenes with the carbon end bearing the Ar substituent; R=H, CH_3, Ph; ‡possibly via a less reactive organometallic reagent.*

The advantage of this approach would be the ability to substitute the chlorine on the phosphorus for other groups [7,44-52].

4.11.3 Potential Synthons for Phosphaalkynes

With 2 α-hydrogen atoms on the carbon, it may be possible to eliminate two moles of HCl to generate the respective phosphaalkyne.

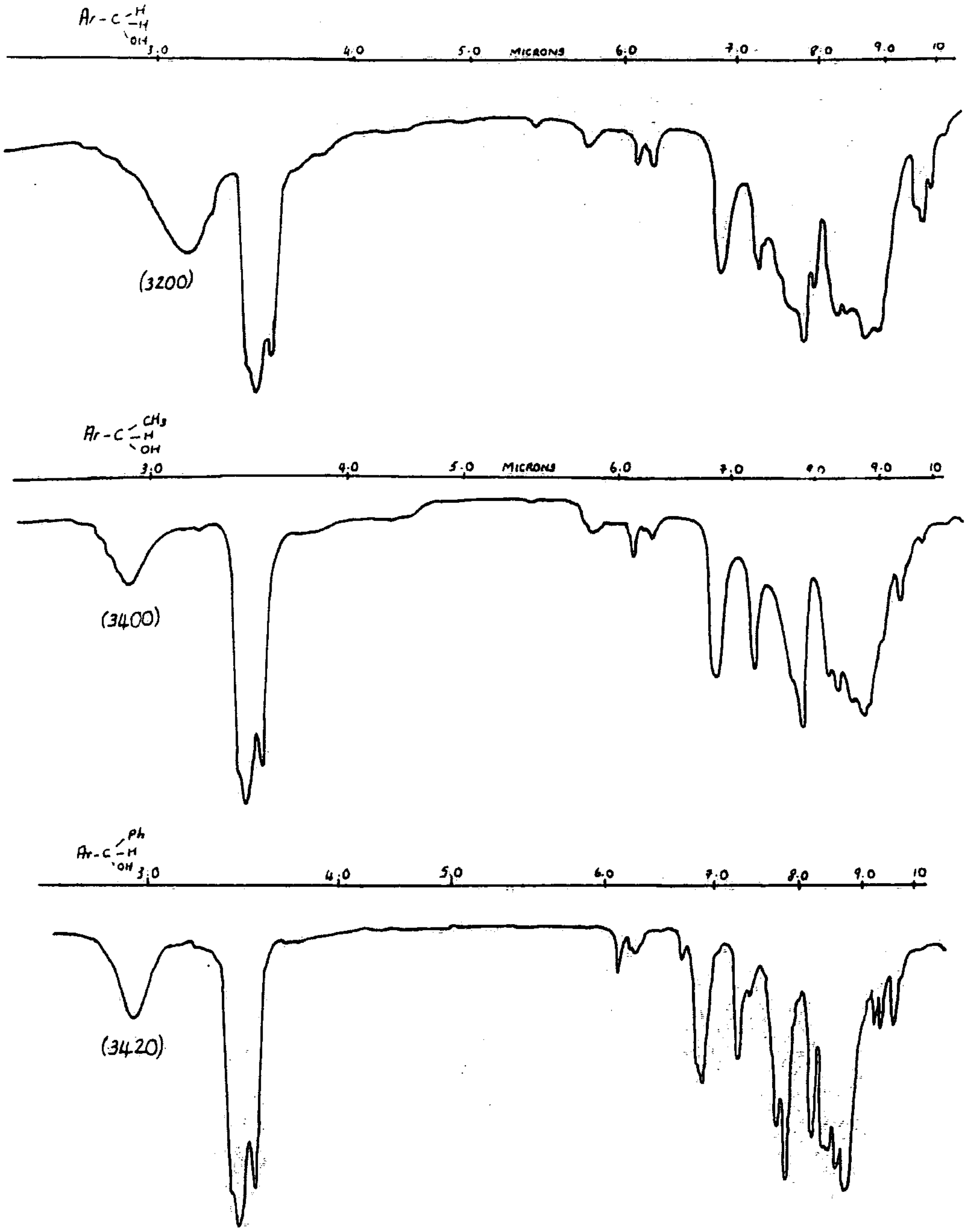

Figure 4.16: *IR film spectra of the alcohols (42), (43) and (44).*

$$\mathrm{ArCH_2Br} \xrightarrow{\mathrm{Mg}} \mathrm{ArCH_2MgBr} \xrightarrow{\frac{1}{2}\mathrm{CdCl_2}} \tfrac{1}{2}(\mathrm{ArCH_2})_2\mathrm{Cd} \xrightarrow{\mathrm{PCl_3}}$$

$$\mathrm{ArCH_2{-}PCl_2} \xrightarrow{-\mathrm{HCl}} \mathrm{Ar(H)C{=}PCl} \xrightarrow{-\mathrm{HCl}} \mathrm{Ar{-}C{\equiv}P} \qquad (4.13)$$

Phosphaalkyne preparation (Equations 4.13) and reactivity has attracted much attention, for example their synthesis [71-73] and reactivity (3 + 2 cycloaddition) [74].

4.11.4 The Alcohols

With the alcohols, ArC(OH)HR it was interesting to consider the interaction between the hydroxyl group and the fluorine atoms on the ortho-trifluoromethyl groups, to determine the extent of the intra- or inter-molecular hydrogen-bonding by infrared spectroscopy [75]. Figure 4.16 illustrates the decreasing effect of hydrogen-bonding in the series of compounds: $\mathrm{ArCH_2(OH)}$ (42) (ν_{OH} 3200 $\mathrm{cm^{-1}}$), $\mathrm{ArCH(CH_3)(OH)}$ (43) (ν_{OH} 3400 $\mathrm{cm^{-1}}$) and ArCH(Ph)(OH) (44) (ν_{OH} 3420 $\mathrm{cm^{-1}}$).

Crystals of $\mathrm{ArCH_2OH}$ and $\mathrm{ArCH(CH_3)(OH)}$ have been obtained. By X-ray structure elucidation it may be possible to determine quantitative data on the HO···F distance.

With these systems and $\mathrm{ArCH_3}$ the broad lines in the ^{19}F NMR were attributed to a significant interaction between the hydrogen and the fluorine, illustrated for $\mathrm{ArCH_3}$ (Figure 4.17), and presumably slowing down the equivalencing of the $\mathrm{CF_3}$ groups by rotation. These systems merit further investigation by temperature-dependence ^{19}F NMR studies.

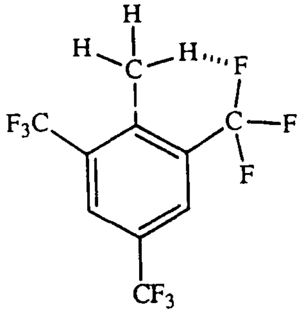

Figure 4.17: *H-F interaction in ArCH3 (41).*

4.12 EXPERIMENTAL PROCEDURES

4.12.1 Preparation of $ArPF_2$ from Ph_2CHLi·TMEDA and $ArPCl_2$

Ph_2CHLi·TMEDA was synthesised as described in the literature [56]. Ph_2CHLi·TMEDA (100 ml, 10 mmol, 0.1 M in THF) was added dropwise over 10 minutes to a stirred solution of $ArPCl_2$ (3.28g, 10 mmol) in THF (150 ml) at -78°C. The solution became deep brown with addition of the first drop of the lithio derivative. The mixture was allowed to warm to room temperature. NMR data on the solution gave: ^{31}P δ: +473 [Ar_2P_2 (19)], +184.6 ppm [t of sept, $ArPF_2$ (3)] $^1J_{PF}$ 1179.5 Hz, $^4J_{PF}$ 50.8 Hz; ^{19}F δ: -56.3 (t,o-CF_3) $^4J_{PF}$ + $^5J_{PF}$ 45 Hz, -63.8 ppm (p-CF_3) [Ar_2P_2 (19)]; -55.5 (d of t,6F) $^4J_{PF}$ 50.6 Hz $^5J_{FF}$ 18.6 Hz, -64.5 (s,3F), -90.9 ppm (d of sept,2F) $^1J_{PF}$ 1179 Hz $^5J_{FF}$ 18.6 Hz [$ArPF_2$ (3)]. The ^{31}P NMR spectrum indicated a conversion to $ArPF_2$ of approximately 65% (w.r.t. $ArPCl_2$). The Et_2O (35.5°C), THF (67°C) and TMEDA (120°C) were removed at atmospheric pressure, and the $ArPF_2$ was collected by distillation at reduced pressure, bpt. 54°C (8 mm Hg). Yield was 1.92g (55%). Exactly similar results were obtained with $PhCH_2Li$·TMEDA (0.1 M solution).

4.12.2 Preparation of $ArP(CHCl_2)Cl$

4.12.2.1 Via the Lithio Species, $CHLiCl_2$

$$CH_2Cl_2 \xrightarrow{BuLi} CHLiCl_2 \xrightarrow{ArPCl_2} ArP(CHCl_2)Cl$$

$CHLiCl_2$ was prepared as described in the literature [76,77]. BuLi (5.2 ml, 13.0 mmol, 2.5 M solution in hexane) was added dropwise over 5 minutes to a stirred solution of CH_2Cl_2 (1.0g, 0.75 ml, 11.8 mmol) in THF:Et_2O:petroleum ether (4:1:1 v/v, 150 ml) at -130 ^{o}C (pentane/liquid nitrogen slush). This lithio reagent was added to a stirred solution of $ArPCl_2$ (5.0g, 13.0 mmol) in Et_2O (50 ml) at -140 ^{o}C. The reaction mixture turned red and was allowed to warm to room temperature. A white precipitate was formed and filtered off. The solvent was removed *in vacuo* yielding a crude yellow oil.

The ^{31}P NMR showed three peaks corresponding to $ArPCl_2$ (12) (+145.4 ppm), the required $ArP(CHCl_2)Cl$ (39) (+63.6 ppm) and $ArP(CHCl_2)_2$ (+6.5 ppm). The tertiary phosphine $ArP(CHCl_2)_2$ was removed as a solid by crystallisation from diethylether at -40 ^{o}C. The product $ArP(CHCl_2)Cl$ was distilled at 68 ^{o}C (0.1 mm Hg) as a clear oil. Yield was 2.1g (41%); Analysis found: C, 27.32; H, 1.08. Required for $C_{10}H_3Cl_3F_9P$: C, 27.80; H, 0.70%; ^{31}P ($CDCl_3$) δ: 63.6 ppm (septet) $^{4}J_{PF}$ 49.8 Hz; ^{19}F δ: -54.7 (d,6F), -64.8 (s,3F) ppm.

4.12.2.2 Via the Organocadmium Reagent

$$2CH_2Cl_2 \xrightarrow{BuLi} 2CHLiCl_2 \xrightarrow{CdCl_2} (CHCl_2)_2Cd \xrightarrow{2ArPCl_2} 2ArP(CHCl_2)Cl$$

$CHLiCl_2$ (*ca.* 11.8 mmol in 150 ml Et_2O) was prepared as described in Section 4.12.2.1. $CdCl_2$ (1.08g, 5.9 mmol) was added directly to the stirred solution of $CHLiCl_2$ (Et_2O) at -130 °C. The reaction mixture was allowed to reach 0°C and stirred for 1 hour, followed by the addition in one portion of $ArPCl_2$ (4.60g, 12.0 mmol) in Et_2O (50 ml). The solution was refluxed for 1 hour, allowed to cool to room temperature, filtered and concentrated *in vacuo*. A single signal (septet) was observed in the ^{31}P NMR at 63.6 ppm. The compound was distilled as a clear oil, bpt.68 °C (0.1 mm Hg). Yield was 1.49g (65%). Characterisation data were as presented in Section 4.12.2.1.

4.12.3 Preparation of $ArP{=}C(Cl)_2$ (31)

$$ArP(CHCl_2)Cl \ (39) \xrightarrow[-DBU.HCl]{DBU} Ar{-}P{=}C(Cl)_2 \ (31)$$

DBU (0.58 ml, 3.74 mmol) in THF (10 ml) was added dropwise over 5 minutes to a stirred solution of $ArP(CHCl_2)Cl$ (39) (1.61g, 3.74 mmol) in THF (25 ml) at 0 °C. The solution was allowed to warm to room temperature. It became yellow with a white insoluble precipitate (DBU.HCl), which was removed by filtration. THF was removed by distillation at atmospheric pressure, and the product collected as a clear oil at 76 °C (0.7 mm Hg). Yield was 0.88g (59.6%). Analysis found: C, 30.55; H, 0.92. Required for $C_{10}H_2Cl_2F_9P$: C, 30.41; H, 0.51%; UV-Vis (CCl_4) λ_{max}: 327, 227 nm; MS (Intensity%) EI: 394 [13.1, $ArP{=}C(Cl)_2^+$], 359 [100,$Ar{-}P{=}CCl^+$]; ^{31}P ($CDCl_3$) δ: +202.9 ppm (septet)

${}^4J_{PF}$ 21.4 Hz; ${}^{19}F$ ($CDCl_3$) δ: -61.0 (d,6F) ${}^4J_{PF}$ 21.4 Hz, -65.1 (s,3F) ppm; ${}^{13}C$ ($CDCl_3$) δ: 164.4 (d) ${}^1J_{PC}$ 45.4 Hz, 140.0 (q,CF_3) ${}^1J_{CF}$ 30.3 Hz, 150.0 (q,CF_3), 127.1 (s,ArCH ring), 125.0 (q,CF_3), 121.0 (q,CF_3) ppm. ${}^1J_{CF}$ not resolved.

4.12.4 Preparation of $PhCH_2PCl_2$

4.12.4.1 Via $(Et_2N)_2PCl$

$$(Et_2N)_2PCl \xrightarrow{PhCH_2MgBr} (Et_2N)_2P(CH_2Ph) \xrightarrow[-2\ Et_2NH_2^+Cl^-]{2HCl} Cl_2P(CH_2Ph)$$

$PhCH_2MgBr$ (12.8 ml, 1 M solution in Et_2O, 12.8 mmol) was added dropwise to a stirred solution of $(Et_2N)_2PCl$ (2.7g, 12.8 mmol) in Et_2O (40 ml) at 0 °C. The mixture was allowed to reach room temperature, and the LiCl removed by filtration. The ${}^{31}P$ NMR of the filtrate showed the presence of $[(Et_2N)_2P(CH_2Ph)]$ at +90.9 ppm. The mixture was cooled to -10 °C, while HCl gas was slowly bubbled through it. Copious amounts of white amine salt were formed (an average rate of 2 bubbles per second for 10 minutes allowed quantitative conversion with respect to the ${}^{31}P$ NMR of $PhCH_2PCl_2$), ${}^{31}P$ δ: 175.2 ppm. Pentane (100 ml) was added to precipitate the amine salt, which was subsequently removed by filtration. The pentane and ether were removed by distillation, and $PhCH_2PCl_2$ was collected at 118 °C (12 mm Hg). Yield was 1.5g (61%). Results agree well with Weil *et al.* [78].

4.12.4.2 Via the Organocadmium Reagent

$$R_2Cd + 2PCl_3 \longrightarrow 2RPCl_2 + CdCl_2 \quad (R = PhCH_2)$$

$CdCl_2$ (4.58g, 25 mmol) in Et_2O (25 ml) as a slurry was added in one portion to a stirred solution of Ph CH_2MgBr (50 ml, 1 M solution, 50 mmol) in Et_2O at 0 °C. This solution was stirred at 0 °C for 2 hours, followed by the addition of PCl_3 (6.9g, 4.4 ml, 50 mmol) in Et_2O (40 ml). The mixture was refluxed for 1 hour before cooling to ambient temperature, filtering and removing Et_2O and excess PCl_3 by distillation at atmospheric pressure. $PhCH_2PCl_2$ was distilled as a pure oil at 118 °C (12 mm Hg) [78]. Yield was 4.0g (41%). ^{31}P NMR δ: +175.2 (s) ppm.

4.12.5 Preparation of ArP(CH_2Ph)Cl (37)

4.12.5.1 From ArLi on $PhCH_2PCl_2$

$$PhCH_2PCl_2 \xrightarrow{ArLi} ArP(CH_2Ph)Cl \ (37)$$

ArLi (0.25 M, 46 ml, 11.5 mmol) in Et_2O was added dropwise over 5 minutes to a stirred solution of $PhCH_2PCl_2$ (2.2g, 11.3 mmol) in Et_2O (50 ml) at -78 °C. The reaction mixture was allowed to warm to room temperature. LiCl was removed by filtration and the filtrate concentrated *in vacuo* to yield a crude yellow oil (4.2g, 85%). This was purified by vacuum distillation. A colourless oil was collected at 122 °C (0.3 mm Hg). Yield 3.7g (75%). Analysis found: C, 43.82; H, 2.00; Required for $C_{16}H_9ClF_9P$: C, 43.81; H, 2.07%; IR (Film): 3100 (w,ArCH), 3000-2030 (m,CH), 1630 and 1570 (m,ArPh,C=C), 1380 (m,P-CH), 900 (m,C-H), 540 (m, P-Cl) cm^{-1}; ^{31}P ($CDCl_3$) δ: 86.4 ppm (septet) $^4J_{PF}$ 52.3 Hz; ^{19}F ($CDCl_3$)

δ: -54.2 (d,6F), -64.6 (s,3F) ppm. A slight excess of ArLi was added to compensate for a small amount of amine salt remaining in solution.

4.12.5.2 Via $(PhCH_2)_2Cd$ on $ArPCl_2$

$$2PhCH_2MgBr \xrightarrow{CdCl_2} (PhCH_2)_2Cd \xrightarrow{2ArPCl_2} 2ArP(PhCH_2)Cl \quad (37)$$

$PhCH_2MgBr$ (11.0 ml, 1 M Et_2O solution, 11.0 mmol) was added dropwise over 5 minutes to a stirred suspension of $CdCl_2$ (1g, 5.5 mmol) in Et_2O (50 ml) at 0 °C. The solution was stirred at 0°C for 1 hour, followed by the addition in one portion of $ArPCl_2$ (4.25g, 11.1 mmol) in Et_2O (40 ml). The mixture was brought to reflux for a period of 4 hours, and then cooled to room temperature, filtered and the filtrate concentrated *in vacuo*. The residual yellow oil was purified by vacuum distillation, bpt. 122 °C (0.3 mm Hg). Yield was 3.1g (64%). Characterisation data were as presented in Section 4.12.5.1.

4.12.6 Preparation of ArP=CH(Ph) (32)

$$ArP(CH_2Ph)Cl \ (37) \xrightarrow{DBU} ArP{=}CH(Ph) \ (32)$$

DBU (0.33 ml, 2.2 mmol) in THF (10 ml) was added over 5 minutes to a stirred solution of $ArP(CH_2Ph)Cl$ (965 mg, 2.2 mmol) in THF (20 ml) at 0 °C. The solution became green. It was allowed to warm to room temperature and the insoluble DBU.HCl salt was removed by filtration. The ^{31}P NMR of the filtrate showed a downfield signal at δ 218.1 ppm (septet) $^4J_{PF}$ 23.7 Hz, attributed to the presence of ArP=CH(Ph) (a quantitative conversion with respect to the ^{31}P NMR); UV-Visible (THF) λ_{max} 327, 225 nm. The THF was removed *in vacuo* to yield a brown decomposition product. ^{31}P NMR δ: 0.9 (intense singlet), 10.8, 19.2 and 24.4 ppm. The phosphaalkene, Ar-P=CH(Ph) (32) did not appear to be stable to isolation. The coordination chemistry of this species in solution has been investigated (Chapter 5).

4.12.7 Preparation of $ArP(Me_3SiCH_2)Cl$ (36)

$$2Me_3SiCH_2MgBr \xrightarrow{CdCl_2} (Me_3SiCH_2)_2Cd \xrightarrow{2ArPCl_2} 2ArP(Cl)(CH_2SiMe_3)$$

Me_3SiCH_2MgBr (40 ml, 1 M Et_2O solution, 40 mmol) was added dropwise over 5 minutes to a stirred solution of $CdCl_2$ (3.7g, 20.1 mmol) in Et_2O (50 ml) at 0 °C. The reaction mixture was stirred at this temperature for 1 hour. The resultant pale yellow solution containing $(Me_3SiCH_2)_2Cd$ was added in one portion to a stirred solution of $ArPCl_2$ (16.8g, 43.8 mmol) in Et_2O (40 ml) at room temperature. The mixture was brought gradually to reflux for a period of 4 hours. The precipitate was removed by filtration and the resulting filtrate concentrated by the removal of the solvent *in vacuo* to yield 15.2g crude yellow oil. This was purified by vacuum distillation. The first fraction was unreacted $ArPCl_2$, bpt. 62 °C (0.5 mm Hg); ^{31}P δ: +145 ppm (septet) $^4J_{PF}$ 61 Hz; and the product was isolated as the second fraction, a very pale yellow oil, bpt. 84 °C (0.5 mm Hg). Yield was 9.2g (53%). Higher yields may have been obtainable *via* the direct use of the Grignard on $ArPCl_2$. It seems possible that the relative bulk of the trimethylsilylmethyl group could allow mono-substitution, *cf*. the synthesis of $Me_3SiCH_2PCl_2$ *via* the direct action of Grignard on PCl_3 [79]. Analysis found: C, 36.50; H, 3.30; Required for $C_{13}H_{13}ClF_9PSi$: C, 36.00; H, 2.78%; MS (Intensity%) EI: 434 [24.5, $ArPCl(CH_2SiMe_3)^+$]; ^{31}P ($CDCl_3$) δ: +92.1 ppm (septet) $^4J_{PF}$ 51.8 Hz; ^{19}F δ: -54.7 (d,6F) $^4J_{PF}$ 51.8 Hz, -64.0 (s,3F) ppm.

4.12.8 Preparation of ArP=C(SiMe$_3$)H (33)

$$\mathrm{ArP(CH_2SiMe_3)Cl}\ (36)\ \xrightarrow[\mathrm{-DBU.HCl}]{\mathrm{DBU}}\ \mathrm{ArP{=}C(SiMe_3)H}\ (33)$$

DBU (0.52 ml, 3.5 mmol) in THF (10 ml) was added dropwise over 5 minutes to a stirred solution of ArP(CH$_2$SiMe$_3$)Cl (1.52g, 3.5 mmol) in THF (25 ml) at 0 $^{\circ}$C. A brown solution and a precipitate formed. The solid was removed by filtration. The solvent was removed *in vacuo* to yield a yellow oil. Crude yield was 1.1g (77%). IR (Film) ν_{max}: 3100 (w,ArCH), 2960 (w,Me/C-H alkyl), 1650 and 1625 (m,Ar/C=C), 1380 (w,P=C), 1280-1000 (s,CF$_3$), 850-800 (m,SiCH$_3$), 700 and 685 (s,CF$_3$) cm^{-1}; UV-Vis (CCl$_4$) λ_{max}: 325, 260 nm; ^{31}P (CDCl$_3$) δ: +287.9 ppm (septet) $^4J_{PF}$ 26.5 Hz; ^{19}F (CDCl$_3$) δ: -56.7 (d,6F) $^4J_{PF}$ 26.5 Hz, -64.1 (s,3F) ppm; ^{13}C (CDCl$_3$) δ: 157.5 $^1J_{PC}$ 118.6,[1] 137.6 Hz (quaternary C on ring), 130.2 (ArCH ring), 124.6 (quaternary C-Ar ring), 2.2 (Si$\underline{\mathrm{Me}}_3$) ppm.

4.12.9 Preparation of ArP(CH=CH$_2$)Cl (38)

$$\mathrm{2CH_2{=}CHMgBr} + \mathrm{CdCl_2} \longrightarrow \mathrm{(CH_2{=}CH)_2Cd} \xrightarrow{\mathrm{ArPCl_2}} \mathrm{ArP(CH{=}CH_2)Cl}\ (38)$$

CH$_2$=CHMgBr (60 ml, 1 M solution in Et$_2$O, 60 mmol) was added dropwise over 5 minutes to a stirred suspension of CdCl$_2$ (5.5g, 30 mmol) in Et$_2$O (50 ml) at 0 $^{\circ}$C. A dark brown solution was formed which was stirred at 0 $^{\circ}$C for 1 hour, followed by the addition of ArPCl$_2$ (23.0g, 60 mmol) in Et$_2$O (40 ml) in one portion. The mixture was refluxed for 4 hours. The solid was filtered off, and the filtrate concentrated *in*

---

[1] The ^{13}C NMR was recorded in deuterated THF. The signals ascribed to ring-CH and the CF$_3$ and CH$_3$ groups, were evident. This doublet, (attributed to the P=C) however, could not be assigned unambiguously.

vacuo. The residual brown oil was purified by vacuum distillation. It is important to heat uniformly. Any excessive heat caused decomposition and the formation of white fumes. First fraction [$ArPCl_2$]: bpt. 62 ^{o}C (0.1 mm Hg). Second fraction [product $ArP(CH{=}CH_2)Cl$]: bpt. 68-70 ^{o}C (0.1 mm Hg). Yield 11.4g (51%). Analysis found: C, 35.44; H, 1.52; Required for $C_{11}H_5ClF_9P$: C, 35.27; H, 1.34%; ^{31}P ($CDCl_3$) δ: +68.7 ppm (septet) $^{4}J_{PF}$ 51.4 Hz: ^{19}F δ: -54.2 (d,6F) $^{4}J_{PF}$ 51.4 Hz, -64.2 (s,3F) ppm.

4.12.10 Attempted Reaction of $ArP(CH{=}CH_2)Cl$ (38) with DBU

$$\mathrm{ArP(CH{=}CH_2)Cl}\ (38)\ \xrightarrow{\mathrm{DBU}}\ ?$$

DBU (1.4 ml, 9.4 mmol) in THF (10 ml) was added dropwise over 5 minutes to a stirred solution of $ArP(CH{=}CH_2)Cl$ (3.5g, 9.3 mmol) in THF (50 ml) at 0 ^{o}C. A green solution was formed, and a solid which was filtered off. The ^{31}P NMR of the filtrate gave a clean spectrum $^{31}P\{^{1}H\}$ δ: +221.3 ppm (septet) $^{4}J_{PF}$ 20.0 Hz; ^{19}F δ: -55.2 (d,6F), -64.1 (s,3F) ppm. The filtrate was concentrated *in vacuo*. The residual brown oil showed ^{31}P δ: *ca*. 26 and 33 ppm, attributed to decomposition.

4.12.11 Attempted Reaction of Phosphide on Ph_2CCl_2

$$\mathrm{ArPH_2}\ (15)\ \xrightarrow{-78^{o}C}\ \mathrm{ArPHLi}\ \overset{\mathrm{Ph_2CCl_2}}{\relbar\relbar\mathrm{X}\!\rightarrow}\ \mathrm{ArP(H)CCl(Ph)_2}$$

BuLi (2.7 ml, 6.8 mmol, 2.5 M in hexane) was added dropwise over 5 minutes to a stirred solution of $ArPH_2$ (2.1g, 6.7 mmol) in THF (40 ml) at -78 ^{o}C. The solution turned black immediately. The solution was stirred at -78 ^{o}C for 20 minutes, followed by the dropwise addition over

5 minutes of dichlorodiphenylmethane, Ph_2CCl_2 (1.6g, 1.3 ml, 6.7 mmol) in THF (20 ml). The reaction mixture was allowed to reach room temperature. This yielded a deep brown/black solution with the presence of a fine white precipitate. The ^{31}P NMR showed no reaction with Ph_2CCl_2 - attributed to ArPH(Li) decomposition before coupling with Ph_2CCl_2. ^{31}P NMR showed a very poor broad signal at δ +32 ppm.

4.12.12 Preparation of ArP(CH_3)Cl (40)

$$CH_3PCl_2 + ArLi\ (2) \longrightarrow ArP(CH_3)Cl\ (40)$$

ArLi (30 ml, 26 mmol, 0.86 M in Et_2O) was added dropwise over 5 minutes to a stirred solution of CH_3PCl_2 (3.0g, 26 mmol) in Et_2O (120 ml) at -78 °C. The solution was allowed to warm to room temperature. A yellow solution was formed with a white insoluble precipitate. This was removed by filtration and the filtrate concentrated *in vacuo* to yield a crude yellow oil. This was purified by vacuum distillation, bpt. 66-67 °C (0.1 mm Hg), yield of clear oil was 5.6g (59%); Analysis found: C, 33.57; H, 1.57; Required for $C_{10}H_5ClF_9P$: C, 33.13; H, 1.39%; ^{31}P ($CDCl_3$) δ: +83.5 ppm (septet) $^4J_{PF}$ 54.1 Hz; ^{19}F δ: -54.4 (d,6F), -64.4 (s,3F) ppm.

4.12.13 Attempted Abstraction of HCl from $ArP(CH_3)Cl$

4.12.13.1 Reaction with DBU

$$ArP(CH_3)Cl\ (40) + DBU \longrightarrow ?$$

DBU (0.28 ml, 1.9 mmol) in THF (10 ml) was added dropwise over 2 minutes to a stirred solution of $(CH_3)PArCl$ (0.65g, 1.8 mmol) in THF (20 ml) at room temperature. A dark brown solution was formed. $^{31}P\{^1H\}$ δ: 46.2 (doublet of septets) J 294.6 (d), 15.6 (septet), -22.4 (septet) J 32.4, -39 ppm, species unassigned.

4.12.13.2 Reaction with DABCO

$$ArP(CH_3)Cl\ (40) + DABCO \longrightarrow ?$$

DABCO (0.21g, 1.9 mmol) in THF (10 ml) was added dropwise over 2 minutes to a stirred solution of $ArP(CH_3)Cl$ (0.65g, 1.8 mmol) in THF (20 ml) at room temperature. A brown solution was obtained. $^{31}P\{^1H\}$ δ: +12.2 (s), +19.2 (s), 45.4 (s), species unassigned.

4.12.13.3 Reaction with LDA

$$ArP(CH_3)Cl\ (40) + LDA \longrightarrow ?$$

LDA was prepared as follows: BuLi (10 ml, 25 mmol, 2.5 M in hexane) was added dropwise to a stirred solution of $^iPr_2NH$ (3.5 ml, 2.5g, 25 mmol) in Et_2O (30 ml) at 0 °C. This was stirred at room temperature for 1 hour.

The as-prepared LDA solution (25 mmol) was added dropwise over 5 minutes to a stirred solution of ArP(CH_3)Cl (9.1g, 25 mmol) in THF (25 ml) at 0 ^{o}C. The reaction mixture was allowed to reach room temperature and stirred for 1 hour. A white precipitate and a black solution was formed. The solid was removed by filtration. The $^{31}P\{^{1}H\}$ NMR of the filtrate showed a complex set of signals. The major product occurred at δ -82.3 ppm (an apparent triplet) J 183.5 Hz.

4.12.14 Coupling Reactions of ArPCl$_2$

4.12.14.1 With Mg/CCl$_4$

$$\mathrm{ArPCl_2}\ (12) + 2\mathrm{Mg/CCl_4} \longrightarrow$$

Magnesium turnings (0.40g, 16.5 mmol) were added to a stirred solution of ArPCl$_2$ (3.1g, 8.0 mmol) and CCl$_4$ (1.2g, 0.77 ml, 8.0 mmol) in THF (20 ml) at room temperature. ^{31}P NMR of the brown solution: +201.6 ppm $^{4}J_{PF}$ 21.8 Hz [Ar-P=C(Cl)$_2$]; 145 ppm $^{4}J_{PF}$ 61.4 Hz [ArPCl$_2$].

4.12.14.2 With Mg/CH$_2$Cl$_2$

$$\mathrm{ArPCl_2}\ (12) + 2\mathrm{Mg/CH_2Cl_2} \longrightarrow$$

Magnesium turnings (0.2g, 8.2 mmol) were added to a stirred solution of ArPCl$_2$ (1.5g, 3.9 mmol) and CH$_2$Cl$_2$ (0.33g, 0.25 ml, 3.9 mmol) in THF (25 ml) at room temperature. A dark brown solution was formed. $^{31}P\{^{1}H\}$ δ: +473 ppm [Ar$_2$P$_2$]; +255.3 ppm (septet) $^{4}J_{PF}$ 44.1 Hz ["Ar-P=CH$_2$"].

4.12.14.3 With Mg/Ph_2CCl_2

$$ArPCl_2\ (12) + 2Mg/Ph_2CCl_2 \longrightarrow$$

Magnesium turnings (0.23g, 9.46 mmol) were added to a stirred solution of $ArPCl_2$ (1.72g, 4.5 mmol) and Ph_2CCl_2 (1.1g, 0.86 ml, 4.5 mmol) in THF (25 ml) at room temperature. A deep brown solution and copious amounts of solid were produced. $^{31}P\{^1H\}$ δ: +473 ppm $[Ar_2P_2]$; +145 ppm $^4J_{PF}$ 61.4 Hz $[ArPCl_2]$.

4.12.15 Coupling Reactions of $ArPH_2$

4.12.15.1 With $DBU/CHCl_3$

$$ArPH_2\ (15) + 2DBU/CHCl_3 \longrightarrow$$

DBU (0.69 ml, 4.61 mmol) in THF (15 ml) was added dropwise over 5 minutes to a stirred solution of $ArPH_2$ (15) (0.72g, 2.3 mmol) and $HCCl_3$ (0.27g, 0.18 ml, 2.3 mmol) in THF (25 ml) at 0 °C. A yellow solution and a solid was formed which turned deep brown at room temperature. ^{31}P NMR δ: -83.3 and -88.9 ppm (singlets, intensity ratio 3:1). $^4J_{PF}$ unresolved.

4.12.15.2 With DBU/Ph_2CCl_2

$$ArPH_2\ (15) + 2DBU/Ph_2CCl_2 \longrightarrow$$

DBU (0.78 ml, 5.2 mmol) in THF (15 ml) was added dropwise over 5 minutes to a stirred solution of $ArPH_2$ (15) (0.81g, 2.6 mmol) and Ph_2CCl_2 (0.62g, 0.50 ml, 2.6 mmol) in THF (25 ml) at 0 °C. A dark brown solution and a solid was formed. ^{31}P NMR δ: 200.6 $^4J_{PF}$ 23Hz (small signal), -0.4 (s), -83.3 and -88.9 (singlets) $^4J_{PF}$ unresolved. The latter two were the major signals and had intensities in the ratio 3:1. Further addition of DBU (0.1 ml, 0.6 mmol) resulted in the replacement of the peaks at -83.3 and -88.9 ppm by a signal due to the symmetrical diphosphene, Ar_2P_2 (19) (δ: +473 ppm $^4J_{PF}$ + $^5J_{PF}$ 45.0 Hz).

4.12.16 Attempted Substitution of Chlorine in $ArP{=}C(Cl)_2$

4.12.16.1 By Me_3Si

$$\mathrm{ArP{=}C(Cl)_2}\ (31)\ \xrightarrow{\mathrm{BuLi}}\ [\mathrm{ArP{=}C(Li)(Cl)}]\ \xrightarrow{\mathrm{Me_3SiCl}}\!\!\!\!\mathrm{X}\!\!\rightarrow\ \mathrm{ArP{=}C(SiMe_3)Cl}$$

BuLi (0.52 ml, 1.3 mmol, 2.5 M in hexane) was added dropwise over 1 minute to a stirred solution of $ArP{=}C(Cl)_2$ (0.5g, 1.3 mmol) in THF (20 ml) at -78 °C. The solution immediately turned black. The mixture was stirred for 20 minutes at -78 °C followed by the dropwise addition over 2 minutes of Me_3SiCl (0.16 ml, 1.3 mmol) in THF (10 ml). The black solution was allowed to warm to room temperature. A fine white precipitate was observed. ^{31}P NMR δ: 37.1 ppm, line width (half height) = 10 ppm (decomposition)!

4.12.16.2 By Ar

$$\mathrm{ArP{=}C(Cl)_2} + \mathrm{ArLi}\ -\!\!-\!\!-\mathrm{X}\!\!-\!\!-\!\!\rightarrow\ \mathrm{ArP{=}C(Cl)Ar}$$

ArLi (2.4 ml, 1.3 mmol, 0.54 M solution in Et_2O) was added dropwise to a stirred solution of $ArP{=}C(Cl)_2$ (0.5g, 1.3 mmol) in THF (10 ml) at -10 °C. The deep brown solution formed was stirred at room temperature for 30 minutes. ^{31}P NMR showed a peak corresponding to $ArP=C(Cl)_2$ only [δ: 202 ppm $^4J_{PF}$ 23 Hz] whilst the ^{19}F spectrum also showed the presence of ArCl [δ: -65.0 (s,6F,o-CF_3), -65.4 (s,3F,p-CF_3)] [61].

4.12.17 Reaction of $ArPH_2$ with PhCHO

$$ArPH_2 + PhCHO \xrightarrow{X} ArP{=}CH_2 + H_2O$$

A catalytic quantity of toluene sulphonic acid was added to a stirred mixture of $ArPH_2$ (15) (1.21g, 3.8 mmol) and PhCHO (0.40g, 0.38 ml, 3.8 mmol) in THF (25 ml). This mixture was refluxed for 8 hours. The ^{31}P NMR indicated that no reaction had occurred [δ: -139.8 ppm (t of sept) $^1J_{PH}$ 217.9 Hz $^4J_{PF}$ 28.9 Hz].

4.12.18 Reaction of $ArPH_2$ with $CHCl_3$

$$ArPH_2 + HCCl_3 \xrightarrow{2KOH} ?$$

Powdered semi-conductor grade KOH (0.71g, 12.6 mmol) was added to a stirred solution of $ArPH_2$ (1.97g, 6.3 mmol) and spectroscopic grade chloroform (0.75g, 0.50 ml, 6.3 mmol) in THF (30 ml) at room temperature. The reaction was exothermic and the solution became jet black. The ^{31}P and ^{19}F NMR were recorded, each indicative of ring decomposition: ^{31}P δ: 1.8 (s) ppm; ^{19}F δ: -55 to -58 ppm (very broad).

4.12.19 Preparation of $ArCH_3$ (41)

$$ArLi + CH_3I \longrightarrow ArCH_3\ (41) + LiI$$

A solution of ArLi (100 ml, 40 mmol, 0.4 M in Et_2O) was added dropwise over 5 minutes to a stirred solution of methyl iodide (6.24g, 44 mmol) in ether (50 ml) at room temperature. No apparent precipitate was formed, attributed to the solubility of LiI in Et_2O. (The slight purple colour of the solution was probably due to the liberation of iodine). The ether and the excess methyl iodide were separated by distillation at atmospheric pressure and the product distilled as a colourless oil, bpt. 123°C (760 mm Hg); Analysis found: C, 40.53; H, 1.07; Required for $C_{10}H_5F_9$: C, 40.56; H, 1.70%; IR (Film) ν_{max}: 3100 (w,ArCH), 1390 (m,CH_3 alkyl), 1400-1000 (s,C-F) cm^{-1}; ^{19}F ($CDCl_3$) δ: -62.21 (s,6F), -64.12 (s,3F) ppm; ^1H ($CDCl_3$) δ: 7.84 (s,2H,Ar ring), 2.40 (s,3H,CH_3) ppm.

4.12.20 Preparation of $ArCH_2OH$ (42)

$$ArLi + H_2CO \longrightarrow ArCH_2O^-Li^+ \xrightarrow{HCl} ArCH_2OH + LiCl$$

Paraformaldehyde (6g, 0.2 mole) was heated to 120°C (decomposition temperature) under reduced pressure (0.1 mm Hg). The formaldehyde monomer was passed through a glass wool filter cooled to -48°C in $CaCl_2$/ice mixture to remove particles of polymer, then dried by passage over P_2O_5 and condensed into Et_2O (250 ml). The formaldehyde is only sparingly soluble in ether, and on cooling to room temperature some re-polymerises. ArLi (0.02M) in Et_2O (50 ml) was added dropwise to a stirred solution of the formaldehyde in Et_2O (250 ml) over 10 minutes at

0^oC (ice bath). Sufficient formaldehyde remained in solution to react quantitatively, according to the ^{19}F NMR recorded. The reaction mixture was stirred at room temperature for one hour. HCl (50 ml, 2 M) was then added in one portion and the mixture shaken vigorously for 30 minutes, after which it was poured onto crushed ice (35 g) and the product extracted into ether (100 ml). The ether layer was separated, dried ($MgSO_4$) and evaporated at reduced pressure to yield a viscous oil, which distilled under reduced pressure at 60^oC (0.2 mm Hg). The oil, when redissolved in Et_2O (5 ml) and allowing the ether to evaporate slowly over a period of 24 hours, gave rhombic crystals. Yield was 2.6g (41%). Analysis found: C, 38.22; H, 1.39; Required for $C_{10}H_5F_9O$: C, 38.48; H, 1.61%; MS EI: 291 [ArC^+], 273, 263, 244 [ring fragmentation]; CI^+: 312 [$ArC(OH)H_2^+$], 291, 273, 263, 244 [ring fragmentation]; CI^-: 292, 272; ^{19}F ($CDCl_3$) δ: -55.5 (s,6F), -60.4 (s,3F) ppm; ^1H ($CDCl_3$) δ: 7.8 (s,2H,Ar ring), 4.6 (s,2H,CH_2-alkyl), 2.0 (s,broad,1H,OH) ppm.

IR figure 4.16

Initially the formaldehyde (0.6g, 1 equivalent) was condensed directly into the ArLi solution (0.02 mole in 50 ml Et_2O) at -78^oC. However, as this solution warmed to room temperature it exploded. This was possibly due to the basic nature of the ArLi inducing rapid polymerisation of the formaldehyde. In all cases extreme care must be taken.

4.12.21 Preparation of $ArC(CH_3)H(OH)$ (43)

$$ArLi + CH_3(H)C{=}O \longrightarrow ArCHO^-(CH_3)Li^+ \xrightarrow{HCl} Ar(CH_3)H(OH)$$

A solution of ArLi (150 ml, 40 mmol, 0.4 M in Et_2O) was added dropwise over 5 minutes to a stirred solution of ethanal (3.1g, 0.07 mole) cooled to -78^oC. The reaction mixture was stirred vigorously at room temperature for two hours. HCl (50 ml, 2 M) was then added in one portion and the mixture shaken vigorously for 30 minutes, after which it was poured onto crushed ice (30 g) and the product extracted into Et_2O (50 ml). The ether layer was separated, dried ($MgSO_4$) and evaporated at reduced pressure to yield a viscous oil. This was distilled, bpt. 75°C (0.4 mm Hg). The oil was dissolved in Et_2O (5 ml) and the solvent allowed to evaporate slowly, giving a pure white solid. Yield was 7.8g (40%). Analysis found: C, 40.53; H, 2.07; Required for $C_{11}H_7F_9O$: C, 40.51; H, 2.16%; IR (Nujol) ν_{max}: 3400 (s,broad,OH), 3100 (w,ArCH), 3000-2900 (m,CH alkyl), 1730, 1640, 1560 (m,C=CAr), 1400-1300 (s,C-F), 1060 (m,ν_{C-O}) cm^{-1}; ^{19}F ($CDCl_3$) δ: -56.83 (s,6F,o-CF_3), -63.77 (s,3F, p-CF_3) ppm; ^1H ($CDCl_3$) δ: 8.19 (s,2H,Ar ring), 5.61 (q,1H,CH) $^3J_{HH}$ 6.61 Hz, 2.65 (s,broad,OH), 1.67 ppm (d,3H,CH_3) $^3J_{HH}$ 6.61 Hz. IR figure 4.16

4.12.22 Preparation of ArC(Ph)H(OH) (44)

A solution of ArLi (65 ml, 26 mmol, 0.4 M in Et_2O) was added dropwise over 5 minutes to a stirred solution of benzaldehyde (3.5g, 33 mmol) in Et_2O (100 ml) at -78°C. The reaction mixture was stirred at room temperature for one hour . HCl (50 ml, 2 M) was then added in one portion and the mixture shaken vigorously for 30 minutes, after which it was poured onto crushed ice (20 g) and the product extracted with Et_2O (50 ml). The ether layer was separated, dried ($MgSO_4$) and evaporated at reduced pressure to yield a viscous oil. This was purified by crystallisation by the addition of Et_2O (10 ml) and allowing its slow evaporation over 8 hours. A powdery white solid was obtained. Yield was 6.41g (63%). MS (Intensity%) EI: 388 [100,ArC(Ph)H(OH)$^+$], 371 [ArC(Ph)H$^+$], 374, 309 [ArCH(OH)$^+$]; CI$^+$: 388 [ArC(Ph)H(OH)$^+$], 371 [ArC(Ph)H$^+$], 262 [(Ar-F)$^+$]; ^{19}F ($CDCl_3$) δ: -58.40 (s,6F), -61.25 (s,3F) ppm; ^1H ($CDCl_3$) δ: 8.27 (2H,Ar ring), 7.32 (3H,PhCH), 7.12 (2H,PhCH), 6.61 (s,1H,CH)[2], 1.95 (s,broad,1H,OH); ^{13}C ($CDCl_3$) δ: 141 ($ArCF_3$), 132 ($ArCF_3$), 126 (ArCH arom), 125 (ArCH ring), 65 (CH) ppm. IR figure 4.16

4.12.23 Preparation of $ArCH_2Br$ (45)

4.12.23.1 Via $Ph_3PBr^+Br^-$ salt

$$Ph_3P\ (CCl_4) \xrightarrow{Br_2} Ph_3PBr^+Br^-\ (xs) + ArCH_2OH \longrightarrow ArCH_2Br$$

The $Ph_3PBr^+Br^-$ salt was precipitated and washed with carbon tetrachloride. A three-fold excess of $Ph_3PBr^+Br^-$ (3.3g, 7.8 mmol) was added to a stirred solution of $ArCH_2OH$ (0.82g, 2.6 mmol) in acetonitrile (20 ml). The mixture was refluxed for a period of two hours. The ^{19}F and ^1H NMR spectra showed the conversion to be very low (*ca.* 20%).

4.12.23.2 Via $C_2(Cl_2Br)_2$

$$ArCH_2OH + C_2(Cl_2Br)_2 + PPh_3 \longrightarrow ArCH_2Br + Ph_3PO + Cl_2C{=}CCl_2 + HBr$$

Ph_3P (0.92g, 3.5 mmol) was added as a solid to a stirred solution of $ArCH_2OH$ (1g, 3.2 mmol) at 0^oC. 1,2-dibromo-tetrachloroethane (1.15g, 3.53 mmol) in Et_2O (15 ml) was added dropwise over 5 minutes. A white solid precipitated immediately. The reaction mixture was stirred at room temperature for 1 hour. The solution was filtered and the solvent removed *in vacuo*. The bromo compound was distilled from the remaining solid/product mixture to give a clear oil, bpt. 40^oC (0.1 mm Hg). Yield was 0.5g (41.5%). Analysis found: C, 32.45; H, 0.73; Required for $C_{10}H_4BrF_9$: C, 32.03; H, 1.07%; IR (Film) ν_{max}: 3100 (w,ArCH), 3000 (m,

---

[2] correct shielding for the surrounding substituents.

CH_2), 1480 (m,C-H), 1400-1000 (s,C-F) cm^{-1}; MS (Intensity%) EI: 374 [$ArCH_2Br^+$], 355 [$(ArCH_2Br-F)^+$], 295 [100,$ArCH_2^+$]; CI^+: 312 (100), 272; CI^-: 374 [$ArCH_2Br^-$], 310, 292, 272, 79 [Br^-]; ^{19}F ($CDCl_3$) δ: -55.94 (s,6F), -60.18 (s,3F) ppm; ^1H ($CDCl_3$) δ: 7.66 (s,2H,Ar ring), 4.20 (s,2H,CH_2 alkyl) ppm.

4.12.24 Preparation of $ArCH_2MgBr$ (48)

$$ArCH_2Br \xrightarrow[Mg]{THF} ArCH_2MgBr$$

Magnesium (0.32g, 13 mmol) was added to a stirred solution of $ArCH_2Br$ (0.5g, 1.3 mmol) in THF (10 ml). This mixture was refluxed for five minutes, during which time it became deep brown. This reagent was used *in situ* for the preparation of $ArCH_2PCl_2$ (49), via the organocadmium derivative.

4.12.25 Preparation of '$ArCH_2PCl_2$' (49)

$ArCH_2MgBr$ (*ca.* 0.5 g, 1.3 mmol) in THF (15 ml) (prepared as described in Section 4.12.24), was added dropwise to a stirred solution of $CdCl_2$ (0.12g, 0.65 mmol) in THF (35 ml) at 0 °C. The solution was stirred for 1 hour at 0 °C, followed by the addition of excess PCl_3 (0.26g, 0.17 ml, 1.9 mmol) in THF (15 ml). The yellow solution was refluxed for 2 hours, filtered and the solvent and PCl_3 (excess) removed *in vacuo*, yielding a crude yellow oil. Yield was 0.25g (48%); ^{31}P δ: +178 ppm (singlet). Further data are required for assignment.

4.12.26 Reaction of '$ArCH_2PCl_2$' with DBU

$$ArCH_2PCl_2 \longrightarrow ArC{\equiv}P \ (?)$$

DBU (0.18 ml, 1.2 mmol) in THF (10 ml) was added dropwise over 2 minutes to a stirred solution of the crude phosphine '$ArCH_2PCl_2$' (0.48g, 1.2 mmol) in THF (15 ml) at 0 °C. A bright green solution and white precipitate was formed. ^{31}P NMR δ: -15.2, -10.8, -5.6, -1.7 ppm. These signals could not be assigned.

4.13 REFERENCES

1. R. Appel, F. Knoll and I. Ruppert, *Angew.Chem. Int.Ed.Engl.*, 20, 731-744 (1981).

2. a) K. Dimroth and P. Hoffmann, *Angew.Chem.*, 76, 433 (1964).

   b) K. Dimroth and P. Hoffmann, *Angew.Chem. Int.Ed.Engl.*, 3, 384 (1964).

3. a) R. Allman, *Angew.Chem.*, 77, 134 (1965).

   b) R. Allman, *Angew.Chem. Int.Ed.Engl.*, 4, 150 (1965).

4. a) G. Märkl, *Angew.Chem.*, 78, 907 (1966).

   b) G. Märkl, *Angew.Chem. Int.Ed.Engl.*, 5, 846 (1966).

5. A.J. Ashe, *J.Amer.Chem.Soc.*, 93, 3293 (1971).

6. G. Becker, *Z.Anorg.Allgem.Chem.*, 423, 242 (1976).

7. L.N. Markovskii and V.D. Romanenko, *Z.Obs.Khim.*, 56(2), 253-269 (1986).

8. Th. A. van der Knapp, Th. C. Klebach, F. Visser, F. Bickelhaupt, P. Ros, E.J. Baerends, C.H. Stam and M. Konijn, *Tetrahedron*, 40(4), 765-776 (1984).

9. O.I. Kolodiazhnyi, I.V. Shevtchenko and V.P. Kukhar', *Phosphorus and Sulphur*, 30, 433-436 (1987).

10. Th. A. Van der Knapp and F. Bickelhaupt, *Chem.Ber.*, 117, 915-924 (1984).

11. R. Appel, C. Casser and M. Immenkeppel, *Tetrahedron Lett.*, 26(30), 3551-3554 (1985).

12. A.A. Prishchenko, A.V. Gromov, Yu N. Luzikov, A.A. Borisenko, E.I. Lozhko, K. Klaus and I.F. Lutsenko, *Z.Obs.Khim.*, 54(7), 1520-1527 (1984).

13. Th. A. Van der Knapp and F. Bickelhaupt, ***Phosphorus and Sulphur***, 21, 227-236 (1984).

14. K. Issleib, H. Schmidt and C. Wirkner, *Z.Chem.*, 21(10), 357-358 (1981).

15. H. Oehme and E. Leissring, *Z.Chem.*, 19, 416 (1979).

16. H. Eshtiagh-Hosseini, H.W. Kroto, J.F. Nixon, S. Brownstein, J.R. Morton and K.F. Preston, *J.Chem.Soc.Chem.Commun.*, 653-654 (1979).

17. H.Eshtiagh-Hosseini, H.W. Kroto, J.F. Nixon and O. Ohashi, *J.Organometallic Chem.*, 296, 351-355 (1985).

18. J. Grobe, D. Le Van, J. Schulze and J. Szameitat, ***Phosphorus and Sulphur***, 28, 239-252 (1986).

19. H. Eshtiagh-Hosseini, H.W. Kroto, J.F. Nixon and O. Ohashi, *J.Organometallic Chem.*, 181, C1-C3 (1979).

20. M. Binnewies, J. Grobe and D. Le Van, *Z.Naturforsch*, 40b, 927-933 (1985).

21. J. Grobe, D. Le Van, J. Nientiedt and J. Szameitat, ***Phosphorus and Sulphur***, 30, 401-404 (1987).

22. J. Grobe, J. Szameitat and M. Möller, *J.Organometallic Chem.*, 344, 61-69 (1988).

23. J. Grobe and J. Szameitat, *Z.Naturforsch*, 41b, 974-980 (1986).

24. G. Becker and O. Mundt, *Z.Anorg.Allgem.Chem.*, 462, 130-142 (1980).

25. G. Becker, W. Uhl and H.I. Wessely, *Z.Anorg.Allgem.Chem.*, 479, 41-56 (1981).

26. K. Issleib, H. Schmidt and E. Leissring, *Z.Chem.*, 26(11), 406-407 (1986).

27. V.D. Romanenko, A.V. Ruban, M.I. Povolotskii, L.K. Polyachenko and L.N. Markovskii, *Z.Obs.Khim.*, 56(5), 1186-1187 (1986).

28. T. Van der Does and F. Bickelhaupt, ***Phosphorus and Sulphur***, 30, 515-518 (1987).

29. M. Yoshifuji, K. Toyota, I. Matsuda, T. Niitsu, N. Inamoto, K. Hirotsu and T. Higushi, ***Tetrahedron***, 44(5), 1363-1367 (1988).

30. R. Appel and M. Immenkeppel, *Z.Anorg.Allgem.Chem.*, 553, 7-14 (1987).

31. R. Appel, C. Casser, M. Immenkeppel and R. Knoch, *Angew.Chem. Int.Ed.Engl.*, 23(11), 895-896 (1984).

32. H. Oehme, E. Lessring and H. Meyer, *Tetrahedron Lett.*, 21, 1141-1144 (1980).

33. G. Becker, G. Gresser and W. Uhl, *Z.Anorg.Allgem.Chem.*, 463, 144-148 (1980).

34. R. Appel, B. Laubach and M. Siray, *Tetrahedron Lett.*, 25(39), 4447-4448 (1984).

35. R. Appel, F. Knoch, B. Laubach and R. Sievers, *Chem.Ber.*, 116, 1873-1879 (1983).

36. G. Becker, M. Rössler and W. Uhl, *Z.Anorg.Allgem.Chem.*, 473, 7-19 (1981).

37. G. Becker, *Z.Anorg.Allgem.Chem.*, 423, 242-254 (1976).

38. A.R. Barron, A.H. Cowley and S.W. Hall, *J.Chem.Soc.Chem.Commun.*, 980-981 (1987).

39. M. Regitz and T. Allspach, *Chem.Ber.*, 120, 1269-1270 (1987).

40. L. Weber, K. Reizig and G. Meine, *Z.Naturforsch*, 40b, 1698-1702 (1985).

41. F. Zurmühlen and M. Regitz, *J.Organometallic Chem.*, 332, C1-C5 (1987).

42. R. Appel, V. Winkhaus and F. Knoch, *Chem.Ber.*, 120, 125-129 (1987).

43. A.R. Barron and A.H. Cowley, *J.Chem.Soc.Chem.Commun.*, 1092-1093 (1987).

44. V.D. Romanenko, T.V. Sarina, N.V. Kolotilo and L.N. Markovskii, *Z.Obs.Khim.*, 55(5), 1188-1190 (1985).

45. R. Appel, J. Menzel and F. Knoch, *Chem.Ber.*, 118, 4068-4072 (1985).

46. L.N. Markovskii and V.D. Romanenko, *Z.Obs.Khim.*, 57(1), 3-31 (1987).

47. R. Appel and U. Kündgen, *Angew.Chem. Int.Ed.Engl.*, 21(3), 219-220 (1982).

48. R. Appel, U. Kündgen and F. Knoch, *Chem.Ber.*, 118, 1352-1370 (1985).

49. R. Appel, C. Casser and F. Knoch, *Chem.Ber.*, 119, 2609-2614 (1986).

50. R. Appel, S. Korte, M. Halstenberg and F. Knoch, *Chem.Ber.*, 115, 3610-3617 (1982).

51. L.N. Markovskii, V.D. Romanenko, A.V. Ruban and L.K. Polyachenko, *Z.Obs.Khim.*, 56(8), 1907-1908 (1986).

52. a) V.P. Kukhar', I.V. Shevchenko and O.I. Kolod yazhnyi, *Z.Obs. Khim.*, 55(2), 264-271 (1985).

b) O.I. Kolodnyazhnyi, I.V. Shevchenko and V.P. Kukhar', *Z.Obs. Khim.*, 55(8), 1862-1863 (1985).

53. R. Appel, J. Menzel and F. Knoch, *Z.Anorg.Allgem.Chem.*, 534, 100-108 (1986).

54. J. Grobe, D. Le Van, J. Nientiedt, B. Krebs and M. Dartmann, *Chem.Ber.*, 121, 655-664 (1988).

55. a) R.B. Fox, *J.Amer.Chem.Soc.*, 72, 4147 (1950).

b) T. Weil, B. Prijs and H. Erlenmeyer, *Helv.Chim.Acta*, 35, 1412 (1952).

56. B.J. Wakefield, "*Best Synthetic Methods*", Organolithium Methods, Academic Press, Chapter 3, 21 (1988).

57. J. Escudié, C. Couret, H. Ranaivonjatovo, M. Lazraq and J. Satgé, *Phosphorus and Sulphur*, 31, 27 (1987).

58. J. Escudié, Personal Communication, April 1989.

59. W. Kirmse, *Series of Monographs Carbene Chemistry*, Academic Press, New York and London, 1, 200 (1964).

60. a) G.E. Carr, R.D. Chambers, T.F. Holmes and D.G. Parker, *J.Organometallic Chem.*, 325, 13 (1987).

b) L.N. Markovskii and V.D. Romanenko, *Z.Obs. Khim.*, 56(11), 2433-2443 (1986).

c) I.F. Lutsenko, A.A. Prishchenko, A.A. Borisenko and Z.S. Novikova, *Doklady Akademii Nauk. SSR.*, 256(6), 1401-1405 (1981).

61. G.E. Carr, Ph.D. Thesis, University of Durham, 260 (1986).

62. M.J. Hopkinson, H.W. Kroto, J.F. Nixon and N.P.C. Simmons, *J.Chem.Soc.Chem.Commun.*, 513 (1976).

63. M. Yoshifuji, K. Toyota, K. Shibayama and N. Inamoto, *Tetrahedron Lett.*, 25(17), 1809-1812 (1984).

64. R. Appel, P. Fölling, B. Josten, M. Siray, V. Winkhaus and F. Knoch, *Angew.Chem. Int.Ed.Engl.*, 23(8), 619-620 (1984).

65. R. Appel, V. Winkhaus and F. Knoch, *Chem.Ber.*, 119, 2466-2472 (1986).

66. M. Yoshifuji, K. Toyota, N. Inamoto, K. Hirotsu, T. Higuchi and S. Nagase, *Phosphorus and Sulphur*, 25, 237-243 (1985).

67. G. Märkl and P. Kreitmeier, *Angew.Chem. Int.Ed.Engl.*, 27(10), 1360-1361 (1988).

68. B.A. Boyd, R.T. Thoma, W.H. Watson and R.H. Neilson, *Organometallics*, 7, 572-574 (1988).

69. F. Mercier, C. Hugel-Le Goff and F. Mathey, *Tetrahedron Lett.*, 30(18), 2397-2398 (1989).

70. H.W. Roesky, M. Scholtz, M. Noltemeyer and F.T. Edelmann, *Inorg. Chem.*, 28, 3829-3830 (1989).

71. R. Appel, F. Knoll and I. Ruppert, *Angew.Chem. Int.Ed.Engl.*, 20, 731-744 (1981).

72. R. Appel, G. Maier, H.P. Reisenauer and A. Westerhaus, *Angew.Chem. Int.Ed.Engl.*, 20(2), 197 (1981).

73. T. Allspach, M. Regitz, G. Becker and W. Becker, *Synthesis*, 31-36 (1986).

74. W. Rösch and M. Regitz, *Angew.Chem. Int.Ed.Engl.*, 23(11), 900-901 (1984).

75. D.H. Williams and I. Flemming, "*Spectroscopic Methods in Organic Chemistry*", McGraw-Hill Book Company UK Ltd., 4th Edition, London (1987).

76. G. Kobrich and W. Drischel, *Angew.Chem.*, 76, 536 (1964).

77. G. Kobrich and W. Drischel, *Angew.Chem. Int.Ed.Engl.*, 3, 513 (1964).

78. Th. Weil, B. Prijs and H. Erlenmeyer, *Helv.Chim.Acta*, 35, 1314-1318 (1953).

79. D. Seyferth and W. Freyer, *J.Amer.Chem.Soc.*, 26, 2604-2605 (1961).

CHAPTER FIVE

THE COORDINATION CHEMISTRY OF NEW PHOSPHINES, DIPHOSPHENES AND PHOSPHAALKENES

5.1 INTRODUCTION: DONOR PROPERTIES OF PHOSPHORUS COMPOUNDS

The great majority of the elements are known to form at least a few complexes with phosphorus donors [1] (Figure 5.1). In particular the platinum complexes of some of these species may have exciting applications as anti-tumour agents. The anti-tumour properties of platinum(II), for example, cisplatin$^{(TM)}$ [*cis*–$Cl_2(NH_3)_2Pt$]* and related compounds are well known [2]. The lack of success in attempting to replace nitrogen-containing ligands by phosphorus donors in complexes of this type, has been attributed to the strong *trans* effect exerted in dichloro–Pt(II) compounds. It has been suggested [3] that the subtle σ-donor and π-acceptor properties of fluorophosphines within these systems may give rise to improved anti-tumour properties.

Aspects of the coordination chemistry of phosphines, phosphaalkenes and diphosphenes, all bearing the 2,4,6-tris(trifluoromethyl)phenyl substituent are presented here, together with a very preliminary investigation of the ligative behaviour of the phosphorus/boron containing nitrileimine (Section 5.4).

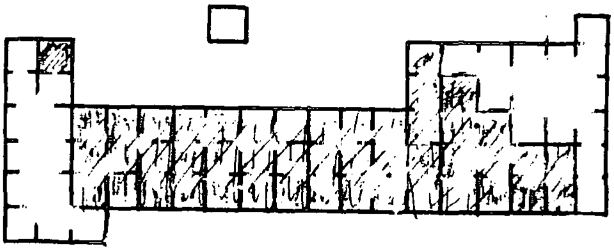

Figure 5.1: *Elements known to form complexes with phosphorus donors.*

* N.B. Correct format for metal complex formulae is [MX_2(L)( )] etc.

5.1.1 Diphosphenes

The coordination chemistry of the new diphosphene $[(CF_3)_3C_6H_2P]_2$ (19) is of considerable interest because of the presence of the strongly electron withdrawing substituents as compared with the well established supermesityl group [4] (see Chapter 3).

The coordination chemistry of the diphosphene is complicated by the fact that it can utilise more than one type of bonding mode. Table 5.1 illustrates the possible bonding types, with reference to specific examples under each classification. A brief discussion of the energy levels in diphosphenes involved in coordination is now presented.

Ab initio calculations on the parent system HP=PH [23] show the HOMO as being representative of the lone pair of electrons on the phosphorus. The three diphosphenes Ar_2P_2 (19) , $ArAr'P_2$ (20) and Ar'_2P_2 (24) were considered. Ar'_2P_2 (24) appeared very unreactive toward coordination [24a]. In contrast, coordination complexes of Ar_2P_2 (19) and $ArAr'P_2$ (21) have been obtained in this work. The MNDO calculations (Section 3.7) were carried out in an attempt to rationalise these differences. However, each showed the HOMO to be the lone pair of electrons, and the HOMO-1 the π "P=P" as expected. The geometry from the MNDO calculation on Ar'_2P_2 (24) was verified by comparison with its known X-ray structure [24b]. There appear to be no significant orbital differences between the three species. It may therefore be valuable to reinvestigate the coordination potential of Ar'_2P_2. (It must not be overlooked that the apparent difference in observed reactivity may be attributed to d-orbital involvement, the concept of which is not incorporated into the MNDO approximation).

	ML_n	R	REF
A η^2 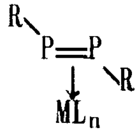	Mo(η^5-C_5H_5)$_2$	H	5
	Pt(PPh$_3$)$_2$	C_6F_5	5
	Ni(PEt$_3$)$_2$	SiMe$_3$	5
	Pd(dppe)	C_6H_5	5
	Ni[R$_4$P$_2$(CH$_2$)$_2$]‡	SiMe$_3$	6
	Ni[R$_4$P$_2$(CH$_2$)$_2$]‡	Me	6
	Ni[R$_4$P$_2$(CH$_2$)$_2$]‡	t-Bu	6
	Ni[R$_4$P$_2$(CH$_2$)$_2$]‡	Ph	6
	Ni(^{n}Bu$_3$P)$_2$	Supermes,^{t}BuN(H)	7
	Ni(Me$_3$P)$_2$	SiMe$_3$	8
	Ni(Et$_3$P)$_2$	CMe$_3$	8
		Ph	8
		Me	8
	Cp$_2$TaH	Ph	9
B η^1 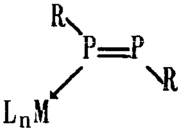	Cr(CO)$_5$	Supermes, mes	10
	Mo(CO)$_5$	Supermes, mes	10
	W(CO)$_5$	Supermes, mes	10
	Cr(CO)$_5$	(Me$_3$Si)$_2$CH	11
	Ni(CO)$_3$	Supermes, RNH	7
	Fe(CO)$_4$	Supermes	12
	Ni(CO)$_3$	Supermes	12
C bis-η^1 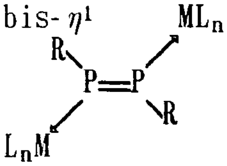	Fe(CO)$_4$	(SiMe$_3$)$_2$CH	13
	Fe(CO)$_4$	(SiMe$_3$)$_2$N	13
	Fe(CO)$_4$	Mes	13
	V(η^5-C_5H_5)(CO)$_3$	Mes	14
	Cr(CO)$_5$	Ph	15
D bis-$\eta^1\eta^2$ 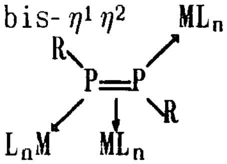	Cr(CO)$_5$	Ph	15
	Cr(CO)$_5$	t‸^{n}Bu	16,17
	W(CO)$_5$	Ph	16
E $\eta^1\eta^2$ 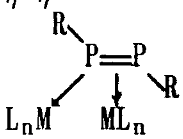	Fe(CO)$_4$	OSupermes	11
	Fe(CO)$_4$	Ph	18
	Fe(CO)$_4$	Me$_2$C$_2$PN$_2$	19
F 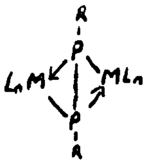	Mo(CO)$_2$(η^5-C_5H_5)	Ph	20
	Mo(CO)$_2$(η^5-C_5H_5)	CH(SiMe$_3$)$_2$	20, 21
G 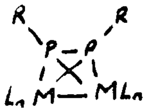	Fe(CO)$_3$	t-Bu	22

Table 5.1: *The modes of coordination of diphosphenes; ‡R=Et, C_6H_{11}.*

5.1.2 Phosphaalkenes

The coordination types for phosphaalkenes so far recognized together with some selective examples are given in Table 5.2. This chemistry has been extensively reviewed by J.F. Nixon [34].

	MLn	R_1	R_2	R_3	REF
A. Terminal Phosphorus (η^1)					
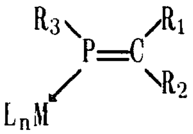	$Cr(CO)_5$	Ph	Ph	Mes	25
	cis-$PtCl_2(PEt_3)$	Ph	Ph	Mes	26
	$Fe(CO)_4$	Ph	$SiMe_3$	Supermes	27
	$Fe(CO)_4$	Me_3Si	Me_3Si	$N(SiMe_3)_2$	28
	$RhCl(PPh_3)_2$	Me_3Si	Me_3Si	F	29
B. Bridging Phosphorus ($\eta^1\mu^2$)					
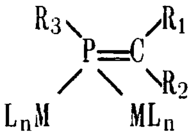	$Cr(CO)_5$	$Me_2C_4PH_3$ (dimer)			30
C. η^2-Type					
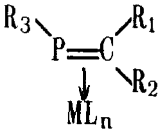	Ni(bipy)	Ph	Ph	$Me_2C_6H_3$	31
	$Fe(CO)_4$	H	H	Supermes	32
	$Ni(PMe_3)_2$	$SiMe_3$	$SiMe_3$	$(Me_3Si)_2CH$	33
D. $\eta^1\eta^2$-Type					
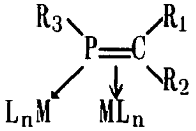	$Fe(CO)_4$	H	H	Supermes	32
	$Fe(CO)_4$	^tBu	H	^tBu	5,34‡
E. Cluster Stabilised					
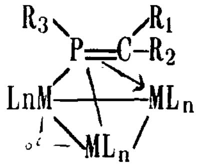	$Fe(CO)_3$	H	H	p-$MeOC_6H_4$	34,35

Table 5.2: *The modes of coordination of phosphaalkenes; ‡page 1344.*

Energy Levels

The phosphorus lone pair σ-orbital and the π-orbital of the P=C bond are the highest occupied molecular orbitals of nearly equal energy [36-38]. The level of the lowest π^* is relatively low. This enables high versatility, whereby coordination may occur in a DCD synergic σ-donating π-backbonding side on η^2 mode, or *via* a lone pair with the formation of a σ-coordinate bond. A very interesting illustration of these two bonding modes is the establishment of the following equilibrium [36-39]:

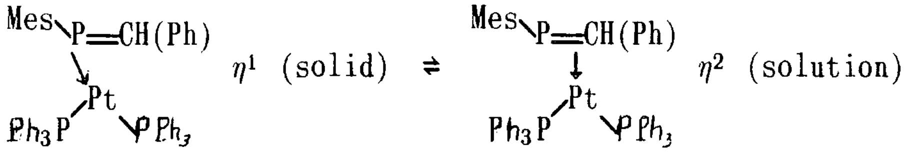

5.1.3 Phosphaalkynes

It is worth offering a comparison here with the phosphaalkyne system. The HOMO is of the π-type with the phosphorus lone pair a lot lower in energy. Phosphaalkynes characteristically give the η^2-mode of coordination [34,40,41], although following η^2-coordination the π-orbital energy may be sufficiently lowered to allow η^1-coordination, indeed some examples of this are known [42].

5.2 COORDINATION WITH THE CIS Pt(II) DIMER

5.2.1 Results

Complexes were prepared of the Pt(II) derivative $[(Et_3P)PtCl_2]_2$ [43] with the following phosphorus containing species: ArP=PAr (19), ArP=PAr' (20), $ArPF_2$ (3), $ArPH_2$ (15), $ArPCl_2$ (12), ArP=CH(Ph) (32), $ArP{=}CH(SiMe_3)$ (33) and $ArP{=}C(Cl)_2$ (31) and results are presented in Table 5.3.

COMPOUND			$^1J(PPt)$	^{31}P
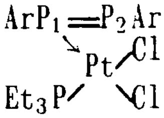 $\mathrm{ArP_1{=}P_2Ar}$ Pt Cl $\mathrm{Et_3P}$ Cl	(51)	cis	2602.9	346.6_1 337.2_2 †534.3
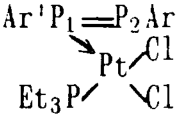 $\mathrm{Ar'P_1{=}P_2Ar}$ Pt Cl $\mathrm{Et_3P}$ Cl	(52)	cis	2550.0	$*343.7_2$ $*386.4_1$ †501.2
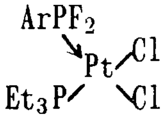 $\mathrm{ArPF_2}$ Pt Cl $\mathrm{Et_3P}$ Cl	(53)	cis	6252.1	124.0
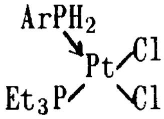 $\mathrm{ArPH_2}$ Pt Cl $\mathrm{Et_3P}$ Cl	(54)	cis	3809.1	-74.2
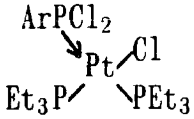 $\mathrm{ArPCl_2}$ Pt Cl $\mathrm{Et_3P}$ $\mathrm{PEt_3}$	(55)	trans	2885.8 ‡679.0	135.8
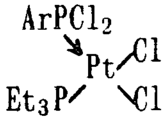 $\mathrm{ArPCl_2}$ Pt Cl $\mathrm{Et_3P}$ Cl	(56)	cis	5511.0	90.3
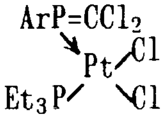 $\mathrm{ArP{=}CCl_2}$ Pt Cl $\mathrm{Et_3P}$ Cl	(57)	cis	5006.4	152.1
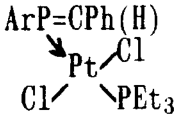 $\mathrm{ArP{=}CPh(H)}$ Pt Cl Cl $\mathrm{PEt_3}$	(58)	trans	2456.5 ‡569.5	178.6
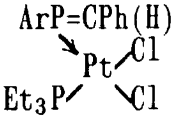 $\mathrm{ArP{=}CPh(H)}$ Pt Cl $\mathrm{Et_3P}$ Cl	(59)	cis	4599.6	149.6
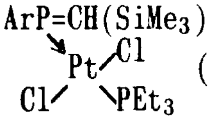 $\mathrm{ArP{=}CH(SiMe_3)}$ Pt Cl Cl $\mathrm{PEt_3}$	(60)	trans	3714.0 ‡787	245.1

Table 5.3: *Square-planar complexes obtained ; ‡$^2J(PP)$ coupling; *it is not possible to distinguish whether Pt is attached to P_1 or P_2; †$^1J(P_1P_2)$ coupling.*

Their facile synthesis involved the addition at ambient temperature of 0.5 equivalents of the cisplatinum (II) dimer $Cl_4Pt_2(PEt_3)_2$ to 1 equivalent of the phosphorus compound in CH_2Cl_2, with stirring. The formation of the diphosphene complex was interesting, since with Cl_2Pt-$(PhCN)_2$ at ambient temperature there was no evidence of coordination. The complexes (51)-(54),(56), (57) and (59) (Table 5.3) were obtained as crystalline white solids, and according to their ^{31}P NMR spectral data ($^1J_{PPt}$ large) have η^1-coordination and are all of *cis* configuration, deduced from their small $^2J_{PP_{cis}}$ coupling [44]. In general the crystals were soluble in $CDCl_3$. ^{31}P NMR data for some of these complexes is presented in Figure 5.2 (where the following abbreviations are used: T/C = *trans/cis* isomers, S = starting material, I = impurity). Figure 5.3 illustrates selected mass spectra for these platinum complexes. The high melting point before decomposition may be the reason for the observation of the important fragmentation ions including the molecular ion. The crystal structure of $ArPCl_2[PtCl_2(PEt_3)]$ (58) has been obtained (Figure 5.4).

The magnitude of $^1J_{PPt}$ in phosphine complexes has been shown to be proportional to the s-character of the phosphorus lone pair [26]. A further effect is that within complexes where the second phosphorus ligand is *cis* to PEt_3, the $^1J_{PPt}$ value is larger than when the two phosphorus ligands are *trans* to each other. In the latter case the ligands compete for electrons giving a strong *trans* influence [45] and hence reducing the $^1J_{PPt}$ coupling.

The sequence of phosphorus ligands in terms of increasing $^1J_{PPt}$ values (~2000 to ~7000) is as follows, for the *cis* square planar complexes:

$$\underset{(52)}{ArP{=}PAr'} < \underset{(51)}{ArP{=}PAr} < \underset{(54)}{ArPH_2} < \underset{(59)}{ArP{=}CH(Ph)} < \underset{(57)}{ArP{=}CCl_2} < \underset{(56)}{ArPCl_2} < \underset{(53)}{ArPF_2}$$

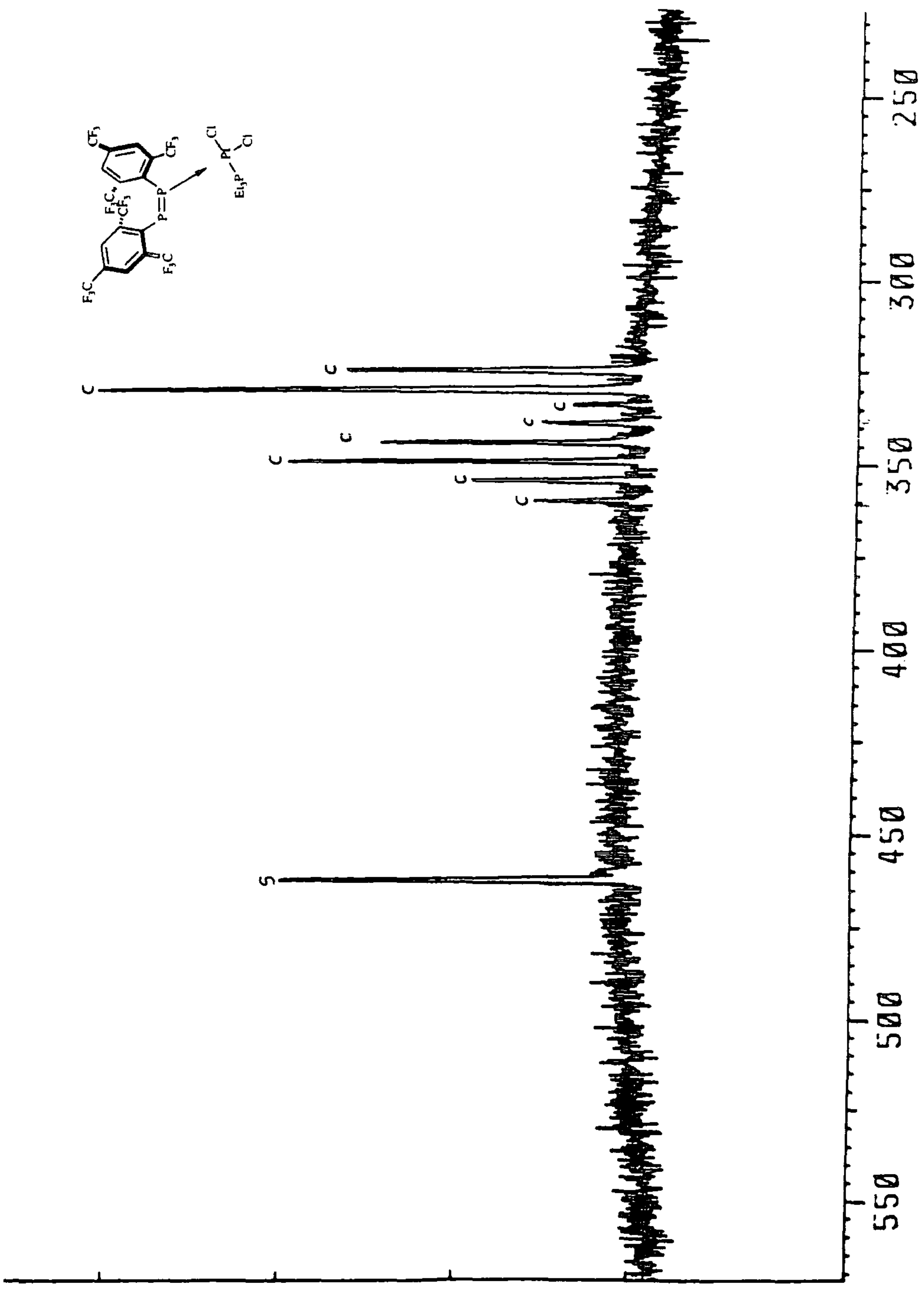

Figure 5.2a: ${}^{31}P$ *NMR spectrum of cis-ArP=PAr[PtCl$_2$(PEt$_3$)] (51) in CDCl$_3$; an expansion of the downfield region of the spectrum, nb. some diphosphene remains uncoordinated.*

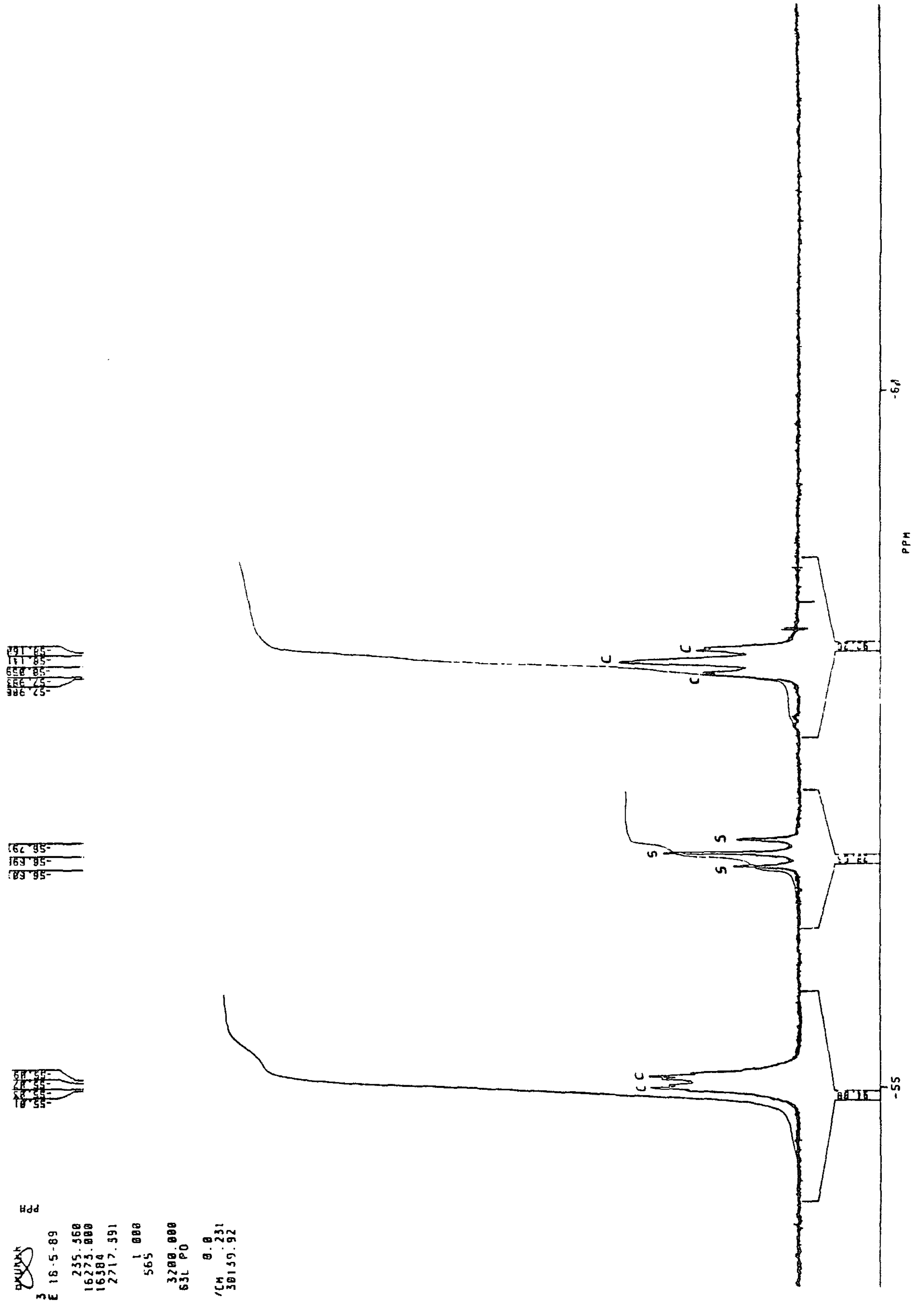

Figure 5.2b: ^{19}F *NMR spectrum of ArP=PAr[PtCl$_2$(PEt$_3$)] (51) in CDCl$_3$; an expansion of the signals due to the o-CF$_3$ groups.*

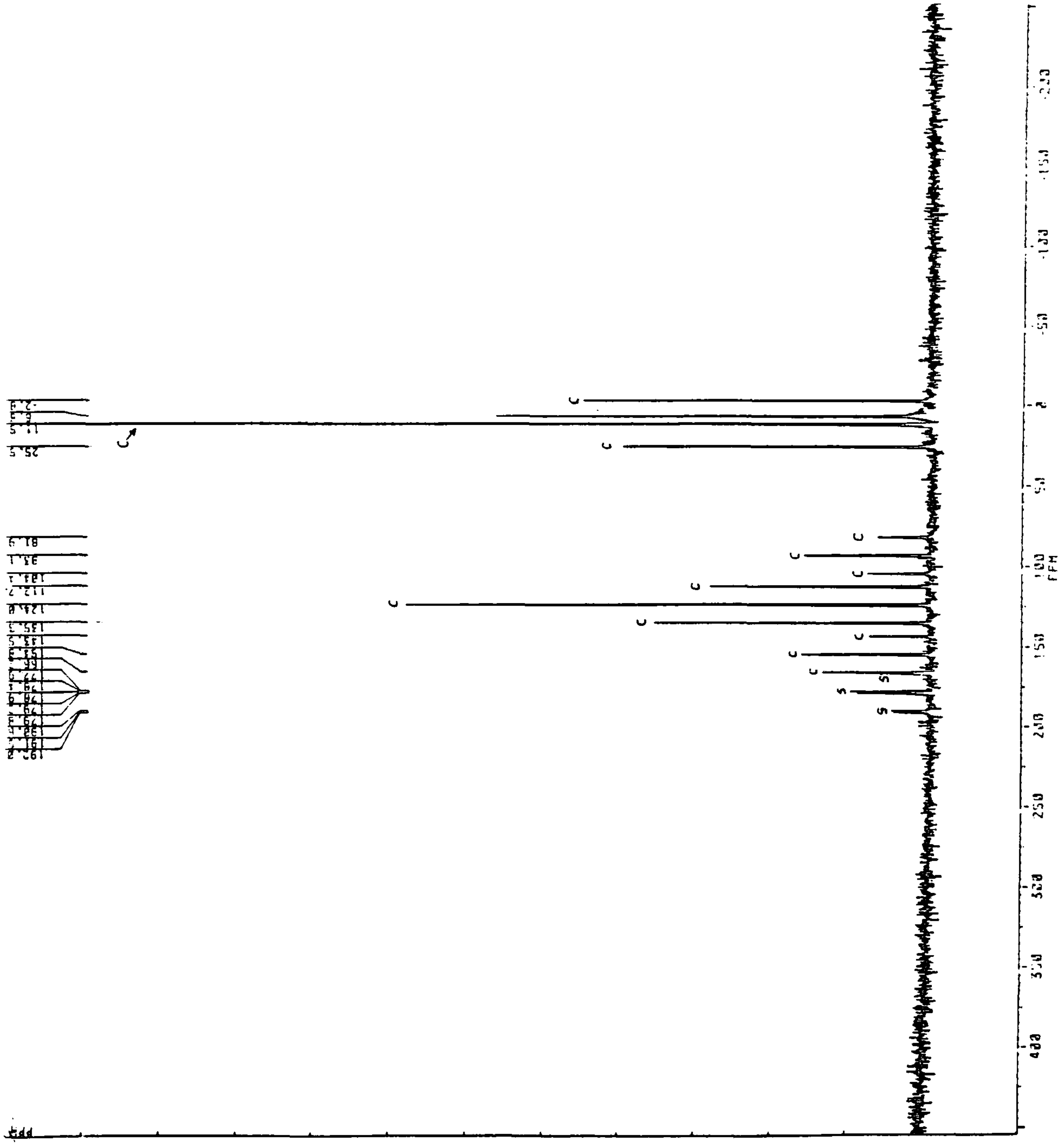

Figure 5.2c: ^{31}P NMR spectrum of cis-ArPF$_2$[PtCl$_2$(PEt$_3$)] (53) in CH$_2$Cl$_2$.

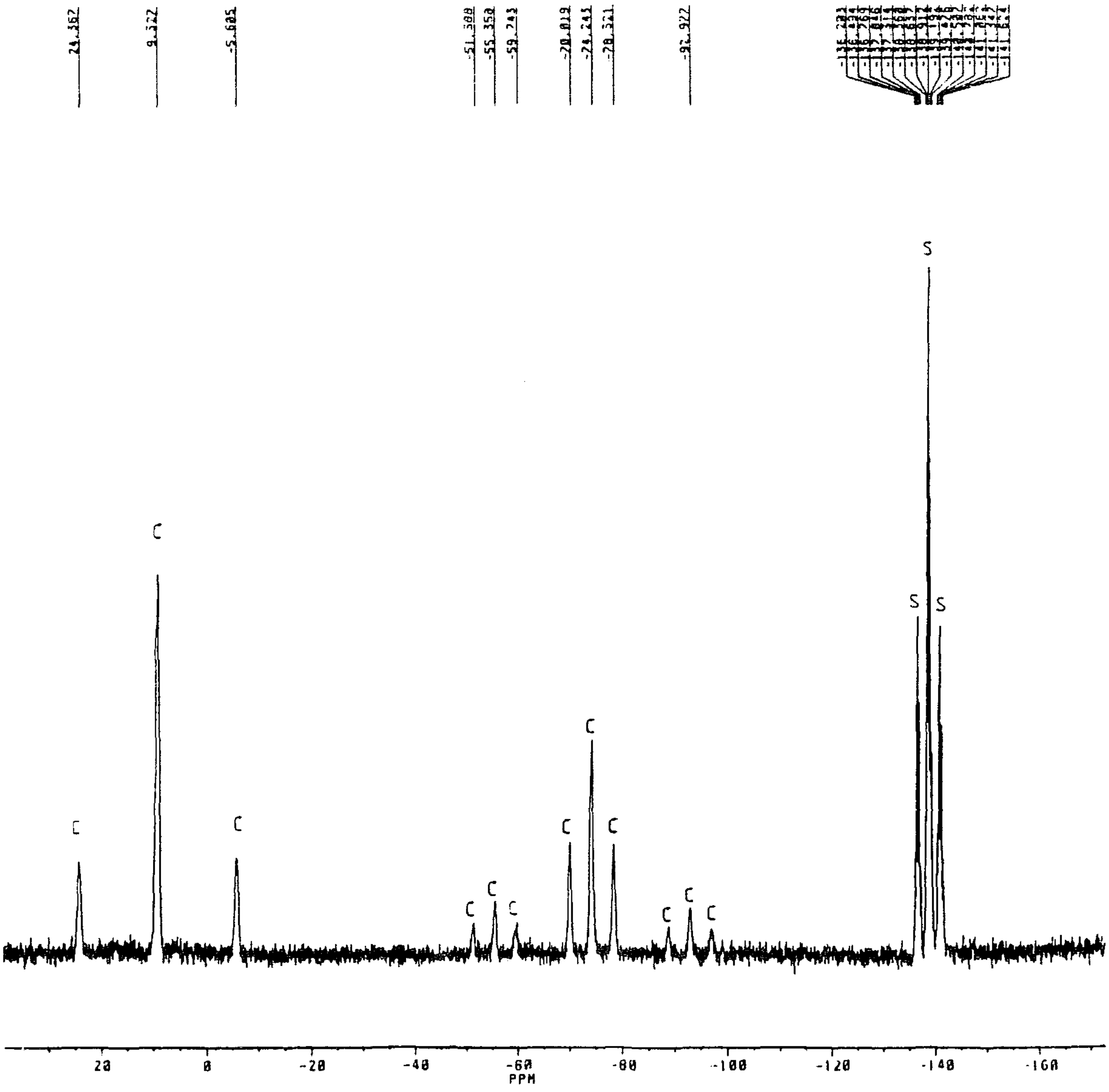

Figure 5.2d: ^{31}P *NMR spectrum of cis-*$ArPH_2[PtCl_2(PEt_3)]$ *(54) in* $CDCl_3$*; coupled to hydrogen.*

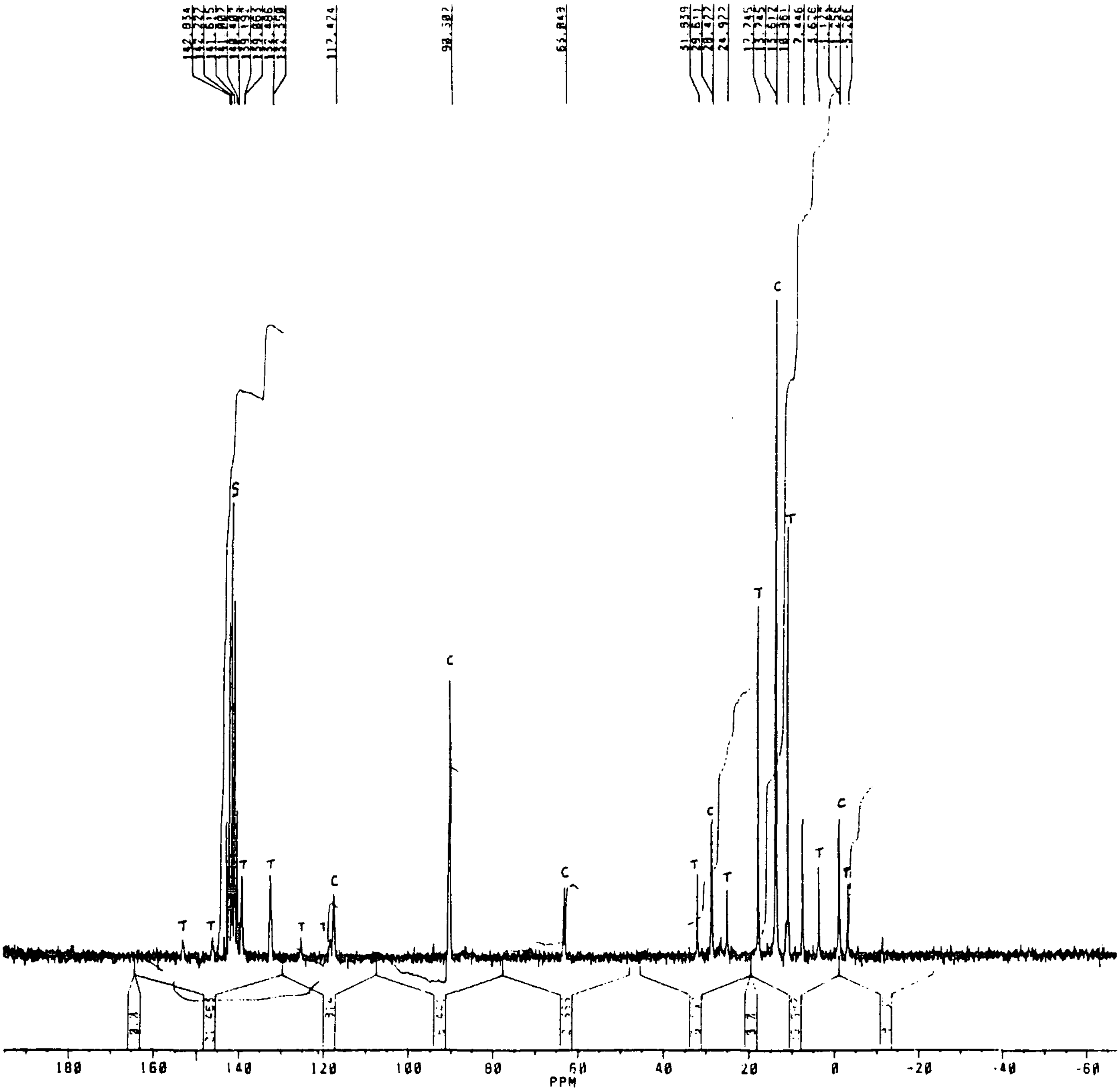

Figure 5.2e: ^{31}P *NMR spectrum of* $ArPCl_2[PtCl_2(PEt_3)]$ *(55) and (56) in* $CDCl_3$*; illustrates the presence of the trans isomer (55) and the cis isomer (56).*

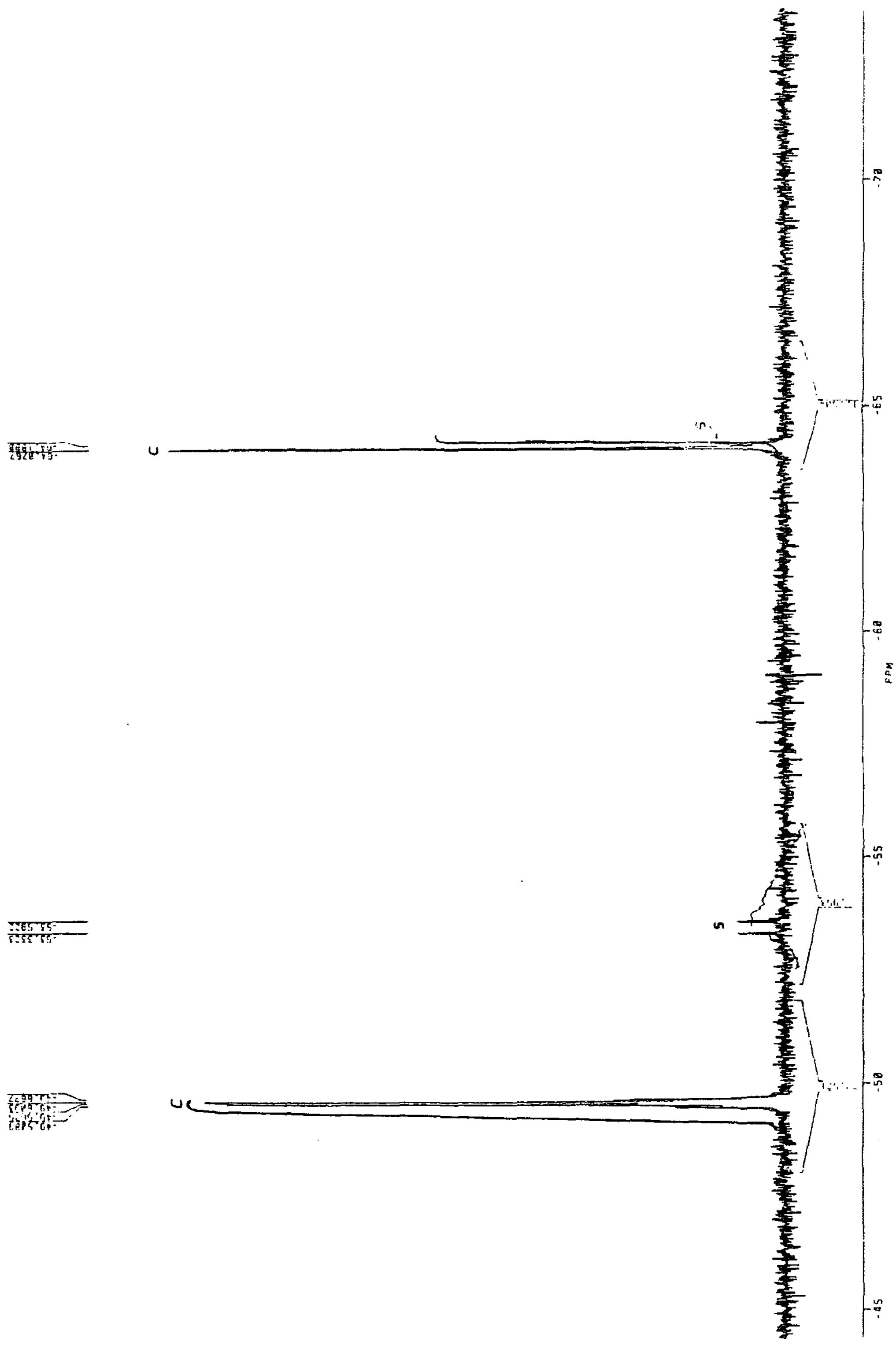

Figure 5.2f: ^{19}F NMR spectrum of cis-ArPCl$_2$[PtCl$_2$(PEt$_3$)] (56) in CDCl$_3$.

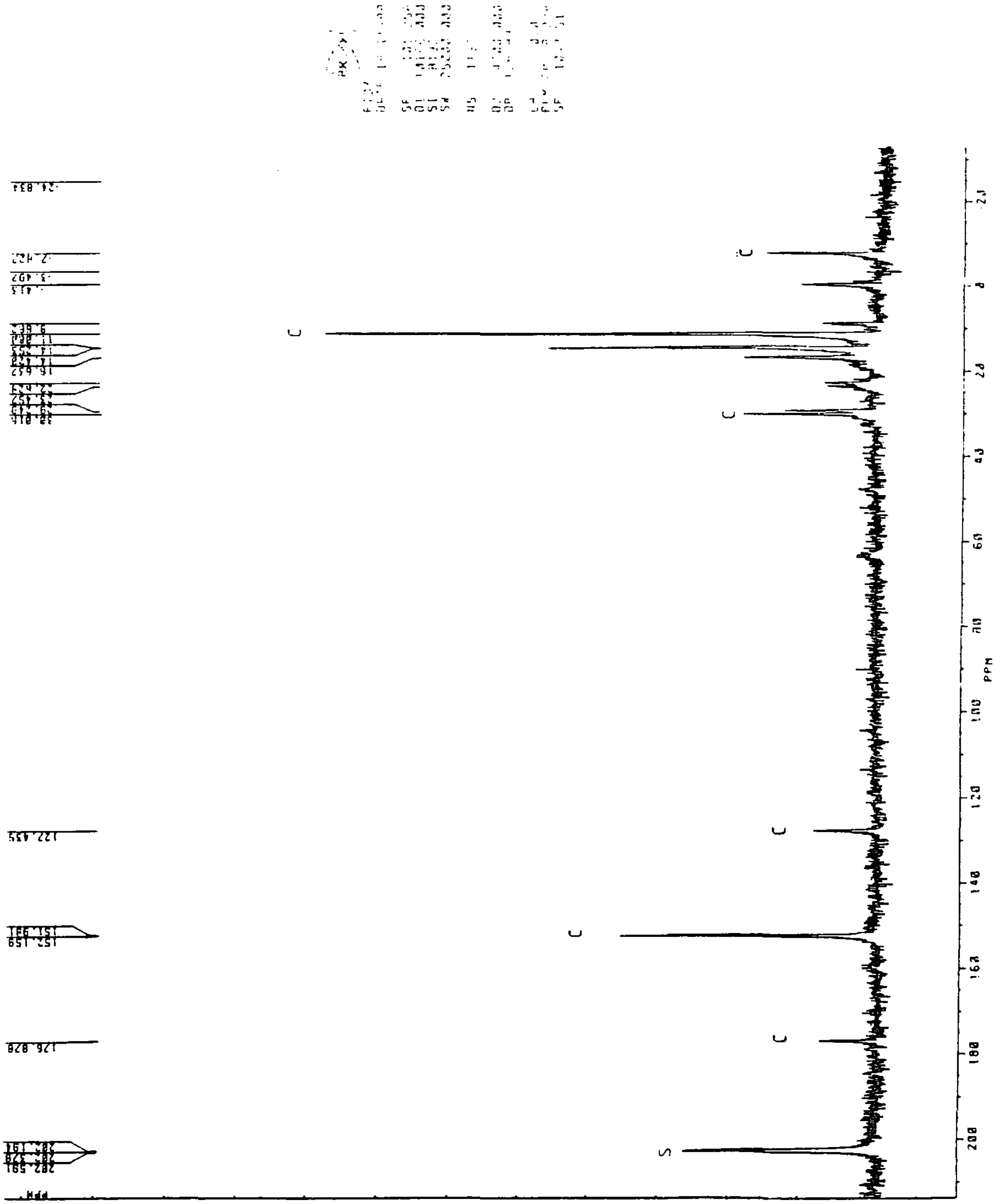

Figure 5.2g: ^{31}P *NMR spectrum of* $cis\text{-}ArP{=}C(Cl)_2[PtCl_2(PEt_3)]$ *(57) in* $CDCl_3$.

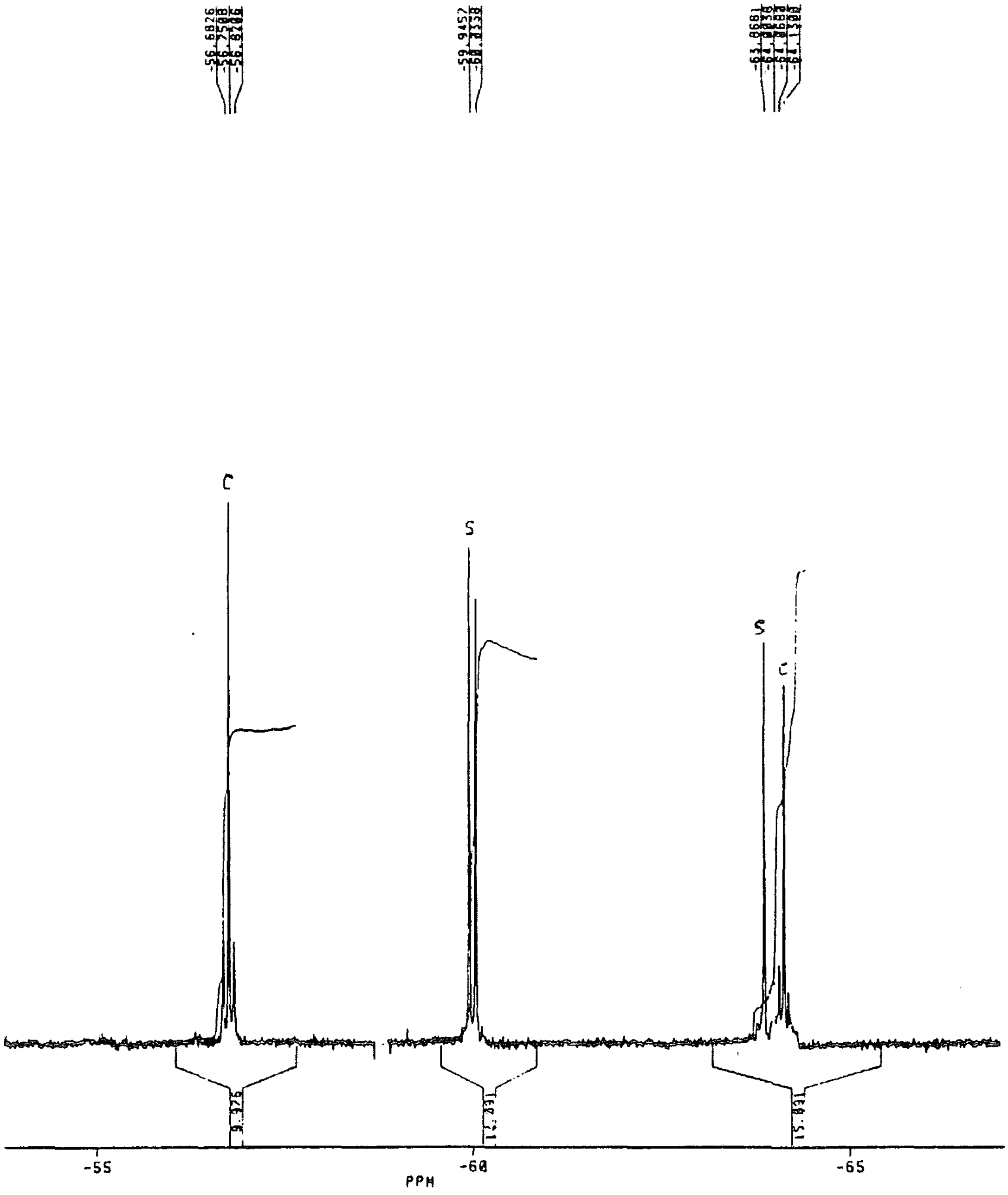

Figure 5.2h: ^{19}F *NMR spectrum of cis-ArP=C(Cl)$_2$[PtCl$_2$(PEt$_3$)] (57) in CDCl$_3$.*

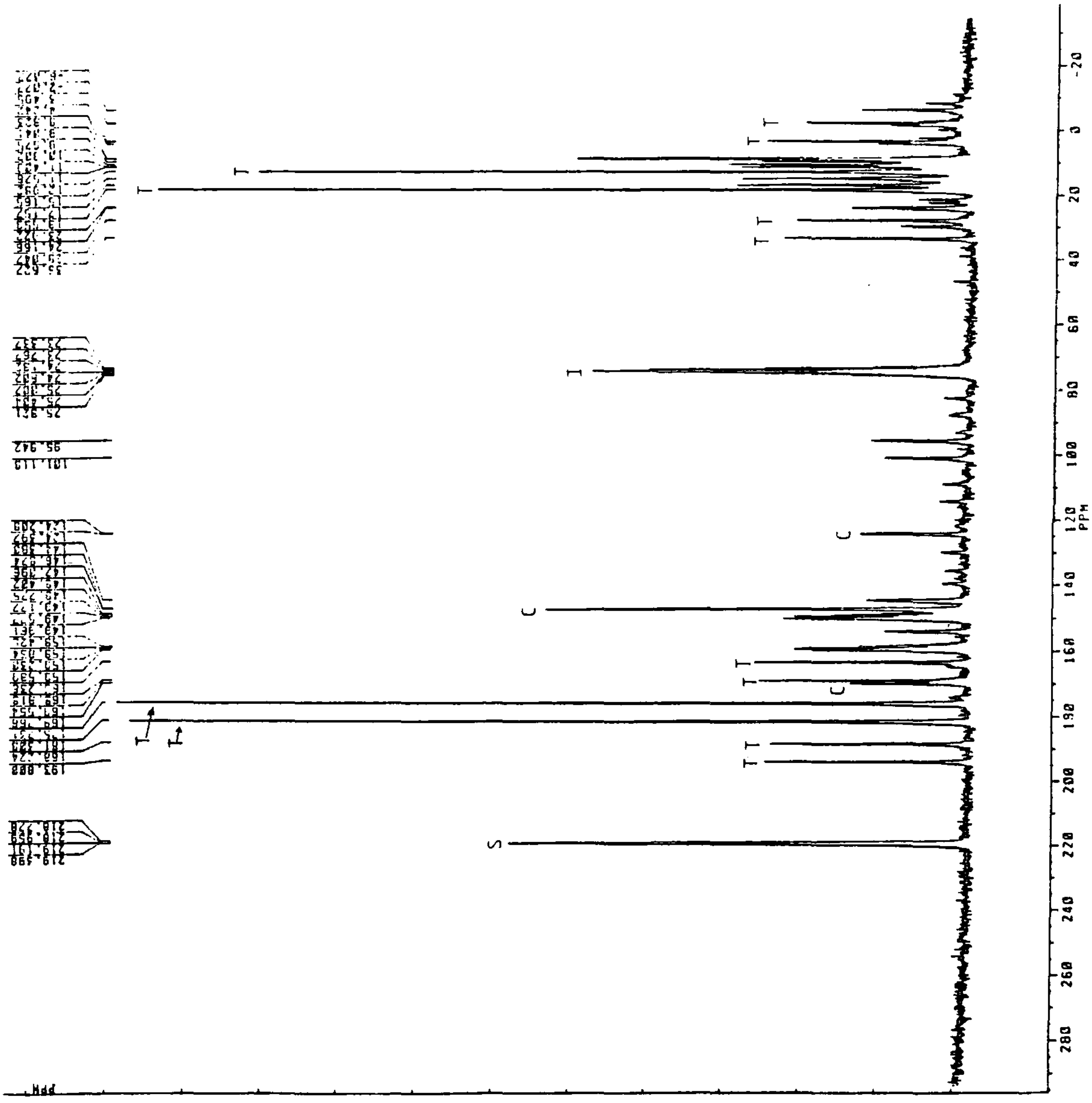

Figure 5.2i: ^{31}P NMR spectrum of $ArP=C(Ph)(H)[PtCl_2(PEt_3)]$ (58) and (59) in THF; both the trans isomer (58) and the cis isomer (59) are present.

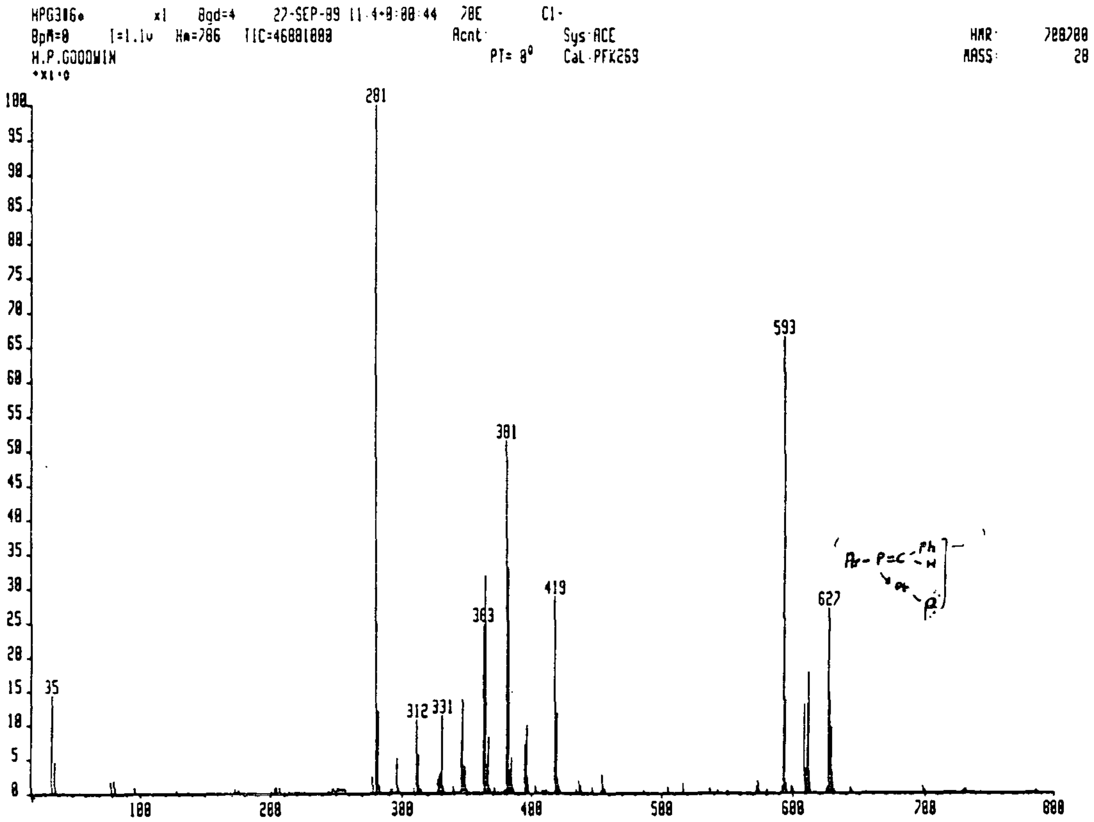

Mass	% Base
34.93	14.29
36.93	4.40
78.87	1.72
80.87	1.86
95.86	0.82
127.83	0.37
172.94	0.62
174.96	0.37
200.85	0.37
202.81	0.83
204.81	0.89
206.82	0.71
244.82	0.30
244.89	0.31
246.71	0.21
246.82	0.61
248.77	0.68
250.69	0.21
250.78	0.71
252.73	0.37
252.81	0.63
254.75	0.41
254.84	0.59
256.81	0.45
277.94	2.34
280.23	0.38
280.94	100.00
281.95	11.84
282.96	1.02
290.80	0.49
292.81	0.38
294.89	0.23
296.94	4.98
297.93	0.52
298.03	0.27
308.95	0.73
311.92	10.67
312.93	5.45
313.96	0.32
314.95	0.40
326.95	0.30
327.92	1.98
328.98	0.49
329.91	2.71
330.92	11.27
331.91	0.79
339.08	0.71
344.93	0.37
345.88	7.24
346.90	13.55
347.89	3.75
348.89	3.68
349.89	0.25
362.89	24.55
363.89	2.16
364.88	31.71
365.88	3.89
366.89	8.00
367.88	0.47
370.99	0.79
378.89	0.42
379.96	0.34
380.86	51.35
381.86	5.04
382.85	32.74
383.86	3.17
384.86	5.07
385.88	0.65
395.18	6.94
396.18	9.79
397.17	2.14
402.98	0.95
408.92	0.28
411.23	0.24
418.98	28.59
420.00	11.50
421.00	1.95
422.00	0.71
434.96	0.68
436.96	1.65
437.99	0.99
447.18	0.75
453.92	0.32
454.96	2.57
455.96	0.44
457.00	0.45
486.02	0.34
504.98	0.83
516.94	1.44
536.86	0.32
536.98	0.56
542.98	0.28
543.05	0.30
550.00	0.34
571.99	0.89
572.97	0.37
573.97	1.67
580.15	0.40
591.98	0.93
592.35	0.23
592.99	66.25
593.99	13.48
595.00	1.44
599.16	0.87
600.18	0.76
608.99	12.80
610.00	3.26
610.98	12.67
611.99	17.80
612.98	3.10
625.01	0.82
626.96	26.82
627.98	14.51
628.96	9.38
629.98	2.81
630.97	0.40
643.01	0.83
643.98	0.34
699.09	0.90
700.02	0.27

Figure 5.3a: *The mass spectrum of* '$ArP=C(Ph)(H)[PtCl_2(PEt_3)]$' *(59)*

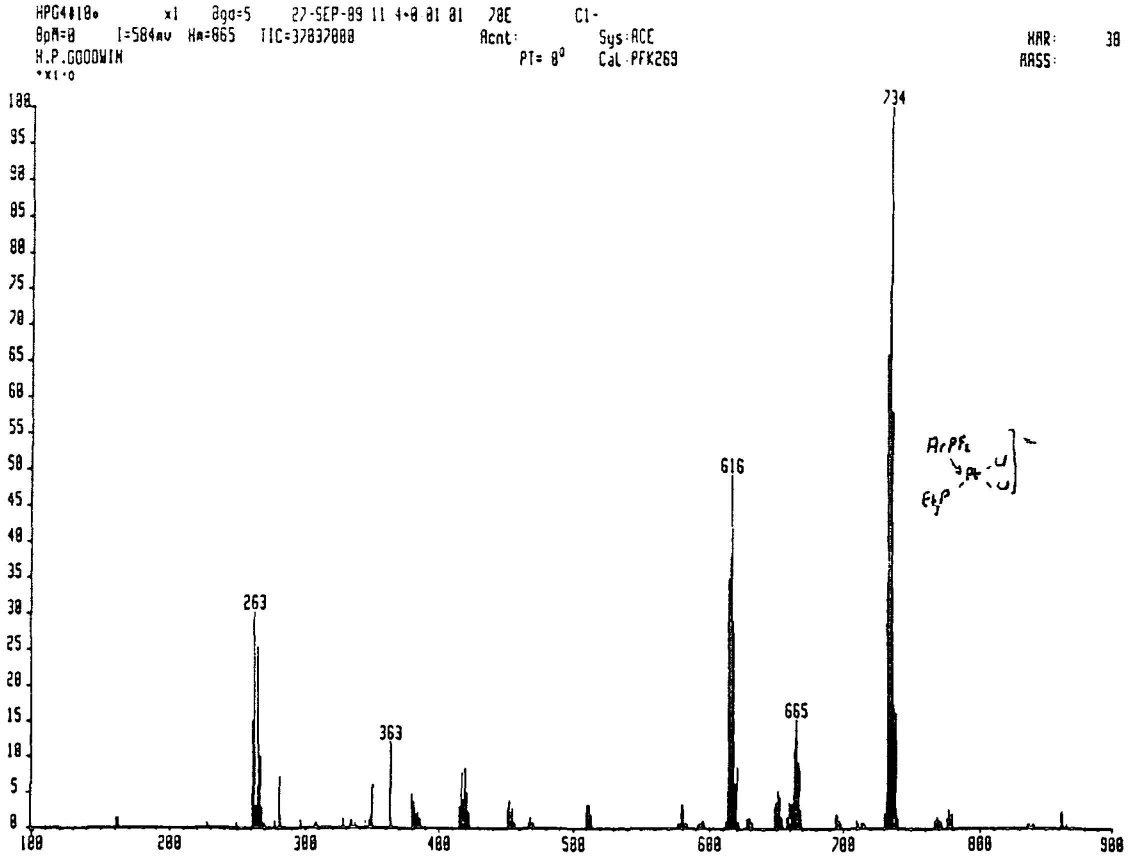

Mass	% Base	
336.83	0.60	
344.89	0.84	
346.90	0.84	
348.87	1.70	
349.88	5.90	
362.87	12.01	
363.90	1.17	
378.82	4.75	
379.85	0.78	
380.82	3.65	
381.85	2.77	
382.87	1.75	
383.86	2.14	
384.88	1.28	
385.89	1.15	
414.79	2.92	
416.84	7.73	
417.87	3.78	
418.86	8.27	
419.87	4.54	
420.86	4.88	
421.86	1.85	
422 88	2.14	
450.90	2.38	
451.88	2.79	
452.89	3.78	
453.87	2.19	
454.88	2.66	
456 78	0 78	
466.88	0.65	
467.89	0.57	
468.88	1.44	
469.88	0.57	
470.89	0.57	
509.86	2.11	
510.86	3.21	
511.87	3.24	
512.87	0.99	
513.87	1.77	
576.81	0.60	
576.91	0.68	
577.82	0.68	
578.86	2.17	
579.88	3.24	
580.85	2.56	
581.89	0.52	
582.79	0.57	
582.94	0.63	
591.74	0.47	
592.95	0.52	
593.84	0.68	
594.84	0.94	
595.80	0.55	
595.93	0.89	
611.85	0.97	
613.84	34.77	
614.84	37.82	
615.84	49.26	
616.84	27.51	
617.84	28.74	
618.84	6.11	
619.85	8.54	
620.80	0.70	
620.94	0.55	
621.87	0.94	
628.02	1.15	
629.00	1.28	
629.99	1.44	
631.04	0.70	
631.95	0.78	
648.83	2.92	
649.84	3.55	
650.84	5.22	
651.84	3.26	
652.85	4.18	
653.83	0.94	
654.85	1.49	
657.82	1.46	
658.83	1.33	
659.84	3.60	
660.85	3.37	
661.84	2.66	
662.98	10.96	
663.98	12.27	
664.99	15.14	
665.99	9.08	
667.00	8.09	
667.99	2.14	
669.00	2.40	
694.02	1.36	
694.99	1.88	
696.00	1.75	
696.87	0.89	
697.08	0.70	
697.97	0.50	
698.14	0.78	
710.01	0.97	
710.92	0.65	
712.97	0.68	
713.97	0.68	
714.94	0.60	
715.94	0.34	
730.04	1.96	
731.02	1.49	
732.02	65.73	
733.01	74.52	F
734.02	100.00	F
735.02	54.53	
736.02	57.95	
737.04	17.07	
738.04	[illegible]5.00	
739.03	2.53	
740.05	1.38	
767.08	0.97	
768.01	0.99	
769.01	1.49	
769.97	1.04	
771.04	0.76	
771.96	0.86	
772.88	0.55	
773.06	0.34	
776.02	1.44	
776.88	0.86	
777.15	1.31	
778.00	2.61	
779.00	1.72	
780.03	2.04	
835.67	0.52	
836.85	0.47	
839.84	0.50	
840.83	0.44	
861.33	1.77	
862.35	2.30	
863.43	1.62	
865.39	0.44	
865.54	0.44	

Figure 5.3b: *The mass spectrum of* $ArPF_2[PtCl_2(PEt_3)]$ *(53)*

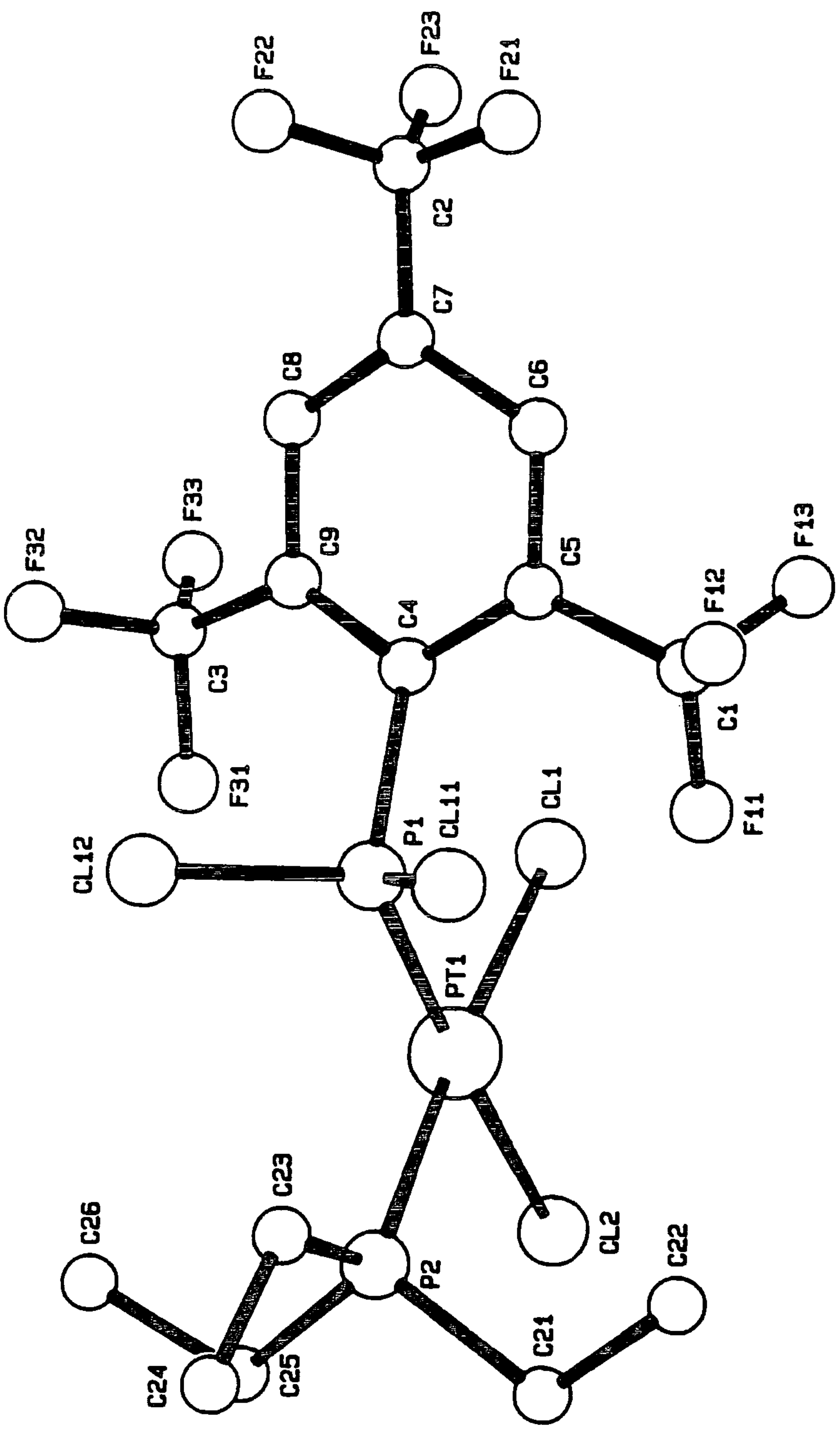

Figure 5.4a: *The crystal structure of* $ArPCl_2[PtCl_2(PEt_3)]$ *(58); the cis conformation is evident; Bond lengths: Pt-Cl(1) = 2.349Å, slightly longer than Pt-Cl(2) (2.322Å); Pt-P(1) = 2.162Å, slightly shorter than Pt-P(2) (2.263Å) and characteristic of* η^1*-coordination.*

Tabelle	Kristall- und Verfeinerungsdaten
Verbindung	DILLON5
Kristallsystem	monoklin
Raumgruppe	P2(1)/C
a	13.984(3)
b	13.876(3)
c	14.620(3)
alpha	90.00
beta	107.85(3)
gamma	90.00
Volumen	2700.3(22)
Z	4
F(000)	1488
M	783.14
D(ber)	1.93
Kristallgroesse (mm)	0.25x0.20x0.10
Messtemperatur (C)	20
Strahlung	Mo-Kalpha
Wellenlaenge	0.71073
Absorptionskoeffizient	58.337
Absorptionskorrektur	empirisch
Maximale Transmission (%)	40.18
Minimale Transmission (%)	26.17
Scan-Methode	Omega-Scan
2Theta-Messbereich	3.00 bis 45.00
[sin(theta)/lamna]max	0.538
hkl-Messbereich	-14, 14/ 0, 14/-15, 0
Messgeschwindigkeit	1.16 bis 5.03
Reflexbreite	0.96 + 0.35tan(theta)
gemessene Reflexe	3652
beobachtete Reflexe	2862
Ablehnungskriterium	Tobs < 2.00sig(Tobs)
R(int)	0.037
Parameterzahl	281
R	0.056
Rw	0.058
Instabilitaetsfaktor p	0.014
Letzter Shift/esd	0.02
Restelektronendichte	2.25

Figure 5.4b: *Crystal packing data for* $ArPCl_2[PtCl_2(PEt_3)]$ *(58)*

Tabelle
----

i Bindungslaengen (Å)

CL(1)	-PT(1)	2.349(5)	CL(2)	-PT(1)	2.322(5)
P(1)	-PT(1)	2.162(5)	P(2)	-PT(1)	2.263(5)
P(1)	-CL(11)	2.006(8)	P(1)	-CL(12)	2.016(9)
C(4)	-P(1)	1.866(20)	C(21)	-P(2)	1.859(20)
C(23)	-P(2)	1.807(19)	C(25)	-P(2)	1.841(21)
C(1)	-F(11)	1.303(34)	C(1)	-F(12)	1.363(31)
C(1)	-F(13)	1.340(38)	C(2)	-F(21)	1.316(4)
C(2)	-F(22)	1.316(4)	C(2)	-F(23)	1.316(4)
C(3)	-F(31)	1.305(24)	C(3)	-F(32)	1.334(25)
C(3)	-F(33)	1.276(28)	C(5)	-C(1)	1.554(39)
C(7)	-C(2)	1.510(1)	C(9)	-C(3)	1.496(31)
C(5)	-C(4)	1.326(29)	C(9)	-C(4)	1.380(29)
C(6)	-C(5)	1.420(29)	C(7)	-C(6)	1.440(32)
C(8)	-C(7)	1.373(29)	C(9)	-C(8)	1.386(28)
C(22)	-C(21)	1.561(33)	C(24)	-C(23)	1.544(26)
C(26)	-C(25)	1.515(33)			

Tabelle
----

ii Bindungswinkel (°)

CL(2)	-PT(1)	-CL(1)	88.3(2)	P(1)	-PT(1)	-CL(1)	87.4(2)
P(1)	-PT(1)	-CL(2)	176.2(2)	P(2)	-PT(1)	-CL(1)	173.6(2)
P(2)	-PT(1)	-CL(2)	84.9(2)	P(2)	-PT(1)	-P(1)	98.9(2)
CL(11)	-P(1)	-PT(1)	116.3(3)	CL(12)	-P(1)	-PT(1)	117.8(3)
CL(12)	-P(1)	-CL(11)	97.6(4)	C(4)	-P(1)	-PT(1)	119.5(7)
C(4)	-P(1)	-CL(11)	101.0(7)	C(4)	-P(1)	-CL(12)	100.5(7)
C(21)	-P(2)	-PT(1)	111.4(8)	C(23)	-P(2)	-PT(1)	118.0(6)
C(23)	-P(2)	-C(21)	105.3(10)	C(25)	-P(2)	-PT(1)	108.3(8)
C(25)	-P(2)	-C(21)	105.4(11)	C(25)	-P(2)	-C(23)	107.7(10)
F(12)	-C(1)	-F(11)	106.6(27)	F(13)	-C(1)	-F(11)	111.7(30)
F(13)	-C(1)	-F(12)	102.8(27)	C(5)	-C(1)	-F(11)	114.8(26)
C(5)	-C(1)	-F(12)	108.5(27)	C(5)	-C(1)	-F(13)	111.6(28)
F(22)	-C(2)	-F(21)	109.3(4)	F(23)	-C(2)	-F(21)	109.4(4)
F(23)	-C(2)	-F(22)	109.4(4)	C(7)	-C(2)	-F(21)	109.4(4)
C(7)	-C(2)	-F(22)	109.6(4)	C(7)	-C(2)	-F(23)	109.6(4)
F(32)	-C(3)	-F(31)	105.8(19)	F(33)	-C(3)	-F(31)	107.7(22)
F(33)	-C(3)	-F(32)	108.0(23)	C(9)	-C(3)	-F(31)	112.7(21)
C(9)	-C(3)	-F(32)	108.9(21)	C(9)	-C(3)	-F(33)	113.3(19)
C(5)	-C(4)	-P(1)	120.3(18)	C(9)	-C(4)	-P(1)	119.5(15)
C(9)	-C(4)	-C(5)	118.6(19)	C(4)	-C(5)	-C(1)	124.7(22)
C(6)	-C(5)	-C(1)	109.5(24)	C(6)	-C(5)	-C(4)	124.7(23)
C(7)	-C(6)	-C(5)	117.0(21)	C(6)	-C(7)	-C(2)	120.8(13)
C(3)	-C(7)	-C(2)	124.6(14)	C(8)	-C(7)	-C(6)	114.4(15)
C(9)	-C(8)	-C(7)	126.0(21)	C(4)	-C(9)	-C(3)	129.2(19)
C(8)	-C(9)	-C(3)	112.0(21)	C(8)	-C(9)	-C(4)	117.6(21)
C(22)	-C(21)	-P(2)	108.3(15)	C(24)	-C(23)	-P(2)	112.9(14)
C(26)	-C(25)	-P(2)	110.1(17)				

Figure 5.4c: *(i) Bond lengths and (ii) bond angles for* $ArPCl_2[PtCl_2(PEt_3)]$ *(58).*

As has been discussed above all the compounds which have been isolated here appear to be square planar and of *cis* η^1-conformation.[1] With the phosphines $ArPH_2$ (15), $ArPF_2$ (3) and $ArPCl_2$ (12), it is only in the latter case that an initial observation of the *trans* isomer [Figure 5.2(e)] was observed in the ^{31}P NMR, possibly attributed to the increased crowding around phosphorus in this species, with non-bonded repulsions being reduced in the *trans* configuration. It would be of interest to extend this investigation to the coordination of Ar_2PCl (14). A similar behaviour is observed for ArP=CH(Ph) and $ArP{=}CH(SiMe_3)$ [see Figure 5.2(i)] and has been shown in other examples [26,46]. The ^{31}P NMR data on the *trans* complex of $ArP{=}CH(SiMe_3)$ (60) was obtained after a period of 6 hours in solution. It would have been interesting to record the data following a longer time period. In these examples [Figures 5.2(e,i)] the initial magnitude of $^{1}J_{PPt}$ and $^{2}J_{PP_{cis}}$ lie in the expected range for mutually *trans* PR_3 ligands attached to Pt(II) [26,46].

With the diphosphenes Ar_2P_2 (19) and $ArAr'P_2$ (20) only the η^1 *cis* isomers are observed, similarly with the phosphaalkene $ArP{=}CCl_2$ (31). It is possible that the *trans* isomer is favoured kinetically in all these reaction but is not observed where a possible rapid rate of conversion to the *cis* form occurs. It has been well established that the *cis* isomer is the thermodynamically more stable [26,47]. This is attributed to the more effective overlap of the d-orbital at the metal centre in the *cis* configuration than in the *trans*. An interesting example where no isomerisation to the cis form occurs, thought to be due to the steric demand of the substituents, is illustrated in Figure 5.5 [48].

---

[1] **Spectroscopic characteristics**: η^1: $^{1}J(PtP)$ large, small change in the ^{31}P chemical shift; η^2: large coordination shift, small $^{1}J(PPt)$. The greater shielding is attributed to a rise in electron concentration at the phosphorus resulting from the π-back donation from metal to phosphorus, decreasing the s-contribution to the bonding between Pt and P.

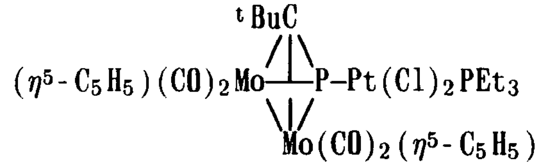

$$(\eta^5\text{-}C_5H_5)(CO)_2Mo(\mu\text{-}C^tBu)(\mu\text{-}P\text{-}Pt(Cl)_2PEt_3)Mo(CO)_2(\eta^5\text{-}C_5H_5)$$

Figure 5.5: *Square planar complex retaining the trans configuration.*

5.2.2 The Pt(II) Complex of the Symmetrical Diphosphene

The ^{19}F NMR of the η^1 square planar complex of the symmetrical diphosphene is particularly interesting. Figures 5.2(a,b) illustrate the ^{19}F and ^{31}P expansion at P(1&2)(51). An apparent $^{9}J_{FF}$ coupling may be observed between the fluorine atoms on C_A and C_B (Figure 5.6) (a through-space effect), with the fine coupling observed in Figure 5.2(b). This observation may be interpreted as inferring a "Z" configuration in the complex (Figure 5.6). However, it may also be the result of a secondary spectrum caused by fluorine coupling with platinum.

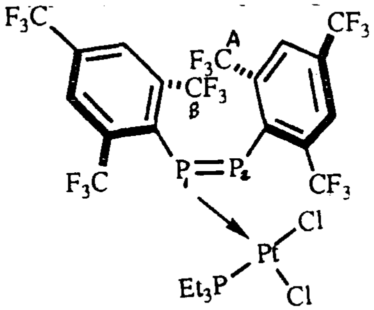

Figure 5.6: *Proposed configuration of η^1-coordinated Ar_2P_2 (51).*

The isomerisation to the Z form postulated may be a result of the lowering of the barrier to isomerisation on coordination[49]. Beautiful crystals could be grown, a sample of which has been submitted for X-ray crystal structure determination. From the ^{19}F and ^{31}P NMR data on the unsymmetrical species ArP=PAr' it was not possible to determine which phosphorus was coordinated. Crystals were obtained but unfortunately these proved to be unsuitable for X-ray analysis.

In previous examples [10] the reaction of a metal fragment, for example $M(CO)_5$, with an unsymmetrical diphosphene has resulted in coordination to the less hindered site (*eg*. Equation 5.1).

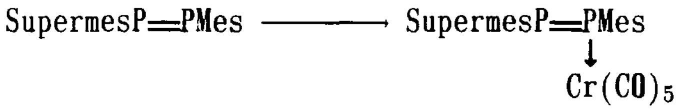

$$\text{SupermesP}{=}\text{PMes} \longrightarrow \text{SupermesP}{=}\underset{\displaystyle \text{Cr(CO)}_5}{\underset{\downarrow}{\text{PMes}}} \qquad (5.1)$$

However the MNDO calculation on the species ArP=PAr' (20) suggests the more positive charge resides on the phosphorus with the smaller group attached. It may therefore be anticipated that in this situation coordination to the more sterically hindered phosphorus may be observed.

5.3 PHOSPHORUS LIGAND COMPLEXES OF Pt(0) COMPOUNDS

5.3.1 Introduction

The aim of this part of the work was to investigate a possible η^2 mode of coordination for the symmetrical diphosphene (19). This involved the reaction of the diphosphene Ar_2P_2 (19) with a Pt(0) complex [*cf*. Section 5.2, η^1 diphosphene coordination with Pt(II)].

A broad overview of some examples where specific conditions have influenced a particular coordination mode is presented here. Calculations on the theoretical model compound $(H_3P)_2PtH_2$ [50] showed that it is the d_{xz} orbital on platinum which is responsible for electron transfer from the metal *via* π back-bonding to the π^*-orbital of "the ligand" PH_3 in both the η^1 and η^2 bonding modes.

(1) Changing ligands on the coordinating metal to decrease the L-M-L interligand bond angle activates effectively and selectively the d_{xz} metal orbital. This transfers electrons to the reactant H_2 with the effect that the Pt-H bonds are strengthened [50]. It can

be deduced that the larger interligand bond angle, imposed by a change from PPh_3 in $Pt(PPh_3)_2MesP{=}CPh_2$ to the more sterically demanding PCy_3 ligand, stabilises the d_{xz} orbital of the PtL_2 fragment to the effect of decreasing the π-back donation component in Pt⋯P=C hence η^1 predominates (Figure 5.7) [50].

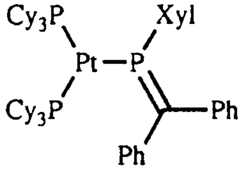

Figure 5.7: *A phosphaalkene in η^1-coordination mode.*

Alternatively, reducing the L-M-L angle results in extensive electron transfer from the destabilised Pt d_{xz} orbital to the π^* orbital of P=C in a square planar complex. This can be achieved by the use of a chelating ligand with a suitable bite angle. For example *bipy* N-Ni-N (Figure 5.8) [31,50].

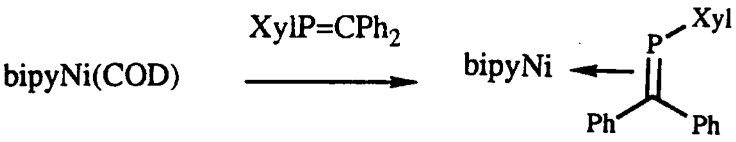

Figure 5.8: *A phosphaalkene in η^2-coordination mode; COD = 1,5-cyclooctadiene; Xyl = 2,6-dimethylphenyl; Bipy = 2,2'-bipyridine.*

This example combines the smallest L-M-L interligand bond angle with the largest P=C bond lengthening, indicating an extensive π-backbonding component.

(2) Ligands with π-acceptor properties on the metal, for example CO, reduce the ability of the metal to interact datively with the π^* LUMO of the phosphaalkene destabilising η^2, *eg*. $Ni(CO)_3[\eta^1\text{-}XylP{=}C(Ph)_2]$. Weakly π-accepting ligands *eg* bipy, promote η^2 (Figure 5.8) [50].

(3) Metal oxidation state. The lower the oxidation state of the metal (electron rich) the greater the electron donation from the metal d_{xz} orbital to the π^* orbital of the "ligand" (*eg*. P=C, P=P) favouring η^2.

(4) Changing the nature of the ligand on the phosphaalkene. When the $(PPh_3)_2Pt$ unit is kept constant, but the relative accessibility of $\sigma(P)$ and $\pi(P{=}C)$ is influenced by a change in the phosphaalkene stereochemistry, the η^1/η^2 balance is disturbed [39,50]. Example (A) illustrates η^2 bonding (Figure 5.9), the η^1 bonding mode is less favourable than in (B) because of repulsion between the fluorene H(1) or H(8) and $Pt(PPh_3)_2$.

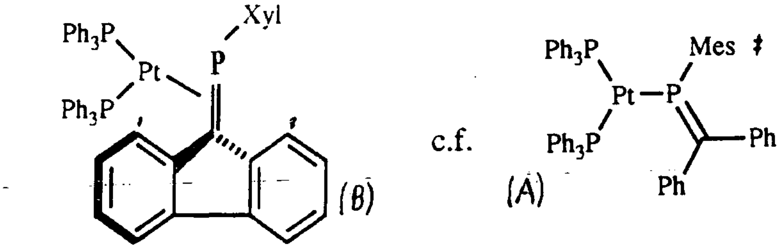

Figure 5.9: *Examples of η^1 (A) and η^2 (B) coordination modes in phosphaalkenes; ‡in the solid state.*

An example whereby the ligands on the metal were designed specifically to promote η^1-coordination of a phosphaalkyne is in the displacement of dinitrogen by Bu$C{\equiv}P$ from *trans*-$[M(N_2)_2\cdot(R'_2PCH_2CH_2PR'_2)_2]$ (M ≡ Mo, R ≡ ^tBu, R' ≡ p-ClC_6H_4) [51].

5.3.2 The Reaction of Pt(0)-Complex (61) with Ar_2P_2 (19)

The Pt(0) species (61) used in the reaction with the symmetrical diphosphene Ar_2P_2 (19) is shown in Figure 5.10. This zero-valent Pt-ethene complex of 2,2-dimethyl-4,5-bis(diphenylphosphinomethyl)-1,3-dioxolan has recently been applied as a chiral derivatising agent for the ^{31}P NMR assay of the enantiomeric purity of certain alkenes and allenes [52].

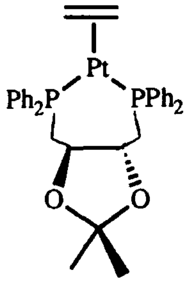

Figure 5.10: *Pt(0) complex (61).*

This complex was used primarily because of its availability. The presence of a chelating ligand and the metal oxidation state of zero, act to favour η^2-coordination [discussed in Section 5.3.1, (1) and (3)]. The mixture of the Pt(0) complex and the diphosphene was stirred at ambient temperature in THF. To obtain any evidence of coordination gentle heating to 35 ^oC was necessary. The results obtained were not conclusive, however, as an unresolved peak was obtained at +251 ppm in the ^{31}P NMR. This was attributed to η^2-coordination, giving a characteristic upfield shift, and a corresponding decrease in the $^1J_{PPt}$ coupling. In this instance since the expected value of $^1J_{PPt}$ was ~60 Hz, resolution would not be observed with a sweep width of 500ppm (23.50 ppm cm^{-1}). This compound did not appear to be stable in solution. Decomposition to $ArPH_2$ and other reduction products was evident, with the probable formation of metallic Pt(0), since a grey solid was seen to precipitate in the reaction vessel. The preliminary stages of this area of work show some promise and could be developed with the aim of isolating the product, and varying the nature of the Pt(0) species used.

5.4 COORDINATION CHEMISTRY OF THE BORON/PHOSPHORUS CONTAINING NITRILEIMINE

The reaction of the boron-phosphorus containing nitrileimine (62) (Chapter 11) with the Pt(II) complex $(PEt_3)_2Pt_2Cl_4$ was carried out with

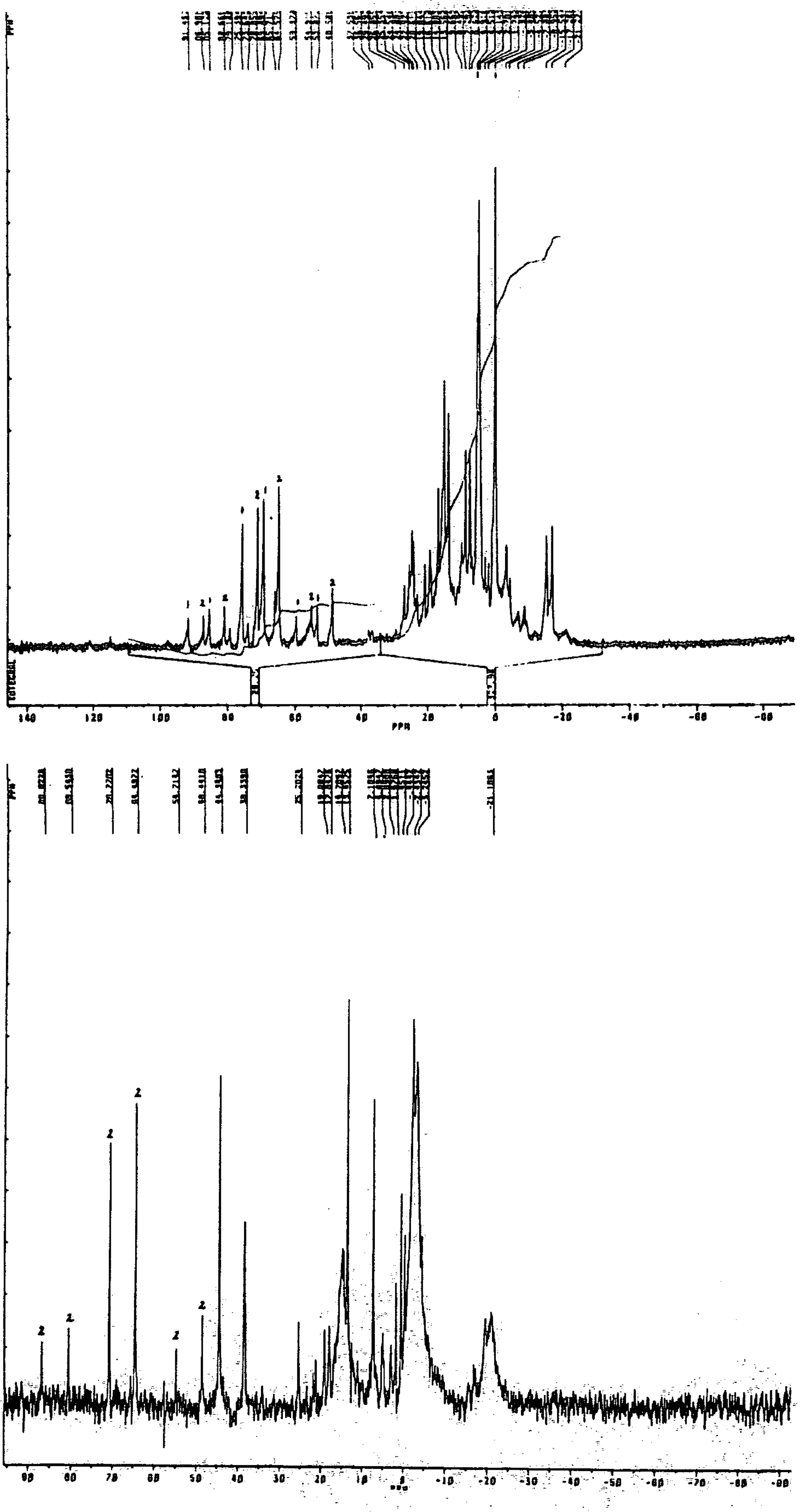

Figure 5.13: *NMR spectra of nitrileimine (62) with $[PtCl_2(PEt_3)]_2$ in THF recorded (a) after 1 hour; (b) after 12 hours; these two spectra are related by time dependence only.*

the aim of providing structural information on the nitrileimine as a ligand and its behaviour in coordination chemistry. Possible modes of coordination are illustrated in Figure 5.11.

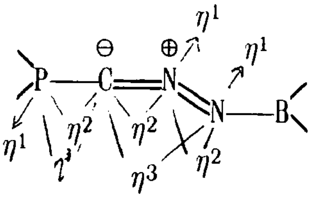

Figure 5.11: *Possible mode of coordination of nitrileimine (62).*

There is evidence for η^1-coordination by phosphorus in the nitrileimine from the magnitude of the $^1J_{PPt}$ value, which is *ca.* 3251.0 Hz.[2] Another isomer may be possible by rearrangement of the nitrileimine around C^* (Figure 5.12), but presumably retaining the *trans* P-Pt-P arrangement as $^2J_{PP}$ coupling is observed of magnitude 635 Hz. The two possible conformations of the nitrileimine are shown in Figure 5.12.

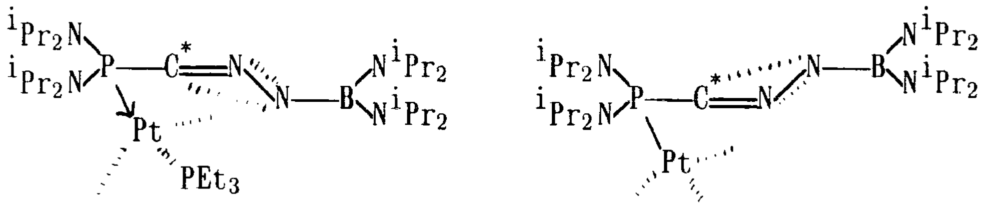

Figure 5.12: *Proposed isomeric forms of (62) in Pt(II) complex.*

A shift downfield is observed on coordination (Figure 5.13) (*cf.* low field shift on coordination of the phosphorus species, Table 5.3).

---

[2] Expected range for η^1 $^1J(PPt)$ is 3000-4000 Hz (ref.44).

This preliminary study simply serves to promote work in this area. This is a new ligand type, and from the indication here would merit further investigation.

5.5 OCTAHEDRAL COMPLEXES OF THE SYMMETRICAL DIPHOSPHENE WITH THE TRANSITION METAL IN ZERO OXIDATION STATE

5.5.1 Synthesis

The diphosphene, Ar_2P_2 (19) was reacted with the following species: $Mo(CO)_5 \cdot THF$, $Cr(CO)_5 \cdot THF$ and $W(CO)_5 \cdot THF$. The types of coordination by diphosphene displacement of THF were deduced primarily from the ^{31}P and ^{19}F NMR data the former of which is presented in Table 5.4.

COMPOUND		δ ^{31}P	$^{1}J_{PP}$
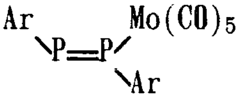	(63)	412.7 407.7	510
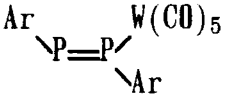	(64)	386.5 359.9	478 ‡292.8
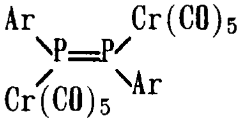	(65)	428.4	---

Table 5.4: *^{31}P NMR data for η^1 coordination complexes; ‡$J(^{183}W-^{31}P)$.*

Preparation of transition metal derivatives of ArP=PAr

a) $Mo(CO)_6 \xrightarrow{h\upsilon\text{, THF}} Mo(CO)_5.THF$

b)

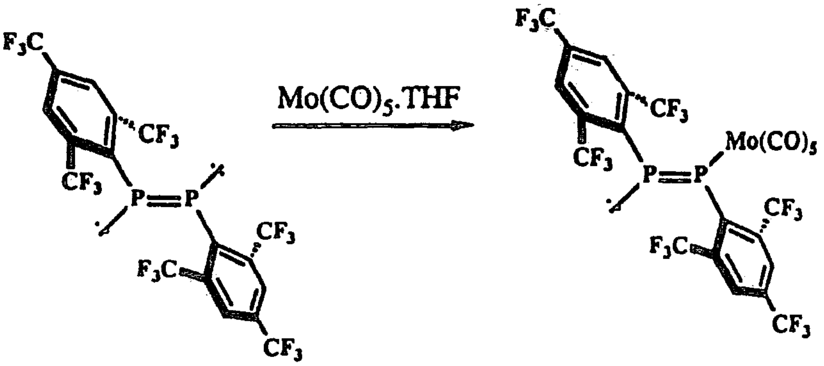

^{31}P N.M.R.

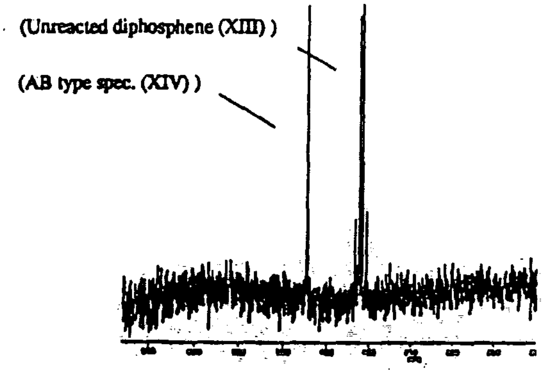

^{31}P N.M.R.

$\delta^{31}P_1$ 412.7 , $^{1}J_{P\text{-}P}$ 510.
$\delta^{31}P_2$ 407.7.
[P-F coupling unresolved.]

^{19}F N.M.R.

$\delta^{19}F_1$ -54.6 (6F), $\delta^{19}F$ -65.1 (6F)
$\delta^{19}F_2$ -58.9 (6F)

(Only one phosphorus coordinates to the molybdenum by its' lone pair in an η^1 fashion making the two rings inequivalent. This shows up distinctly in the ^{31}P N.M.R. as an AB pattern resulting from phosphorus-phosphorus' coupling.Some uncoordinated diphosphene is present.) .

Figure 5.15: ^{31}P *NMR spectrum of ArP=PAr[Mo(CO)$_5$] (63) in THF.*

5.5.2 Results

It appeared that the η^1 mode of coordination was observed exclusively. The molybdenum complex (63) was isolated pure as deep-red needle-like crystals which were characterised by ^{31}P NMR (Figure 5.15), ^{19}F NMR (Figure 5.16), IR and elemental analysis for carbon and hydrogen (Section 5.6.14). Mass spectrometry here however caused problems, as did that of the tungsten and chromium complexes. Accurate mass spectra were unobtainable because of contamination within the mass spectrometer.

The crystals of the molybdenum complex (63) have been submitted for an X-ray analysis, from which it will be possible to assign unambiguously the configuration as E or Z. The E form is proposed, as depicted in Table 5.4.

Complex (64) was characterised by its ^{31}P NMR spectrum and its characteristic tungsten-phosphorus coupling (^{183}W: 14% abundance), verifying the phosphorus as the donor atom [53].

The formation of the symmetrical complex (65) has been postulated to explain the singlet observed in the ^{31}P NMR spectrum (Figure 5.17). This centrosymmetric complex with a phosphorus-phosphorus double bond is proposed in preference to the η^2-type complex. The basis for this assignment is discussed below. Deep brown/orange crystals of (65) were obtained, and have also been submitted for X-ray analysis, although separation difficulties may make this impossible. (The microanalysis was inaccurate due to the presence of $Cr(CO)_6$ which appeared to co-crystallise). The downfield ^{31}P shift and UV spectrum support the bis-η^1 structure presented. The E conformation was assigned because of the expected steric demand of the Ar substituent. In the absence of a crystal structure, however, it was not possible to confirm this assignment unambiguously.

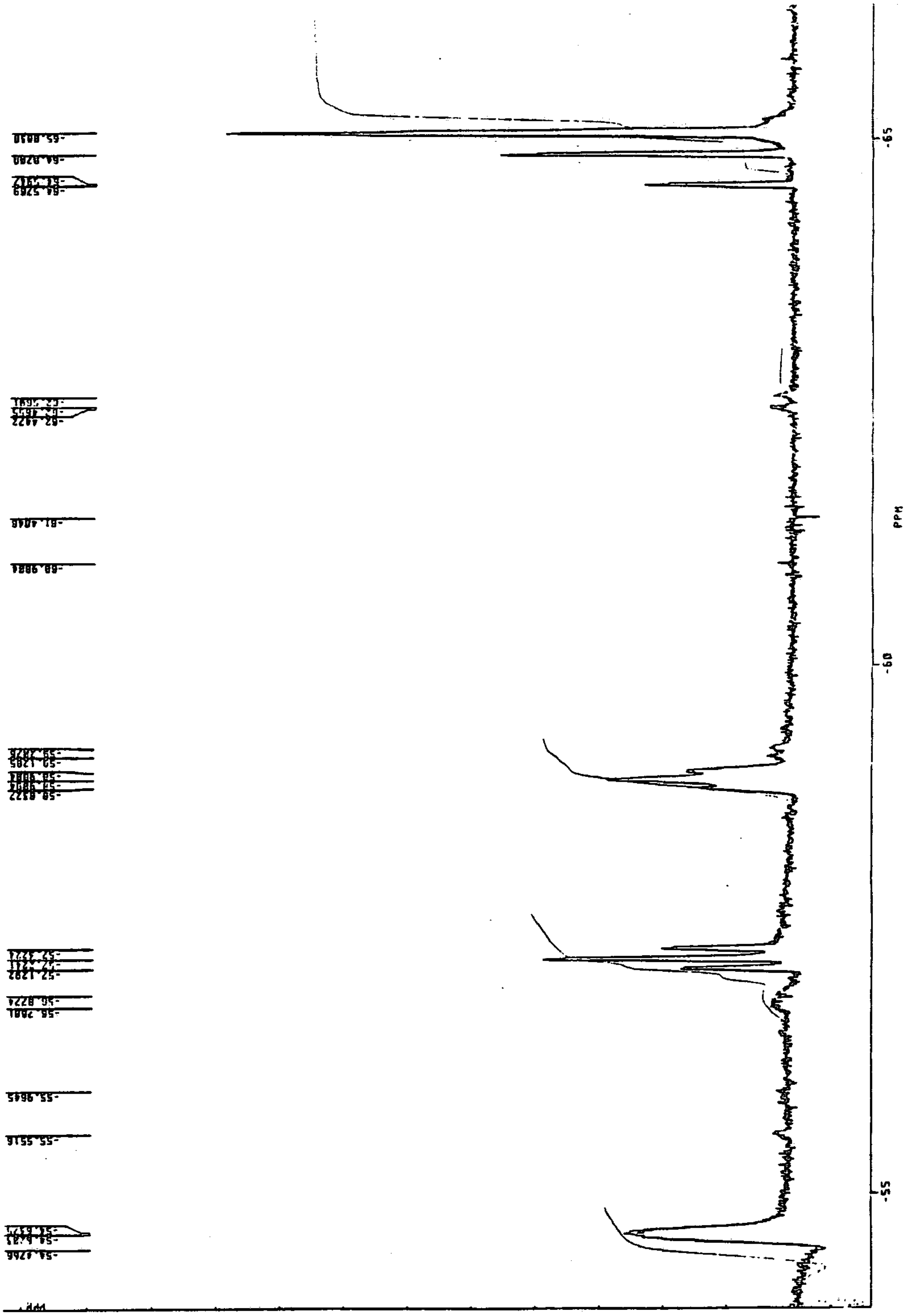

Figure 5.16: ^{19}F *NMR spectrum of ArP=PAr[Mo(CO)$_5$] (63) in THF; some uncoordinated diphosphene is also present.*

Interestingly, there was no evidence of the initial mono η^1 complex, even with a reaction stoichiometry of one $Cr(CO)_5 \cdot THF$ to one diphosphene (19). This yielded unreacted diphosphene and complex (65) only (see Figure 5.17). A possible explanation may be the ability of the chromium pentacarbonyl moiety to line up in conjugation with the phosphorus-phosphorus double bond. Being Cr(0) and hence electron-rich, it can donate into the P=P bonding system, with concomitant increase in the reactivity of the second lone pair. Preferential reaction here would therefore explain why no mono-coordinated intermediate is observed. This difference in behaviour compared with the molybdenum and tungsten derivatives may be a result of their increase in size, disallowing such extensive overlap with the π-system. This is possibly also partially reflected in the shielding of the phosphorus (Table 5.4 and Figure 5.18).

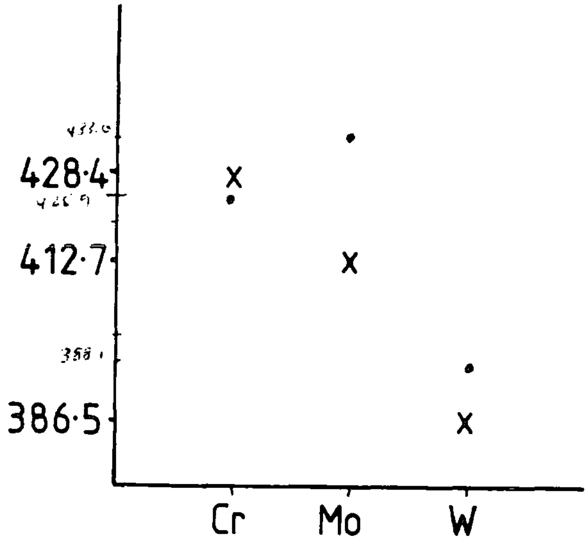

Figure 5.18: ^{31}P *shift of complex; ‡values of similar complexes for the diphosphene* $(Me_3SiCH_2)_2P_2$ *have been included for comparative purposes.* (9)

The assumption has been made that the most shielded phosphorus is directly coordinated to the metal. Similar complexes have been isolated with other diphosphenes [53-55]. It is worth considering a possible interpretation for the mode of coordination of complex (65) in terms of

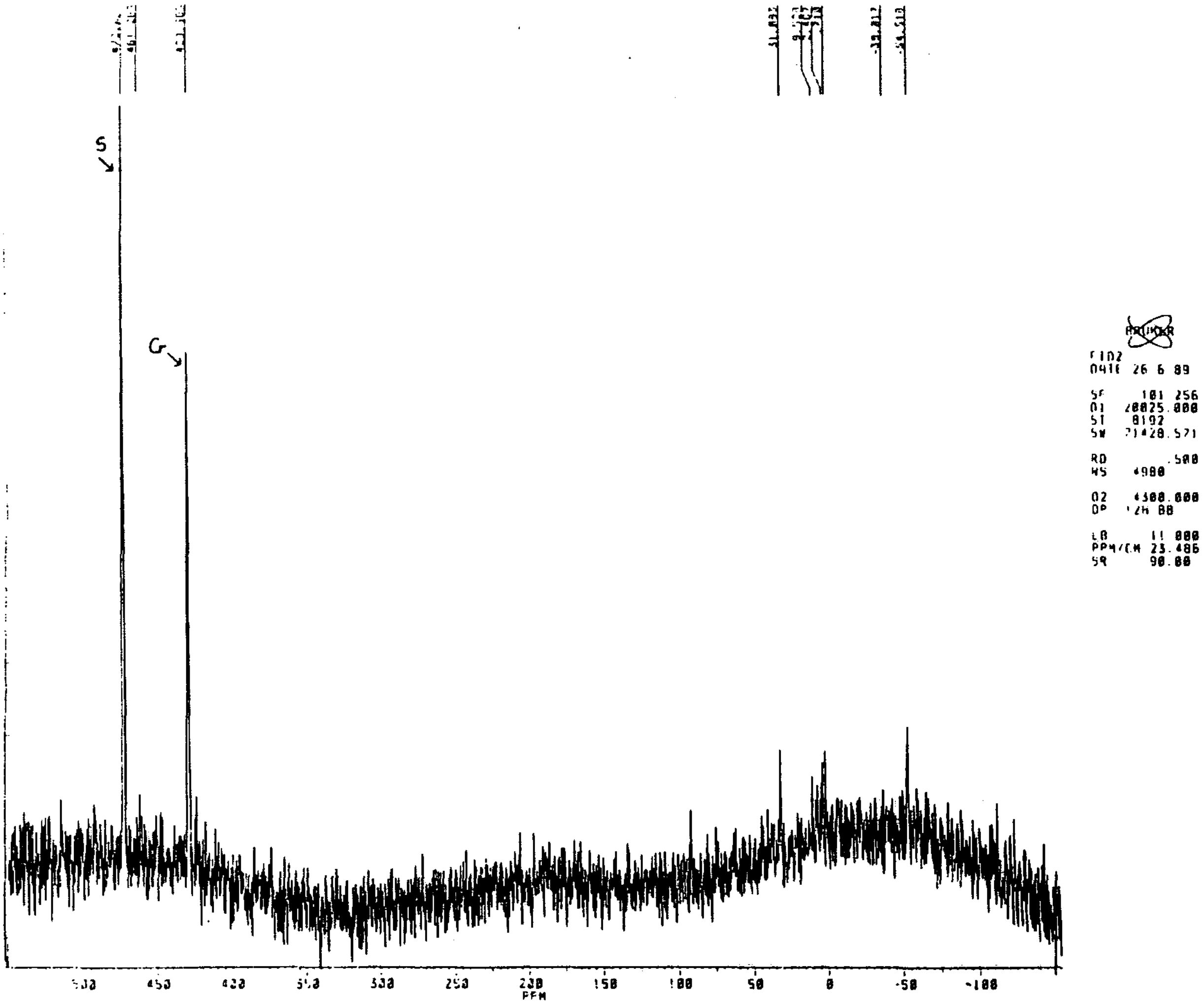

Figure 5.17: *^{31}P NMR spectrum of $ArP{=}PAr[Cr(CO)_5]_2$ (65) in THF; some unreacted Ar_2P_2 (19).*

an η^6 bonding mode to a $Cr(CO)_3$ fragment *via* the aromatic ring. This coordination type has been verified with the very sterically crowded diphosphene, $(SupermesP)_2$ [10,56]. The η^1 coordination of $Cr(CO)_5$ in (65) appears justified in terms of the reaction conditions employed. (For 'ring-coordination' there is an increase in the harshness of the conditions used [56], for example *via* refluxing in dioxane). The η^6-arene coordination complex would also be considered unlikely in this situation, due to the electron deficiency of the Ar ring system, when compared with that of the supermesityl derivative.

In general, the end-on η^1 coordination of the $M(CO)_5$ group ($M \equiv Cr$, Mo, W) would not be expected to exert an influence on the bond order of "P=P", although it acts to shield slightly the phosphorus nuclei, as reflected by the shift of the resonances to lower frequency (Table 5.4 and Figure 5.18).

5.5.3 Complex Stability

The molybdenum complex, $Ar_2P_2{\cdot}Mo(CO)_5$ (63) appeared relatively stable in air over a period of weeks. Exposure of the deep brown complex, $Ar_2P_2{\cdot}[Cr(CO)_5]_2$(65) to the atmosphere over a few hours caused a green colouration, attributed to the oxidation of Cr(0) to Cr(III). Isolatation of the tungsten derivative (64) was not successful (Section 5.6.16).

5.5.4 Relative Rates of Coordination of $M(CO)_5$ (M = W, Cr, Mo)

It was of interest to study the relative rates of coordination of the metal pentacarbonyl fragments, $M(CO)_5$ with the diphosphene, Ar_2P_2 (19) with respect to the gradual size increase Cr, Mo, W, as the group is descended.

The procedure followed initial generation of the THF adduct by irradiation of the metal hexacarbonyl in THF [25] for a standard period of 8 hours. The adduct was formed as a preliminary stage to avoid any rate dependence on this. It was used in a two-fold excess with the diphosphene (19). The ^{31}P NMR of each sample was recorded in subsequent 5 hour intervals. For chromium only, there was evidence of reaction after the first time interval. A small singlet (+428.4 ppm), corresponding to *ca*. 5% conversion and indicative of η^1 bis coordination (65), was evident in the ^{31}P NMR (Table 5.5 and Figure 5.19). However, after 20 hours a 30% conversion to the η^1 $Mo(CO)_5Ar_2P_2$ (63), 10% to $W(CO)_5Ar_2P_2$ (64) and 45% conversion to $Ar_2P_2[Cr(CO)_5]_2$ (65) was observed. A general observation of higher reactivity of the smaller $Cr(CO)_5$ fragment, with intermediate reactivity of $Mo(CO)_5$, and significantly reduced reactivity of $W(CO)_5$ is apparent. Improved yields of the order of 20% (see Sections 5.6.14-5.6.16) of complexes (63)-(65) were obtained by *in situ* irradiation of a mixture of the metal hexacarbonyl (2-fold excess) with the diphosphene in THF, and exactly analogous NMR data were obtained. It is worth mentioning here that irradiation of $ArPH_2$ in the presence of a two-fold excess of $Mo(CO)_6$ in THF, appeared to generate $ArPH_2[Mo(CO)_5]$ (66) (see Experimental, Section 5.6.13). It is likely that these reactions also proceed *via* the initial THF adduct, although direct displacement of carbon monoxide cannot be ruled out [50b]..

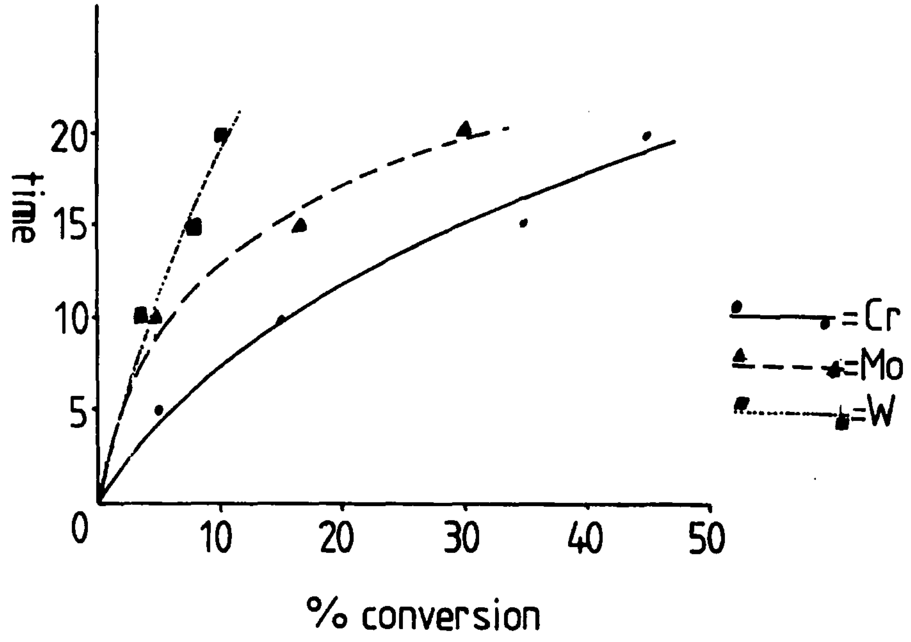

Figure 5.19: *Rate of reaction of $M(CO)_5$ (M = Mo, Cr, W) with Ar_2P_2 (19).*

	% CONVERSION TO COORD.COMPLEX‡		
TIME (hrs)	Cr (65)	Mo (63)	W (64)
5	~5	---	---
10	~15	5	4
15	~35	17	8
20	45	30	10

Table 5.5: *Rate of reaction of $M(CO)_5$ (M = Mo, Cr, W) with Ar_2P_2 (19); ‡derived from ^{31}P NMR.*

5.6 EXPERIMENTAL DETAILS

5.6.1 Preparation of $ArPF_2[(PEt_3)PtCl_2]$ (53)

$$ArPF_2\ (3) + 1/2Cl_4Pt_2(PEt_3)_2 \longrightarrow ArPF_2[(PEt_3)PtCl_2]\ (53)$$

$(PEt_3)_2Pt_2Cl_4$ (768 mg, 1.0 mmol) was added to a stirred solution of $ArPF_2$ (0.7g, 2.0 mmol) in CH_2Cl_2 (15 ml) at room temperature. A clear pale yellow solution was formed. This was cooled to -40 ^oC to give white crystals. Yield was 800 mg (54%). This solid was recrystallised again from CH_2Cl_2 (5 ml) to obtain a sample suitable for X-ray analysis. The *cis* isomer was isolated. Mpt. 190 ^oC; ^{31}P ($CDCl_3$) δ: +124.0 ppm ('pseudo triplet' of triplets), $^1J_{PPt}$ +6252.1, $^1J_{PF}$ 1146.1 Hz; (LIGAND PEt_3): +11.5 ppm ('pseudo triplet'), $^1J_{PPt}$ 2876.9 Hz; ^{19}F δ: -55.3 to -55.6 ppm (o-CF_3,6F,very complex '2nd order'), -64.4 (p-CF_3,3F); MS [Intensity%] CI$^-$: 733 [100,$ArPF_2(Et_3PPtCl_2)^-$], 616 [49,$ArPF_2(PtCl_2)^-$].

5.6.2 Preparation of $ArPH_2[(PEt_3)PtCl_2]$ (54)

$$ArPH_2\ (15) + 1/2Cl_4Pt_2(PEt_3)_2 \longrightarrow ArPH_2[(PEt_3)PtCl_2]\ (54)$$

$(PEt_3)_2Pt_2Cl_4$ (500 mg, 0.65 mmol) was added to a stirred solution of $ArPH_2$ (0.41g, 1.30 mmol) in CH_2Cl_2 (20 ml) at room temperature. This was stirred for 1 hour. The pale yellow solution was cooled to -40 ^oC with the precipitation of clear crystals. Yield of the *cis* isomer was 800 mg (88%). These have been submitted for X-ray analysis. Mpt. 310-312 ^oC; ^{31}P ($CDCl_3$) δ: -74.2 ppm ('pseudo triplet' of triplets), $^1J_{PPt}$ +3809.1, $^1J_{PH}$ 412.9, $^2J_{PP}$ 20.6 Hz; (LIGAND PEt_3): +9.3 ppm ('pseudo triplet'), $^1J_{PPt}$ 3034.8, $^2J_{PP}$ 20.6 Hz; ^{19}F δ: -50 to -60 ppm (o-CF_3,6F,very complex '2nd order' spectrum), -64.6 ppm (p-CF_3,3F); MS [Intensity%] CI$^-$: 314 [100,$ArPH_2^-$].

5.6.3 Preparation of $ArPCl_2[(PEt_3)PtCl_2]$ (56)

$$ArPCl_2\ (12) + 1/2(PEt_3)_2Pt_2Cl_4 \longrightarrow ArPCl_2[(PEt_3)PtCl_2]\ (56)$$

$(PEt_3)_2Pt_2Cl_4$ (500 mg, 0.65 mmol) was added to a stirred solution of $ArPCl_2$ (500 mg, 1.3 mmol) in CH_2Cl_2 (20 ml) at room temperature. The mixture was stirred for 1.5 hours. The ^{31}P NMR showed no evidence of coordination. The solution was warmed to 35 ^oC for 2 hr. A low conversion (*ca.* 5%) to the *trans* isomer of the desired complex was observed. After a further two hours complete conversion to the *cis* isomer was detected. The pale yellow solution was cooled to -40 ^oC giving pale yellow crystals. Yield was 350 mg (35%). An X-ray analysis was obtained on these crystals (Figure 5.4). *Trans* isomer: ^{31}P ($CDCl_3$) δ: +135.8 ppm ('pseudo triplet' of doublets), $^1J_{PPt}$ 2885.8, $^2J_{PP}$ 679.0 Hz; (LIGAND PEt_3): 14.3 ppm ('pseudo triplet' of doublets), $^1J_{PPt}$ +2840.0, $^2J_{PP}$ +694.8 Hz. *Cis* isomer: ^{31}P ($CDCl_3$) δ: +90.3 ppm ('pseudo triplet'), $^1J_{PPt}$ 5511.0 Hz; (LIGAND PEt_3): 13.6 ppm ('pseudo triplet'), $^1J_{PPt}$ 2756.3 Hz; ^{19}F δ: -49.0 ppm (o-CF_3,apparent AB, 4 lines unusually deshielded), -64.1 ppm (p-CF_3); ^1H δ: 7.18 (2H,CH on Ar), 2.21 (6H, CH_2/Et), 1.17 (9H,CH_3/Et) ppm.

The apparent quartet observed in the ^{19}F NMR may be assigned to fluorine splitting by platinum [Figure 5.2(f)], and further splitting by phosphorus (Figure 5.20). If these were of similar magnitude this would offer an explanation for the pseudo quartet observed. If this explanation is valid the values are $^4J_{PF}$ 27.6 Hz and $^5J_{PtF}$ *ca.* 24.2 Hz. This is supported by a very similar value of $^5J_{PtF}$ (32.5 Hz) for the phosphaalkene coordination $ArP{=}C(Cl)_2[Et_3PPtCl_2]$ (57) (Section 5.6.6). The crystal structure data for complex (56) are presented in Figure 5.4.

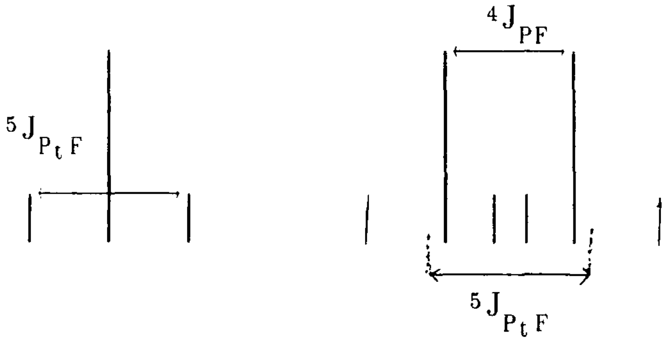

Figure 5.20: *Predicted coupling pattern for* $ArPCl_2[(PEt_3)PtCl_2]$ *(56)*

5.6.4 Preparation of $Ar_2P_2[(PEt_3)PtCl_2]$ (51)

$$ArP{=}PAr\ (19) + 1/2(PEt_3)_2Pt_2Cl_4 \longrightarrow Ar_2P_2[(PEt_3)PtCl_2]\ (51)$$

$(PEt_3)_2Pt_2Cl_4$ (461 mg, 0.60 mmol) was added to a stirred solution of ArP=PAr (0.81g, 1.3 mmol) in CH_2Cl_2 (25 ml) at room temperature. The pale yellow solution was stirred for 1 hr, and then cooled to -40 ^oC to give pale yellow crystals. Yield was 0.84g (64%). These crystals were submitted for X-ray analysis. ^{31}P ($CDCl_3$) δ: P_1 +346.6 ppm ('pseudo triplet' of doublets), $^1J_{PPt}$ 2602.9, $^2J_{PP}$ 534.3 Hz, P_2 337.2 ppm (doublet), $^2J_{PP}$ 534.3 Hz; (LIGAND PEt_3): +9.5 ppm ('pseudo triplet'), $^1J_{PPt}$ 4024.3 Hz; ^{19}F ($CDCl_3$) δ: -55.9 (d of t,o-CF_3), -57.9 (t of d, o-CF_3), -63.7 (s,p-CF_3), -63.9 (s,p-CF_3) ppm, '$^9J_{FF}$ +5.2 Hz',[3] (between the o-CF_3 groups on opposite rings), ['J_{PF} 18 Hz', from the ^{19}F NMR (Section 5.2.2) it appears that one set of the o-CF_3 groups on one ring is seeing two phosphorus atoms to split it into a real triplet, whilst the other is seeing one phosphorus atom resulting in a doublet].

---

[3] or this may be attributed to a second order fine coupling with platinum [Figure 5.2(b)].

5.6.5 **Preparation of ArP=PAr'$[(PEt_3)PtCl_2]$ (52)**

ArP=PAr' (20) + $1/2(PEt_3)_2Pt_2Cl_4 \longrightarrow$ ArP=PAr'$[(PEt_3)PtCl_2]$ (52)

$(PEt_3)_2Pt_2Cl_4$ (0.58g, 0.76 mmol) was added to a stirred solution of ArP=PAr' (0.85g, 1.5 mmol) at room temperature. This mixture was stirred for 1 hr. The solution was cooled to -40 ^oC, and the η^1 complex isolated as small transparent crystals which were submitted for X-ray analysis, but no suitable crystals were obtained. Yield was 0.62g (64%). From the ^{19}F and ^{31}P NMR it was not possible to determine which phosphorus the platinum was coordinated to, so an X-ray structure would have been of particular interest here. ^{31}P δ: 386.4 ppm, $^1J_{PPt}$ 2550.0 Hz, P_1 +343.7 ppm, $^1J_{PP}$ 501.2 Hz; ^{19}F ($CDCl_3$) δ: very complex spectrum: -55 to -60 (o-CF_3,12F), -64.0 (p-CF_3,3F) ppm.

5.6.6 **Preparation of ArP=C(Cl)$_2[(PEt_3)PtCl_2]$ (57)**

ArP=C(Cl)$_2$ (31) + $1/2(PEt_3)_2Pt_2Cl_4 \longrightarrow$ ArP=C(Cl)$_2[(PEt_3)PtCl_2]$ (57)

$(PEt_3)_2Pt_2Cl_4$ (461 mg, 0.60 mmol) was added to a stirred solution of ArP=C(Cl)$_2$ (474 mg, 1.2 mmol) in CH_2Cl_2 (10 ml) at room temperature. The mixture was stirred for one hour. The pale yellow solution was cooled to -40 ^oC. Clear transparent plates were isolated and submitted for X-ray analysis. Yield was 390 mg (42%). *Cis* isomer: ^{31}P δ: 152.1 ('pseudo triplet'), $^1J_{PPt}$ 5006.4 Hz, $^2J_{PP}$ +18 Hz; (LIGAND PEt_3): +11.1, $^1J_{PPt}$ 3831.8 Hz; ^{19}F δ: -56.8, $^5J_{PtF}$ 32.5 Hz (pseudo triplet,o-CF_3), -63.0 (s,p-CF_3) ppm.

5.6.7 Preparation of *trans*- and *cis*-ArP=C(Ph)H[$(PEt_3)PtCl_2$] (58,59)

$$\text{ArP=CH(Ph) (32)} + 1/2(PEt_3)_2Pt_2Cl_4 \longrightarrow \text{ArP=CH(Ph)}[(PEt_3)PtCl_2]$$

$\left.\begin{matrix}(58)\\(59)\end{matrix}\right\}$ *trans*
cis

$(PEt_3)_2Pt_2Cl_4$ (400 mg, 0.52 mmol) was added to a stirred solution of ArP=CH(Ph) (*ca.* 440 mg, 1.1 mmol) in THF[4] (15 ml) at room temperature. The solution was stirred for 0.5 hours. The ^{31}P NMR showed the presence of two isomers. After the mixture was stirred for 2 hr. only the *cis* isomer was detected. The pale yellow solution was cooled to -40 ^oC and white crystals were precipitated. Yield was 0.41g (47%). *Trans* isomer: ^{31}P (THF) δ: +178.6 ppm ('pseudo triplet' of doublets), $^1J_{PPt}$ 2456.5, $^2J_{PP}$ 569.5 Hz; (LIGAND PEt_3): 15.8 ppm ('pseudo triplet' of doublets), $^1J_{PPt}$ +3253.4, $^2J_{PP}$ 569 Hz. *Cis* isomer: ^{31}P (THF) δ: +149.6 ppm ('pseudo triplet'), $^1J_{PPt}$ 4599.6 Hz; (LIGAND PEt_3): 9.86 ppm, $^1J_{PPt}$ 3219.1 Hz; MS (Intensity%) CI$^-$: 635 [26.8,ArP=CH(Ph)PtP$^-$], 593 [66], 381 [51,$Et_3PPtCl_2^-$], 312 [10.7,ArP$^-$], 331; ^{19}F δ: The ^{19}F NMR is complex, but as observed in the ^{31}P NMR (Figure 5.2) there are some impurities, which appear to contain fluorine, however a pseudo triplet at -64.1 ppm is evident and a tentative value of $^5J_{PtF}$ 31.8 Hz may be derived. There is also a peak at -67.2 ppm corresponding to the p-CF_3 groups. The $^5J_{PtF}$ value here is notably similar to the values obtained for compounds (56) and (57).

---

[4] A THF solution of the phosphaalkene ArP=CH(Ph) had to be used since it was unstable to isolation.

5.6.8 Preparation of *trans*-ArP=CH(SiMe$_3$)[(PEt$_3$)PtCl$_2$] (60)

$$\text{ArP=CH(SiMe}_3\text{) (33) + (PEt}_3\text{)}_2\text{Pt}_2\text{Cl}_4 \longrightarrow \text{ArP=CH(SiMe}_3\text{)[(PEt}_3\text{)PtCl}_2\text{] (60)}$$

(PEt$_3$)$_2$Pt$_2$Cl$_4$ (400 mg, 0.52 mmol) was added to a stirred solution of ArP=CH(SiMe$_3$) (*ca.* 0.1g, 0.25 mmol) in THF (10 ml). This was stirred at room temperature for 6 hrs. The ^{31}P NMR showed the *trans* isomer. Conversion (w.r.t. ^{31}P NMR) was 78%. ^{31}P (THF) δ: +245.1 ppm, $^1J_{PPt}$ 3714.0, $^2J_{PP}$ 788.0 Hz; (LIGAND PEt$_3$): 15.4 ppm, $^1J_{PPt}$ 3000, $^2J_{PP}$ 787 Hz.

5.6.9 Reaction of Ar$_2$P$_2$ (19) with the Pt(0) Complex (61)

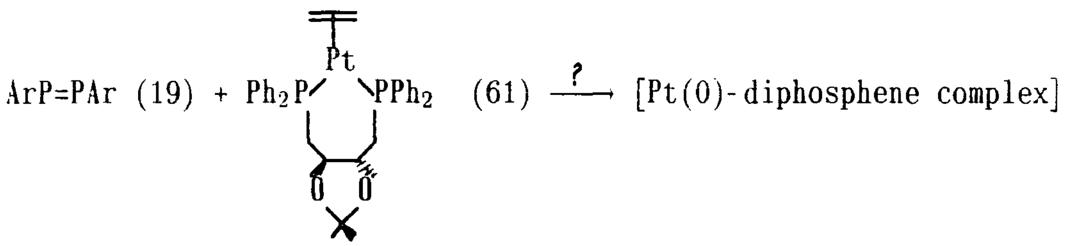

The Pt(0) complex (61) (150 mg, 0.22 mmol) was added to a stirred solution of ArP=PAr (0.137g, 0.21 mmol) in THF (25 ml) at room temperature. No reaction was observed after stirring for 2hr. This solution was warmed gently with a hair-dryer. The ^{31}P NMR showed a peak at 251 ppm : phosphorus ligand +6.3 ppm, $^1J_{PPt}$ 3189.9 Hz. There were small peaks at -189, -0.5 and -2.4 (s) possibly from a reduction product such as ArPH$_2$, since a small amount of grey metallic solid was observed, which could have been platinum metal. The ^{19}F NMR spectrum showed unreacted diphosphene with an apparent triplet at -52.3 ppm. This may be attributed to the η^2 complex: a $^4J_{PF}$ + $^5J_{PF}$ value of 79 Hz may be tentatively assigned.

5.6.10 Preparation of bis-benzonitrile-Pt(II) chloride [57]

$PtCl_2$ (1.1g, 4.1 mmol) was dissolved in a minimum of hot benzonitrile (15 ml, 100 ^{o}C). After filtering, this solution was cooled to give a heavy precipitate of $(PhCN)_2PtCl_2$ (1.89g, 4.0 mmol) collected by filtration. A further crop of crystals was obtained by diluting the filtrate with low boiling point petroleum ether. Yield was 98%. The product was recrystallised from benzene.

5.6.11 Addition of $(PhCN)_2PtCl_2$ to Ar_2P_2 (19)

$$(PhCN)_2PtCl_2\ (xs) + ArP{=}PAr\ (19) \xrightarrow{\quad X \quad}$$

ArP=PAr (0.42g, 0.67 mmol) in CH_2Cl_2 (10 ml) was added to a stirred solution of $(PhCN)_2PtCl_2$ (0.51g, 1.1 mmol) in CH_2Cl_2 (20 ml) at room temperature. This was stirred for 4hr. ^{31}P NMR showed no reaction (+473.8 ppm).

5.6.12 Reaction of nitrileimine (62) with $[(PEt_3)PtCl_2]$

$$(^{i}Pr_2N)_2P\text{-}C{=}N{=}N\text{-}B(N^{i}Pr_2)\ (62) \xrightarrow[CH_2Cl_2]{Cl_4Pt_2(PEt_3)_2}$$

$(PEt_3)_2Pt_2Cl_4$ (0.51g, 0.66 mmol) was added at room temperature to a solution of nitrileimine $(^{i}Pr_2N)_2P\text{-}C{=}N{=}N\text{-}B(N^{i}Pr_2)$ (0.82g, 1.7 mmol) and stirring was continued for 1 hr. The resultant yellow solution gave a complex ^{31}P NMR spectrum [Figure 5.13(a)] which simplified after 12 hours [Figure 5.13(b)]. The IR showed no nitrileimine absorption. On cooling the CH_2Cl_2 solution to -40 ^{o}C no crystals were obtained. ^{31}P (THF) δ_1: 72.24 ppm, $^{1}J_{PPt}$ 3247.6 Hz, $^{2}J_{PP}$ 637.9 Hz; δ_2: +67.73 ppm,

$^{1}J_{PPt}$ 3251.0 Hz. Figure 5.13(b) showed δ_1 only.

5.6.13 Preparation of $ArPH_2[Mo(CO)_5]$ (66) in solution

$$ArPH_2 \ (15) + Mo(CO)_6 \xrightarrow[h\nu]{THF} ArPH_2[Mo(CO)_5] \ (66)$$

$Mo(CO)_6$ (2.0g, 7.6 mmol) was added to a stirred solution of $ArPH_2$ (1.2g, 3.8 mmol) at room temperature in a quartz vessel. This mixture was irradiated for 1.5 hr. at 254 nm (Hg lamp). A deep-red solution was formed. The product was not isolated. The ^{31}P NMR showed an approximate 55% conversion to the postulated η^1 coordination complex. ^{31}P (THF) δ: -78.2 ppm (d of t), $^{1}J_{PH}$ +354.0, $^{4}J_{PF}$ +17.0 Hz; ^{19}F (THF) δ: -58.6 (d of t,o-CF_3), $^{4}J_{PF}$ +17.0, $^{5}J_{FH}$ 3.1 Hz, -64.2 (p-CF_3) ppm.

5.6.14 Preparation of $ArP{=}PAr[Mo(CO)_5]$ (63)

$$ArP{=}PAr \ (19) + Mo(CO)_6 \xrightarrow[h\nu]{THF} ArP{=}PAr[Mo(CO)_5] \ (63)$$

ArP=PAr (0.61g, 1.0 mmol) in THF (10 ml) was added to a stirred suspension of $Mo(CO)_6$ (0.53g, 2.0 mmol) in THF (15 ml) in a quartz tube at room temperature. This mixture was irradiated for 12 hr at 254 nm, giving a dark-red solution. All the volatile material was removed *in vacuo* and the reddish oil was extracted with pentane (20 ml). This was cooled to -40 ^{o}C and dark red crystals were obtained. Yield was 0.57g (66%). Analysis found: C, 32.45; H, 0.73; Required for $C_{23}H_4F_{18}O_5P_2Mo$: C.32.09; H, 0.47%; ^{31}P ($CDCl_3$) δ: +412.7 (d), +407.7 (d) ppm, $^{1}J_{PP}$ 510 Hz; ^{19}F ($CDCl_3$) δ: -54.9 (6F), -58.9 (6F) (apparent triplet, coupling 18.05 Hz, finer coupling 7 Hz), -65.1 (6F) ppm (see Figure 5.16); IR

(Nujol) ν_{max}: 2000 (s), 1980 (s), 1960 (s), 1945 (s,ν_{CO}), 1450 and 1370 (s,C-F), 590 (w,"P=P") cm^{-1}.

5.6.15 Preparation of ArP=PAr$[Cr(CO)_5]_2$

$$ArP{=}PAr\ (19)\ +\ 2Cr(CO)_6\ \xrightarrow[h\nu]{THF}\ ArP{=}PAr[Cr(CO)_5]_2\quad (65)$$

ArP=PAr (1.5g, 2.4 mmol) in THF (10 ml) was added to a stirred suspension of $Cr(CO)_6$ (1.06g, 4.8 mmol) in a quartz vessel in THF (50 ml) at room temperature. This mixture was irradiated at 254 nm (Hg lamp) for 12 hr. All the volatiles were removed from the resulting deep-red solution *in vacuo*. Pentane (10 ml) was added, and the mixture was cooled to -40 °C. A crystalline dark red solid was precipitated. Yield was 1.6g (66% assuming molecular formula as ArP=PAr$[Cr(CO)_5]_2$). ^{31}P (THF) δ: +428.4 (singlet); IR (Nujol) ν_{max}: 3100 (w,CHAr), 2080 (w,sharp), 2000 (w), 1985 (w), 1950 (s,ν_{CO}), 1460 (m,ArC=C), 1380 (w,ArC=C), 1260 (s), 1200-1000 (s,C-F), 800 (s), 700-650 (m,"P=P") cm^{-1}; UV-Vis λ_{max} (Abs): 291 (0.39), 261 (0.69).

5.6.16 Preparation of ArP=PAr$[W(CO)_5]$ (64)

$$ArP{=}PAr\ (19)\ +\ W(CO)_6\ \xrightarrow[h\nu]{THF}\ ArP{=}PAr[W(CO)_5]\quad (64)$$

ArP=PAr (0.81g, 1.3 mmol) in THF (10 ml) was added to a stirred suspension of $W(CO)_6$ (0.91g, 2.6 mmol) in THF (50 ml) in a quartz vessel at room temperature. The mixture was irradiated at 254 nm (Hg lamp) for 12 hr. The solution became deep-red. ^{31}P NMR showed a low yield (~30%) of the proposed η^1-coordination complex had formed. All the volatiles were removed *in vacuo* to give a black oil. Pentane (5 ml) was added. The solution was cooled to -40 ^{o}C, and a colourless solid was isolated containing no fluorine or phosphorus, deduced to be unreacted $W(CO)_6$. ^{31}P (THF) δ_1: +386.5 ppm (doublet); δ_2: +359.9 ppm (doublet), $J_{^{183}W-^{31}P}$ 292.8 Hz, $^{1}J_{PP}$ +478 Hz; IR (Nujol) ν_{max}: 2200 (w), 2080 (m), 1980 (m) and 1950 (s,br) (all ν_{CO}) cm^{-1}; ^{19}F δ: *ca.* (br) -58.7 (o-CF_3), *ca.* -65.0 (p-CF_3) ppm.

5.6.17 Preparation of ArP=PAr[Mo(CO)$_5$] (63)

$$Mo(CO)_6 \xrightarrow[h\nu]{THF} Mo(CO)_5\cdot THF + ArP{=}PAr \longrightarrow ArP{=}PAr[Mo(CO)_5] \quad (63)$$

$Mo(CO)_6$ (0.3g, 1.1 mmol) in THF (50 ml) was irradiated at 254 nm (Hg lamp) for 4 hr. ArP=PAr (0.62g, 1.0 mmol) in THF (10 ml) was added to this pale yellow solution, and the mixture stirred for 20 hr. at room temperature to give a deep-red solution. The solvent was removed *in vacuo*, and the resultant red oil was extracted with pentane (10 ml). This was cooled to -40 ^{o}C. A dark red solid was obtained. Yield was 0.26g (30%). Characterisation data appear in Section 5.6.14.

5.6.18 Preparation of ArP=PAr[Cr(CO)$_5$]$_2$ (65)

$$2Cr(CO)_6 \xrightarrow[h\nu]{THF} 2Cr(CO)_5\cdot THF + ArP{=}PAr \longrightarrow ArP{=}PAr[Cr(CO)_5]_2 \quad (65)$$

$Cr(CO)_6$ (0.48g, 2.2 mmol) in THF (50 ml) was irradiated at 254 nm (Hg lamp) for 4 hr. ArP=PAr (0.62g, 1.0 mmol) in THF (10 ml) was added to this clear yellow solution. The mixture was stirred for 20 hr. at room temperature to give a deep-red solution. Yield (from ^{31}P NMR measurement) was *ca*. 45%. All the volatile material was removed *in vacuo*, and the resulting red/orange oil was extracted into pentane (10 ml). This was cooled to -40 °C. Deep red needle-like crystals were obtained. Yield was 0.37g (37% w.r.t. 1 equivalent of diphosphene assuming the molecular formula to be $ArP{=}PAr[Cr(CO)_5]_2$). Characterisation data appear in Section 5.6.15.

5.6.19 Preparation of $ArP{=}PAr[W(CO)_5]$ (64)

$$W(CO)_6 \xrightarrow[h\nu]{THF} W(CO)_5 \cdot THF + ArP{=}PAr \longrightarrow ArP{=}PAr[W(CO)_5]\ (64)$$

$W(CO)_6$ (0.4g, 1.1 mmol) in THF (50 ml) was irradiated at 254 nm (Hg lamp) for 4 hr. ArP=PAr (0.62g, 1.0 mmol) was added. The mixture was stirred for 20 hr. to give a dark-red solution. The solvent was removed *in vacuo*. The residual brown oil was extracted into pentane (20 ml) and cooled to -40 °C. A dark-red solid was precipitated, however under magnification this appeared to contain a white solid attributed to unreacted $W(CO)_6$ ~10% recovery w.r.t. ^{31}P NMR. Characterisation data appear in Section 5.6.16.

5.7 REFERENCES

1. L.M. Venanzi, *Pure and Applied Chemistry*, 52, 1117-1129 (1980).
2. F.A. Cotton and G. Wilkinson, *Advanced Inorganic Chemistry*, John Wiley and Sons, Fourth Edition, p.64 (1980).
3. L. Heuer and R. Schmutzler, *J.Fluorine Chem.*, 39, 197-216 (1988).
4. M. Yoshifuji, I. Shima, N. Inamoto, K. Hirotsu and T. Higushi, *J.Amer.Chem.Soc.*, 103, 4587 (1981).
5. O.J. Scherer, *Angew.Chem. Int.Ed.Engl.*, 24, 924-943 (1985).

6. a) H. Schäfer and D. Binder, *Z.Anorg.Allg.Chem.*, 557, 45-58 (1988).

   b) H. Schäfer, D. Binder and D. Fenske, *Angew.Chem. Int.Ed.Engl.*, 24(6), 522 (1985).

   c) H. Schäfer, D. Binder, B. Deppisch and G. Mattern, *Z.Anorg. Allg.Chem.*, 546, 79-98 (1987).

7. E. Niecke, B. Kramer and M. Nieger, *Angew.Chem. Int.Ed.Engl.*, 28, 215 (1989).

8. H. Schäfer and D. Binder, *Z.Anorg.Allg.Chem.*, 546, 55-78 (1987).

9. J.C. Leblanc and C. Moïse, *J.Organometallic Chem.*, 364, C3-C4 (1989).

10. M. Yoshifuji, T. Hashida, K. Shibayama and N. Inamoto, *Chem.Lett.*, 287-290 (1985).

11. K.M. Flynn, H. Hope, B.D. Murray, M.M. Olmstead and P.P. Power, *J.Amer.Chem.Soc.*, 105, 7750 (1983).

12. A.H. Cowley, J.E. Kilduff, J.G. Lasch, N.C. Norman, M. Pakulski, F. Ando and T.C. Wright, *J.Amer.Chem.Soc.*, 105, 7751-7752 (1983).

13. R.A. Bartlett, H.V.R. Dias, K.M. Flynn, M.M. Olmstead and P.P. Power, *J.Amer.Chem.Soc.*, 109, 5699-5703 (1987).

14. R.A. Bartlett, H.V.R. Dias and P.P. Power, *J.Organometallic Chem.*, 362, 87-94 (1989).

15. A.M. Caminade, C. Couret, J. Escudié and M. Koenig, *J.Chem.Soc. Chem.Commun.*, 1622 (1984).

16. G. Huttner, J. Borm and L. Zsolnai, *J.Organometallic Chem.*, 304, 309-321 (1986).

17. J. Borm, G. Huttner and L. Zsolnai, *Angew.Chem. Int.Ed.Engl.*, 24(12), 1069-1070 (1985).

18. A.M. Caminade, J.P. Majoral, M. Sanchez, R. Mathieu, S. Attali and A. Grand, *Organometallics*, 6, 1459-1465 (1987).

19. A.G. del Pozo, A.M. Caminade, F. Dahan, J.P. Majoral and R. Mathieu, *J.Chem.Soc.Chem.Commun.*, 574 (1988).

20. D. Fenske and K. Merzweiler, *Angew.Chem. Int.Ed.Engl.*, 25(4), 338 (1986).

21. A.H. Cowley, D.M. Giolando, C.M. Nunn, M. Pakulski, D. Westmoreland and N.C. Norman, *J.Chem.Soc.Dalton Trans.*, 2127 (1988).

22. H. Vahrenkamp and D. Wolters, *Angew.Chem. Int.Ed.Engl.*, 22(2), 154 (1983).

23. a) T.-K. Ha, M.T. Nguyen and P. Ruelle, *Chem.Phys.*, 87, 23-29 (1984).

b) V. Galasso, *Chem.Phys.*, 83, 407-413 (1984).

c) T.L. Allen, A.C. Scheiner, Y. Yamagushi and H.F. Schaefer (III) *Chem.Phys.Lett.*, 12, 154-158 (1977).

d) T.L. Allen, A.C. Scheiner, Y. Yamagushi and H.F. Schaefer (III) *J.Amer.Chem.Soc.*, 108, 7579-7588 (1986).

e) M.T. Nguyen, *Chem.Phys.Lett.*, 135(1,2), 73-77 (1987).

24. a) J. Escudié, Personal communication to author, August 1988.

b) A. Dubourg, J.-P. Declercq, H. Ranaivonjatovo, J. Escudié, C. Couret and M. Lazraq, *Acta Cryst.*, C44, 2004 (1988).

25. T.C. Klebach, R. Lourens, F. Bickelhaupt, C.H. Stam and A. Van-Herk, *J.Organometallic Chem.*, 210, 211-221 (1981).

26. H.W. Kroto, J.F. Nixon, M.J. Taylor, A.A. Frew and K.W. Muir, *Polyhedron*, 1(1), 89-95 (1982).

27. a) R. Appel and C. Casser, *Tetrahedron Lett.*, 25, 4109 (1984).

b) R. Appel, C. Casser, M. Immenkeppel and F. Knoch, *Angew.Chem.*, 96, 905 (1984).

28. R.H. Neilson, R.J. Thomas, I. Vickovic and W.H. Watson, *Organometallic*, 3, 1132 (1984).

29. P.B. Hitchcock, M.F. Meidine, J.F. Nixon, H. Wang, D. Gudat and E. Niecke, *J.Organometallic Chem.*, 368, C29-C32 (1989).

30. S. Holand, C. Charrier, F. Mathey, J. Fischer and A. Mitschler, *J.Amer.Chem.Soc.*, 106, 826 (1984).

31. Th.A. van der Knapp, L.W. Jenneskens, H.J. Meeuwissen F. Bickelhaupt, D. Walther, E. Dinjus, E. Uhlig and A.L. Spek, *J.Organometallic Chem.*, 254, C33-C36 (1983).

32. R. Appel, C. Casser and F. Knoch, *J.Organometallic Chem.*, 293, 213 (1985).

33. A.H. Cowley, R.A. Jones, C.A. Stuart, A.L. Stewart, J.L. Atwood, W.E. Hunter and H.-M. Zhang, *J.Amer.Chem.Soc.*, 105, 3737-3738 (1983).

34. J.F. Nixon, *Chem.Rev.*, 88, 1327-1362 (1988).

35. K. Knoll, G. Huttner, M. Wasiucionek and L. Zsolnai, *Angew.Chem.*, 96, 708 (1984); *Angew.Chem. Int.Ed.Engl.*, 23, 739 (1984).

36. C. Thomson, *J.Chem.Soc.Chem.Commun.*, 322 (1977).

37. W.W. Schoeller and E. Niecke, *J.Chem.Soc.Chem.Commun.*, 569 (1982).

38. J.C.T.R. Burckett St. Laurent, P.B. Hitchcock, M.A. King, H.W. Kroto, M.F. Meidine, S.I. Klein, S.I. Al-Resayes, R.J. Suffolk and J.F. Nixon, ***Phosphorus and Sulphur***, 18, 259-262 (1983).

39. a) T.A. van der Knapp, F. Bickelhaupt, J.G. Kraaykamp, G. van Koten, J.P.C. Bernards, H.T. Edzes, W.S. Veeman, E. de Boer and E.J. Baerends, *Organometallic*, 3, 1804-1811 (1984).

b) H.W. Kroto, S.I. Klein, M.F. Meidine, J.F. Nixon, R.K. Harris, K.J. Packer and P. Reams, *J.Organometallic Chem.*, 280, 281-287 (1985).

40. J.C.T.R. Burckett St. Laurent, M.A. King, H.W. Kroto, J.F. Nixon and R.J. Suffolk, *J.Chem.Soc.Dalton Trans.*, 755 (1983).

41. J.C.T.R. Burckett St. Laurent, P.B. Hitchcock, H.W. Kroto and J.F. Nixon, *J.Chem.Soc.Chem.Commun.*, 1141 (1981).

42. J.C.T.R. Burckett St. Laurent, P.B. Hitchcock, H.W. Kroto, M.F. Meidine and J.F. Nixon, *J.Organometallic Chem.*, 238, C82 (1982).

43. This dimer was very kindly supplied by Professor J.F. Nixon of Sussex University.

44. M.F. Meidine, C.J. Meir, S. Morton and J.F. Nixon, *J. Organometallic Chem.*, 297, 255 (1985).

45. E. Cartmell and G.W.A. Fowles, "*Valency and Molecular Structure*", Fourth Edition, Butterworths, Chapter 11, p.282 (1983); and references therein.

46. H. Eshtiagh-Hosseini, H.W. Kroto, J.F. Nixon, M.J. Maah and M.J. Taylor, *J.Chem.Soc.Chem.Commun.*, 199-200 (1981).

47. a) J. Chatt and R.G. Wilkins, *J.Chem.Soc.*, 273-278 (1952).

b) J. Chatt and R.G. Wilkins, *J.Chem.Soc.*, 525-529 (1956).

48. M.F. Meidine, C.J. Meir, S. Morton and J.F. Nixon, *J. Organometallic Chem.*, 297, 255-263 (1985).

49. M. Yoshifuji, T. Hashida, N. Inamoto, K. Hirotsu, T. Horriuchi, T. Higuchi, K. Ito and S. Nagase, *Angew.Chem. Int.Ed.Engl.*, 24(3), 211-212 (1985).

50. a) J.G. Kraaijkamp, G. van Koten, T.A. van der Knapp and F. Bickelhaupt, *Organometallics*, 5, 2014-2020 (1986).

b) T.A. van der Knapp, L.W. Jenneskens, H.J. Meeuwissen, F. Bickelhaupt, D. Walther, E. Dinjus, E. Uhlig and A.L. Spek, *J.Organometallic Chem.*, 254, C33-36 (1983).

51. P.B. Hitchcock, M.J. Maah, J.F. Nixon, J.A. Zora, G.J. Leigh and M.A. Bakar, *Angew.Chem. Int.Ed.Engl.*, 26(5), 474-475 (1987).

52. D. Parker, R.J. Taylor, *Tetrahedron*, 44(8), 2241-2248 (1988).

53. M. Yoshifuji, K. Shibayama, T. Hashida, K. Toyota, M. Niitsu, I. Matsuda, T. Sato and N. Inamoto, *J.Organometallic Chem.*, 311, C63-C67 (1986).

54. J.F. Nixon and A. Pidcock, *Ann.Rev.NMR Spectrosc.*, 2, 345 (1969).

55. T.A. van der Knapp, F. Bickelhaupt, J.G. Kraaykamp, G. van Koten, J.P.C. Bernards, H.T. Edzes, W.S. Veeman, E. de Boer and E.J. Baerends, *Organometallics*, 3, 1804 (1984).

56. M. Yoshifuji and N. Inamoto, *Tetrahedron Lett.*, 24(44), 4855-4858 (1983).

57. F.R. Hartley, *Organometallic Chem.Reviews A.*, 6, 119-137 (1970).

CHAPTER SIX

ACCEPTOR PROPERTIES OF P(III) COMPOUNDS

6.1 INTRODUCTION

A large number of organohalophosphines have been prepared (see Chapter 2), and a large volume of data are available [1]. Many organophosphorus pseudohalides have been isolated [2-6], more recently by R. Ali (1986) and in this work. The acceptor properties of $RP(CN)_2$ have been investigated with R = Me, Ph, Et or C_6F_5 and X = Cl, Br, I or NCS (Equation 6.1) [7,8]. Addition of CN^- to $RP(CN)_2$ (R = Ph, Me and Et), resulted in reductive elimination, yielding the cyanophosphide, $RP(CN)^-$ and cyanogen $(CN)_2$ [9]. This phenomenon is also known in the addition of CN^- to $P(CN)_3$ giving $P(CN)_2^-$ and cyanogen [10].

It is interesting to note that some P(III) trihalides show acceptor properties, behaving as Lewis acids towards halides and pseudohalides, and several anionic derivatives, PX_4^- (X = F, Cl or Br) have been obtained [11-15]. The first phosphoranide isolated (as its Pr_4N^+ salt) was PBr_4^- [16a]. These can be compared with adduct formation (Equation 6.2) [17] and substitution (Equation 6.3) [2-6].

$$RP(CN)_2 + X^- \longrightarrow RP(CN)_2X^- \qquad (6.1)$$

$$MePCl_2 + NMe_3 \longrightarrow MePCl_2NMe_3 \qquad (6.2)$$

$$X^- + MePCl_2 \longrightarrow MePClX + Cl^- \qquad (6.3)$$

These substitution reactions only proceed if X forms stronger bonds to phosphorus in the normal way, *cf*. Equation 6.1 (*eg*. NCS, NCO, N_3, CN). They will not go with Br or I unless some additional driving force is provided, for example with LiI as the reagent, where formation of LiCl in a suitable solvent make the reaction possible.

The acceptor properties of RPX_2 are of particular interest as the resulting phosphoranide may play an important role in nucleophilic substitution at the phosphorus(III) centre, and also in coordination chemistry [8,13,15]. By isolation of the "intermediate" (II) (Equation 6.4) it should be possible by structural determination to obtain an insight into the mechanism of the overall reaction.

$$\underset{(I)}{RPX_2} + Y^- \longrightarrow \underset{(II)}{RPX_2Y^-} \longrightarrow \underset{(III)}{RPXY} + X^- \qquad (6.4)$$

Previous work revealed the X-ray crystallographic structure of some phosphoranides. Some selected examples are given in Table 6.1, including the first structurally determined phosphoranide containing an organo-group $[PhP(CN)_2Cl]^-$.

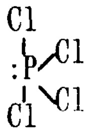
(A)

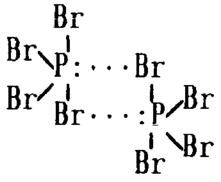
(B)

PHOSPHORANIDE	STRUCTURE	TYPE	REF
Et_4N^+ PCl_4^-	trigonal bipyramid	(A)	13,14
$[Ph_3P{=}CH\text{-}PPh_3]^+$ $P(CN)_3Cl^-$			13
$[Ph_3P{=}CH\text{-}PPh_3]^+$ $P(CN)_2Cl_2^-$			13
Pr_4N^+ PBr_4^- [1]	asymmetric dimer	(B)	13,14,16a
‡ 18C6-Na^+ $P(CN)_3Br^-$	symmetrical dimer with halogen bridges	(B)	13,14
‡ 18C6-Na^+ $P(CN)_3I^-$			13,14
Et_4N^+ $P(CN)_2PhCl^-$	trigonal bipyramid †		18 *

Table 6.1: *Shapes of some phosphoranides; ‡18C6=Na($C_{12}H_{24}O_6$)(THF)$_2$; †similar to PCl_4^- with equatorial Ph group with long (281 pm) axial P–Cl bond; *see Figure 6.2.*

The purpose of this study was aimed at the exploration of the effect of the organo group (R) on the acceptor properties of $RPCl_2$ and $RP(CN)_2$.

---

[1] A very recent publication (ref.16b) with the cation Et_4N^+ illustrates a monomeric structure for the PBr_4^-. An extremely distorted ψ-trigonal bipyramidal structure with axial P-Br distances of 2.970 Å and 2.305 Å. In this case at least the crystal structure is apparently cation dependent.

This area was extensively developed by R. Deng and R. Ali [7,8,18,19]. A brief summary of these groups, alongside previous ones for clarity, is presented in Table 6.2.

$$RPX_2 + Y^- \longrightarrow RPX_2Y^-$$

PRODUCT	R	X	Y	REF
$MeP(CN)_2Cl^-$	Me	CN	Cl	18
$MeP(CN)_2Br^-$	Me	CN	Br	18
$MeP(CN)_2I^-$	Me	CN	I	18
$PhP(CN_2)Cl^-$	Ph	CN	Cl	18
$PhP(CN)_2Br^-$	Ph	CN	Br	18
$PhP(CN)_2I^-$	Ph	CN	I	18
$C_6F_5P(Cl)_3^-$	C_6F_5	Cl	Cl	19
$C_6F_5P(NCS)_3^-$	C_6F_5	NCS	NCS	19
$C_6F_5P(CN)_2Cl^-$	C_6F_5	CN	Cl	20

Table 6.2

In these examples the use of cyanide increases the positive charge at phosphorus in the phosphine, and delocalises the negative charge at the phosphorus centre in the resulting phosphoranide, *eg.* ($R_2\overset{+}{P}{=}C{=}N^-$). It has been shown that the use of a sufficiently electron with-drawing group on phosphorus, *eg.* for $C_6F_5PCl_2$, allows the acceptor properties without the need for cyanide [19].

6.2 FURTHER ACCEPTOR PROPERTIES OF RPX_2 ($X \equiv Cl, CN$)

This study involved the R groups Ar [Ar = 2,4,6-$(CF_3)_3C_6H_2$] and CF_3 and the results are presented in Tables 6.3 and 6.5 respectively. Cl^- was used since it gives the greatest limiting shift.

6.2.1 Results for R ≡ Ar

REACTION	RESULT	^{31}P NMR
$ArPCl_2$ (12) $\xrightarrow{Cl^-}$	no reaction	[145 ppm, $^4J(PF)$ 61 Hz]
$ArP(CN)_2$ (16) $\xrightarrow{Cl^-}$	$ArP(CN)_2Cl^-$ (67)	[-137.4 ppm, $^4J(PF)$ 34.5 Hz]
$ArP(CN)_2$ (16) $\xrightarrow{CN^-}$	no reaction	[-86.8 ppm, $^4J(PF)$ 40.0 Hz]

Table 6.3: *Acceptor properties of* $ArPX_2$ *(*$X \equiv CN, Cl$*).*

The ^{31}P NMR values obtained on successive addition of Cl^- (Et_4NCl) to the dicyanophosphine (16) are presented in Table 6.4. The results were attributed to the setting up of the equilibrium shown in Equation 6.5.

$$ArP(CN)_2\ (16) + Cl^- \rightleftharpoons ArP(CN)_2Cl^-\ (67) \qquad (6.5)$$

MOLAR RATIO Cl^- : $ArP(CN)_2$ (16)	^{31}P NMR (δ/ppm)
0.5	-103.5
1.0	-120.2
1.2	-129.2
1.5	-137.4
2.0	-137.4

Table 6.4: *"Limiting Shift".*

The limiting shift was achieved here only when the tetraethylammonium chloride was in excess (~ 1.5 fold). This effect is illustrated graphically in Figure 6.1.

It has been shown that C_6F_5 is more strongly electron withdrawing in nature than the aryl substituent [21]. This may account for the non-acceptor properties of $ArPCl_2$ (12) compared with the phosphoranide formation by $C_6F_5PCl_2$. This may also be attributed to the greater steric demand of the aryl substituent. The predominance of this factor may account for the fact that no phosphoranide was observed on reaction of

$ArP(CN)_2$ (16) with cyanide (Table 6.3). Numerous attempts at low temperature crystallisation of $[Et_4N][ArP(CN)_2Cl]$ (67) were made, but these were not successful.

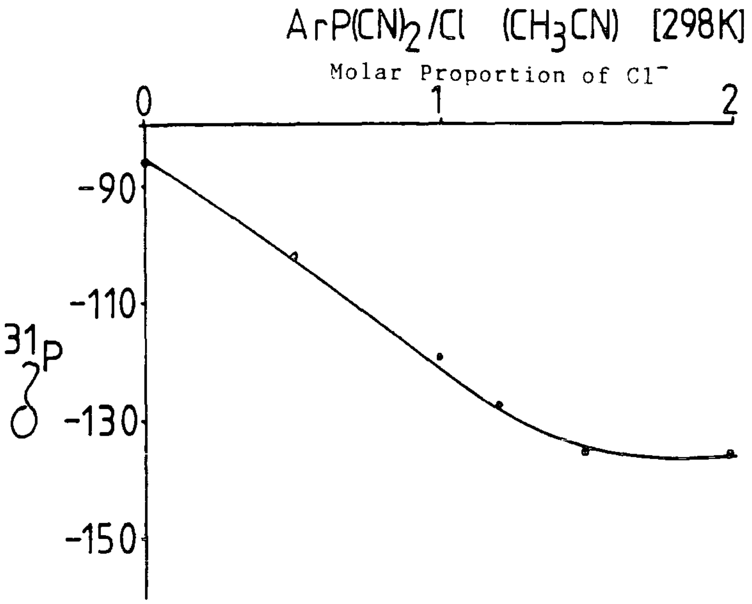

Figure 6.1: *Successive addition of Cl⁻ to the dicyanophosphine $ArP(CN)_2$ (16).*

Structural details of (67) would be of particular interest because of the electron-withdrawing nature of the aryl group and its size - it may occupy the axial position in the trigonal bipyramid. The general rule of apicophilicity[2] places the most electronegative group axial. As discussed, the only other known structural parameters of a phosphoranide containing an organo-group are for $PhP(CN)_2Cl^-$ [18]; here this balance of steric and electronic properties of R is not so pronounced. The very recent publication of the crystal structure of this species has been presented (Figure 6.2).

---

[2] The change in energy when two groups exchange apical and equatorial positions in a trigonal bipyramid.

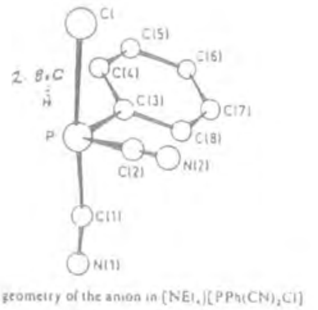

Figure 6.2: *Recently published X-ray structure of $PhP(CN)_2Cl^-$.*

6.2.2 MNDO Calculation

The results of a MNDO calculation on the species $ArP(CN)_2Cl^-$ (67) are presented in Figure 6.3. The aryl group is axial and as expected orientated slightly toward the equatorial lone pair. Poor results were obtained, as expected from this calculation on the phosphoranide (67) since the phosphorus is hypervalent, and the MNDO calculation fails to consider d-orbital involvement (calculated P-Cl length = 2.2Å). The expected P-Cl bond length in phosphoranides is of the order of 2.85Å in PCl_4^- and 2.81Å in $PhP(CN)_2Cl^-$ [18].

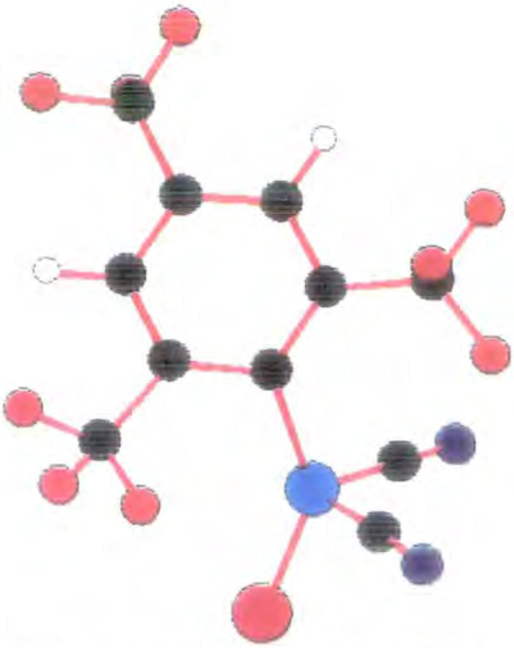

Figure 6.3: *MNDO calculation results for $ArP(CN)_2Cl^-$ (67).*

Figures 6.2 and 6.3 illustrate the cyanide to be definitely less apicophilic than halogen (Cl, Br). In the specific case of $P(CN)_3X^-$, $(X \equiv Br, I)$ dimerisation prevents the CN group from being forced into an apical position [13].

6.2.3 Results for R ≡ CF_3

Addition of Et_4NCN to $CF_3P(CN)_2$ (68) expected to possess high acceptor properties does not show the phosphoranide $CF_3P(CN)_3^-$ (69). However, a downfield signal at +77 ppm was present with the concomitant disappearance of $CF_3P(CN)_2$ (68). Results are presented in Table 6.5 and illustrated in Figure 6.4. An extension of this work could involve the addition of Cl^- to $CF_3P(CN)_2$ (68). This would be expected to accept to form the respective phosphoranide.

SPECIES	^{31}P NMR (δ/ppm)	COUPLING $^2J(PF)$/Hz
CF_3PCl_2 (13)	133.47	7.9
$CF_3P(CN)_2$ (68)	-80	89
$[CF_3PCN]^-$ (70)	+77	43.1

Table 6.5

The quartet at +77 ppm is assigned to the cyanophosphide, $[CF_3PCN]^-$ (70) (Equation 6.6). The overall reaction and the ^{31}P NMR parameters are shown in Equation 6.6 and Table 6.5 respectively, with the phosphoranide (69) proposed as the intermediate.

$$CF_3P(CN)_2\ (68) \xrightarrow{CN^-} CF_3P(CN)_3^-\ (69) \longrightarrow [CF_3PCN]^-\ (70) + (CN)_2 \qquad (6.6)$$

The brown colouration of the solution was attributed to rapid cyanogen polymerisation providing the driving force for the reaction.

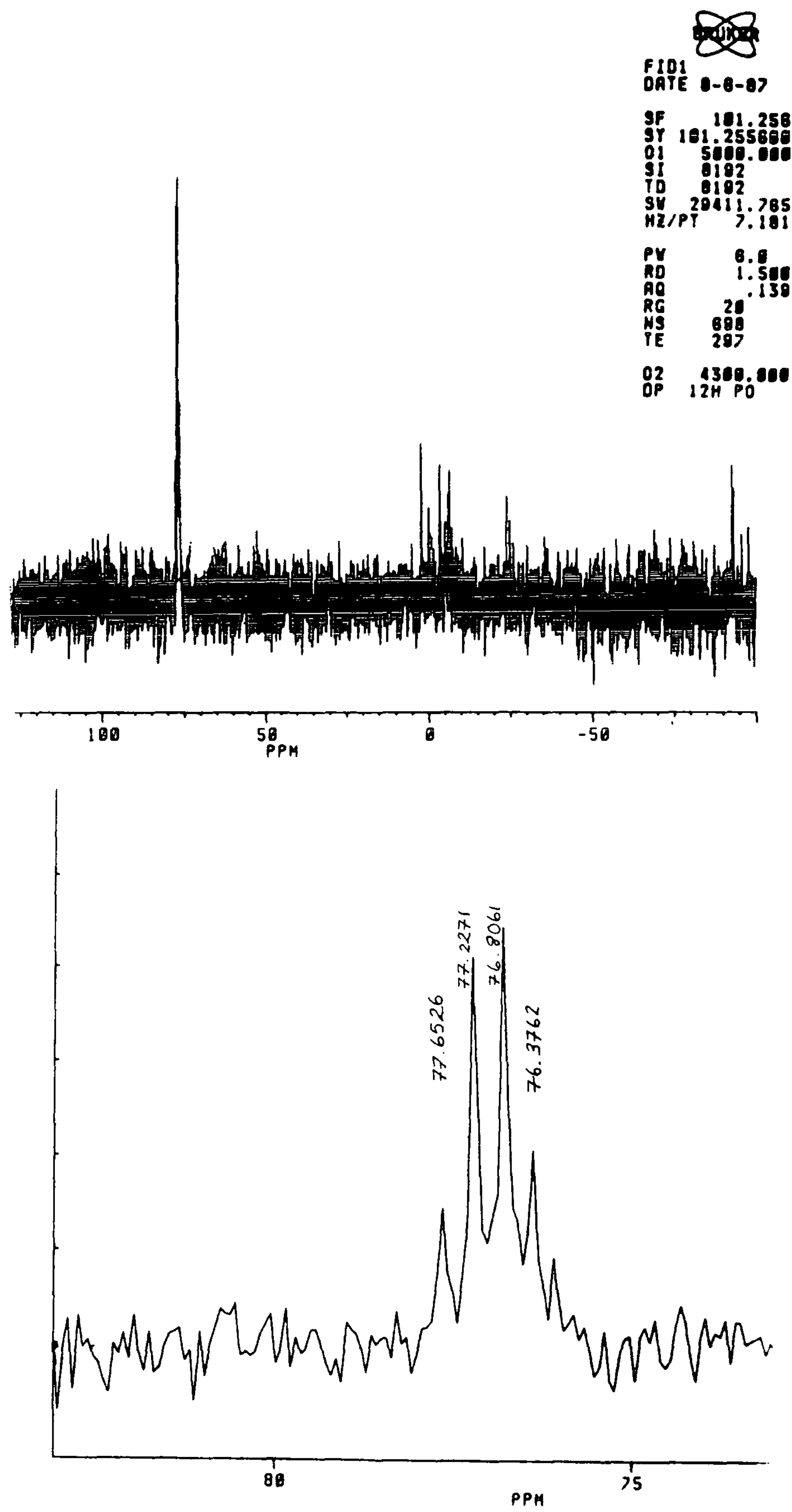

Figure 6.4: *The addition of Bu_4NCN to $CF_3P(CN)_2$ (68) with the apparent formation of the cyanophosphide, $[CF_3PCN]^-$ (70).*

The species was not stable to isolation. This may be compared with other phosphides [9]. This was considered unusual since the presence of the electronegative CF_3 groups would be expected to stabilise the anion.

The particular interest in the nature of the Ar group led us to explore the acceptor properties of the boron derivatives (4,73) (Chapter 8). No acceptance was observed in the case of either $ArBCl_2$ or Ar_2BCl.

6.3 AN AMINO GROUP AS THE ORGANO SUBSTITUENT

The nature of R_2N in this context was considered for the first time. Reactions were carried out with R_2NPCl_2 and $(R_2N)_2PCl$, and their cyanide derivatives, the analogous chloroboron systems were also considered. With the following systems no acceptance properties with Cl^- were observed even by decreasing the group size on nitrogen, indicating that the steric effects do not appear to be significant. $(^iPr_2N)_2PCl$ (^{31}P δ: 139.9 ppm)[22]; $(^iPr_2N)_2PCN$ (^{31}P δ: 30.0 ppm)[23]; $^iPr_2NPCl_2$ (^{31}P δ: 167.7 ppm)[24]; $^iPr_2NP(CN)_2$ (^{31}P δ: -19.3 ppm); $(Et_2N)_2PCl$ (^{31}P δ: 147.9 ppm)[24]; $(Et_2N)_2PCN$ (^{31}P δ: 29.5 ppm)[22]; Et_2NPCl_2 (^{31}P δ: 160.8 ppm)[24]; $Et_2NP(CN)_2$ (^{31}P δ: -17.1 ppm)[22]; $(Et_2N)_2BCl$ (^{11}B δ: +28.4 ppm)[25]; $(Et_2N)BCl_2$ (^{11}B δ: +23.3 ppm)[25] (see Section 6.4.11).

It had been expected that the boron derivatives would accept more readily because of their greater Lewis acidity. The fact that no acceptor properties were observed can possibly be attributed to lone pair back donation from nitrogen to boron, *ie.*.

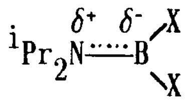

R_2N is used universally in the stabilisation of 2 coordinate boron and phosphorus cations (borinium and phosphenium moieties) [26].

6.4 EXPERIMENTAL DETAILS

6.4.1 Preparation of $ArP(CN)_2$ (16)

$$ArPCl_2\ (12) + 2AgCN \longrightarrow ArP(CN)_2\ (16) + 2AgCl$$

$ArPCl_2$ was prepared as described in Section 2.3.3 AgCN (1.1g, 8.2 mmol) was added to a stirred solution of $ArPCl_2$ (1.51g, 3.96 mmol) in CH_3CN (20 ml) at room temperature. This mixture was gradually brought to reflux. After refluxing for 2 hours complete conversion to $ArP(CN)_2$ was verified by the ^{31}P NMR of -86.8 ppm, $^4J_{PF}$ 40.0 Hz. CH_3CN was removed *in vacuo*, and the product was extracted into Et_2O. Extraction into pentane gave very poor yields due to the low solubility of $ArP(CN)_2$ in this solvent. The insoluble silver salts were removed by filtration, and the pentane removed *in vacuo* to yield a white solid. Extreme care had to be taken on manipulation due to its extreme sensitivity to hydrolysis giving peaks in the ^{31}P NMR at approx 0 ppm. The initial AgCN added must be stored with rigorous exclusion of light and moisture, since a poor AgCN sample (grey Ag deposits) gave very poor results even when added in excess. Best yields were obtained from a fresh sample. From the above preparation, $ArP(CN)_2$ (16) (0.7g, 49%) was obtained as a white solid. Mpt. > 75 ^oC (dec); Analysis found: C, 36.33; H, 0.60; N, 7.39; Required for $C_{11}H_2F_9N_2P$: C, 36.28; H, 0.55; N, 7.69%; IR (Nujol) ν_{max}: 3120 (m,C aromatic), 2190 (s,CN), 1850 (m), 1630 (m), 1585 (m), 1480-800 (s,CF_3) cm^{-1}; MS (Intensity%) EI: 364 [10.3,($ArP(CN)_2^+$)], 83 [100,($P(CN)_2^+$)]; CI^+: 364 [10.3,($ArP(CN)_2^+$)], 83 [100,($P(CN)_2^+$)]; ^{31}P δ:

-87.2 ppm (septet) $^4J_{PF}$ 40.6 Hz; ^{19}F δ: -54.9 (d,6F) $^4J_{PF}$ 40.6 Hz, -64.1 (s,3F) ppm.

6.4.2 Attempted Preparation of $ArP(CN)_2$ (16) *via* $ArPCl_2$/LiCN

$$ArPCl_2\ (12) + LiCN\ (xs) \xrightarrow[\quad X \quad]{DMF} ArP(CN)_2\ (16)$$

A solution of lithium cyanide (22 ml, 11 mmol, 0.5M in DMF) was added dropwise over 5 minutes to a stirred solution of $ArPCl_2$ (2.1g, 5.4 mmol) in CH_3CN (25 ml) at room temperature. This was refluxed for 2 hours. The recording of the ^{31}P NMR showed a singlet species at 4.97 ppm, attributed to complete hydrolysis of material. LiCN·DMF solution was commercially available [Aldrich Cat.No. 24,660-3].

6.4.3 Preparation of $ArP(CN)_2Cl^-$ (67)

$$ArP(CN)_2\ (16) + Cl^- \longrightarrow ArP(CN)_2Cl^-\ (67)$$

$Et_4N^+Cl^-$ (0.27g, 1.63 mmol) in CH_3CN (10 ml) was added dropwise to a stirred solution of $ArP(CN)_2$ (1.2g, 3.3 mmol) in CH_3CN (25 ml) at room temperature. The reaction mixture was stirred for 1 hour. Successive 0.5 equivalents of $Et_4N^+Cl^-$ (0.27g, 1.63 mmol) in CH_3CN (10 ml) were added, and the reaction mixture stirred for 1 hour after each addition. The ^{31}P NMR was recorded after each stage. Results and graph are shown in Section 6.2.1. Removal of the CH_3CN *in vacuo* yielded a sticky oil, and addition of a minimum volume of CH_2Cl_2 (*ca.* 5 ml), and cooling to -40 °C over one week gave no precipitation (it was hoped that the greater solubility of $Et_4N^+Cl^-$ in CH_2Cl_2 would keep it in solution).

The C,H,N elemental analysis showed that the compound obtained was not pure (%C ~7% too low and similarly low value for %N).
With respect to the ^{31}P NMR an almost quantitative yield of the phosphoranide was achieved: ^{31}P δ: -137.4 ppm (septet) $^{4}J_{PF}$ 34.5 Hz.

6.4.4 Attempted Preparation of Bu_4N^+ $ArP(CN)_3^-$

$$ArP(CN)_2\ (16) + Bu_4N^+CN^-\ (xs) \longrightarrow ArP(CN)_3^-$$

Bu_4NCN (1.1g, 4.1 mmol) in CH_3CN (10 ml) was added dropwise over 5 minutes to a stirred solution of $ArP(CN)_2$ (1.2g, 3.3 mmol) in CH_3CN (25 ml). This mixture was stirred at ambient temperature for 6 hours. No reaction was detected in the ^{31}P NMR. ^{31}P (CH_3CN) δ: -86.8 ppm (septet) $^{4}J_{PF}$ 40 Hz (unchanged starting material).

6.4.5 Preparation of CF_3PCl_2 *via* $CF_3P(Et_2N)_2$

CF_3PCl_2 was prepared by the method of Volbach and Ruppert [29] and also the method of Ruppert [30]. In this work the experiment was modified to involve CF_3I in place of CF_3Br. Both gave satisfactory results, but the CF_3I was superior, as expected from the weaker C-I bond strength. Yields of the latter were of the order of 70-75%. The two methods (Equations 6.7 and 6.8) differ only in that the first involves attack of PCl_3 on $(Et_2N)_3P$ to form equimolar quantities of each starting material.

$$5(Et_2N)_3P + PCl_3 \longrightarrow 3(Et_2N)_3P + 3(Et_2N)_2PCl \xrightarrow{3CF_3X} 3[(Et_2N)_3PCl]^+X^- + 3CF_3P(NEt_2)_2\ (X = I,\ Br) \qquad (6.7)$$

$$(Et_2N)_2PCl + (Et_2N)_3P \xrightarrow{CF_3X} [(Et_2N)_3PCl]^+X^- + CF_3P(NEt_2)_2 \qquad (6.8)$$

The first method (Equation 6.7) stated the use of diethyl carbonate as the solvent, although some results were obtained in hexane using the other method (Equation 6.8). This gave lower yields and CH_2Cl_2 was superior. Some explanation for the lack of success of the non-polar solvent can be gained from the postulate of Volbach and Ruppert [29] concerning the formation of an ionic intermediate, $(Et_2N)_3PBr^+CF_3^-$. This may be unfavourable in hexane which did not appear capable of keeping all the reactants in a single homogeneous phase. This effect is obviously dominant over the insolubility of $(Et_2N)_3PCl^+Br^-$ driving the reaction to completion. In hexane, reactions were carried out at temperatures below the boiling points of the CF_3X ($X \equiv$ Br, I) species, which did not appear to be reactive at these temperatures. The more polar solvents allowed the CF_3I and CF_3Br to be introduced at higher temperatures without boiling off.

The product $CF_3P(Et_2N)_2$ was separated from oxides and side products. The applicability of GLC was tested on a small sample - it showed a good peak separation, but proved to be an unsuitable technique for such an air-sensitive compound. Purification was best achieved by low temperature crystallisation, allowing the precipitation of unwanted oxides in a small volume of hexane. The filtrate was treated *in situ* with gaseous HCl to yield CF_3PCl_2 (a one pot reaction sequence). The CF_3PCl_2 was then distilled from the hexane, bpt. 36 ^oC (760 mm Hg) [31]; ^{31}P δ: 133.5 ppm, $^2J_{PF}$ 79.9 Hz.

6.4.6 Preparation of $CF_3P(CN)_2$ (68)

$$CF_3PCl_2 \xrightarrow{2AgCN} CF_3P(CN)_2 \ (68)$$

CF_3PCl_2 (1.5g, 8.8 mmol) in CH_3CN (25 ml) was added to a slight excess of AgCN (*ca*. 2.5g, 18.7 mmol, 2.4 equivalents). This mixture was stirred for at least 4 hours and the reaction was monitored by ^{31}P NMR. It appeared that several exchange equilibria were established, *eg*. signals were observed at ^{31}P δ: -70 ppm, $^4J_{PF}$ 40 Hz, -74 ppm, $^4J_{PF}$ 46 Hz. After 4 hours a limiting NMR chemical shift was recorded (^{31}P δ: -80.1 ppm, $^2J_{PF}$ 89.0 Hz; ^{19}F δ: -52.2 ppm). This agrees well with the previously recorded NMR parameters [32-33]. CH_3CN was removed *in vacuo*, and the product was extracted into pentane. The pentane was removed to give an oil in approximately 45% yield (0.6g).

6.4.7 Preparation of $[Et_4N][CF_3PCN]$ (70)

$$CF_3P(CN)_2 \ (68) + 3CN^- \longrightarrow [CF_3PCN]^- \ (70) + (CN)_2 + 2Cl^-$$

A solution of $CF_3P(CN)_2$ (0.7g, 4.6 mmol) in CH_3CN (20 ml) and 1.1 equivalents of Bu_4NCN (1.36g, 5.1 mmol), stirred at room temperature for 2 hours did not give the expected upfield shift corresponding to $CF_3P(CN)_3^-$. The solution turned brown. A peak downfield was seen in the ^{31}P NMR (+77 ppm $^2J_{PF}$ 43.1 Hz) with the disappearance of the peak at -80.1 ppm (corresponding to starting material) (see Figure 6.4). This peak was attributed to $[Bu_4N^+][CF_3PCN^-]$ caused by loss of cyanogen - its rapid polymerisation causing colouring of the solution. Removal of the solvent, and redissolving the resulting sticky brown oil in a minimum volume of CH_3CN on cooling gave no precipitation, and neither did dropwise addition of pentane. Re-observation of the ^{31}P NMR spectrum indicated decomposition, possibly polymerisation or hydrolysis, giving a ^{31}P shift of approximately 0 ppm.

6.4.8 Preparation of $(^{i}Pr_2N)_2PCl$ and $(Et_2N)_2PCl$

$$PCl_3 + 4R_2NH \longrightarrow (R_2N)_2PCl + 2R_2NH_2^+Cl^- \quad (R = {}^{i}Pr,\ Et)$$

These were prepared according to N.D.A.H. Khabbass [27]. A low boiling point petroleum was used for the solvent system, however, since this allows its facile removal *in vacuo*. ^{31}P NMR data for $(^{i}Pr_2N)_2PCl$ and $(Et_2N)_2PCl$ agree well with previously published results [1], δ: +147.9 and +139.9 ppm, respectively.

6.4.9 Preparation of $(^{i}Pr_2N)PCl_2$ and $(Et_2N)PCl_2$

$$PCl_3 + 2R_2NH \longrightarrow R_2NPCl_2 + R_2NH_2^+Cl^-$$

These were prepared similarly, according to King and Sadanani (1985) [24]. $^{i}Pr_2NPCl_2$ [21,22], bpt. 75-80 ^oC (3.5 mm Hg); ^{31}P δ: +167.7 ppm. Et_2NPCl_2 [24,27], bpt. 68-70 ^oC (3.5 mm Hg); ^{31}P δ: +160.8 ppm.

6.4.10 Preparation of $(Et_2N)_3P$

$$6Et_2NH + PCl_3 \xrightarrow{Et_2O} (Et_2N)_3P + 3Et_2NH_2^+Cl^-$$

Hexaethylphosphorus triamide was prepared according to A. Michaelis [28] and also commercially available from Aldrich [Cat. 25,318-9]. Bpt. 85-90 ^oC (10 mm Hg); ^{31}P δ: +117.4 ppm.

6.4.11 Preparation of $(Et_2N)_2BCl$ and $(Et_2N)BCl_2$

$(Et_2N)_2BCl$ was prepared according to W. Gerrard *et al.*[25b], and $(Et_2N)BCl_2$ according to A.J. Banister [25c]. ^{11}B NMR shifts were verified from known data [25a]. $(Et_2N)_2BCl$, bpt. 83-85°C (16 mm Hg) [25b]; ^{11}B δ: 28.4 ppm. $(Et_2N)BCl_2$, bpt. 75-75.5°C (63-64 mm Hg) [25c]; ^{11}B δ: +23.3 ppm [25a]. Preparation of the $^iPr_2N$ derivatives is described in Chapter 11 and the disubstituted derivative in Chapter 9.

6.4.12 Preparation of Cyanide Derivatives

The solvent used in the preparation of the cyanide derivative was CH_3CN since CH_2Cl_2 may possibly exchange Cl^- with CN^-, lowering the effective cyanide concentration. The general technique of extracting the cyanide derivative into pentane allows separation from hydrolysis products at this stage.

6.4.12.1 Preparation of $^iPr_2NP(CN)_2$

$$^iPr_2NPCl_2 + 2\ AgCN \xrightarrow{MeCN} {}^iPr_2NP(CN)_2$$

Silver cyanide (7.65g, 57 mmol) was added to a stirred solution of $^iPr_2NPCl_2$ (5.66g, 28 mmol) in CH_3CN (50 ml) at room temperature. This was refluxed for 16 hours until quantitative conversion to the dicyanide was verified by ^{31}P NMR. The solvent was removed *in vacuo* and the product extracted into pentane (25 ml). The insoluble silver salts were removed by filtration and the pentane *in vacuo* to yield a thermally unstable whitish oil. Yield of crude product was 3.2g (63%). ^{31}P δ: -19.29 ppm.

6.4.12.2 Preparation of $Et_2NP(CN)_2$

$$Et_2NPCl_2 + 2\ AgCN \longrightarrow Et_2NP(CN)_2$$

The experimental procedure and molar quantities are exactly analogous to that described for $^{i}Pr_2NP(CN)_2$ (Section 6.4.12.1), however, for this stage it was purified by vacuum distillation. A clear oil was obtained in 60% yield. Bpt. 71 °C (0.5 mm Hg); ^{31}P δ: -17.1 ppm [22].

6.4.12.3 Preparation of $(Et_2N)_2PCN$

$$(Et_2N)_2PCl + AgCN \longrightarrow AgCl + (Et_2N)_2P(CN)$$

A similar preparation to the dicyanide analogues however a stoichiometry AgCN : $(^{i}Pr_2N)_2PCl$ = 1:1 is required. This was distilled as an oil, yield 50%. Bpt. 66-68 °C (1 mm Hg) [22]; ^{31}P δ: 30.2 ppm.

6.4.12.4 Preparation of $(^{i}Pr_2N)_2PCN$

$$(^{i}Pr_2N)_2PCl + AgCN \longrightarrow (^{i}Pr_2N)_2P(CN) + AgCl$$

Crude yield 55%, ^{31}P δ: +30.0 ppm. This was also obtained as a by-product from hydrolysis occurring in the nitrileimine species (62) (Chapter 11) [23], ^{31}P δ: +29.5 ppm.

6.4.13 Addition of X^-

In a typical experiment to investigate the acceptance of X^- [where $X = CN^-$ $(Bu_4N^+CN^-)$, Cl^- $(Et_4N^+Cl^-)$, the cyanide or chlorophosphorus derivative (0.01 mol) was dissolved in CH_3CN. To this was added $Et_4N^+Cl^-$ or $Bu_4N^+CN^-$ (1 equivalent), and the mixture stirred for a period of 6 hours at room temperature. The NMR was recorded. No X^- acceptance of species bearing R_2N groups was observed.

6.5 REFERENCES

1. M.M. Crutchfield, C.H. Dungan, J.H. Letcher, V. Mark and J.R. van Wazer, "*^{31}P Nuclear Magnetic Resonance*", John Wiley and Sons (1967).
2. F.W. Bennett, H.J. Emeleus and R.N. Haszeldine, *J.Chem.Soc.*, 1565 (1953).
3. M. Fild, *Z.Naturforsch*, 23b, 604 (1968).
4. M. Fild, O. Glemser and I. Hollenburg, *Naturwiss*, 53, 130 (1966).
5. L. Maier, *Helv.Chim.Acta*, 46, 2667 (1963).
6. R. Ali and K.B. Dillon, *Polyhedron*, 5(6), 1197-1199 (1986).
7. R.M.K. Deng, Ph.D. Thesis, Durham University (1981).
8. R.M.K. Deng, K.B. Dillon and A.W.G. Platt, *Phosphorus and Sulphur*, 18, 93-96 (1983).
9. R.M.K. Deng and K.B. Dillon, *J.Chem.Soc.Chem.Commun.*, 1170 (1981).
10. A. Schmidpeter and F. Zwaschka, *Angew.Chem. Int.Ed.Engl.*, 16, 704 (1977).
11. A.W.G. Platt, Ph.D. Thesis, Durham University (1980).
12. A. Schmidpeter and F. Zwaschka, *Angew.Chem. Int.Ed.Engl.*, 18, 411 (1979).
13. W.S. Sheldrick, A. Schmidpeter, F. Zwaschka, K.B. Dillon, A.W.G. Platt and T.C. Waddington, *J.Chem.Soc.Dalton Trans.*, 413 (1981).
14. K.B. Dillon, A.W.G. Platt, A. Schmidpeter, F. Zwaschka and W.S. Sheldrick, Z. Anorg. Allg. Chem., 488, 7 (1982).
15. R. Ali and K.B. Dillon, *Phosphorus and Sulphur*, 30, 139-142 (1987).
16. a) K.B. Dillon and T.C. Waddington, *J.Chem.Soc.Chem.Commun.*, 1317 (1969).

    b) W.S. Sheldrick and J. Kiefer, *Z.Naturforsch B.*, 44b, 609-611 (1989).

17. R.P. Holmes and R.P. Wagner, *Inorg.Chem.*, 2, 384 (1963).

18. R.M.K. Deng, K.B. Dillon and W.S. Sheldrick, *J.Chem.Soc.Dalton Trans.*, in press (1990).

19. R. Ali, Ph.D. Thesis, Durham University (1986).

20. Work by J. Lincoln, University of Durham, 1986-1987.

21. G.E. Carr, R.D. Chambers, T.F. Holmes and D.G. Parker, *J.Organometallic Chem.*, 325, 13 (1987).

22. D. Kiessling, K.-P. Knackmuss, H. Schicht, F. Winn and R. Schöllner, *J.für Praktische Chemie*, 315(4), 577-586 (1973).

23. A. Baceiredo and G. Bertrand, *Phosphorus and Sulphur*, 26, 57-62 (1986).

24. R.B. King and N.D. Sadanani, *Synth.React.Inorg.Met.Org.Chem.*, 15(2), 149-153 (1985).

25. a) H. Nöth and H. Vahrenkamp, *Chem.Ber.*, 1049-1067 (1966).

    b) W. Gerrard, M.F. Lappert and C.A. Pearce, *J.Chem.Soc.*, 381-386 (1957).

    c) A.J. Banister, N.N. Greenwood, B.P. Straughan and J. Walker, *J.Chem.Soc.*, 995-1000 (1964).

26. P. Kölle and H. Nöth, *Chem.Rev.*, 85, 399-418 (1985).

27. A.H. Khabbass, Ph.D. Thesis, Durham University (1981).

28. a) A. Michaelis, *Ann.Chem.Liebigs*, 326, 154 (1903).

    b) J.R. van Wazer and L. Maier, *J.Amer.Chem.Soc.*, 56, 811 (1964).

29. W. Volbach and I. Ruppert, *Tetrahedron Lett.*, 24(49), 5509-5512 (1983).

30. I. Ruppert, *International Conference on Phosphorus Chemistry*, Bonn, Abstracts of Posters, August 31st-September 6th, 1986.

31. F.W. Bennett, H.J. Emeléus and R.N. Haszeldine, *J.Chem.Soc.*, 1565-1571 (1953).

32. I.H. Sabherwal and A.B. Burg, *Inorg.Chem.*, 11, 3138 (1972).

33. R.C. Dobbie, P.D. Gosling and B.P. Straughan, *J.Chem.Soc.Dalton Trans.*, 2368-2373 (1975).

CHAPTER SEVEN

HALO AND DIHALOSTIBINES AND THE ATTEMPTED FORMATION OF OTHER LOW COORDINATED, MULTIPLY-BONDED COMPOUNDS

7.1 ORGANOANTIMONY COMPOUNDS

7.1.1 Introduction

Halostibines, R_2SbX and dihalostibines, $RSbX_2$ (where R = alkyl, aryl and X = halogen), can be prepared by standard methods [1]. For example the stibine $(Me_3Si)_2CHSbCl_2$ may be prepared by treatment of $SbCl_3$ with $(Me_3Si)_2CHMgCl$ in Et_2O [2], and the synthetic route to Ph_2SbF [3] has been described. An interesting cyclisation yielding an antimony heterocycle resulted from the attempted synthesis of 2,4,6-$(^tBu)_3C_6H_2SbCl_2$ by treatment of 2,4,6-$(^tBu)_3C_6H_2Li$ with $SbCl_3$ [4].

7.1.2 New Organoantimony Compounds

$ArSbCl_2$ and Ar_2SbCl were prepared *via* the classical procedure (Equations 7.1 and 7.2) (see Figure 7.1).

$$\text{ArLi (2)} + SbCl_3 \longrightarrow ArSbCl_2 \text{ (71)} \tag{7.1}$$

$$\text{2ArLi (2)} + SbCl_3 \longrightarrow Ar_2SbCl \text{ (72)} \tag{7.2}$$

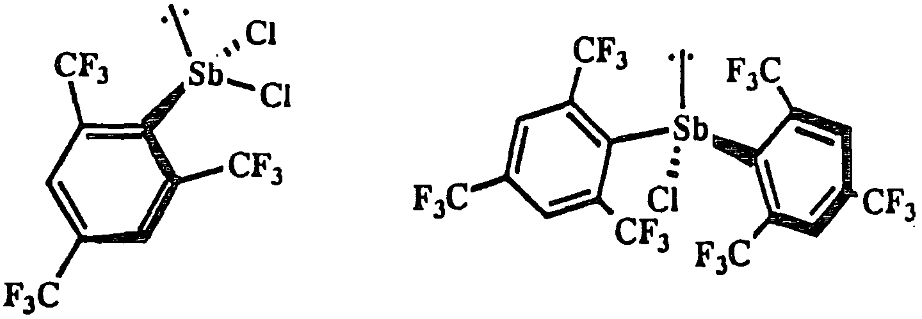

Figure 7.1: *$ArSbCl_2$ (71) and Ar_2SbCl (72).*

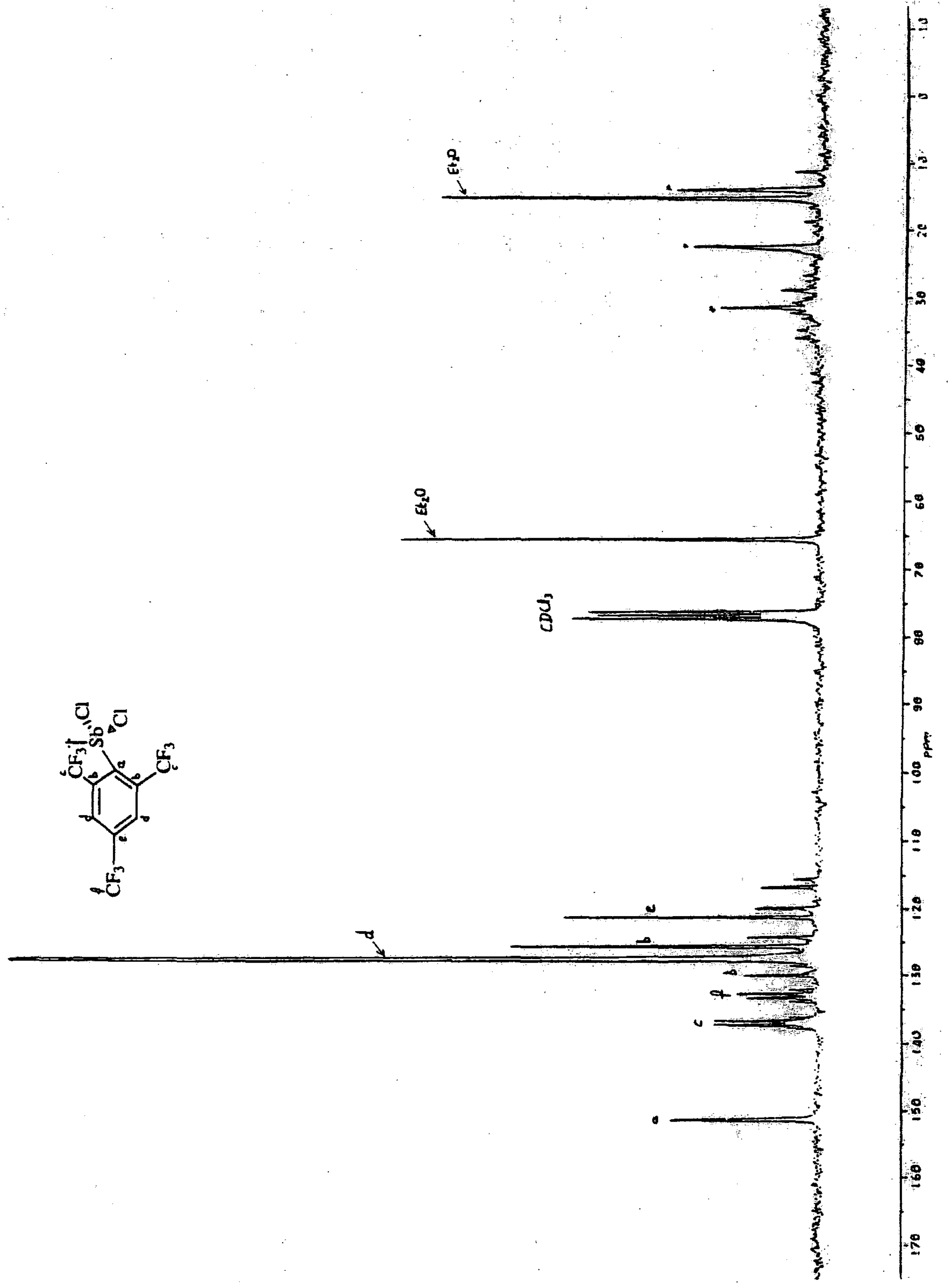

Figure 7.2: $^{13}C\{^{1}H\}$ NMR spectrum of $ArSbCl_2$ (71) in $CDCl_3$.

The reactions were carried out in diethyl ether. The fact that $SbCl_3$ is insoluble in non-polar solvents allowed the product to be extracted into pentane. High yields of these compounds were obtained. With slow controlled addition of ArLi to the required stoichiometric amount of $SbCl_3$ at low temperature, it was possible to substitute selectively chlorine for aryl, avoiding a loss of yield by tertiary stibine formation.

The high instability of $ArSbCl_2$ (71) caused a great many problems. It was possible by preparing, and then immediately recording its spectral parameters, and elemental analysis (its sensitivity precluded a very accurate analysis), to characterise it. However, even in the inert atmosphere of the glove box, the powdery yellow solid visibly decomposed to a reddish viscous oil. This was also confirmed by L. Weber [5]. In contrast, Ar_2SbCl (72) was stable in storage indefinitely under an inert atmosphere at room temperature. The ^{13}C NMR of $ArSbCl_2$ (71) in $CDCl_3$ (illustrating the presence of Et_2O) is shown in Figure 7.2 and the mass spectra of $ArSbCl_2$ (71) and Ar_2SbCl (72) in Figures 7.3 and 7.4 respectively.

7.2 ATTEMPTED FORMATION OF OTHER LOW-COORDINATE, MULTIPLY BONDED SPECIES

7.2.1 Introduction

The use of bulky aryl and alkyl substituents has allowed the isolation of low coordinate, multiply bonded Group (V) compounds with the general formula R'-X=Y-R" [2,6,7]. Some examples are presented in Table 7.1.

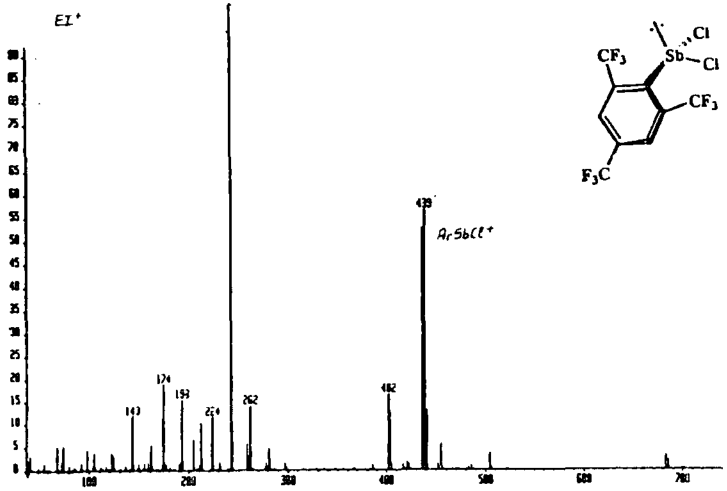

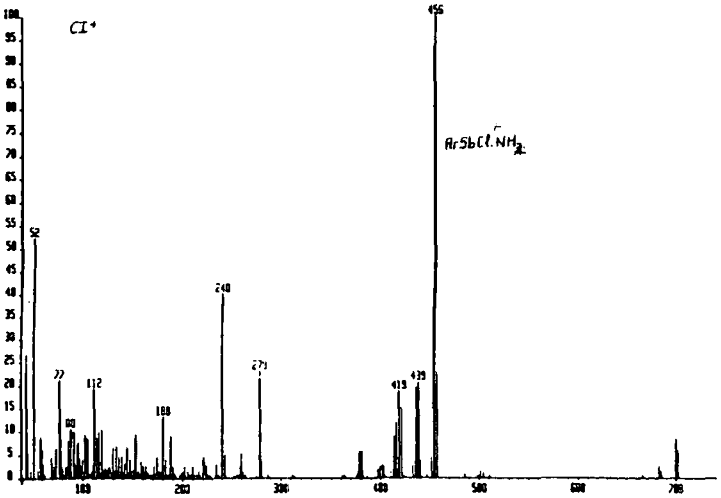

EI⁺

Mass	% Base	
396.93	0.16	
401.83	16.51	
402.83	1.46	
403.82	12.77	
404.86	1.58	
405.90	0.11	
416.93	1.14	
417.84	0.37	
419.80	0.31	
420.83	1.65	
421.82	0.28	
422.82	1.28	
423.82	0.11	
435.92	28.91	F
436.81	52.93	F
437.80	5.44	F
438.80	56.71	F
439.80	5.26	
440.79	13.06	
441.80	1.13	
451.90	1.25	
452.88	0.27	
453.92	0.43	
454.93	5.61	
455.93	1.13	
456.93	0.11	
466.94	0.17	
470.91	0.25	
480.76	0.29	
482.75	0.56	
484.78	0.20	
485.92	0.95	
486.93	0.16	
504.94	3.51	
505.95	0.65	
520.94	0.18	
682.90	3.02	
683.92	0.57	
684.90	2.01	
685.88	0.38	
698.82	0.29	
700.86	0.21	

CI⁺

Mass	% Base
259.99	0.39
279.12	1.65
280.13	0.26
377.07	0.11
378.87	0.42
379.88	0.18
380.87	0.42
381.90	0.13
397.87	0.13
399.88	0.17
401.83	0.19
403.79	0.16
410.87	0.11
412.87	0.12
413.84	0.64
414.85	0.11
415.83	0.85
416.89	0.12
417.86	0.30
418.88	1.34
419.89	0.54
420.86	1.08
421.90	0.33
432.97	0.19
435.94	0.32
436.77	1.40
437.85	0.27
438.77	1.48
439.82	0.23
440.76	0.29
451.98	0.33
453.86	6.70
454.86	0.77
455.85	7.14
456.87	0.80
457.85	1.65
458.86	0.16
682.77	0.17
684.73	0.10
699.92	0.60
700.94	0.11
701.93	0.42

Figure 7.3: *Mass spectrum of ArSbCl$_2$ (71).*

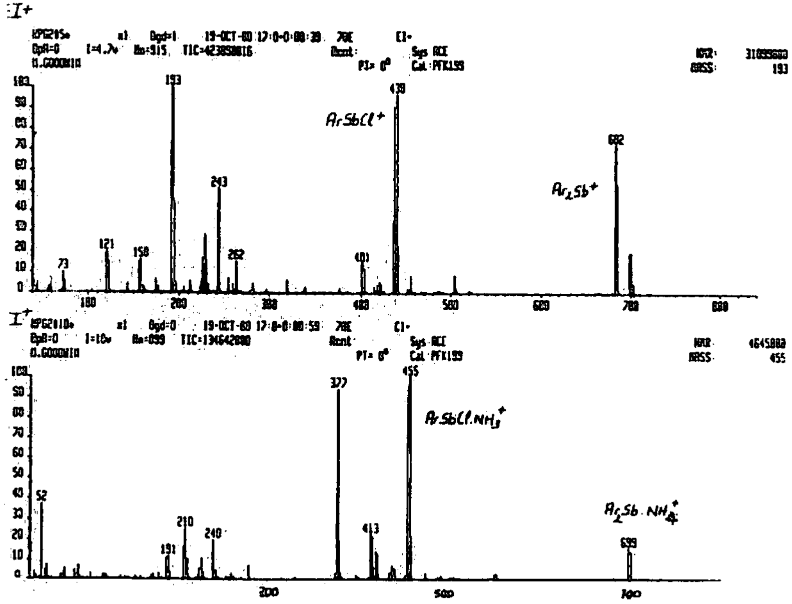

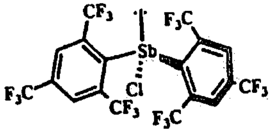

EI+

	% Base					
376.74	2 19	436 33	90 44 F	683 27	14 58	718 26
401.41	14 36	436 49	8 02 F	684 27	52.74	720 28
402.41	2.10	437.36	9 15 F	685.28	10.77	721.36
403.41	11.43	438.34	96.29 F	686.29	1.12	722.35
404.44	1.45	439.35	9.00	698.24	19.32	752 21
414.79	2.70	440.35	22.48	699.25	3.96	752.28
416.15	1.24	441.35	2.00	700.25	19.55	756.23
416.47	1.19	451.44	2.16	701.25	4.17	803.62
418.14	3.90	454.44	8.06	702.24	4.96	822.18
420.14	5 38	455.45	1.40	702.47	0.08	845.29
420 39	5 23	485.43	1.06	703.25	0.67	850 85
422.13	3 88	504.43	8.40	703.79	0.05	851.90
422 39	4.28	505.44	1 52	704.29	0.15	870.90
424 13	1 59	520.38	1.01	708.33	0.12	882 33
435 47	34 14 F	682.27	72 52	710.36	0.14	815.68

CI+

207.60	1.19
209.60	1 79
239.73	1 39
376.82	6.65
377.81	1.43
412.86	1.58
414.85	1.49
418 50	1.01
452.88	4.76 F
453.42	6.78 F
453.89	1.84 F
455.40	7.09
457.41	1.52
699.39	1.15
700 38	0.27
701 39	1.00
70[illegible]	0.19
703 [illegible]	0.03

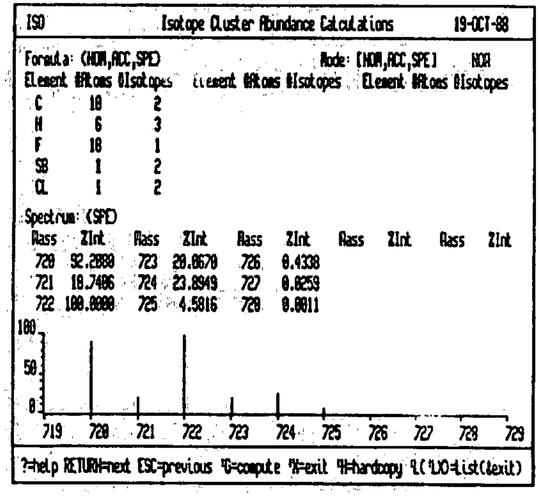

```
ISO                    Isotope Cluster Abundance Calculations            19-OCT-88

Formula: (NOM,ACC,SPE)                              Mode: [NOM,ACC,SPE]    NOM
Element #Atoms #Isotopes   Element #Atoms #Isotopes   Element #Atoms #Isotopes
  C        18      2
  H         6      3
  F        18      1
  SB        1      2
  CL        1      2

Spectrum: (SPE)
 Mass   %Int     Mass   %Int     Mass   %Int     Mass   %Int     Mass   %Int
  720  92.2880    723  20.8670    726   0.4338
  721  18.7486    724  23.8949    727   0.0259
  722 100.0000    725   4.5816    728   0.0011
```

Figure 7.4: Mass spectrum of Ar_2SbCl (72).

$$R'XCl_2 + R''YH_2 \xrightarrow{DBU} R'X{=}YR''$$

R'	R''	X	Y	REF
$(Me_3Si)_2CH$	Supermes	Sb	P	[2,7]‡
$(Me_3Si)_2CH$	Supermes	As	P	[2]*
$(Me_3Si)_2CH$	Supermes	As	As	[6]

$$R'X(SiMe_3)Li + R''_2NYCl_2 \xrightarrow[-Me_3SiCl]{-LiCl} R'X{=}YNR''_2$$

R'	R''	X	Y	REF
Supermes	$tBuMe_2Si$	P	As	[8]
Supermes	$tBuMe_2Si$	P	Sb	[8]
Supermes	$R''_2N \equiv$ tmp	P	B	[9]†

Table 7.1: *Low coordinate, multiply bonded Group (V) compounds; ‡this phosphastibene decomposes to give the symmetrical diphosphene, $(Supermes)_2P_2$ (a source of free phosphinidene! ref.7); *crystal structure reported (ref.7); †The dimer, diphosphadiboretane only. The boraphosphene is generated by thermolysis in the vapour phase.*

It is known that the stability of X=Y decreases for lower groups and higher periods, *ie.* towards the left and bottom of the periodic table. The potential of the Ar group as a steric shield has been illustrated by the formation of the stable diphosphene (19) and the phosphaalkene (31).

Many possible precursors for the preparation of X=Y materials are now available, *ie.* $ArSbCl_2$ (71), $ArPH_2$ (15), $ArPCl_2$ (12), $ArAsF_2$ (prepared by Edelmann *et al.*) [10], and from Group III $ArBCl_2$ (73). (see Chapter 8).

Although it is conceivable that boron may form a symmetrical double bonded species, *ie.* RB=BR, so far no examples of this compound type are known. There are, however, many examples of boron possessing multiply bonded character, for example B=C (see Section 11.3).

7.2.2 Attempted Synthesis of RB=BR (R ≡ Ar, tmp)

Symmetrical coupling of $ArBCl_2$ analogous to that used in the generation of the diphosphene (19) (Section 3.4) was attempted. On addition of bisimidazolidine or magnesium respectively, no B=B double bond was characterised. Since it was considered[1] that the electron-withdrawing nature of the ring might destabilise this system, a parallel reaction was carried out with $tmpBCl_2$ and bisimidazolidine. [The lone pair of the nitrogen substituent is able to participate in bond formation resulting from pπ-pπ overlap with the vacant p-orbital of boron (see Chapter 9)]. This yielded upfield signals in the ^{11}B NMR, attributed to coupling to form tmp(Cl)B–B(Cl)tmp, or a polymeric boron containing material, a possible result of the insufficient bulk of the tmp for the kinetic stabilisation of this species. This may be compared with the inherent instability of SupermesP=Btmp with respect to dimer formation [9].

7.2.3 Attempt to form Phosphastibene and Boraphosphene

The unsymmetrical coupling between $ArPH_2$ (15) and $ArSbCl_2$ (71) or $ArBCl_2$ (73) respectively was also attempted. For the antimony/phosphorus mixture, only the symmetrical diphosphene was characterised. In each case the required product did not appear to be formed. Since, (with both the boron and antimony systems) an apparent change in the appearance of the product occurred on warming the mixture to room temperature, it may be interesting to monitor initial product formation at low temperature. An attempted rationalisation of the observations made is presented in

---

[1] The absence of Lewis acid/base behaviour may be attributed to the presence of too much steric hindrance.

Section 7.3.

The Ar substituent may prove effective in stabilising these species, and it may be possible to extend the work to give a route to the distibene and, using the arsenic derivative, to the diarsene. It might also prove to be a precursor to the first B=B double bond. This exciting new area is currently under investigation by P. Paetzold and many other research groups.

7.3 SOME GENERAL OBSERVATIONS ON $ArPH_2$ COUPLING REACTIONS

7.3.1 Introduction

Many varied coupling reactions between $ArPH_2$ (15) and chlorine species were carried out, with the aim of obtaining unsymmetrical diphosphenes (Section 3.8), phosphaalkenes (Section 4.3), phosphastibenes (Section 7.2.3) and other low-coordinate species.

7.3.2 Results

A common observation in these reactions was the appearance of two peaks (septets) at -84 ppm and -89 ppm in the ^{31}P NMR, or the presence of the symmetrical diphosphene, Ar_2P_2 (19) in place of the desired product. In the specific case of $C_6Cl_5PCl_2$ (23) the peaks at -84 and -89 ppm were discovered (by ^{31}P NMR observation) to convert completely to the symmetrical diphosphene (19) on warming to room temperature. A similar observation with the system Ph_2CCl_2, $ArPH_2$ (15) and DBU, was the appearance of resonances at -84 and -89 ppm, and rapid conversion to the symmetrical diphosphene (^{31}P δ: +473 ppm) on addition of a further 0.5 equivalents of DBU.

The two peaks around -87 ppm were also observed with the substituent Ar' [2,6-bis(trifluoromethyl)phenyl], but these were shifted slightly upfield. This observation was made in attempted Ar'PH_2 coupling reactions with Ar_2SnCl_2 and Ar'$AsCl_2$ to form the phosphastannene and phosphaarsene respectively [11]. Interestingly, these peaks were also observed in the gamma source irradiation of Ar'PH_2 in CCl_4 [11] [together with other products attributed to Ar'P(H)Cl and Ar'P(H)CCl_3].

Specific examples and the conditions in which these species predominate, are presented in the relevant experimental sections of this thesis, whilst a summary of this information appears in Table 7.2.

Each of the two observed peaks appeared to be split into a doublet by P-H coupling, and further split into septets by coupling with the fluorine atoms of the ortho-CF_3 groups (indicative of an Ar group and a hydrogen attached to phosphorus). The upfield chemical shift also indicates the presence of hydrogen.

The assignment of the species to the general formula, ArP(H)P(H)Ar was made. With this structure an *asymmetry* must be considered which may account for the two peaks seen close together in the ^{31}P NMR. The shifts could possibly be attributed to the *meso* and *racemic* forms illustrated in Figure 7.5.

Figure 7.5: *The possible isomeric forms of ArP(H)P(H)Ar.*

Consistently the peak furthest upfield was lower in intensity, and there is no evidence as to which is the major and which is the minor product formed. The optical activity of similar compounds, for example

CHLORINATED COMPOUND	MAJOR ^{31}P NMR PEAKS δ/ppm	$^{4}J(PF)$	CONDITIONS	SECTION /REF
$^{t}BuPCl_2$	473	‡	RT/4h	3.8
$C_6F_5PCl_2$	473	‡	RT	3.8
$C_6F_5PCl_2$	-83.8 (3P) -89.2 (1P)	22 NR	-40 ^{o}C	3.8
$C_6Cl_5PCl_2$	472	‡	RT	3.8
CH_2Cl_2	-84.4 (4P) -89.4 (3P)	NR NR	RT/1h	4.3
Ph_2CCl_2	-83.3 (3P) -88.9 (1P)	25.4 25.0	RT/2DBU	4.3
Ph_2CCl_2	473	‡	2.5DBU	4.3
$ArSbCl_2$	473	‡	RT/4h	7.2
$ArBCl_2$	473	‡	RT/4h	7.2
$Ar'AsCl_2$ *	-84.0	24.5 192†	RT/THF	[11]
	-90.1	25.3 167†		
$Ar'AsCl_2$ *	473		$CDCl_3$ extract	
Ar_2SnCl_2	-84.0 (3P)	24.5 192†	RT/THF	[11]
	-90.0 (1P)	25.3 167†		
CCl_4	-84.0	24.5 192†	γ irradiated	[11]
	-90.0	25.3 167†		

Table 7.2: *Results of coupling $ArPH_2$ (top) and $Ar'PH_2$ (bottom) with various chlorinated compounds; ‡$^{4}J(PF)$ + $^{5}J(PF)$ = 45 Hz; DBU in equivalents; *^{19}F δ: -57.7 ppm (major); -57.4 (minor); †$^{1}J(PH)$ coupling.*

with supermes substituents, does not appear to have been extensively studied [2]. However, the supermes derivative has been isolated [13,14] and shows interesting spectral parameters. This derivative was obtained by the reduction of the diphosphene Supermes_2P_2 [14], which indeed may be a route *via* Ar_2P_2 (19) to isolate and fully characterise the ArP(H)P(H)Ar species.

7.3.3 **Mechanism**

It is very difficult to write a mechanism for the formation of this product, and the formation of the symmetrical diphosphene. Only starting materials are observed with $ArPH_2$ and DBU *in situ*, hence a chlorine source is implicated in the mechanism. A radical process cannot be ruled out on the present evidence, however. Further mechanistic studies are certainly required to understand this system fully.

7.3.4 **Reaction Rate**

The phosphorus-phosphorus bond appears to form in each case much faster than the desired 'P-X' material. However derivatives, for example, $\text{SupermesP=SbCH(SiMe}_3)_2$ [2] and $\text{SupermesP=AsCH(SiMe}_3)_2$ [2], can be formed successfully *via* a similar route.

To form unsymmetrical species with the Ar or Ar' substituent on 'PH_2' it appears that it is necessary to promote coupling with the other component. One possibility would be *via* the phosphide, ArP(H)Li. However, this has already been shown to be inherently unstable with Ar or Ar' (Section 4.3). The formation of the 'P-P' species is a result of the presence of $ArPH_2$, hence it may be worthwhile reversing the coupling substituents, for example *via* $ArXH_2$ and $ArPCl_2$.

This predominant 'P-P' symmetrical coupling appears to interfere in many of these reactions. However, it is interesting to note that coupling between $ArPH_2$ and the $^iPr_2N$- , Ar'- and Mes- derivatives of 'PCl_2' resulted in the formation of the unsymmetrical diphosphene.

7.4 EXPERIMENTAL

7.4.1 Preparation of $ArSbCl_2$ (71)

$$ArLi\ (2) + 1.3SbCl_3 \longrightarrow ArSbCl_2\ (71)$$

ArLi/ArH (100 ml, 45 mmol, 0.45 M solution in Et_2O) was added dropwise over 10 minutes to a stirred solution of antimony trichloride (10.8g, 47.3 mmol) in Et_2O (50 ml) at -78 ^oC. An orange/brown solution was formed with no visible precipitation of LiCl. The reaction mixture was stirred for 2 hours at room temperature. Pentane (150 ml) was added to the reaction mixture and shaken vigorously. Two apparent layers formed. The lower dense brown oil gave no signal in the ^{19}F NMR so this was attributed to excess $SbCl_3$ (and LiCl). The pentane was removed *in vacuo* from the upper layer, yielding a yellow powdery solid which was recrystallised from CH_2Cl_2 (25 ml). Yield was *ca.* 12.2g (57%). As an isolated solid this is extremely unstable. Any amount of exposure to the atmosphere in the glove box caused it to turn from a yellow solid to a red oil. This instability may have led to an inaccuracy in the elemental analysis. The ^{121}Sb NMR spectrum was not useful, showing only a very broad absorption due to the low symmetry of $ArSbCl_2$.

However, from the ^{13}C NMR, Et_2O appears to have remained coordinated. This would also partially account for the elemental analysis obtained (high %carbon). It seemed unlikely, however, that ether of coordination would be retained after the extraction of the solid into pentane. Mpt. >62 ^{o}C (dec). Analysis found: C, 26.87; H, 0.98; Required for $C_9H_2F_9SbCl_2$: C, 22.82; H, 0.43%; Required for $C_9H_2F_9SbCl_2\cdot(1/2Et_2O)$: C, 25.86; H, 1.38%; Required for $C_9H_2F_9SbCl_2\cdot(Et_2O)$: C, 28.50; H, 2.21%; IR (Nujol) ν_{max}: 3100 (w,ArCH), 2900(CH), 1630 and 1570 (m,C=C/Ar), 1400-1000 (s,C-F), ~900 (m,CH ring), 700 (s,CF_3) cm^{-1}; UV-Visible (CCl_4) $\lambda_{max}(\epsilon)$: 273 (52093.0) nm; MS (Intensity%) EI: 439 [56.7,$ArSbCl^+$], 402 [16.5, $ArSb^+$], 262 [10,$(Ar-F)^+$], 243 [100,$(Ar-2F)^+$]; ^{19}F δ: -55.6 (s,6F), -64.9 (s,3F) ppm; ^{13}C δ: 151.3 (s, slightly broadened, possibly due to its attachment to Sb), 136.9 (q,CF_3) $^1J_{CF}$ 33.7 Hz, 132.9 (q,CF_3) $^1J_{CF}$ 35.0 Hz, 127.5 (d,CH) $^1J_{CH}$ 284 Hz, 125.6 (s,quaternary C on Ar ring), 121.2 (s,quaternary C on Ar ring), 67.4 (Et_2O), 17.1 (Et_2O) ppm.

7.4.2 Preparation of Ar_2SbCl (72)

$$2ArLi + SbCl_3 \longrightarrow Ar_2SbCl\ (72) + 2LiCl.$$

ArLi (100 ml, 45 mmol, 0.45 M solution in Et_2O) was added dropwise over 10 minutes to a stirred solution of $SbCl_3$ (5.1g, 22.4 mmol) in Et_2O (50 ml) at -78 ^{o}C. The reaction mixture was allowed to reach room temperature, filtered and the solvent removed *in vacuo* to give a reddish amorphous solid, crude yield 10g (62%). This was recrystallised in a minimum volume of CH_2Cl_2 (15 ml) at low temperature (-40 ^{o}C) to yield pale yellow crystals. Filtration at low temperature gave maximum yields of *ca.* 7.6g (45-50%). The isolated solid was very sensitive even to the atmosphere of the glove box, but appeared more stable than the analogous $ArSbCl_2$. Crystals suitable for X-ray analysis were obtained and have been submitted, mounted in Lindemann (0.3 μm) capillaries. Mpt. 195-196 ^{o}C; Analysis found: C, 30.07; H, 0.48; Cl, 5.31; Required for

$C_{18}H_4F_{18}SbCl$: C, 30.05; H, 0.56; Cl, 4.93%; IR (Nujol) ν_{max}: 3100 (w,ArCH), 1630 and 1570 (m,C=C/Ar), 1400-1000 (s,C-F), ~900 (m,CH/Ar) cm^{-1}; UV-Visible (CCl_4) λ_{max} (ϵ): 273 (27368.4) nm; MS (Intensity%) EI: 718 [0.16,Ar_2SbCl^+], 682 [72.5,Ar_2Sb^+], 438 [96.3,$ArSbCl^+$], 401 [14.41,$ArSb^+$], 262 [$(Ar-F)^+$], 243 [100,$(Ar-2F)^+$]; CI^+: 699[2] [1.15, $(Ar_2SbCl-F)^+$], 454 [100,($ArSbCl\cdot NH_3^+$)]; ^{19}F ($CDCl_3$) δ: -55.4 (s,12F), -64.0 (s,6F) ppm.

7.4.3 Attempted Reactions of $ArBCl_2$ to form ArB=BAr

7.4.3.1 With Bisimidazolidine

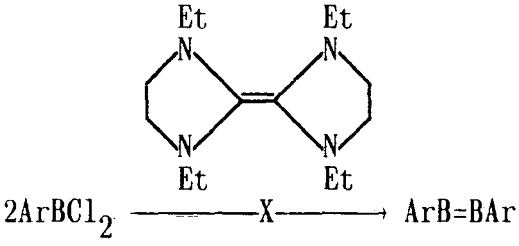

A solution of bisimidazolidine (1.1g, 4.4 mmol) in toluene (10 ml) was added dropwise over 5 minutes to a stirred solution of $ArBCl_2$ (3.2g, 8.8 mmol) in toluene (25 ml) cooled to 0^oC. No apparent reaction occurred, and the solution remained a clear yellow colour. ^{11}B (toluene) δ: 26 pm; ^{19}F δ: -56.6 (o-CF_3), -63.8 (p-CF_3). This is indicative of unchanged $ArBCl_2$. On warming to room temperature and refluxing for 6 hours, there was still no apparent reaction.

---

[2] Isotopic pattern as expected for one Sb and one Cl, *ie.* intensities: 19.32, 3.96, 19.55, 4.17 and 4.96%

7.4.3.2 With Magnesium

$$2\mathrm{ArBCl_2}\ \overset{2\mathrm{Mg}}{\text{—X→}}\ \mathrm{ArB{=}BAr}$$

Magnesium (0.08g, 3.3 mmol) was added in one portion to a stirred solution of $\mathrm{ArBCl_2}$ (1.21g, 3.3 mmol) in THF (40 ml) at ambient temperature. This mixture was refluxed for ten hours. No apparent reaction occurred. The change in colour of the solution from pale yellow to a pale grey suspension, was attributed to the presence of magnesium. ^{11}B NMR (THF) δ: +26 ppm; ^{19}F δ: -56.4 (o-$\mathrm{CF_3}$), -63.6 (p-$\mathrm{CF_3}$) ppm. $\mathrm{ArBCl_2}$ appears to remain unchanged.

7.4.4 Attempted Preparation of tmpB=Btmp

$$2\mathrm{tmpBCl_2}\ \overset{\text{bisimidazolidine}}{\text{————?————→}}\ \mathrm{tmpB{=}Btmp}$$

Bisimidazolidine (1.89g, 7.5 mmol) in toluene (15 ml) was added dropwise over 5 minutes to a stirred solution of $\mathrm{tmpBCl_2}$ (2.9g, 13.0 mmol) in toluene (25ml) at 0°C. The solution turned dark orange with no obvious precipitate. ^{11}B NMR (toluene) δ: +33.4 (small signal,unchanged $\mathrm{tmpBCl_2}$), +16.1 (major signal,tmp(Cl)B-B(Cl)tmp?), +2.0 (small signal). On warming to room temperature no change in the NMR spectrum was observed.

7.4.5 Attempted Preparation of ArP=SbAr

$$ArPH_2 + ArSbCl_2 \xrightarrow[\text{X}]{2DBU} ArP{=}SbAr$$

DBU (0.93g, 0.91 ml, 6.1 mmol) in THF (15 ml) was added dropwise over 5 minutes to a stirred solution of $ArSbCl_2$ (1.42g, 3.0 mmol) and $ArPH_2$ (0.94g, 3.0 mmol) in THF (50ml) at 0°C. The solution became deep brown and a precipitate formed. On warming to room temperature it became clear and pale yellow in colour. $^{31}P\{^1H\}$ (THF) δ: +473.4 ppm $^4J_{PF}$ + $^5J_{PF}$ 45 Hz [major signal, symmetrical diphosphene (19) (see Section 3.5 for data)], small peaks at +174 and +67.5 ppm were also observed.

7.4.6 Attempted Preparation of ArP=BAr

DBU (1.32g, 1.30 ml, 8.7 mmol) in THF (15 ml) was added dropwise over 5 minutes to a stirred solution of $ArBCl_2$ (1.56g, 4.3 mmol) and $ArPH_2$ (1.35g, 4.3 mmol) in THF (50ml) at -60°C. The reaction mixture became red after addition of the first drop of DBU solution, and some solid was evident. On warming the solution to room temperature it became clear and pale yellow in colour. ^{31}P (THF) δ: +473.4 ppm $^4J_{PF}$ + $^5J_{PF}$ 45 Hz [major signal, symmetrical diphosphene (19)], -0.45 ppm (small unassigned peak); ^{19}F δ: -56.4 (s,o-CF_3), -63.4 (s,p-CF_3). (+ diphosphene)

7.5 REFERENCES

1. N.N. Greenwood and A. Earnshaw, "*Chemistry of the Elements*", Pergamon Press, Oxford, 695 (1984).

2. A.H. Cowley, J.G. Lasch, N.C. Norman, M. Pakulski and B.R. Whittlesey, *J.Chem.Soc.Chem.Commun.*, 881-882 (1983).

3. S.P. Bone and D.B. Sowerby, *J.Chem.Soc.Dalton Trans.*, 1430-1433 (1979).

4. A.H. Cowley, N.C. Norman, M. Pakulski, D.L. Bricker and D.H. Russell, *J.Amer.Chem.Soc.*, 107, 8211-8218 (1985).

5. L. Weber, Private Communication to K.B. Dillon (1989).

6. A.H. Cowley, J.G. Lasch, N.C. Norman and M. Pakulski, *J.Amer. Chem.Soc.*, 105, 5500 (1983).

7. A.H. Cowley, J.E. Kilduff, J.G. Lasch, S.K. Mehrotra, N.C. Norman, M. Pakulski, B.R. Whittlesey, J.L. Atwood and W.E. Hunter, *Inorg. Chem.*, 23, 2582-2583 (1984).

8. V.D. Romanenko, E.O. Klebanskii and L.N. Markovskii, *Z.Obs.Khim.*, 55(9), 2141-2 (1985).

9. A.M. Arif, J.E. Bloggs, A.H. Cowley, J.-G. Lee, M. Pakulski and J.M. Power, *J.Amer.Chem.Soc.*, 108, 6083-6084 (1986).

10. M. Scholz, H.W. Roesky, D. Stalke, K. Keller and F.T. Edelmann, *J. Organometallic Chem.*, 366, 73-85 (1989).

11. Dr. K.B. Dillon and T. Straw, unpublished work, University of Durham (1989).

12. C. Couret, J. Escudié, J. Satgé, A. Raharinirina and J.D. Andriamizaka, *J.Amer.Chem.Soc.*, 107, 8280-8281 (1985).

13. A.H. Cowley , J.E. Kilduff, T.H. Newman and M. Pakulski, *J.Amer. Chem.Soc.*, 104, 5820 (1982).

14. M. Yoshifuji, K. Shibayama, N. Inamoto and T. Watanabe, *Chem. Lett.*, 585-588 (1983).

CHAPTER EIGHT

ARYL BORON HALIDES

8.1 INTRODUCTION

The most important methods for the preparation of alkyl (and aryl) boron dihalides and dialkyl (and diaryl) boron halides have depended essentially on one of the following three procedures [1].

(1) The interaction of organometallic compounds with boron halides or substituted boron halides (Equations 8.1-8.5) [1-3].

(2) The reaction of trialkylborons or amino dialkyl borons with halogenating agents (Equation 8.6) [1].

(3) The reaction of boronic or boronous acid with boron halides (Equation 8.7) [1].

$$Zn(C_6H_5)_2 + BF_3 \longrightarrow C_6H_5ZnF + C_6H_5BF_2 \qquad (8.1)$$

$$Zn(Me)_2 + BF_3 \longrightarrow MeZnF + MeBF_2 \qquad (8.2)$$

$$ArHgX + BX_3 \longrightarrow ArBX_2 + HgX_2 \ (X = Cl, Br) \qquad (8.3)$$

$$Al(Me)_3 + 3BBr_3 \longrightarrow 3\ MeBBr_2 + AlBr_3 \qquad (8.4)$$

$$Me_3SnC_6F_5 + 2BCl_3 \longrightarrow Me_2SnCl_2 + MeBCl_2 + C_6F_5BCl_2 \qquad (8.5)$$

$$B(Bu)_3 + HBr \xrightarrow{-BuH} Bu_2BBr \qquad (8.6)$$

$$(MeBO)_3 + 2BF_3 \longrightarrow 3MeBF_2 + B_2O_3 \qquad (8.7)$$

8.2 Ar SUBSTITUTED ORGANOBORON

It was of particular interest,with respect to its electronic and steric effects to investigate the effect of attaching the Ar group to boron. Attempts to synthesise the Ar_2B^+ borinium ion are described in Section 9.6.

Three species have been prepared: (i) $ArBCl_2$ (73); (ii) Ar_2BCl (4) and (iii) Ar_3B (75). These compounds will now be considered in sequence.

8.2.1 '$ArBCl_2$' (73)

Many attempts were made to synthesise $ArBCl_2$ (73). The general route involved the addition of ArLi to BCl_3. This gave interesting results with a distinctive competing decomposition reaction evident. The presence of direct B-F bonds was observed in the ^{19}F and ^{11}B NMR spectra, (the only source of fluorine being the CF_3 groups on the ring). A possible mechanism for the formation of the B-F bonds is illustrated in Figure 8.1.

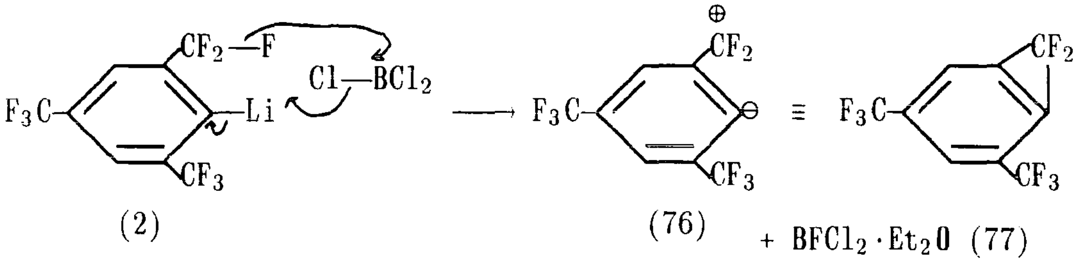

Figure 8.1: *The proposed effect of BCl_3 on ArLi (2).*

The existence of species (77) was verified by setting up an equilibrium between $BF_3 \cdot Et_2O$ and $BCl_3 \cdot Et_2O$, generating species of identical chemical shift, splitting patterns and distinctive B-F couplings [4].

The MNDO calculation on ArLi (2) (Section 1.3) showed extensive interaction between the lithium and the fluorine, weakening the carbon-fluorine bond. The reaction proposed (Figure 8.1) must be a consequence of the presence of lithium, since no reaction was observed with ArH in the presence of an excess of BCl_3.

This decomposition process (Figure 8.1) may be attributed to the interaction of the electrons on the fluorines in ArLi with the empty orbital on boron, and the thermodynamic favourability of forming a boron-fluorine bond.

The proximity of the fluorines to the boron centre in $ArBCl_2$ (73) may allow $p\pi$-interaction, resulting in the partial occupation of the

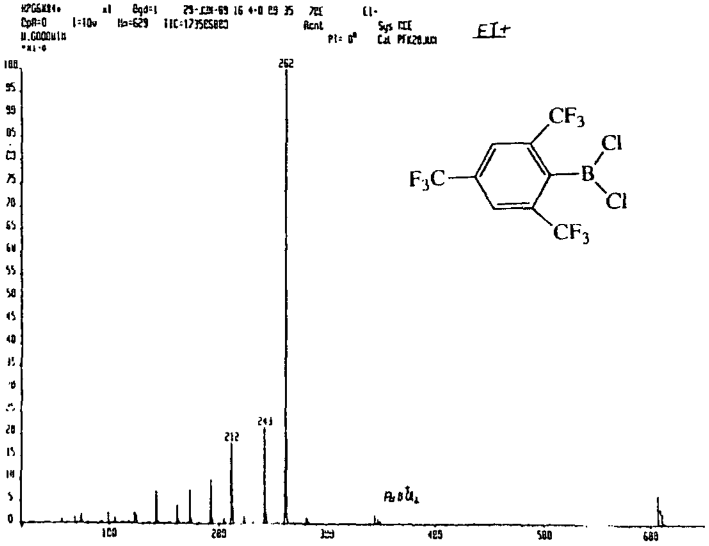

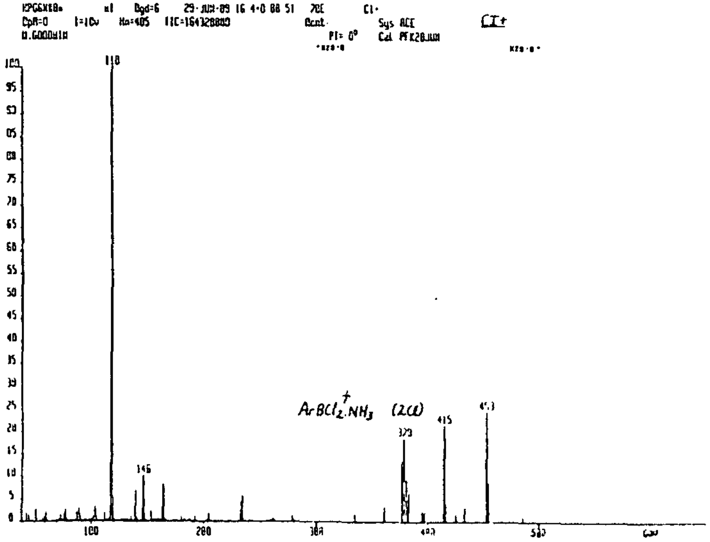

EI+

261.93	100 00 FU
262 94	19 15
263 96	1 00
269 04	0 11
278 97	0 15
280 96	1 34
281 97	1 04
283 00	0 11
339 11	0 23
344 88	1 93
345 88	0 18
346 88	1 05
347 88	0 28
348 88	0 79
377.19	0 16
415 25	0 19
435 95	0 23
504.97	0 13
606 87	6 54
607 87	1 19
608 87	3 53
609 86	1 13
610 86	2 57
611 86	0 41
612 86	0 10
625 88	0 11

CI+

377 21	0 38
378 95	0 51
380.95	0 26
382 94	0 18
415 26	0 59
416 26	0 11
453 34	0 67
454.35	0 23

Figure 8.2: Mass spectral data for ArBCl$_2$ (73).

fourth covalency of boron. This reasoning may account for the anomaly of the more shielded nature of the ^{11}B NMR chemical shift for $ArBCl_2$ (73), and the unusual small variation in chemical shift with a directly coordinating solvent, *ie.* $ArBCl_2$, ^{11}B (Et_2O) δ: +27 ppm; (CH_2Cl_2) δ: +32 ppm ($\Delta\delta$ = +5 ppm). This can be compared with BCl_3, ^{11}B (Et_2O) δ: +11 ppm; (CH_2Cl_2) δ: +47 ppm ($\Delta\delta$ = +36 ppm).

A dimeric structure may also be proposed, offering an explanation for the two points above, and possibly explaining the small peaks to higher mass in the mass spectrum (Figure 8.2). However, this would seem unlikely as further examples of symmetrically bridged halogeno organoboron compounds have not been reported in the literature. The steric demand of the aryl group would also be expected to disfavour the tetrahedral configuration demanded by a dimeric conformation (Figure 8.3).

It should be noted that once the species $BFCl_2 \cdot Et_2O$ (77), $BF_2Cl \cdot Et_2O$ *etc.*, and $ArBCl_2$ (73) are present together in solution there is considerable scope for boron-halogen exchange (see Chapter 10). The result of this exchange is seen in the possible presence of "$ArBF_2$" in the reaction mixture (Figure 8.4). The reaction of $ArBCl_2$ and SbF_3 (Section 8.9.4.1) gave similar distinctive ^{19}F NMR parameters attributed to $ArBF_2$ which was not isolated (Figure 8.4).

The ^{19}F NMR (Figures 8.3 and 8.4) shows $Et_2O \cdot BFCl_2$ (77), and the "CF_3", "CF_2" regions appear very complex. Other species may possibly be as shown in Figure 8.5.

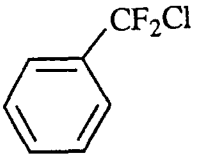

Figure 8.5: *Species possibly indicated by ^{19}F NMR from the reaction of ArLi with BCl_3.*

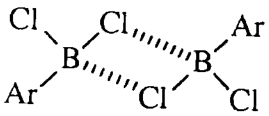

Figure 8.3: *Possible dimeric configuration of* $ArBCl_2$ *(73).*

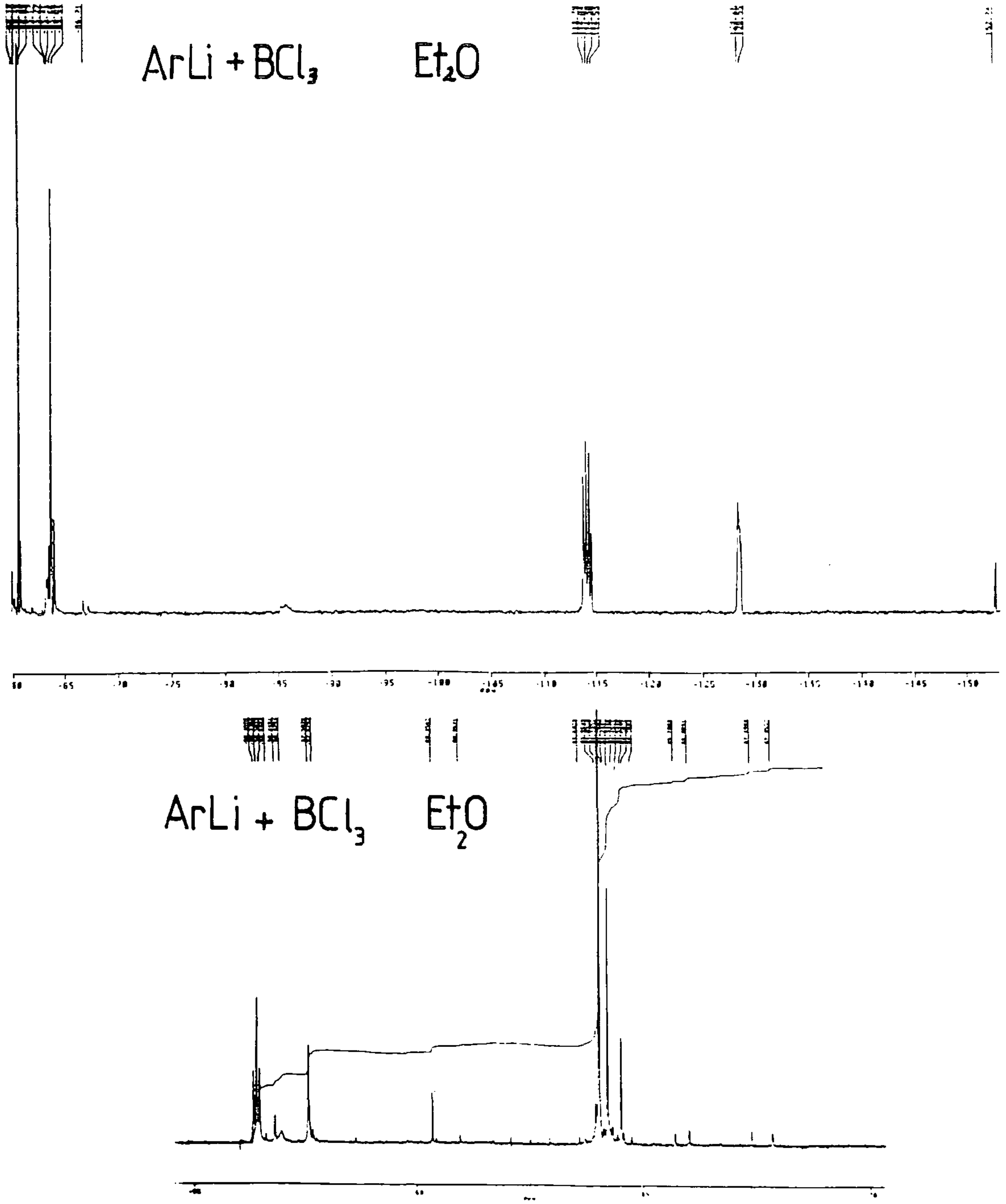

Figure 8.4: ^{19}F *NMR spectra: Addition of ArLi to* BCl_3*.*

This major side-reaction has been indicated. However, it was possible to isolate $ArBCl_2$ (73) pure from this reaction, presumably as shown in Equation 8.8 (possibly with a contribution from the reaction shown in Equation 8.9). Indeed lithium fluoride and chloride were found in the precipitate.

$$ArLi\ (2) + BCl_3 \longrightarrow ArBCl_2\ (73) + LiCl \qquad (8.8)$$

$$BFCl_2{\cdot}Et_2O\ (77) + ArLi \longrightarrow ArBCl_2\ (73) + LiF \qquad (8.9)$$

8.2.2 Ar_2BCl (4)

The preparation of Ar_2BCl by the use of an excess of Arli showed a similar side reaction, attributed to the same effect. Again "B-F" species and specifically "$ArBF_2$" were evident in the reaction. However, yields of Ar_2BCl were significantly higher than in the attempts at the synthesis of $ArBCl_2$ making a satisfactory preparative route to Ar_2BCl.

Interestingly the action of $ArBCl_2$ with ArLi was found to act in a similar way to BCl_3 (Figure 8.6).

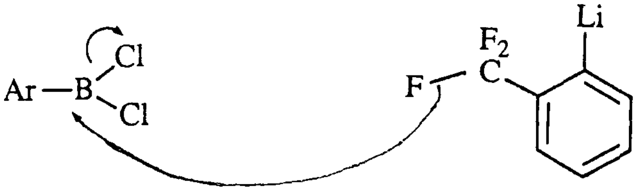

(73) (2)

Figure 8.6: *Action of ArLi on $ArBCl_2$.*

This reaction has a much lower significance, possibly due to the fluorine : boron intramolecular interaction reducing the electrophilic character of the boron. An MNDO calculation on Ar_2BCl together with its ^{11}B and ^{19}F NMR data is presented in Section 8.7, Figures 8.18 and 8.19.

8.3 BORON-FLUORINE DERIVATIVES

To develop this chemistry further an attempt was made at the standard $ArBF_2$ preparation by the reaction of ArLi with $BF_3 \cdot Et_2O$ [5]. Since BF_3 is a weaker Lewis acid than BCl_3, the breaking of a B-F bond is possibly unfavourable. (The products formed in this process must also be considered.)

If the side-reaction described earlier (Section 8.2) occurs in this system, as one fluorine leaves this boron another fluorine goes back on (Figure 8.7).

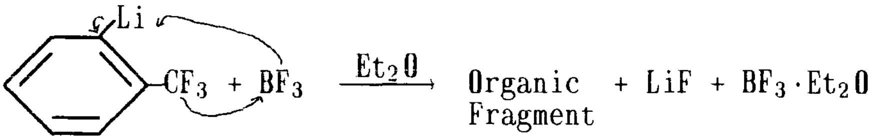

(2)

Figure 8.7: *The proposed interaction of BF_3 with ArLi.*

No $ArBF_2$ was observed. A brown inhomogeneous material was isolated which unfortunately could not be fully characterised. The ^{19}F spectrum indicated a number of products present with a very complex "CF_3" region. No precipitate was visible from this reaction, possibly because the "LiF" generated is solubilised in an "active" form [6].

It can be concluded that BF_3 seems to be acting to decompose *catalytically* the Ar ring system. Even with a 1:1 stoichiometric ratio of ArLi : $Et_2O \cdot BF_3$, substantial amounts of BF_3 appeared to remain in the reaction mixture from the ^{19}F NMR, adding further weight to this hypothesis (Figure 8.8). Further evidence can be found from earlier work [7] illustrating the decomposition of CF_3BF_2 to give BF_3 (Figure 8.9). (Crystals of $ArBCl_2$ (73) and Ar_2BCl (74) were isolated from the methods described, and were submitted for X-ray analysis.)

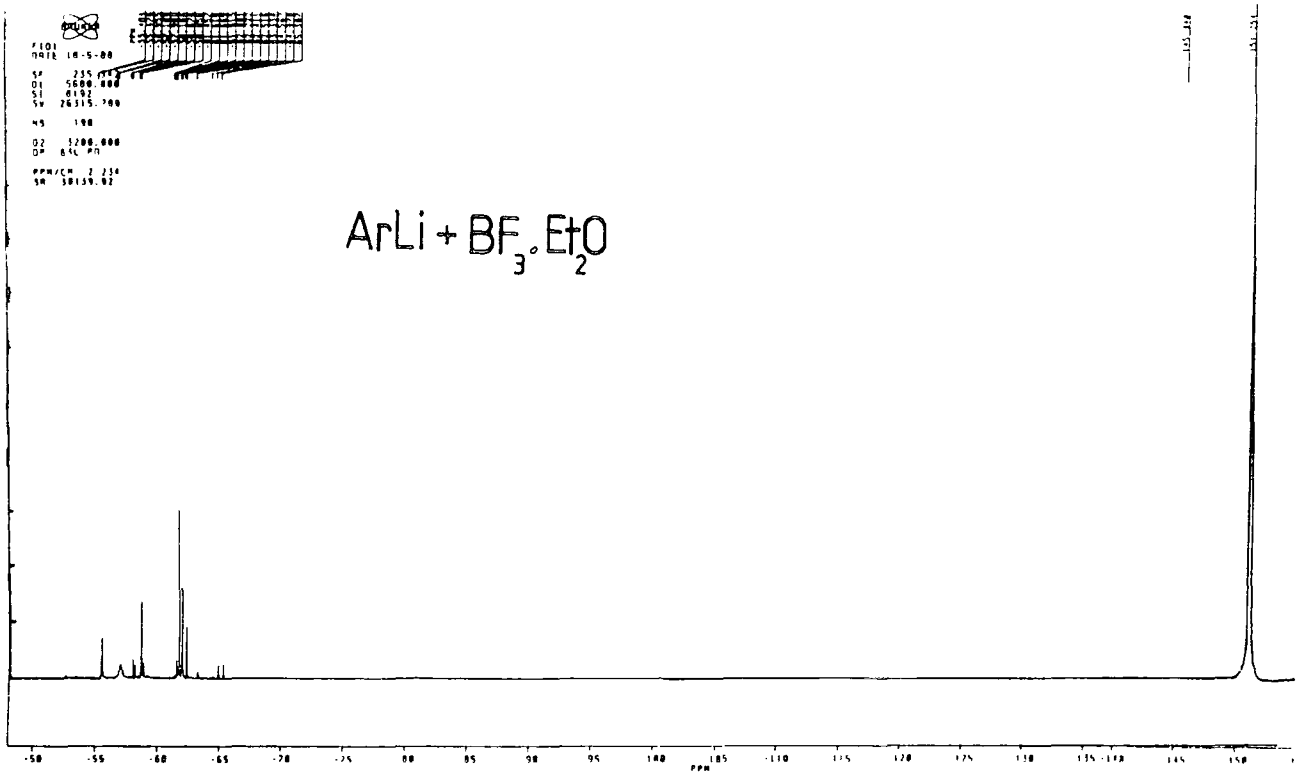

Figure 8.8: ^{19}*F NMR spectrum for the reaction ArLi* + $BF_3\cdot Et_2O$.

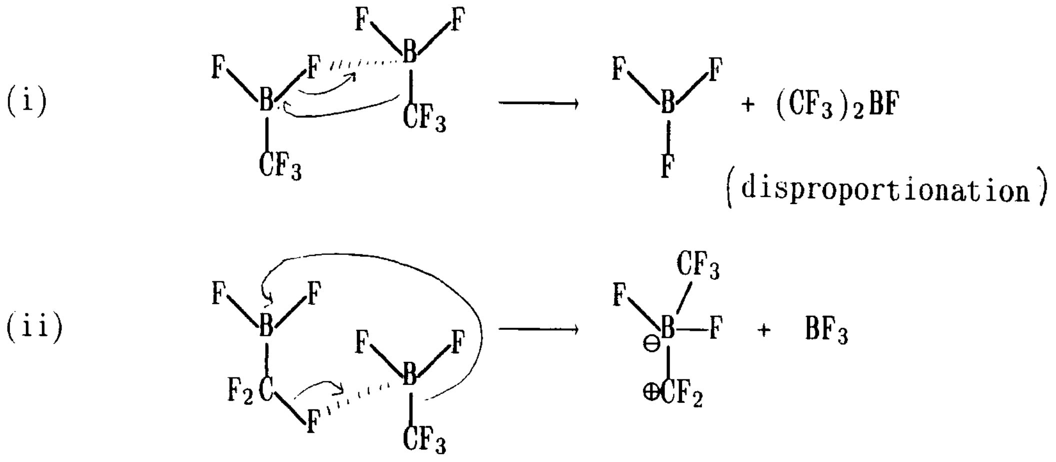

Figure 8.9: *Decomposition of* CF_3BF_2.

An interesting area of research which may be further pursued in the light of this finding would be the possible synthetic use of BF_3 or BCl_3 in the catalytic elimination of LiF from other species, with CF_3 similarly displaced from Li, for example:

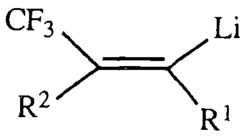

The low yield of $ArBCl_2$ led to the exploration of a different synthetic route (Section 8.4).

8.4 ORGANOTIN DERIVATIVES

8.4.1 Trimethyl Ar Tin (78)

$ArSnMe_3$ (78) was synthesised *via* the reaction of the ArLi precursor with Me_3SnCl, and distilled as a colourless oil. It was hoped to initiate exchange between the Ar group and chlorine on boron trichloride. In the compound $PhSnMe_3$, Ph would be expected to exchange before Me [9]. The ease of Sn-X cleavage by halogens, or other reagents varies with the nature of the organic group - generally increasing in the sequence [9] (Bu being the most stable):

Bu < Pr < Et < Me < vinyl < Ph < Bz < allyl < CH_2CN < CH_2CO_2R

Based on this hypothesis, $ArSnMe_3$ and BCl_3 were mixed. No exchange was observed in Et_2O [10]. A more polar solvent was required, such as CH_2Cl_2.

In CH_2Cl_2 a peak in the ^{11}B NMR indicative of $MeBCl_2$ [4] with a chemical shift of +62.3 ppm was clearly seen, with the ^{19}F spectrum indicating the formation of a different Ar-containing species attributed to $ArSnMe_2Cl$ (79). Very recent work on a similar exchange system between boron and tin (R = allyl) has been reported [11].

To indicate whether the new Ar species had the Ar group attached to tin or boron, a ^{119}Sn NMR spectrum should have been recorded. However, the volatility of the boron species (removed *in vacuo*), giving a shift in the ^{11}B NMR at +62 ppm suggested it was $MeBCl_2$, and therefore the Me group had been transferred first. The reaction appeared to proceed as shown in Figure 8.10.

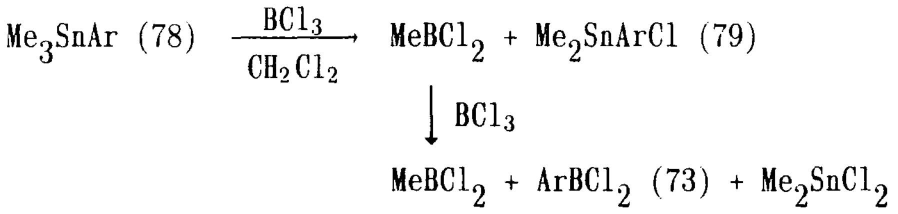

$$\begin{tikzcd} \mathrm{Me_3SnAr}\ (78) \arrow[r, "\mathrm{BCl_3}", "\mathrm{CH_2Cl_2}"'] & \mathrm{MeBCl_2} + \mathrm{Me_2SnArCl}\ (79) \arrow[d, "\mathrm{BCl_3}"] \\ & \mathrm{MeBCl_2} + \mathrm{ArBCl_2}\ (73) + \mathrm{Me_2SnCl_2} \end{tikzcd}$$

Figure 8.10: *Reaction of* $ArSnMe_3$ *(78) with* BCl_3 *in* CH_2Cl_2.

The signal at +32 ppm in the ^{11}B NMR was assigned to $ArBCl_2$ (73). The slight deshielding was attributed to CH_2Cl_2 being less coordinating than Et_2O (*NB.* No further Me exchange appears to occur from Me_2SnCl_2 - this species appeared to be stable in solution)[9,10]. Many tin compounds of the general formula R_3SnX or R_2SnX_2 are strongly associated with bridging X groups raising the coordination number of tin to 5, 6 or 7 [9].

8.4.2 Tributyl Ar Tin (80)

By the use of Bu_3SnAr (80) it was hoped to reduce and possibly eliminate the problem of smaller group migration, since ^{n}Bu appeared to form the most stable "tin-carbon" bond in the sequence (Section 8.4.1) [9]. Butyl with a larger steric requirement will make it more difficult for the two species to approach in the postulated transition state (Figure 8.11).

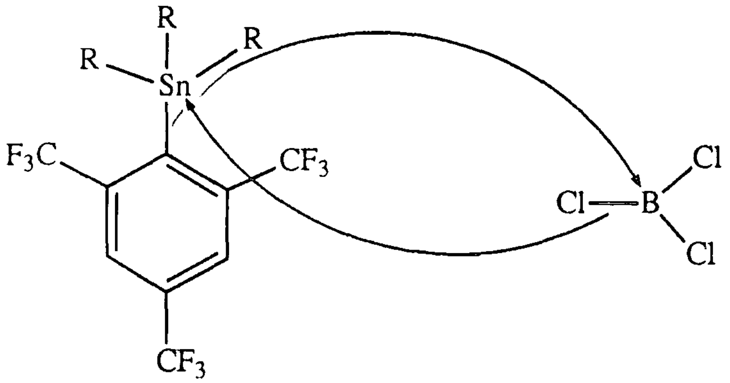

(80) R=Bu (78) R=Me

Figure 8.11: *The Ar tin derivative with BCl_3.*

Bu_3SnAr (80) was isolated and vacuum distilled as a clean oil and as a new Ar-containing tin derivative. In ether no exchange with BCl_3 was observed, as expected from the previous example [10]. With CH_2Cl_2 even by refluxing no Ar or Bu group transference was apparent.

In both reactions involving Bu_3SnAr (80) and Me_3SnAr (78) with BCl_3 a symmetrical peak at *ca.* -64 ppm in the ^{19}F NMR appeared, indicative of ArH, a possible result of destannylation.

8.4.3 Other Possible Tin Derivatives

The synthesis of $ArSnCl_3$, Ar_2SnCl_2 (which may also be a precursor for a diaryl substituted phosphastannene), Ar_4Sn *etc.* would eliminate the complications of methyl group migrations. However, their use as synthons would be dependent on the ability of the aryl group to migrate in these systems, and a plausible synthetic route to their preparation. For example, there may be steric limitations to the formation of Ar_4Sn, and once prepared, for example with $(C_6F_5)_4Sn$ [7] it may be too unreactive to provide a useful route to $Ar'BCl_2$ ($Ar' = C_6F_5$). However, this would be an interesting system for further investigation.

It is appropriate to mention here the observed reaction of $ArSnMe_3$ (78) with iodine, and a possible rationalisation of its lack of reactivity. The reaction is outlined in Figure 8.12.

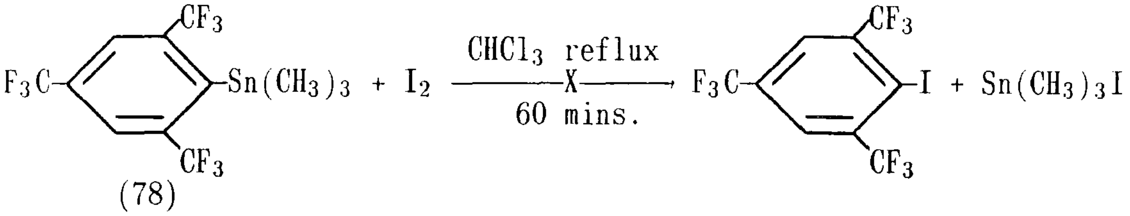

(78)

Figure 8.12: *Attempted reaction of $ArSnMe_3$ with iodine.*

It was reported [12a] that even after refluxing, neither dissipation of the iodine colouration nor formation of the iodo derivative was observed. The tin-carbon bond strength may be enhanced by the three trifluoromethyl groups, as the reaction is an example of electrophilic aromatic substitution which is hindered by electron withdrawing substituents. The cyclic transition state proposed (Figure 8.13) would also be difficult to achieve in the presence of two bulky ortho substituents [12b].

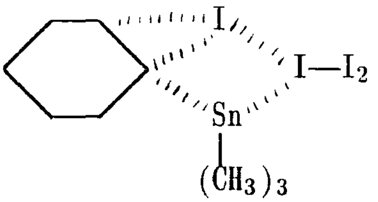

Figure 8.13: *Interaction of iodine with $ArSnMe_3$ (78); (aromatic electrons omitted for simplicity).*

With the boron trichloride reaction, however, its greater electrophilicity and smaller size, together with its ability to partially complex with fluorine drawing it into the reaction, were anticipated to overcome some of the problems observed in the iodine case (*ie.* repulsion by large diffuse electron clouds). The poor yields obtained in the boron case (Section 8.4.1) may be a direct result of the high tin-carbon bond strength.

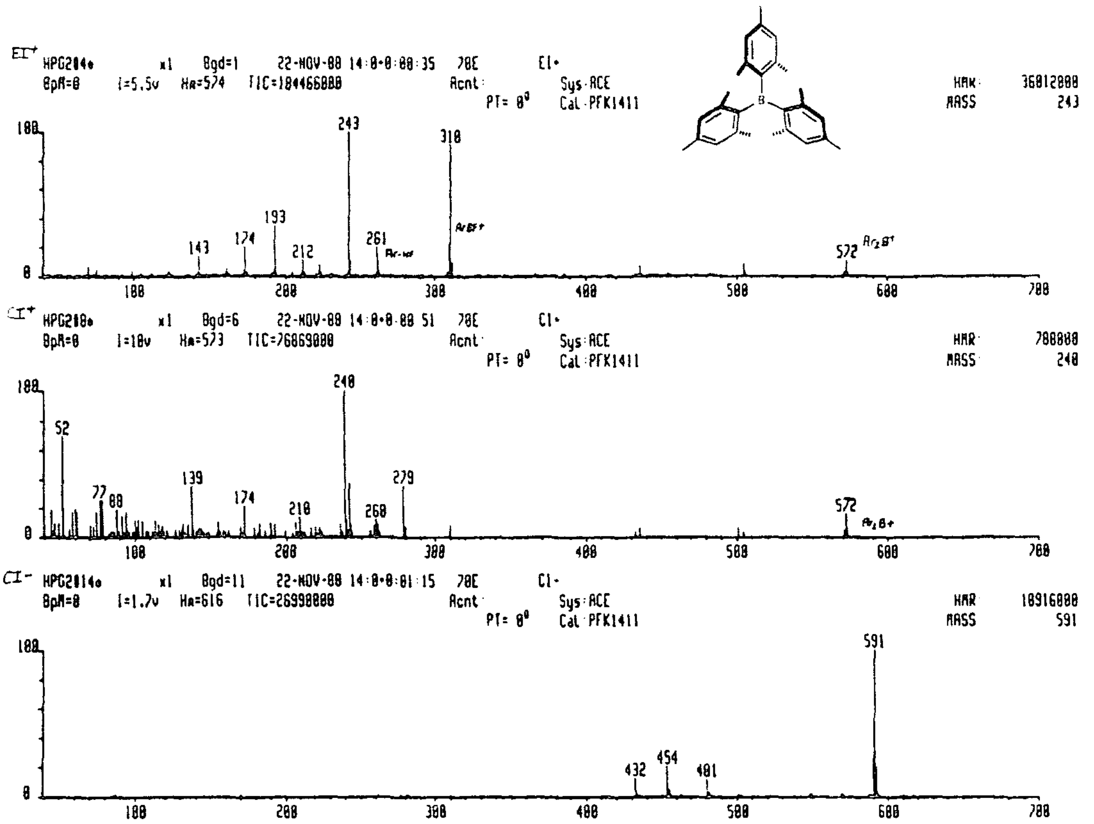

EI+

551.18	0.06
568.99	0.04
569.11	0.26
570.09	1.02
571.09	2.52
571.71	0.05
572.08	10.19
572.36	0.08
572.75	0.05
573.09	2.01
574.11	0:16

CI+

432.34	0.04
435.27	0.07
501.14	0.03
501.25	0.07
504.11	0.03
571.11	0.06
572.12	0.18
573.12	0.07

CI−

		453.74	0.16			
431.82	0.14	454.17	20.26	588.39	0.12	
432.21	12.50	454.87	0.18	588.49	0.19	
432.90	0.16	455.18	4.40	588.66	0.29	
433.00	0.34	456.21	0.43	589.93	26.37	F
433.22	2.64	463.17	0.39	590.97	100.00	F
434.22	0.65	464.17	0.14	591.98	19.60	F
435.22	0.65	480.07	0.26	592.52	0.21	
436.21	0.26	480.18	0.30	592.96	2.33	
450.27	0.19	480.77	0.18	594.00	0.17	
453.04	0.28	481.13	11.36	609.02	0.22	
453.18	0.49	482.12	2.45	609.95	0.81	
453.54	0.16	483.12	0.41	610.92	0.16	
453.63	0.17	483.23	0.26	616.95	0.38	
		484.17	0.19			

Figure 8.15: *Mass spectral data for Ar_3B (75).*

8.5 PREPARATION OF Ar_3B (75)

The new aryl zinc compound, ArZnCl (81) was prepared by classical methods [13] and reacted stoichiometrically with BCl_3. Vacuum distillation of this mixture however, yielded a low melting point solid which was characterised as Ar_3B (75) (Equation 8.10).

$$3ArBCl_2\ (73) \rightleftharpoons Ar_3B\ (75) + 2BCl_{3\ (v)} \qquad (8.10)$$

Many such disproportionation reactions are known in organohalo boron chemistry [14,15]. A possible mechanism is shown in Figure 8.14, and Figures 8.15 and 8.16 illustrate, respectively, mass spectral and ^{13}C NMR data for the Ar_3B species.

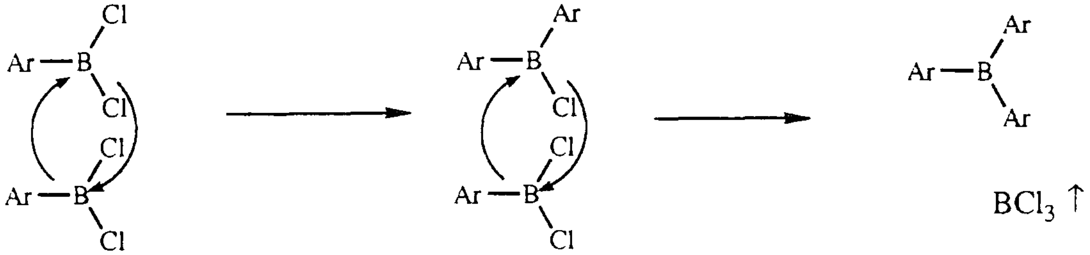

Figure 8.14: *Possible reaction mechanism for formation of* Ar_3B.

Addition of ArZnCl (81) to BCl_3 gave no apparent reaction at room temperature. No "B-F" decomposition species were evident. Refluxing may promote the required substitution reaction. However, these results appear to suggest that an organometallic derivative of intermediate reactivity between the organolithium and organozinc species is required. Attempts to generate the ArMgCl Grignard by ArLi addition to magnesium chloride failed (Section 8.9.9.1).

Recently a possible route to the Grignard ArMgBr was discovered in the literature [16] generating $MgBr_2$ *in situ* (Section 9.9.9.2). This may also be *via* the formation of ArBr, however the synthetic route to ArBr *via* the direct action of bromine on ArLi gave consistently low yields

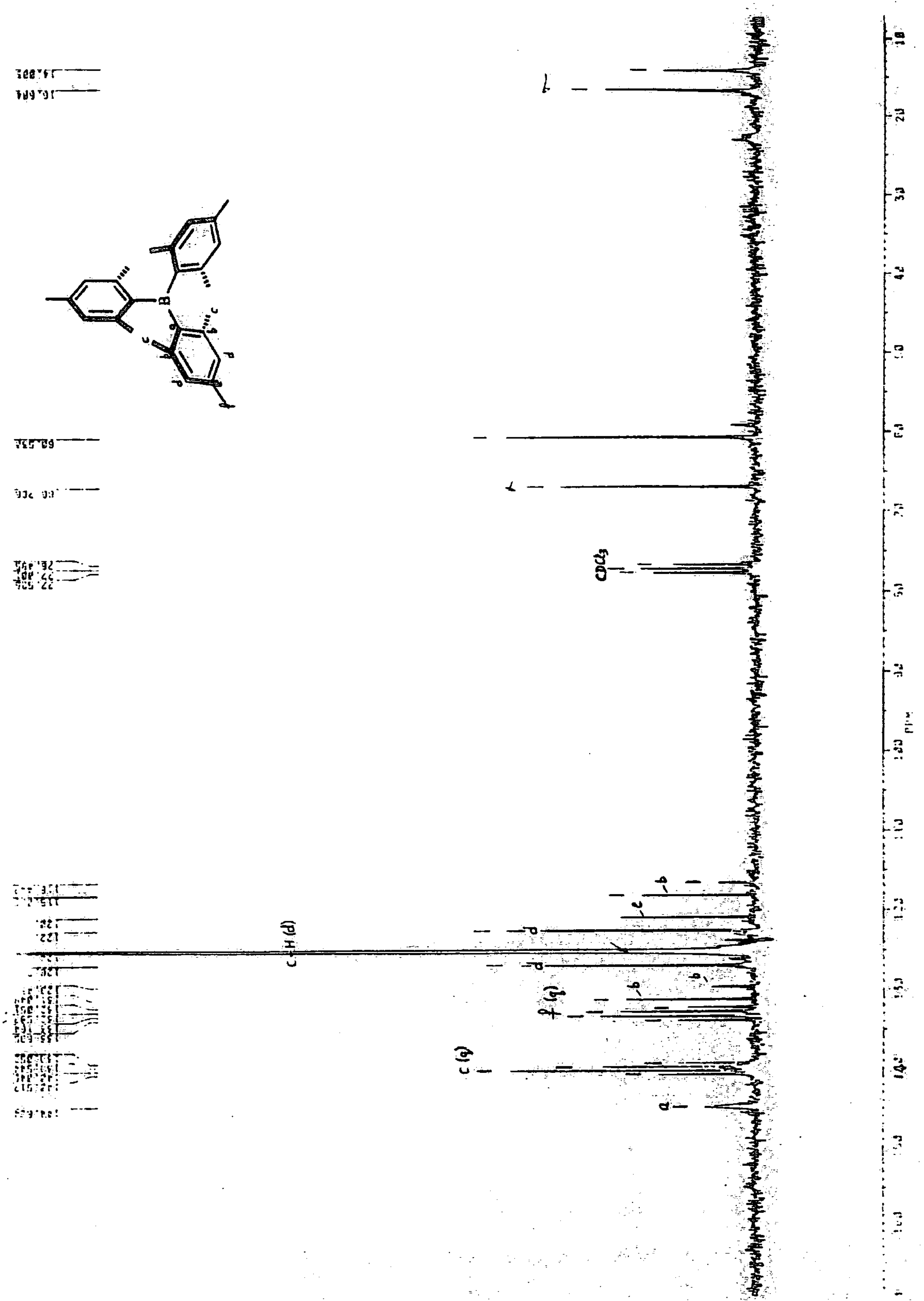

Figure 8.16: *Partially decoupled* ^{13}C *NMR spectrum for* Ar_3B *(75) in* $CDCl_3$.

(~12%) [8]. [A possible steric limitation to Grignard formation may also exist]. This organometallic reagent should be further pursued to allow a possible high yield synthetic route to $Ar_{3-n}BX_n$ by preventing decomposition *via* attack at the trifluoromethyl groups.

8.6 HYDROLYSIS OF Ar_2BCl (4)

Ar_2BCl was hydrolysed (Equation 8.11) and the ^{19}F NMR spectrum was monitored, with no attempt made to isolate the product. The ortho-CF_3 groups appeared to be equivalent although, of course, the rings may still be spatially inequivalent and simply have coincident chemical shifts.

$$Ar_2BCl\ (74) + H_2O \longrightarrow \text{"}Ar_2B\text{–}OH\text{"} \tag{8.11}$$

8.7 COMPARISON OF $Ar_{3-n}BCl_n$ (n = 1-3) SPECIES: STRUCTURE AND NMR PARAMETERS

A direct comparison of the physical data of the three Ar-substituted derivatives is presented in Table 8.1.

COMPOUND	^{11}B (δ/ppm)	^{19}F (δ/ppm)	MPt
$ArBCl_2$ (73)	27 (Et_2O) 31 (CH_2Cl_2)	-56.3 (o-CF_3) -63.9 (p-CF_3)	62-64
Ar_2BCl (74)	47 (Et_2O)	-57.5 (o-CF_3) -57.6 (o-CF_3) -64.6 (p-CF_3)	71-73
Ar_3B (75)	31 (Et_2O)	-63.3 (o-CF_3) -64.8 (p-CF_3)	40-41 ‡

Table 8.1: *Comparative physical data for the three Ar-substituted boron derivatives; ‡compare with Mes_3B (190 °C) (ref.4).*

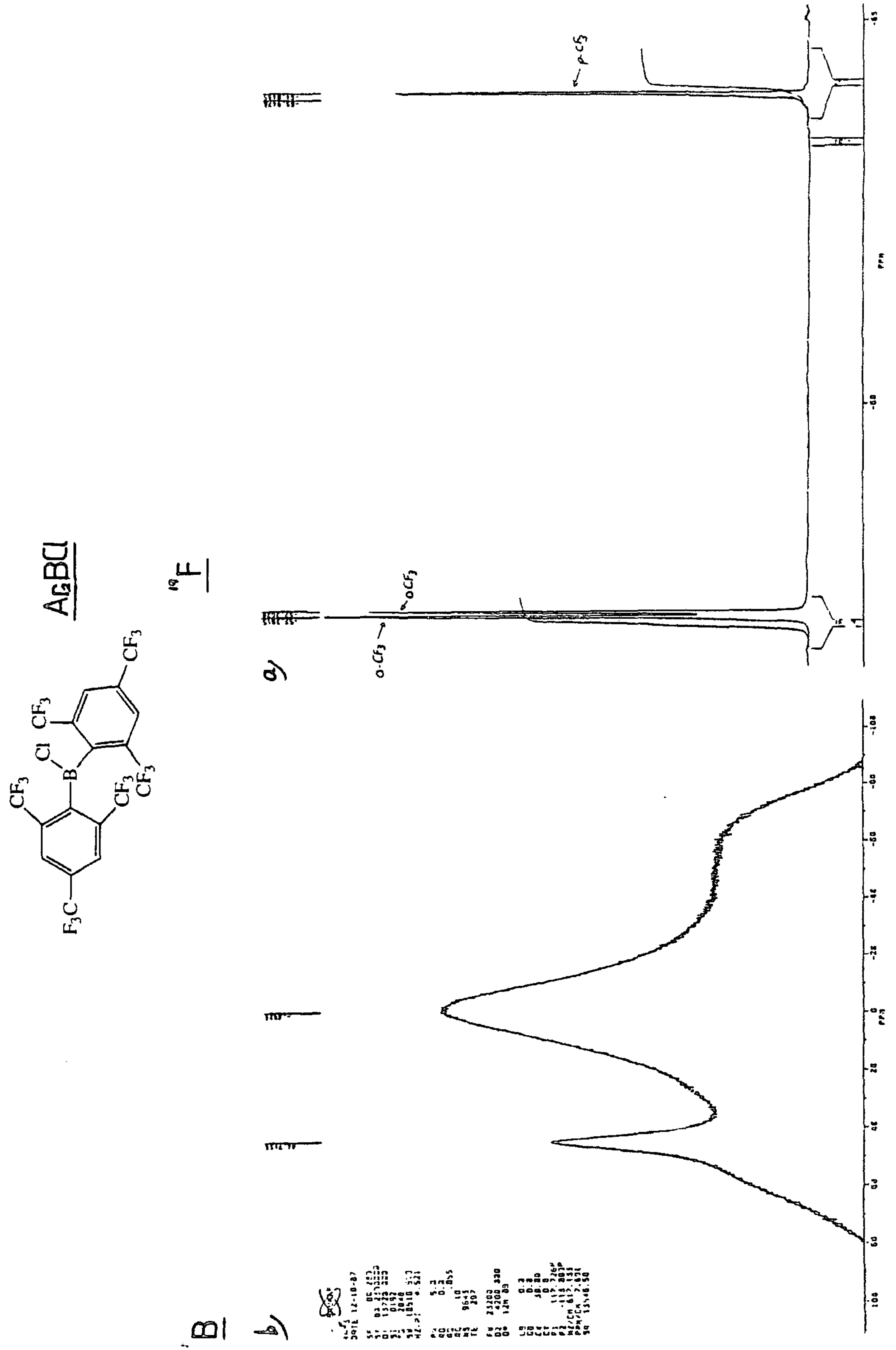

Figure 8.18: (a) ^{19}F and (b) ^{11}B NMR spectra of Ar_2BCl (4) in $CDCl_3$.

The graph represents the trend in ^{11}B NMR shifts on progressive substitution of chlorine for Ar in BCl_3. Values for the corresponding ethyl and diethylamino derivatives are given for comparative purposes (Figure 8.17).

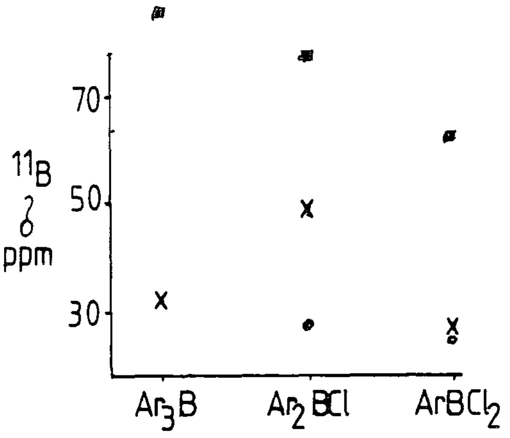

Figure 8.17: *Correlation of* ^{11}B *NMR shifts in the Ar* (x), Et$_2$*N* (●) *and* Et (▪) *systems.*

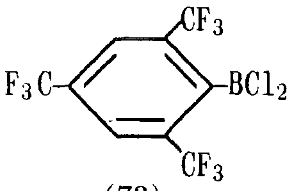

(73)

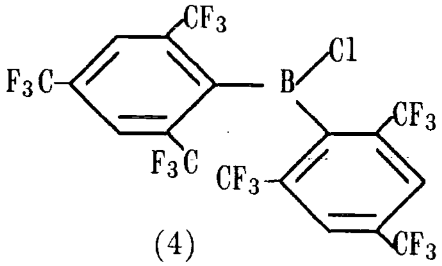

(4)

The unexpected shielding of the ^{11}B NMR value for compound (73) is attributed to occupancy of the fourth valency of boron by electron donation from the ortho fluorine atoms.

The ^{19}F NMR spectrum of (4) (Figure 8.18) clearly shows two distinctive types of ortho-CF_3 group. The MNDO calculation diagnoses this effect to two inequivalent rings. The results of these calculations are shown in Figure 8.19.

The equivalence of the ortho-CF_3 groups in Ar_3B (75) is attributed to the symmetrical orientation of the three rings (twisting out of plane), *cf.* Mes_3B (82) (Figure 8.20) [4]. The low melting point of Ar_3B may be attributed to a crystal-packing effect.

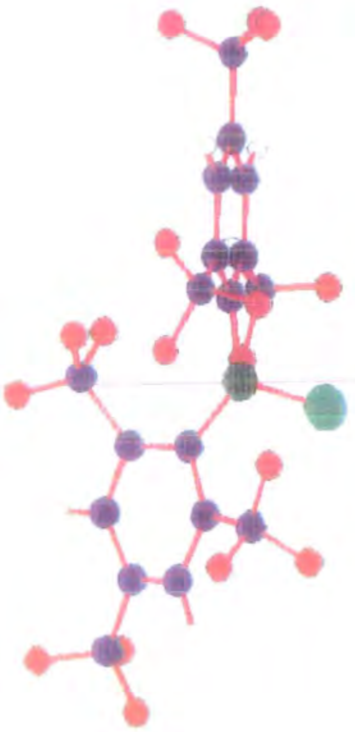

Figure 8.19: *Results of MNDO calculation on Ar_2BCl (4).*

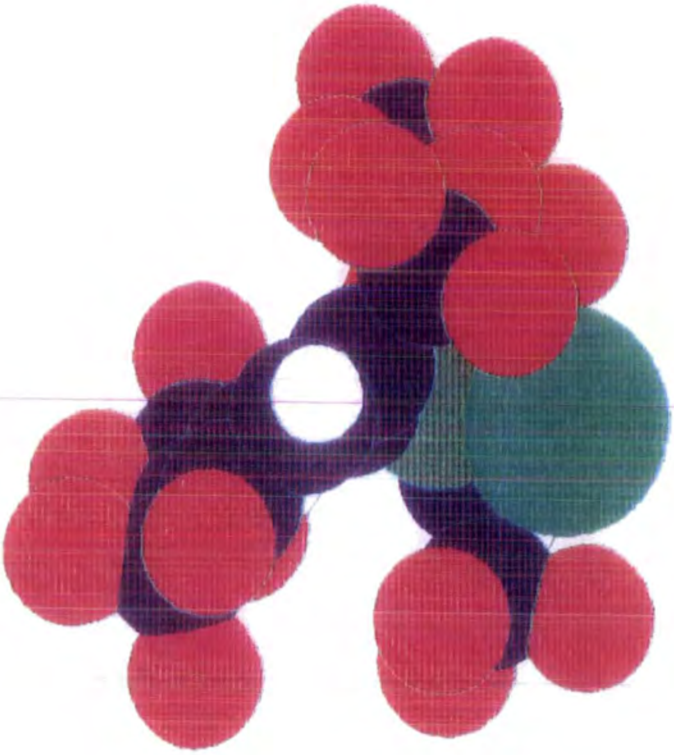

Figure 8.19: *Results of MNDO calculation on Ar_2BCl (4).*

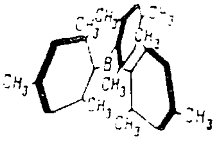

Figure 8.20: *Orientation of the mesityl rings in Mes$_3$B (82).*

8.8 ^{11}B NMR SPECTRA: A GENERAL DISCUSSION

Broad signals were obtained for all the Ar containing organoboron species. This is due to the quadrupolar relaxation of the boron nucleus (I = 3/2), although more serious quadrupolar relaxation is seen in trigonal than in tetrahedral derivatives. It is interesting to compare the line widths obtained in these systems with those for isolated borates (Chapter 10). The electron density is important in determining the shifts but both the inductive (-I) and perhaps most significantly the mesomeric effects also play their part [4].

8.9 EXPERIMENTAL DETAILS

8.9.1 Preparation of ArBCl$_2$ (73)

8.9.1.1 With Excess BCl$_3$

ArLi (100 ml, 45 mmol,0.45 M in Et$_2$O) was added dropwise over 5 minutes to a stirred solution of BCl$_3$ (5.0 ml, 6.8g, 58 mmol) condensed into Et$_2$O (70 ml) at -40 ^{o}C, and the mixture was maintained at this temperature during addition. Copious amounts of white solid were precipitated. The solution was allowed to reach room temperature over a period of one hour and stirred continuously. Removal of the solid by filtration gave a clear yellow-green coloured solution. The ^{11}B NMR spectrum showed clear evidence of "B-F" species. ^{19}F NMR δ: -114.2 (4 equal lines) $^{1}J_{BF}$ 58 Hz, -128.4 (unresolved), -152 (s), -54.1 (t,o-CF_3) $^{5}J_{FF}$ 15.8 Hz, -64.2 (s,p-CF_3),"$ArBF_2$" . The large singlet at -64.0 ppm present was attributed to ArH (1).

The solution was pumped under hard vacuum (0.01 mm Hg) for 1 hour to remove all the volatile material. The resulting sticky green residue could be redissolved in CH_2Cl_2 (*ca.* 10 ml), or alternatively diethylether, and cooled overnight to -40 ^{o}C (if no solid precipitated at low temperature the solvent could be slowly removed *in vacuo* and the product fell out of the solution as a whitish/yellow solid). The solid was isolated by filtration under rigorously anhydrous conditions and washed to pure white crystals by several aliquots of pentane. Very poor yields were obtained, approximately 1.9g (12%) (for improved yields see Section 8.9.1.2). The precipitate obtained at the first stage was analysed and found to contain lithium, fluorine and chlorine,[1] attributed to LiF and LiCl elimination. Mpt. 62-64 ^{o}C; Analysis found: C, 29.58; H, 0.52; Required for $C_9H_2F_9BCl_2$: C, 29.79; H, 0.55%; IR (Nujol) ν_{max}: 3100 (w,ArCH), 1630 and 1570 (s,ArC=C), 1400-1000 (s,C-F,CF_3), ~900 (m,ArCH), 1037 (m,B-Cl), 705 and 690 (m,CF_3) cm^{-1}; MS (Intensity%) EI: 362 (low intensity,$ArBCl_2^+$), 262 (100,Ar-F), 243 (ring fragmentation), 212; CI^+: 379 (0.51,$ArBCl_2^+NH_3$); ^{11}B (Et_2O) δ: 27 ppm, (CH_2Cl_2) δ: 32 (s,broad) ppm; ^{19}F (CH_2Cl_2) δ: -56.3 (6F,o-CF_3), -63.9 (3F,p-CF_3) ppm; (Et_2O) δ: -57.4 (6F,o-CF_3), -64.4 (3F,p-CF_3) ppm; (THF) δ: -56.4 (6F,o-CF_3), -62.7 (3F,p-CF_3) ppm.

---

[1] F^- : $Fe(NCS)_6^{2-}$ test;
Cl^- : silver nitrate test;
Li : flame test.

8.9.1.2 Improved Synthesis of $ArBCl_2$

ArLi (100 ml, 45 mmol, 0.45 **M** in Et_2O) was added dropwise over 10 minutes to a stirred solution of BCl_3 (45 ml, 45 mmol, 1 **M** solution in hexane) at -10 ^oC. This was stirred for 30 minutes and allowed to reach room temperature. The ^{11}B NMR spectrum confirmed the presence of $ArBCl_2$, $BFCl_2\cdot Et_2O$ and $BF_3\cdot Et_2O$. A greater attack at CF_3 results in the presence of an excess (1.3 equivalents) of boron trichloride (Section 8.9.1.1). The solid filtered from the reaction was found to contain fluorine, reinforcing the belief that the reaction mechanism involved LiF and LiCl elimination (Section 8.2.1). $ArBCl_2$ was isolated as described earlier (Section 8.9.1.1), and the yield was 5.2g (32%).

8.9.2 Reaction of $BF_3\cdot Et_2O$ and $BCl_3\cdot Et_2O$

$BF_3\cdot Et_2O$ (0.2 ml, 1.63 mmol) was added dropwise over 2 minutes to a stirred solution of $BCl_3\cdot Et_2O$ (1.63 ml, 1.63 mmol, 1 **M**) in ether (10 ml) at room temperature. The mixture was stirred for 10 minutes before the ^{11}B NMR spectrum was recorded. ^{11}B δ: 10.62 (s,$BCl_3.Et_2O$), 7.87 (d, $BCl_2F\cdot Et_2O$) $^1J_{BF}$ 57.0 Hz, 3.88 (t,$BClF_2\cdot Et_2O$) $^1J_{BF}$ 29.1 Hz, 0.0 (s, $BF_3\cdot Et_2O$) ppm.

8.9.3 Reaction of ArH and BCl_3

$$\mathrm{ArH} + \mathrm{BCl_3} \not\longrightarrow$$

BCl_3 (1.72g, 1.26 ml, 14.7 mmol) was condensed into a stirred solution of ArH (4.1g, 14.6 mmol) in Et_2O (30 ml) at -10 ^oC. The reaction mixture was allowed to reach room temperature and stirred for 4 hours. There was no visible reaction, even after refluxing for 2 hours. ^{19}F (Et_2O) δ: -62 ppm (s,ArH); ^{11}B (Et_2O) δ: 11 ppm (unreacted BCl_3)[4].

8.9.4 Preparation of '$ArBF_2$'

8.9.4.1 From $ArBCl_2$

$$ArBCl_2 + SbF_3 \longrightarrow ArBF_2$$

$ArBCl_2$ (0.42g, 1.2 mmol) in Et_2O (25 ml) was added to a stirred suspension of SbF_3 (0.24g, 1.32 mmol) in Et_2O (10 ml) at room temperature. This mixture was brought gradually to reflux for 2 hours. ^{19}F δ: -54.1 (t,o-CF_3) $^5J_{FF}$ 15.8 Hz, -64.2 (s,p-CF_3) ppm.

8.9.4.2 Attempt From ArLi and $BF_3 \cdot Et_2O$

$$ArLi + BF_3 \cdot Et_2O \xrightarrow{X} ArBF_2$$

ArLi (17.2 ml, 7.74 mmol, 0.45 M) was added dropwise to a stirred solution of $BF_3.Et_2O$ (0.95 ml, 7.74 mmol) in Et_2O (35 ml) at -20 ^oC. The reaction mixture was stirred for 1/2 hour at -20 ^oC and then warmed to room temperature. The ^{19}F spectrum was very complex in the "CF_3" region (from -55 to -65 ppm) with a large peak at -151 ppm attributed to $BF_3 \cdot Et_2O$ (see Figure 8.8). $BF_3 \cdot Et_2O$ appeared to catalyse decomposition of ArLi (2).

8.9.5 Preparation of Ar_2BCl (74)

8.9.5.1 From ArLi and BCl_3

$$3ArLi\ (2) + BCl_3 \longrightarrow Ar_2BCl\ (74)\ \text{(major product)}$$

A solution of BCl_3 (22 ml, 22 mmol, 1 M in hexane) was added dropwise over 5 minutes to a stirred solution of ArLi (67 mmol, 0.45 M) in Et_2O (150 ml) at -10 ^oC. A visible precipitate was formed instantly on addition. The reaction mixture was allowed to reach room temperature. The ^{11}B NMR showed the presence of two boron species assigned to $ArBCl_2$ and Ar_2BCl. The insoluble solid (LiCl/"LiF") was removed by filtration and the pale brown filtrate concentrated in volume on the vacuum line. With about 30 ml Et_2O remaining, the solution was cooled to -40 ^oC. Ar_2BCl (pale brown solid) precipitated immediately. The solution was maintained at low temperature for 2 hours to maximise yields, filtered at low temperature, and the resultant solid washed with a small volume of petrol, giving a pure white solid which was fully characterised. Yield was 5.2g (39%). Mpt. 71-73 ^oC. Ar_2BCl was also stable to sublimation at 38 ^oC (0.5 mm Hg). Analysis found: C, 35.81; H, 0.31; B, 1.26; Cl, 5.23; Required for $C_{18}H_4F_{18}BCl$: C, 35.53; H, 0.66; B, 1.77; Cl, 5.82%; IR (Nujol) ν_{max}: 3640 (m,OH hydrolysis), 3100 (w,ArCH), 1400-1000 (s,C-F), 1350 (m,B-Cl), 700 (m,CF_3) cm^{-1}; UV-Visible (CCl_4) $\lambda_{max}(\epsilon)$: 270 (2200) nm; MS (Intensity%) EI: 608 (12.1,Ar_2BCl^+), 262 (100,$Ar-F^+$), [peak higher masses: 871 (1B, 1Cl) 4.0 low intensity]; CI^+: 573 (1.4,Ar_2B^+), 248 (100); ^{11}B (CH_2Cl_2) δ: 47 ppm (s,broad); ^{19}F δ: -57.5 (s), -57.6 (s) (12F,o-$CF_3^{a,b}$), -64.6 (s,3F,p-CF_3) ppm.

A small sample (2.1g, 3.5 mmol) was recrystallised from CH_2Cl_2 (5 ml) at -40 ^oC to give crystals suitable for X-ray analysis. These were mounted for this purpose.

8.9.5.2 From ArLi and ArBCl$_2$

It was thought that, to avoid the problem of excess of BCl$_3$, it would be possible, despite its isolation in low yield, to use ArBCl$_2$ in a direct reaction with ArLi (Section 8.2.2). An ether solution of ArLi (6.2 ml, 3.4 mmol, 0.55 M) was added dropwise over 5 minutes to a stirred solution of ArBCl$_2$ (1.1g, 3.0 mmol) in Et$_2$O (50 ml) at -10 ^{o}C. The formation of Ar$_2$BCl was confirmed by ^{19}F and ^{11}B NMR data only, and some "B-F" species were also present in solution.

8.9.6 Reactions of ArSnMe$_3$ (78) with BCl$_3$

ArSnMe$_3$ was made and isolated according to Chambers *et al.*[9], distilled as a colourless oil, bpt. 50 ^{o}C (0.5 mm Hg); ^{19}F δ: -58.5 (6F,o-CF$_3$), -64.4 (3F,p-CF$_3$) ppm.

ArSnMe$_3$ (2.62g, 5.9 mmol) in CH$_2$Cl$_2$ (20 ml) was added dropwise over 5 minutes to a stirred solution of BCl$_3$ (6 ml, 6 mmol, 1 M in CH$_2$Cl$_2$) in additional CH$_2$Cl$_2$ (10 ml) at -40 ^{o}C. The solution immediately turned blue-green on addition. It was stirred for 1/2 hour, allowed to reach room temperature and stirred for a further 2 hours. ^{11}B δ: 62 ppm ("MeBCl$_2$") [4]; ^{19}F δ: -57.4 (6F,o-CF$_3$), -64.4 (3F,p-CF$_3$) ppm ("Me$_2$SnArCl") (no coupling by ^{119}Sn was observed). All volatiles were removed *in vacuo* by pumping for 30 minutes. The ^{11}B NMR peak at +62 ppm almost disappeared.

A further portion of BCl$_3$ (6 ml, 6 mmol, 1M solution in CH$_2$Cl$_2$) was added dropwise to the stirred solution, cooled to -20 ^{o}C. This was allowed to reach room temperature over 20 minutes and a ^{11}B signal corresponding to $ArBCl_2$ was observed. ^{11}B (CH_2Cl_2) δ: +31 (s,broad), +42.6 (s,broad,unreacted BCl_3), +62.3 (s,weak,$MeBCl_2$) ppm [4].

The excess BCl_3 and the remaining $MeBCl_2$ was removed *in vacuo* over 1 hour to yield Me_2SnCl_2, $Me_2SnArCl$ and $ArBCl_2$ as a black oil. It did not appear worthwhile to isolate $ArBCl_2$ from this mixture.

8.9.7 Preparation of Bu_3SnAr (80)

$$Bu_3SnCl + ArLi \longrightarrow Bu_3SnAr \ (80)$$

ArLi (47 ml, 36 mmol, 0.77 M solution in Et_2O) was added dropwise over 5 minutes to a stirred solution of Bu_3SnCl (9.8 ml, 11.7g, 36 mmol) in diethylether (120 ml) at -10 °C. A white precipitate was formed immediately. This was removed by filtration and the filtrate concentrated to yield a heavy yellow oil, purified by vacuum distillation, bpt. 124 °C (0.1 mm Hg). Yield was 17.4g (85%). ^{119}Sn δ: -11.8 (s) ppm; ^{13}C ($CDCl_3$) δ: 125.1 (ArCH ring), 137.5 (o-CF_3) $^1J_{CF}$ 33 Hz, 130.2 (p-CF_3) $^1J_{CF}$ 35 Hz, *ca*. 40 (C on Sn) $^1J_{CSn}$ not resolved, 28.7 ppm (C Bu); ^{19}F δ: -56.1 (6F,o-CF_3), -64.0 (3F,p-CF_3) ppm.

26.0
17.2
13.2

8.9.8 Reaction of Bu_3SnAr (80) with BCl_3

$$Bu_3SnAr \ (80) + BCl_3 \xrightarrow{\quad X \quad} ArBCl_2 + Bu_3SnCl$$

$ArSnBu_3$ (5.62g, 9.8 mmol) in CH_2Cl_2 (10 ml) was added dropwise to a stirred solution of BCl_3 (0.93 ml, 1.27g, 10.8 mmol, 1.1 equivalents) in CH_2Cl_2 (50 ml). This solution was refluxed overnight and no evidence of butyl group transfer was observed. ^{11}B (CH_2Cl_2) δ: 42.6 ppm (unreacted BCl_3); ^{19}F δ: -56.1, -64.0 ppm ($ArSnBu_3$).

8.9.9 Attempted Preparation of a Grignard Reagent

8.9.9.1 From ArLi and $MgCl_2$

$$ArLi + MgCl_2 \longrightarrow ArMgCl + LiCl$$

ArLi/Et_2O (0.57 M, 7.3mmol was added dropwise to a stirred suspension of anhydrous $MgCl_2$ (0.7g, 7.3 mmol) in Et_2O (20 ml) at room temperature. The reaction mixture was stirred for 1 hour. The ^{19}F NMR showed complete hydrolysis of the ArLi forming ArH. ^{19}F (Et_2O) δ: -64 ppm (ArH). $MgCl_2$ was rigorously dried by heating to 110 ^{o}C *in vacuo* for 6 hours. However, the solid appeared to retain sufficient water of crystallisation to make this reaction ineffective.

8.9.9.2 Possible Generation of ArMgBr

Anhydrous $MgBr_2$ may be prepared *in situ* by the reaction of magnesium with bromine, 1,2 dibromoethane or $HgBr_2 \cdot THF$, to give a two phase system, the dense lower phase containing a $MgBr_2 \cdot THF$ complex [16].

8.9.10 Preparation of ArZnCl (81)

$$ArLi + ZnCl_2 \longrightarrow ArZnCl\ (81)$$

ArLi (50 ml, 35 mmol, 0.7 M) was added dropwise over 5 minutes to a stirred solution of $ZnCl_2$ (4.8g, 35 mmol) in ether (50 ml) at room temperature. This mixture was stirred for two hours. ^{19}F NMR δ: -62.0 (6F,o-CF_3), -64.1(3F,p-CF_3) ppm. Quantitative conversion with respect to the ^{19}F NMR. This reagent was used *in situ*.

8.9.11 Preparation of Ar_3B (75)

$$3ArZnCl + BCl_3 \longrightarrow [ArBCl_2] \longrightarrow Ar_3B + 3ZnCl_2$$

The ArZnCl-ether solution (*ca.* 35 mmol) was added dropwise to a stirred solution of BCl_3 (4.1g, 3.0 ml, 35 mmol) in ether (70 ml) at -10 ^oC. This mixture was allowed to reach room temperature and stirred for 2 hours. The Et_2O was removed *in vacuo* and the residue distilled to give a pale yellow oil, bpt. 84 ^oC (0.1 mm Hg), which solidified in the receiving vessel. This appeared to be Ar_3B (75) presumably formed *via* the disproportionation of $ArBCl_2$. No B-F species were observed. Yield was 4.2g (42% w.r.t ArZnCl). Mpt. 40-41 ^oC. Analysis found (%C is slightly low): C, 36.08; H, 0.72; B, 1.26; Cl, 0%; Required for $C_{27}H_6B$: C, 37.97; H, 0.71; B, 1.27%; UV-Visible (CCl_4) $\lambda_{max}(\epsilon)$: 262.5 (3975.5) nm; MS (Intensity%) EI: 573 (10.2,Ar_2B^+), 310 (65,$ArBF^+$), 261 (25) and 243 (100,ring fragmentation); CI^+: 573 (0.18,Ar_2B^+), 279 (25) and 240 (100,ring fragmentation); CI^-: 591 (100,Ar_2BF^-); ^{11}B ($CDCl_3$) δ: 31 ppm (s,broad); ^{19}F ($CDCl_3$) δ: -63.32 (s,6F), -64.76 (s,3F) ppm; ^1H ($CDCl_3$) δ: 8.1 (s) ppm; ^{13}C ($CDCl_3$) δ: 144.62 (s,broad,B-$\underline{C}$), 139.80 $^1J_{CF}$ 31.51 Hz (q,$\underline{C}F_3C$), 132.88 $^1J_{CF}$ 34.47 Hz (q,$\underline{C}F_3C$), 124.91 $^1J_{CH}$ 270.58 Hz (d, CH), 120.76 (s,CF_3-$\underline{C}$), 118.05 (s,CF_3-C), 116.45 (s,CF_3-C) ppm (Figure 8.16).

8.9.12 Hydrolysis of Ar_2BCl (4)

$$Ar_2BCl \xrightarrow{H_2O} "Ar_2BOH"$$

Excess H_2O (5 ml) was added to a stirred solution of Ar_2BCl (0.25g, 0.4 mmol) in CH_2Cl_2 (10 ml). The ^{19}F NMR was recorded. The o-CF_3 groups appear to be equivalent. ^{19}F δ: -57.1 (o-CF_3), -64.1 (p-CF_3) ppm.

8.10 REFERENCES

1. a) M.F. Lappert, *Chem.Rev.*, 1024 (1956) and references therein.

   b) M.F. Lappert and M.K. Majumdar, *J.Organometallic Chem.*, 6, 316-332 (1966).

2. E. Wiberg and W. Ruschman, *Chem.Ber.*, 7, 1583-1591 (1937).

3. W. Gerrard, M. Howarth, E.F. Mooney and D.E. Pratt, *J.Chem.Soc.*, 1582-1584 (1963).

4. H. Nöth and B. Wrackmeyer, "*Nuclear Magnetic Resonance Spectroscopy of Boron Compounds*", Springer-Verlag, Berlin, Heidelberg, New York, 9, 109 (1978).

5. H.C. Brown, *J.Amer.Chem.Soc.*, 67, 374 (1945).

6. Personal comunication, Professor R.D. Chambers, Durham University (1989).

7. R.D. Chambers and T. Chivers, *J.Chem.Soc.*,3933 (1965).

8. G.E. Carr, R.D. Chambers, T.F. Holmes and D.G. Parker, *J.Organometallic Chem.*, 325, 13 (1987).

9. a) N.N. Greenwood and A. Earnshaw, "*Chemistry of the Elements*", Pergamon Press, Oxford, New York, 10, 461 (1984).

   b) P. Powell, "*Principles of Organometallic Chemistry*", 2nd Edition, Chapman and Hall, London, New York, p.102-103 (1988).

10. K.B. Dillon and G.F. Hewitson, *Polyhedron*, 3(8), 957-962 (1984).

11. P. Harston, J.L. Wardell, D. Marton, G. Tagliavini and P.J. Smith, *Inorg.Chim.Acta*, 162, 245-250 (1989).

12. a) G.E. Carr, Ph.D. Thesis, Durham University (1986).

    b) R.W. Bott, C. Eaborn and J.A. Waters, *J.Chem.Soc.*, 687 (1963).

13. J.S. Thayer, "*Organometallic Chemistry: An Overview*", VCH Publishers Ltd., p.16 (1988) and references therein.

14. P.A. McCusker, G.F. Hennion and E.C. Ashby, *J.Amer.Chem.Soc.*, 79, 5192-5194 (1957).

15. E. Gipstein, P.R. Kippiv, M.A. Higgins and B.F. Clark, *J.Organometallic Chem.*, 26, 2947-2950 (1961).

16. B.J. Wakefield, "*Organolithium Methods, Best Synthetic Methods*", Academic Press, p.163 (1988).

CHAPTER NINE

BORINIUM CHEMISTRY

9.1 INTRODUCTION

The most prolific researchers within the field of borinium chemistry are H. Nöth and co-workers. Recently (1985) he has provided a comprehensive review on borinium $R\text{-}\overset{+}{B}\text{-}R$ (83) and borenium $R_2B^+\leftarrow D$ (84) ions [1]. The boron cation ($-\overset{+}{B}-$) has only two electrons available for bonding, therefore, in the case of (84) an electron pair must be supplied by a suitable ligand. It is clear that the coordination of boron is correlated with the size and nature of R, D and X [2]. Studies on systems of type (84) have been carried out to define a three coordinate range in the ^{11}B NMR spectrum [2] [$X = Cl^-$, $SO_3CF_3^-$]. The molecular orbital approach to these structures has been explored by Nöth and Kölle (1985) [1]. The importance of back-bonding from π-electron rich species and a steric shield for stability is emphasised. This situation is exactly paralleled with phosphenium cations [3].

Aromatic species also seem capable of some degree of stabilisation[1,4]. Borinium ion preparations can be classified into four groups. A brief survey under each classification is given below.

9.1.1 **Boron-Halogen Heterolysis**

$$R_2BX + MX_3 \longrightarrow R_2B^+MX_4^-$$

This method, which involves the use of a Lewis acid to remove a halogen as X^- [1], is employed in this work. Further examples are illustrated in Figure 9.1.

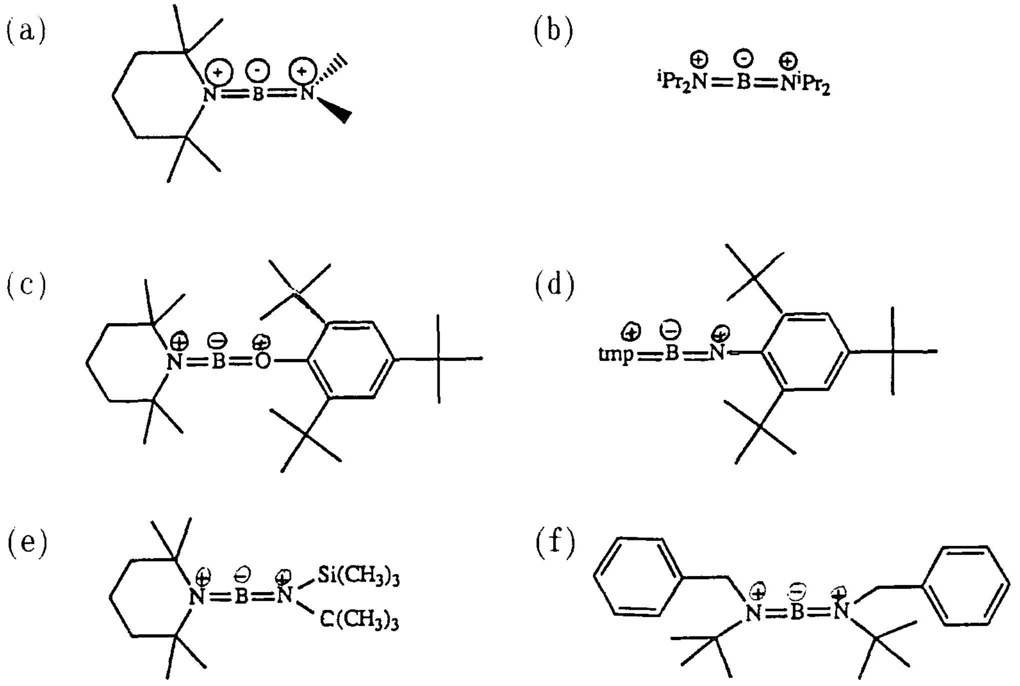

Figure 9.1: *Borinium ions formed by boron-halogen heterolysis; (a) 1981 (refs.4b,4h); (b) 1982 (ref.4h); (c) 1983 (refs.2,5); (d) 1983 (ref.2); (e) 1985 (ref.6); and (f) 1986 (ref.7,8).*

9.1.2 Electrophilic Attack

This includes, for example, attack on aminoboranes by the use of a suitable electrophile [1,6] (Equation 9.1).

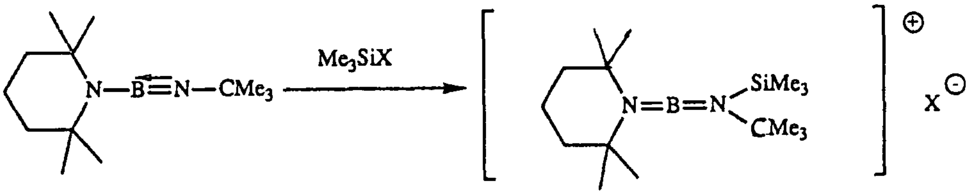

(9.1)

9.1.3 Nucleophilic Attack

Addition of a nucleophile may form borenium ions by displacement of a good anionic leaving group [1,9] (Equation 9.2).

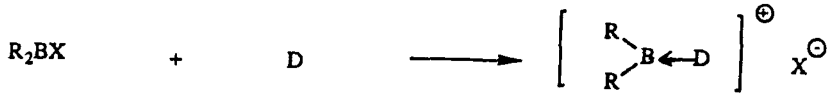

$$R_2BX + D \longrightarrow \left[R_2B \leftarrow D \right]^{\oplus} X^{\ominus} \qquad (9.2)$$

9.1.4 Metathesis

The bulk of tmp is essential for this reaction; (Equation 9.3) [1,10] (for example with $^{i}Pr_2N$ the bisamino boron triflate is formed) (see also Chapter 11).

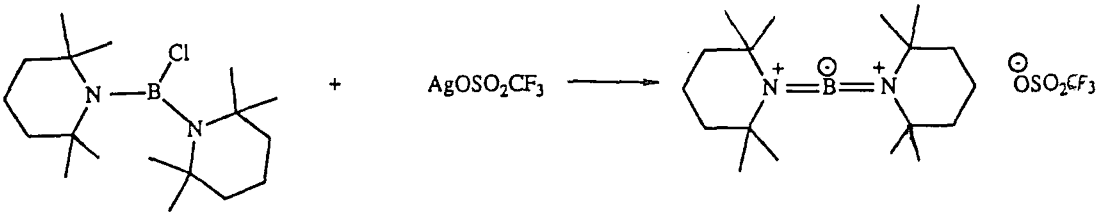

(9.3)

9.2 OVERVIEW

Routes to stable two coordinate boron cations similar to those prepared by Nöth 1985 [1] have been investigated. A range of Lewis acids were used for the abstraction of Cl^- from R_2BCl. The potential of Ar [2,4,6-tris(trifluoromethyl)phenyl] as a steric shield has been recognised (Chapters 1, 3 and 4). It was of interest to see if it could stabilise the respective borinium ion, *ie.* Ar_2B^+ (85).

9.3 MNDO CALCULATION ON Ar_2B^+ (85)

An MNDO calculation related these properties and allowed an insight into the feasibility of the proposed structure of Ar_2B^+ (85). The results are given in Figure 9.2.

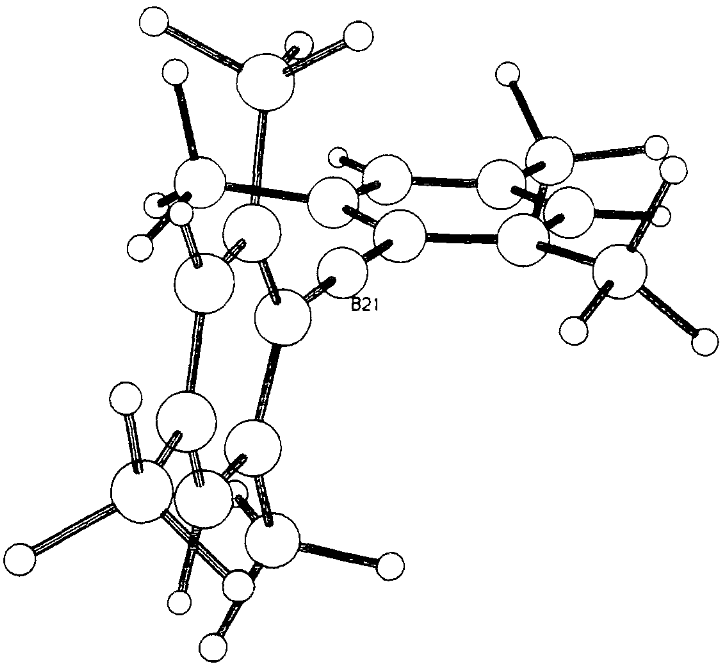

Figure 9.2: *MNDO calculation results for the postulated borinium ion, Ar_2B^+ (85).*

$\mathrm{Ar}\text{-}\overset{178^\circ}{\widehat{\mathrm{B}}}\text{-}\mathrm{Ar}$ Ar-B length 1.474Å

9.4 BORINIUM ION SYNTHESIS

To allow a direct comparison of techniques and NMR interpretation a series of borinium ions were synthesised. The bis amino substituted boron halide was prepared either by simple addition of the amine to BCl_3, where the steric strain was low enough to allow this [4h,11], or by the addition of the lithium derivative to BCl_3 (in the cases of tmp and Ar) [10]. The resulting compounds (Table 9.1) were treated with $SbCl_5$, $AlCl_3$, $TiCl_4$ and BCl_3.

In cases with tmp_2BCl (86) and $(^iPr_2N)_2BCl$ (87), the best results were achieved with $AlCl_3$, although $SbCl_5$ was also effective in a number of examples (see Table 9.1). However, this often gave intractable black solids which appeared to contain the borinium ion with respect to the ^{11}B NMR, but purification from these systems proved difficult. The driving force of these reactions is the thermodynamic favourability of the formation of a 4th bond to aluminium, or a 6th bond to antimony. With the use of BCl_3 as the Lewis acid, B-Cl bond forming counteracts B-Cl breaking [2].

LEWIS ACID	SOLVENT (25°C)	^{11}B δ	SPECIES	
$[(^iPr_2N)_2BCl]$				
---	CH_2Cl_2	30.7	$(^iPr_2N)_2BCl$	(87)
$AlCl_3$	CH_2Cl_2	37.0	$(^iPr_2N)_2B^+AlCl_4^-$	(88)
$SbCl_5$	CH_2Cl_2	30.7	$(^iPr_2N)_2BCl$	(87)
$SbCl_5$	no solvent	36.4	$(^iPr_2N)_2B^+SbCl_6^-$	(89)
		4.0	‡	
BCl_3	CH_2Cl_2	42.6	BCl_3	
		30.7	$(^iPr_2N)_2BCl$	(87)
$[(tmp)_2BCl]$				
---	CH_2Cl_2	34.5	$(tmp)_2B+$	(90)
		26.0	"$tmp_2BCl_2^-$"	
---	CH_2Cl_2 (40°C)	32.5	tmp_2BCl	(86)
$AlCl_3$	CH_2Cl_2	35.6	$(tmp)_2B^+AlCl_4^-$	(91)
$SbCl_3$	CH_2Cl_2	35.6	$(tmp)_2B^+SbCl_6^-$	(92)

Table 9.1: *Experimental results for borinium ion synthesis (refs.4h,10); ‡small peak: possibly hydrolysis.*

9.5 STRUCTURAL CONSIDERATIONS

A downfield shift relative to that of the 3-coordinate precursor (86) or (87) is indicative of two coordinate cation formation, although the magnitude is less than that which might have been expected. This is attributed to electron donation by the amine groups into both vacant orbitals [1,4h,10].

In the starting bisaminoboron chloride, nitrogen to boron $p\pi$-$p\pi$ backbonding is reduced [1,4h]. A theoretical study of electron delocalisation in the amino-borane system is available [12]. On abstraction of X^- a geometric change to linearity decreases the steric strain with concomitant increase in stabilisation by $p\pi$-$p\pi$ backbonding.

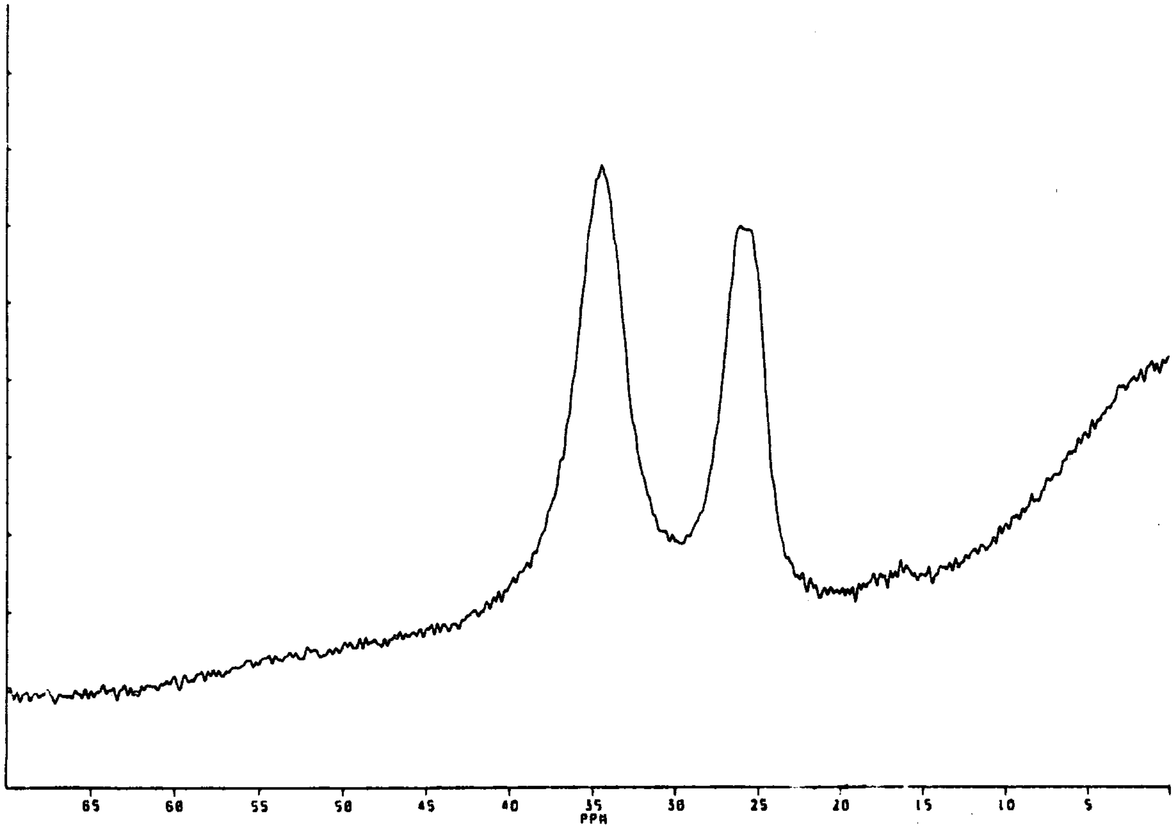

Figure 9.4: ^{11}B *NMR Spectrum of* $(tmp)_2BCl$ *(90) (298K,* CH_2Cl_2*).*

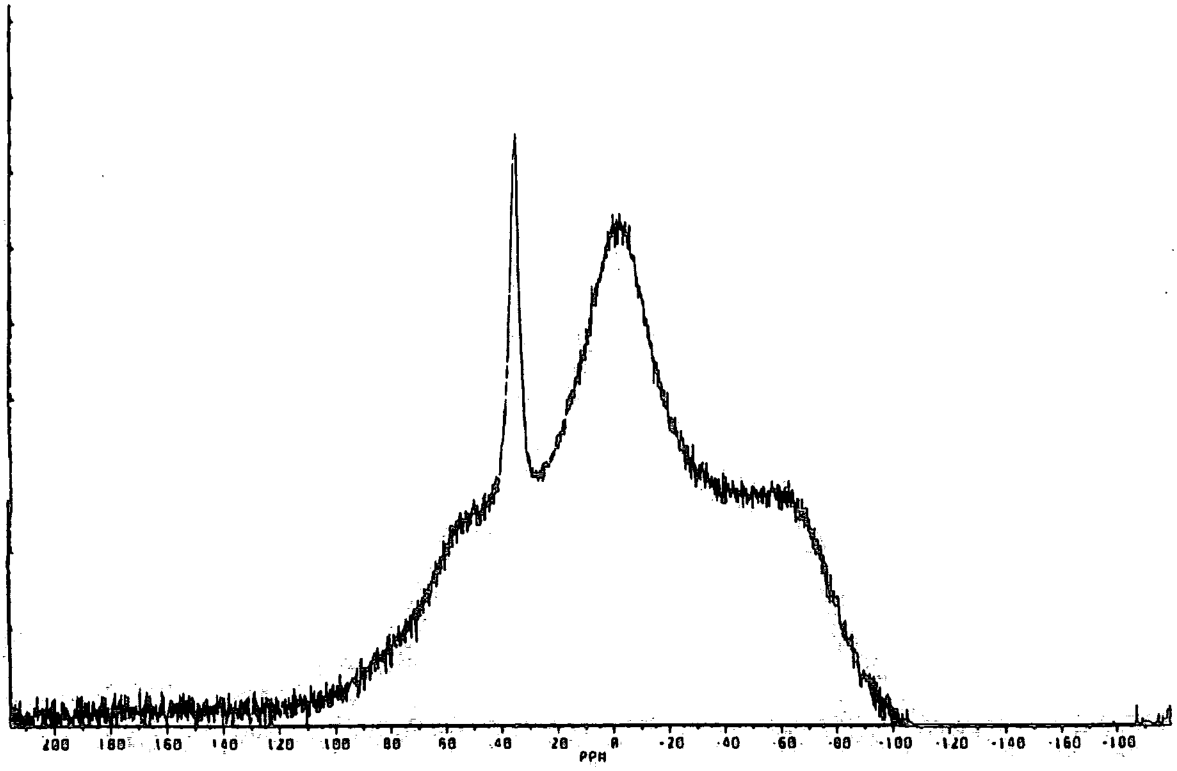

Figure 9.5: ^{11}B *NMR Spectrum of* $(tmp)_2B^+AlCl_4^-$ *(91) (298K,* CH_2Cl_2*).*

The situation for $(tmp)_2B^+$ is exactly analogous (Figure 9.3) [10].

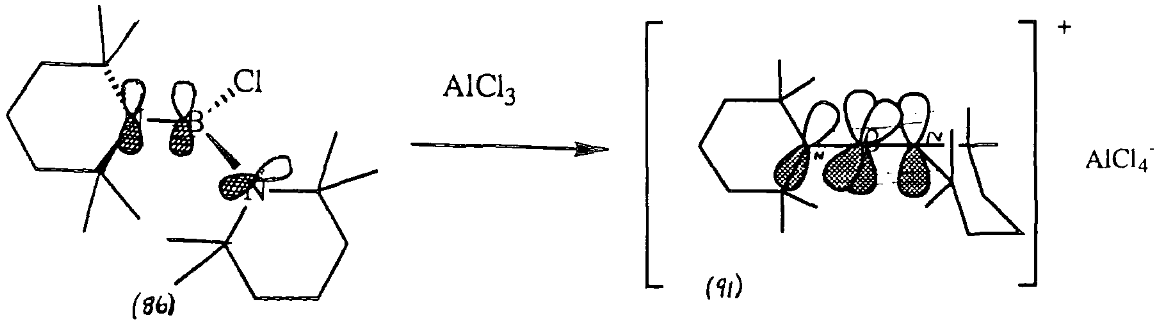

Figure 9.3: *Borinium ion stabilisation by pπ-pπ backbonding.*

It is of interest to note that, in the case of $(tmp)_2BCl$ (86), the cation appeared to be present at normal temperatures in the absence of a Lewis acid (Figure 9.4). The more shielded species may be attributed to $(tmp)_2BCl_2^-$, although on the basis of the results obtained in Chapter 6, the chloroboron species (86) would not be expected to accept Cl^-. The ^{11}B chemical shift is not as shielded as would be anticipated for a 4-coordinate boron species. Raising the temperature to 40 °C gave coalescence of these two peaks yielding an ^{11}B peak corresponding to the expected shift for $(tmp)_2BCl$ (86) [10]. Further temperature dependent studies to low values may prove interesting. On addition of $AlCl_3$ the characteristic deshielded peak due to the cation was observed [10] (Figure 9.5). The general reaction R_2BCl with Lewis acid was found to be most efficient at low temperature.

The two coordinate boron cations (88) and (91) did not decompose significantly when left in solution in CH_2Cl_2 for two weeks at ambient temperature. The results (Table 9.1) indicate $AlCl_3$, CH_2Cl_2 and low temperatures gave superior results. These were therefore the conditions used in the attempted generation of $Ar_2B^+AlCl_4^-$ (85) from Ar_2BCl (74).

9.6 ATTEMPTED SYNTHESIS OF Ar_2B^+ (85)

The solution of Ar_2BCl in CH_2Cl_2 turned black on addition of $AlCl_3$, but both ^{11}B NMR and ^{19}F NMR showed only the characteristics of unchanged Ar_2BCl, (*ie.* an equivalence of o-CF_3 groups on borinium ion formation, releasing the steric strain would be predicted). Notwithstanding the bulk of the Ar group and the electron clouds around the fluorines which could act to stabilise the two coordinate cation, the instability may arise from the electron withdrawing nature of the ring. In previous examples (Table 9.1) π-electron donation stabilised the two coordinate boron. The carbon fragment can play a stabilising role [4], for example the downfield ^{13}C shift of the system shown in Figure 9.6 [4b] not only indicates cation formation but also charge delocalisation with a considerable contribution of the canonical forms (C) and (F) [4b].

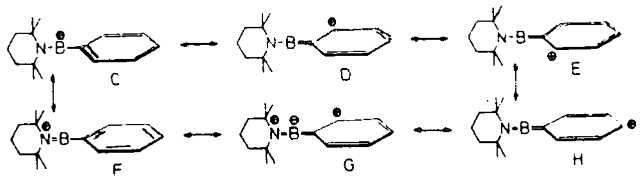

Figure 9.6: *A contribution to borinium ion stabilisation by a carbon substituent.*

A similar stabilisation by a carbon fragment in a borenium system [4i] is shown in Figure 9.7. This moiety has been shown also to stabilise a boron-carbon double bond [4a].

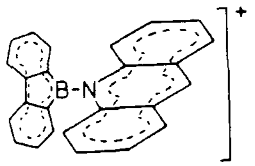

Figure 9.7

Borenium ion with a carbon substituent.

The Ar_2B^+ cation does not form in this way but it is evident in the mass spectra of both Ar_2BCl (74) and Ar_3B (75), illustrating that Ar_2B^+ can be formed by electron bombardment of these organoboron species. This is an interesting observation but proves only that the lifetime of this species is sufficient to be detected by the mass spectrometer, *ie.* of the order of approximately $10^{-10} \rightarrow 10^{-3}$ seconds [13].

It would be interesting to study these systems with a "C-B-C" backbone, and of particular interest to succeed with the reaction:

$$Mes_2BF + AlCl_3 \longrightarrow Mes_2B^+AlCl_3F^-.$$

So far [2] a bis tertiary butyl boron or even a bis mesityl boron has eluded detection. SbF_5 or even PF_5 may prove better F^- acceptors than $AlCl_3$. Perhaps by the use of the more bulky supermesityl group this may be possible. However, a synthetic route to the starting material must be available, and possibly this area of work should initially be attempted at low temperature.

Preparation of the initial R_2BF derivative may be advantageous for two reasons: (i) the limited space around B in the initial R_2BX starting material, and (ii) thermodynamic favourability of M-F bond formation (where M = Sb, Al).

Large groups, *eg.* Supermes, Mes are already known in the stabilisation of two coordinate B (Figure 9.8).

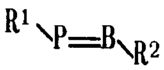

Figure 9.8: *A phosphaborene; R^1 = Supermes (ref.14); R^2 = tmp.*

9.7 EXPERIMENTAL DETAILS

9.7.1 Synthesis of R_2BCl and $R_2B^+AlCl_4^-$ (R ≡ tmp, $^iPr_2N$)

$(^iPr_2N)_2BCl$ and $(^iPr_2N)_2B^+AlCl_4^-$ were synthesised according to Higashi *et al.*[4h] and $(tmp)_2BCl$ and $(tmp)_2B^+AlCl_4^-$ according to Nöth *et al.*[10]. The two borinium ions were isolated pure from low temperature crystallisation from CH_2Cl_2. ^{13}C and ^1H data are presented in Table 9.2 and ^{11}B NMR data in the text.

^1H (δ/ppm)	^{13}C (δ/ppm)
$(^iPr_2N)_2BCl$ (C_6D_6) (87)‡	
3.3(1H,sept,7.0Hz) 1.0(6H,d,7.0Hz)	60.9(s) 25.0(s)
$(^iPr_2N)_2B^+$ $AlCl_4^-$ (C_6D_6) (88)	
3.7(1H,sept,6.5Hz) 1.4(6H,d,6.5Hz)	51.9(s) 23.0(s)
$(tmp)_2BCl$ (C_6D_6) (86)	
1.4(12H,ring H) 1.5(24H,$C\underline{H}_3$)	54.9($\underline{C}$-CH_3) 40.4(ring C) 32.8($\underline{C}H_3$) 17.9(ring C)
tmp_2B^+ $AlCl_4^-$ (91)	
1.7(12H,ring H) 1.55(24H,$C\underline{H}_3$)	58.1($\underline{C}$-CH_3) 37.3(ring C) 30.9($\underline{C}H_3$) 16.1(ring C)

Table 9.2: *^1H and ^{13}C NMR data for compounds (86)-(88)and (91); agrees well with Nöth et al.(ref.4h,10); ‡MS (Intensity%) EI: 247 [50,$(M+1)^+$], 211 [100,$(M-Cl)^+$], 102; CI^- : 269 [100,rearrangement of $^iPr_2N$ groups on boron).*

9.7.2 Preparation of $(^{i}Pr_2N)_2B^{+}SbCl_6^{-}$ (89)

The best synthetic route to this borinium ion was by mixing in 1:1 stoichiometry at room temperature $SbCl_5$ (2.79g, 9.3 mmol) and $(^{i}Pr_2N)_2BCl$ (2.3g, 9.3 mmol) as neat liquids (no results were obtained in solution - see Table 9.1).

9.7.3 Preparation of $(tmp)_2B^{+}SbCl_6^{-}$ (92)

$SbCl_5$ (3.3g, 11.0 mmol) in CH_2Cl_2 (15 ml) was added dropwise to a stirred solution of $(tmp)_2BCl$ (3.6g, 11.0 mmol) in CH_2Cl_2 (40 ml) at room temperature. This yielded a deep brown/black solution, with quantitative conversion to the borinium ion according to the ^{11}B NMR [4h].

9.7.4 Attempted Preparation of $R_2B^{+}BCl_4^{-}$ ($R \equiv {}^{i}Pr_2N$, tmp)

Reaction of $(tmp)_2BCl$ and $(^{i}Pr_2N)_2BCl$ with BCl_3 respectively at room temperature (1:1 stoichiometry) 12 mmol quantities in CH_2Cl_2 (60 ml) gave no evidence of cation formation [2] (Table 9.1). (after reaction work up.)

Ar_2BCl (4) was synthesised *via* the route described in Section 8.9.5.

9.7.5 Attempted Preparation of $Ar_2B^{+}AlCl_4^{-}$ (85)

$$Ar_2BCl\ (4) \xrightarrow{AlCl_3} Ar_2B^{+}AlCl_4^{-}\ (85)$$

Freshly sublimed $AlCl_3$ (*ca.* 0.4g, 3 mmol) was added as a slurry in CH_2Cl_2 (10 ml) to a stirred solution of Ar_2BCl (1.71g, 2.8 mmol) in CH_2Cl_2 (15 ml) at -20 °C. The reaction mixture became deep brown. It was allowed gradually to reach room temperature and stirred for 4 hours. Any unreacted $AlCl_3$ and other solids were removed by filtration, and the ^{11}B solution spectrum of the filtrate recorded (CH_2Cl_2).

This gave ^{11}B +47 ppm (broad singlet) and a characteristic ^{19}F NMR indicative of unreacted starting material. ^{19}F δ: -58.4, -58.5 ppm (o-CF_3) and -65.2 ppm (p-CF_3). No borinium ion formation, *ie.* no apparent Cl^- abstraction, was observed. A few peaks (-137, -131 ppm) in the ^{19}F NMR may be indicative of $AlCl_3$ attack at the fluorine site (CF_3) on the ring.

9.8 REFERENCES

1. P. Kölle and H. Nöth, *Chem.Rev.*, 85, 399-418 (1985), and references therein.

2. H. Nöth, S. Weber, B. Rasthofer, Ch. Narula and A. Konstantinov, *Pure and Applied Chemistry*, 55(9), 1453-1461 (1983).

3. a) A.H. Cowley, M.C. Cushner, M. Lattman, M.L. McKee, J.S. Szobota and J.C. Wilburn, *Pure and Applied Chemistry*, 52, 789-797 (1980) and references therein.

   b) Dr. Bartsch (University of Sussex), Seminar at Durham University, 6th May, 1987 "*Low Coordinated Phosphorus Compounds*".

4. a) B. Glaser and H. Nöth, *Angew.Chem. Int.Ed.Engl.*, 24(5), 416-417 (1985).

   b) H. Nöth, R. Staudigl and H.U. Wagner, *Inorg.Chem.*, 21, 706-716 (1982).

   c) H. Nöth and R. Staudigl, *Angew.Chem. Int.Ed.Engl.*, 20(9), 794-795 (1981).

   d) J.M. Davidson and C.M. French, *J.Chem.Soc.*, 114-117 (1958).

   e) J.M. Davidson and C.M. French, *J.Chem.Soc.*, 3364-3372 (1962).

   f) D.R. Armstrong and P.G. Perkins, *J.Chem.Soc.A.*, 1026-1031 (1966).

   g) R.B. Moodie and B. Ellul, *Chemistry and Industry*, 767-768, May 7th, 1966.

   h) J. Higashi, A.D. Eastman and R.W. Parry, *Inorg.Chem.*, 21, 716-720 (1982).

i) D. Männig, H. Nöth, H. Prigge and A.-R. Rotsch, *J.Organometallic Chem.*, 310, 1-20 (1986).

5. H. Nöth, *Nachr.Chem.Tech.Lab.*, 32(11), 956-959 (1984).

6. H. Nöth and S. Weber, *Chem.Ber.*, 118, 2144 (1985).

7. P. Kölle and H. Nöth, *Chem. Ber.*, 119, 313-324 (1986).

8. P. Kölle and H. Nöth, *Chem. Ber.*, 119, 3849-3855 (1986).

9. C.K. Narula and H. Nöth, *Inorg.Chem.*, 23, 4147 (1984).

10. H. Nöth, B. Rasthofer and S. Weber, *Z.Naturforsch.*, 39b, 1058-1068 (1984).

11. a) D.W. Aubrey, W. Gerrard and E.F. Mooney, *J.Chem.Soc.(London),* 1784 (1962).

    b) D.W. Aubrey, M.F. Lappert and M.K. Majumda, *J.Chem.Soc.*, 4088-4094 (1962).

12. K. Niedenzu and J.W. Dawson, *J.Amer.Chem.Soc.*, 82, 4223-4228 (1960).

13. R.M. Silverstein G.C. Bassler and T.C. Morrill, "*Spectroscopic Identification of Organic Compounds*", 4th Edition, John Wiley and Sons, 8 (1981).

14. a) A.H. Cowley, *Phosphorus and Sulphur*, 30, 129-133 (1987).

    b) A.M. Arif, J.E. Boggs, A.H. Cowley, J.G. Lee, M. Pakulski and J.M. Power, *J.Amer.Chem.Soc.*, 108, 6083-6084 (1986).

CHAPTER TEN

NMR STUDY OF TETRAHEDRAL COMPLEXES OF BORON(III)

10.1 INTRODUCTION

The aim of these preliminary investigations was to detect substitution products by ^{11}B NMR, and to study factors which affect exchange within four coordinated borate anions; For example, solvent, temperature, substituents, cation and concentration. If the exchange rate is slow on the NMR timescale, each species possesses a distinctive chemical shift which can be predicted by the pairwise interaction calculation, provided that the shifts of three members of the series are known (Section 10.12) [1].

The present study involved the observation of BX_4^- (X = F, Cl, Br, I) with a variety of counterions [*eg.* Bu_4N^+, Et_4N^+, $C_6F_5PX_3^+$ (X ≡ Br or Cl)]. The major interest was their behaviour in the presence of the anions competing for coordination (NCS^-, CN^-, N_3^-, NCO^-). Three approaches were used to prepare the substitution products:

1. Addition of a metal (Ag^+, Cs^+) salt of the anion required, to $R_4N^+BX_4^-$ (X ≡ Cl, Br, I). This is preferred when the substitution product is to be isolated, as it is easy to remove the insoluble metal halide.
2. The reaction of the three-coordinated boron species, for example BI_3 or BBr_3 with $Z^{\oplus}X^{\ominus}$ where X is one of the substituting anions.
3. With the B/F system the strength of the B–F bond may preclude substitution into the boron fluorides, *ie.* BF_4^-, hence "reverse" substitution was employed in which fluoride was substituted into the $B(NCS)_4^-$ system. It was however possible to establish this system *via* $BF_3{\cdot}Et_2O$ + LiNCS (see Section 10.9.1).

10.2 SOLVENT TYPE

The original solvent used in the BCl_4^- systems was nitromethane, but with BI_4^- complex spectra were observed, possibly due to solvent interaction yielding black insoluble products. This led to an exploration of a range of solvents (Table 10.1) in an attempt to diagnose their effect, and ultimately obtain a solvent of optimum utility - allowing sufficient solubility of the reactants (possessing a high enough dielectric constant), while not becoming too involved in the reaction by either coordination to the boron [Figure 10.1(a)], or by reaction with one of the pseudo-halogeno anions: CN^- interaction with CH_2Br_2 may generate the CH_2BrCN species which could act as a coordinating moiety and become involved in the system [Figure 10.1(b)]. Any attack of the anion on the solvent will reduce the concentration of the anion. Its effective concentration may therefore become insufficient to make formation of the four-coordinated species possible. Halogen exchange is significant with BBr_4^- in CH_2Cl_2 (Table 10.1).

(a) (b)

Figure 10.1

The reverse substitution of F^- into $R_4N^+B(NCS)_4^-$ involved the use of caesium fluoride for which the optimum solvent was tetraglyme, since CsF is sufficiently soluble in it, and F^- is not too solvated to prevent its action as a nucleophile. Thus the choice of solvent is crucial if unwanted interactions are to be minimised.

SOLVENT	COMMENTS
CH_2Cl_2	Best results with $R_4N^+BCl_4^-$. With $R_4N^+BI_4^-$, $R_4N^+BBr_4^-$, some chloride ion incorporated into the system, see effect on ^{11}B NMR (below). With the cyanide system, CN^- attack on the solvent is possible.
CH_2Br_2	Best results with $R_4N^+BBr_4^-$.
CH_2I_2	Best results with $R_4N^+BI_4^-$.
$PhNO_2$	Best results in the case of $C_6F_5PBr_3^+$, $C_6F_5PCl_3^+$, $ArPCl_3^+$ etc. Large cations which are of very limited solubility in the halogenated solvents.
PhCN CH_3CN	These solvents strongly interact with 3-coordinate boron species.
Fluorobenzene	Good solvent for $R_4N^+BX_4^-$ ($X \equiv I, Br, Cl$) No apparent interaction.
Tetraglyme	Ideal for F^- (see Section 10.9.1).

SPECIES	SOLVENT	^{31}P δ(ppm)	COMMENTS	REF
BI_3	CH_3CN	-85.1	coordinates: $CH_3CN \cdot BI_3$	
BI_3	PhCN	-85.3	coordinates: $PhCN \cdot BI_3$	
BI_3	CH_2Cl_2	7.1	left overnight $\equiv BCl_4$	
BI_3	CH_2I_2	-5.6		
BI_4^-	Hexane	16.2	Decomposition $(BI)_x$!	[4]
BI_4^-	CH_3CN	16.0	Decomposition !	
BI_4^-	PhCN	-127.7		
BI_4^-	CH_2Cl_2	-127.7	NMR recorded immediately	
BI_4^-	CH_2Cl_2	7.1	Salt left stirring in CH_2Cl_2 overnight $\equiv BCl_4$-	
BI_4^-	CH_2I_2	-126.7	Stable at RT > 1 week	
BBr_3	PhCN	-19.8	coordinates: $PhCN \cdot BBr_3$	
BBr_3	CH_3CN	-19.8	coordinates: $CH_3CN \cdot BBr_3$	
BBr_4^-	CH_2Cl_2	-24.5	BBr_4^- (left overnight)	[2]
		-14.9	BBr_3Cl^-	
		-6.5	$BBr_2Cl_2^-$	
		0.71	$BBrCl_3^-$	
		6.6	BCl_4^-	

Table 10.1: *General solvent properties (above); solvent effects on ^{11}B chemical shifts (below).*

10.3 MECHANISMS OF EXCHANGE OR SUBSTITUTION IN BX_4^-

Several possible methods have been postulated [2] including (i) dissociation to produce the trihalide and free anion, $BX_4^- \rightleftharpoons BX_3 + X^-$ and (ii) nucleophilic attack of X^- on BY_4^-. The former can be followed by recombination (Equation 10.1) or exchange *via* a bridged species (Equation 10.2), whilst the latter would clearly involve a double negative charge in the transition state (Equation 10.3).

$$BX_3 + Y^{\ominus} \rightleftharpoons BX_3Y^{\ominus} \qquad (10.1)$$

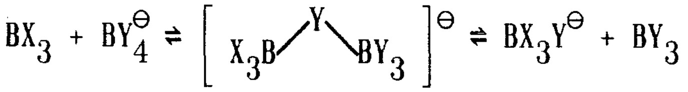

$$BX_3 + BY_4^{\ominus} \rightleftharpoons \left[X_3B{-}Y{-}BY_3 \right]^{\ominus} \rightleftharpoons BX_3Y^{\ominus} + BY_3 \qquad (10.2)$$

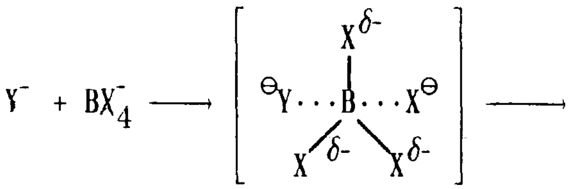

(10.3)

10.4 REACTION OF $R_4N^+BX_4^-$ (X ≡ Br, I, Cl) WITH N_3^-, NCO^-, CN^-

In the present work initial investigations involved the salt $R_4N^+BBr_4^-$ (R ≡ Et) with CN^-, NCO^- and N_3^-. Results are presented in Section 10.4.1. A small number of averaged peaks was obtained and no pairwise correlation fitted [1], hence an exchanging process was postulated. Similar exchanging systems were found with $R_4N^+BI_4^-$ and CN^-, NCO^- and N_3^- respectively, for which results are described in Section 10.4.2.

10.4.1 Tetraethylammonium Tetrabromoborate

Selected results are presented (Table 10.2) for the $Et_4N^+BBr_4^-$ system with the anions CN^-, NCO^- and N_3^- competing for coordination.

SYSTEM	SOLVENT	^{11}B NMR (ppm) ‡
$Et_4N^+BBr_4^-$ + AgCN	CH_3CN	+2.0(m), +0.2(m), -24.0(s) [1]
$Et_4N^+BBr_4^-$ + Bu_4NN_3	CH_2Br_2	+2.2(m), -2.2(m), -10.0(m), -24.1(s)
$Et_4N^+BBr_4^-$ + AgNCO	CH_2Br_2	-14.5(m), -19.0(m), -24.5(m)

Table 10.2: *The bromoborate systems with CN^-, N_3^-, NCO^-; ‡parentheses indicate signal intensity.*

In the cyanide system the results (Table 10.2) illustrate the effect of addition of 1 equivalent of cyanide. If two equivalents are added, signals on average occur at +4.0, +0.2 and -23.0 ppm. In the postulated exchange equilibrium (Equation 10.4) stabilisation of the three coordinate boron by π-bonding may be effected, *via* the possible resonance form $>B^{\ominus}=C=N^{\oplus}$.

$$BBr_3CN^- \rightleftharpoons BBr_3 + CN^- \rightleftharpoons BBr_2CN + Br^- \qquad (10.4)$$

Attempts to generate the BBr_4^- systems by addition of the anion to BBr_3 in PhCN failed. The solvent appeared to compete effectively with the anion for the three-coordinate boron species, complicating the spectral interpretation (Table 10.1).

---

[1] The exchanging process appears to shift the peak corresponding to BBr_4^- only slightly from its expected position. This may be a result of its higher concentration than any other one substitution product present.

10.4.2 Tetrapropylammonium Tetraiodoborate

Selected results are presented (Table 10.3) for the $Pr_4N^+BI_4^-$ system with the anions CN^-, NCO^- and N_3^- competing for coordination. BI_4^- decomposes in acetonitrile (see Table 10.1). It should be noted here that the thiocyanate (NCS) ligand substituted into all the haloboron systems to yield the complete set of anions in each case, however thiocyanate (NCS) appears to be an exceptional ligand and will be considered separately (Section 10.9).

SYSTEM	SOLVENT	^{11}B NMR (ppm) ‡
$Pr_4N^+BI_4^-$ + AgCN	CH_2I_2	-128.7(m), -89.0(w)*, -84.0(w)*
BI_3 + $Bu_4N^+CN^-$	CH_2I_2	-101.1(m), -88.7(w)*, -84.9(m)* -33.9(m)
BI_3 + $Bu_4N^+N_3^-$	CH_2I_2	-126.3(m), -85.8(m)*
BI_3 + $Et_4N^+NCO^-$	CH_2I_2	-126.0(m), -89(m)*, -84(m)*, -49(m)

Table 10.3: *The iodoborate systems with CN^-, N_3^-, NCO^-; ‡parentheses indicate signal intensity; *signals are unassigned but are common to each system.*

In view of the fact that R. Ali [3] had not observed the exchange phenomenon in her experiment with BCl_4^- and AgCN, the rapid exchange observed here was somewhat surprising. Initially it was postulated that the difference could be due to the lower strengths of the boron-bromine and boron-iodine bonds, in comparison with boron-chlorine. However, when the system $R_4N^+BCl_4^-$ was investigated (Section 10.4.3) similarly rapid exchange was again observed.

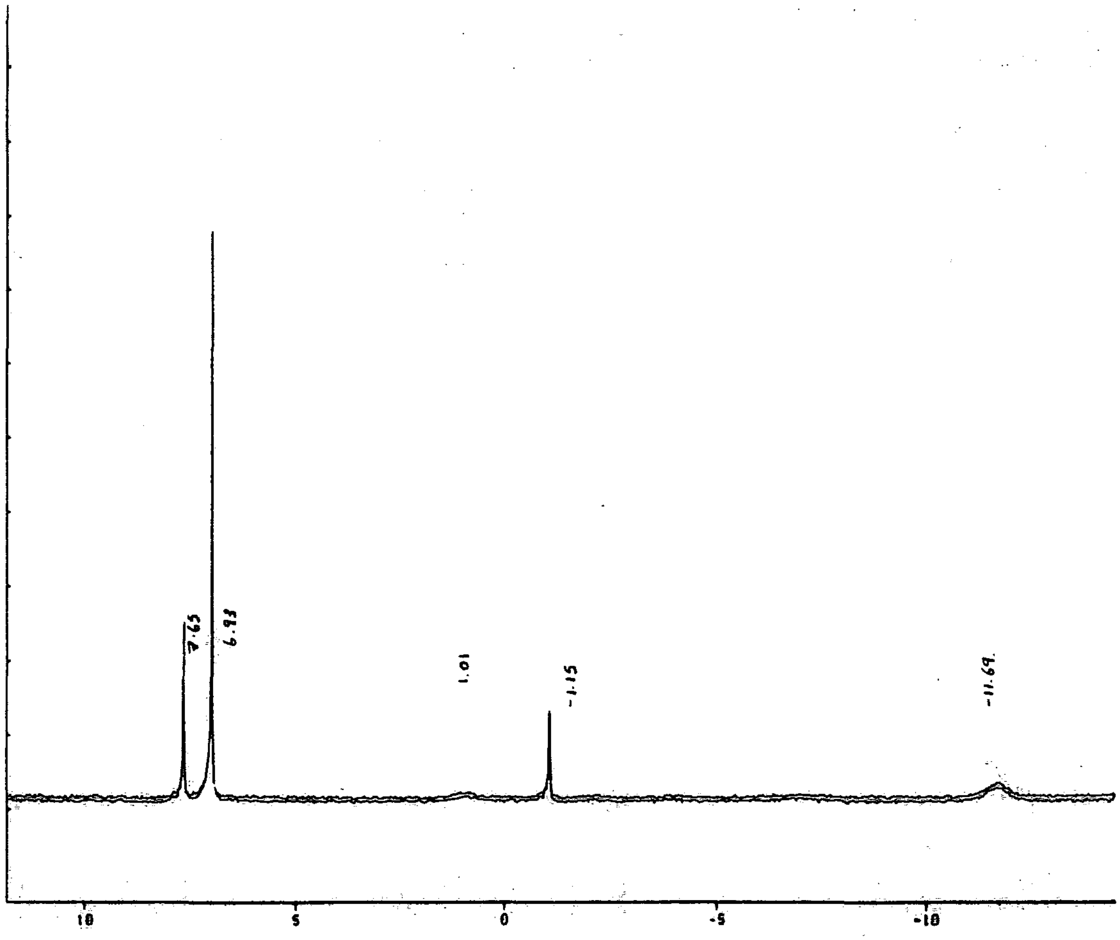

Figure 10.1a: *One dimensional ^{11}B NMR spectra for the system $BCl_4^- Et_4N^+ + Et_4N^+NCO^-$ in CH_2Cl_2.*

10.4.3 Tetraethylammonium Tetrachloroborate

Selected results are presented (Table 10.4) for the $Et_4N^+BCl_4^-$ system with the anions CN^-, NCO^- and N_3^- competing for coordination.

SYSTEM	SOLVENT	^{11}B NMR (ppm) ‡	REF
$Et_4N^+BCl_4^-$ + AgCN	CH_3CN	+2.0(m), -2.0(m)	[4]
$Et_4N^+BCl_4^-$ + $Bu_4N^+N_3^-$	CH_2Cl_2	0.0(m), -4.2(m)	
$Et_4N^+BCl_4^-$ + $Et_4N^+NCO^-$	CH_2Cl_2	7.6(m), 6.9(s), 1.0(w,br), -1.1(m), -11.7(m)†	

Table 10.4: *The chloroborate systems with CN^-, N_3^-, NCO^-; ‡parentheses indicate signal intensity; †See Figure 10.1;*

In the isocyanate system there exists the possibility of coordination through oxygen or nitrogen, *linkage isomerism* [5], since the donor atoms are both hard centres. None of the peaks could be assigned to definite substitution products by application of the pairwise interaction calculation. For example, if the assumption of unique nitrogen coordination is made and the signal at 7.6 ppm is assigned to BCl_4^-, -11.7 ppm to $B(NCO)_4^-$ and +6.9 ppm to the first substitution product $B(NCO)Cl_3^-$, the calculated values for the two intermediate substitution products are 3.6 ppm $[B(NCO)_2Cl_2^-]$ and -2.6 ppm $[B(NCO)_3Cl^-]$. (In principle, of course, NCO^- could give ^{14}N coupling, and may provide a means of distinguishing oxygen and nitrogen bonded isomers, if J-values could be measured).

The ^{11}B 2-D NMR [6-10] spectrum confirmed the presence of seven different boron species and the existence of exchange. A possible exchange mechanism is shown in Equation 10.5. The ^{11}B NMR spectrum is illustrated in Figure 10.1(a) and the 2D NMR spectrum in Figure 10.1(b).

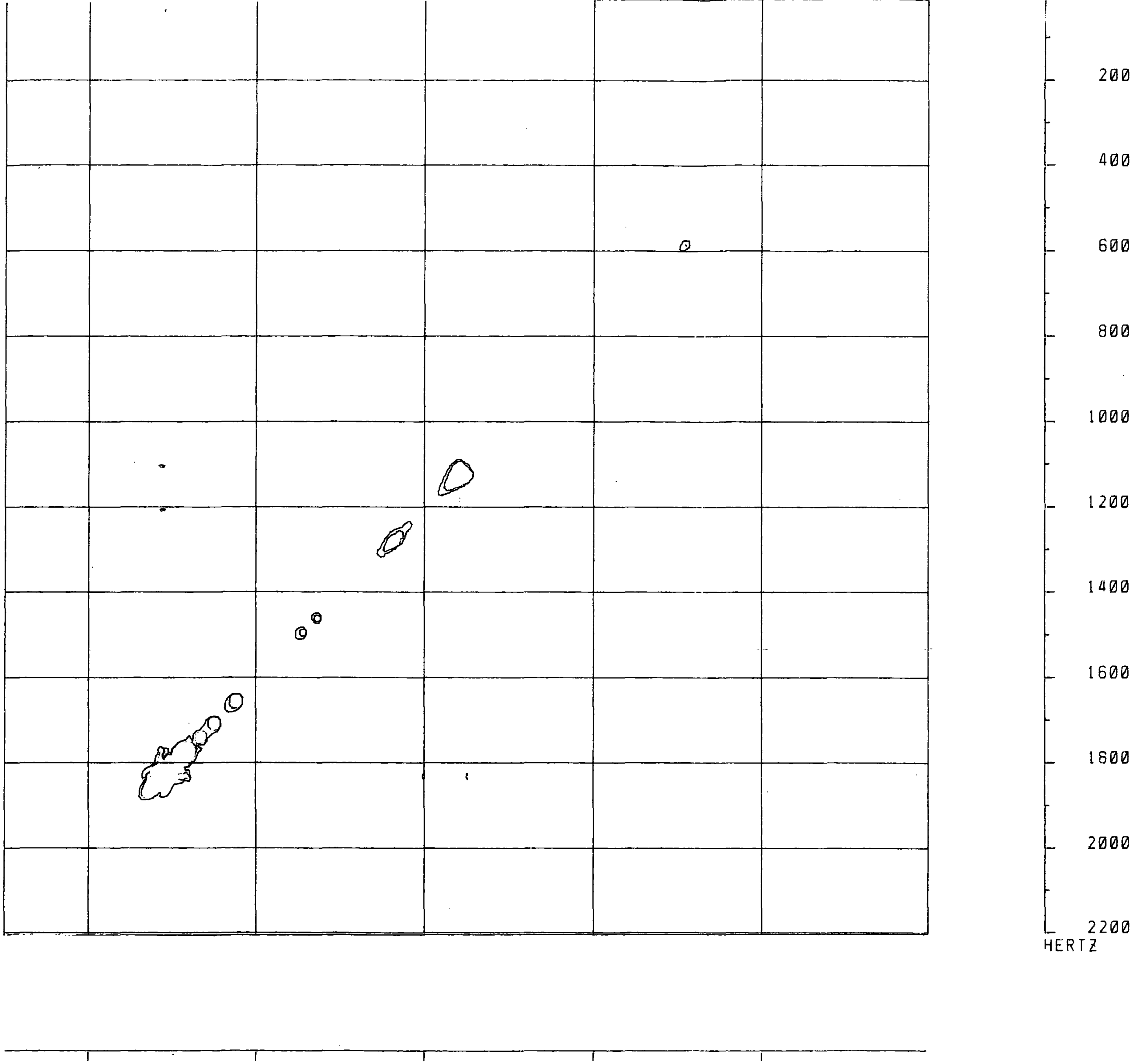

```
HELEN.SMX
AU PROG:
 NOESY.AU
DATE 31-3-87

SI2      512
SI1      256
SW2   2202.643
SW1   1101.322
ND0        1


WDW2      Q
WDW1      Q
SSB2      0
SSB1      0
MC2       M
PLIM ROW:
F1       27.451
F2         .107
AND COLUMN:
F1       27.451
F2         .107

O1      .150000
P1          22.
D0      .000001
P2          22.
D9      .050000
P3          22.
RD      0.0
PW           0.
DE         283.
NS        1024
DS           4
NE         128
IN      .000454
V9          10
```

Figure 10.1b: *Two dimensional* ^{11}B *NMR spectra for the system* $BCl_3 \cdot Et_2O + Et_4N^+NCO^-$ *in* CH_2Cl_2.

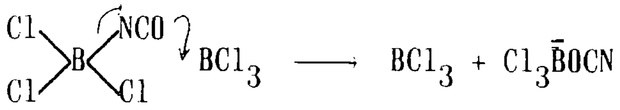

$$Cl_2BCl(NCO) \cdot BCl_3 \longrightarrow BCl_3 + Cl_3\bar{B}OCN \qquad (10.5)$$

10.5 EFFECT OF CHANGING TEMPERATURE AND CONCENTRATION

Warming gave no change in the NMR for any of the systems where it was attempted. It was avoided for the tetraiodoborate systems since decomposition of this species is inevitable. The effect of cooling the system $Et_4N^+BBr_4^-/AgCN$ in CH_2Br_2 to -60°C was also investigated, in an attempt to slow the exchange sufficiently to allow the observation of the substitution products. No change was detected from the results given in Section 10.2.1.

Variation in concentration from 0.5 equivalent with respect to the tetrahaloborate present to a three-fold excess gave an exactly similar exchange phenomenon, with peaks slightly shifted (see example, Section 10.4.1). The concentrations used in a typical exchange experiment were in general of the order of 50-70 mg cm^{-3}.

10.6 EFFECT OF CHANGING COUNTERION WITH THE BCl_4^- SYSTEM

Since R. Ali [3] had used $C_6F_5PCl_3^+$ as the counterion it seemed that it could be the nature of the counter-cation, rather than the halogen involved which affects the tendency of the X^- ion to exchange with other ligands in the BX_4^- anion. The next obvious step was to investigate the effect of changing the cation.

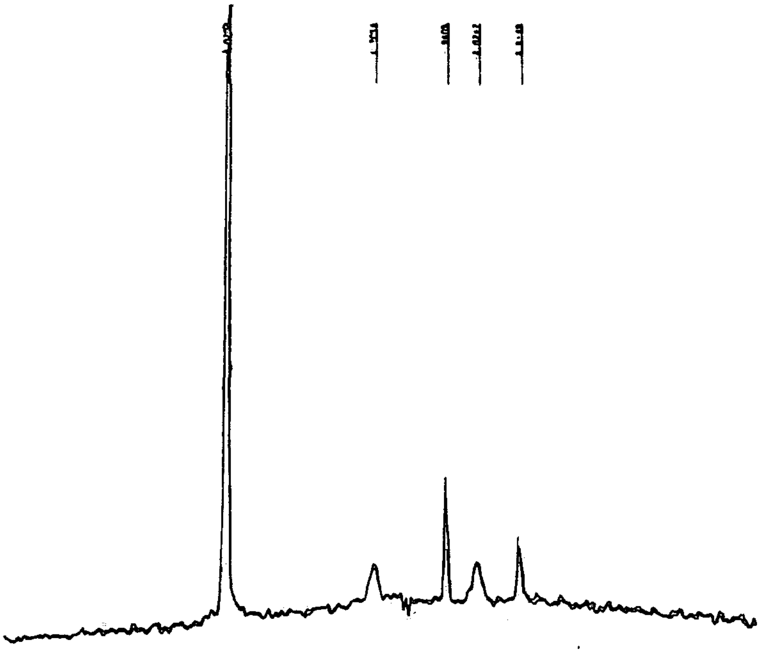

Figure 10.2a: *One dimensional ^{11}B NMR spectra for the system $Ph_4P^+BCl_4^-$ + $AgCN$ in CH_3CN.*

10.6.1 Ph_4P^+ Cation

$Ph_4P^+BCl_4^-$ (93) was synthesised. This appeared to reduce the exchange rate with CN^-, since five peaks were evident (Table 10.5), but shifted slightly downfield from their expected positions (as calculated from pairwise interactions) [see Figure 10.2(a)]. A two-dimensional (2-D) NMR spectrum of this system [Figure 10.2(b)] showed evidence of exchange. Exchange is evident between 'BCl_4^-' and the first substitution species, and between 'BCl_4^-' and the second species. All the exchange has been associated with 'BCl_4^-', possibly because of its greater intensity observed in the 1-D NMR spectrum [Figure 10.2(a)]. Exchanges between other species may not be detectable due to their relatively low concentrations.

SYSTEM	SOLVENT	^{11}B NMR (ppm) ‡
$Ph_4P^+BCl_4^-$ (93) + AgCN	CH_3CN	7.1(s), 1.7(w), -0.9(w), -2.1(w), -3.6(w)

Table 10.5: *The chloroborate system (93) with CN^- (Ph_4P^+ counterion); ‡Values calculated by pairwise interactions assuming BCl_4^- 7.1 ppm; $B(CN)_4^-$ -3.6 ppm; BCl_3CN^- 1.7 ppm; $BCl_2(CN)_2^-$ -1.9 ppm and $B(CN)_3Cl^-$ -3.6 ppm; parentheses indicate signal intensity;.*

10.6.2 $C_6F_5PCl_3^+$ Cation

The reaction shown in Equation 10.6 was carried out, and results were exactly analogous to those reported by R. Ali [3], namely, $B(CN)_4^-$ -9.0(m) ppm, $B(CN)_3Cl^-$ -3.4(m) ppm, $B(CN)_2Cl_2^-$ +0.6(s) ppm, $B(CN)Cl_3^-$ +4.5(s) ppm and BCl_4^- +7.7(m) ppm [assuming $B(CN)_4^-$ -9.0 ppm, $B(CN)_3Cl^-$ -3.4 ppm and BCl_4^- +7.7 ppm]. The calculated results for $B(CN)_2Cl_2^-$ (0.7 ppm) and $B(CN)Cl_3^-$ (+4.5 ppm) from pairwise interaction, agree well with

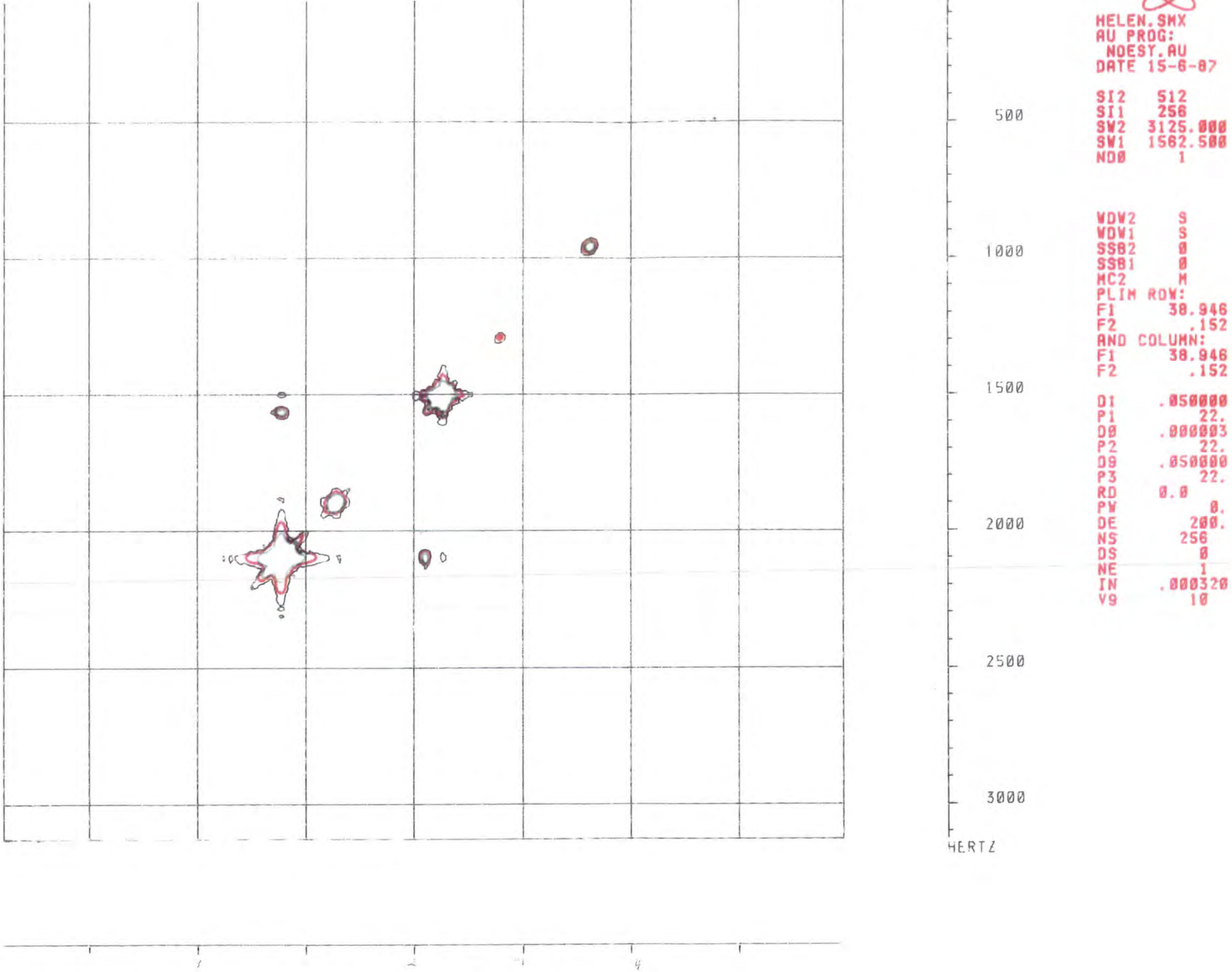

```
HELEN.SMX
AU PROG:
 NOESY.AU
DATE 15-6-87

SI2     512
SI1     256
SW2   3125.000
SW1   1562.500
ND0       1

WDW2      S
WDW1      S
SSB2      0
SSB1      0
MC2       M
PLIM ROW:
F1      38.946
F2        .152
AND COLUMN:
F1      38.946
F2        .152

D1     .050000
P1         22.
D0     .000003
P2         22.
D9     .050000
P3         22.
RD     0.0
PW          0.
DE        200.
NS        256
DS          0
NE          1
IN     .000320
V9         10
```

Figure 10.2b: *Two dimensional* ^{11}B *NMR spectra for the system* $Ph_4P^+BCl_4^-$ + *AgCN in* CH_3CN.

the data obtained by experiment, and with previous reported data [2].

$$C_6F_5PCl_3^+BCl_4^- \ (94) + AgCN \xrightarrow{PhNO_2} \qquad (10.6)$$

10.6.3 $ArPCl_3^+$ Cation

Because of the significant interest in the Ar substituent, 2,4,6-tristrifluoromethylphenyl, the system $ArPCl_3^+BCl_4^-$ (95) was explored with cyanide, and three of the substitution products were observed in the ^{11}B NMR at ambient temperature (Table 10.6). It should be noted that with a large excess of CN^-, substitution into $ArPCl_3^+$ causes decomposition to $ArPCl_2$ (12) [verified by the ^{31}P NMR data δ +145 ppm (septet) $^4J_{PF}$ +62.4 Hz (see Chapter 2)], possibly *via* the elimination of ClCN.

^{11}B NMR δ(ppm)		ANIONIC SPECIES
EXPT	CALC‡	
-9.5	(-9.5)	$B(CN)_4^-$
-3.4	(-3.4)	$B(CN)_3Cl^-$
0.5	1.5	$B(CN)_2Cl_2^-$
---	5.2	$B(CN)Cl_3^-$
7.7	(7.7)	BCl_4^-

Table 10.6: *^{11}B NMR data for $ArPCl_3^+BCl_4^-$ (95) + AgCN ($PhNO_2$); ‡calculated by pairwise interaction (ref.1) using the bracketed values.*

10.7 BROMINE SYSTEMS: $C_6F_5PBr_3^+$ Cation

To investigate BBr_4^- systems, $C_6F_5PBr_3^+BBr_4^-$ (96) was prepared according to Equation 10.7 [3].

$$C_6F_5Br \xrightarrow{Mg} C_6F_5MgBr + PBr_3 \longrightarrow C_6F_5PBr_2 \xrightarrow{Br_2}$$

$$C_6F_5PBr_4 \xrightarrow{BBr_3} C_6F_5PBr_3^+BBr_4^- \ (96) \qquad (10.7)$$

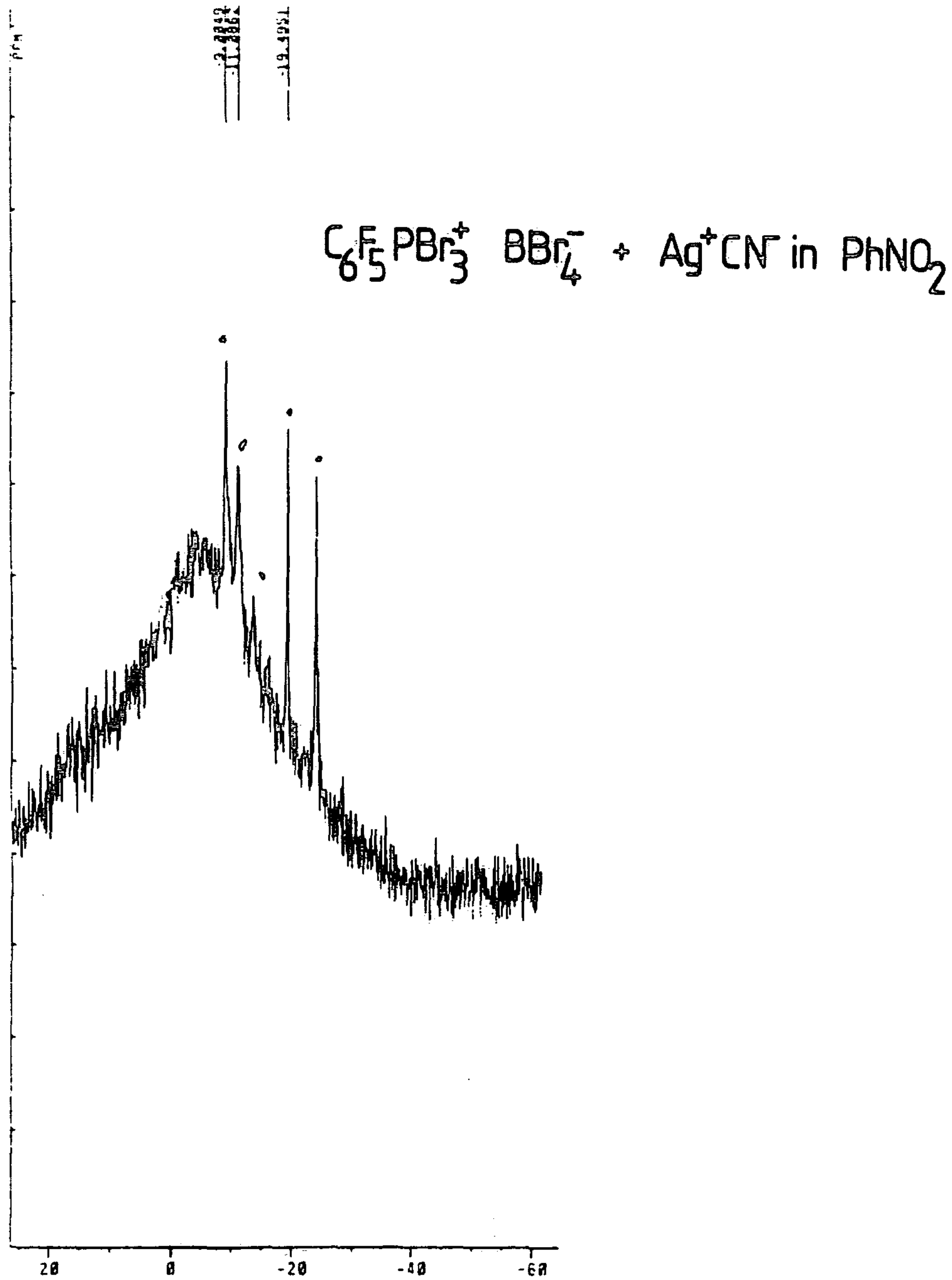

Figure 10.3: *^{11}B NMR data for $C_6F_5PBr_4{}^+BBr_4{}^-$ + AgCN ($PhNO_2$); the observed broad background was attributed to the poor solubility of the salt.*

Additionally it was hoped, by synthesis of $C_6F_5PI_3^+BI_4^-$ (97) to extend this work to the iodide systems. Unfortunately, the instability of these P(V) cations severely limited their usefulness. In $PhNO_2$ apparent dissociation of the tetrabromoborate salt occurred, giving a signal at +21 ppm in the ^{31}P NMR. This suggested the formation of $C_6F_5PBr_2$ which then complexed with the BBr_3 present (Equation 10.8).

$$C_6F_5PBr_3^+BBr_4^- \longrightarrow C_6F_5PBr_2 + BBr_3 + Br_2 \longrightarrow C_6F_5PBr_2{\cdot}BBr_3\ (98) \qquad (10.8)$$

This agreed well with data obtained by R. Ali [3]. Numerous efforts were made to generate $C_6F_5PBr_3^+BBr_4^-$ and to substitute with CN^-. On one occasion the P(V) cation remained intact while all the substitution products in the ^{11}B NMR spectrum were observed (Figure 10.3). (Table 10.7)

^{11}B NMR δ(ppm)		ANIONIC SPECIES
EXPT	CALC‡	
-9.0	(-9.0)	$B(CN)_4^-$
-11.1	(-11.1)	$B(CN)_3Br^-$
-13.8	-14.3	$B(CN)_2Br_2^-$
-19.5	-18.7	$B(CN)Br_3^-$
-24.2	(-24.2)	BBr_4^-

Table 10.7: *^{11}B NMR data for $C_6F_5PBr_4^+BBr_4^-$ + AgCN ($PhNO_2$); ‡calculated by pairwise interaction methods (ref.1) using the bracketed values.*

10.8 THE WHOLE SYSTEM

10.8.1 Introduction

$$A^+ + BX^- \xrightarrow{C^+D^-}$$

If A^+ can affect the exchange rate then the added cation C^+ must also be considered. It has already been seen that the rate of exchange can be affected by the B-X (X = I, Br, Cl, F) bond strength, and the ability of X to back-donate π-electrons [2]. D^- can also affect the rate of exchange. For example, the properties of NCS^- make it an exceptional nucleophile (Section 10.9). Substitution into the cationic species, $C_6F_5PCl_3^+$, $ArPCl_3^+$, is inevitable in the presence of powerful nucleophiles. This inherent change in the cation affects its nature, and therefore presumably its effect on $BX_nY_{4-n}^-$.

The discussion which follows is highly speculative and requires more experimental work before it can be considered complete. However, since this piece of work was not the focus of the thesis it was not considered appropriate to pursue this further in the limited time available.

10.8.2 Discussion of the Results

The most prominent difference between the two groups is the much larger proportion of halogen in the Type 2, and thus presumably the presence of electron withdrawing groups makes the P^+ centre more electropositive (*ie.* an increase in the formal positive charge at phosphorus). The cations in this latter group also appear to be larger.

Et_4N^+ Ph_4P^+	TYPE 1 allows rapid exchange in anion
$C_6F_5PX_3^+$ $C_6H_2(CF_3)_3PX_3^+$	TYPE 2 inhibits rapid exchange in anion

It may well be that the smaller cations also allow a close approach of boron, helping to remove X^- from it (see possible exchange mechanism, Section 10.3), whereas the larger cations cannot associate so readily with the borate anion (reduced polarisation) (Figure 10.4). On the other hand the cations in the second group might have been expected to be effective in X^- removal from boron, in view of the greater electron withdrawing nature of the halogen atoms. (There could however be more repulsion between X on boron and electronegative ligands on phosphorus, which would more than counteract the increased positive charge at phosphorus mentioned above. The ions are φ-tetrahedral, so the P^+ would be quite well shielded. This does not accord with the following proposal).

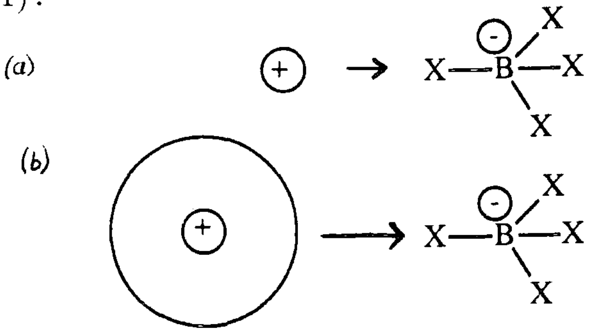

Figure 10.4: *Cation/anion association; (a) allows a close approach; (b) very little association.*

It is hard to envisage why these halogenated cations should inhibit the exchange unless somehow they stabilise a very strong ion pairing with the counterion, possibly *via* a halogen bridge (Figure 10.5). Thus, if the electron withdrawal from phosphorus were sufficiently strong this would also inhibit the loss of a chloride ion from boron either directly, or *via* a bridging mechanism as required by the exchange mechanism (Section 10.3). The existence of such a large attachment to one side of the BCl_4^- anion would also block the formation, (unlikely in any case), of the transition state required by Method 2. Such an arrangement could explain the inhibition of rapid exchange and still permit substitution to take place at a much lower rate. Indeed, since the overall ion pair is neutral, (hence removing the objection to Method 2), the whole cation with Cl^- could act as a leaving group in a possible S_N2 substitution process.

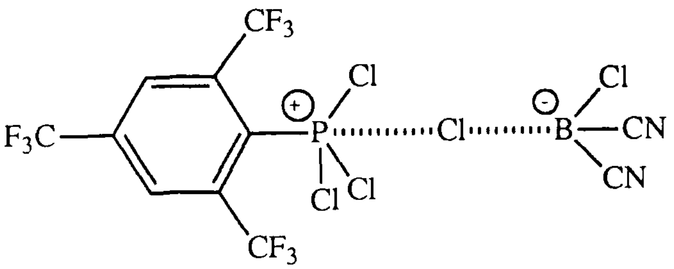

Figure 10.5: *Proposed ion-pair with a halogen bridge.*

If these cations of Type 2 do indeed form such stable ion pairs this would explain why the subsequent addition of a Type 1 cation to the system, for example in the form $R_4N^+CN^-$, does not cause exchange to commence. It would be possible to check this hypothesis further by adding Type 2 cations (with a convenient anion also) to an exchanging system when the exchange should be inhibited. This has not yet been attempted.

10.9 THE THIOCYANATE SYSTEM

The thiocyanate anion, NCS^- , substitutes into BX_4^- (X = F, Cl, Br and I), exchanging on a slow enough timescale with respect to the NMR to allow the observation of the ^{11}B NMR signals corresponding to <u>all</u> of the substitution products. These systems will now be considered.

10.9.1 The F^-/NCS^- Borate System

This was achieved by the addition of LiNCS to $BF_3 \cdot Et_2O$, and conversely by the addition of F^- (CsF) in tetraglyme to $Et_4N^+B(NCS)_4^-$. Initially, only signals corresponding to $B(NCS)F_3^-$, BF_4^- and $B(NCS)_4^-$ were present, but after warming to 35 °C all the substitution products were clearly observed. The shifts agree well with those calculated by the pairwise interaction method. A 2-D NMR spectrum showed no evidence of

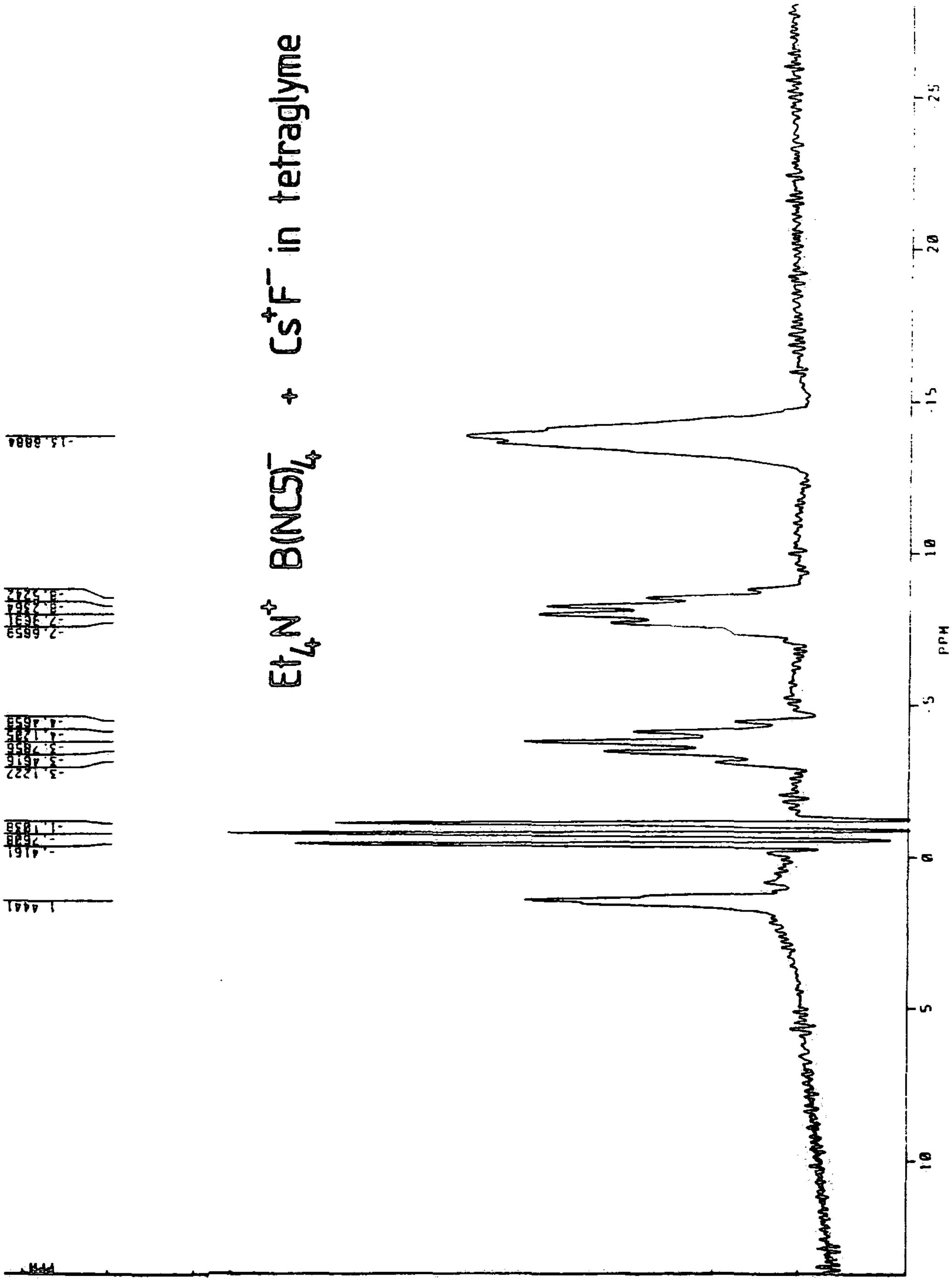

Figure 10.6: *One dimensional* ^{11}B *NMR data for* $Et_4N^+B(NCS)_4^-$ + *CsF in tetraglyme, illustrating* $^1J(BN)$ *coupling.*

exchange, as expected.

Boron-nitrogen ($^{1}J_{BN}$) coupling was evident in the 1-D ^{11}B NMR spectrum (Figure 10.6). This phenomenon was previously observed in the similar system boron-chlorine-NCS [3]. Assignment was made (Table 10.8) entirely to boron-nitrogen coupling, since no $^{1}J_{BF}$ could be resolved in the ^{19}F NMR spectrum. *However*, before a final conclusion can be reached, further work would be desirable on resolution in the ^{19}F NMR since the possibility may exist of the observed splitting pattern resulting from both $^{1}J_{BF}$ and $^{1}J_{BN}$. The $^{1}J'_{BN}$ values derived look reasonable by comparison with those for BCl_4^-/NCS^-, where B-F coupling is impossible.

The sharp signal of BF_4^- is in agreement with its high symmetry, and the small coupling constants associated with highly fluorinated boron systems [2].

^{11}B NMR δ(ppm)		ANIONIC SPECIES	$^{1}J_{BN}$ (Hz)	^{19}F NMR (/ppm)*
EXPT	CALC‡			
-17.4	(-17.4)	$B(NCS)_4^-$	20.1	---
-11.7	(-11.7)	$B(NCS)_3F^-$	22.4	-142.7
-7.0	-7.2	$B(NCS)_2F_2^-$	26.9	-145.9
-3.9	-3.8	$B(NCS)F_3^-$	27.6	-147.1
-1.6	(-1.6)	BF_4^-	----	-158.4

Table 10.8: *^{11}B NMR data for $Et_4N^+B(NCS)_4^-$ + CsF (tetraglyme); ‡calculated by pairwise interaction methods (ref.1) using the bracketed values; *no $^{1}J(BF)$ resolved.*

10.9.2 $Et_4N^+BCl_4^-$ with NCS^-

The full set of substitution products was obtained from the tetraalkylammonium tetrachloroborate system with thiocyanate. This data has been previously reported by R. Ali [3], however her work involved the cation $C_6F_5PCl_3^+$. The results here (Table 10.9) agree well with this data. A 2-D NMR was carried out on this system and no evidence of exchange was observed. This system was also achieved with the new cation $ArPCl_3^+$ and the results are presented in Table 10.10.

^{11}B NMR δ(ppm)		ANIONIC SPECIES	$^1J_{BN}$ * (Hz)
EXPT	CALC‡		
-17.1	(-17.1)	$B(NCS)_4^-$	----
-12.7	(-12.7)	$B(NCS)_3Cl^-$	----
-7.2	-7.2	$B(NCS)_2Cl_2^-$	----
-0.7	-0.6	$B(NCS)Cl_3^-$	23
7.0	(7.0)	BCl_4^-	----

Table 10.9: *^{11}B NMR data for $Et_4N^+BCl_4^-$ + AgNCS (CH_2Cl_2); ‡calculated by pairwise interaction methods (ref.1) using the bracketed values; *$^1J(BN)$ resolved only for the first substitution product in this system.*

^{11}B NMR δ(ppm)		ANIONIC SPECIES	$^1J_{BN}$ (Hz)
EXPT	CALC‡		
-17.2	(-17.2)	$B(NCS)_4^-$	NR
-12.9	-15.6	$B(NCS)_3Cl^-$	24.5
-7.2	-10.9	$B(NCS)_2Cl_2^-$	25.6
-3.2	(-3.2)	$B(NCS)Cl_3^-$	25.3
+7.7	(+7.7)	BCl_4^-	----

Table 10.10: *^{11}B NMR data for $ArPCl_3^+BCl_4^-$ + AgNCS (CH_2Cl_2); ‡calculated by pairwise interaction methods (ref.1) using the bracketed values; NR=not resolved.*

10.9.3 $Et_4N^+BBr_4^-$ With NCS^-

The analogous system with bromide was obtained by the addition of AgNCS to $Et_4N^+BBr_4^-$ in CH_2Br_2. $J(^{11}B-^{14}N)$ coupling was observed in this system (Table 10.11) but only for the first substitution product.

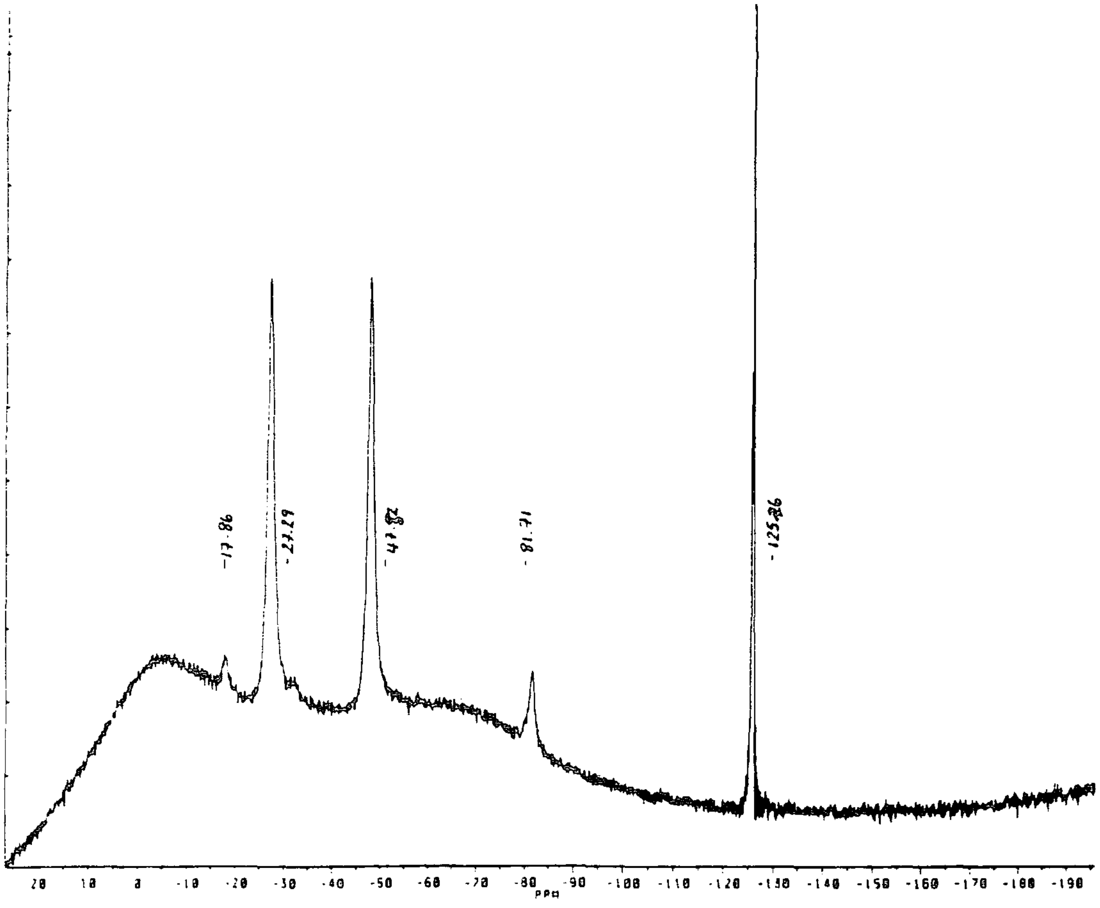

Figure 10.7: *One dimensional ^{11}B NMR spectra for the system $BI_3 + Et_4N^+NCS^-$ in CH_2I_2.*

^{11}B NMR δ(ppm)		ANIONIC SPECIES	$^1J_{BN}$ (Hz)
EXPT	CALC‡		
-17.7	(-17.7)	$B(NCS)_4^-$	
-17.0	(-17.0)	$B(NCS)_3Br^-$	*
-18.5	-17.9	$B(NCS)_2Br_2^-$	*
-20.9	-20.3	$B(NCS)Br_3^-$	21.0
-24.3	(-24.3)	BBr_4^-	

Table 10.11: *^{11}B NMR data for $Et_4N^+BBr_4^-$ + AgNCS (CH_2Br_2); ‡calculated by pairwise interaction methods (ref.1) using the bracketed values; *no $^1J(BN)$ coupling resolved.*

10.9.4 $Et_4N^+NCS^-$ With BI_3

The iodo-thiocyanatoborate system was produced by the addition of $Et_4N^+NCS^-$ to BI_3 in CH_2I_2 and the results are presented in Table 10.12.

^{11}B NMR δ(ppm)		ANIONIC SPECIES
EXPT	CALC‡	
-17.9	(-17.9)	$B(NCS)_4^-$
-27.3	(-27.3)	$B(NCS)_3I^-$
-47.5	-48.4	$B(NCS)_2I_2^-$
-81.7	-81.3	$B(NCS)I_3^-$
-125.8	(-125.8)	BI_4^-

Table 10.12: *^{11}B NMR data for $Et_4N^+NCS^-$ + BI_3 (CH_2I_2); ‡calculated by pairwise interaction methods (ref.1) using the bracketed values; for 1-D spectrum see Figure 10.7.*

The two intermediate substitution products $Et_4N^+B(NCS)_2I_2^-$ and $Et_4N^+B(NCS)_3I^-$ were not always observed, although they must have been formed to allow the generation of $B(NCS)_4^-$. Heating was avoided, because of the inherent instability of BI_4^-.

No $^1J_{BN}$ coupling was observed. This was attributed to the greater quadrupolar relaxation induced by ^{127}I (I = 5/2) compared with ^{35}Cl (I = 3/2), and ^{79}Br or ^{81}Br (I = 3/2).

10.10 THE F^-/CN^- BORATE SYSTEM

The first cyano-substituted product was obtained by the addition of LiCN to $BF_3 \cdot Et_2O$. An excess of lithium cyanide gave no evidence of further substitution, but the addition of $Bu_4N^+CN^-$ caused this to take place (see Table 10.13).

^{11}B NMR δ(ppm)				ANIONIC SPECIES
EXPT	$^1J_{BF}$ (multiplicity)		CALC‡	
-9.0†	----		(-9.0)	$B(CN)_4^-$
----	----		-7.4	$B(CN)_3F^-$
-6.6	41.4	triplet	-5.5	$B(CN)_2F_2^-$
-3.4	27.1	quartet	(-3.4)	$B(CN)F_3^-$
-1.1	1.0	singlet [2]	(-1.1)	BF_4^-

Table 10.13: *^{11}B NMR data for $BF_3 \cdot Et_2O$ + LiCN + $Bu_4N^+CN^-$ (Et_2O/ CH_2Cl_2); †obtained from $C_6F_5PCl_3^+$ $B(CN)_4^-$ (ref.3); ‡by pairwise interaction.*

Addition of $Et_4N^+NCO^-$ and $Bu_4N^+CN^-$ respectively to $BF_3 \cdot Et_2O$ gave in each case a few peaks around 0 ppm, attributed to exchange.

In the systems with counterions such as $ArPCl_3^+$ or $C_6F_5PBr_3^+$ this work could be extended to observe directly, anion substitution into these cations, using ^{31}P NMR.

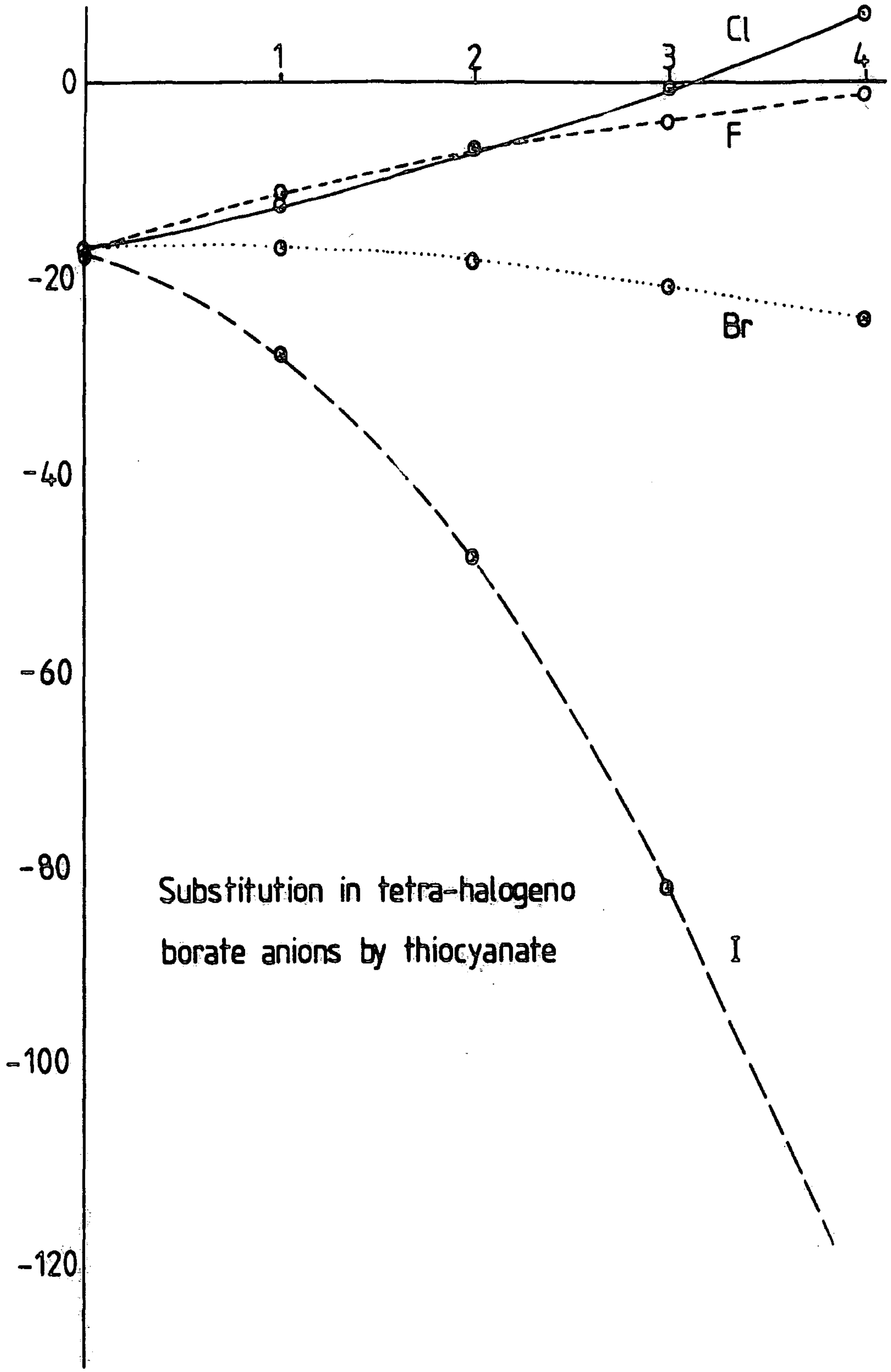

Graph 10.1: *^{11}B NMR data for the BX_4^- ($X \equiv F$, Cl, Br, I) and NCS^- systems.*

10.11 SPECTRAL CHARACTERISTICS

10.11.1 Introduction

The shift pattern BX_4^-, BX_3Y^- ... BY_4^- inclusive should not be assumed to be sequential. For example, this is illustrated in the BBr_4^--NCS^- system: -17.7, -17.0, -18.5, -20.9 and -24.3 ppm.

The quadrupolar moment of boron (I = 3/2) tends to broaden the lines in the NMR, with the sharpest lines corresponding to the most symmetrically substituted systems. Some of the results of this work have been presented in graphical form (Graphs 10.1-10.4). No variation in linewidth with the nature of the attached halogens was observed. This may be compared with P(III) halides, in which iodides give sharper lines than bromides, which in turn are sharper than those from chlorides. This is attributed to the size of the quadrupole moments.

10.11.2 Graph 10.1: BX_4^- (X ≡ Cl, Br, I, F) and NCS^-

This displays data for the tetrafluoro-, chloro-, bromo- and iodoborate systems with thiocyanate anions. It clearly illustrates the variation in chemical shift range for the different halogeno compounds. The much larger span for the iodide containing system is evident. The non-sequential shift order for the bromide species has been noted above.

In general for the series chloride, bromide and iodide, there is a greater degree of shielding as the halogen group is descended. An exception exists for the fluoride, whereby towards the end of the substitution system (more fluorine) the species become more shielded than for the analogous chloride compounds. As fluorine is smaller and more electron withdrawing this must be attributed to an increase in the

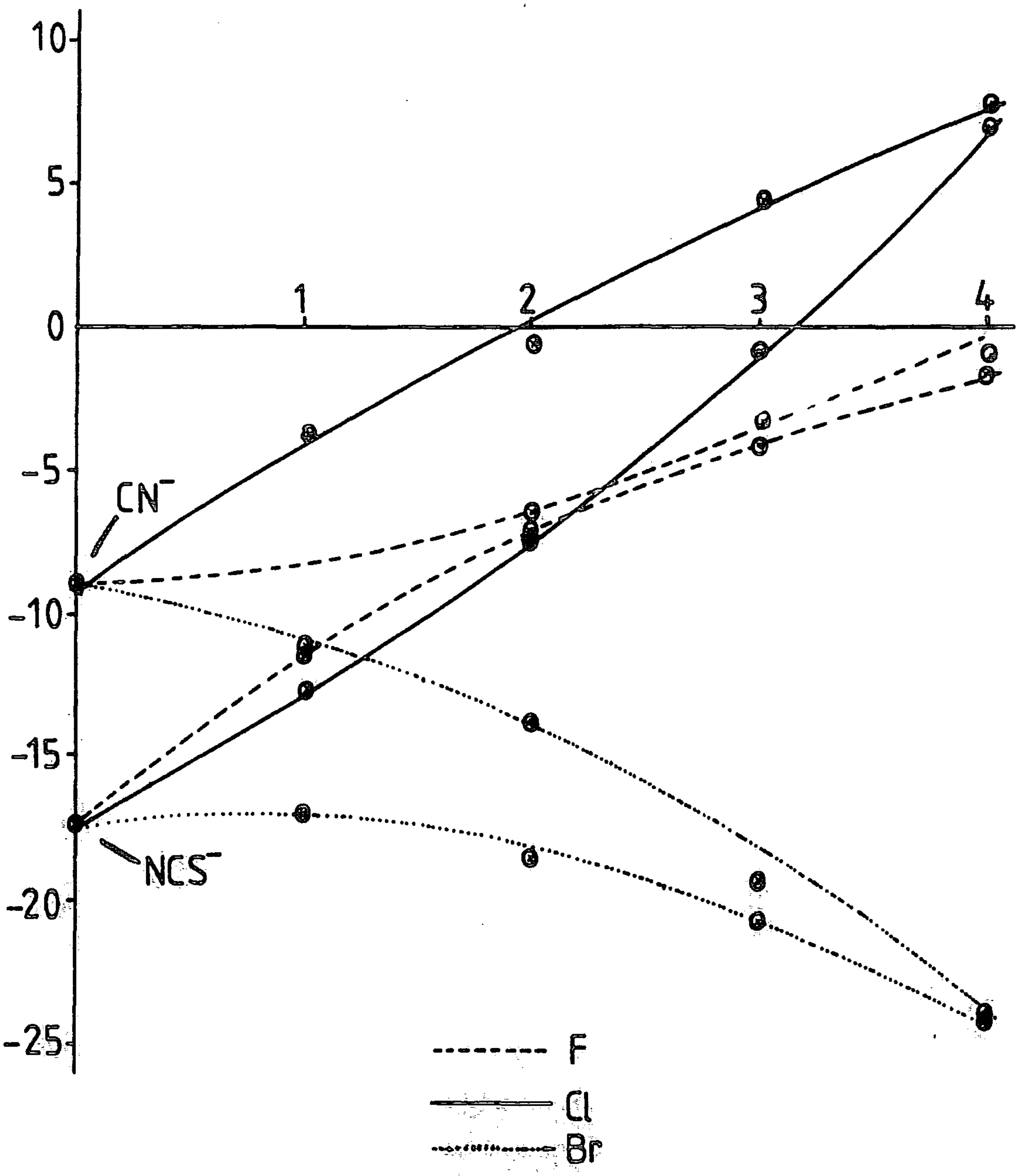

Graph 10.2: *^{11}B NMR data for the BX_4^- ($X \equiv Cl, Br, I$), CN^- and NCS^- systems.*

effective p-orbital overlap with boron. This is also illustrated by BF_4^- (+1.5) being more shielded than BCl_4^- (+6.6).

10.11.3 Graph 10.2: BX_4^- ($X \equiv F, Cl, Br$) and CN^-, NCS^-

This displays substitution in tetrahalogenoborate anions by thiocyanate and cyanide respectively. The graph allows a direct comparison of the thiocyanate and cyanide systems. The iodo- derivatives are omitted since values for the iodo-cyanoborate species were unobtainable.

The order of the cyano systems is chloride, fluoride and bromide, with respect to an increase in shielding at the boron centre: for exactly similar reasons as proposed in the thiocyanate system.

10.11.4 Graph 10.3: $^1J_{BN}$ Coupling in the B/F/NCS System

This illustrates the novel $^1J_{BN}$ coupling in the thiocyanate borate system, with fluoride, chloride and limited data with the bromide system. In the fluoride system an apparent decrease in $^1J_{BN}$ coupling exists, as the number of nitrogen atoms increases.

10.11.5 Graph 10.4: $^1J_{BF}$ Coupling in the B/F/CN System

This shows $^1J_{BF}$ coupling in the new cyano-fluoroborate system. The well-known phenomenon is illustrated, of coupling constant decrease with an increase in the number of fluorine atoms [2].

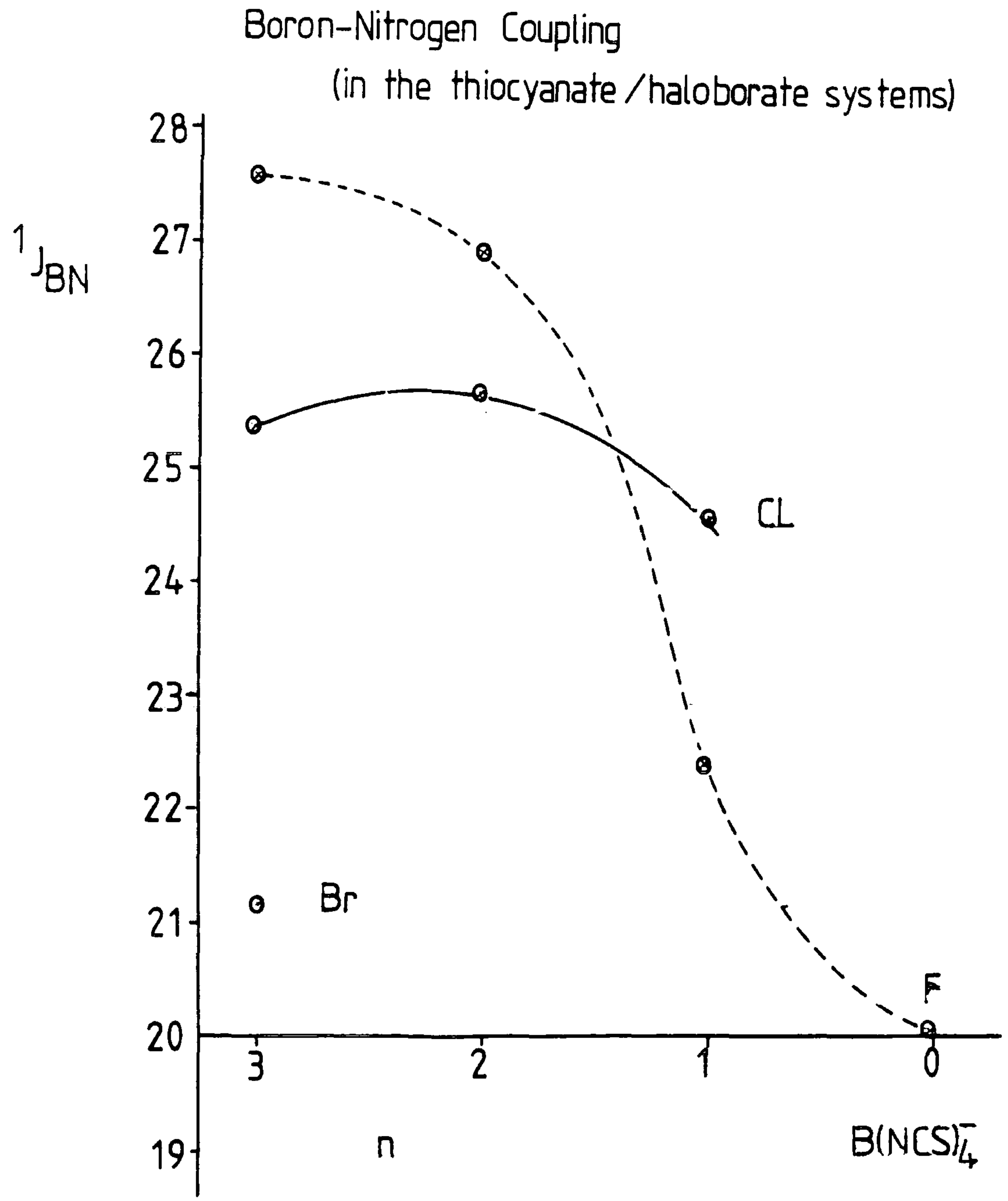

Graph 10.3: $^1J(BN)$ *coupling in* BX_4^- *(*$X \equiv F, Cl$*) and* NCS^- *systems.*

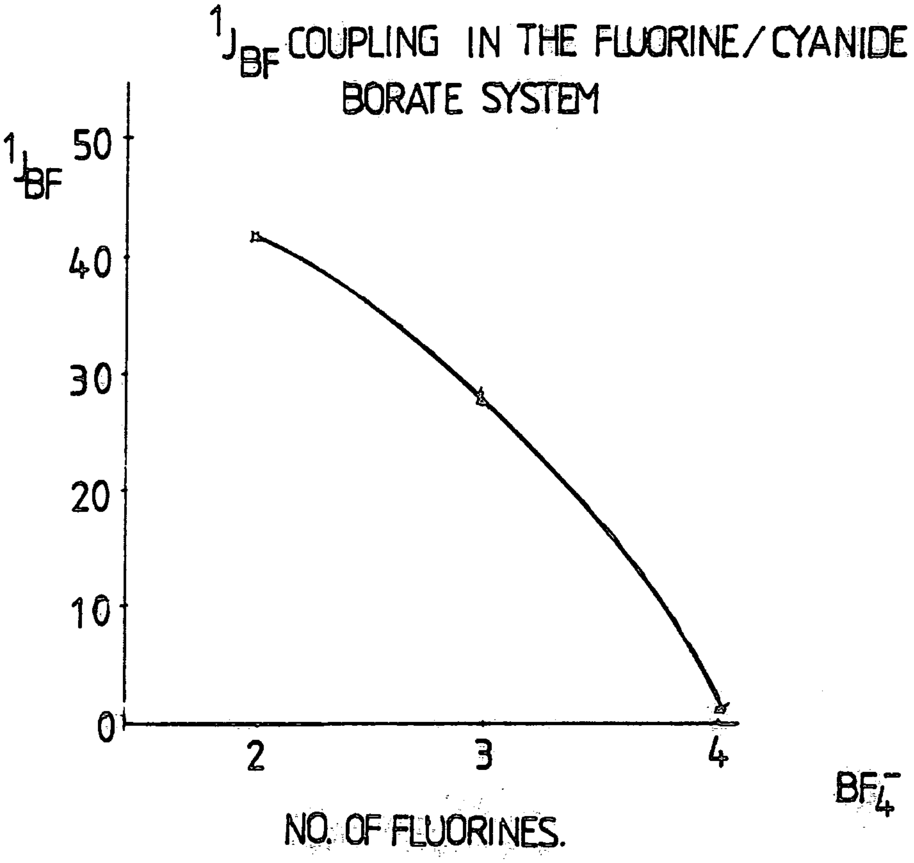

Graph 10.4: $^1J(BF)$ *coupling values for the B/F/NCS system.*

10.12 CALCULATION OF CHEMICAL SHIFTS FROM PAIRWISE ADDIVITY CONSTANTS

Chemical shifts of various nuclei have been observed which are pairwise additive with respect to the substituent groups [1]. For example the chemical shift can be expressed as:

$$\delta = \Sigma\, \eta_{i,j}$$

where $\eta_{i,j}$ is a parameter associated with substituents i and j and independent of all other substituents. The sum is taken over all substituents about a central atom excluding the nucleus observed in the NMR experiment, for example:

$$BF_2(NCS)_2^-: \qquad {}^{11}B\ \delta = \eta_{F,F} + 4\eta_{F,NCS} + \eta_{NCS,NCS}$$

where $\eta_{i,j}$ is different for each nucleus observed - theoretical justification for this rule is given in detail elsewhere [11]. Pairwise contributions arise because the wave function of each substituent group suffers a linear correction due to the presence of each neighbouring substituent group [1]. This work involves the use of the pairwise substitution products in the system BX_4^-/Y^-. Errors in these calculations may originate from deviations in the geometry of the species under consideration. This correlation by pairwise additivity relations provides useful confirmations of the resonance assignments. (The pairwise interaction calculation is obviously more useful for the octahedral systems, because more predictions can be made from the same amount of data.)

10.13 TWO DIMENSIONAL EXCHANGE NMR

2-D correlated experiments have been used to provide a map of coherent interactions, for example ^{11}B NMR for boranes [12-15]. Two dimensional exchange spectroscopy provides a map of incoherent interactions such as chemical exchange or magnetisation exchange arising from the Nuclear Overhauser Effect (NOE). Many examples of the elucidation of chemical exchange networks by 2-D NMR spectroscopy are known, for example using the techniques for proton [6], deuterium [7] and carbon (^{13}C) [8].

An additional fixed time, called the mixing time, T_m, is introduced in 2-D exchange spectroscopy to allow exchange of magnetisation *via* incoherent interactions. The pulse sequence for 2-D exchange spectroscopy is shown in Figure 10.8.

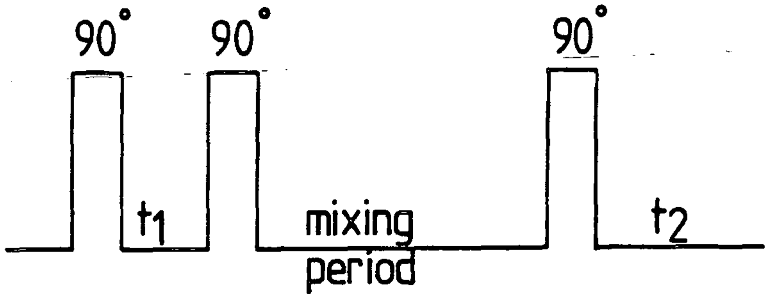

Figure 10.8: *The basic 2-D exchange pulse sequence.*

The first 90^0 pulse flips the net magnetisation vector in the x-y plane and causes each spin to precess at its characteristic frequency during the evolution period. This effectively labels each spin according to its initial precession frequency during t_1. In a 2-D NOE experiment, dipole-dipole coupled nuclei exchange magnetisation *via* the NOE during the mixing period T_m. This period has a constant value, chosen to be approximately equal to the spin-lattice relaxation time T_1. In this work, *a chemical exchange experiment*, magnetisation exchange occurs during the mixing period *as a consequence of chemical exchange.*

In both cases, the final frequency is detected during the detection period of length t_2 (2-D spectrum obtained by running this sequence at many values of t_1). The species which did not exchange magnetisation during the mixing period have the same initial and final frequencies. Hence, diagonal peaks occur along the diagonal line. This is clearly illustrated in Figures 10.1(b) and 10.2(b). [*NB*. Figure 10.1(b) shows more than five species present on the diagonal as a consequence of ligand isomerisation]. Those species exchanging magnetisation during the mixing period have final frequencies that differ from their initial frequencies. This exchange gives rise to off-diagonal peaks connecting spins related by a NOE or chemical exchange. The latter is clearly illustrated in Figures 10.1(b) and 10.2(b). These off-diagonal peaks generally occur in pairs that are symmetric about the diagonal peaks. **By matching all pairs of off-diagonal peaks, the complete exchange network can be seen in a single experiment.**

The resultant exchange spectrum depends critically on the magnitude of the mixing time, and the cross-peak intensities reflect the amount of exchange that takes place during τ_m. Hence, an interesting development of this work would be an investigation of the build-up rate of cross-peak intensities in 2-D exchange spectra obtained with different mixing times, providing a *direct* measure of the exchange rate [10].

NB. The pulse sequence (Figure 10.8) used in this work is identical to NOESY, but for the modification of the mixing time. For NOESY this is the spin-lattice relaxation time, and for the 2-D exchange experiment, as applied here for the pseudohaloborate system, it is simply **guesswork to obtain a mixing period of the same sort of order as the exchange process.**

10.14 EXPERIMENTAL

10.14.1 General Points

Lithium azide (LiN_3) was prepared according to the method of A.W.G. Platt [16], a method adapted by Dr. C. Ludman (University of Durham, 1980). Tetrabutylammonium azide (Bu_4NN_3) and lithium thiocyanate (LiNCS) were prepared as described by A. Marshall [17].

In the simple tetrahalogenoborate salt preparations, at the final stage of solvent removal, the solid appeared to be oily. A small volume of petroleum ether (30-40) was therefore added. The resulting suspension was stirred for several hours, before the petrol was removed *in vacuo* to yield a pure dry powdery solid.

10.14.2 Preparation of $Et_4N^+BCl_4^-$

$$Et_4N^+Cl^- + BCl_3 \longrightarrow Et_4N^+BCl_4^-$$

Boron trichloride (1.41g, 1.0 ml, 12 mmol) was condensed into a stirred solution of tetraethylammonium chloride (2.0g, 12 mmol) at -20 ^{0}C. The reaction mixture was stirred for 1 hour at room temperature. The solvent was removed *in vacuo* to yield a pure white salt $Et_4N^+BCl_4^-$. Yield was 2.5g (74%). ^{11}B (CH_2Cl_2) δ: + 6.6 ppm. This agrees well with known data [2,3].

10.14.3 Preparation of $Et_4N^+BBr_4^-$

$$Et_4N^+Br^- + BBr_3 \longrightarrow Et_4N^+BBr_4^-$$

Boron tribromide (1.5 ml, 15.9 mmol) in CH_2Br_2 (15 ml) was added dropwise over 5 minutes to a stirred solution of tetraethylammonium bromide (3.3g, 15.9 mmol) in CH_2Br_2 (20 ml) at room temperature. The mixture was stirred for 1 hour. The solvent was removed *in vacuo* to yield a pale brown powdery solid. This was washed with 4 aliquots of cold pentane (5 ml) to give a pure white salt. Yield was 6.2g (84%). ^{11}B NMR (CH_2Br_2) δ: -24 ppm, *cf.* published data [2,3]. The use of CH_2Br_2 in place of CH_2Cl_2 prevented chloride incorporation into the product [2].

10.14.4 Preparation of $Pr_4N^+BI_4^-$

$$Pr_4N^+I^- + BI_3 \longrightarrow Pr_4N^+BI_4^-$$

A solution of tetrapropylammonium iodide (1.9g, 6.1 mmol) in CH_2I_2 (35 ml) was added dropwise over 5 minutes to a stirred solution of boron triiodide (2.4g, 6.1 mmol) in CH_2I_2 (20 ml) at 0 °C (the mixture became pale purple attributed to the evolution of iodine, though this was minimised by keeping the reaction mixture in the dark). The mixture was stirred at 0 °C for 30 minutes, before the solvent was removed *in vacuo* yielding a pale purple/brown solid. This was washed with 2 aliquots (10 ml) cold pentane to give a yellow solid. Yield was 2.2 g (51%). ^{11}B (CH_2Cl_2) δ: -127 ppm, *cf.* published data [2,3].

10.14.5 Preparation of $Et_4N^+B(NCS)_4^-$

$$Et_4N^+BCl_4^- \xrightarrow{4AgNCS} Et_4N^+B(NCS)_4^- + 4AgCl$$

AgNCS (2.90g, 17.5 mmol) was added to a stirred solution of $Et_4N^+BCl_4^-$ (1.21g, 4.3 mmol) in CH_2Cl_2 (35 ml) at room temperature. This was stirred for four hours. The completion of the reaction was confirmed by ^{11}B NMR -17.0 ppm [3,18]. AgCl was removed by filtration, and the dichloromethane *in vacuo*, to yield a pale yellow solid. Yield was 1.24g (77%). $^1J_{BN}$ 23.2 Hz [3] (9 lines).

10.14.6 Preparation of $Ph_4P^+BCl_4^-$ (93)

$$Ph_4\overset{+}{P}\overset{-}{Cl} + BCl_3 \longrightarrow Ph_4P^+BCl_4^-$$

Tetraphenylphosphonium chloride (7.96g, 21.3 mmol) in CH_2Cl_2 (25 ml) was added dropwise over 10 minutes to a stirred solution of boron trichloride (2.5g, 1.8 ml, 21.3 mmol) which had been condensed into CH_2Cl_2 (35 ml) at -20 ^{0}C, and maintained at this temperature. The reaction mixture was allowed to reach room temperature, and stirred for 1 hour before the removal of the solvent *in vacuo* to yield a white solid. Yield was 6.7g (64%). ^{11}B NMR (CH_2Cl_2) δ: +6.6 ppm, *cf.* published data [2,3].

10.14.7 Preparation of $ArPCl_3^+BCl_4^-$ (95)

$$ArPCl_2 \xrightarrow{Cl_2} ArPCl_4 \xrightarrow{BCl_3} ArPCl_3^+BCl_4^- \text{ (95)}$$

This was prepared by T.Straw [19]. ^{31}P (CH_2Cl_2) δ: 97.1 ppm; ^{11}B (CH_2Cl_2) δ: +6.6 ppm.

10.14.8 Preparation of $C_6F_5PBr_3^+BBr_4^-$ (96)

This reaction followed work by R. Ali [3]. It consisted of four stages:

$$C_6F_5Br + Mg \xrightarrow{Et_2O} C_6F_5MgBr$$

$$C_6F_5MgBr + PBr_3 \xrightarrow{Et_2O} C_6F_5PBr_2 + MgBr_2$$

$$C_6F_5PBr_2 + Br_2 \xrightarrow{CCl_4} C_6F_5PBr_4$$

$$C_6F_5PBr_4 + BBr_3 \longrightarrow C_6F_5PBr_3^+BBr_4^- \ (96)$$

It was observed that the use of dibromomethane in the place of dichloromethane at stage 4 allowed higher yields of the order of 65% - avoiding any incorporation of chloride by exchange with the solvent. $C_6F_5PBr_3^+BBr_4^-$: ^{11}B ($PhNO_2$) δ: -24 ppm; ^{31}P ($PhNO_2$) δ: -38 ppm; MS (Intensity%) EI: 438 (20,$C_6F_5PBr_3^+$), 358 (100,$C_6F_5PBr_2^+$), 277 (22,$C_6F_5PBr^+$).

10.14.9 Chloride Systems

10.14.9.1 Reaction of $Et_4N^+BCl_4^-$ With AgNCS (CH_2Cl_2)

AgNCS (0.85g, 5.12 mmol) was added to a stirred solution of $Et_4N^+BCl_4^-$ (1.45g, 5.12 mmol) in CH_2Cl_2 (10 ml) at room temperature. Results are described in Section 10.9.2.

10.14.9.2 Reaction of $Et_4N^+BCl_4^-$ With AgCN (CH_3CN)

AgCN (0.47g, 3.51 mmol) was added to a stirred solution of $Et_4N^+BCl_4^-$ (0.99g, 3.51 mmol) in CH_3CN (15 ml) at room temperature. The mixture was filtered and the ^{11}B NMR of the filtrate showed two major peaks (which could not be assigned to any of the expected substitution products) near 0 ppm [4]. Results are described in Section 10.4.3.

10.14.9.3 Reaction of $Et_4N^+BCl_4^-$ With $Et_4N^+NCO^-$ (CH_2Cl_2)

Et_4NNCO (0.87g, 5.06 mmol) was added to a stirred solution of $Et_4N^+BCl_4^-$ (1.43g, 5.06 mmol) in CH_2Cl_2 (35 ml) at room temperature. The reaction mixture was stirred for 30 minutes. More than five peaks were observed in the ^{11}B NMR. Results are described in Section 10.4.3.

10.14.9.4 Attempted Preparation of $B(CN)_4^-$ Salts

It was not possible to isolate $Et_4N^+B(CN)_4^-$ by the addition of four equivalents of cyanide to $Et_4N^+BCl_4^-$ in acetonitrile, since the substitution products exchange. The same problem was encountered with KCN and BCl_3. Signals in the ^{11}B NMR were observed at 0 and -4.1 ppm (Section 10.4.3)

An exactly similar phenomenon exists on refluxing 4.1 equivalents AgCN and $Et_4N^+BCl_4^-$ in $PhNO_2$. This gave an average ^{11}B NMR chemical shift of -0.51 ppm indicative of rapid exchange:

$$BX_3(C_6H_5NO_2) + Y^- \rightleftharpoons BX_3Y^- + BX_2Y_2^- + BXY_3^- + BY_4^- + C_6H_5NO_2$$ [4]

10.14.9.5 Preparation of $Ag^+B(CN)_4^-$

This was carried out according to Bessler *et al.*[20] using BCl_3 (1.42g, 1.0 ml, 12.1 mmol) and AgCN (6.5g, 49 mmol) (*ie.* in the ratio 1:4) in a carius tube at 150-160 °C for 2 hours. The solid obtained was insoluble and had a very poor analysis; Found: C, 6.39; H, 2.05; N, 14.67; Required: C, 21.57; H, 0.00; N, 25.1%. By following the procedure [21] with BCl_3 in slight excess, similarly poor results were obtained.

10.14.9.6 Reaction of $Ph_4P^+BCl_4^-$ With AgCN (CH_3CN)

AgCN (0.35g, 2.58 mmol) was added to a stirred solution of $Ph_4P^+BCl_4^-$ (1.27g, 2.58 mmol) in CH_3CN (25 ml) at room temperature. The ^{11}B NMR showed 5 peaks (discussed in Section 10.6.1).

10.14.9.7 Reaction of $ArPCl_3^+BCl_4^-$ With AgNCS ($PhNO_2$)

AgNCS (0.35g, 2.1 mmol) was added to a stirred solution of $ArPCl_3^+BCl_4^-$ (1.2g, 2.1 mmol) in $PhNO_2$ (20 ml). ^{11}B data is detailed in Section 10.9.2 . Thiocyanate substitution in the P(V) cation was also observed. ^{31}P ($PhNO_2$) δ: +97 [$ArPCl_3^+$], +26 [$ArPCl_2(NCS)]^+$, +2.2 ['$ArPCl(NCS)_2$'$]^+$, -30.1 ['$ArP(NCS)_3^+$'] ppm. An excess of thiocyanate resulted in decomposition, and the observation of $ArPCl_2$ [^{31}P NMR δ: +145 ppm $^4J_{PF}$ 62.4 Hz].

10.14.9.8 Reaction of $ArPCl_3^+BCl_4^-$ With AgCN ($PhNO_2$)

AgCN (0.34g, 2.54 mmol) was added to a stirred solution of $ArPCl_3^+BCl_4^-$ (1.45g, 2.54 mmol) in $PhNO_2$[2] (15 ml). This mixture was filtered and the ^{11}B NMR of the filtrate recorded. Results are discussed in Section 10.6.3 . An excess of silver cyanide caused decomposition of the cation ($ArPCl_3^+$) generating $ArPCl_2$ [^{31}P NMR δ: +145 ppm, $^4J_{PF}$ 62 Hz] possibly *via* ClCN elimination.

---

[2] $PhNO_2$ is required to bring the salt into solution.

10.14.10 Bromide Systems

10.14.10.1 Reaction of $Et_4N^+BBr_4^-$ With AgNCS (CH_2Br_2)

AgNCS (0.25g, 1.5 mmol) was added to a stirred solution of $Et_4N^+BBr_4^-$ (0.69g, 1.5 mmol) in CH_2Br_2 (20 ml). The solution was stirred at room temperature for 10 minutes before filtration, and recording the ^{11}B NMR. Addition of further AgNCS (0.75g, 4.5 mmol) and stirring at room temperature for 1 hour showed quantitative conversion to $Et_4N^+B(NCS)_4^-$ with respect to the ^{11}B NMR. (Section 10.9.3)

10.14.10.2 Reaction of $Et_4N^+BBr_4^-$ With AgCN (CH_3CN)

AgCN (0.17g, 1.3 mmol) was added to a stirred solution of $Et_4N^+BBr_4^-$ (0.60g, 1.3 mmol) in CH_3CN (25 ml) at room temperature. The reaction mixture was stirred for 10 minutes. Results are discussed in Section 10.4.1. After a further 2 hours there was no change in the ^{11}B NMR.

10.14.10.3 Reaction of $Et_4N^+BBr_4^-$ With $Bu_4N^+N_3^-$ (CH_2Br_2)

Bu_4NN_3 (0.2g, 0.7 mmol) was added to a stirred solution of $Et_4N^+BBr_4^-$ (0.33g, 0.7 mmol) in CH_2Br_2 (20 ml) at room temperature. The reaction mixture was stirred for 30 minutes. Results are described in Section 10.4.1. The peaks to higher field may indicate loss of nitrogen (*ie. via* $Br_3B{-}N{-}\overset{\curvearrowleft}{N}^{+}{\equiv}N$).

10.14.10.4 Reaction of $Et_4N^+BBr_4^-$ With $Et_4N^+NCO^-$ (CH_2Br_2)

$Et_4\overset{+}{N}NC\bar{O}$ (0.63g, 3.7 mmol) was added to a stirred solution of $Et_4N^+BBr_4^-$ (1.72g, 3.7 mmol) in CH_2Br_2 (25 ml) at room temperature. The reaction mixture was stirred for 30 minutes. The results are discussed in Section 10.4.1.

10.14.10.5 Reaction of $C_6F_5PBr_3^+BBr_4^-$ With AgCN ($PhNO_2$)

The salt was prepared according to R. Ali [3]. AgCN (0.3g, 2.2 mmol) was added to a stirred solution of $C_6F_5PBr_3^+BBr_4^-$ (1.67g, 2.2 mmol) in $PhNO_2$[3] (20 ml) at 0 ^{o}C. This mixture was allowed to reach room temperature and its ^{11}B NMR was recorded immediately. Results are discussed in Section 10.7.

10.14.11 Iodide Systems

10.14.11.1 Reaction of $Pr_4N^+BI_4^-$ With AgNCS (CH_2I_2)

AgNCS (0.26g, 1.6 mmol), was added to a stirred solution of $Pr_4N^+BI_4^-$ (1.1g, 1.6 mmol) in CH_2I_2 (25 ml) at 0 ^{o}C. This reaction mixture was allowed to reach room temperature and stirred for 30 minutes. Results are discussed in Section 10.9.4.

---

[3] $PhNO_2$ was required to dissolve $C_6F_5PBr_3{}^+BBr_4{}^-$ salt.

10.14.11.2 Reaction of BI_3 With $Et_4N^+NCS^-$ (CH_2I_2)

Et_4NNCS (1.2g, 6.4 mmol) was added to a stirred solution of BI_3 (2.5g, 6.4 mmol) in CH_2I_2 (25 ml) at 0 °C. This was stirred at room temperature for 30 minutes. Results are discussed in Section 10.9.4

Decomposition within the cyanoiodo systems was minimised by weighing out the required quantities of $R_4N^+BI_4^-$ or BI_3, and AgCN or Bu_4NCN in one vessel at 0 °C under nitrogen. The required solvent was then added by syringe or condensed into the mixture. (The two solids do not react until they are brought into solution).

10.14.11.3 Reaction of $Pr_4N^+BI_4^-$ With AgCN (CH_2I_2)

CH_2I_2 (25 ml) was condensed onto a mixture of $Pr_4N^+BI_4^-$ (1.1g, 1.6 mmol) and AgCN (0.21g, 1.6 mmol) at -78 °C. The reaction mixture was allowed to gradually reach room temperature and stirred for 30 minutes. Results are discussed in Section 10.4.2.

10.14.11.4 Reaction of BI_3 With $Bu_4N^+CN^-$ (CH_2I_2)

CH_2I_2 (25 ml) was condensed onto a mixture of BI_3 (0.9g, 2.3 mmol) and $Bu_4N^+CN^-$ (0.62g, 2.3 mmol) at -78 °C. The reaction mixture was allowed to warm to room temperature and stirred for 30 minutes. Results are discussed in Section 10.4.2.

10.14.11.5 Reaction of BI_3 With $Bu_4N^+N_3^-$ (CH_2I_2)

CH_2I_2 (25 ml) was condensed onto a mixture of BI_3 (1.0g, 2.6 mmol) and $Bu_4N^+N_3^-$ (0.74g, 2.6 mmol) at -78 °C. The reaction mixture was stirred and allowed to reach room temperature. Results are discussed in Section 10.4.2.

10.14.11.6 Reaction of BI_3 With $Et_4N^+NCO^-$ (CH_2I_2)

CH_2I_2 (25 ml) was condensed onto a mixture of BI_3 (0.62g, 1.6 mmol) and $Et_4N^+NCO^-$ (0.27g, 1.6 mmol) at -78 °C. The reaction mixture was stirred and allowed to reach room temperature. Results are discussed in Section 10.4.2.

10.14.12 Fluoride Systems

10.14.12.1 Reaction of $Et_4N^+B(NCS)_4^-$ With CsF (tetraglyme)

CsF (0.68g, 4.5 mmol) was added to a stirred solution of $Et_4N^+B(NCS)_4^-$ (1.67g, 4.5 mmol) in tetraglyme (25 ml) at room temperature. The reaction mixture was stirred for 1 hour. Results are discussed in Section 10.9.1.

10.14.12.2 Reaction of $BF_3 \cdot Et_2O$ With LiCN and Bu_4NCN (DMF/Et_2O)

LiCN (0.5 M solution in DMF, 7.04 ml, 3.5 mmol) was added dropwise to a stirred solution of $BF_3 \cdot Et_2O$ (0.5g, 0.4 ml, 3.5 mmol) in CH_2Cl_2 (15 ml) at room temperature. The reaction mixture was stirred for 30 minutes. Results are discussed in Section 10.10 . The first substitution product $NCBF_3^- Li^+$ was observed. For further substitution $Bu_4N^+CN^-$ (0.94g, 3.5 mmol) was added, and stirred for 30 minutes. Results are discussed in Section 10.10.

10.14.12.3 Reaction of $BF_3 \cdot Et_2O$ With $Bu_4N^+N_3^-$ (CH_2Cl_2)

$BF_3 \cdot Et_2O$ (0.62g, 0.54 ml, 4.4 mmol) in CH_2Cl_2 (10 ml) was added dropwise over 5 minutes to a stirred solution of Bu_4NN_3 (1.25g, 4.4 mmol) in CH_2Cl_2 (15 ml) at room temperature. The reaction mixture was stirred for 30 minutes before recording its ^{11}B NMR. A peak at +3.2 ppm was observed, and attributed to loss of Et_2O coordination of the BF_3 in CH_2Cl_2. (Section 10.10)

10.14.12.4 Reaction of $BF_3 \cdot Et_2O$ With $Et_4N^+NCO^-$ (CH_2Cl_2)

$Et_4\overset{+}{N}NC\bar{O}$ (0.70g, 4.1 mmol) was added to a stirred solution of $BF_3 \cdot Et_2O$ (0.58g, 0.50 ml, 4.1 mmol) in CH_2Cl_2 (15 ml) at room temperature. The solution was stirred for 30 minutes. An ^{11}B NMR signal at +3.27 ppm was attributed to BF_3 in solution. Results are discussed in Section 10.10.

10.15 REFERENCES

1. T. Vladimiroff and E.R. Malin owski, *J.Chem.Phys.*, 46, 1830 (1967).
2. J.S. Hartman and G.T. Schrobilgen, *Inorg.Chem.*, 11(5), 940 (1972).
3. R. Ali, Ph.D Thesis, Univeristy of Durham (1986).
4. H. Landesman and R.E. Williams, *J.Amer.Chem.Soc.*, 83, 2663 (1961).
5. F.A. Cotton and G. Wilkinson, *Advanced Inorganic Chemistry*, Fourth Edition, John Wiley and Sons, p.64 (1980).

6. B.H. Meier and R.R. Ernst, *J.Amer.Chem.Soc.*, 101(21), 6441-6442 (1979).

7. C. Boeffel, Z. Luz, R. Poupko and H. Zimmermann, *J.Mag.Resonance*, 85, 329-336 (1989).

8. Y. Huang, S. Macura and R.R. Ernst, *J.Amer.Chem.Soc.*, 103, 5327-5333 (1981).

9. "*NMR Spectroscopy Techniques*", Practical Spectroscopy Series, Eds. C. Dybowski and R.L. Lichter, Marcel Dekker Inc., New York and Basel, 5, 150 (1987).

10. J. Jeener, B.H. Meier, P. Bachman and R.R. Ernst, *J.Chem.Phys.*, 71, 4246 (1979).

11. J.G. Andrade, T. Clark, J. Chandrasekhar and P. von Ragué Schleyer, *Tetrahedron Lett.*, 22(31), 2957-2960 (1981).

12. D.C. Meina, J.H. Morris and D. Reed, *Polyhedron*, 5(10), 1639-1643 (1986).

13. G.B. Jacobsen, D.G. Meina, J.H. Morris, C. Thomson, S.J. Andrews, D. Reed and A.J. Welch, *J.Chem.Soc.Dalton Trans.*, 1645-1654 (1985).

14. D. Reed, *J.Chem.Research*, 198-199 (1984).

15. T.L. Venable, W.C. Hutton and R.N. Grimes, *J.Amer.Chem.Soc.*, 106, 29-37 (1984).

16. A.W.G. Platt, Ph.D Thesis, Univeristy of Durham, page 8 (1980).

17. A. Marshall, Ph.D Thesis, Univeristy of Durham (1982).

18. V.H. Binder, *Z.Anorg.Allgem.Chem.*, 383, 279-284 (1971).

19. Preparation by T. Straw, unpublished work, University of Durham (1989).

20. V.E. Bessler and J. Goubeau, *Z.Anorg.Allgem.Chem.*, 352, 67-76 (1967).

21. V.E. Bessler, *Z.Anorg.Allgem.Chem.*, 430, 38-42 (1977).

CHAPTER ELEVEN

THE CHEMISTRY OF BORON IN NITRILEIMINES

11.1 INTRODUCTION TO NITRILEIMINES

This section is prefaced with a brief historical perspective on nitrileimine chemistry.

1934 The action of triphenylmethylsodium on diazomethane resulted in the discovery of the linear isomer iso-diazomethane[1] [1]:

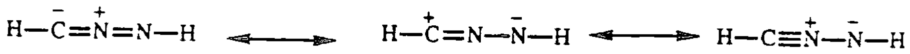

$$H-\overset{-}{C}=\overset{+}{N}=N-H \longleftrightarrow H-\overset{+}{C}=N-\overset{-}{N}-H \longleftrightarrow H-C\equiv\overset{+}{N}-\overset{-}{N}-H$$

1959 Thermal breakdown of 2,5-disubstituted tetrazoles yields nitrileimines as reactive intermediates [2]:

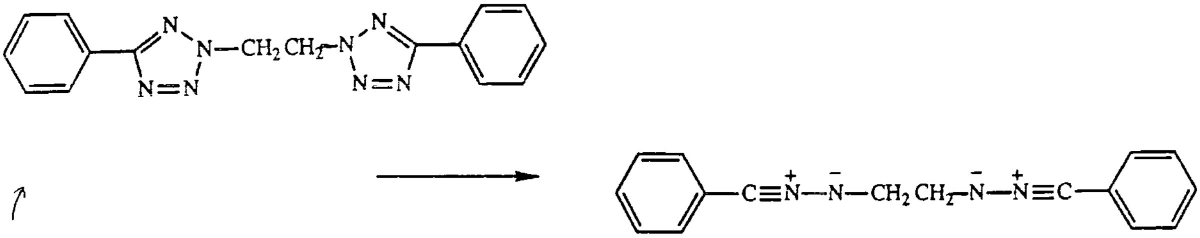

This method has developed as a usual route to unstable nitrileimines [3] and has been used recently (1989) [4] in the generation of the following bis-nitrileimine:

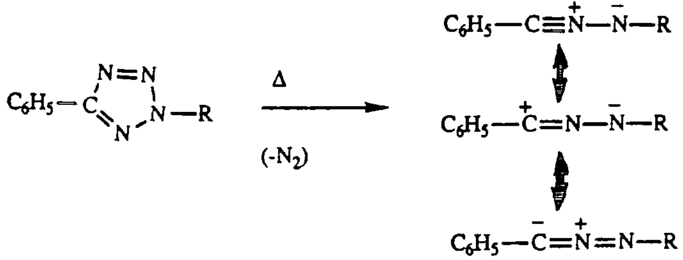

The same workers showed that nitrileimines can also be formed by 1,3-dehydrochlorination of a suitable compound [2]:

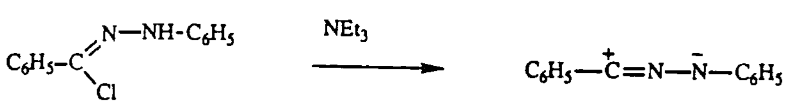

1966 The chemistry of iso-diazomethane was reviewed [5].

---

[1] It is of interest to note the apparent kinetic control of these reactions. Protonation occurs rapidly at the more nucleophilic nitrogen giving rise to the thermodynamically less stable isomer (Section 11.4.3)

1969 Pyrolysis of potassium mesitylazomesityl-nitromethane generated a non-isolable nitrileimine which was trapped by 1,3-dipolar cycloaddition and identified [6]:

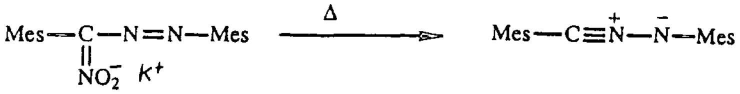

$$\mathrm{Mes{-}\underset{\underset{NO_2^-\ K^+}{\|}}{C}{-}N{=}N{-}Mes} \xrightarrow{\Delta} \mathrm{Mes{-}C{\equiv}\overset{+}{N}{-}\overset{-}{N}{-}Mes}$$

1980 The first nitrileimine to be generated by photolysis was characterised spectroscopically [7]:

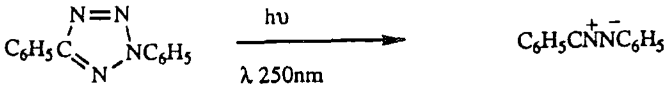

1985 The first direct spectroscopic characterisation of a substituted nitrileimine generated thermally. Spectroscopic evidence for the existence of discrete nitrileimine molecules in the gas phase was obtained. The problem of isomerisation of N-substituted compounds to azines and carbodiimides was overcome by the use of a silyl derivative [8]:

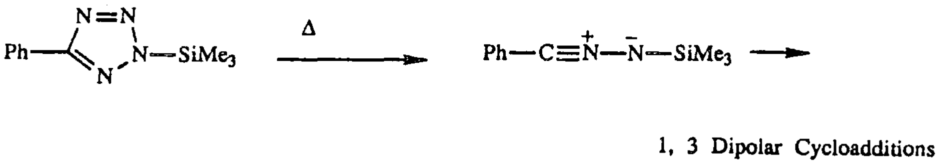

1988 Synthesis of the first stable nitrileimine *via* the phosphorus diazo compound:

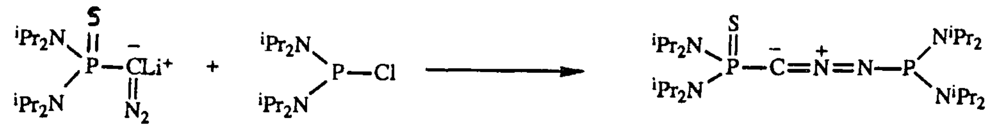

In summary, the parent nitrileimine was discovered in 1934 [1], the first substituted nitrileimine was shown to have independent existence spectroscopically in 1980 [7] and a report of the first stable nitrileimine to be successfully isolated was made in 1988 [9].

The chemistry of the nitrileimines is multifaceted. They have the potential to behave as acids or bases, as electrophiles or nucleophiles, as 1,3-dipoles or a carbene source (see Section 11.8).

11.2 CARBODIIMIDES

1980 Carbodiimides are accessible *via* a Wolff rearrangement of a nitrileimine (Section 11.7) [10], *eg.*

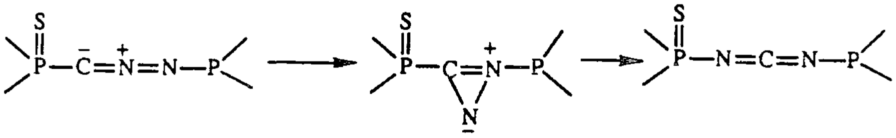

1988 A direct synthesis for carbodiimides is *via* the following route [11]:

$$C_6F_5\text{-}N{=}CCl_2 \xrightarrow{RNH_2} C_6F_5N{=}C{=}NR$$

1989 The discovery of a synthesis for C=C conjugated carbodiimides by aza-Wittig reaction of iminophosphoranes with isocyanate [12]:

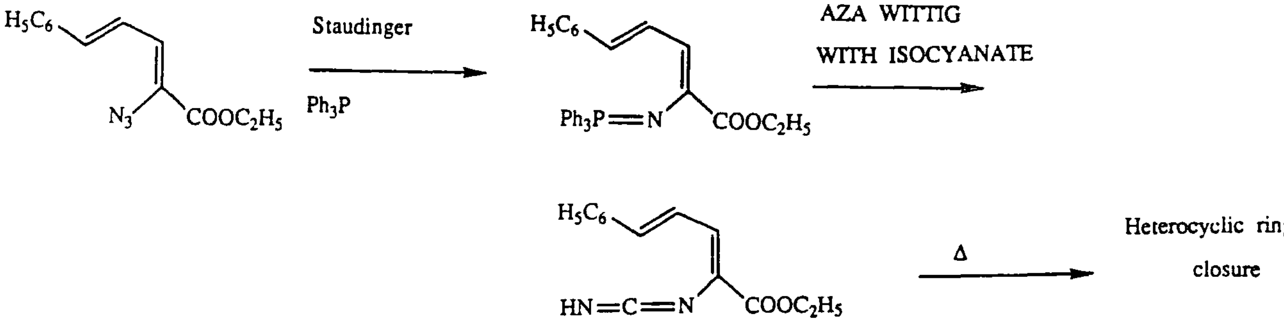

The preferred geometry of carbodiimides is analogous to that found in allenes [13] with orthogonal π-systems:

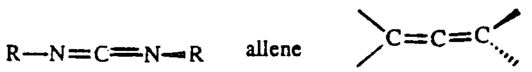

A brief consideration of the reactivity of carbodiimides should include its use in the synthesis of phosphaalkenes (Chapter 4) by the route shown below [14]:

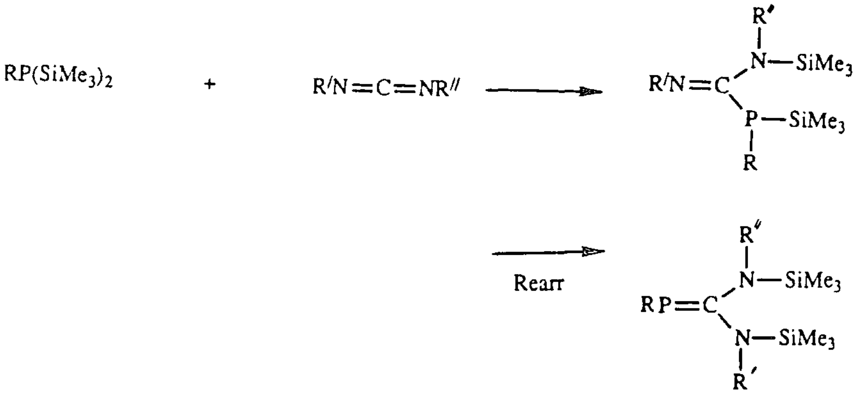

An interesting use for carbodiimides is in the alignment of peptides in a micellar system [15].

The current study aimed to cover stable nitrileimine synthesis, including their rearrangement to carbodiimides and their reactivity as 1,3-dipoles. An attempt was also made to form a boron diazo species.

11.3 BORON DIAZO COMPOUNDS

Boron diazo compounds to date have only been postulated as reactive intermediates [16] for example:

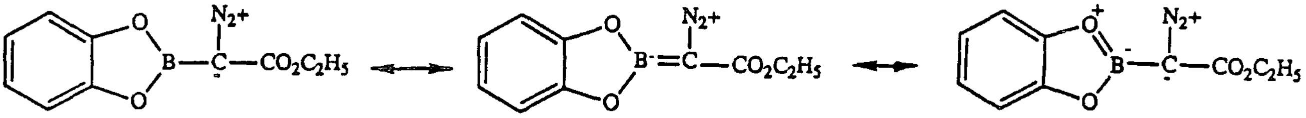

A number of different avenues have been explored in the attempt to obtain diazo compounds of boron and, although success cannot be claimed in the overall goal many interesting and novel observations have been possible *en route* (Section 11.10).

The main reason for attempting such a synthesis is that a stable diazo compounds could provide a starting point for a wide range of boron compounds. It could provide, above all in line with the interest in the chemistry of low coordinated species, a possible route *via* the carbene to a B=C double bond, *ie*.

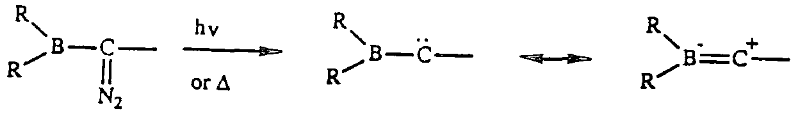

Recent work in this area includes the synthesis of alkylalkylideneboranes [$R-B=CA_2$ where R = Me, ^tBu; A = $SiMe_3$] by elimination of AOMe at 560 °C and 490 °C respectively [17]:

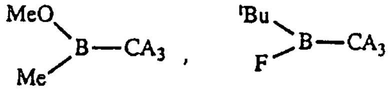

Other work includes the synthesis of aminomethylene boranes [18]:

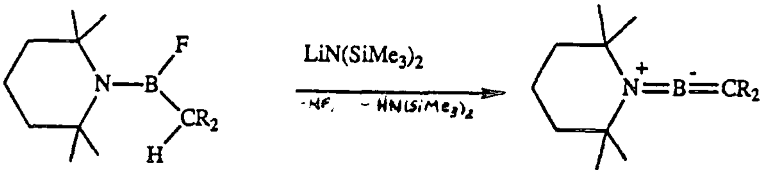

Helm and Nöth [19] demonstrated the high reactivity of B=C double bonds towards 2+2 and 2+3 cycloaddition. Berndt *et al.* [20] have developed the chemistry of borolithium alkanes [postulated as boron stabilised carbanions with a boratoalkene structure (11.1a)], and have prepared the first stable diboryldilithiomethane established as having a 1,3-diboratoallene structure (11.1b):

(11.1a)

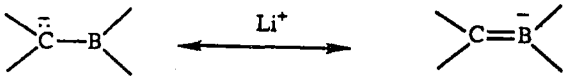

(11.1b)

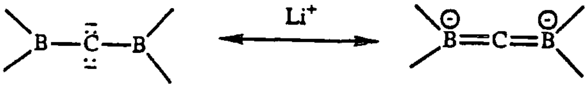

11.4 NITRILEIMINES VIA DIAZO COMPOUNDS

One of the principal routes to nitrileimines is *via* the diazo compound [9].

11.4.1 Synthesis of Diazo Compounds

A major problem in the synthesis of diazo compounds is their susceptibility to the Staudinger reaction [21]. This was comprehensively reviewed up to 1981 [22]. In order to prevent P(III)-diazo compounds following the Staudinger process (Figure 11.1) bulky substituent groups must be employed to block reaction with the lone electron pair on the phosphorus atom [23]. The bisdiisopropylamino group is frequently used for this purpose [23].

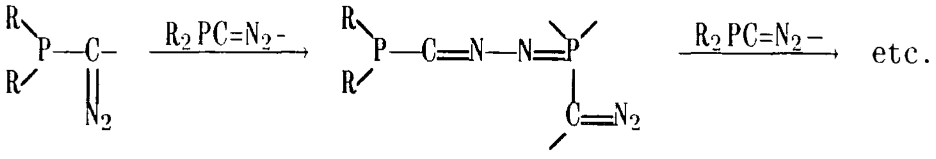

Figure 11.1: *The Staudinger process.*

It is interesting to contrast this problem with the facile synthesis of P(V)-diazo compounds [24] (Figure 11.2).

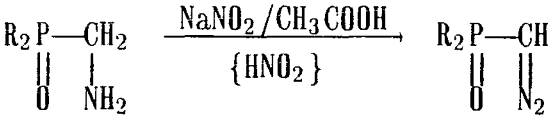

$$R_2\underset{\displaystyle O}{\underset{\|}{P}}-\underset{\displaystyle NH_2}{\underset{|}{CH_2}} \xrightarrow[\{HNO_2\}]{NaNO_2/CH_3COOH} R_2\underset{\displaystyle O}{\underset{\|}{P}}-\underset{\displaystyle N_2}{\underset{\|}{CH}}$$

Figure 11.2: *P(V) diazo compound synthesis.*

In this case the R groups can be small since there is no lone pair of electrons on the phosphorus atom to permit the Staudinger reaction to interfere. However, the "Curtius" rearrangement [25-27] is still possible as in the P(III) case on generation of the carbene, and is prevented by the use of R groups such as -OEt [28].

11.4.2 The Diazo Route to Nitrileimines

The diazo compounds described here are from work of the Toulouse research group led by G. Bertrand [24,29], with whom the author has collaborated.

The starting material is usually diazomethane itself prepared by a standard reaction (Equation 11.1) [30]. The diazomethane in ether is then silylated using trimethyl-silyltriflate (Equation 11.2) [31]. The diazo compound is then lithiated. At this stage there are theoretically two possible sites for electrophilic attack, the carbon or nitrogen as indicated (Equation 11.3). As the reaction scheme shows the product is formed entirely by electrophilic attack at the carbon.

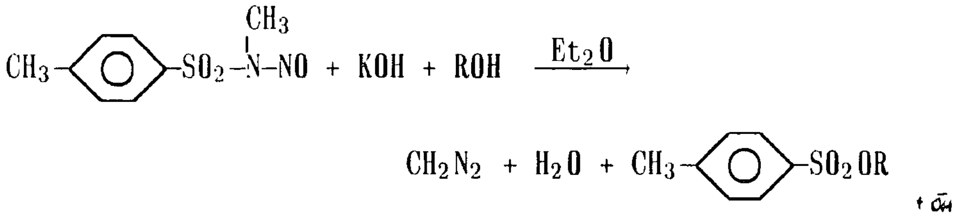

(11.1)

$$CH_2N_2 + Me_3Si\text{-}OSO_2CF_3 \xrightarrow[Et_2O]{^iPr_2NEt} Me_3SiCH(N_2)\ (99) + {}^iPr_2NHEt^+CF_3SO_3^- \quad (11.2)$$

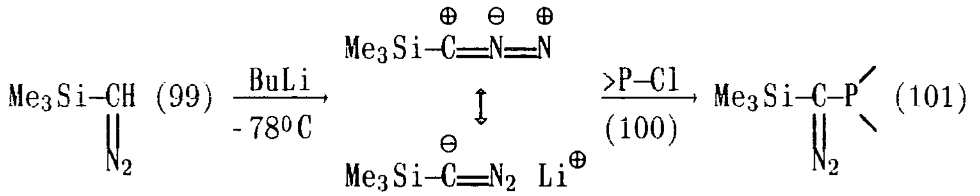

(11.3)

The Me_3Si– group is easily cleaved by aqueous methanol to generate the required compound, $(^iPr_2N)_2P\text{–}CH{=}N_2$ (102). The chemistry of this compound was explored in relation to its reactions with boron derivatives (Experimental data, Section 11.13). Previous work by Bertrand *et al.*[9] clearly showed that in reactions with acyl chlorides, N-acylation strongly competes with C-acylation. In the case of the P(III) compound the final product is partly the result of attack at C (Figure 11.3). The P(V) analogue with S attached to the lone pair of P [Figure 11.3(ii)] provides an example of the N-acylated product.

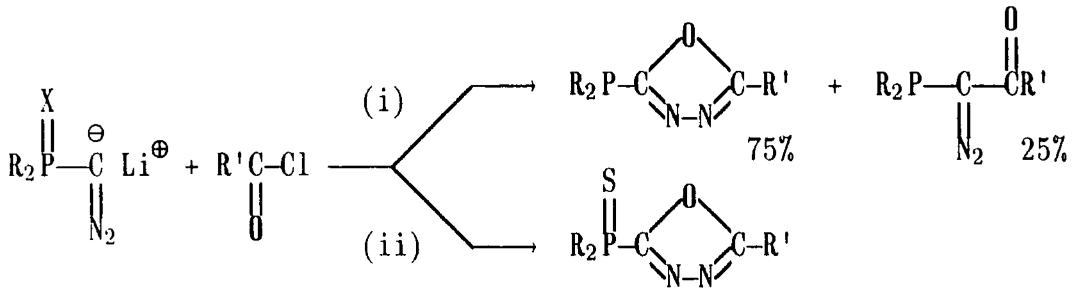

Figure 11.3: *Reaction of the lithio derivative of a phosphorus diazo compound with acyl chloride; (i) X = lone pair (103); (ii) X = (=S) (105).*

An exactly parallel pair of reactions is shown with P(III) monochlorides [9] (Figure 11.4). In the case of these compounds it is clear that in terms of the final product, P(V) gives result of attack at nitrogen and P(III) gives result of attack at carbon.

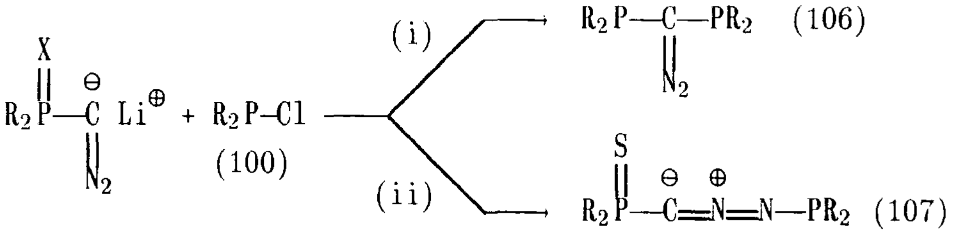

Figure 11.4: *Reaction of the lithio derivative of a phosphorus diazo compound with a P(III) monochloride; (i) X = lone pair (103); (ii) X = (=S) (105).*

11.4.3 Extension to Boron-Containing Compounds

The reaction between the lithio P(III) diazo compound with bis-di-isopropylaminoboron chloride was explored. This resulted in the formation of the new stable nitrileimine (Equation 11.4).

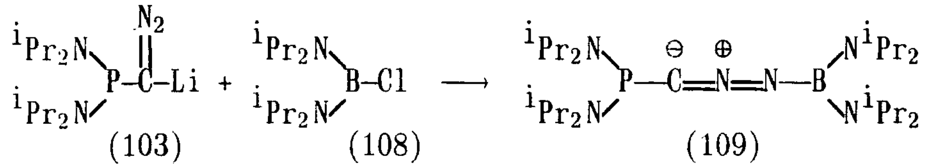

(11.4)

Selected spectroscopic data for the nitrileimine (109) are presented in Table 11.1, and full experimental details are given in Section 11.13.1.

The formation of compound (109) by the reaction sequence above illustrates *quite a different behaviour of the P(III) compound* from that described in Figure 11.4. Perhaps this reaction may be attributed to the high level of crowding around the boron. This is further evidence that the nitrileimine is the kinetically stabilised/preferred product [1,32].

^1H NMR		^{13}C NMR	
δ /ppm	Coupling /Hz	δ /ppm	Coupling /Hz
3.36 (sept,4H,CH/B)	$^3J(HH)$ 6.7	61.87 (d,1C,C=N)	$^1J(PC)$ 48.3
3.37 (d/s,4H,CH/P)	$^3J(HH)$ 6.6	49.25 (d,4C,$P\underline{C}HMe$)	$^2J(PC)$ 11.8
1.33 (d,24H,CH_3/B)	$^3J(HH)$ 6.7	46.49 (s,4C,CH/B)	
1.16 (d,12H,CH_3/P)	$^3J(HH)$ 6.6	24.04 (d,4C,CH_3/P)	$^3J(PC)$ 5.6
1.05 (d,12H,CH_3/P)	$^3J(HH)$ 6.6	23.71 (s,8C,CH_3/B)	
		23.63 (d,4C,CH_3/P)	$^3J(PC)$ 4.3

Table 11.1: *^1H and ^{13}C NMR data (C_6D_6) for nitrileimine (109); d/s=doublet of septets.*

The addition of a stoichiometric equivalent of sulphur to (109) gave nitrileimine (110) (Equation 11.5).

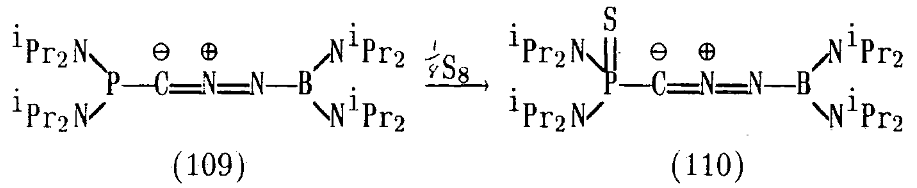
(11.5)

Furthermore, the P(V)-diazo compound (104) was synthesised *via* the three stages described above (Section 11.4.2) followed by the addition of sulphur and purification by column chromatography [9] before lithiation. Nitrileimine (110) was also synthesised independently (Equation 11.6). This also led to attack at nitrogen. Selected spectroscopic data on nitrileimine (110) are given in Table 11.2, and full experimental details in Section 11.13.2.

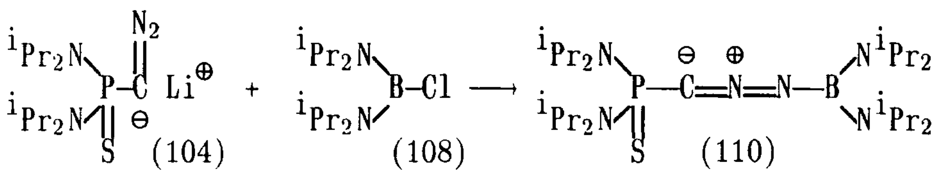
(11.6)

^{1}H NMR		^{13}C NMR	
δ /ppm	Coupling /Hz	δ /ppm	Coupling /Hz
3.60 (mult,6H,4CH/B, 2CH/P)		57.42 (d,1C,C=N)	^{1}J(PC) 125.28
		48.07	
3.39 (mult,2H,CH/P)		47.27 (d,4C,CH/P)	^{2}J(PC) ~40.0
1.34 (d,12H,CH_3/P)	^{3}J(HH) 6.5	46.66 (s,4C,CH/B)	
1.28 (d,24H,CH_3/B)	^{3}J(HH) 6.6	23.72 (s,8C,CH_3/B)	
1.19 (d,12H,CH_3/P)	^{3}J(HH) 6.7	23.70 (s,2C,CH_3/P)	
		23.49 (s,2C,CH_3/P)	
		22.91 (s,2C,CH_3/P)	
		22.55 (s,2C,CH_3/P)	

Table 11.2: *^{1}H and ^{13}C NMR data (C_6D_6) for nitrileimine (110).*

11.5 NITRILEIMINES WITH CARBON SUBSTITUENTS ON BORON

It was of interest to look at the behaviour of groups on boron forming B-C bonds, *eg*.

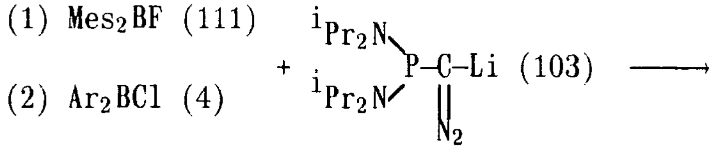

$$\begin{matrix}(1)\ Mes_2BF\ (111)\\(2)\ Ar_2BCl\ (4)\end{matrix} + ({}^{i}Pr_2N)_2P{-}\underset{\overset{\|}{N_2}}{C}{-}Li\ (103) \longrightarrow$$

where Ar = 2,4,6-tris(trifluoromethyl)phenyl.

Both of these groups are relatively large and hence would be expected to stabilise the nitrileimine structure. In (1) with (103), the reaction mixture turned deep pink with an infra-red absorption characteristic of a nitrileimine, a ^{31}P shift of +44ppm, but lithium fluoride did not separate (Experimental, Section 11.13.5).

Reaction (2) with (103) formed a black oil which was attributed to the attack of the lithium compound on the CF_3 groups. Even the reverse addition of the lithium compound to the boron monochloride gave a similar decomposition product (Section 11.13.6).

It is unfortunate that separation and full characterisation of these products did not prove to be possible.

11.6 BORON AND SILICON CONTAINING STABLE NITRILEIMINES

In a similar way the first nitrileimine containing both boron and silicon was prepared (Equation 11.7).

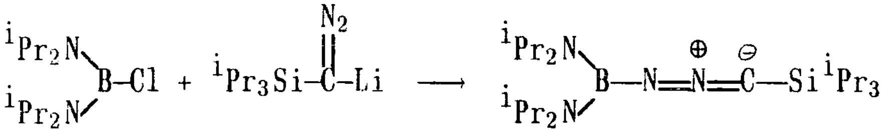

(108) (112) (113) (11.7)

Selected spectroscopic data for the nitrileimine (113) are presented in Table 11.3, and full experimental details are given in Section 11.13.7. The size of the groups attached to silicon appears to control the course of the reaction since when isopropyl groups are replaced by methyl, completely different products are obtained (See Section 11.13.19).

^{1}H NMR		^{13}C NMR
δ /ppm	Coupling /Hz	δ /ppm
3.61 (sept,2H,CH/B)	^3J(HH) 6.9	47.06 (s,2C,CH/B)
3.41 (sept,2H,CH/B)	^3J(HH) 6.9	46.33 (s,2C,CH/B)
1.31 (d,12H,CH_3/B)	^3J(HH) 6.6	23.40 (s,4C,CH_3/B)
1.19 (d,12H,CH_3/B)	^3J(HH) 6.8	23.25 (s,4C,CH_3/B)
1.04 (s,18H,CH_3/Si)‡		18.25 (s,6C,CH_3/Si)
		11.83 (s,3C,CH/Si)

Table 11.3: *^{1}H and ^{13}C NMR data (C_6D_6) for nitrileimine (113); ‡Underneath the propyl signal, 3H.*

11.7 SYNTHESIS OF CARBODIIMIDES FROM NITRILEIMINES

Irradiation of nitrileimines (109), (110) and (113) at 300 nm and 250 nm gave carbodiimides (114), (115) and (116) respectively. Formulae and selected spectroscopic data for these are given in Tables 11.4-11.6, with full experimental details in Sections 11.13.8 (114), 11.13.9 (115) and 11.13.10 (116).

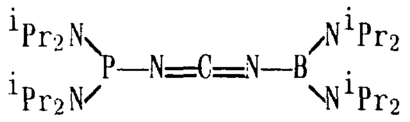

(114)

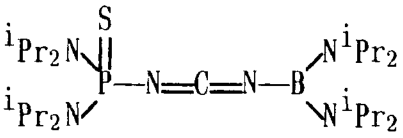

(115)

[also via (114) + 1/8S$_8$]

^{1}H NMR		^{13}C NMR	
δ /ppm	Coupling /Hz	δ /ppm	Coupling /Hz
3.61 (d,sept,4H,CH/P)	^{3}J(HH) ~6‡	46.29 (s,4C,CH/B)	
3.39 (sept,8H,CH/B)	^{3}J(HH) ~6	45.79 (d,4C,CH/P)	^{2}J(PC) 12.53
1.35 (d,12H,CH$_3$/P)	^{3}J(HH) 6.7	~24.4 (4xs,8C,CH$_3$/P†)	
1.24 (d,24H,CH$_3$/B)	^{3}J(HH) 6.7	~23.9 (s,8C,CH$_3$/B)	
1.20 (d,12H,CH$_3$/P)			

Table 11.4: *^{1}H and ^{13}C NMR data (C$_6$D$_6$) for carbodiimide (114); ‡^{3}J(PH) is not resolved; †Inequivalent.*

^{1}H NMR		^{13}C NMR	
δ /ppm	Coupling /Hz	δ /ppm	Coupling /Hz
3.53 (d,sept,8H,CH/P)	^{3}J(HH) ~6‡	46.16 (s,4C,CH/B)	
3.32 (sept,8H,CH/B)	^{3}J(HH) ~6	45.70 (d,4C,CH/P)	^{3}J(PC) 69†
1.18 (d,12H,CH$_3$/P)	^{3}J(HH) 6.6	23.73 (s,8C,CH$_3$/B)	
1.13 (d,24H,CH$_3$/B)	^{3}J(HH) 6.7	23.39 (s,8C,CH$_3$/P)	
1.02 (d,12H,CH$_3$/P)	^{3}J(HH) 6.3	22.54	
		22.27	

Table 11.5: *^{1}H and ^{13}C NMR data (C$_6$D$_6$) for carbodiimide (115); ‡^{3}J(PH) is not resolved; †Or small ^{3}J(PC) and 2 singlets.*

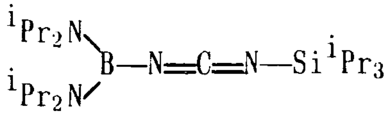

$({}^{i}Pr_2N)_2B{-}N{=}C{=}N{-}Si{}^{i}Pr_3$ (116)

¹H NMR		¹³C NMR
δ /ppm	Coupling /Hz	δ /ppm
3.46(mult,8H,CH/B)		84.6 (weak*,1C,N=C=N?)
1.93(mult,8H,CH/Si)		~48 (s's,11C,CH/ⁱPr,B/Si)
1.18(d's,24H,CH_3/B)	$^3J(HH)$ 2.9	20 (s,8C,CH_3/B)‡
1.13(d,18H,CH_3/Si)	---	~14 (s's,6C,CH_3/Si)
		11

Table 11.6: *¹H and ¹³C NMR data (C_6D_6) for carbodiimide (116); *not well defined; ‡possibly CH/Si carbon.*

A possible mechanism for this rearrangement has been proposed [10] which postulates an aziridine intermediate. This is outlined in Figure 11.5. It seems likely that the rearrangement of the B/Si nitrileimine (113) occurs similarly.

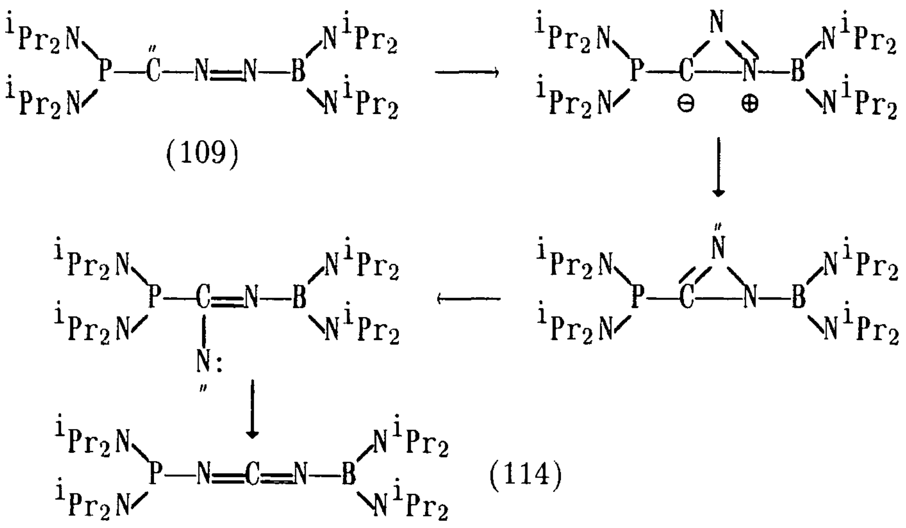

Figure 11.5: *Proposed mechanism for rearrangement of (109) to (104).*

Further information has been sought from a theoretical perspective using MNDO calculations. The details of the calculation and further discussion are given in Section (11.12). They predict a significant interaction between C(1) and N(3) with a partial bond of order 0.3, *ie.*

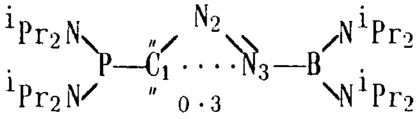

Thus, in the ground state, the C(1)–N(3) bond required in the rearrangement has already begun to form.

The nitrileimine rearrangement to carbodiimide *via* the nitrene intermediate is very similar to the well-known Wolff rearrangement (which involves the migration of an alkyl or aryl group to an electron deficient carbon centre), and the analogous migration to an electron deficient nitrogen *eg.* a nitrene which is a feature of the Hof mann reaction. Both of these are discussed by Sykes [34] and are represented in Figure 11.6.

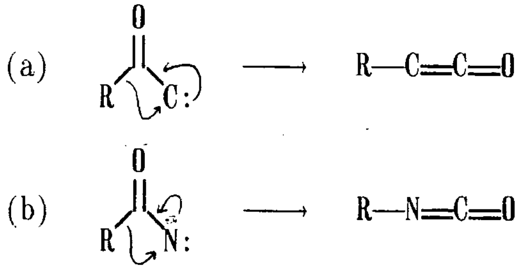

Figure 11.6: *(a) The Wolff rearrangement; (b) The Hofmann reaction.*

In contrast to the expected rearrangement of nitrileimine (109) to the carbodiimide (114), ***on one occasion***, photolysis at 250 nm resulted in a species with ^{31}P shift at +139 ppm [35] possibly in line with the proposed structure (117):

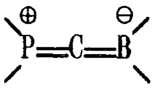

(117)

An alternative synthesis of this proposed structure (117) involved the addition of an electron donating substituent to boron thus increasing the negative charge here and forcing the rearrangement to this part of the molecule. The reaction of nitrileimine (109) with triethylamine after several days stirring at room temperature gave a ^{31}P

shift of +139 ppm. The nitrileimine absorption was also found to be absent from the infrared spectrum. By using a smaller attacking amine (trimethylamine), it was hoped to increase the rate of reaction. However, decomposition resulted and the product was not identified (Section 11.13.11/12).

The rearrangement from nitrileimine to the postulated carbene species may proceed *via* the diazo compound (118) as a key intermediate, followed by the loss of nitrogen [Figure 11.7].

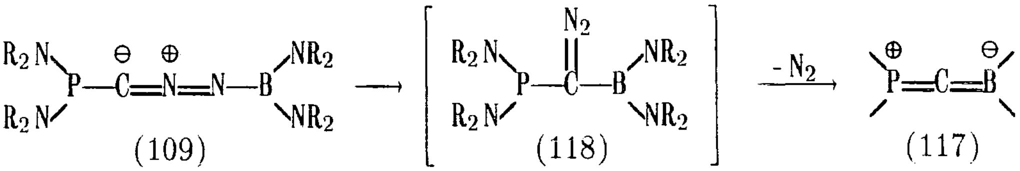

Figure 11.7: *Possible mechanism for conversion of (109) to (117).*

11.8 1,3-DIPOLAR CYCLOADDITION CHEMISTRY

1,3 dipolar cycloaddition is a versatile method for the stereo- and regio-selective synthesis of penta-atomic heterocyclic rings [9,36-40]. The nitrileimine structure has four delocalised electrons distributed over three atoms and thus is electron rich. Consequently some of the higher energy orbitals are occupied. Nitrileimines readily form cycloadducts with electron poor alkenes (dienophiles). Consider the series of dienophiles (Figure 11.8).

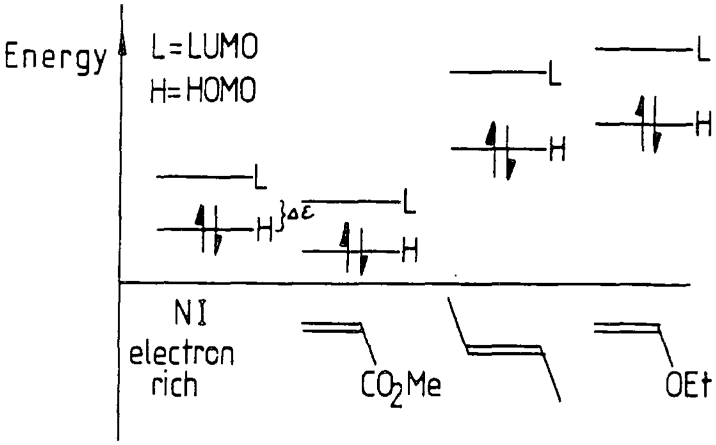

Figure 11.8: *HOMO and LUMO representation of a series of dienophiles (ref.41).*

Donation of electrons occurs from HOMO of the nitrileimine to the LUMO of the alkene. Hence, the greater the electron deficiency of the alkene, the smaller the value of Δε and the more favourable is the reaction.

Cycloaddition reactions were studied with nitrileimines (109), (110) and (113) in conjunction with the dienophiles-methyl fumarate (119) and methyl acrylate (120), *eg.* nitrileimine (109) with methyl fumarate gave cyclo-adduct (121) (Equation 11.8). Selected spectroscopic data for the cycloadduct (121) are presented in Table 11.7 with full experimental details in Section 11.13.13.

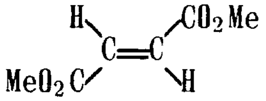
(119)

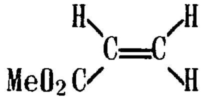
(120)

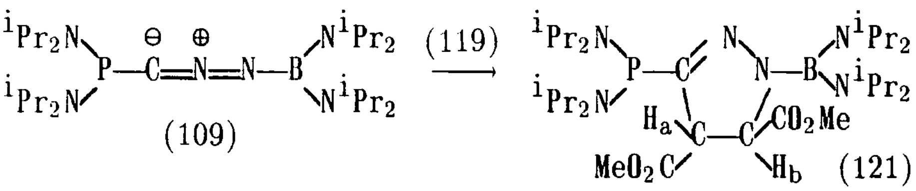
(109)
(121)

(11.8)

The P(V) species (110) reacts similarly to give (122) (Equation 11.9). The boron-silicon containing nitrileimine (113) produces an analogous adduct (123) (Equation 11.10). Cycloadduct (122) can also be made by reaction of (121) and sulphur (Equation 11.11).

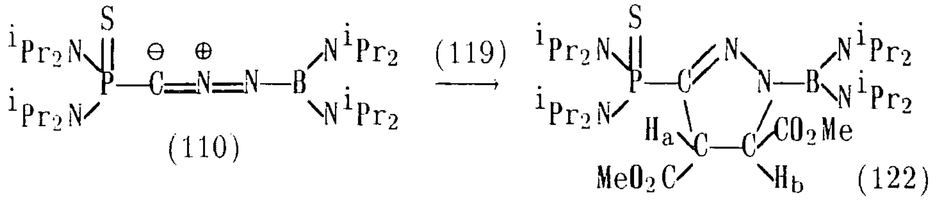

(11.9)

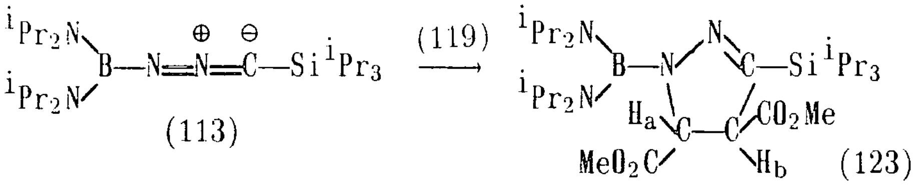

(11.10)

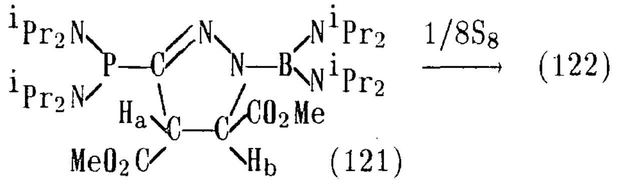

(11.11)

Selected spectroscopic data for the cycloadducts (122) and (123) are presented in Table 11.8 with full experimental details in Sections 11.13.14 and 11.13.15 respectively.

^1H NMR		^{13}C NMR	
δ /ppm	Coupling /Hz	δ /ppm	Coupling /Hz
4.74 (d.d,1H,H_a)	$^3J(H_aH_b)$ 7.02	173.42 (s,1C,C=O)	
	$^3J(PH_a)$ 1.44	171.71 (s,1C,C=O)	
3.97 (d.d,1H,H_b)	$^3J(H_aH_b)$ 6.94	146.71 (d,1C,C=N)	$^2J(PC)$ 17.4
	$^4J(PH_b)$ 1.42	64.51(d,1C,C-ring)	$^3J(PC)$ 3.86
3.73 (s,3H,CO_2Me)		60.16 (s,1C,OMe)	
3.65 (s,3H,CO_2Me)		59.57 (s,1C,OMe)	
3.57 (mult,8H,CH/B+P)		52.05 (d,1C,C-ring)	$^2J(PC)$ 8.0
1.23 (d,6H,CH_3/P)	$^3J(HH)$ 7.06	47.95 (s,4C,CH/B)	
1.18 ('d',6H,CH_3/P)	---	47.83 ('d',2C,CH/P)	
1.15 (d,24H,CH_3/B)	$^3J(HH)$ 7.03	47.67 ('d',2C,CH/P)	
1.06 (d,6H,CH_3/P)	$^3J(HH)$ 6.61	26.79 (impurity)	
1.02 (d,6H,CH_3/P)	$^3J(HH)$ 6.58	24.08, 23.99 (x2), 23.91,	‡
		23.76, 23.68 (x2), 23.56	
		23.41 (s,8C,CH_3/B)	

Table 11.7: *^1H and ^{13}C NMR data (C_6D_6) for cycloadduct (121); ‡all singlet peaks (CH_3/P).*

^1H NMR		^{13}C NMR	
δ /ppm	Coupling /Hz	δ /ppm	Coupling /Hz
4.62 (d.d,1H,H_b)	$^3J(H_aH_b)$ 4.5‡	172.19 (s,1C,C=O)	
4.22 (d.d,1H,H_a)	$^3J(H_aH_b)$ 4.5‡	171.38 (s,1C,C=O)	
4.06 (mult,6H,*)	$^3J(HH)$ 7.0	143.27 (d,1C,C=N)	$^1J(PC)$ 158.2
3.82 (mult,2H,CH/P)		66.05(d,1C,C-ring)	$^3J(PC)$ 3.6
3.73 (s,3H,$CO_2\underline{Me}$)		56.97(d,1C,C-ring)	$^2J(PC)$ 26.0
3.69 (s,3H,$CO_2\underline{Me}$)		52.35, 48.13 (2xs,2C,OMe)	
1.39, 1.37, 1.34, 1.26 (d,24H,CH_3/P)	$^3J(HH)$ ~7†	47.14 (d,2C,CH/P)	$^2J(PC)$ 5.1
		46.98 (d,2C,CH/P)	$^2J(PC)$ 6.9
		26.76 (s,4C,CH/B)	
1.15(d,24H,CH_3/B)	$^3J(HH)$ 6.7	24.34, 24.28, 24.22, 24.18 (4xs,6C,CH_3P)	
		23.32 (s,8C,CH_3/B)	
5.01 (d,1H,H_a)	$^3J(H_aH_b)$ 4.8	172.71 (s,1C,C=O)	
4.24 (d,1H,H_b)	$^3J(H_aH_b)$ 4.8	171.03 (s,1C,C=O)	
3.85 (sept,2H,CH/B)	$^3J(HH)$ ~6	164.93 (s,C=O,**)	
3.40 (sept,2H,CH/B)	$^3J(HH)$ ~6	143.26 (s,1C,C=N)	
3.31 (s,3H,OMe ring)		133.40 (s,C=C,sym. fumarate)	
3.29 (s,3H,OMe ring)		64.13 (s,2C,CH/B)	
3.26 (s,**)		61.32 (s,2C,CH/B)	
~1.5 (mult,3H,CH/Si)		51.58 (s,1C,OMe ring)	
1.37 (d,6H,CH_3/B)	$^3J(HH)$ 6.58	48.47 (s,OMe,**)	
1.29 (d,6H,CH_3/B)	$^3J(HH)$ 6.88	47.29 (s,1C,CH/B)	
1.18 (d,6H,CH_3/B)	$^3J(HH)$ 6.78	27.10 (s,2C,CH_3/B)	
1.14 (d,6H,CH_3/B)	$^3J(HH)$ 5.71	23.79 (s,2C,CH_3/B)	
1.05 (d,18H,CH_3/Si)	$^3J(HH)$ 5.88	23.48 (s,6C,CH_3/Si)	
		18.90 (s,2C,CH_3/B)	
		18.80 (s,2C,CH_3B)	
		12.13 (s,3C,CH/Si)	

Table 11.8: *^1H and ^{13}C NMR data (C_6D_6) for cycloadducts (122) (above) and (123) (below); ‡$^3J(PH)$ not resolved; *Ratio CH/B:CH/P = 2:1; **unreacted fumarate starting material; †Complex.*

11.8.1 Stereochemical Considerations

The methyl fumarate molecule has the *trans* configuration [Figure 11.9(a)]. If a single stage reaction occurs it would be expected that the *trans* configuration would be preserved in the product (121) [Figure 11.9(b)].

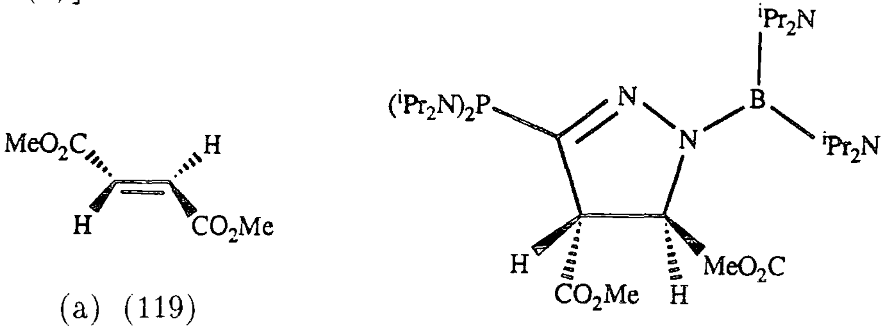

(a) (119)

(b) (121)

Figure 11.9: *Title; (a) trans configuration of methyl fumarate; (b) retention of configuration in the product.*

Evidence that this is the case is provided by the large coupling constant of $^3J_{H_aH_b}$ (Table 11.9) (values are of the order of staggered hydrogen atoms in iso-propyl).

COMPOUND		$^3J(H_aH_b)$/Hz
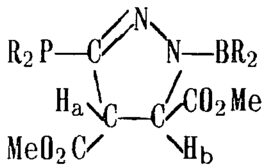	(121)	~ 7.0
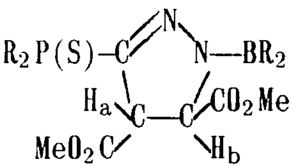	(122)	4.5
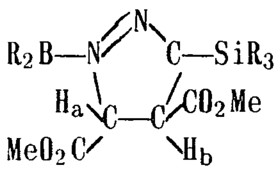	(123)	4.8

Table 11.9: *$J(H_aH_b)$ coupling constants for cycloadducts (121)-(123).*

11.8.2 Regiospecificity

Reactions with the unsymmetrical methyl acrylate (120) allowed a study of regiospecificity in this system. Isomers were formed in the ratio 3:1 (Figure 11.10). Selected spectroscopic data for the cycloadducts (124) and (125) are presented in Table 11.10 with full experimental details in Section 11.13.16.

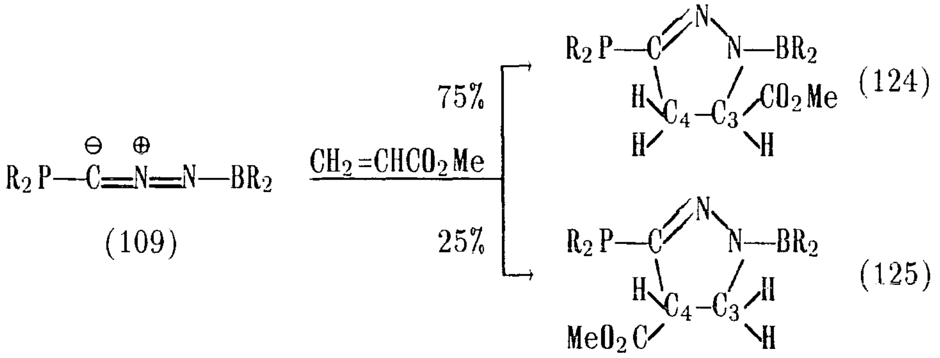

Figure 11.10: *Reaction of nitrileimine (109) with methyl acrylate (120).*

^{1}H NMR		^{13}C NMR	
δ /ppm	Coupling /Hz	δ /ppm	Coupling /Hz
4.58 (d.d,1H,H_x)	$^3J(H_bH_x)$ 7.58	174.47(s,1C,C=O)	
	$^3J(H_aH_x)$12.06	152.06(d,1C,C=N)	^1J(PC) 5.68
~3.8 (mult,8H,CH/B+P)		60.36(d,1C,C•/CO$_2$Me)	^3J(PC) 5.38
~3.5 (mult,2H,H_aH_b)		48.28(s,1C,CO$_2$Me)	
3.33 (s,3H,CO$_2$Me)		42.53(d,1C,CH$_2$•)	^2J(PC) 41.12
~1.3 (s,18H,CH$_3$/P)		~48 (d's,8C,CH/P)	
~1.3 (s,18H,CH$_3$/B)		~27 (s,8C,CH/B)	
		24 (8xs,16C,CH$_3$/P)	
*3.4 (s,3H,OMe)		23 (s,16C,CH/B)	
		*172.70(s,1C,C=O)	
		*150.22(d,1C,C=N)	^1J(PC) 13.9
		* 54.61(d,1C,CH$_2$•)	^2J(PC) 36.9
		* 52.46(d,1C,CO$_2$Me•)	^3J(PC) 2.97
		* 51.3 (s,1C,CO$_2$Me)	

Table 11.10: *^{1}H and ^{13}C NMR data (C_6D_6) for cycloadduct (124); *Data for 25% isomer (125); • = on ring.*

The formation of these two regioisomers may be explained by consideration of the HOMO of the nitrileimine (Figure 11.11).

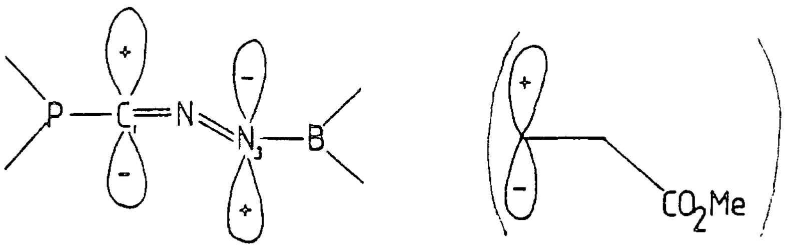

Figure 11.11: *HOMO for nitrileimine (109).*

The large coefficients on C(1) and N(3) allow the alkene to add in either orientation. The site of the larger **HOMO** density coefficient corresponds to the more electronegative terminus (the expected site of attack by the electrophile). The site of the largest LUMO coefficient is the least negative terminus and provides the site for attack by the nucleophile [41]. The isomers (124) and (125) can be distinguished by ^{13}C NMR spectroscopy. In (124), C(3) is more deshielded with a smaller $^{3}J_{PC}$ coupling constant. In (125), the most deshielded carbon is C(4) and this has the larger coupling with phosphorus [*cf.* C(3)] (see Figure 11.10, and for spectra, Figure 11.20).

With the presence of boron it is important to consider electron back-donation from nitrogen to boron. The geometry at the nitrogen is determined by the degree to which the nitrogen lone pair back-donates. The possibility of two rotamers exists, with boron fixed up or down with respect to the nitrileimine backbone. However since these could not be detected in the case of the reaction with methyl fumarate, the diagnosis of the presence of two regioisomers in this case is justified (together with the ^{13}C NMR evidence).

Since (124) is the predominant isomer, 'fixing' of the geometry at boron does *not* appear to be significant. The isomers were not separated but each was distinguished by ^{13}C NMR spectroscopy. Separation using column chromatography was considered but was judged inappropriate owing to the sensitivity of the boron to air and traces of moisture. Removing the boron from the system by cleaving the B-N bond (Figure 11.12) may provide a possible route to adduct separation and isolation.

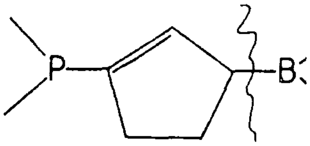

Figure 11.12: *Possible removal of boron from the compound.*

It is very interesting to note that in the case of the sulphur containing P(V) nitrileimine (110) only one isomer was formed by cycloaddition with methyl acrylate (120) (Equation 11.12, R = ^{i}Pr). This [and the predominance of isomer (124) with the P(III) nitrileimine] is attributed to the steric bulk at phosphorus. In the case of P(V) the presence of the sulphur atom provides sufficient bulk to prevent the formation of any of the isomer with the ester group on the same side of the molecule as the phosphorus.

The addition of elemental sulphur to isomers (124) and (125) in the P(III) case produced one isomer only (Equation 11.13). It seems that the cycloaddition may be reversible thus providing the route for the conversion of isomer (125) into the more stable form (Equation 11.14). If sulphur only added to isomer (124), it would have been expected that the phosphorus shift of (125) would still have been evident. This was not observed.

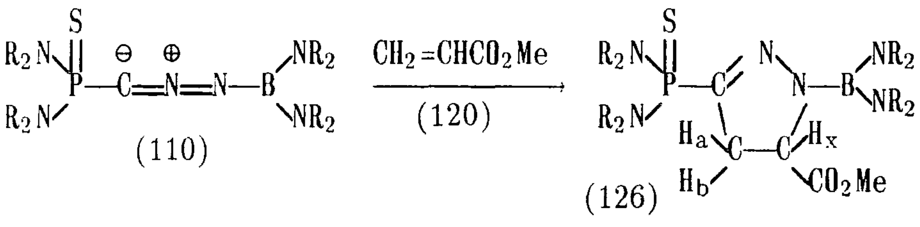

(11.12)

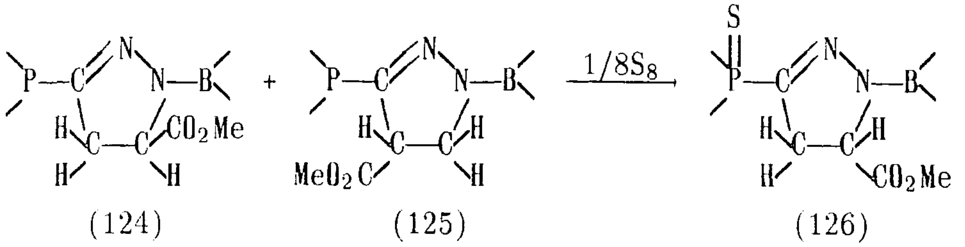

(11.13)

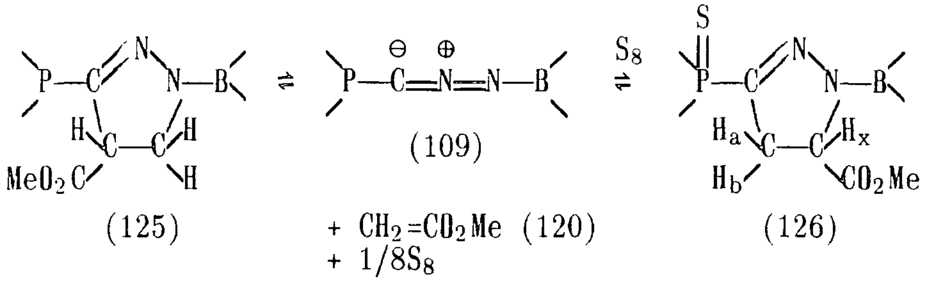

(11.14)

Selected spectroscopic data for the cycloadduct (126) are presented in Table 11.11 with full experimental details in Section 11.13.17.

^1H NMR		^{13}C NMR	
δ /ppm	Coupling /Hz	δ /ppm	Coupling /Hz
4.55 (d.d,1H,H_x)	$^3J(H_bH_x)$ 5.3	174.0 (s,1C,C=O)	
	$^3J(H_aH_x)$13.4	147.5 (d,1C,C=N)	$^1J(PC)$ 150.9
3.9 (mult,8H,CH/P)	$^3J(HH)$ ~6.6	60.8 (d,1C,$CHCO_2Me$)	$^3J(PC)$ 3
3.7 (mult,8H,CH/B)	$^3J(HH)$ ~6.6	~41.4 (d,1C,CH_2•)	$^2J(PC)$ 23.2
3.5 3.4 (mult,2H,CH_2•)		47 (d's,8C,CH/P)	$^2J(PC)$ ----
		~28 (s,8C,CH/B)	
3.28 (s,3H,CO_2Me)		26.5 (s,16C,CH_3/B)	
1.5 1.3 (d's,24H,CH_3/P)	$^3J(HH)$ ~6.8	~24 (8xs,16C,CH/P)	
1.2 (d,24H,CH_3/B)	$^3J(HH)$ ~6		

Table 11.11: *^1H and ^{13}C NMR data (C_6D_6) for cycloadduct (126); •=ring.*

An interesting extension of this work would involve a study of the reaction of nitrileimine (113) with CH_2=$CHCO_2Me$ (120) in order to investigate the regiochemistry involved.

11.9 REACTION OF NITRILEIMINE (109) WITH TETRACHLOROORTHOQUINONE

Orthoquinones are known to react across double bonds and to form P(V) species [42]. Nitrileimine (109) was reacted successively with sequential molar equivalents of tetrachloroorthoquinone (127). No products were isolated, so the attempted rationalisation is based on ^{31}P NMR and infrared data only (Table 11.12).

11.9.1 Results

Addition of one equivalent of (127) caused loss of the nitrileimine absorption in the infrared and a ^{31}P NMR shift was obtained in the P(III) region. Two equivalents gave a characteristic P(V) ^{31}P chemical shift at -36 ppm. In addition, a white precipitate was formed too insoluble to allow solution NMR spectroscopy.

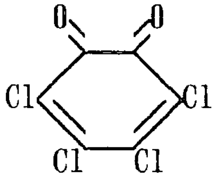

(127)

EQUIV.OF (127)	^{31}P NMR (δ/ppm)	IR OBSERVATIONS
1	+103	No NI absorption
2	-36	No NI absorption
3	+19	Decomposition

Table 11.12: *Addition of TCOQ to nitrileimine (NI) (109).*

11.9.2 Possible Reaction Mechanism

A possible reaction mechanism for this system is presented in Figure 11.13(a). From a model of this system it appears that this seven membered ring would be possible without substantial strain [Figure

11.13(b)]. Other possibilities to account for the observed experimental data include 6 membered rings [Figure 11.13(c)].

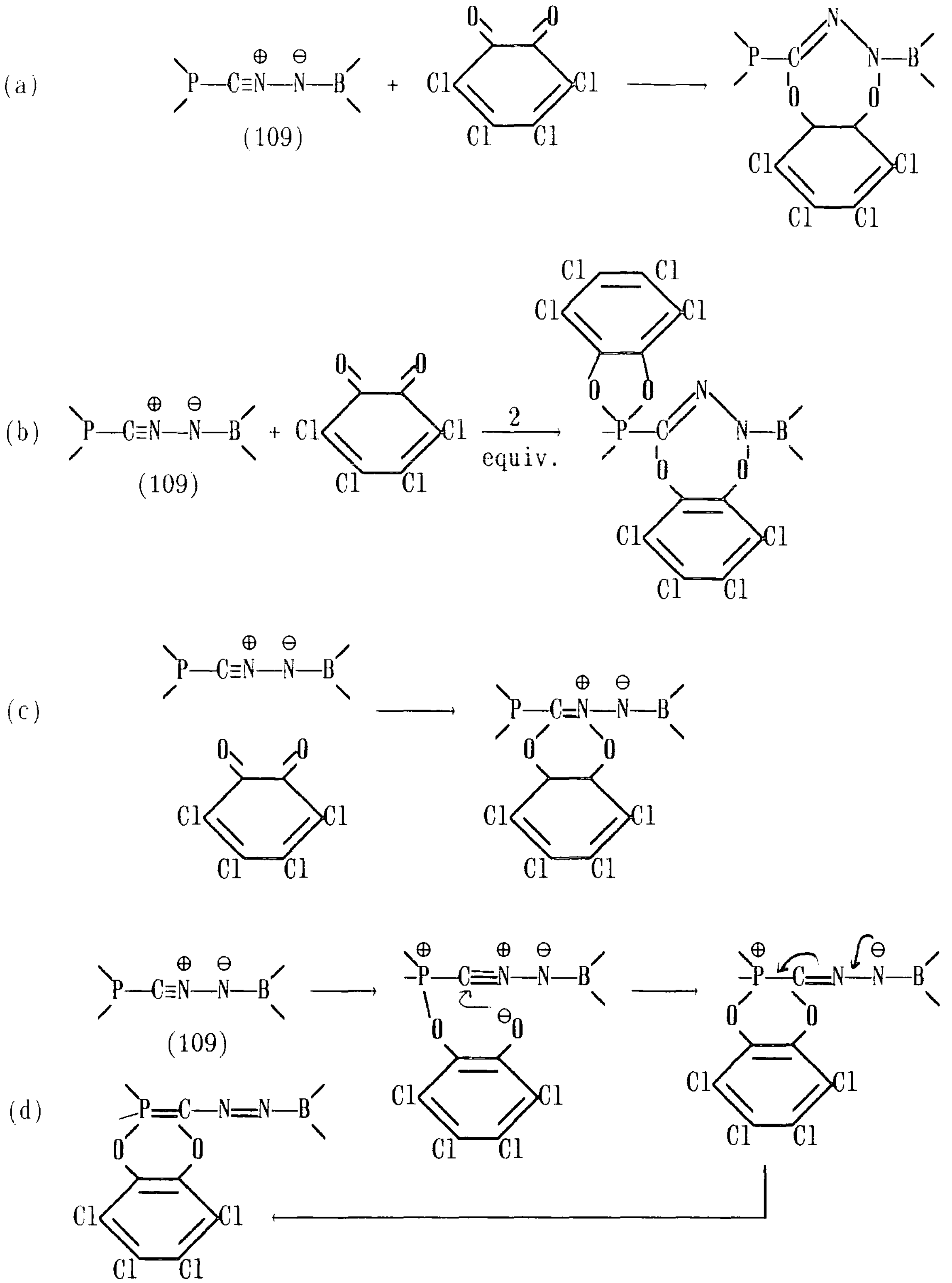

Figure 11.13: *Proposed reaction mechanism for TCOQ (127) and nitrileimine (109).*

11.10 PROPOSED SYNTHETIC ROUTES TO 'BORON-DIAZO' COMPOUNDS

To date, no stable boron diazo species are known, some possible guidelines for their synthesis are considered here.

11.10.1 Increasing Negative Charge at Boron

Increasing the negative charge at the boron of the nitrileimine can be achieved, for example, by reaction with a tertiary amine. It appears that this causes rearrangement to $>\overset{+}{P}{=}C{=}\overset{-}{B}<$ (117), possibly *via* an unstable diazo compound which eliminates N_2 (Section 11.7). It is difficult to see how the diazo compound can be stabilised at the same time as destabilisation of the nitrileimine. A similar reaction could be tried with nitrileimine (113):

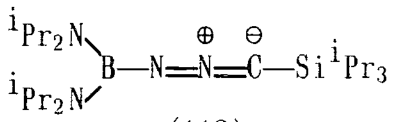

$({}^iPr_2N)_2B{-}N{=}\overset{\oplus}{N}{=}\overset{\ominus}{C}{-}Si{}^iPr_3$

(113)

11.10.2 Reduction in Substituent Size

Reduction of the group size on boron was done in an attempt to disfavour the formation of a nitrileimine. A direct analogy to work by Bertrand *et al.*[32], with the phosphorus derivatives [Figure 11.14(a)]. With smaller dimethylamino groups on phosphorus, the reaction proceeds as shown in Figure 11.14(b).

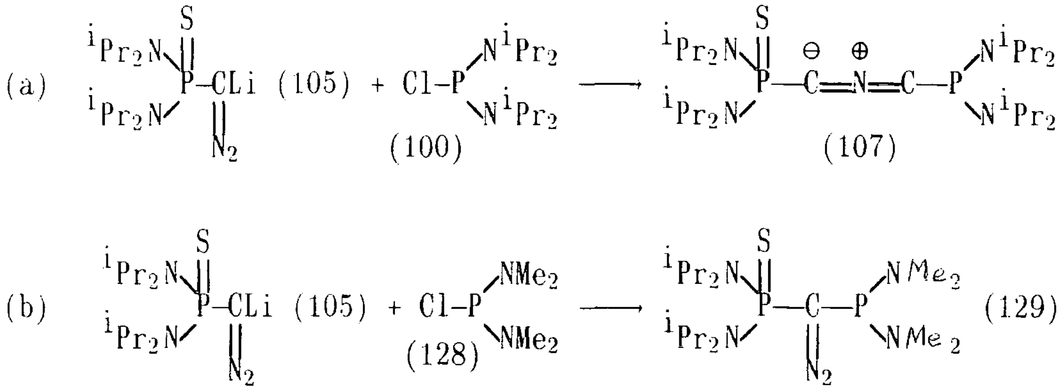

Figure 11.14: *The effect of reducing substituent size at phosphorus.*

The reaction of $(^iPr_2N)_2PC(N_2)Li$ (103) with $(Me_2N)_2BCl$ (130) did not give the expected results (Section 11.13.20). A peak at +139 ppm in the ^{31}P NMR was observed, thought possibly to be due to $>\overset{+}{P}{=}C{=}\overset{-}{B}<$ (117). On cooling crystals were formed and isolated. The NMR shift varied depending on the solvent: 135.0 ppm (THF), 138.5 ppm (pentane) and 140.5 ppm ($CDCl_3$). The ^1H and ^{13}C NMR data clearly indicated that the solid was $(^iPr_2N)_2PCl$ (100).

Repetition of this experiment gave a diazo absorption in the infrared and a ^{31}P NMR shift as expected for $>P{-}C(N_2){-}P<$ (106). This was further identified by its characteristic shift on addition of sulphur, giving two further ^{31}P NMR signals corresponding to $>P(S){-}C(N_2){-}P<$ (129) and $>P(S){-}C(N_2){-}P(S)<$ (131) [32]. On addition of sulphur another peak also formed upfield at +50 pm, presumably due to the phosphorus and boron containing material. A shift to high field on addition of sulphur appears to be characteristic of a diazo species [32], and to low field of a nitrileimine species, *cf.* compounds (107) and (129). The infrared spectrum showed a broad absorption centred around 2100 cm^{-1} (it may be the nitrileimine species had formed due to B-N thermodynamic favourability).

In the presence of sulphur it was hoped to isolate the phosphorus-boron containing material by low temperature crystallisation, but no solid was obtained. Repetition of this experiment gave totally reproducible results.

It has proved very difficult to postulate a mechanism with the formation of bis(diisopropylamino)phosphorus(III) chloride, $({}^{i}Pr_2N)_2PCl$ (100). This reaction does not occur with the larger diisopropylamino groups on boron, only with the smaller dimethylamino groups, hence with more room around the boron, a 4-coordinated intermediate may be postulated (*cf.* Equations 11.15 and 11.16). A possible mechanism is shown in Figure 11.15. This rearrangement would also explain the appearance of $>PC(N_2)P<$ (106) by coupling of bis(diisopropylamino)phosphorus(III) chloride (100) with $>PC(N_2)Li$ (103). The other ^{31}P NMR signal must be generated *via* a different route.

$$({}^{i}Pr_2N)_2BCl \xrightarrow{AlCl_3} ({}^{i}Pr_2N)_2B^+ \ AlCl_4^- \qquad (11.15)$$

$$(Me_2N)_2BCl \xrightarrow{AlCl_3} (Me_2N)_2BCl\cdot AlCl_3 \qquad (11.16)$$

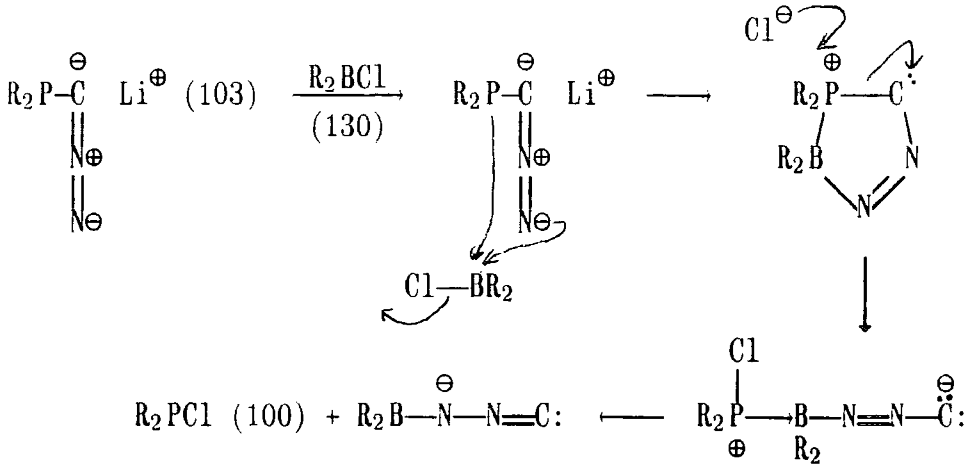

Figure 11.15: *Proposed mechanism for reaction of the phosphorus diazo compound (103) with $(Me_2N)_2BCl$ (130).*

It may be possible to prevent rearrangement *via* a four-coordinate intermediate by starting with four-coordinate boron (Equation 11.17).

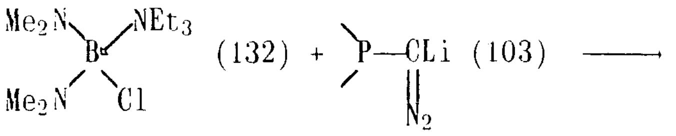

(132) + (103) (11.17)

11.10.3 Reduction of Group Size at Both Boron and Silicon

The reaction of the lithio diazo compound (112) with the boron halide has previously been shown to give a stable nitrileimine (Equation 11.7, see Section 11.6). Reduction of the size of the groups on silicon (*eg.* replacing $-Si^iPr_3$ with $-SiMe_3$) gave a complex reaction mixture, which had a broad absorption in the infrared around 2400-2000 cm^{-1}, and many peaks around 30-20 ppm in the ^{11}B NMR spectrum (possibly due to some diazo compound and some nitrileimine).

With the phosphorus diazo compound (103), reducing the size of the groups on boron has been investigated. This also led to a mixture of products (see earlier in this section).

In support of this experimental data an interesting reaction to try would involve reduction of the group size at silicon and boron, possibly kinetically favouring the diazo compound (Equation 11.18). *The presence of smaller groups may prevent bulky groups "pushing off" the* N_2.

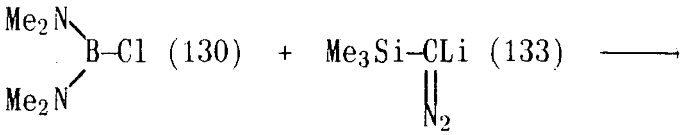

(130) + (133) (11.18)

11.10.4 Reaction Between Boron Triflate and Diazomethane

A reaction analogous to that used to form $Me_3SiC(N_2)H$ (99), by direct interaction of a covalent boron triflate [43] with diazomethane was attempted (Equation 11.19).

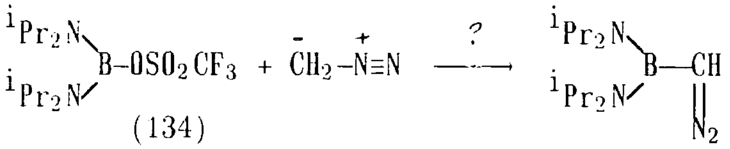

(134)

(11.19)

$PrNEt_2$ was added to scavenge for triflate, as for the trimethylsilyl derivative (99), preventing the following displacement of N_2 by precipitation of the salt:

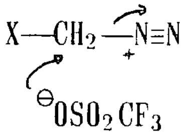

On reaction at -78 °C a yellow solution was formed with a white precipitate. As the temperature rose > -20 °C an apparent rapid polymerisation occurred, yielding a white apparently 'air stable' solid with a clear overlying liquid. The insoluble nature of this polymer limited spectroscopic data (Section 11.13.21).

It is known that if R_2BCl acts as an electron pair acceptor, formation of polymethylene may result with the initial step involving the coordination of the $-CH_2$ group of the diazomethane with the acceptor orbital (Equation 11.20) [44].

$$X_3B + H_2\overset{\ominus}{C}—\overset{\oplus}{N}\equiv N \longrightarrow X_3\overset{\ominus}{B}—CH_2—\overset{\oplus}{N}\equiv N \qquad (11.20)$$

This is followed by fast subsequent steps by elimination of N_2 and polymerisation. It is therefore clear that the less the boron species acts as an electron acceptor, the more likely it is to prevent this reaction.

Nitrogen: electron-donating substituents, bis(diisopropylamino), ($^{i}Pr_2N$) groups on boron are already in use. However, perhaps the bulk of the groups could be increased, for example to tetramethylpiperidine (tmp) groups. This will donate to the empty orbital on boron, and may be large enough to prevent polymerisation. However, the use of tmp groups makes the triflate ionic: $[(tmp)_2B^+][CF_3OSO_2^-]$ [43]. It is debatable whether this will make it more susceptible to attack since once the CH_2N_2 has reacted, the molecule will be covalent.

11.10.5 Conclusion

There appears to be a conflict as to whether small groups or large groups (Sections 11.10.3 and 11.10.4 respectively) would stabilise the boron-diazo compound.

<u>11.11 DIAZO-CARBENE CHEMISTRY WITH Ar GROUPS ON PHOSPHORUS</u>

Photolysis of the diazo compound $(^iPr_2N)_2PC(N_2)SiMe_3$ (101) or thermal elimination of N_2 at 250 °C under vacuum generates the stable carbene (Equation 11.21) [45-47]. It was of interest to look at the possible electronic and steric stabilisation of a carbene bearing the Ar group, 2,4,6-tris(trifluoromethyl)phenyl . The reaction (Equation 11.22) was therefore undertaken.

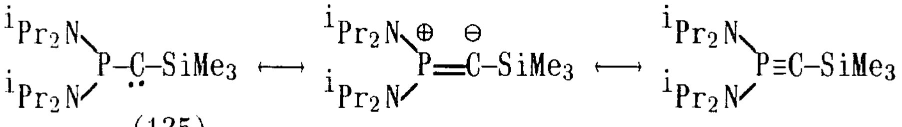

(135)

(11.21)

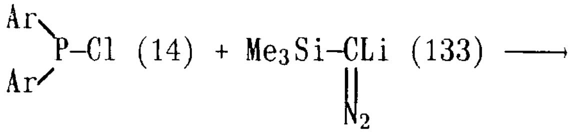

(11.22)

On dropwise addition of the Ar_2PCl (14) solution in ether to (133) at -78° in THF, a black oil was obtained which was attributed to possible 'Li' attack at the Ar ring fluorine atoms. There may also be a steric barrier to the introduction of this group, since the synthesis of 'Ar_3P' is not possible (attributed to the limited room around the tetrahedral phosphorus, see Chapter 2).

To avoid the Ar compound being in an excess of the lithium species, reverse addition was carried out with exactly similar results. The LiCl was inseparable. The ^{31}P NMR spectrum showed a 13 line splitting pattern at -8 ppm and a similar multiplet signal at -70 ppm. (A diazo absorption was present in the infrared spectrum). Attributing the former to $Ar_2P{-}C(N_2)SiMe_3$ (136), the peak at -70 ppm may correspond to a stable *carbene* (137) formed at room temperature.

Gentle heating and also photolysis of this mixture caused the signal at -8 ppm to disappear, reinforcing the diazo nature of this species. However, a marked increase in the signal at -70 ppm was not clear, perhaps due to the low concentration involved (Section 11.13.22).

This synthetic route is not satisfactory and the possibility of the peak at -70 ppm corresponding to Ar_2PH cannot be ruled out. It may be possible to avoid attack at the fluorine atom by generating a less reactive derivative, for example *via* a Grignard reagent [the solution put forward for a high yield synthetic route to Ar containing organoboron species (Chapter 8)]. The steric bulk of the Ar group may stabilise carbene (137) and aid its formation by N_2 elimination:

$$Ar_2\overset{\oplus}{P}{=}\overset{\ominus}{C}{-}SiMe_3 \longleftrightarrow Ar_2P{\equiv}C{-}SiMe_3 \quad (137)$$

11.12 MNDO CALCULATIONS

11.12.1 Introduction

The following calculations were done using MNDO as implemented in MOPAC version 5. In order to keep the calculations tractable, the model fragments (138), (139) and (140) have been used. This has the implication that the results have qualitative rather than quantitative value.

$H_2P{-}C{-}N{-}N{-}BH_2$ (138)

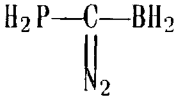

$H_2P{-}\underset{\|}{C}{-}BH_2$ (N_2 below C) (139)

$H_2P{-}C{-}BH_2$ (140) triplet (t) + singlet (s)

MNDO does *not* take into account contributions from d-orbitals [48-50], but it is known to give good results for P(III) species. H-substituents were used in the three systems, since with diisopropylamino there are too many atoms to carry out a reasonable calculation.

By replacing $^{i}Pr_2N$ with H, the steric effects of this group have been lost, together with the electronic effect of the nitrogen back-donating into boron. Although these parameters may alter the situation, a concept of the bonding involved is possible. The geometry has been optimised with no initial symmetry parameters.

11.12.2 Nitrileimine (138)

A previous calculation has been carried out on the parent nitrileimine, H_2CNNH [51].

For nitrileimine (138) the predicted final heat of formation is +56.8 kcal mol^{-1} and its ionisation potential is 10.16 eV.

Final Geometry

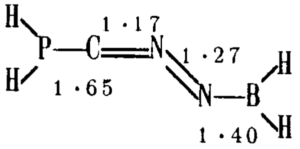

[*cf*. 1.72Å in the diazo]

HOMO (delocalised)

To summarise the nature of the HOMO, N(3): node (no contribution); N(6): large negative value, bigger and opposite to C(2); B: contribution in phase with nitrogen but a smaller value.

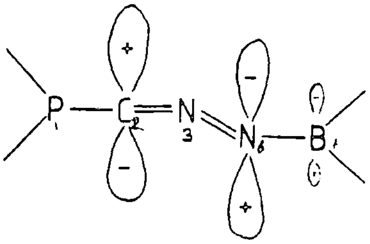

Bond Order

Calculated bond orders are: C(2)-N(3) = 2.5; C(2)-N(6) = 0.3 and N(6)-B(7) = 1.32.

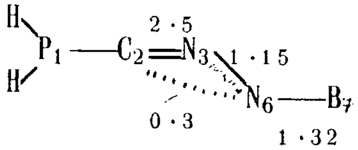

Valency

This indicates that the nitrogen lone pair is donating into the boron, however with $(^{i}PrN)_2B$, with two nitrogens already donating into boron this may be significantly lower. To summarise the results, N(3): expanded valency (more like the nitrilium ion); C(2): reduced valency (3.8) and N(6): reduced valency (2.86).

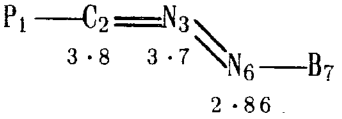

Localised Bonding Orbitals

(A consideration of orbitals lower in energy than these involves the σ-framework.)

Energy/eV	
-11.63	(N lone pair)
-15.27	(C-N π bond)
-15.75	(2 degenerate B-H bonds)
-16.24	(2 degenerate P-H bonds)

The boron-nitrogen bond (1.71Å) has contributions from the nitrogen lone pair and the σ-bond. The rest are effectively 2 centre bonds. The top localised orbital is the nitrogen lone pair donating into the boron The orbital below this in energy is the C(2)-N(3) π-bond. The most representative structure can be drawn with nitrogen in an expanded valency:

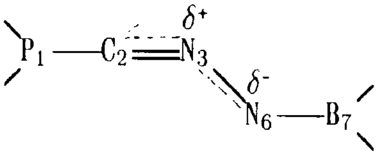

However, other canonical forms are important, for example, $C{\equiv}\overset{+}{N}{-}\overset{-}{N}$.

Nitrileimine Molecular Charge

This charge distribution will change with $^{i}Pr_2N$ groups on the boron and phosphorus. The boron here is not charged. *When amine substituents are present on boron this may not be the case.* [Perhaps by making the boron negatively charged the nitrileimine could be destabilised to form the diazo. This argument has been discussed previously (Section 11.1.1)].

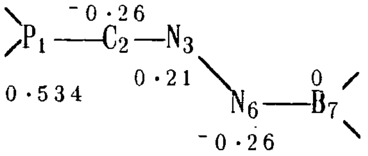

The next stage would be to do a similar calculation but with nitrogen substituents in place of the hydrogen atoms, *ie.* using the nitrileimine compound $(H_2N)_2P{-}C{=}N{=}N{-}B(NH_2)_2$ (141). This work is at present underway.

11.12.3 Calculation on Diazo (139)

The calculated heat of formation = 43.73 kcal mol^{-1}, *nb.* the diazo is 13 kcal more stable than the nitrileimine (however, the more steric demand of $^{i}Pr_2N$ and its inductive effect may counteract this, hence the difference in heats of formation of the two structures may not be so pronounced).

The calculated ionisation energy is 9.6eV, *cf.* 10.1 eV for the nitrileimine (in the diazo compound the slightly higher lying orbitals make it easier to ionise by 0.5 eV).

Molecular Geometry

Calculated bond lengths and angles are as follows: P-H = 1.34Å and B-H = 1.16Å (*cf.* 1.33Å and 1.17Å respectively in the nitrileimine); P-C = 1.72Å (larger than in the nitrileimine). The carbon atom is effectively flat with the P, B, N and C all in the same plane. The C(2)-N(3)-N(6) fragment is virtually linear. The C-N bond (1.36Å) is short, with some double-bonded character, and the N-N (1.12Å) close to that of molecular nitrogen, so it appears that the structure can be represented by the fragment, C-N≡N. The C-B bond is short (1.46Å) due to the negative charge donated from carbon to the boron vacant orbital. This effect would probably be reduced with nitrogen substituents on the boron.

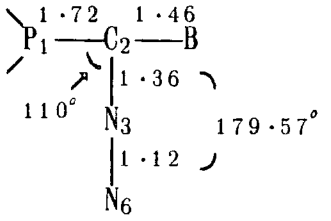

(139)

Highest Delocalised Molecular Orbital

The C-N-N π-system is basically delocalised into the boron atom. The next orbital energy level down is the phosphorus lone pair, followed by the B-H bonds in the delocalised orbital scheme.

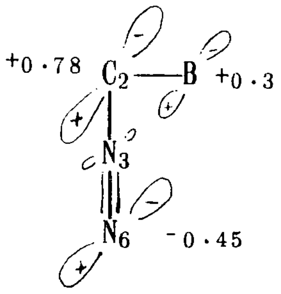

Charges

Here the carbon is more negatively charged than in the nitrileimine species.

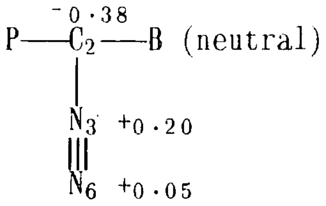

Bond Order and Valencies

The structure is almost N≡N so it is fairly unstable to the loss of N_2. N(3): has expanded valency, N^+ (3.7); P: normal valence; C: valence is reduced (3.58), it is on its way to becoming a carbene.

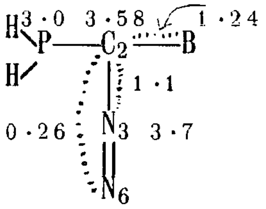

Diazo Localised Molecular Orbital

The electrons on carbon donate into boron (*cf.* the nitrileimine in which the nitrogen lone pair donates to the boron).

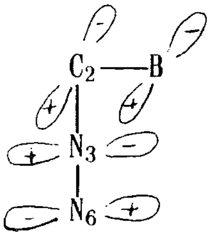

It appears that the diazo fragment is thermodynamically more stable than the nitrileimine. There is no information on the potential surface connecting the nitrileimine and the diazo species.

11.12.4 Triplet State >P–C–B< (140^t) (UHF)[2]

This system has already been calculated using the 3-21G 2nd order Mollerplesset theory [52], which is a much more rigorous calculation than that used here. However, very similar results have been obtained showing that the MNDO is comparable, and is an acceptable method for this system.

The unrestricted Hartree-Fock method treats up and down spin electrons differently with different energies and different orbital shapes, whereas the RHF system treats the up and down spin electrons equally. In this UHF system there are 7 β-electrons and 9 α-electrons, *ie.* 9 up, 7 down occupying different orbitals. The calculated heat of formation is 45.67 kcal mol^{-1}. Its geometry is nearly linear (175 ^{0}):

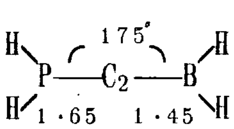

Highest Occupied Molecular Orbital

The two highest (singly occupied) orbitals have energies of -9.6 and -10.9, both α(up) spin. They are not degenerate. There is one electron in C(y), and one in C(z) and the latter can donate into the boron empty orbital so its energy is slightly lower.

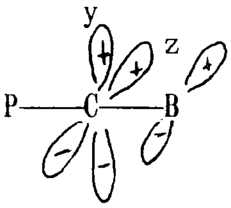

---

[2] The heats of formation here cannot be compared with the nitrileimine and the diazo compounds as these were calculated with RHF. Unrestricted Hartree-Fock (UHF) is used here since it gives an accurate picture of the electron spin distribution.

Charges

The C-B bond is σ-polarised, the negative charge resides on the carbon, π-donation is possible from only one electron to boron. With the Unrestricted Hartree-Fock (UHF) treatment, the amount bond orders are inaccurate is proportional to the amount of spin.
The spin *is* significant here and therefore bond orders *cannot* be accurately determined.

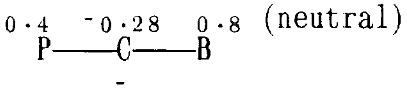

$$\overset{0\cdot4}{P}-\underset{-}{\overset{-0\cdot28}{C}}-\overset{0\cdot8}{B}\ \text{(neutral)}$$

Spin and Valency

Some spin is transferred to boron from donation by the p_z orbital on carbon. The expected value of the spin is 2, in the calculation it appears as 2.0239, hence there is no substantial spin contamination. The $C(p_z)$ orbital has slightly less spin than the $C(p_y)$ as it has transferred some spin to the boron.

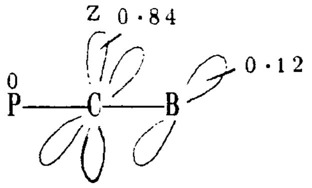

Spin

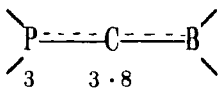

Valency

11.12.5 Singlet State >P–C–B< (140^S) (UHF)

A comparison of UHF type calculations can only be made with similar UHF calculations, *cf.* the triplet state. Heat of formation is 44 kcal mol^{-1}, so the singlet state is calculated to be slightly more stable than the triplet state. [8 doubly filled energy levels - all electron paired and therefore a different geometry is obtained]. The C-B bond length is shortened as the *two* electrons on the carbene carbon atom can donate into the boron empty orbital, increasing the bond order and hence the negative charge at boron.

Geometry and HOMO

Molecular geometry and the highest occupied molecular orbital are depicted below. Two electrons overlap with the boron orbital. The HOMO-1 (next highest molecular orbital) is the lone pair on the phosphorus.

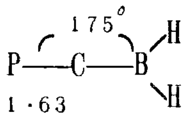

Geometry

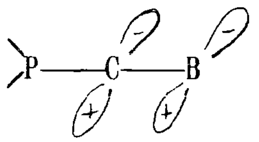

HOMO

Atomic Charges, Bond Order and Valency

More negative charge resides on boron due to more π-donation (*cf.* the triplet case). Bond orders for the singlet case cannot be compared with those in the triplet, since the UHF treatment for the triplet state precluded their calculation (Section 11.12.4). The bond order of P-C is 1.12 (slightly multiple bonded) whilst for B-C it is 1.74 (almost a B=C bond). The carbon valency of 3.09 corresponds to a significant valency decrease (*ie.* singlet carbon). The boron valency is 3.6 (*ie.* significantly increased). There are no unpaired electrons therefore it is possible to consider the ***localised orbitals***, as represented by a lone pair of electrons on carbon donating into boron. The next energy level down is the phosphorus lone pair.

The heat of formation for the diazo species (139) cannot be directly compared to that of the carbene (140) since even though by *definition* the heat of formation of N_2 is zero, the entropy must also be taken into account which will be large and positive.

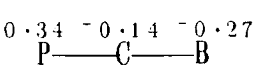

Charges

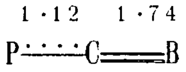

Bond Order

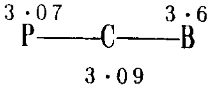

Valency

11.13 EXPERIMENTAL DETAILS

11.13.1 Preparation of (109)

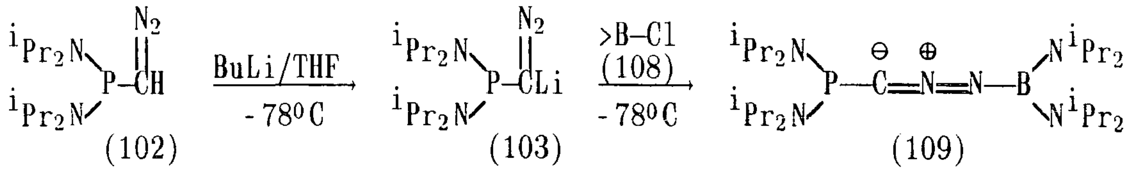

A solution of (102) (2g, 7.4 mmol) in THF (25 ml) was cooled to -78 ^{o}C and to it was added *n*-BuLi (4.6 ml, 7.4 mmol, 1.6 M), dropwise *via* syringe. The solution was stirred at -78 ^{o}C for 30 min, followed by the dropwise addition of bis-(diisopropylamino)boron chloride (108) (2 ml, 1.8g, 7.4 mmol, 1 equivalent) in THF (20 ml). The temperature was maintained at -78 ^{o}C until the addition was complete (15 mins) and then was allowed to slowly return to ambient temperature over a period of 2h. The THF was removed *in vacuo* and pentane (20 ml) was added to precipitate the LiCl formed in the reaction. The salts were removed by filtration and the filtrate was concentrated *in vacuo* to give (109) as a yellow oil (pure by ^{31}P NMR). Yield was 3.5g (98%) with some unreacted $(^{i}Pr_2N)_2BCl$ (108); bpt. 113 ^{o}C (0.2 mm Hg); IR (pentane) ν_{max}: 2100 cm^{-1}; MS (Intensity%) EI: 282 [100, $^{i}Pr_2N$-PC(N_2)B-$N^{i}Pr_2$]; ^{11}B δ: 29 ppm (s,broad); ^{31}P δ: 45.1 ppm. ^{1}H and ^{13}C NMR spectral data are presented in Table 11.1 (Section 11.4.3) (see also Figure 11.16).

11.13.2 Preparations of (110)

11.13.2.1 From Nitrileimine (109) and Sulphur

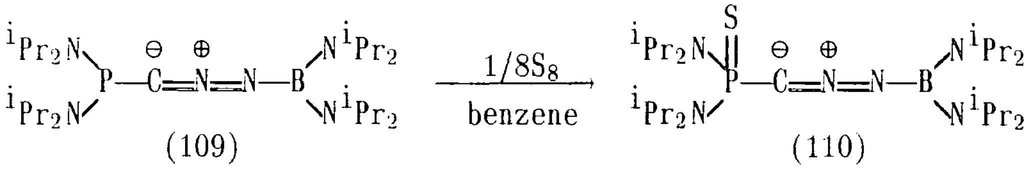

A solution of nitrileimine (109) (1g, 2.1 mmol) in benzene (25 ml) was placed in a 100 ml Schlenk tube. To this solution was added sulphur (0.074g, 2.18 mmol, 1.1 equivalents). The reaction mixture was stirred for 1 hour at room temperature, after which complete conversion to (110) was noted by ^{31}P NMR spectroscopy. The solvent was removed *in vacuo* and the product separated from excess sulphur by cooling to -30 °C in pentane (30 ml). Concentration of the filtrate allowed isolation of the pure nitrileimine (110). Yield was 900 mg (83% by weight) with some unreacted $({}^{i}Pr_2N)_2BCl$ (108).

11.13.2.2 From $({}^{i}Pr_2N)_2P(S)CHN_2$ (104)

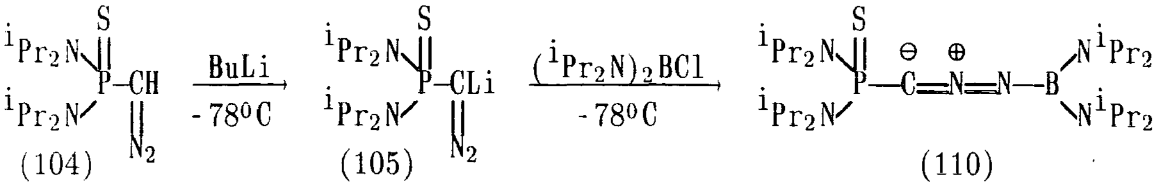

A solution of the yellow crystalline diazo compound (104) (500 mg, 1.6 mmol) in THF (25 ml) was cooled to -78 °C and to it was added ^{n}BuLi (1 ml, 1.6 mmol, 1 equivalent, 1.6 M) dropwise *via* syringe. The solution was stirred at -78 °C for 30 min followed by dropwise addition of bis(diisopropylamino)boron chloride (0.4g, 1.6mmol) in THF (10 ml). The temperature was maintained at -78 °C until the addition was complete (10 min), and then was allowed to slowly return to ambient temperature over a period of 2 hours. The THF was removed *in vacuo* and pentane (20 ml) was added to precipitate the LiCl formed in the reaction. The salts were removed by filtration and the product (110) was isolated as a white solid in pure form by crystallisation from pentane. Yield was 500 mg (61%); IR (C_6D_6) ν_{max}: 2095 cm^{-1}; ^{11}B δ: 27.8 ppm (s,broad); ^{31}P δ: 31.8 ppm (pentet) $^3J_{PH}$ 19.7 Hz. ^1H and ^{13}C NMR spectral data are presented in Table 11.2 (Section 11.4.3) (see also Figure 11.17).

11.13.3 Preparation of Mes$_2$BF

Very low yields were obtained by the use of organozinc compounds and other classical routes to organoboron species (Section 8.1). Higher yields (*ca.* 70%) were obtained by the preparative route, and use of specific apparatus designed by Professor Pelter [53].

Mes$_2$BF: air sensitive white solid, mpt. 70-72°C; bpt. 120-122°C (0.1 mm Hg); ^{11}B (CH_2Cl_2) δ: 53.5 ppm (s,broad).

11.13.4 Attempted Reaction of (111) with (101)

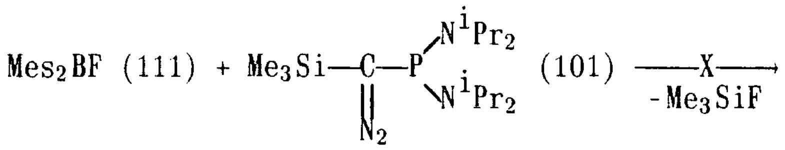

$$Mes_2BF\ (111) + Me_3Si{-}\underset{N_2}{\overset{\|}{C}}{-}P(N^iPr_2)_2\ (101) \xrightarrow[-Me_3SiF]{X}$$

Mes$_2$BF (0.8g, 3 mmol) in THF (10 ml) was added to a solution of phosphorus diazo compound (101) (1.0g, 3 mmol) at room temperature with stirring. After 1 hour, the ^{31}P NMR indicated that no reaction had taken place. The reaction mixture was warmed to 35 °C, and stirred at this temperature for 2 hours and no reaction occurred. The ^{31}P NMR signal (+54 ppm) corresponds to the starting material (101), with the corresponding diazo absorption in the infrared at 2020 cm^{-1}.

11.13.5 Reaction of (102) with (111)

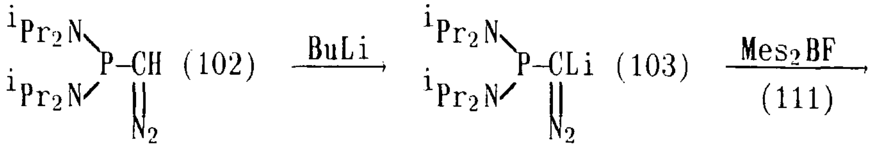

A solution of diazo compound (102) (0.51g, 1.9 mmol) was cooled in THF (25 ml) to -78 ^{o}C. BuLi (0.83 ml, 2.1mmol, 1.1 equivalents, 2.5 M) was added dropwise, and the solution stirred at -78 ^{o}C for 20 mins. Mes_2BF (0.51g, 1.9 mmol) in THF (15 ml) was added dropwise. On addition the solution turned bright pink. The THF was removed *in vacuo* to yield a pink oil. Addition of pentane gave no visible precipitate, and no lithium fluoride was separable. Cooling in pentane to -20 ^{o}C gave an apparent precipitate (LiF!). Filtration gave a pink solution, from which no crystalline product was obtained by cooling to -40 ^{o}C. IR (pentane) ν_{max}: 2120 cm^{-1}; ^{31}P δ: +44.97 ppm; ^{11}B δ: ~40 ppm; (br) ^{1}H NMR spectroscopy indicated a mixture of products.

11.13.6 Reaction of (103) with (4)

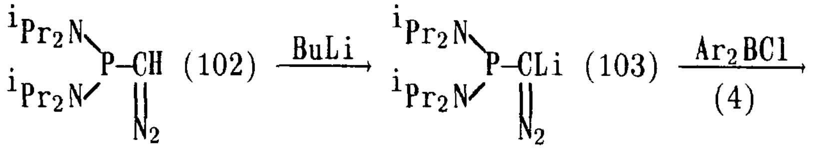

Ar = 2,4,6-tris(trifluoromethyl)benzene

A solution of diazo compound (102) (1.1g, 4.0 mmol) was cooled to -78^{o}C in THF (20 ml). BuLi (1.78 ml, 4.5 mmol, 1.1 equivalents, 2.5 M) was added dropwise, and the solution was stirred at -78 ^{o}C for 20 mins, followed by the dropwise addition of Ar_2BCl (4) (2.43g, 4.0 mmol) dissolved in THF (10 ml). Following the first drop of Ar_2BCl solution, the solution turned black. After complete addition the THF was removed *in vacuo*, and addition of pentane (20 ml) gave no LiCl precipitate. It was inseparable from the black oil. The very poor broad signal in the ^{31}P NMR spectrum (42 ppm) was attributed to decomposition. IR ν_{max}: 1160 cm^{-1} (broad). Reverse addition of the lithio compound to Ar_2BCl gave the same black oil attributed to the same decomposition process.

11.13.7 Preparation of (113)

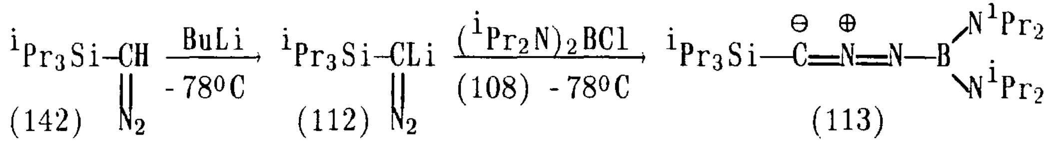

A solution of the diazo compound (142) (0.41g, 2.07 mmol) in THF (25 ml) was cooled to -78 °C, and to it was added $^{n}BuLi$ (1.29 ml, 2.07 mmol, 1 equivalent, 1.6 M) dropwise by syringe. The solution was stirred at -78 °C for 30 min followed by the dropwise addition of bis(diisopropylamino)boron chloride (0.51 ml, 2.07 mmol, 1 equivalent) in THF (10 ml). The temperature was maintained at -78 °C until the addition was complete (10 min) and then was allowed to slowly return to ambient temperature over a period of 2 hours. The THF was removed *in vacuo*, and pentane (10 ml) was added to precipitate the LiCl formed in the reaction. No immediate precipitation occurred, so the solution was cooled to -30 °C overnight to allow its separation. [This problem may have been overcome by the use of a crown ether]. The salts were removed by filtration. The filtrate was concentrated *in vacuo* to give (113) as a pale yellow oil (purified by crystallisation from $CDCl_3$). Yield was 800 mg (95%); IR ν_{max}: 2100 (C=N) cm^{-1}; Mass spectrum (EI) showed small fragments: 96 [100,^{i}Pr-Si]; ^{11}B (C_6D_6) δ: +28.1 (s,broad) ppm; ^{29}Si (C_6D_6) δ: 0.726 (s) ppm. ^{1}H and ^{13}C NMR spectral data are presented in Table 11.3 (Section 11.6) (see also Figure 11.18).

11.13.8 Preparation of (114)

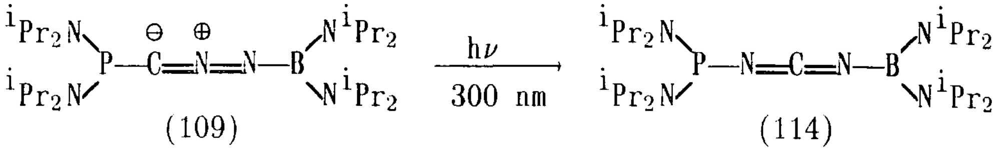

A solution of nitrileimine (109) (200 mg, 0.41 mmol) in d^6-benzene (5 ml) in a 10 mm pyrex NMR tube was irradiated at 300 nm for 12 hours. After irradiation was stopped the ^{31}P NMR spectrum showed complete conversion to a single new product. Removal of the solvent *in vacuo* gave carbodiimide (114) in quantitative yield as a pale yellow oil. Yield was 200 mg (100% by weight); IR (benzene) ν_{max}: 2200 (N=C=N) cm^{-1}; MS (Intensity%) EI: 257 [100,$(^iPr_2N)_2P$-N=C]; 211 [65,$(^iPr_2N)_2B$]; ^{11}B δ: +23 ppm (s,broad); ^{31}P δ: +82 ppm. ^1H and ^{13}C NMR spectral data are presented in Table 11.4 (Section 11.7).

11.13.9 Preparations of (115)

11.13.9.1 From Carbodiimide (114) and Sulphur

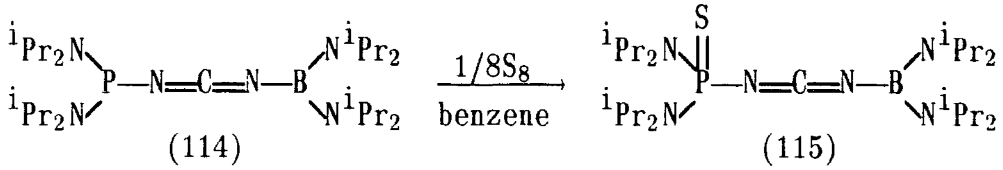

To a solution of the carbodiimide (114) (300 mg, 0.62 mmol) in benzene (15ml) was added sulphur (22 mg, 0.68 mmol, 1.1 equivalents). The reaction mixture was stirred for 1 hour at room temperature. Quantitative conversion to (115) was noted by ^{31}P NMR spectroscopy. The solvent was removed *in vacuo*, and the excess sulphur removed by crystallisation at -30 ^oC in pentane. The carbodiimide (115) was isolated as a yellow oil. Yield was 290 mg (91% by weight).

11.13.9.2 Via Photolysis of Nitrileimine (110)

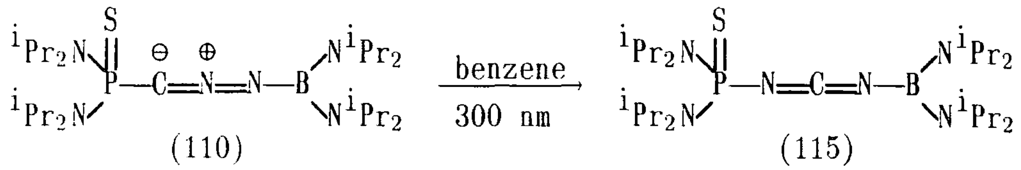

A solution of nitrileimine (110) (400 mg, 0.78 mmol) in d^6-benzene (5 ml) in a 10 mm pyrex NMR tube was irradiated at 300 nm for 12 hours. The solvent was removed *in vacuo*. Addition of pentane and cooling allowed the removal of any impurity by precipitation. Concentration of the filtrate gave the carbodiimide (115) in 60% yield (240 mg); IR (pentane) ν_{max}: 2200 (N=C=N) cm^{-1}; ^{11}B δ: 22 (broad) ppm; ^{31}P δ: 54.5 (pentet) ppm $^3J_{PH}$ 19.4 Hz. ^{1}H and ^{13}C NMR spectral data are presented in Table 11.5 (Section 11.7).

11.13.10 Preparation of (116)

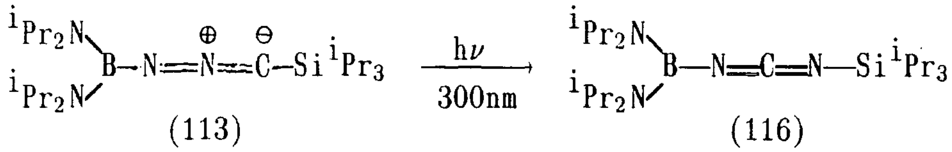

A solution of nitrileimine (113) (400 mg, 0.98 mmol) in d^6-benzene (5 ml) in a 10 mm Pyrex NMR tube was irradiated at 300 nm for 12 hours. The solvent was removed *in vacuo*. Addition of pentane and cooling allowed the removal of a small amount of solid material. The filtrate was concentrated to give the carbodiimide (116). Yield was 344 mg (86%). IR ν_{max}: 2200 cm^{-1}; ^{11}B (C_6D_6) δ: 22.2 ppm; ^{1}H and ^{13}C NMR spectral data are presented in Table 11.6 (Section 11.7).

11.13.11 Reaction of (109) with Et_3N

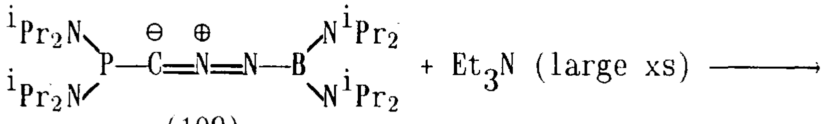

(109)

A solution of the nitrileimine (109) (0.40g, 0.83 mmol) in THF (25 ml) was reacted with Et_3N (0.5g, 5.0 mmol) at room temperature. After stirring for 2 hours there was no evidence of any reaction in the ^{31}P NMR spectrum. After stirring overnight a small peak at +139 ppm was observed and the solution became coloured red. Addition of a further amount of Et_3N (0.5g, 5.0 mmol) and stirring for 2 days gave an apparent quantitative conversion by ^{31}P NMR to a species with a chemical shift of +139 ppm. No absorption remained in the infrared spectrum corresponding to the nitrileimine starting material. The signal at +139 ppm was attributed to the $>\overset{+}{P}=C=\overset{-}{B}<$ moiety (see Section 11.7).

11.13.12 Reaction of (109) with Me_3N

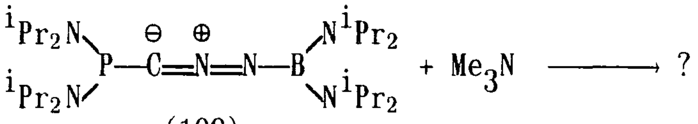

(109)

A ten-fold excess of Me_3N (0.62g, 10.5 mmol) was bubbled through a THF solution (25 ml) containing nitrileimine (109) (0.51g, 1.06 mmol) at room temperature with stirring. No apparent reaction was observed. The solution remained yellow. The ^{31}P NMR signal at ~4 ppm however, showed complete decomposition, and the nitrileimine absorption in the infrared spectrum was lost.

11.13.13 Preparation of (121)

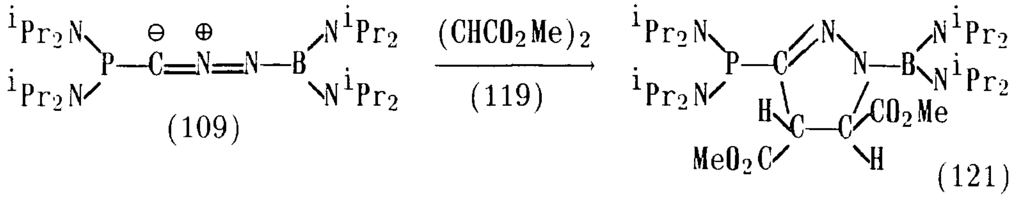

A solution of nitrileimine (109) (0.37g, 0.77 mmol) in benzene (15 ml) was placed in a 100ml Schlenk tube. To this solution was added solid dimethyl fumarate (122 mg, 1.1 equivalents). The reaction mixture was stirred at ambient temperature for 6 hours, after which complete conversion to (121) was noted by ^{31}P NMR spectroscopy. The solvent was removed *in vacuo* and the product was separated from the excess fumarate by crystallisation at -30 ^{0}C from pentane. The cycloadduct (121) was isolated as a pale yellow oil. Yield was 480 mg (99% by weight); IR (pentane) ν_{max}: 1730 (broad,CO_2Me) cm^{-1}; ^{11}B δ: 27.7 ppm (s,broad); ^{31}P δ: 26.7 ppm. ^{1}H and ^{13}C NMR spectral data are presented in Table 11.7 (Section 11.8) (see also Figure 11.19).

11.13.14 Preparations of (122)

11.13.14.1 From Nitrileimine (110) and $(CHCO_2Me)_2$ (119)

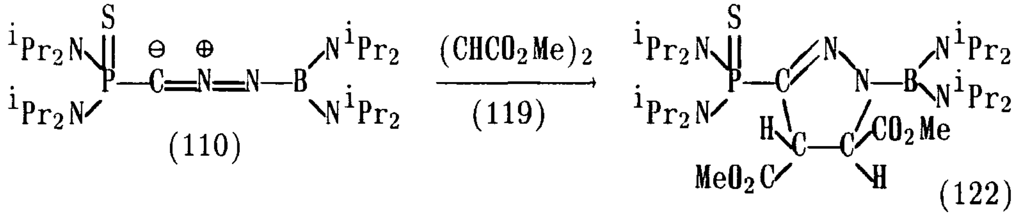

A solution of nitrileimine (110) (500 mg, 0.97 mmol) in benzene (15 ml) was placed in a 100 ml Schlenk tube. To this solution was added solid dimethyl fumarate (0.15g, 1.07 mmol, 1.1 equivalents). The reaction mixture was stirred at ambient temperature for 6 hours, after which the complete conversion to (122) was noted by ^{31}P NMR spectroscopy. The solvent was removed *in vacuo* and the product was separated from the excess fumarate by crystallisation at -30 ^{0}C. Cycloadduct (122) was isolated as a pale yellow oil. Yield was 620 mg (97%). A small impurity was detected from the ^{13}C NMR spectrum.

11.13.14.2 From Cycloadduct (121) and Sulphur

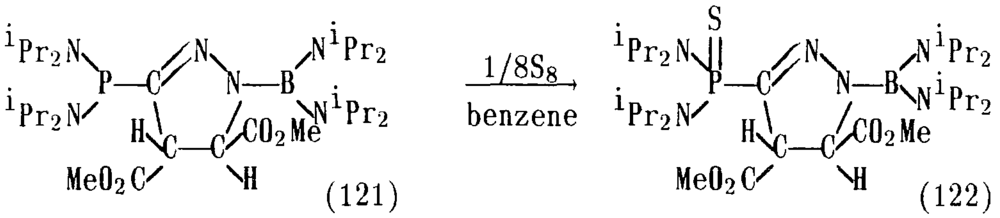

To a solution of cycloadduct (121) (200 mg, 0.32 mmol) in benzene (15 ml) was added sulphur powder (11.2 mg, 0.35 mmol, 1.1 equivalents). The reaction mixture was stirred for 1 hour at room temperature. Quantitative conversion to (122) was noted by ^{31}P NMR spectroscopy. The solvent was removed *in vacuo* and the excess sulphur removed by crystallisation at -30 ^{0}C in pentane. Compound (122) was isolated as a pale yellow oil. Yield was 0.20g (97%); IR (pentane) ν_{max}: 1740 (d,C=0) cm^{-1}; ^{11}B δ: +27 ppm (s,broad); ^{31}P δ: +57 ppm (pentet) $^{3}J_{PH}$ 15.9 Hz. ^{1}H and ^{13}C NMR spectral data are presented in Table 11.8 (Section 11.8) (see also Figure 11.20).

11.13.15 Preparation of (123)

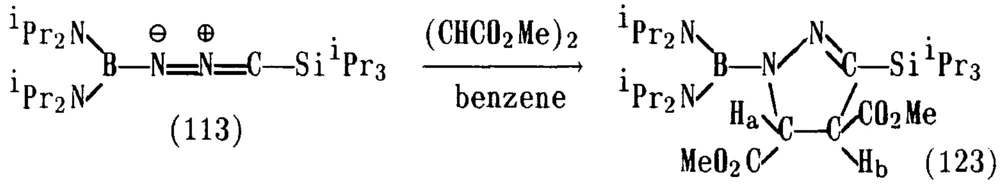

A solution of nitrileimine (113) (500 mg, 1.2 mmol) in benzene (15 ml) was placed in a 100 ml Schlenk tube. To this solution was added solid dimethyl fumarate (194 mg, 1.34 mmol, 1.1 equivalents). The reaction mixture was stirred at ambient temperature for 6 hours, after which complete conversion to (123) was noted by ^{31}P NMR spectroscopy. The solvent was removed *in vacuo*, and the product was separated from the excess fumarate by crystallisation at -30 °C. The cycloadduct (123) was isolated as a pale yellow oil. Yield was 800 mg (spectroscopy suggested that not all the excess fumarate had been removed); IR ν_{max}: 1740 cm^{-1}; ^{11}B (C_6D_6) δ: +28 (s,broad) ppm; ^{29}Si (C_6D_6) δ: 0.705 (s) ppm. ^1H and ^{13}C NMR spectral data are presented in Table 11.8 (Section 11.8) (see also Figure 11.22).

11.13.16 Preparation of (124) and (125)

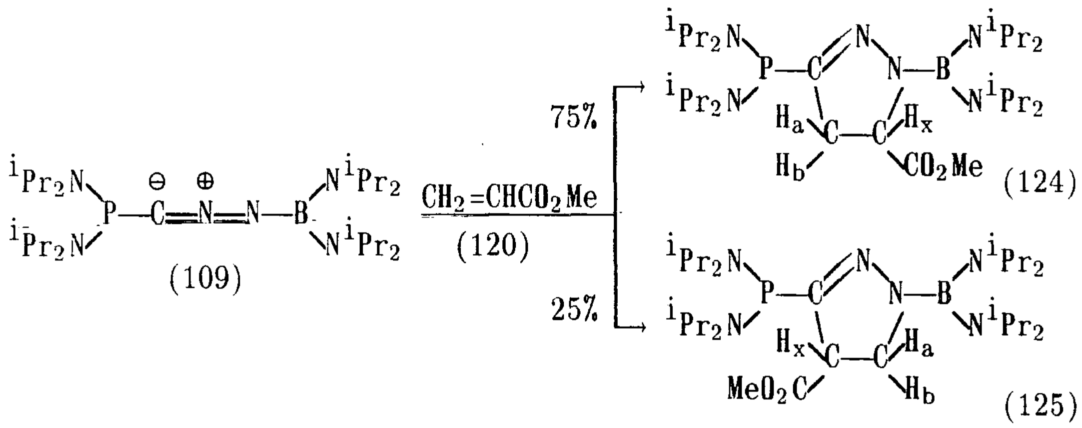

A solution of nitrileimine (109) (500 mg, 1.0 mmol) in benzene (20 ml) was placed in a 100 ml Schlenk tube. To this solution was added dropwise by syringe methyl acrylate (0.09g, 0.1 ml, 1.1 mmol, 1.1 equivalent). The reaction mixture was stirred at ambient temperature for 6 hours after which complete conversion to (124) and (125) was noted by ^{31}P NMR spectroscopy. The solvent and any excess trapping agent was removed *in vacuo*. A mixture of the cycloadduct isomers (124) and (125) was isolated as a pale yellow oil. Yield was 500 mg (88% by weight); IR (pentane) ν_{max}: 1735 (C=O) cm^{-1}; MS EI: 568 [M^+], 468 [$(M-{}^iPr_2N)^+$]; ^{11}B (C_6D_6) δ: 27.9 ppm (broad,both isomers); ^{31}P (C_6D_6) δ: 36.47 $^3J_{PH}$ 9.4 Hz

(75% isomer), 34.43 ppm (25% isomer). ^{1}H and ^{13}C NMR spectral data for both isomers are presented in Table 11.10 (Section 11.8.2).

See also figure 11.20

11.13.17 Preparations of (126)

11.13.17.1 From Nitrileimine (110) and CH_2=$CHCO_2Me$ (120)

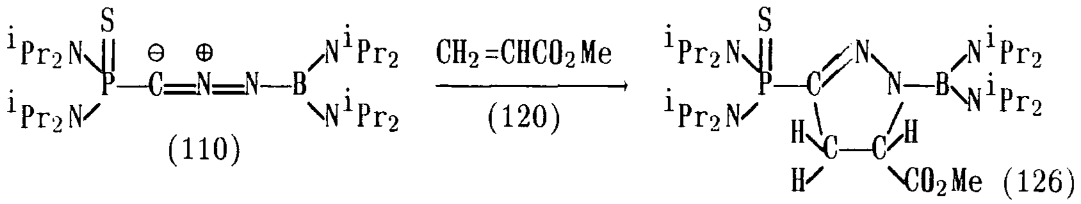

A solution of nitrileimine (110) (450 mg, 0.87 mmol) in benzene (15 ml) was placed in a 100 ml Schlenk tube. To this solution was added dropwise by syringe methyl acrylate (0.09 ml, 1.1 equivalents). The reaction mixture was stirred at ambient temperature for 6 hours after which complete conversion to (126) was noted by ^{31}P NMR spectroscopy. The solvent and any excess trapping agent was removed *in vacuo*. The cycloadduct (126) was isolated as a pale yellow oil. Yield was 525 mg (100% by weight) with a small impurity detected from the ^{13}C NMR spectrum.

11.13.17.2 From Cycloadduct (124)/(125) and Sulphur

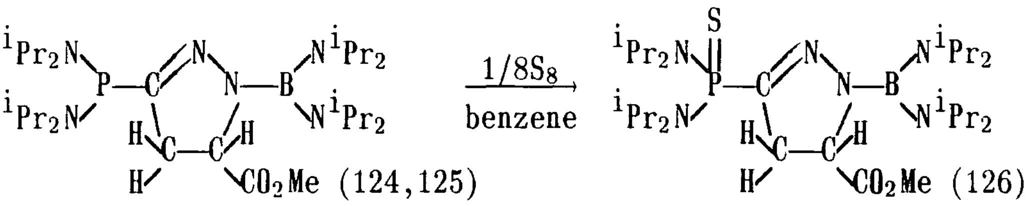

The cycloadduct (126) was also formed by the addition of sulphur (1.1 equivalents) with stirring at ambient temperature for 1 hour to a benzene solution of the isomers (124) and (125). IR (pentane) ν_{max}: 1745 (C=O) cm^{-1}; ^{11}B (C_6D_6) δ: ~28 ppm; ^{31}P (C_6D_6) δ: 57.16 ppm (pentet)

$^3J_{PH}$ 16.3 Hz. ^{1}H and ^{13}C NMR spectral data are presented in Table 11.11 (Section 11.8.2).

11.13.18 Reaction of (109) with (127)

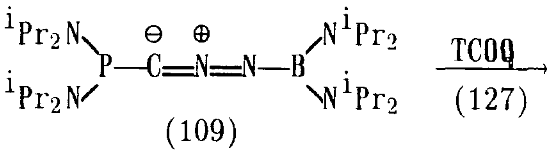

Successive volumes (2 ml) of a solution of the tetrachloroorthoquinone (TCOQ) (0.47g, 1.9 mmol) in benzene were added to a solution of the nitrileimine (109) (900 mg, 1.9 mmol) with stirring at room temperature. The results are shown in Table 11.13.

EQUIV.OF TCOQ	COLOUR OF SOLUTION	^{31}P NMR (δ/ppm)	IR OBSERVATIONS
1	green	+103	No NI absorption
2	red	-36	No NI absorption
3	deep brown	+19	Apparent decomposition

Table 11.13: *The reaction of TCOQ with nitrileimine (NI) (109).*

11.13.19 Reaction of (133) with (108)

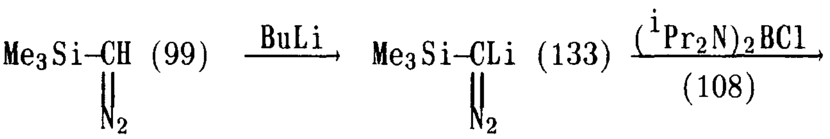

$$\underset{\overset{\|}{N_2}}{Me_3Si\text{-}CH}\ (99)\ \xrightarrow{BuLi}\ \underset{\overset{\|}{N_2}}{Me_3Si\text{-}CLi}\ (133)\ \xrightarrow[(108)]{(^iPr_2N)_2BCl}$$

A solution of trimethylsilyl-diazo compound (99) (820 mg, 7.2 mmol) in THF (25 ml) was cooled to -78 ^{o}C. BuLi (3.2 ml, 7.95 mmol, 1.1 equivalent, 2.5 M) was added dropwise. The reaction mixture was stirred at -78 ^{o}C for 20 min before the addition of $(^iPr_2N)_2BCl$ (1.77g, 7.2 mmol) in THF (10 ml). After complete addition it was allowed to warm to room temperature. The THF was removed *in vacuo* before the addition of pentane (20 ml). A white insoluble precipitate was removed by filtration and the filtrate concentrated by removal of pentane *in vacuo*. IR ν_{max}: 2100-2200 cm^{-1} (broad); ^{11}B δ: 30-35 ppm (many broad peaks).

11.13.20 Reaction of (103) with (130)

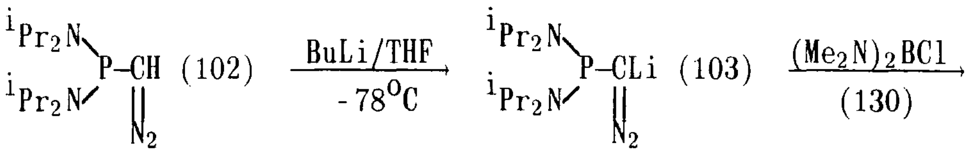

Phosphorus diazo compound (102) (0.52g, 1.9 mmol) was dissolved in THF (25 ml) and cooled to -78 °C. BuLi (0.84 ml, 2.1 mmol, 1.1 equivalents, 2.5 M) was added, followed by stirring at -78 °C for 20 mins. A solution of $(Me_2N)_2BCl$ (0.26g, 1.9 mmol) in THF (15 ml) was added dropwise with stirring. The reaction mixture was allowed to reach room temperature and the THF removed *in vacuo*. Addition of pentane (20 ml) produced a white precipitate. ^{31}P NMR of the resultant filtrate showed a peak at +139 ppm. No diazo or nitrileimine absorptions were observed in the infrared. Cooling the solution to -40 °C gave a crystalline solid whose analysis corresponded to $({}^{i}Pr_2N)_2PCl$ (100); mpt. 96-98 °C. A repeat of this preparation showed the presence of compound $({}^{i}Pr_2N)_2PC(N_2)P(N{}^{i}Pr_2N)_2$ (106) with a characteristic IR absorption at 2010 cm^{-1}. This was further verified by the addition of an excess of elemental sulphur, which was stirred in pentane at room temperature for 1 hour. ^{31}P NMR spectroscopy showed characteristic shifts at 74.5, 72.39 ($^{1}J_{PP}$ 140.1 Hz) and 71.44 ppm [9] corresponding to compounds (129) and (131) respectively, and another peak at +50 ppm thought to correspond to the boron and phosphorus containing species.

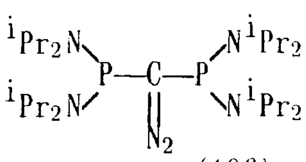
(106)

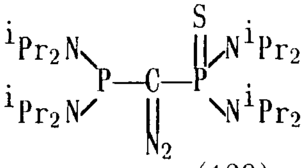
(129)

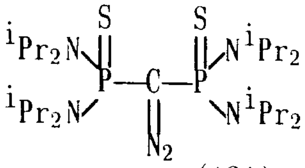
(131)

By cooling the solution to -40 °C it was hoped to separate the product as a solid, however no precipitation occurred. IR ν_{max}: 2780 (N-Me), 2010 (sharp, diazo), 2040, 2095, 2160 (broad) cm^{-1}.

11.13.21 Attempted Reaction of (134) with Diazomethane

$(^iPr_2N)_2B(OSO_2CF_3)$ was synthesised by a route analogous to that used by Narula and Nöth (Equation 11.23) [55].

$$(^iPr_2N)_2BCl + CF_3O_2SO^- Ag^+ \xrightarrow{CH_2Cl_2} (^iPr_2N)_2B(OSO_2CF_3) + AgCl \quad (11.23)$$

(134)

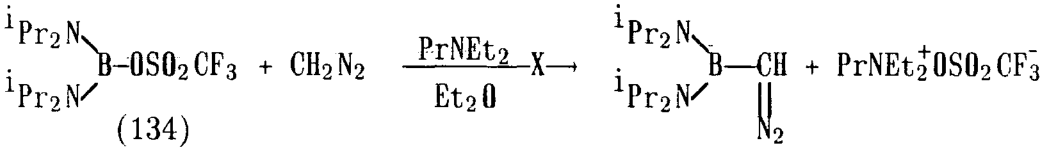

Bis(diisopropylamine)boron triflate (134) (1g, 2.8 mmol) was dissolved in Et_2O (50 ml) followed by the addition of $PrNEt_2$ (0.32g, 2.8 mmol). This mixture was cooled to -78 °C. Diazomethane was generated by the standard route (Section 11.4.2) and obtained as an ether solution (2g in 150 ml, 0.32 M), some of which (10 ml, 3.2 mmol, 1.1 equivalents) was added dropwise by syringe with continual stirring. The solution turned yellow with a white precipitate. On warming to approximately -20 °C there was an apparent rapid polymerisation forming a white solid and clear overlying liquid. The insolubility of the polymer limited the spectral data which could be obtained. The infrared spectrum of the overlying liquid showed no diazo absorption.

11.13.22 Reaction of (133) with (14)

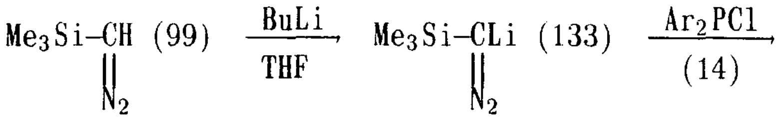

$$\underset{\underset{N_2}{\|}}{\mathrm{Me_3Si{-}CH}}\ (99)\ \xrightarrow[\mathrm{THF}]{\mathrm{BuLi}}\ \underset{\underset{N_2}{\|}}{\mathrm{Me_3Si{-}CLi}}\ (133)\ \xrightarrow[(14)]{\mathrm{Ar_2PCl}}$$

Ar = 2,4,6-tris(trifluoromethyl)benzene

Trimethylsilyldiazo compound (99) (0.5g, 4.4 mmol) was dissolved in THF (25 ml) and cooled to -78 °C. This was stirred continuously while BuLi (1.93 ml, 4.82 mmol, 1.1 equivalents, 2.5 M) was added dropwise. After stirring at -78 °C for 20 mins Ar_2PCl (14) (2.77g, 4 mmol) as a solution in THF (20 ml) was added dropwise. The solution turned black after the addition of just one drop of the phosphorus compound. When addition was complete, the solution was allowed to warm to room temperature and the THF was removed *in vacuo*. On addition of pentane the LiCl appeared inseparable from the viscous black oil. IR ν_{max}: 2010 cm^{-1} (diazo absorption); ^{31}P δ: +77 $^4J_{PF}$ 41 Hz, -8.15 [$Me_3SiC(N_2)PAr_2$ (106)], -70.1 [carbene (137)] ppm.

Warming the reaction mixture to 35 °C caused the signal at -8.15 ppm to disappear. The same result was obtained by exposure to radiation for 30 mins.

Using the same quantities but reversing the addition (to avoid Ar_2PCl being in excess of the lithio compound) gave a similar black oil with the same spectroscopic data.

11.14 SUMMARY OF SPECTROSCOPIC DATA AND SELECTED SPECTRA

A summary of the NMR data of some of these species is presented in Table 11.14, and some selected spectra are shown in Figures 11.16-11.22.

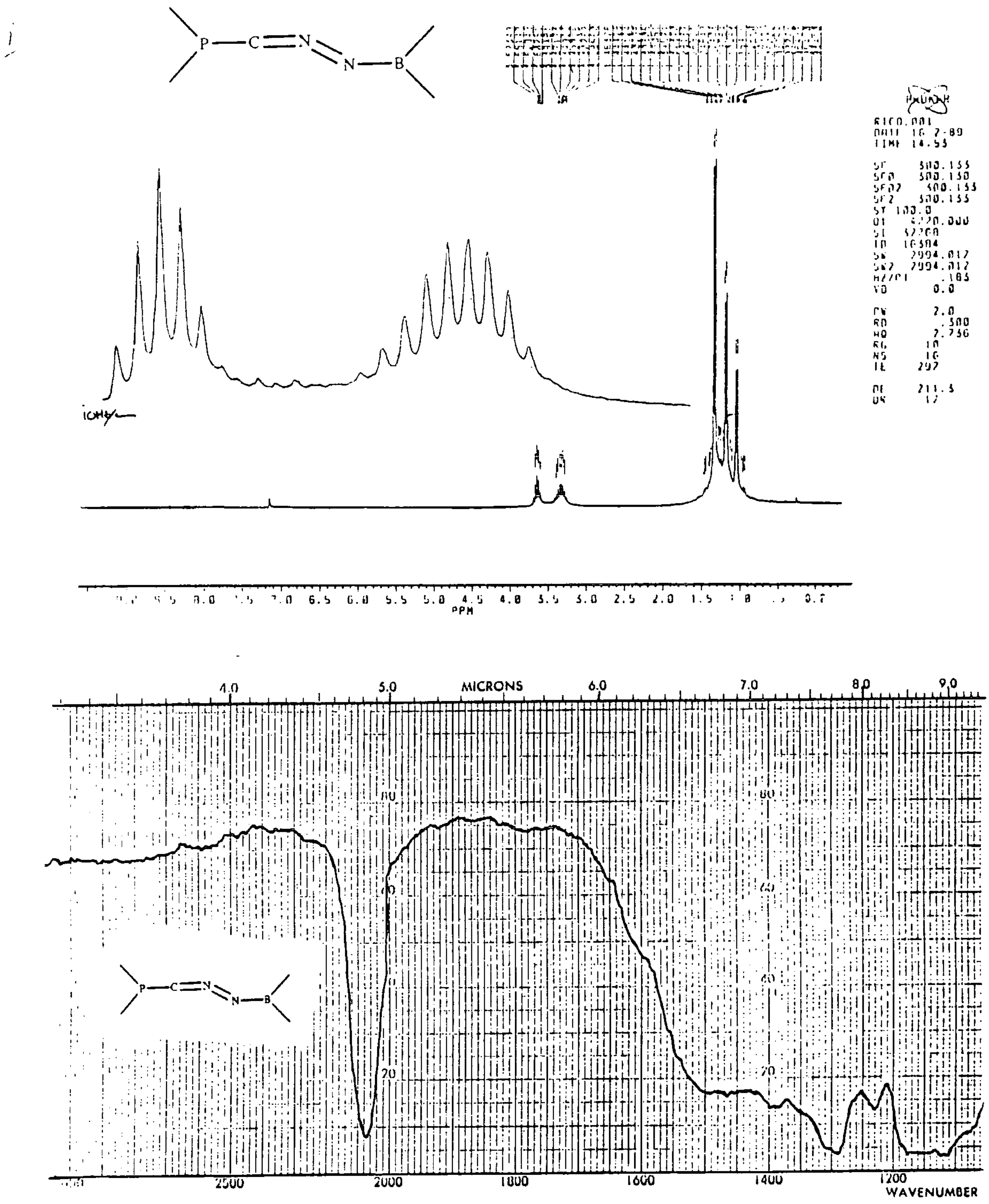

Figure 11.16: *(i) ¹H NMR and (ii) IR (pentane) spectra of nitrileimine (109)*

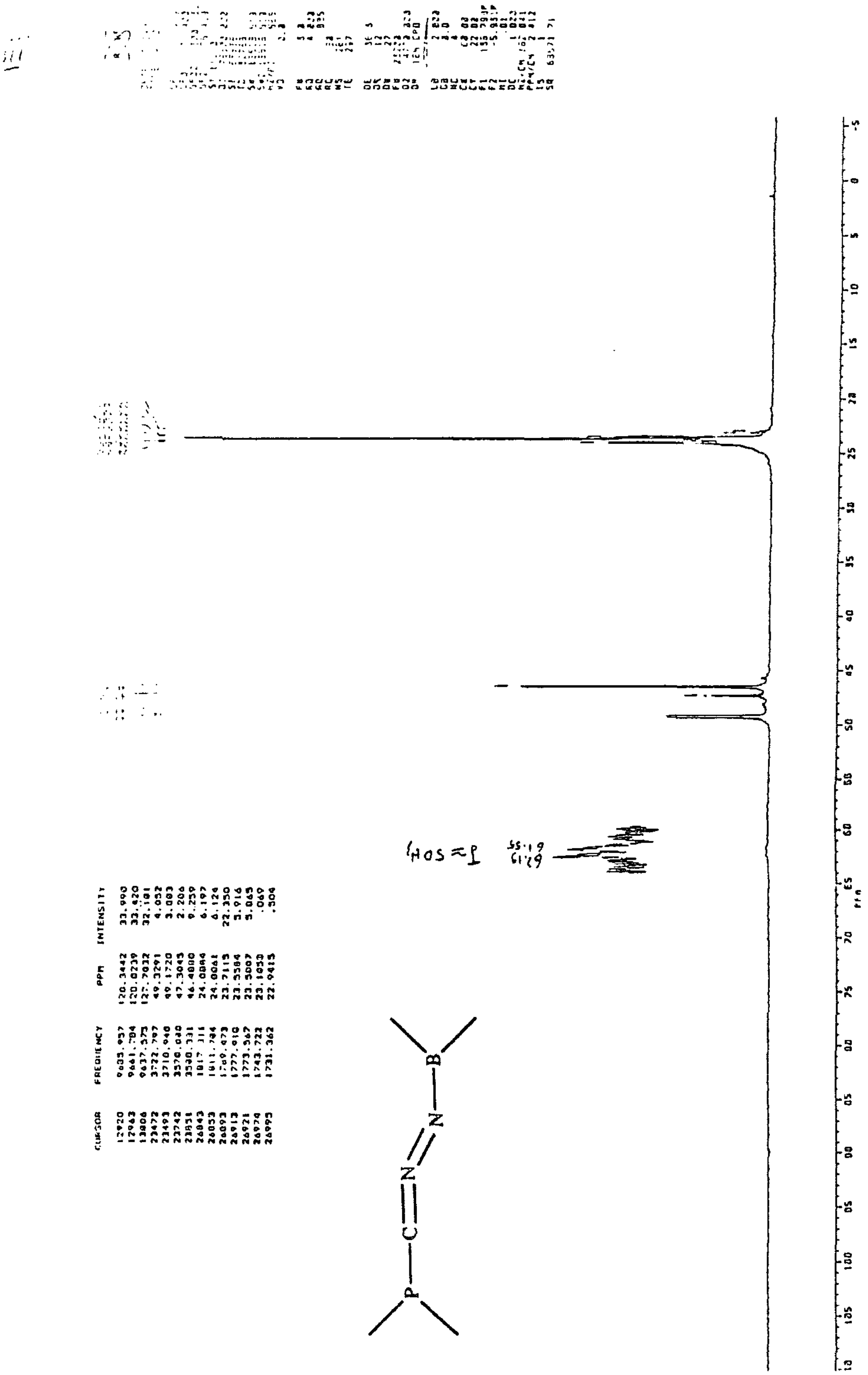

CURSOR	FREQUENCY	PPM	INTENSITY
12920	9685.957	128.3442	33.990
12963	9661.784	128.0239	33.420
13006	9637.575	127.7032	32.101
23472	3722.797	49.3291	4.052
23493	3710.940	49.1720	3.003
23742	3570.040	47.3045	2.206
23851	3502.331	46.4080	9.259
26843	1817.311	24.0084	6.197
26853	1811.784	24.0061	6.124
26893	1789.473	23.7115	22.350
26913	1777.910	23.5584	5.916
26921	1773.567	23.5007	5.065
26974	1743.722	23.1053	.069
26995	1731.362	22.9415	.504

Figure 11.16: *(iii)* ^{13}C *NMR spectrum of nitrileimine (109) in* C_6D_6.
(cont'd)

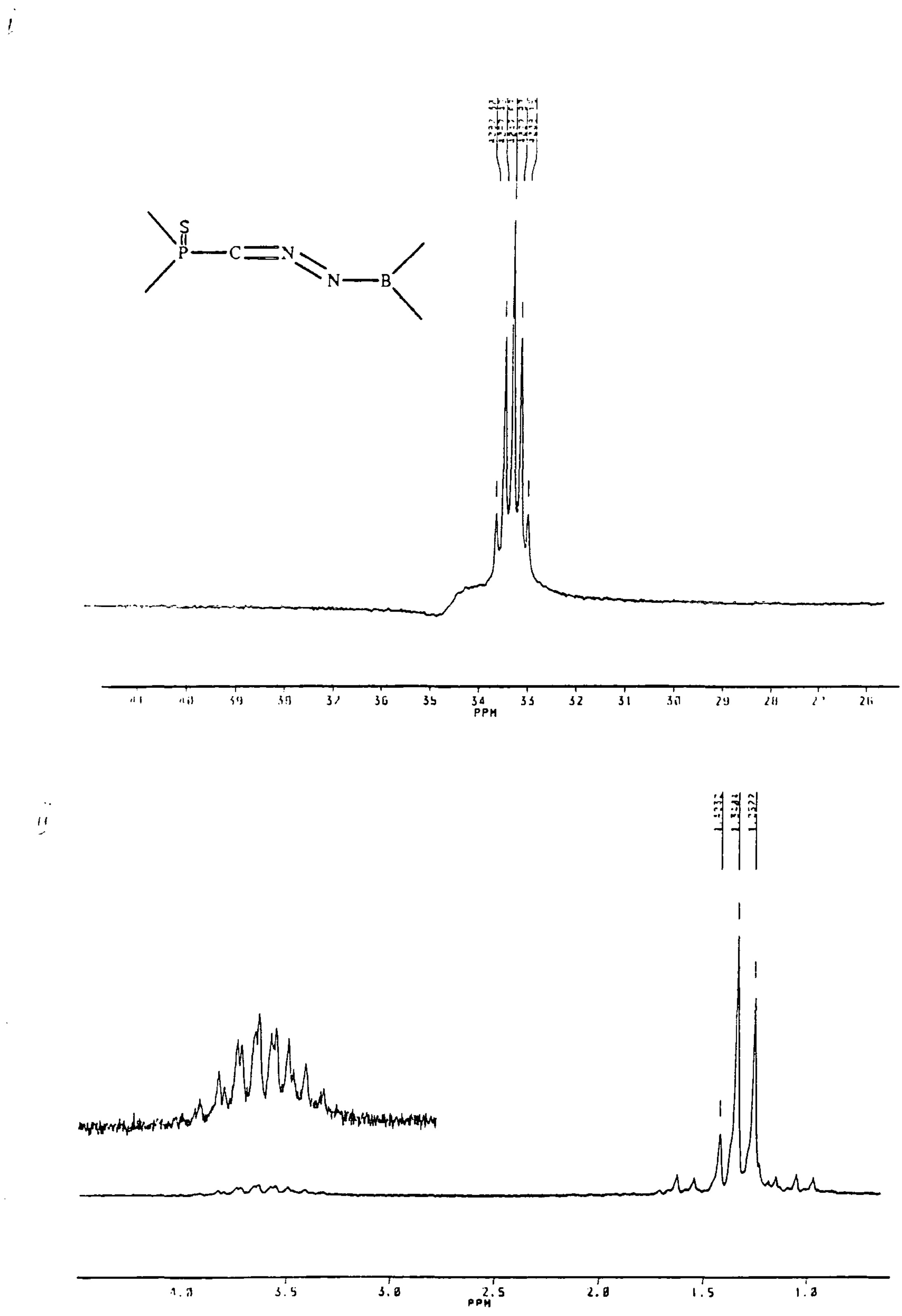

Figure 11.17: (i) ^{31}P and (ii) ^{1}H NMR spectra of nitrileimine (110) in C_6D_6.

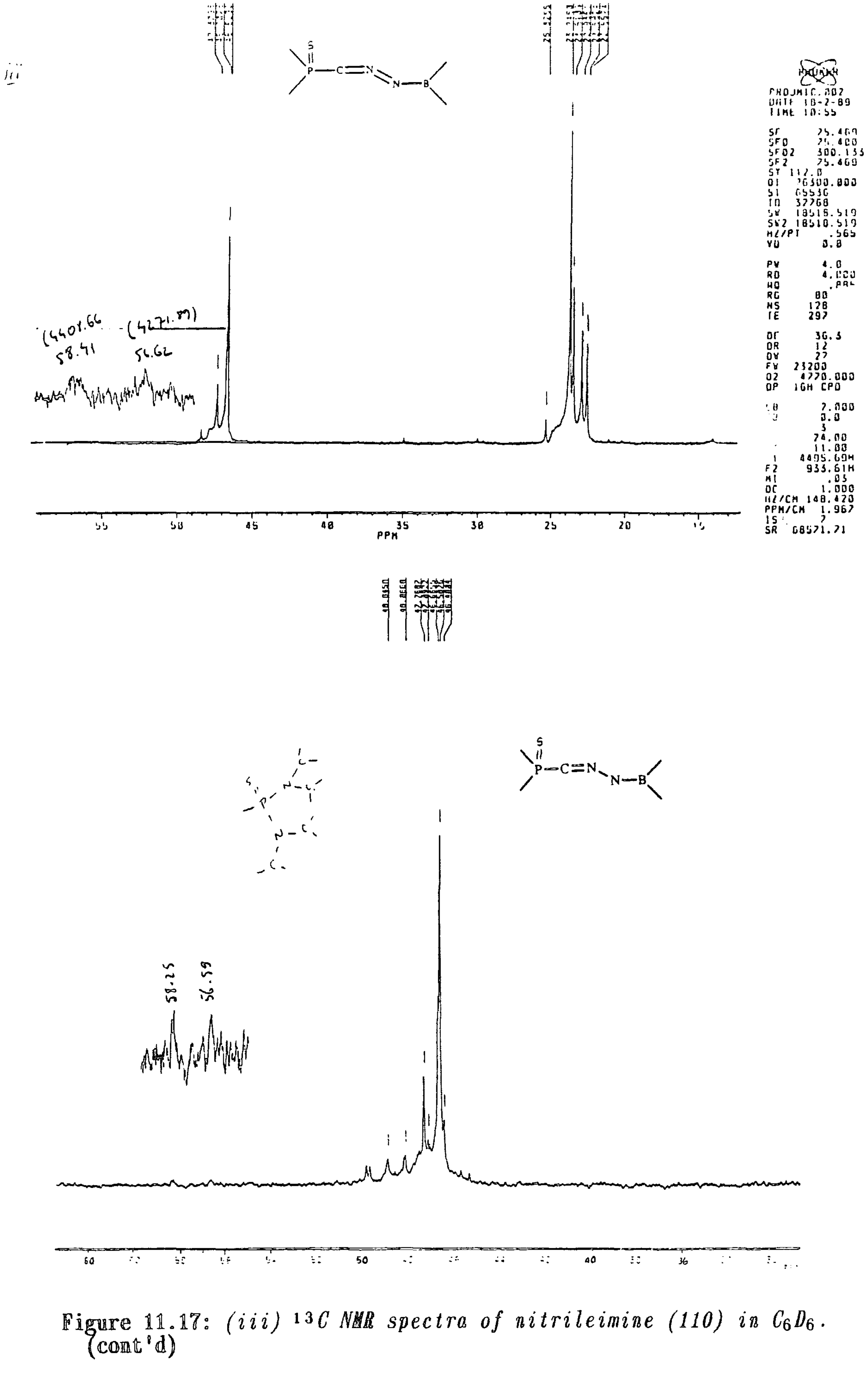

Figure 11.17: (iii) ^{13}C NMR spectra of nitrileimine (110) in C_6D_6. (cont'd)

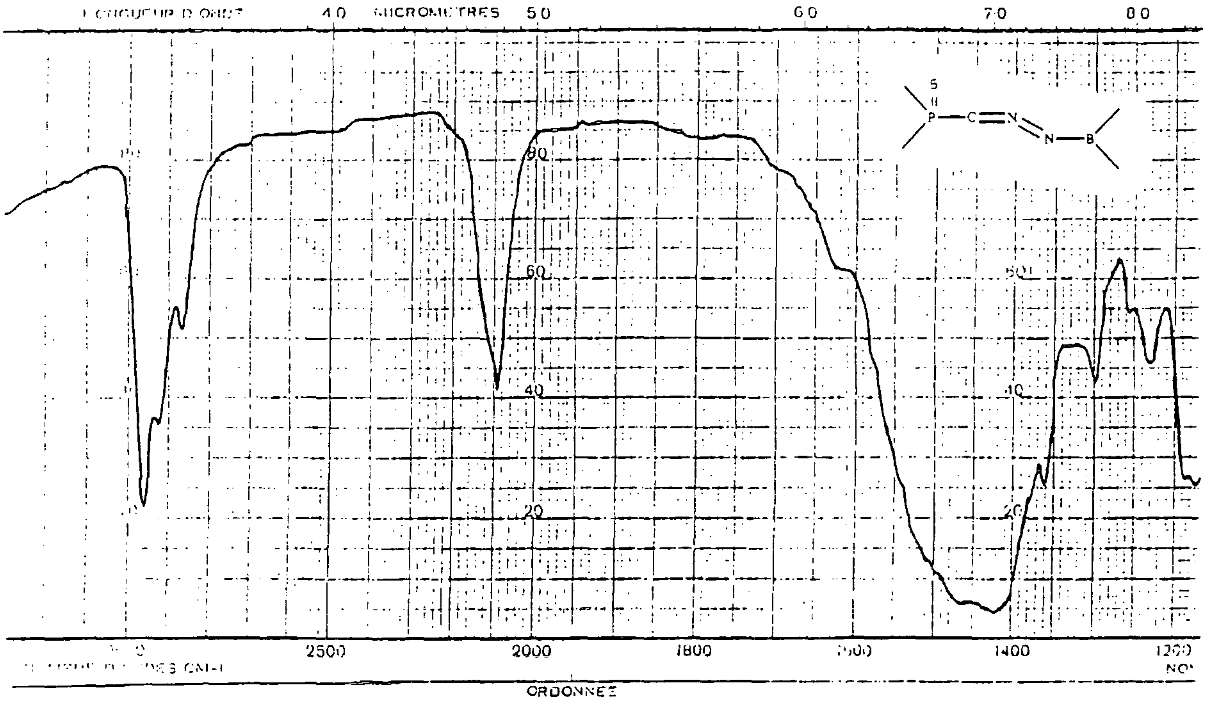

Figure 11.17: *(iv) IR spectrum of nitrileimine (109) (pentane).* (cont'd)

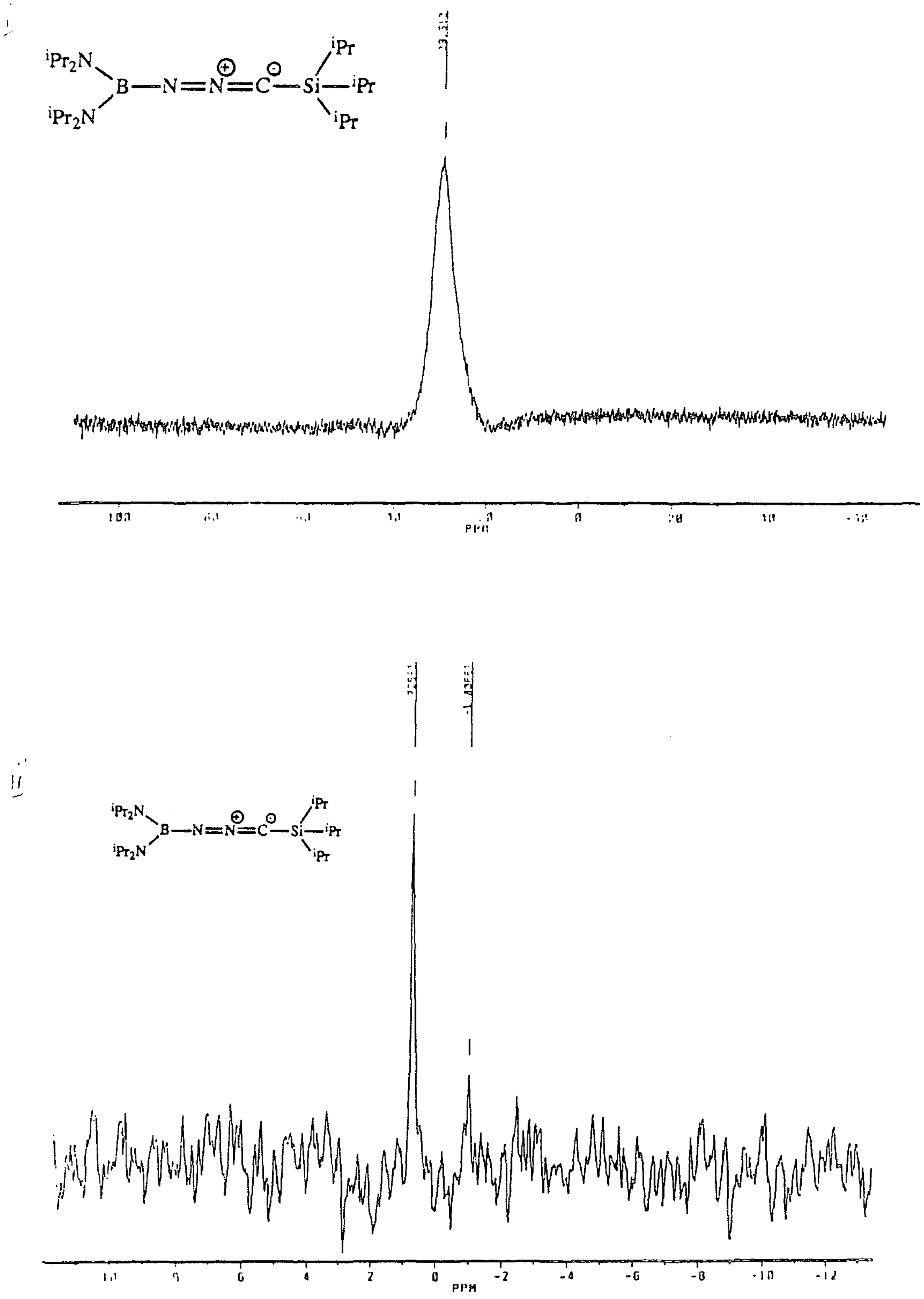

Figure 11.18: *(i) ^{11}B and (ii) ^{29}Si NMR spectra of nitrileimine (113) in C_6D_6.*

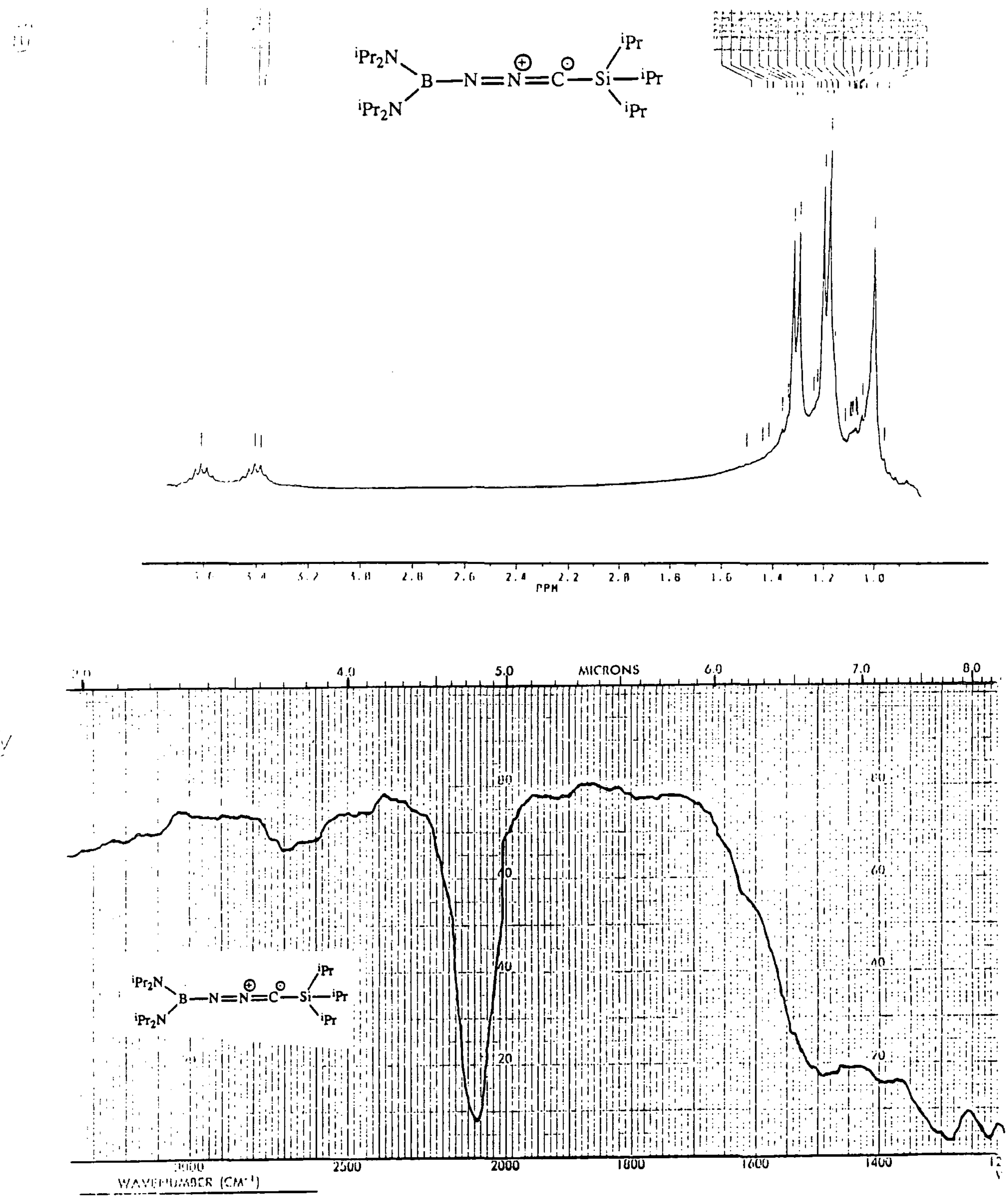

Figure 11.18: *(iii) ${}^1H$ NMR (C_6D_6) and (iv) IR (pentane) spectra*
(cont'd) *of nitrileimine (113).*

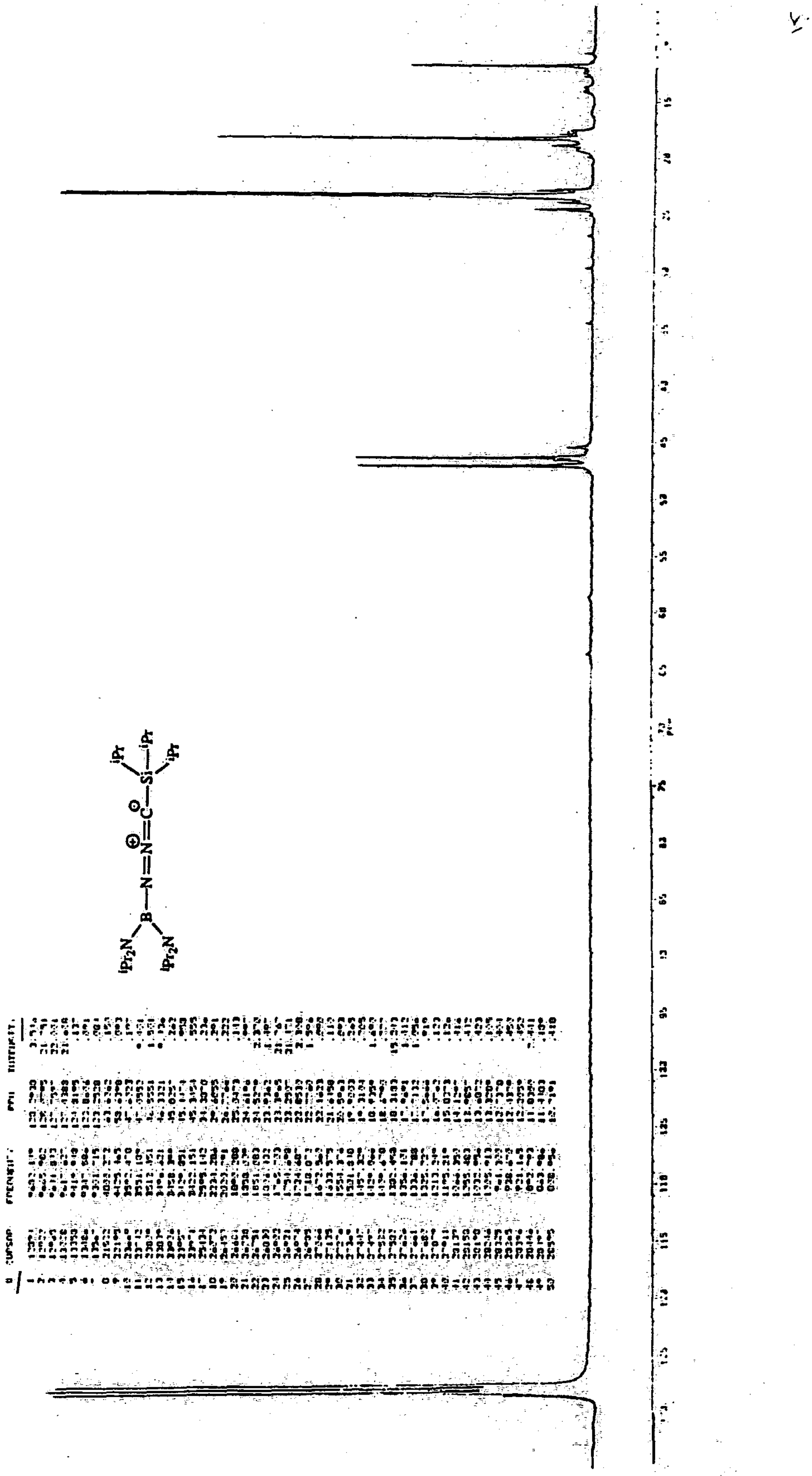

Figure 11.18: *(v)* ^{13}C *NMR spectrum of nitrileimine (113) in* C_6D_6.
(cont'd)

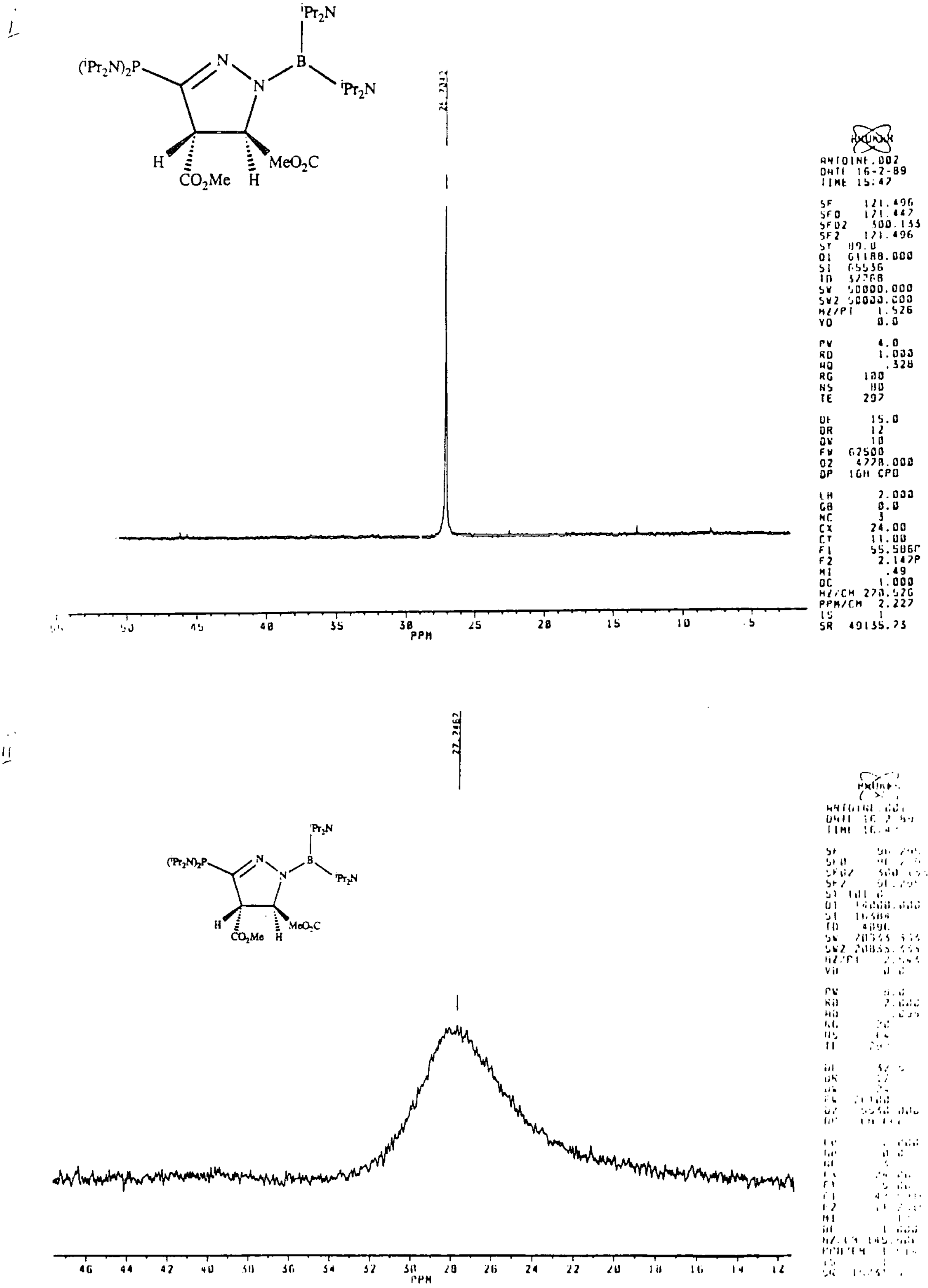

Figure 11.19: *(i) ^{31}P and (ii) ^{11}B NMR spectra of cycloadduct (121) in $CDCl_3$.*

iii

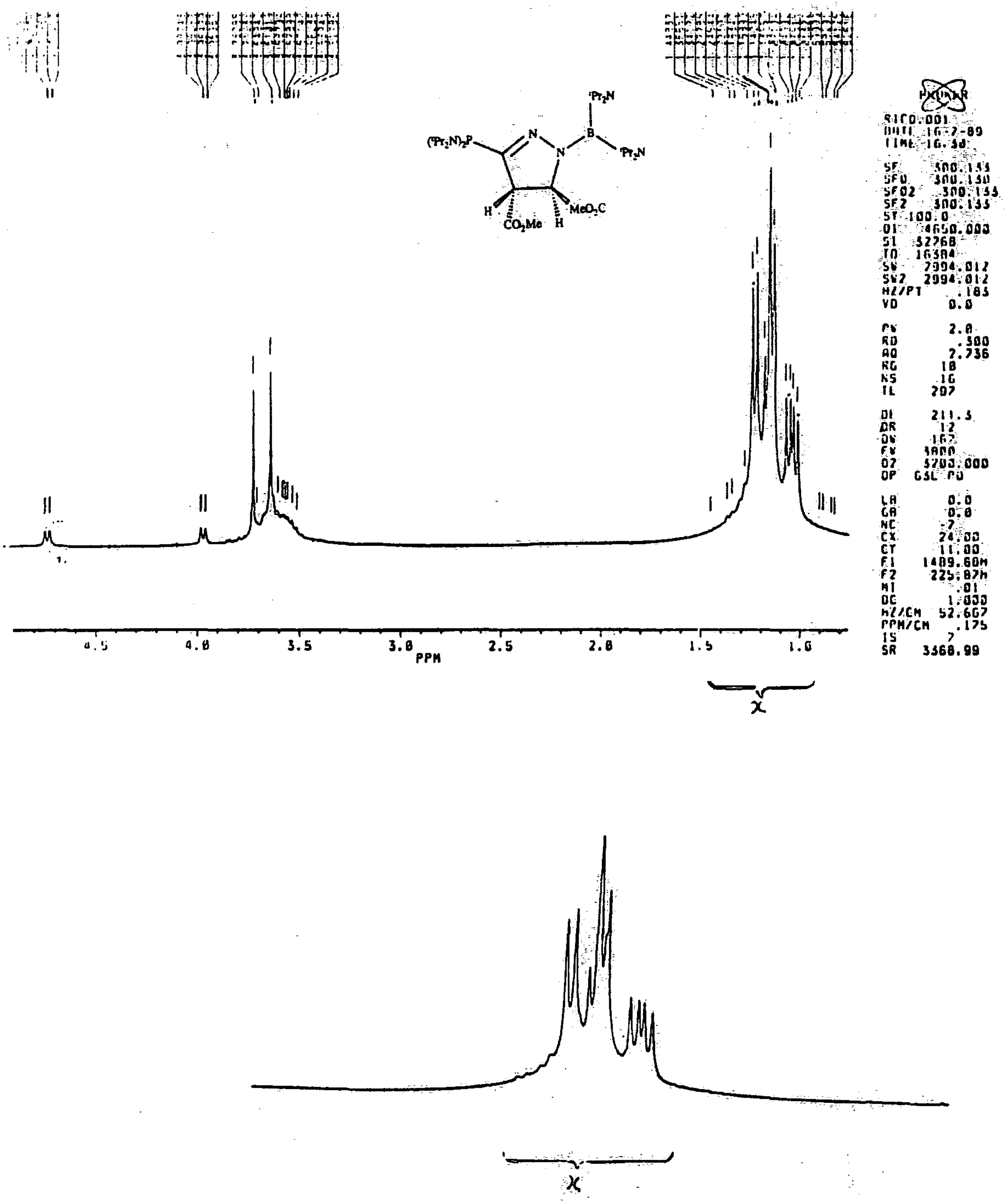

Figure 11.19: *(iii)* ¹*H NMR spectrum of cycloadduct (121) in* $CDCl_3$. (cont'd)

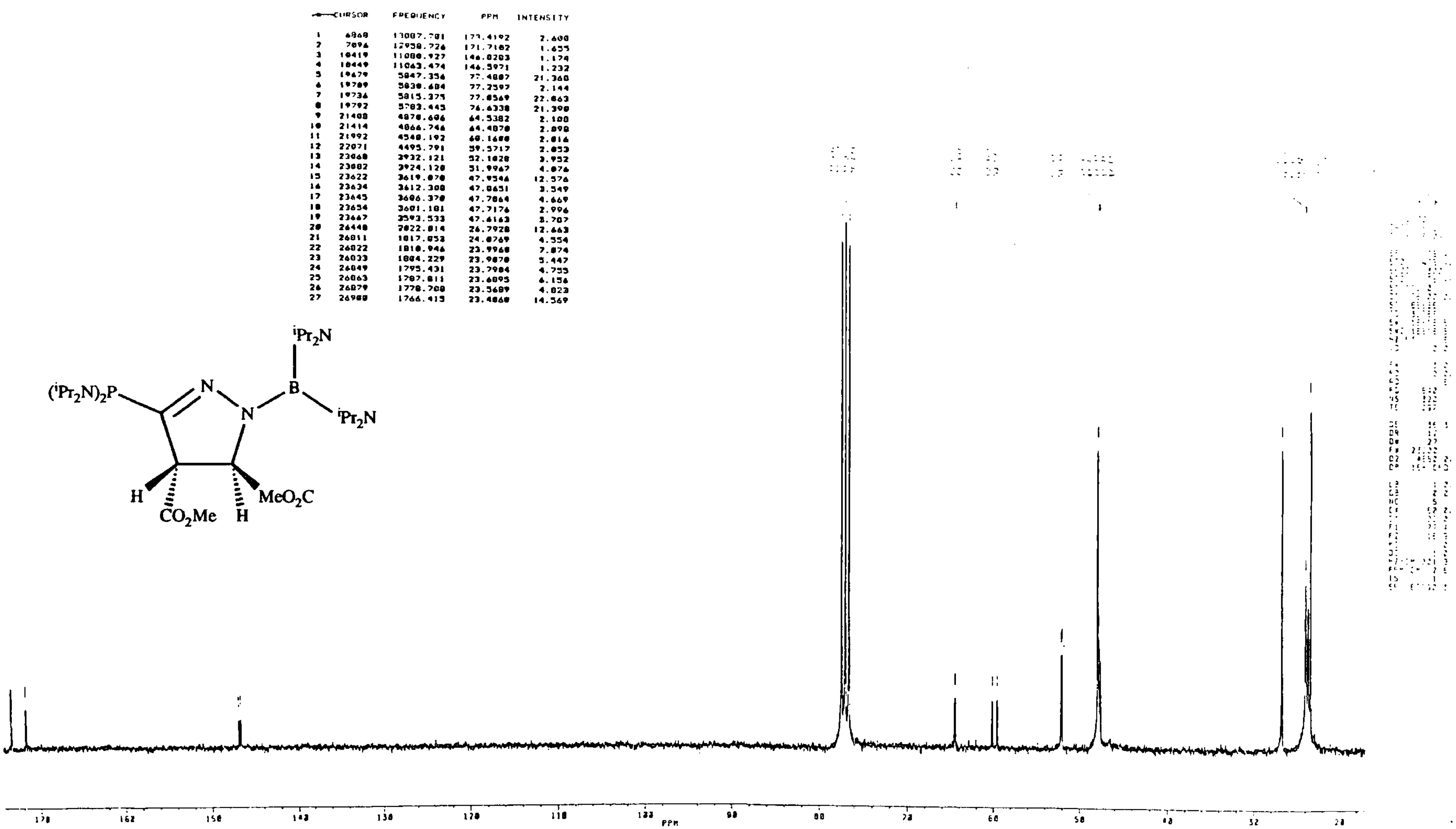

←CURSOR		FREQUENCY	PPM	INTENSITY
1	4868	13087.781	173.4192	2.600
2	7096	12958.726	171.7182	1.655
3	10419	11080.927	146.8203	1.179
4	10449	11043.474	146.5971	1.232
5	19679	5847.356	77.4807	21.360
6	19709	5830.604	77.2597	2.144
7	19736	5815.375	77.0569	22.063
8	19792	5783.445	76.6338	21.390
9	21408	4870.606	64.5382	2.100
10	21414	4866.746	64.4870	2.098
11	21992	4540.192	60.1600	2.016
12	22071	4495.791	59.5717	2.053
13	23068	3932.121	52.1028	3.952
14	23082	3924.120	51.9967	4.076
15	23622	3619.070	47.9546	12.576
16	23634	3612.300	47.8651	3.549
17	23645	3606.370	47.7864	4.669
18	23654	3601.181	47.7176	2.996
19	23667	3593.533	47.6163	8.707
20	26440	2022.014	26.7928	12.663
21	26011	1817.053	24.0769	4.554
22	26022	1810.946	23.9960	7.074
23	26033	1804.229	23.9070	5.447
24	26049	1795.431	23.7904	4.755
25	26063	1787.811	23.6895	6.156
26	26079	1778.700	23.5689	4.023
27	26900	1766.415	23.4060	14.569

Figure 11.19: *(iv)* $^{13}C\{^{1}H\}$ *NMR spectrum of cycloadduct (121) in* $CDCl_3$.
(cont'd)

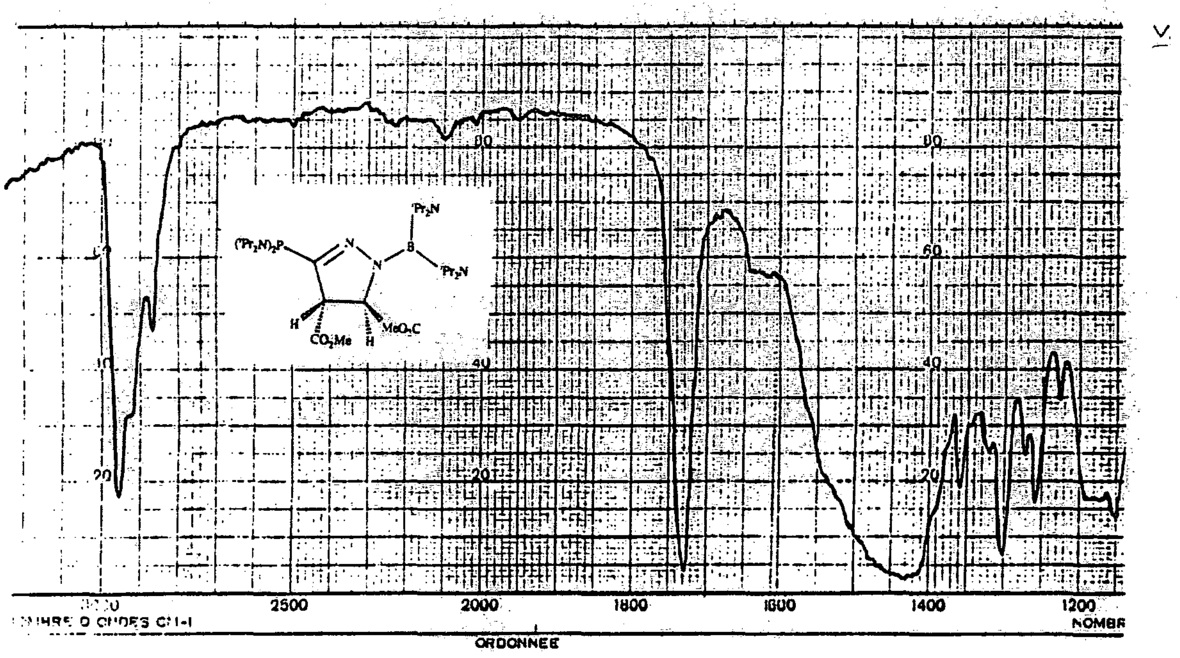

Figure 11.19: *(v) IR spectrum of cycloadduct (121) (pentane).*
(cont'd)

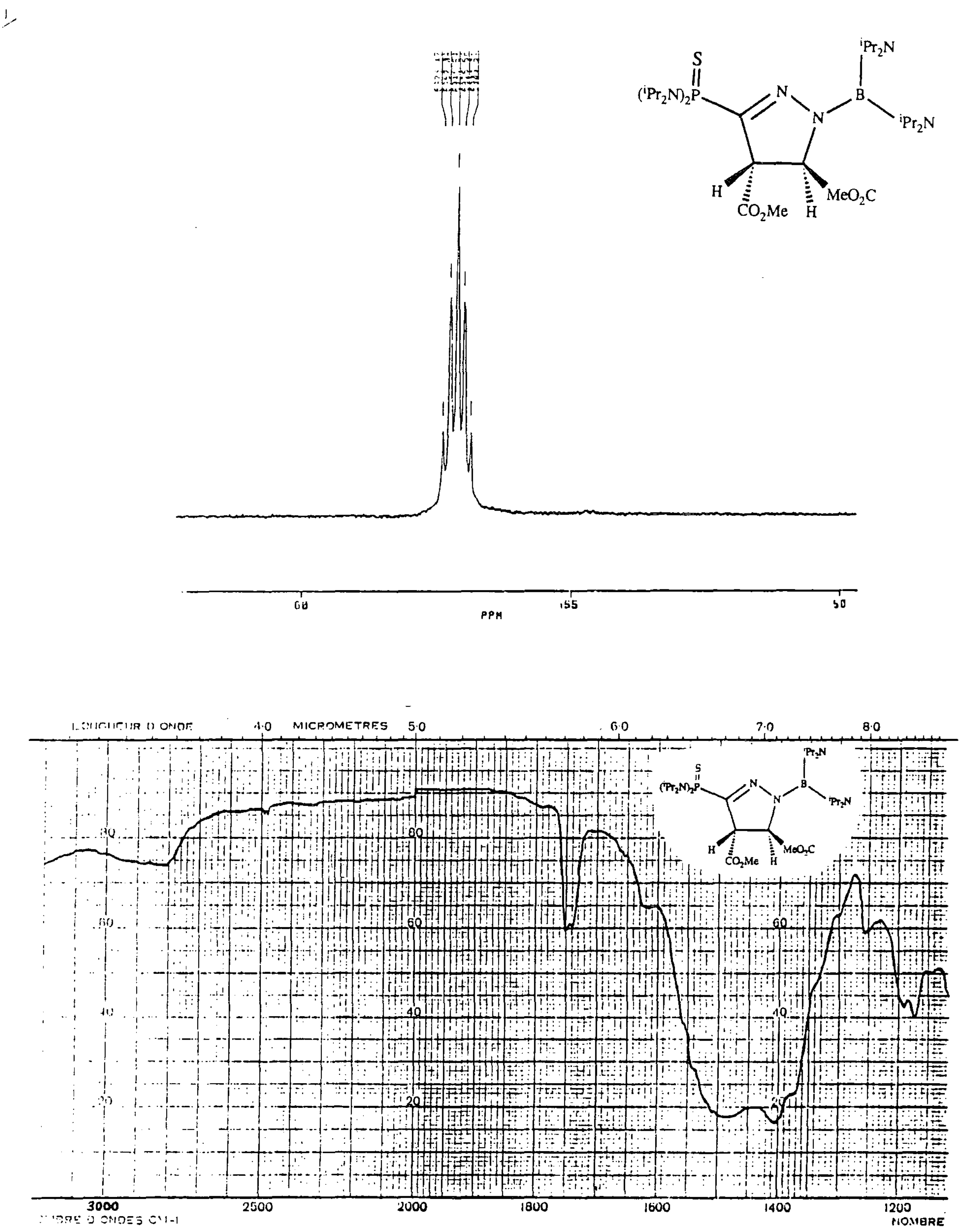

Figure 11.20: *(i)* ^{31}P *($CDCl_3$) and (ii) IR (pentane) spectra of cycloadduct (122).*

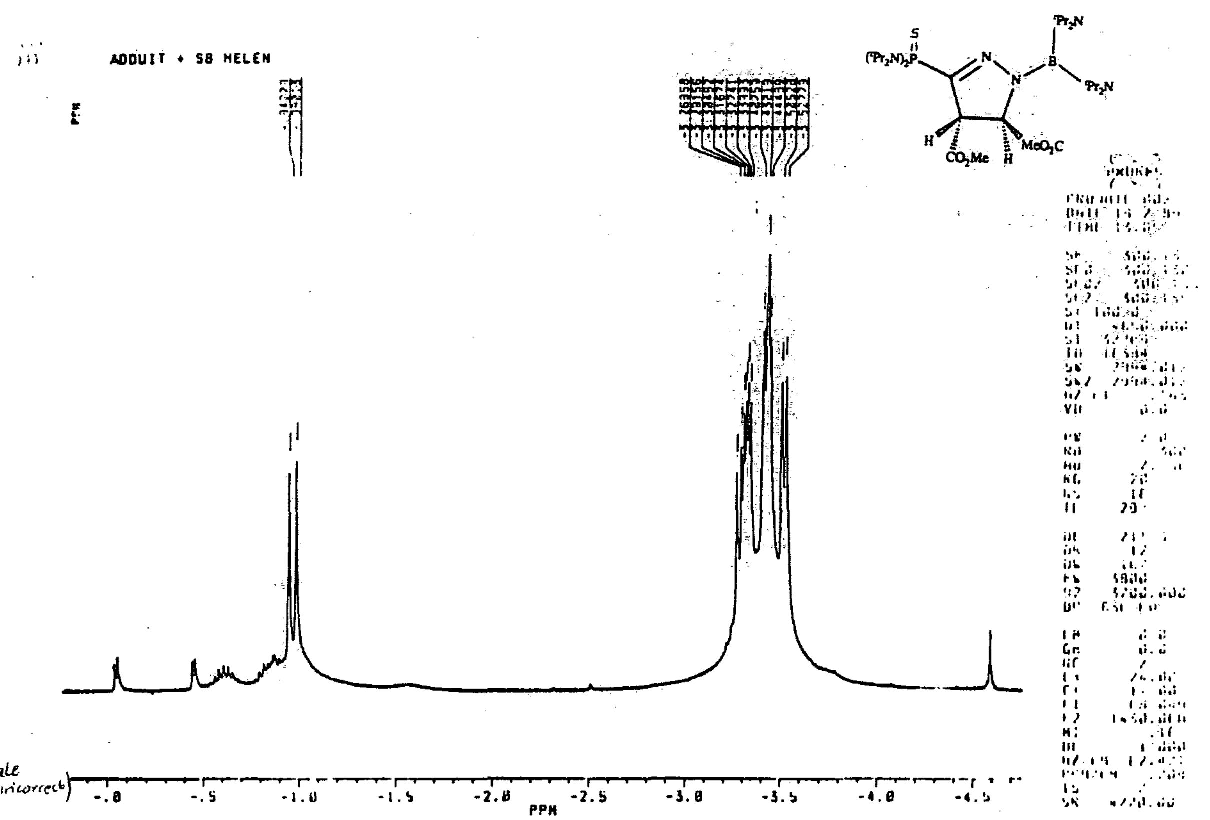

Figure 11.20: *(iii) ^1H NMR spectrum of cycloadduct (122) in $CDCl_3$.* (cont'd)

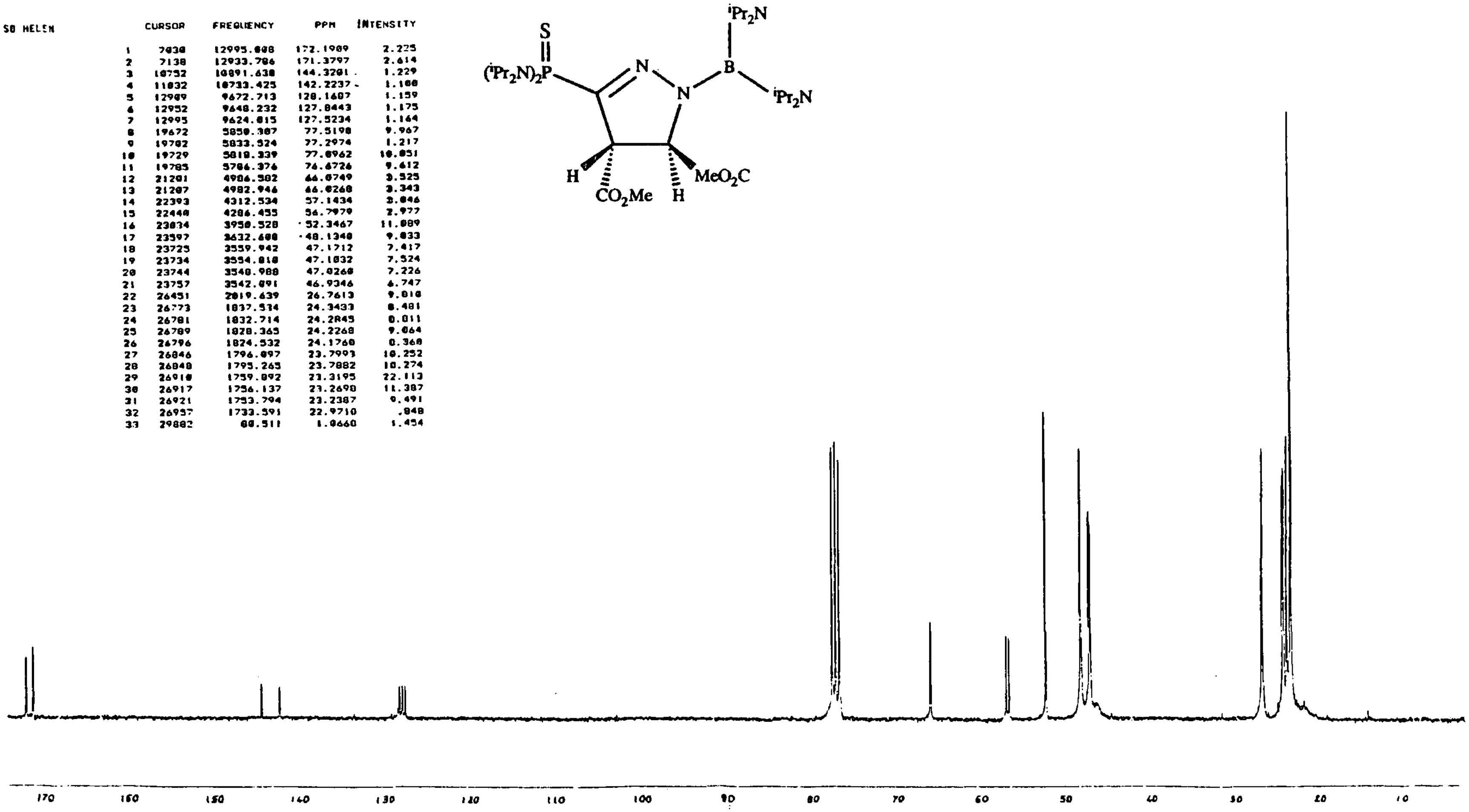

	CURSOR	FREQUENCY	PPM	INTENSITY
1	7030	12995.000	172.1909	2.225
2	7130	12933.786	171.3797	2.614
3	10752	10891.630	144.3201	1.229
4	11032	10733.425	142.2237	1.100
5	12909	9672.713	128.1687	1.159
6	12952	9648.232	127.8443	1.175
7	12995	9624.015	127.5234	1.164
8	19672	5850.307	77.5198	9.967
9	19702	5833.524	77.2974	1.217
10	19729	5818.339	77.0962	10.051
11	19785	5786.376	76.6726	9.612
12	21201	4986.582	66.0749	3.525
13	21207	4982.946	66.0268	3.343
14	22393	4312.534	57.1434	3.046
15	22440	4286.455	56.7979	2.977
16	23034	3950.528	52.3467	11.089
17	23597	3632.600	48.1340	9.033
18	23725	3559.942	47.1712	7.417
19	23734	3554.810	47.1032	7.524
20	23744	3548.988	47.0260	7.226
21	23757	3542.091	46.9346	6.747
22	26451	2019.639	26.7613	9.010
23	26773	1837.534	24.3483	8.481
24	26781	1832.714	24.2845	0.011
25	26789	1828.365	24.2268	9.064
26	26796	1824.532	24.1760	0.360
27	26846	1796.097	23.7993	10.252
28	26848	1795.265	23.7882	10.274
29	26910	1759.892	23.3195	22.113
30	26917	1756.137	23.2698	11.387
31	26921	1753.794	23.2387	9.491
32	26957	1733.591	22.9710	.848
33	29882	80.511	1.0668	1.454

Figure 11.20: *(iv)* ^{13}C *NMR spectrum of cycloadduct (122) in* $CDCl_3$.
(cont'd)

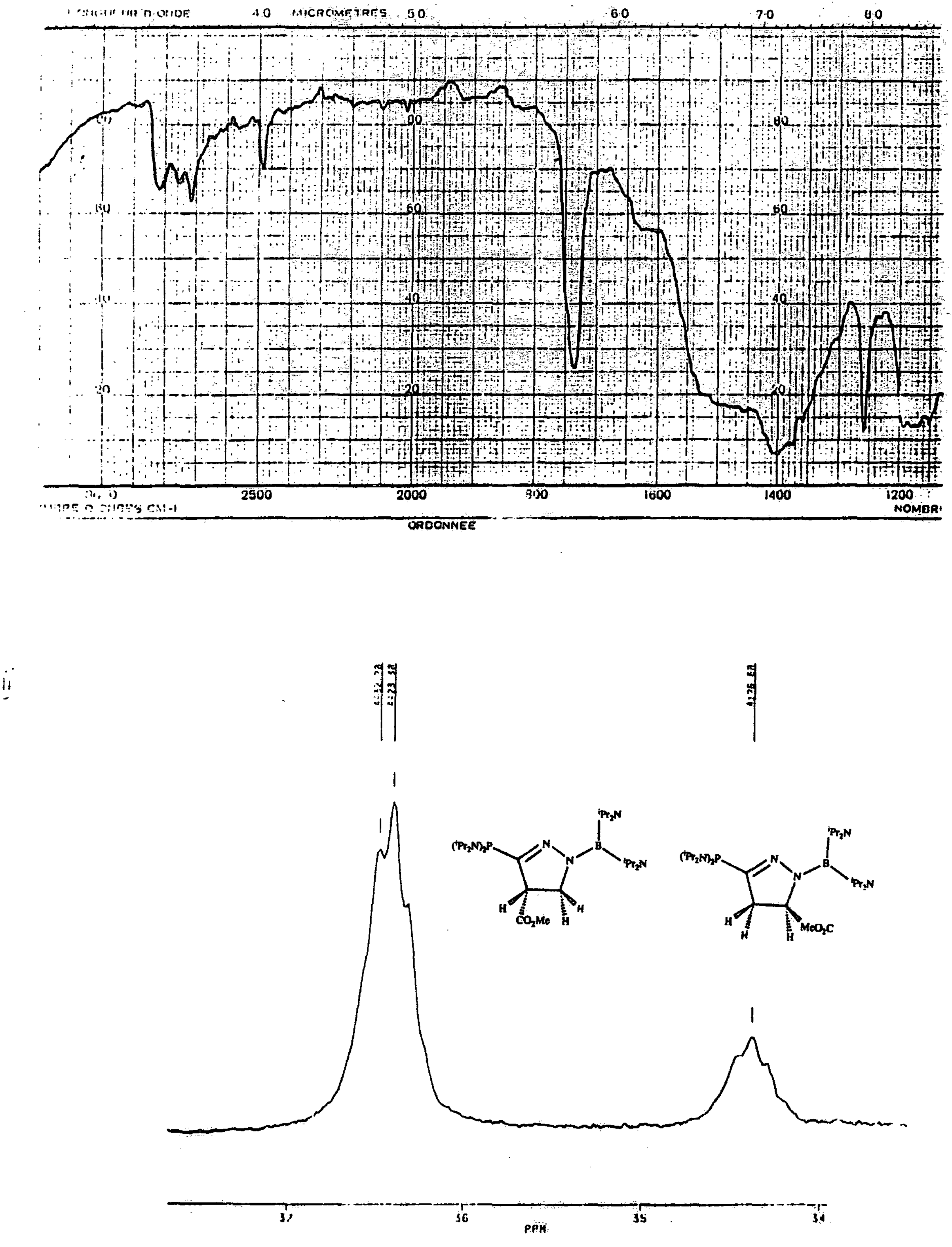

Figure 11.21: *(i) IR (pentane) and (ii) ^{31}P NMR ($CDCl_3$) spectra of cycloadducts (124,125).*

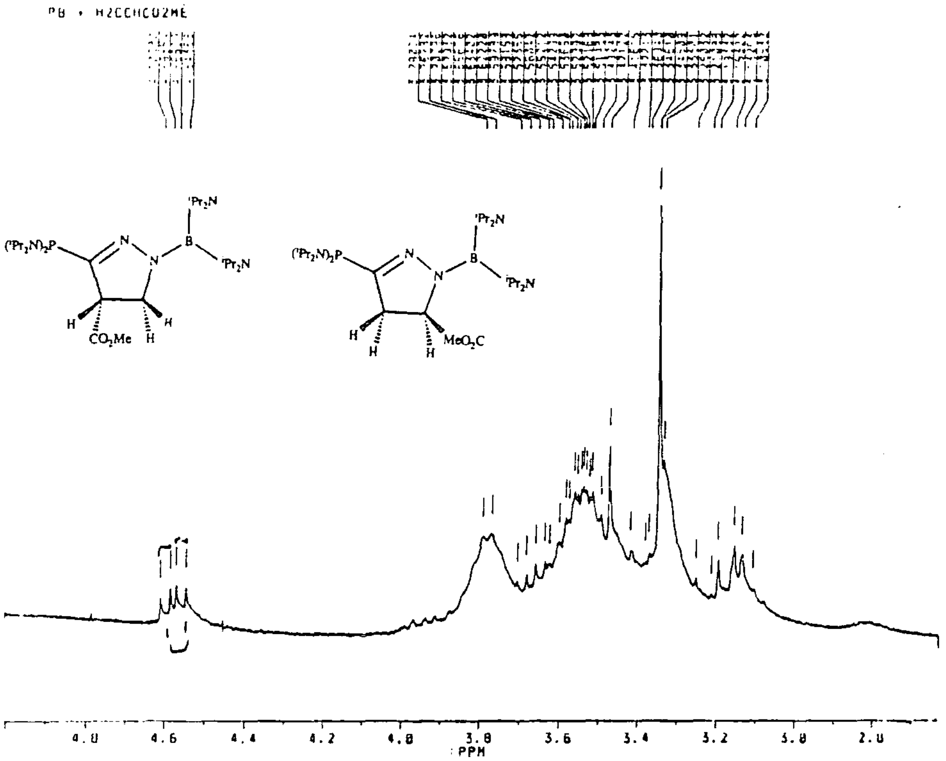

Figure 11.21: *(iii)* ^1H *NMR spectrum of cycloadducts (124,125) in* $CDCl_3$. (cont'd)

iv

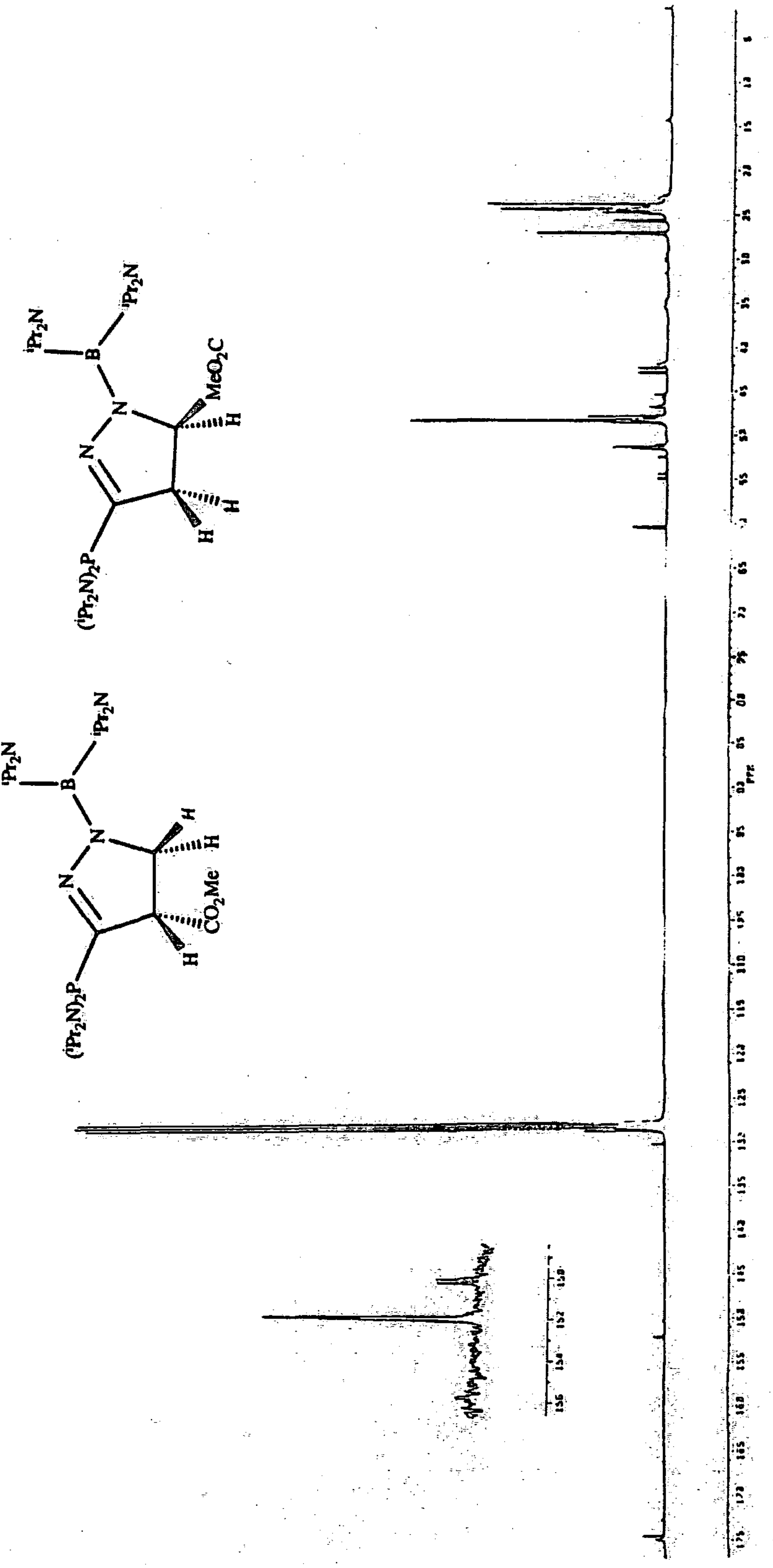

Figure 11.21: (iv) ^{13}C NMR spectrum of cycloadducts (124,125)
(cont'd) in $CDCl_3$.

Figure 11.21: *(v) Mass spectrum cycloadduct mixture (124,125).* (cont'd)

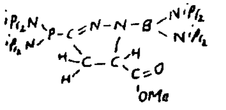

$C_{29}H_{62}N_6O_2PB$:568

BERTRAND REF 2 568 EI
Fichier: BERTRAN3.SPE   Date 04-26-89   Heure 09:43:05
S=33 MB=86 IB=3.82 RT=00:00:35

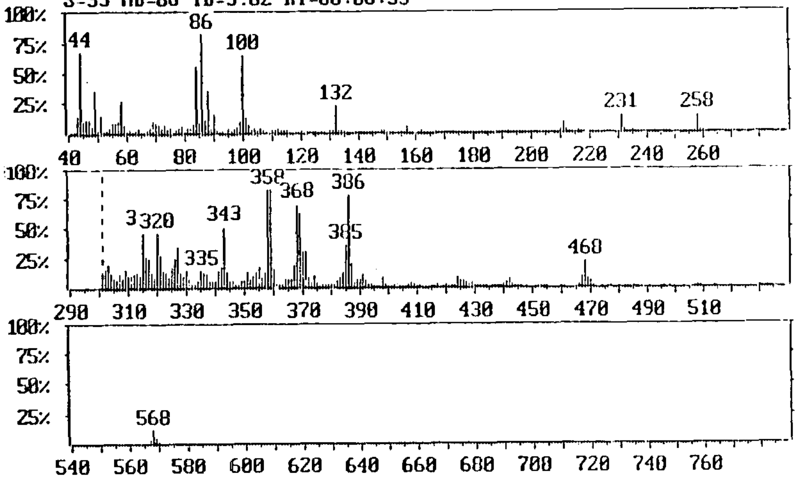

DS=41 FS=587 DA=40 FA=590 N=0 Z=2 S=0.0 Fact[301->650]*128
Liste Spectres > S=33 F=0 Pos=4 Tot=4

Fichier: BERTRAN3.SPE   Date 04-26-89
S=33 MB=86 IB=3.82 RT=00:00:35

Masse	Int(%)	Masse	Int(%)	Masse	Int(%)	Masse	Int(%)
41	0.42	42	0.13	43	13.43	44	66.88
45	9.46	46	10.55	47	10.22	48	5.43
49	34.85	50	2.01	51	13.24	52	0.90
53	2.62	54	3.75	55	8.57	56	8.10
57	9.78	58	26.92	59	7.07	60	1.43
61	1.82	62	0.61	63	2.05	64	3.31
65	0.70	66	0.58	67	2.56	68	3.41
69	9.59	70	8.45	71	6.84	72	3.55
73	7.16	74	3.71	75	3.64	76	0.89
77	2.17	78	4.18	79	4.92	80	1.14
81	3.26	82	3.28	83	6.01	84	55.75
85	8.29	86	100.00	87	10.62	88	35.55
89	3.01	90	15.09	91	2.23	92	1.41
93	1.60	94	1.50	95	3.13	96	2.04
97	4.03	98	5.12	99	8.76	100	64.07
101	11.71	102	6.65	103	1.93	104	3.32
105	2.57	106	4.35	107	2.10	108	1.15
109	2.11	110	1.67	111	2.43	112	4.17
113	2.43	114	2.24	115	2.75	116	1.27
117	1.11	118	0.82	119	1.06	120	2.24
121	1.24	122	1.36	123	0.90	124	0.56
125	1.19	126	0.87	127	0.90	128	1.09
129	1.76	130	2.30	131	1.99	132	22.19
133	2.78	134	1.98	135	1.71	136	0.52
137	0.71	138	0.99	139	1.04	140	1.50
141	1.38	142	0.91	143	0.66	144	0.66
145	0.71	146	0.54	147	0.90	148	1.68
149	1.76	150	0.61	151	0.65	152	0.35
153	0.39	154	0.42	155	0.57	156	1.05
157	5.24	158	0.91	159	1.18	160	0.36
161	0.59	162	1.65	163	0.73	164	0.58
165	0.66	166	0.72	167	1.46	168	0.47
169	0.51	170	0.58	171	0.59	172	0.74
173	0.88	174	0.79	175	0.72	176	0.31
177	0.52	178	0.38	179	0.37	180	0.35
181	0.33	182	0.27	183	0.31	184	0.33
185	0.28	186	0.95	187	0.65	188	0.54
189	0.65	190	0.50	191	0.51	192	0.20
193	0.25	194	0.42	195	0.26	196	0.15
197	0.27	198	0.90	199	0.32	200	0.35
201	0.14	202	0.39	203	0.26	204	0.41
205	0.57	206	0.25	207	1.14	208	0.38
209	0.35	210	1.99	211	7.42	212	1.51
213	0.36	214	0.63	215	0.46	216	2.24
217	0.82	218	1.13	219	0.67	220	0.60
221	0.45	222	0.35	223	0.41	224	0.30
225	0.34	226	0.85	227	1.10	228	0.82
229	0.38	230	1.01	231	13.11	232	2.31
233	1.30	234	0.93	235	1.55	236	0.57
237	0.52	238	0.50	239	0.40	240	0.15
241	0.15	242	1.30	243	0.36	244	0.31
245	0.20	246	0.33	247	0.74	248	0.82
249	0.43	250	0.22	251	0.24	252	0.19
253	0.18	254	0.15	255	0.55	256	1.76
257	1.92	258	13.06	259	1.85	260	1.68
261	0.29	262	0.27	263	0.36	264	0.15
265	0.15	266	0.15	267	0.27	268	0.16
269	0.27	270	0.40	271	0.23	272	0.13
273	0.13	274	0.18	275	0.12	276	0.19
277	0.10	278	0.14	279	0.18	280	0.17
281	0.42	282	0.17	283	0.10	284	0.09
285	0.15	286	0.15	291	0.32	292	0.26
293	0.11	294	0.12	295	0.16	296	0.12
298	0.19	299	0.20	300	0.11	301	0.10
302	0.12	303	0.15	304	0.10	309	0.12
312	0.09	313	0.10	315	0.38	316	0.20
317	0.19	318	0.10	320	0.36	321	0.22
322	0.11	323	0.10	325	0.13	326	0.19
327	0.27	328	0.10	330	0.14	333	0.11
336	0.10	341	0.11	342	0.13	343	0.40
344	0.11	351	0.10	354	0.10	355	0.13
357	0.10	358	3.58	359	0.93	360	0.12
367	0.14	368	0.54	369	0.49	370	0.23
371	0.24	384	0.10	385	0.28	386	0.61
387	0.16	391	0.09	468	0.17	568	0.09

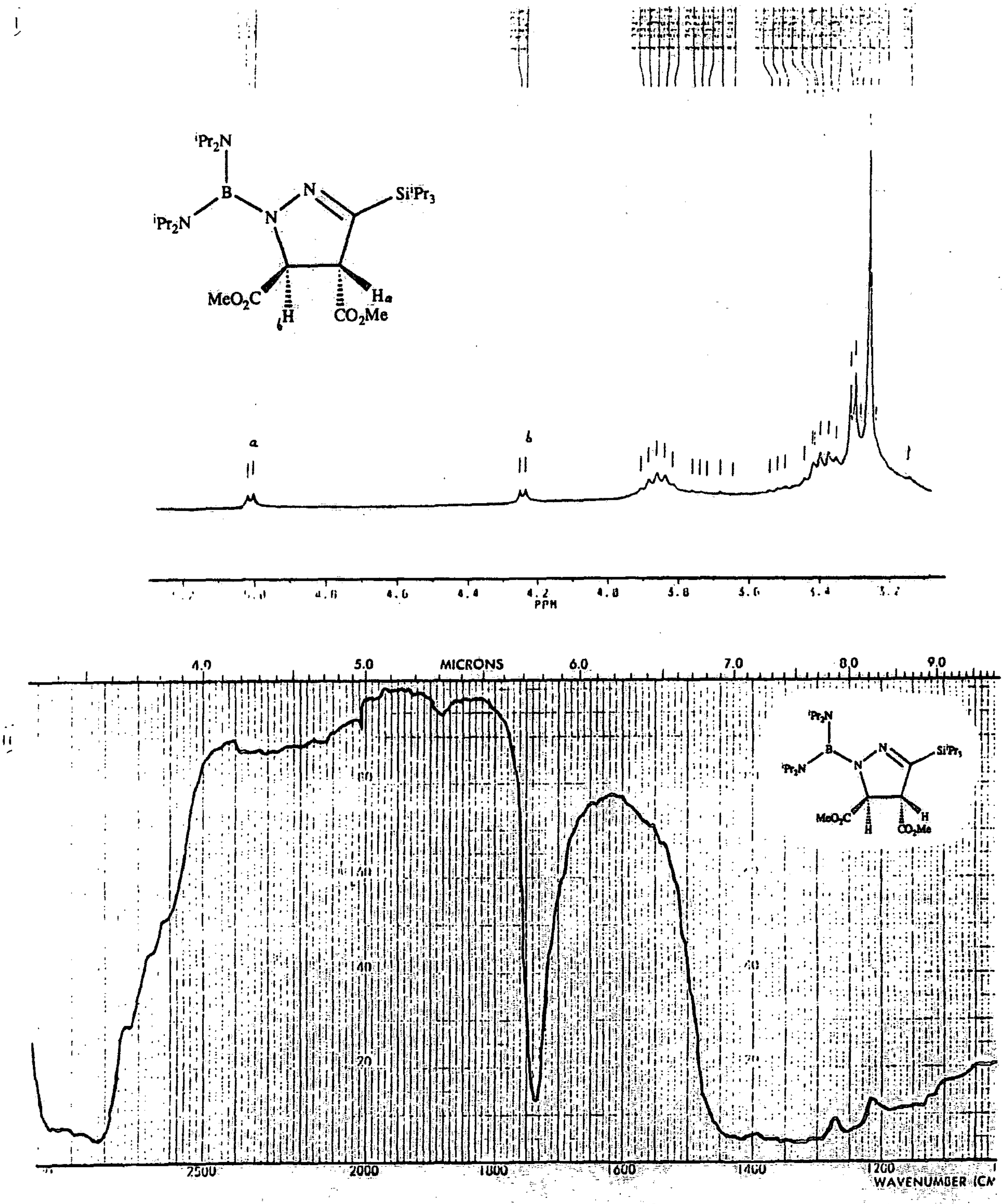

Figure 11.22: *(i) ^1H NMR (C_6D_6) and (ii) IR (pentane) spectra of cycloadduct (123).*

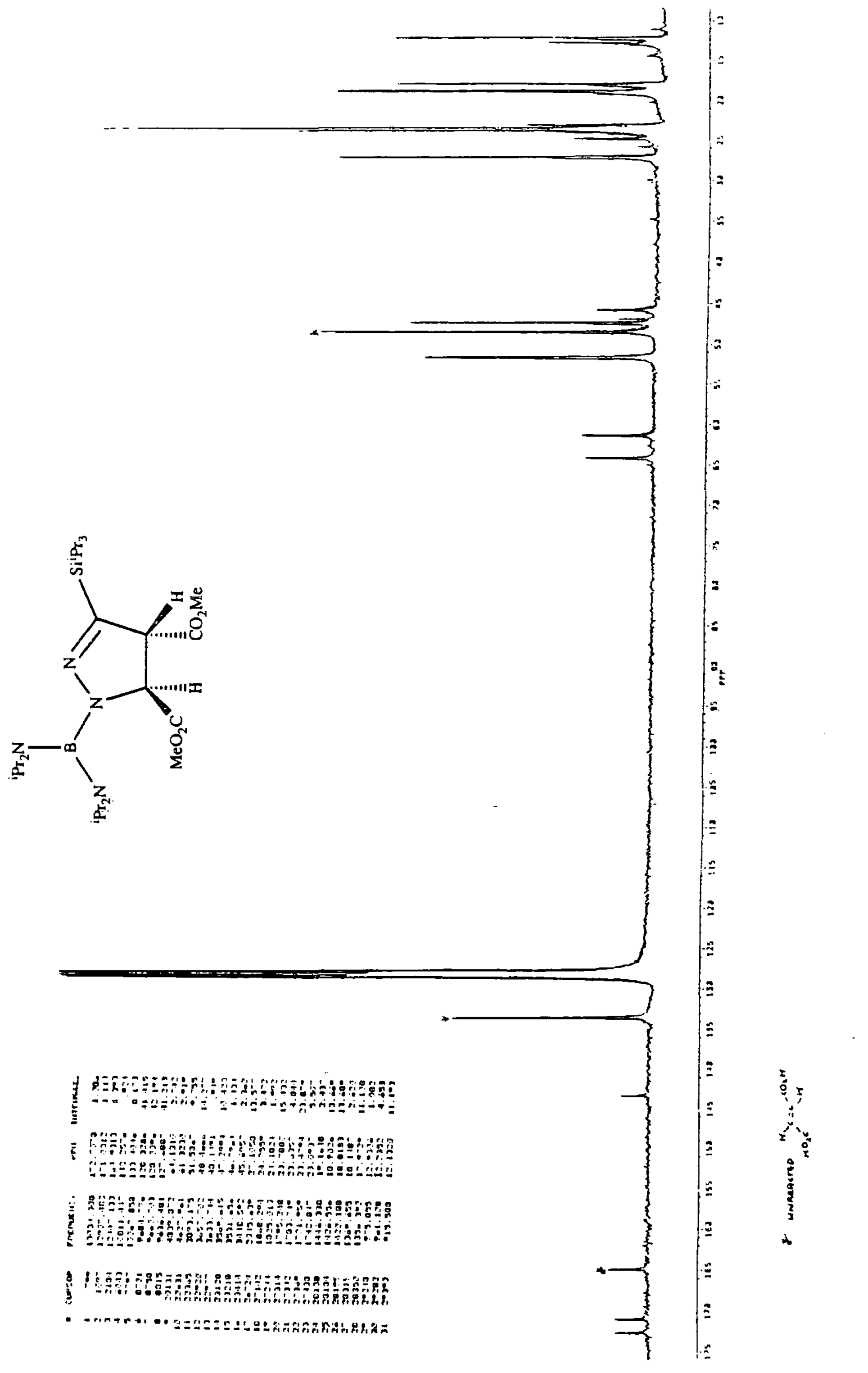

Figure 11.22: (iii) $^{13}C\{^{1}H\}$ NMR spectrum of cycloadduct (123) in $CDCl_3$.
(cont'd)

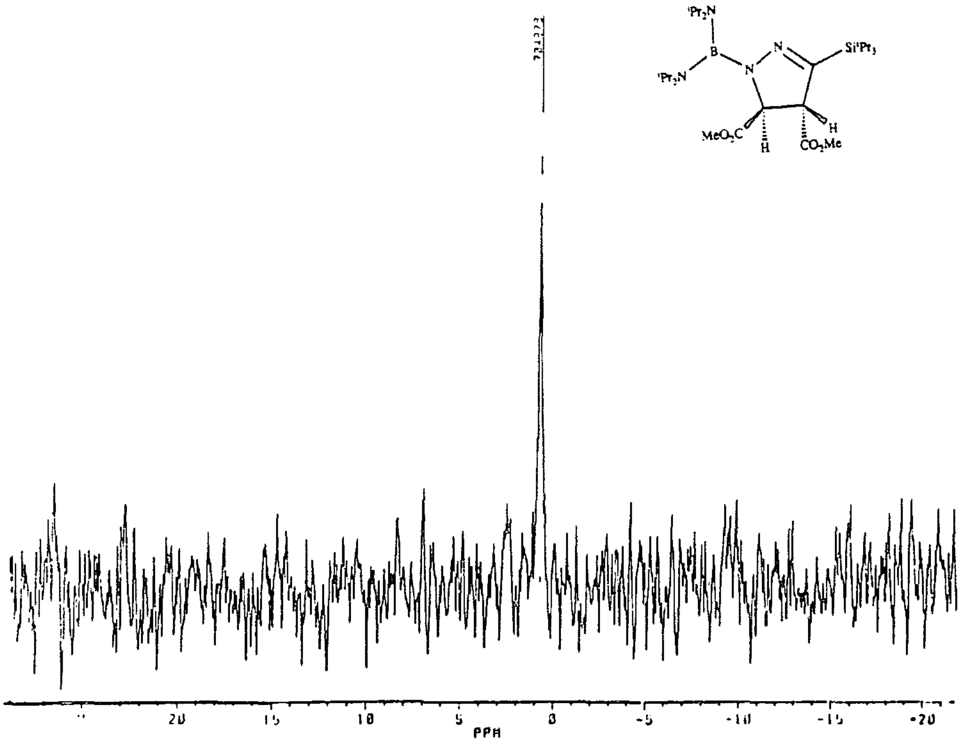

Figure 11.22: *(iv)* ^{29}*Si NMR spectrum of cycloadduct (123) in* $CDCl_3$. (cont'd)

CPD	^{11}B	^{31}P ($^{3}J_{PH}$)	$^{13}C_{CN}$ ($^{1}J_{CP}$)	IR
109	29.07	45.14(----)	61.87(48.3)	2100
110	27.75	31.8 (19.7)	57.42(125)	2095
113	28.1	0.726*		2100
114	23.06	82.96(----)	(-----------)	2200
116	22.2	0.72 *	'84'	2200
121	27.7	26.7 (----)	146.7 (17.4)	1730
122	27.69	57.1 (16.4)	143.27(158)	1750
				1740
123	28	0.705*	143.26	1740
124	27.9	36.4 (9.4)	152 (~6)	1735
125	~25	34.43(----)	~152 (~5)	1735
126	27	57.16(16.2)	147.45(150)	1750

Table 11.14: *NMR parameters for nitrileimines (109)-(113); carbodiimides (114),(116) and cycloadducts (121)-(126);* *^{29}Si *data.*

11.15 REFERENCES

1. E. Muller and H. Dusselhoff, *Annalen*, 512, 250 (1934).

2. R. Huisgen, M. Seidel, J. Sauer, J.W. McFarland and G. Wallbillich, *J.Chem.Soc.Chem.Commun.*, 24, 892-893 (1959).

3. R. Huisgen, J. Sauer and M. Seidel, *Chem.Ber.*, 2503-2509 (1961).

4. P. Weinberg, M. Siegmund, C. Csongár and G. Tomaschewski, *Z.Chem.*, 28(7), 252-253 (1988).

5. J.P. Anselme, *J.Chem.Educt.*, 43(11), 596-598 (1966).

6. C. Grundmann and K. Flory, *Liebigs Ann.Chem.*, 721, 91-100 (1969).

7. N.H. Toubro and A. Holm, *J.Amer.Chem.Soc.*, 2093-2094 (1980).

8. C. Wentrup, S. Fischer, A. Maquestiau and R. Flammang, *Angew.Chem. Int.Ed.Engl.*, 24, 56-57(1985).

9. G. Sicard, A. Baceiredo and G. Bertrand, *J.Amer.Chem.Soc.*, 110, 2663-2664 (1988).

10. S. Fischer and C. Wentrup, *J.Chem.Soc.Chem.Commun.*, 502-503 (1980).

11. I.V. Kolesnikova, T.D. Petrova and V.E. Platonov, *J.Fluorine Chem.*, 40, 217-246 (1988).

12. P. Molina, A. Argues, P.M. Fresneda, M.V. Vinader, M. de la C. Foces-Foces and F.H. Cano, *Chem.Ber.*, 122, 307-313 (1989).

13. M.S. Gordon, M.W. Schmidt and S. Koseki, *Inorg.Chem.*, 28, 2161-2163 (1989).

14. K. Issleib, H. Schmidt and H. Meyer, *J.Organometallic Chem.*, 192, 33-39 (1980).

15. D. Ranganathan, G.P. Singh and S. Ranganathan, *J.Amer.Chem.Soc.*, 111, 1144-1145 (1989)

16. U. Schöllkopf, B. Bánhidai, H. Frasnelli, R. Meyer and H. Beckhaus, *Liebigs Ann.Chem.*, 1767-1783 (1974).

17. R. Boese, P. Paetzold, A. Tapper and R. Ziembinski, *Chem.Ber.*, 122, 1057-1060 (1989).

18. B. Glaser and H. Nöth, *Angew.Chem. Int.Ed.Engl.*, 24(5), 416-417 (1985).

19. S. Helm and H. Nöth, *Angew.Chem. Int.Ed.Engl.*, 27(10), 1331-1336 (1988).

20. M. Pilz, J. Allwohn, R. Hunold, W. Massa and A. Berndt, *Angew. Chem. Int.Ed.Engl.*, 27(10), 1370-1372 (1988).

21. G. Singh and H. Zimmer, *Organomet.Chem.Rev.*, 279 (1967).

22. Yu.G. Gololobov, I.N. Zhmurova and L.F. Kasukhin, *Tetrahedron*, 37, 437-472 (1981).

23. A. Baceiredo, G. Bertrand and G. Sicard, *J.Amer.Chem.Soc.*, 107, 4781-4783 (1985).

24. S. Patai (Ed), "*The Chemistry of Functional Groups: The Chemistry of Diazonium and Diazo Groups, Part 2*", Wiley, New York, 17, 792-802 (1978).

25. S. Patai, "*The Chemistry of the Azido Group*", Wiley-Interscience, New York (1971).

26. W. Lwowski, "*Nitrenes*", Wiley-Interscience, New York (1970).

27. J.P. Ma joral, G. Bertrand, A. Baceiredo and E.O. Mavarez, *Phosphorus and Sulphur*, 27, 75-80 (1986).

28. J.S. Thayer, *Organomet.Chem.Rev.*, 157 (1966).

29. A.M. Jacquey "Memoire devant l'universite Paul Sabatier de Toulouse (Sciences)", 26th June 1986

30. M. Hudlicky, *J.Org.Chem.*, 45, 5377-5378 (1980).

31. M. Martin, *Synth.Comm.*, 13(10), 809-811 (1983).

32. M. Granier, A. Baceiredo and G. Bertrand, *Angew.Chem. Int.Ed. Engl.*, 27(10), 1350-1351 (1988).

33. Synthesised by F. Castan, Toulouse, CNRS (1989).

34. P. Sykes, "*Guidebook to Mechanism in Organic Chemistry*", 5th Edition, Longman, New York, 117-122 (1981).

35. Unpublished Work by A. Igau, Toulouse (CNRS).

36. A.K. Baruah, D. Prajapati and J.S. Sandhu, *Tetrahedron*, 44(19), 6137-6142 (1988).

37. H.M. Hassaneen, H.A. Ead, N.M. Elwan and A.S. Shawali, *Heterocycles*, 27(12), 2857-2862 (1988).

38. T. Fathi, A.N. Dinh Nguyen, G. Schmitt, E. Cerutti and B. Laude, *Tetrahedron*, 44(14), 4527-4536 (1988).

39. G. Märkl, I. Troetsch-Schaller and W. Hölzl, *Tetrahedron Lett.*, 29(7), 785-788 (1988).

40. G. Adembri, A.M. Celli and M. Scotton, *J.Heterocyclic Chem.*, 249(25), 249-251 (1988).

41. a) A. Padwi, (Eds. E.C. Taylor and A. Weissburger), "*1,3-Dipolar Cycloaddition Chemistry*", Wiley Interscience, Chapter 3, 1, 291 (1984).

    b) A. Bojilova, N.A. Rodios and N.E. Alexandrou, *J.Chem.Soc. Perkin.Trans.I*, 3233-3237 (1988).

42. a) R. Schmutzler, O. Stelzer and N. Weferling, *Chem.Ber.*, 121, 391-395 (1988).

    b) G. Bettermann, R. Schmutzler, S. Pohl and U. Thewalt, *Polyhedron*, 6(10), 1823-1831 (1987).

43. H. Nöth, *Nachr.Chem.Tech.Lab.*, 32(11), 956-959 (1984).

44. P. Powell, "*Principles of Organometallic Chemistry*", 2nd Edition, Chapman and Hall, London and New York, page 26 (1988).

45. A. Baceiredo and G. Bertrand, *Phosphorus and Sulphur*, 26, 57-62 (1986).

46. A. Igau, H. Grutzmacher, A. Baceiredo and G. Bertrand, *J.Amer. Chem.Soc.*, 110, 6463-6466 (1988).

47. A. Igau, A. Baceiredo, G. Trinquier and G. Bertrand, *Angew.Chem. Int.Ed.Engl.*, 28(5), 621-622 (1989).

48. G. Frenking, F. Marschner and H. Goetz, *Phosphorus and Sulphur*, 8, 337 (1980).

49. M.J.S. Dewar and S. Olivella, *J.Amer.Chem.Soc.*, 101, 4958 (1979).

50. J.A. Mosbo, R.K. Atkins, P.L. Bock and B.N. Storhoff, *Phosphorus and Sulphur*, 11, 11 (1981).

51. H. Boch, R. Dammel, S. Fischer and C. Wentrup, *Tetrahedron Lett.*, 28(6), 617-620 (1987).

52. G Bertrand, Communication from M. Th. Nguyen (1986).

53. Professor Pelter, personal communication (1988).

54. M.J.S. Gynane, A. Hudson, M.F. Lappert, P.P. Power and H. Goldwhite, *J.Chem.Soc.Dalton Trans.*, 2428-2433 (1980).

55. C.K. Narula and H. Nöth, *Inorg.Chem.*, 23, 4147-4152 (1984).

CHAPTER TWELVE

CONCLUSION

12.1 CONCLUSION

The Ar group has been shown to be effective in stabilising low coordinate phosphorus compounds. Some interesting coordination complexes have been isolated, and the crystal structure of $ArPCl_2[Pt(PEt_3)Cl_2]$ (57) has been obtained.

Work has begun in the area of low coordinate compounds containing boron and antimony, and some potentially useful starting materials have been obtained. Some progress has been made in the areas of halogenoborate and phosphoranide chemistry.

It is perhaps noteworthy that many of the Ar compounds illustrate 'through space coupling' some of the values of which are presented in Table 12.1. This data has been provided to a student of Stafford Polytechnic to help with a more direct study on the specific properties which influence these values.

Some new nitrileimines and heterocycles derived from these starting materials have been obtained, and the rearrangement of nitrileimines to carbodiimides by photolysis has been explored. This work has been extended to phosphorus and boron diazo compounds. Much of the above investigation has been supported by a parallel theoretical calculation of the molecular parameters by MNDO.

COMPOUND	NUMBER	$^{4}J_{PF}$	$^{5}J_{PF}$	$^{5}J_{FH}$	$^{5}J_{FF}$	$^{5}J_{PtF}$
$\mathrm{ArPCl_2}$	(12)	62.0				
$\mathrm{ArP(CN)_2}$	(16)	40.6				
$\mathrm{ArPH_2}$	(15)	28.9		5.5		
$\mathrm{ArPF_2}$	(3)	50.6			18.6	
$\mathrm{Ar_2PCl}$	(14)	42.0				
$\mathrm{ArP(Me)Cl}$	(40)	54.1				
$\mathrm{ArP(Et)Cl}$		51.2				
$\mathrm{ArP(Bu)Cl}$		51.1				
$\mathrm{ArP(PhCH_2)Cl}$	(37)	52.3				
$\mathrm{ArP(Me_3SiCH_2)Cl}$	(36)	51.8				
$\mathrm{ArP(CH_2{=}CH)Cl}$	(38)	51.4				
$\mathrm{ArP(CHCl_2)Cl}$	(39)	49.8				
$\mathrm{[ArP(Bu)_2]}$ ‡		43.7				
$\mathrm{[ArP(Me)_2]}$ ‡		33.2				
$\mathrm{[ArP(PhCH_2)_2]}$ ‡		40.0				
$\mathrm{[ArP(CH_2SiMe_3)_2]}$ ‡		46.3				
$\mathrm{[ArP(CH_2{=}CH)_2]}$ ‡		34.4				
$\mathrm{[ArP(CHCl_2)_2]}$ ‡		43.0				
$\mathrm{Ar_2P_2}$	(19)	45.0				
$\mathrm{ArP{=}CH(Ph)}$	(32)	23.7				
$\mathrm{ArP{=}CH(SiMe_3)}$	(33)	26.5				
$\mathrm{ArP{=}C(Cl)_2}$	(31)	21.0				
$\mathrm{ArP{=}C(Cl)[Pt(PEt_3)Cl_2]}$	(57)					32.5
$\mathrm{ArPCl_2[Pt(PEt_3)Cl_2]}$	(56)	27.6				24.2
$\mathrm{ArPH_2[Mo(CO)_5]}$	(66)	17.0		3.1		
$\mathrm{'ArBF_2'}$					15.8	

Table 12.1: *Through-space coupling constants; ‡side product only.*

APPENDIX A

CHARACTERISATION METHODS

A.1 COMPOUND IDENTIFICATION

A.1.1 Mass Spectrometry (MS)

Three techniques were employed: Electron Impact (EI), Positive Ion Chemical Ionisation (CI^+) and Negative Ion Chemical Ionisation (CI^-). For each example the technique used has been specified. Where an isotopic distribution pattern exists the most intense peak has been reported.

A.1.2 Nuclear Magnetic Resonance (NMR) Spectroscopy

Unless otherwise stated, where NMR shifts are quoted these have been obtained on a Bruker AC250 (250 MHz) machine. Frequencies used for specific nuclei include: ^{31}P 101.256 MHz; ^{11}B 80.239 MHz; ^{13}C 62.896 MHz; ^{1}H 250.133 MHz; ^{19}F 235.360 MHz; ^{119}Sn 93.275 MHz and ^{7}Li 97.206 MHz with the following references: ^{31}P H_3PO_4 (external); ^{11}B $BF_3\cdot Et_2O$ (external); ^{1}H TMS (internal); ^{13}C (internal deuterated solvent); ^{19}F (internal $CFCl_3$), ^{119}Sn (external Me_4Sn) and ^{7}Li (1M LiCl solution). In Chapter 11, work was carried out in Toulouse and the spectra were recorded on a Bruker AC200 (200 MHz) machine; ^{11}B 96.295 MHz; ^{31}P 121.496 MHz; ^{13}C 75.469 MHz; ^{1}H 300.133 MHz and ^{29}Si 39.761 MHz.

A.1.3 Vibrational Spectra (IR)

Infrared spectra were recorded on a Perkin-Elmer 577 instrument. The solids were prepared as Nujol mulls between KBr/CsI plates, or as a KBr disc when considered appropriate. The liquids were recorded as thin films, and the solutions in 0.05 mm solution cells with a KBr window.

A.1.4 Ultraviolet-Visible Spectra

The UV-visible spectra were recorded as solutions in CCl_4 or $CHCl_3$ in quartz cells with the solvent system in the reference beam, between 200 nm and 450 nm.

A.1.5 Chemical Analysis

C, H and N analysis were determined by micro-combustion with a Perkin-Elmer 240 instrument. Phosphorus and halogen analyses were carried out by R. Coult. For phosphorus and chlorine a weighed sample was decomposed by fusing in a nickel Parr bomb. The residue was acidified with concentrated nitric acid and made up to 100 mls with distilled water. For phosphorus a suitable aliquot was treated with ammonium molybdate/ammonium vanadate reagent and the absorbance measured at 420 μ using a Unicam SP500 spectrophotometer. Chlorine was determined by potentiometric titration against N/100 silver nitrate solution using Ag/AgCl electrodes in an acetone medium. Bromine and iodine were determined iodometrically following a Schoniger oxygen flask combustion. Metal analysis was achieved by atomic absorption spectrometry.

A.2 APPARATUS

A.2.1 Glove Box

Due to the moisture-sensitive nature of many of the compounds studied, manipulation of materials was carried out under an atmosphere of dry nitrogen. A dry box was used, equipped with two ports. The large port, for sizeable apparatus, was purged for at least 30 minutes before opening to the box. A smaller 'quick-entry' port, suitable for removal of NMR sample tubes and other small apparatus, was purged by excess internal pressure. The laboratory supply of piped nitrogen was further dried by passage through a tower packed with P_2O_5 about 1 metre in length. The external water pump, used for filtering solutions in the box, was protected by a calcium chloride trap, to prevent any water vapour diffusion into the dry box. A further precaution was a dish of P_2O_5 kept exposed in the box to remove any traces of water admitted through the entry ports.

A.2.2 Vacuum and High Pressure Apparatus

Standard vacuum line equipment, and high pressure apparatus (discussed in Chapter 1) was employed.

A.3 REAGENTS

A.3.1 Diazomethane Synthesis

CH_2N_2 was generated by the standard procedure (Chapter 11), using apparatus specially designed to avoid the use of ground glass joints.

A.3.2 Solvent and Reagent Purification

All solvents were dried and purified by standard techniques. For example, chlorocarbons were dried over 4Å mesh molecular sieve and stored under nitrogen. Hydrocarbon solvents were first dried over sodium wire and then stored under nitrogen over freshly activated molecular sieve. Diethylcarbonate was dried over $MgSO_4$. Nitrobenzene was distilled from P_2O_5 and stored over molecular sieve before use. All amines, for example i-Pr_2NH, were dried by distillation from, and storage over, KOH pellets.

The drying procedure for DBU involved refluxing with benzene and subsequent distillation onto activated 4Å molecular sieve. $AlCl_3$ was used directly after sublimation. The deliquescent tetraalkylammonium salts were dried by dissolving them in methanol, stirring, filtering off any insoluble impurities and removing the methanol *in vacuo*. Any residual methanol/water was removed by addition of toluene to form a slurry. This was stirred for 1 hr. before the toluene was removed *in vacuo*. The solid was pumped to dryness. In order to minimise borate hydrolysis, this procedure was repeated several times. Caesium fluoride was finely ground under nitrogen, and dried *in vacuo* at temperatures exceeding 100 ^{o}C for 2 hr. Specific cases in which further purification has been effected have been indicated.

A.4 MNDO CALCULATIONS

The calculations carried out in this work were done using MNDO as implemented in MOPAC version 5.

APPENDIX B

RESEARCH COLLOQUIA, SEMINARS, LECTURES AND CONFERENCES

The Board of Studies in Chemistry requires that each postgraduate research thesis contains an Appendix listing:

(A) All research colloquia, seminars and lectures arranged by the Department of Chemistry during the period of the author's residence as a postgraduate student, including lectures organised by Durham University Chemical Society;

(B) All research conferences attended and work presented by the author during the period when research for the thesis was carried out and

(C) Details of the postgraduate induction course.

(A) RESEARCH COLLOQUIA, SEMINARS AND LECTURES ORGANISED

DURING THE PERIOD: 1986-1987

* ALLEN, Prof. Sir G. (Unilever Research) Biotechnology and the Future of the Chemical Industry	13th November 1986
* BARTSCH, Dr. B. (University of Sussex) Low Co-ordinated Phosphorus Compounds	6th May 1987
BLACKBURN, Dr. M. (University of Sheffield) Phosphonates as Analogues of Biological Phosphate Esters	27th May 1987
BORDWELL, Prof. F.G.(Northeastern University,USA) Carbon Anions, Radicals, Radical Anions and Radical Cations	9th March 1987
CANNING, Dr. N.D.S. (University of Durham) Surface Adsorption Studies of Relevance to Heterogeneous Ammonia Synthesis	26th November 1986
CANNON, Dr. R.D. (University of East Anglia) Electron Transfer in Polynuclear Complexes	11th March 1987
CLEGG, Dr. W. (University of Newcastle-upon-Tyne) Carboxylate Complexes of Zinc; Charting a Structural Jungle	28th January 1987
DÖPP, Prof. D. (University of Duisburg) Cyclo-additions and Cyclo-reversions Involving Captodative Alkenes	5th November 1986
DORFMÜLLER, Prof. T. (University of Bielefeld) Rotational Dynamics in Liquids and Polymers	8th December 1986
GOODGER, Dr. E.M. (Cranfield Inst.Technology) Alternative Fuels for Transport	12th March 1987
GREENWOOD, Prof. N.N. (University of Leeds) Glorious Gaffes in Chemistry	16th October 1986
* HARMER, Dr. M. (I.C.I. Chemicals & Polymer Group) The Role of Organometallics in Advanced Materials	7th May 1987
HUBBERSTEY, Dr. P. (University of Nottingham) Demonstration Lecture on Various Aspects of Alkali Metal Chemistry	5th February 1987
* HUDSON, Prof. R.F. (University of Kent) Aspects of Organophosphorus Chemistry	17th March 1987

HUDSON, Prof. R.F. (University of Kent) Homolytic Rearrangements of Free Radical Stability	18th March 1987
JARMAN, Dr. M. (Institute of Cancer Research) The Design of Anti Cancer Drugs	19th February 1987
KRESPAN, Dr. C. (E.I. Dupont de Nemours) Nickel(0) and Iron(0) as Reagents in Organofluorine Chemistry	26th June 1987
KROTO, Prof. H.W. (University of Sussex) Chemistry in Stars, between Stars and in the Laboratory	23rd October 1986
LEY, Prof. S.V. (Imperial College) Fact and Fantasy in Organic Synthesis	5th March 1987
* MILLER, Dr. J. (Dupont Central Research, USA) Molecular Ferromagnets; Chemistry and Physical Properties	3rd December 1986
MILNE/CHRISTIE, Dr.A./Mr.S.(International Paints) Chemical Serendipity: A Real Life Case Study	20th November 1986
NEWMAN, Dr. R. (University of Oxford) Change and Decay: A Carbon-13 CP/MAS NMR Study of humification and Coalification Processes	4th March 1987
* OTTEWILL, Prof. R.H. (University of Bristol) Colloid Science a Challenging Subject	22nd January 1987
PASYNKIEWICZ, Prof. S. (Technical Univ.,Warsaw) Thermal Decomposition of Methyl Copper and its Reactions with Trialkylaluminium	11th May 1987
ROBERTS, Prof. S.M. (University of Exeter) Synthesis of Novel Antiviral Agents	24th June 1987
RODGERS, Dr. P.J. (I.C.I. Billingham) Industrial Polymers from Bacteria	12th February 1987
SCROWSTON, Dr. R.M. (University of Hull) From Myth and Magic to Modern Medicine	6th November 1986
* SHEPHERD, Dr. T. (University of Durham) Pteridine Natural Products; Synthesis and Use in Chemotherapy	11th February 1987
THOMSON, Prof. A. (University of East Anglia) Metalloproteins and Magneto-optics	4th February 1987
* WILLIAMS, Prof. R.L. (Metropolitan Police Forensic Science) Science and Crime	27th November 1986

WONG, Prof.E.H. (University of New Hampshire,USA) Coordination Chemistry of P-O-P Ligands	29th October 1986
WONG, Prof.E.H. (University of New Hampshire,USA) Symmetrical Shapes from Molecules to Art and Nature	17th February 1987

DURING THE PERIOD: 1987-1988

BAILEY, Dr. P.D. (University of York) Oncogenes	November 1987
* BIRCHALL, Prof. D. (I.C.I. Advanced Materials) Environment Chemistry of Aluminium	25th April 1988
* BORER, Dr. K. (University of Durham Industrial Research Laboratories) The Brighton Bomb - (A Forensic Science View)	18th February 1988
BOSSONS, L. (Durham Chemistry Teachers' Centre) GCSE Practical Assessment	16th March 1988
* BUTLER, Dr. A.R. (University of St.Andrews) Chinese Alchemy	5th November 1987
* CAIRNS-SMITH, Dr. A. (Glasgow University) Clay Minerals and the Origin of Life	28th January 1988
DAVIDSON, Dr. J. (Herriot-Watt University) Metal Promoted Oligomerisation Reactions of Alkynes	November 1987
* GRAHAM, Prof. W.A.G. (University of Alberta, Canada) Rhodium and Iridium Complexes in the Activation of Carbon-Hydrogen Bonds	3rd March 1988
* GRAY, Prof. G.W. (University of Hull) Liquid Crystals and their Applications	22nd October 1987
HARTSHORN, Prof. M.P. (University of Canterbury, New Zealand) Aspects of Ipso-Nitration	7th April 1988
* HOWARD, Dr. J. (I.C.I. Wilton) Chemistry of Non-Equilibrium Processes	3rd December 1987
JONES, Dr. M.E. (Durham Chemistry Teachers' Centre) GCSE Chemistry Post-mortem	29th June 1988
JONES, Dr. M.E. (Durham Chemistry Teachers' Centre) GCE Chemistry A-Level Post-mortem	6th July 1988
KOCH, Prof. H.F. (Ithaca College, U.S.A.) Does the E2 Mechanism Occur in Solution ?	7th March 1988

LACEY, Mr. (Durham Chemistry Teacher's Centre) Double Award Science	9th February 1988
* LUDMAN, Dr. C.J. (Durham University) Explosives	10th December 1987
McDONALD, Dr. W.A. (I.C.I. Wilton) Liquid Crystal Polymers	11th May 1988
* MAJORAL, Prof. J.-P. (Université Paul Sabatier) Stabilisation by Complexation of Short-Lived Phosphorus Species	8th June 1988
MAPLETOFT, Mrs. M. (Durham Chemistry Teachers' Centre) Salters' Chemistry	4th November 1987
NIETO DE CASTRO, Prof. C.A. (University of Lisbon and Imperial College) Transport Properties of Non-Polar Fluids	18th April 1988
* OLAH, Prof. G.A. (University of Southern California) New Aspects of Hydrocarbon Chemistry	29th June 1988
* PALMER, Dr. F. (University of Nottingham) Luminescence (Demonstration Lecture)	21st January 1988
* PINES, Prof. A. (University of California, Berkeley, U.S.A.) Some Magnetic Moments	28th April 1988
* RICHARDSON, Dr. R. (University of Bristol) X-Ray Diffraction from Spread Monolayers	27th April 1988
ROBERTS, Mrs. E. (SATRO Officer for Sunderland) Talk - Durham Chemistry Teachers' Centre - "Links between Industry and Schools"	13th April 1988
* ROBINSON, Dr. J.A. (University of Southampton) Aspects of Antibiotic Biosynthesis	27th April 1988
* ROSE, van Mrs. S. (Geological Museum) Chemistry of Volcanoes	29th October 1987
* SAMMES, Prof. P.G. (Smith, Kline and French) Chemical Aspects of Drug Development	19th December 1987
* SEEBACH, Prof. D. (E.T.H. Zurich) From Synthetic Methods to Mechanistic Insight	12th November 1987
SODEAU, Dr. J. (University of East Anglia) Durham Chemistry Teachers's Centre: "Spray Cans, Smog and Society"	11th May 1988
SWART, Mr. R.M. (I.C.I.) The Interaction of Chemicals with Lipid Bilayers	16th December 1987

* TURNER, Prof. J.J. (University of Nottingham) Catching Organometallic Intermediates	11th February 1988
* UNDERHILL, Prof. A. (University of Bangor) Molecular Electronics	25th February 1988
* WILLIAMS, Dr. D.H. (University of Cambridge) Molecular Recognition	26th November 1987
* WINTER, Dr. M.J. (University of Sheffield) Pyrotechnics (Demonstration Lecture)	15th October 1987

DURING THE PERIOD: 1988-1989

ASHMAN, Mr. A. (Durham Chemistry Teachers' Centre) The Chemical Aspects of the National Curriculum	3rd May 1989
AVEYARD, Dr. R. (University of Hull) Surfactants at your Surface	15th March 1989
AYLETT, Prof. B.J. (Queen Mary College, London) Silicon-Based Chips: The Chemists Contribution	16th February 1989
BALDWIN, Prof. J.E. (Oxford University) Recent Advances in the Bioorganic Chemistry of Penicillin Biosynthesis	9th February 1989
BALDWIN & WALKER, Drs. R.R. and R.W. (Hull University) Combustion: Some Burning Problems	24th November 1988
BOLLEN, Mr. F. (Durham Chemistry Teachers' Centre) Lecture about the use of SATIS in the classroom	18th October 1988
BUTLER, Dr. A.R. (St. Andrews University) Cancer in Linxiam: The Chemical Dimension	15th February 1989
* CADOGAN, Prof. J.I.G., (British Petroleum) From Pure Science to Profit	10th November 1988
CASEY, Dr. M. (University of Salford) Sulphoxides in Stereoselective Synthesis	20th April 1989
WALTERS & CRESSEY, Mr. D. and T. (Durham Chemistry Teachers' Centre) GCSA Chemistry 1988: "A Coroner's Report"	1st February 1989
CRICH, Dr. D. (University College London) Some Novel Uses of Free Radicals in Organic Synthesis	27th April 1989

DINGWALL, Dr. J. (Ciba Geigy) Phosphorus-containing Amino Acids: Biologically Active Natural and Unnatural Products	18th October 1988
ERRINGTON, Dr. R.J. (University of Newcastle-upon-Tyne) Polymetalate Assembly in Organic Solvents	1st March 1989
FREY, Dr. J. (Southampton University) Spectroscopy of the Reaction Path: Photodissociation Raman Spectra of NOCl	11th May 1989
HALL, Prof. L.D. (Addenbrooke's Hospital, Cambridge) NMR - A Window to the Human Body	2nd February 1989
HARDGROVE, Dr. G. (St. Olaf College, U.S.A.) Polymers in the Physical Chemistry Laboratory	December 1988
HARWOOD, Dr. L. (Oxford University) Synthetic Approaches to Phorbols Via Intramolecular Furan Diels-Alder Reactions: Chemistry under Pressure	25th January 1988
JÄGER, Dr. C. (Friedrich-Schiller University GDR) NMR Investigations of Fast Ion Conductors of the NASICOM Type	9th December 1988
* JENNINGS, Prof. R.R. (Warwick University) Chemistry of the Masses	26th January 1989
JOHNSON, Dr. B.F.G. (Cambridge University) The Binary Carbonyls	23rd February 1989
JONES, Dr. M.E. (Durham Chemistry Teachers' Centre) Discussion Session on the National Curriculum	14th June 1989
JONES, Dr. M.E. (Durham Chemistry Teachers' Centre) GCSE and A Level Chemistry 1989	28th June 1989
* LUDMAN, Dr. C.J. (Durham University) The Energetics of Explosives	18th October 1988
MACDOUGALL, Dr. G. (Edinburgh University) Vibrational Spectroscopy of Model Catalytic Systems	22nd February 1989
MARKO, Dr. I. (Sheffield University) Catalytic Asymmetric Osmylation of Olefins	9th March 1989
* McLAUCHLAN, Dr. K.A. (University of Oxford) The Effect of Magnetic Fields on Chemical Reactions	16th November 1988

MOODY, Dr. C.J. (Imperial College) Reactive Intermediates in Heterocyclic Synthesis	17th May 1989
MORTIMER, Dr. C. (Durham Chemistry Teachers' Centre) The Hindenberg Disaster - an Excuse for Some Experiments	14th December 1989
* NICHOLLS, Dr. D. (Durham Chemistry Teachers' Centre) Liquid Air Demonstration	11th July 1989
* PAETZOLD, Prof. P. (Aachen) Iminoboranes $XB{\equiv}NR$: Inorganic Acetylenes ?	23rd May 1989
PAGE, Dr. P.C.B. (University of Liverpool) Stereocontrol of Organic Reactions Using 1,3-dithiane-1-oxides	3rd May 1989
POLA, Prof. J. (Czechoslovak Academy of Sciences) Carbon Dioxide Laser Induced Chemical Reactions - New Pathways in Gas-Phase Chemistry	15th June 1989
* REES, Prof. C.W. (Imperial College London) Some Very Heterocyclic Compounds	27th October 1988
REVELL, Mr. P. (Durham Chemistry Teachers' Centre) Implementing Broad and Balanced Science 11-16	14th March 1989
* SCHMUTZLER, Prof. R. (Technische Universitat Braunschweig) Fluorophosphines Revisited - New Contributions to an Old Theme	6th October 1988
SCHROCK, Prof. R.R. (M.I.T.) Recent Advances in Living Metathesis	13th February 1989
SINGH, Dr. G. (Teeside Polytechnic) Towards Third Generation Anti-Leukaemics	9th November 1988
* SNAITH, Dr. R. (Cambridge University) Egyptian Mummies: What, Where, Why and How ?	1st December 1988
STIBR, Dr. R. (Czechoslovak Academy of Sciences) Recent Developments in the Chemistry of Intermediate-Sited Carboranes	16th May 1989
VON RAGUE SCHLEYER, Prof. P. (Universitat Erlangen Nurnberg) The Fruitful Interplay Between Calculational and Experimental Chemistry	21st October 1988
* WALKER, Dr. R.W. and Dr. R.R. (University of Hull) Combustion - Some Burning Problems	24th November 1988

WELLS, Prof. P.B. (Hull University) 10th May, 1989
Catalyst Characterisation and Activity

* - Indicates Colloquia attended by the author.

(B) CONFERENCES

The author attended and presented a summary of her current research at the Euchem Conference Psiblocs in Paris-Palaiseau (August 1988).

The research work carried out in Toulouse on Nitrileimine and Carbodiimide chemistry was presented at the Conseil Scientifique at the CNRS (June 1989).

The Durham Graduate Symposium was also attended (April 1987).

(C) FIRST YEAR INDUCTION COURSE (OCTOBER 1986)

This course consisted of a series of one hour lectures on the services available in the department:

Departmental Organisation	Dr. E.J.F. Ross
Safety Matters	Dr. M.R. Crampton
Electrical Appliances	Mr. B.T. Barker
Chromatography and Microanalysis	Mr. T.F. Holmes
Atomic Absorption and Inorganic Analysis	Mr. R. Coult
Library Facilities	Mr. R.B. Woodward
Mass Spectrometry	Dr. M. Jones
Nuclear Magnetic Resonance Spectroscopy	Dr. R.S. Matthews
Glass Blowing Technique	Mr. R. Hart Mr. G. Haswell